Scope and Mechanistic Studies of Ruthenium Catalyzed C-N Bond Activation Reactions

Pandula Taepith Kirinde Arachchige
Marquette University

SCOPE AND MECHANISTIC STUDIES OF RUTHENIUM CATALYZED C-N BOND ACTIVATION REACTIONS

by

Pandula T. Kirinde Arachchige B.Sc. (Hons), M.Sc.

A Dissertation Submitted to the Faculty of the Graduate School,

Marquette University,

in Partial Fulfillment of the Requirements for

the Degree of Doctor of Philosophy

Milwaukee, Wisconsin

May 2021

ABSTRACT

SCOPE AND MECHANISTIC STUDIES OF RUTHENIUM CATALYZED C-N BOND ACTIVATION REACTIONS

Pandula T. Kirinde Arachchige B.Sc. (Hons), M.Sc.

Marquette University, 2021

Primary aliphatic amines which are ubiquitous in natural products, traditionally considered as inert to substitution reactions. Recent studies clearly demonstrated that the aliphatic deaminative coupling chemistry can be used to make valuable scaffolds through C–N bond activation on transition metal complexes. The catalytic system generated in situ from the tetranuclear Ru–H complex with a catechol ligand (**2-9**/**2-16**) and independently synthesized ruthenium catecholate complex **2-11** was found to be effective for the direct deaminative coupling of primary amines. The catalytic system formed *in-situ* from the reaction of cationic Ru–H complex **2-10** with 3,4,5,6-tetrachloro-1,2-benzoquinone **2-12** was found to mediate a regioselective deaminative coupling reaction of ketones with amines to form the α-alkylated ketone products. The monitoring of the coupling reaction of acetophenone and 4-methoxybenzylamine showed a rapid formation of $PhC(Me)=NCH_2C_6H_4$-4-OMe, which was slowly converted to the alkylation product. The Hammett plot obtained from the reaction of *para*-substituted imines showed a strong promotional effect by the amine substrates with electron-releasing group ($\rho = -0.96 \pm 0.1$), while the analogous plot obtained from the reaction of *para*-substituted imines with benzylamine showed a moderate promotional effect from the ketone substrates with electron-withdrawing group ($\rho = +0.24 \pm 0.1$). The most significant carbon isotope effect was observed on the α-carbon of the alkylation product ($C_\alpha = 1.020$). The empirical rate law was determined as rate = k_{obs}[imine][Ru] from measuring the kinetics of the alkylation reaction of the isolated imine substrate. A catalytically active Ru-catecholate complex was synthesized and the DFT study revealed a stepwise mechanism of the [1,3]-carbon migration step via the formation of a Ru(IV)-alkyl species. A plausible mechanism of the catalytic alkylation reaction via an intramolecular [1,3]-alkyl migration of Ru-enamine intermediate has been proposed. The in situ formed ruthenium catalytic systems (**2-10**/**2-16**), (**2-10**/**2-12**) and the complex **2-11** was also found to be highly selective for the dehydrogenative/deaminative coupling reactions to form number of pharmaceutically important nitrogen heterocyclic products with amines. The catalytic coupling method provides an operationally simple and chemoselective synthetic protocol without using any reactive reagents or forming wasteful byproducts.

ACKNOWLEDGEMENTS

First and foremost, I give my deepest gratitude to all the wonderful people who enriched my graduate studies at Marquette university. I would like to express my sincere gratitude to my esteemed advisor, Professor Chae Sung YI, for giving me this opportunity at Marquette University. His aspiring guidance, invaluably constructive criticism, friendly advices, help when required at the most appropriate moment and mentorship were vital to my success. I take this opportunity to express my heartiest thanks to the committee members, Professor William A. Donaldson, Professor Adam Fiedler, Professor James R. Gardinier and Professor Chieu D. Tran for their acceptance, service, insightful comments and support throughout my study time. I would like to thank all my teachers at Marquette chemistry and former group members Dr. Nishantha Kalutharage, Dr. Hanbin Lee and Dr. Junghwa Kim for their valuable support. Also, current group members, Dr. Nuwan Pannilawithana, Dulanjali Tennakoon, Xiangyu Chen, Krishna Gnyawali, Aldiyar Shakenov and Dana Stambekova for being dearest friends. In addition, I would like to express my sincere thanks to Dr. S. Lindeman for X-ray diffraction analysis, Dr. Sheng Cai for the technical support on NMR analysis, Mark Bartelt for the technical support, Lori Callaghan for the excellent support on office matters, and Paul Dion for purchasing support.

I am very grateful to all my teachers and colleagues at the *University of Ruhuna, Matara*, Sri Lanka, especially professor P. Ruchira T. Cumaranatunga and Hema M. K. K. Pathirana, who have inspired and encouraged me to choose the academic field as my career and their unconditional support. Also, I am very appreciating for the help I received from professor Tilak P. D. Gamage, professor R. A. Maithreepala, professor H. B. Asanthi, Mr. Samantha Kumarasena and Dr. Elmo Weerakoon on academic and family matters. Also, I will never forget the people and wonderful time I had as a faculty member at University of Ruhuna, Matara, Sri Lanka which always in the highest place in my heart. I deeply respect and admire my high school, *Richmond College*, *Galle*, primary school, *Kirinda Model Primary School*, (කිරින්ද කනිෂ්ඨ විද්‍යාලය) Puhulwella, Matara and all the teachers for the dissemination of knowledge and strength developed in me.

This work would not have been possible without the love, support and lifelong sacrifice made by my late Father, Mr. Darmadasa Kirinde Arachchi and Mother Mrs. Malini Kuruppu Nanayakkara. My Father, the greatest person in my life, my first teacher, who inspired me to be a good citizen and showed me the way of living a simple quality life and installed such a strong foundation to grow and be the independent adult I am today. I am trying my best to follow his philosophy and the path he showed me. I am so lucky to have such a wonderful mother in my life; her unconditional love and care mean everything to me. Thank you, my ever-loving mom, for always being there for me!! I also thankful for my sister Jeewa Kirinde Arachchi, brother-in-law-Dhanushka Weerakoon, and sister-in-law-Nadeeka Hewage and specially brother, Susil Shantha Kirinde Arachchi who took all the responsibilities of the family in the events of my absence. I also thankful for their kids Senuja Thisen Dinusara Weerakoon, Sethuli Vihasna Weerakoon and Sanudi Sri Thanuthmi Kirinde Arachchi, for bringing me joy and hope. I extend my sincere thanks for Darshi and Sri Lankan community living in Milwaukee being with me! Your help and support incredibly helped me when I needed the most. Also, big thank to the wonderful people living in Milwaukee who made me this beautiful city as my home.

I am extremely appreciative for the financial assistance given by National Science Foundation, National Institute of Health, Denis J. O'Brien Foundation, Wehr Foundation and Marquette University, which exclusively supportive to keep my focus and concentration on research work all over the day. Also, I would like to extend my sincere gratitude for all the wonderful people at the Graduate School, Office of International Education, department of chemistry and Marquette University administration. Finally, I am sincerely thankful to all the friends and colleagues for sharing their truthful and illuminating views during my time at Marquette Chemistry.

DEDICATION

My humble effort I dedicated to the memory of my beloved father **Mr. Dharmadasa Kirinde Arachchi**, and mother, **Mrs. Malini Kuruppu Nanayakkara**, for unconditional love, care, guidance and lifelong sacrifice to make me who I am.

Along with all hard working and respected teachers in the world.

TABLE OF CONTENTS

LIST OF TABLES

LIST OF FIGURES

LIST OF SCHEMES

ABBREVIATIONS

iPr – iso-Propyl

tBu – tertiary Butyl

KHMDS – Potassium bis(trimethylsilyl)amide

tBuOK – Potassium tert-butoxide

THF – Tetrahydrofuran

TON – Turn Over Number

TOF – Turn Over Frequency

LiOTf – Lithium Triflate

dpen – Diphenylethylenediamine

DFT – Density-functional theory

DPPB – (1,4-bis(diphenylphosphino)butane)

DMC – Dimethyl Carbonate

C-T – Charge-Transfer

TBDMS – tert-Butyldimethylsilyl

SET – Single Electron Transfer

Bn – Benzyl

Ph – Phenyl

Ar – Aryl

dba – dibenzylideneacetone

acac – Acetylacetone

DMA – Dimethylacetamide

dtbbpy – 4,4′-Di-tert-butyl-2,2′-dipyridyl

Boc – tert-Butyloxycarbonyl

SIPr – 1,3-Bis(2,6-diisopropylphenyl)imidazolidin

THBP – tert-Butyl hydroperoxide

RDS – Rate Determining Step

DTBP – di-tert-butyl peroxide

Cp – Cyclopentadienyl

Cp* – 1,2,3,4,5-Pentamethylcyclopentadienyl

PPh_3 – Triphenylphosphine

PCy_3 – Tricyclohexylphosphine

Me – Methyl

Et – Ethyl

R – Alkyl-, Aryl moiety

Nu – Nucleophile

DMF – Dimethylformamide

TFE – 2,2,2-trifluoroethanol

IMes – 1,3-bis-(2,4,6-trimethylphenyl)imidazole carbene ligand

DPPF – 1,1'-Bis(diphenylphosphino)ferrocene

BINAP – diphenylphosphinobinapthyl

coe – Cyclooctene

NCTS – N-cyano-N-phenyl- p-toluenesulfonamide

t-BuXPhos – 2-Di-tert-butylphosphino-2′,4′,6′-triisopropylbiphenyl

COD – Cyclooctadiene

NMR – Nuclear magnetic resonance

s – singlet

d – doublet

t – triplet

q – quartet

m – multiplet

br – broad

ppm – Parts per million

HRMS – High resolution mass spectroscopy

Chapter 1

Recent Advances on the Development and Synthetic Applications of Catalytic Coupling Methods via C–N Bond Activation

1.1 Introduction

The C−N bond is one of the most abundant chemical bonds found in many organic, and biomacromolecules.[1] The activation and transformation of C−N bonds[2] by using transition-metal catalysis has been emerged as a powerful tool for a variety of C−C bond forming reactions, synthesis of amides and other nitrogen-containing molecules.[3] In a biochemical example, proteins are translated from α-amino acids via the C−N bond formation and the reverse process from proteins to α-amino acids via the amide C−N bond cleavage for biological systems.[4] Compared to catalytic C−H[5] and C−O[6] bond activation reactions, transition-metal catalyzed C−N bond cleavage methods have been considerably underexplored, and has been identified as a new emerging area of organic chemical transformations. While primary and branched amines have been found to be the most prevalent classes of organic compounds, their utilization in C−N bond cleavage reactions has been found to be quite challenging, in part due to relatively high C−N bond dissociation energy and remains a great challenge in the development of catalytic coupling methods via C–N bond cleavage.

Transition metal mediated C–N bond cleavage reactions have been found to be a key step in a number of catalytic coupling methods.[3b, 7] Transition metal catalytic species have been shown to mediate inert C–N bond activation, which then generate new C-C and C-X bonds in the presence of potential electrophilic or nucleophilic species affording desired products as illustrated in **Figure 1.1**.

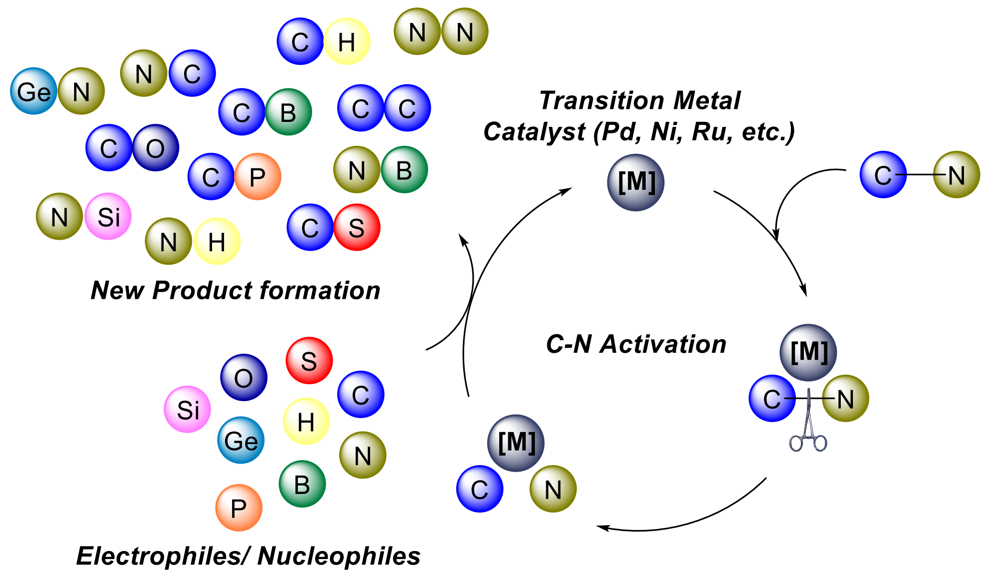

Figure 1.1: Representation of Catalytic C–N Bond Activation and Product Formation

The designing and utilization of catalytic C–N bond cleavage strategy and synthetic applications present a unique challenge due to their inert nature of the unreactive C–N bond and their well-known ability to poison the metal catalysts. In the last decades, many clever and convenient Catalytic C−N cleavage methods approaches have been developed to obtain reliable nitrogen and/or carbon sources. Two main transition metal catalyzed C−N bond activation protocols have been classified, namely: N-containing compounds such as amines, amides having unactivated C−N bonds, and N-containing compounds having activated C−N bonds, such as ammonium salts, diazonium salts, triazoles, strained azaheterocycles.

Fundamental mechanistic understandings on catalytic C−N bond cleavage reactions are immensely valuable not only for establishing the governing factors and fate of the active species, but also in designing the next generation of efficient and greener C−N bond cleavage protocols. Six major pathways have been identified for the transition-metal catalyzed C−N bond cleavage reactions as illustrated in **Scheme 1.1**.[3a, 3b]

a) Oxidative addition

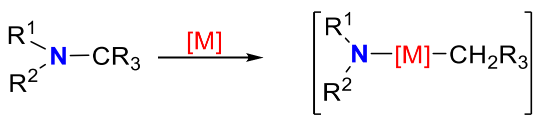

b) C-H bond cleavage triggered C-N activation (via imine species)

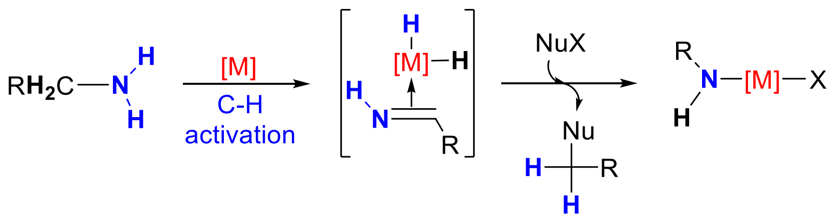

c) C-H bond cleavage triggered C-N activation (via iminium species)

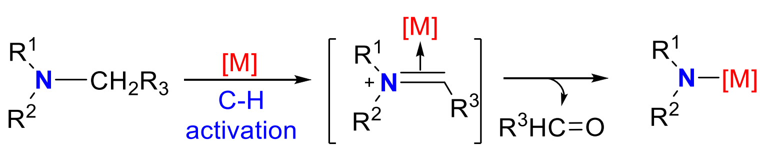

d) Via ammonium ion species

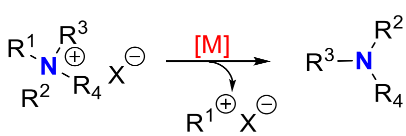

e) *β*-N elimination

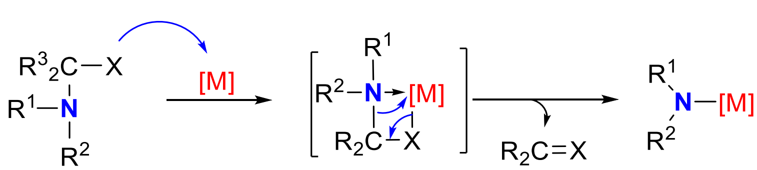

f) Via insertion/de-insertion

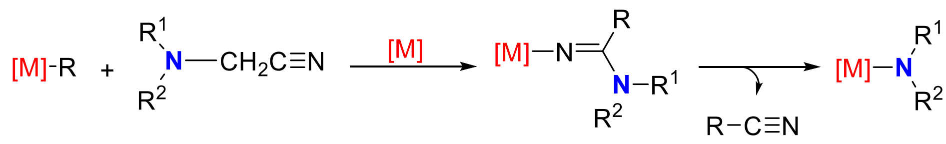

Scheme 1.1: General Mechanistic Pathways for C-N Bond Activation

Selective C−N bond cleavage reactions of sterically non-demanding N-containing compounds, such as amines, amides, and ammonium salts have been commonly achieved, in which their reactivity and selectivity patterns are depend on the substrate structure and reaction conditions. In this chapter, we will discuss the development and synthetic applications of transition-metal catalyzed C−N bond hydrogenolysis, C−C, and C−heteroatom bond forming reactions via C−N bond activation for nitrogen containing compounds reported in last five years. The content is organized according to the types of coupling methods involved in the reactions and mechanistic insights listed in **Scheme 1.1**.

1.2 Catalytic C–N Bond Hydrogenolysis Methods

Hydrogenolysis of C–N bond is an efficient transformation for the synthesis of complex molecules.[8] Since traditional methods mainly employ stoichiometric (and in practice, excess) quantities of hydride reagents, i.e. $LiAlH_4$ at room temperature, they have a number of drawbacks such as the production of stoichiometric amounts of byproducts, loss of important raw materials especially in multi-step synthesis, and lack of chemo-selectivity during the reduction process. Transition metals catalyzed C–N bond hydrogenolysis methods have been shown to provide an alternative strategy for atom efficient, environmentally friendly and economically acceptable solutions to overcome these problems.

1.2.1 Deaminative Hydrogenolysis of Amides

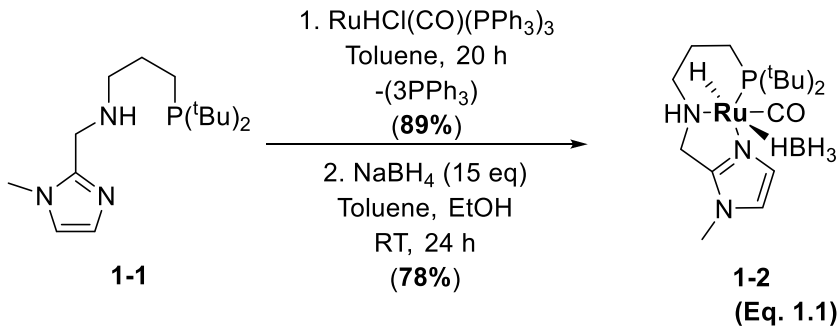

Due to their low reactivity, transition metal catalyzed C−N hydrogenolysis of amides has been considered challenging and scarcely investigated until recent past.[9]

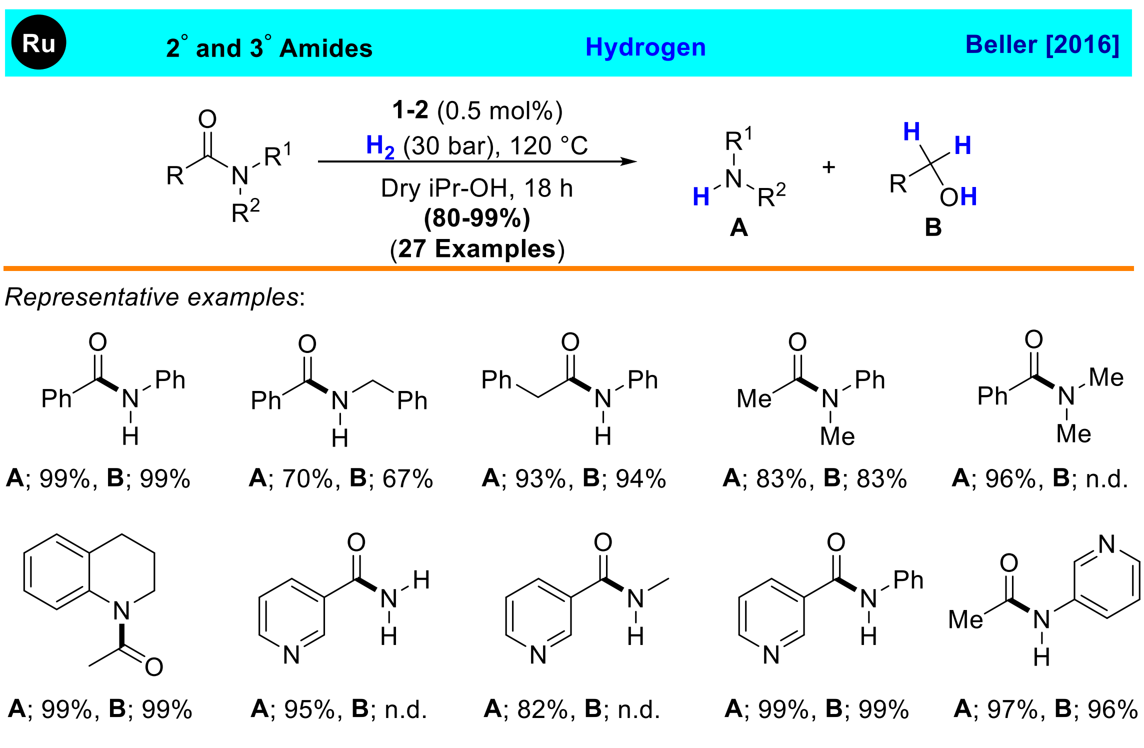

Scheme 1.2: Base Free Hydrogenolysis of Amides Catalyzed by Complex **1-2**

In 2016, Beller group reported ruthenium pincer complex **1-2** bearing an imidazolylaminophosphino ligand **1-1** (**Eq. 1.1**) is an effective catalytic system for the hydrogenolysis of primary and secondary amides to generate corresponding alcohols in good to excellent yields (**Scheme 1.2**).[10] The ruthenium-PNN pincer complex **1-2** alone failed to catalyze the hydrogenolysis reaction for simple amides, but the addition of 10 mol % KO^{t}Bu at 150 °C under 50 bar of H_2 gave satisfactory yields of desired products. The detailed mechanistic and spectroscopic studies suggested the involvement of complexes **1-3** and **1-4** as major species in the catalytic cycle, which are generated from the Ru species **1-5** (**Scheme 1.3**).

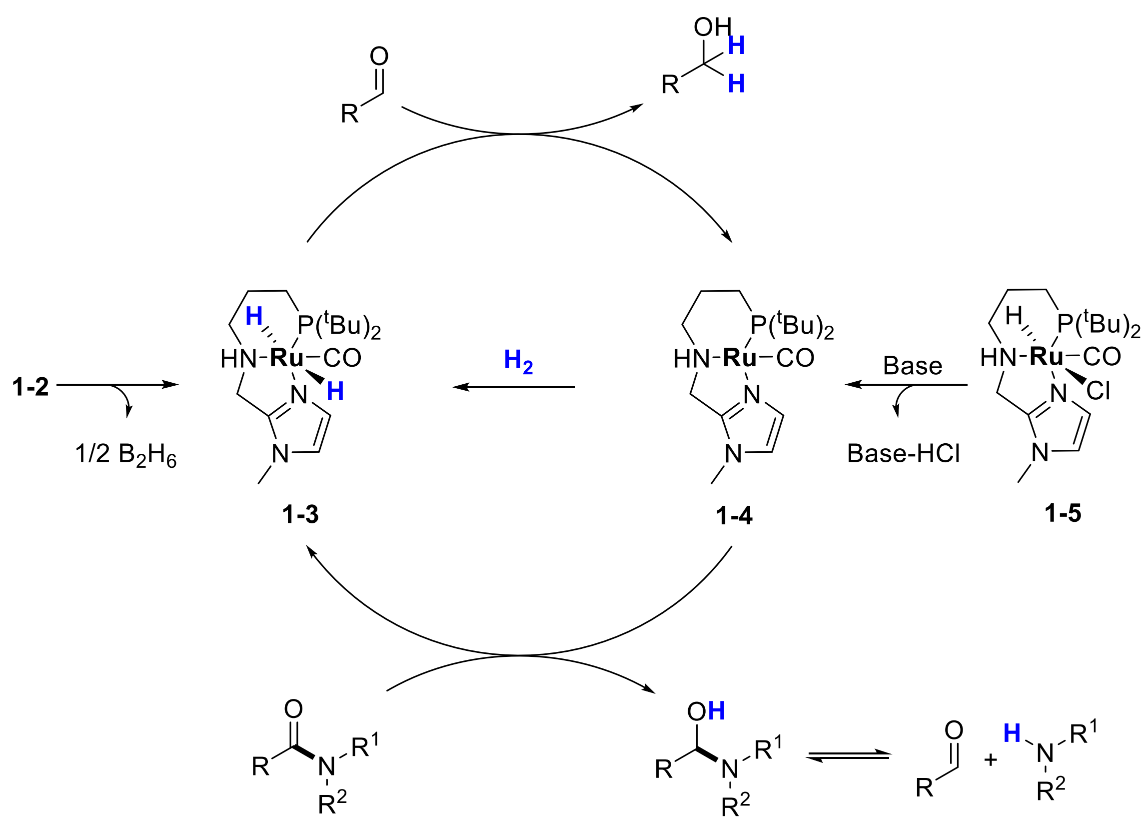

Scheme 1.3: Proposed Catalytic Cycle for Hydrogenolysis of Amides

In 2017, they developed a new catalytic system for hydrogenolysis of amides air stable cationic manganese pincer (Mn-PNN) complex, which was synthesized from the reaction of imidazolylaminophosphino ligand with [$MnBr(CO)_5$] in ethanol at 90 °C. Unprotected amines and alcohols were afforded in 78% – 99% yield with the 4–15 mol% of KO^{t}Bu (**Eq. 1.2**).[11]

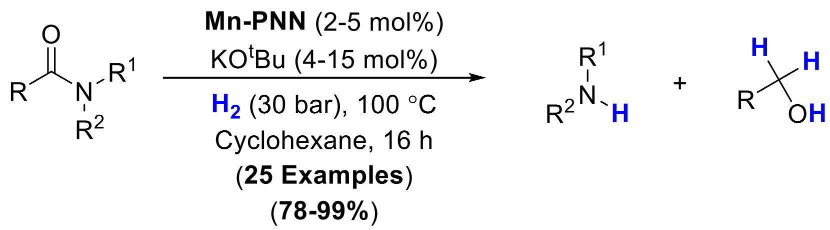

(Eq. 1.2)

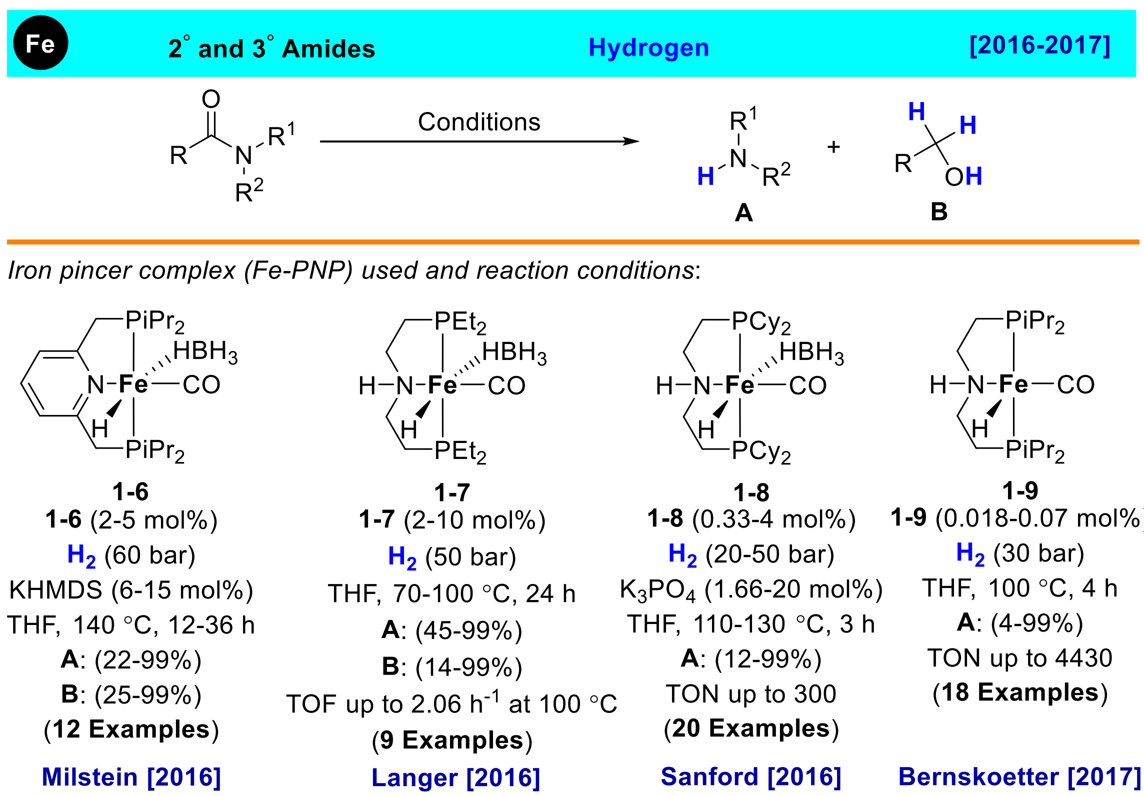

Scheme 1.4: Hydrogenolysis of Amides with Iron Pincer Complexes

A number of iron pincer complexes (**1-6** – **1-9**) have been found to catalyze selective hydrogenolysis of C−N bonds to form alcohols and amine products (**Scheme 1.4**). In 2016, Milstein group reported the first example of homogeneous iron-catalyzed hydrogenolysis of amides by using an iron pincer complex **1-6**. A variety of activated secondary and tertiary N-substituted 2,2,2-trifluoroacetamides have been utilized to form the corresponding amines and trifluoroethanol with moderate to good yields under harsh conditions (60 bar of H_2 at 140 °C) with a 6 mol% of KHMDS and the complex **1-6** as the catalyst (**Scheme 1.4**).[12] In 2016, Langer and coworkers reported hydrogenolysis of nonactivated amides and lactams by using iron pincer catalyst **1-7**. The hydrogenolysis of N-phenylbenzamide with 50 bar of H_2 at 100 °C in dry THF for 24 h cleanly afforded the alcohols and amines (**Scheme 1.4**).[13] Sanford group employed an analogous iron catalyst **1-8** for the hydrogenolysis of both amides and formamides to form the corresponding alcohols and amines up to 300 TON in 3 h.[14] In 2017, Bernskoetter group utilized an analogous iron pincer PNP complexes **1-7** and **1-8** as the catalyst for the hydrogenolysis of amides (**Scheme 1.4**). In this case, a higher activity was observed for secondary formamide derivatives under a slightly lower H_2 pressure (30 bar) and at a low catalyst loading (0.018−0.07 mol%) in THF (4430 TONs). Interestingly, some challenging substrates such as formanilide required 20 equivalents of LiOTf to increase the productivity at 120 °C for 16 h under 60 bar of H_2.[15] Bergens and coworkers achieved a highly enantioselective hydrogenation of racemic α-phenoxy-amides via dynamic kinetic resolution under mild conditions.[16] The catalytic system of *trans*-$RuCl_2$((S,S)-skewphos)((R,R)-dpen) **1-10**, 2-PrONa, and 2-PrOH afforded the corresponding alcohol products in excellent yields and with high enantioselectivity (up to 99% e.e.) (**Eq. 1.3**).

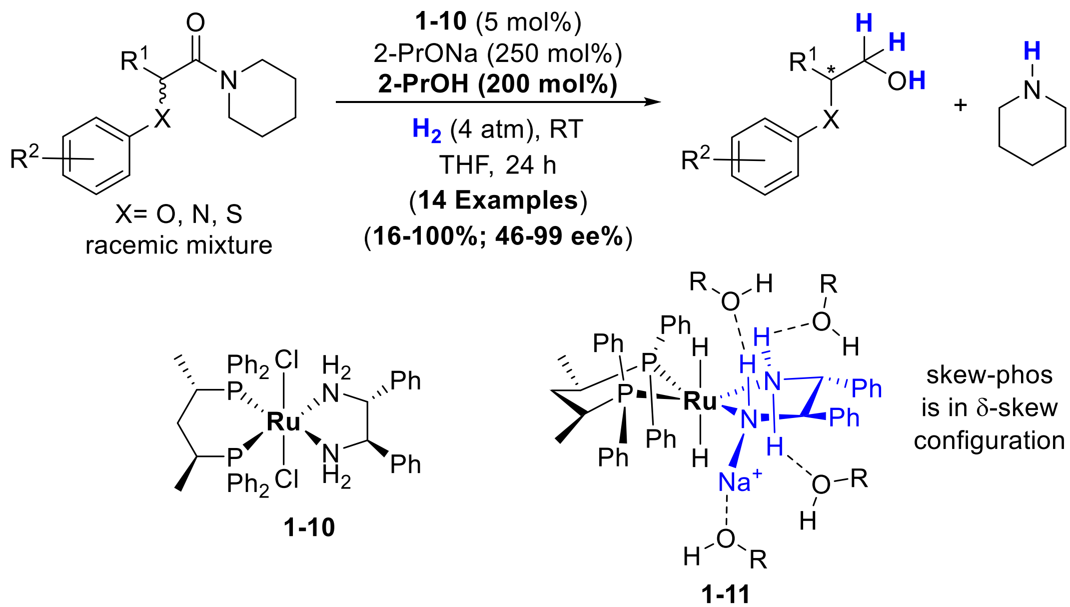

(Eq. 1.3)

Catalyst **1-10** is believed to have possible interactions with primary alcohol products to generate active catalytic species **1-11**. The authors suggested that 2-PrOH is bonded to the diastereomeric transition states of the enantioselective step, favoring one pathway over the other.

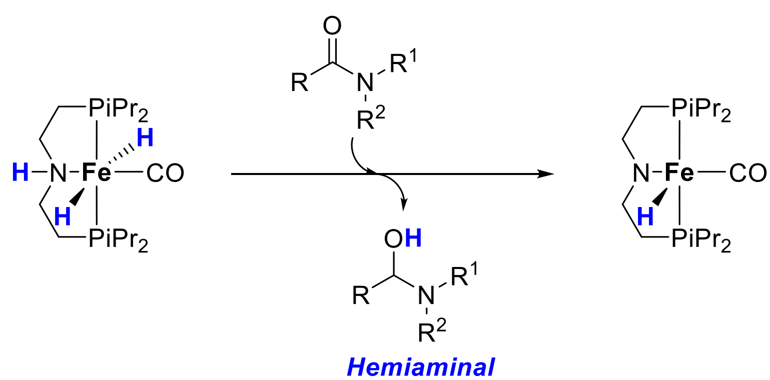

(Eq. 1.4)

Nova group performed with density functional theory (DFT) calculations and microkinetic modeling studies to investigate the mechanism of the iron-catalyzed deaminative hydrogenolysis.[17] This study revealed the "hemiaminal" (**Eq. 1.4**) is the key intermediate in the hydrogenolysis of amides. Turnover limiting step was found to be

C−N bond cleavage of the hemiaminal (**Scheme 1.5**), where, the hydrogenation of electron rich carbonyl substrate was found to be governed by their carbonyl hydrogenation step.

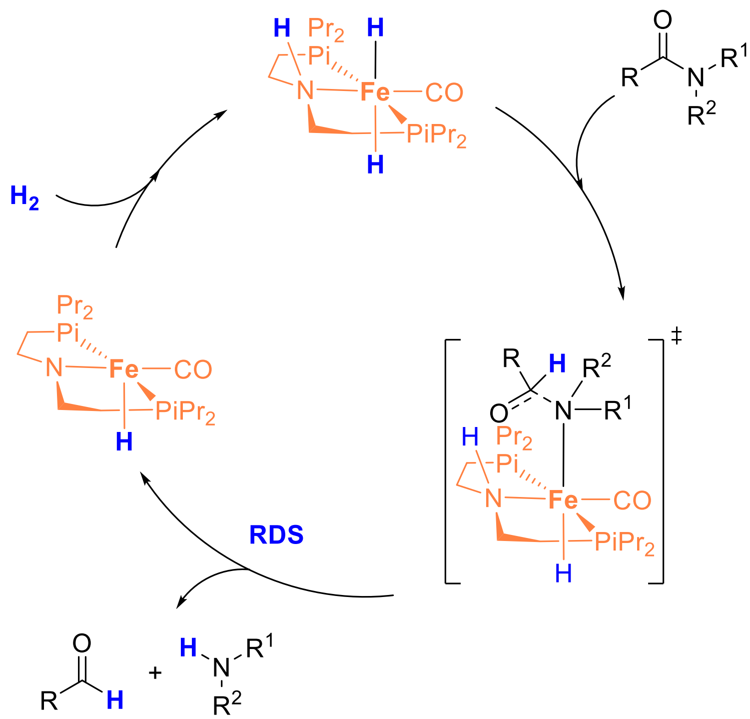

Scheme 1.5: Reaction Mechanism Shown with Hemiaminal Transition State

1.2.2 Deaminative Hydrogenolysis of Carbamates and Urea Derivatives

Milstein group in 2011 first reported a catalytic hydrogenolysis of C–N bond of urea to generate amines and methanol by using bipyridyl-based PNN Ru(II) pincer complex.[18] Later, in 2019, they reported the hydrogenolysis of carbamates and urea derivatives, catalyzed by a manganese pincer complex **1-12**.[19]

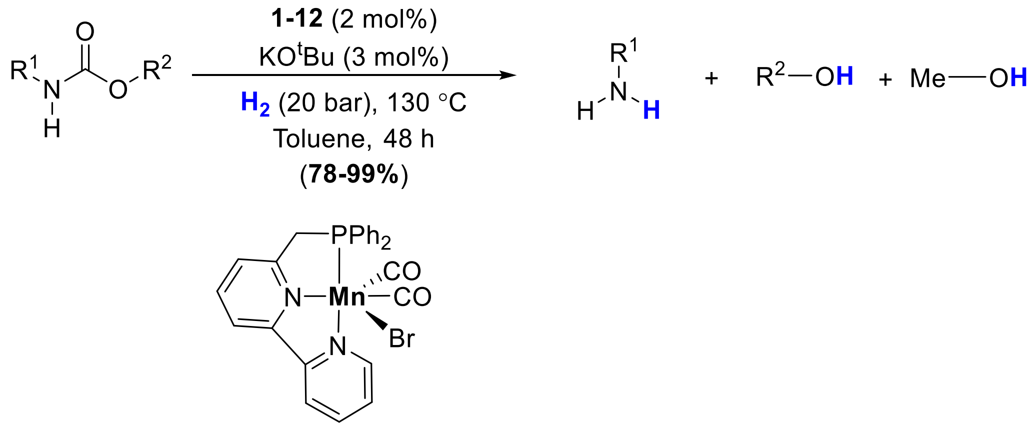

1-12

(Eq. 1.5)

The manganese complex **1-12** (0.02 mmol), ^{t}BuOK (0.03 mmol), carbamate (1 mmol) and H_2 gas (20 bar) in toluene were heated up to 130 °C for 48 hours. The reaction tolerated a variety of linear carbamates bearing aliphatic or aromatic substituents in producing the corresponding amines and alcohols (**Eq. 1.5**). A variety of hydrogenation resistant urea derivatives were hydrogenated to methanol and amines by using slightly modified catalytic conditions: complex **1-12** (3 mol %), KO^{t}Bu (4 mol %), H_2 (20 bar)) at 130 °C for 48 h in THF (**Eq. 1.6**).

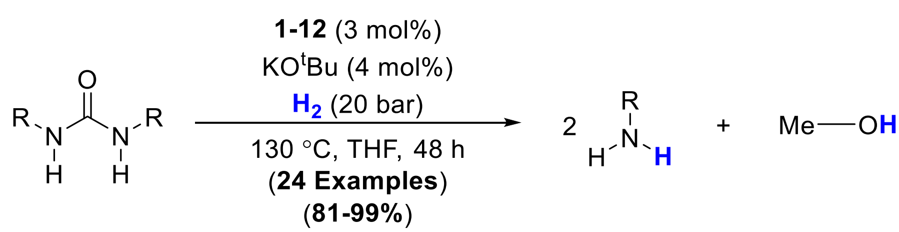

(Eq. 1.6)

The precatalyst **1-12** reacts with the base to generate the dearomatized complex **1-13**, which is then hydrogenated to give the rearomatized hydride complex **1-14**. In support of hemilabile properties of the bipyridine moiety, the urea or carbamate derivatives interact with complex **1-14** to form complex **1-15**. Complex **1-16** is formed from metal−ligand cooperation of the complex **1-15** and the elimination of R^1XH (X = O, NH). Complex **1-16** continues the catalytic cycle by regenerating complex **1-13** with the liberation of N-formamide **1-17**, which then reacts with complex **1-14** to form complex **1-18**, and the elimination of amine via metal−ligand cooperation would form the formaldehyde complex **1-19**. Complex **1-19** reacts with hydrogen to form the methoxide complex **1-20** via complex **1-14**. Finally, methanol is liberated from the complex **1-20** and the regeneration of manganese hydride complex **1-14** through the hydrogenation of complex **1-13** (**Scheme 1.6**). One of the mechanistic experiments was revealed that the introduction of para-formaldehyde corroborates the possibility of generation of complex **1-20** from complex **1-19**.

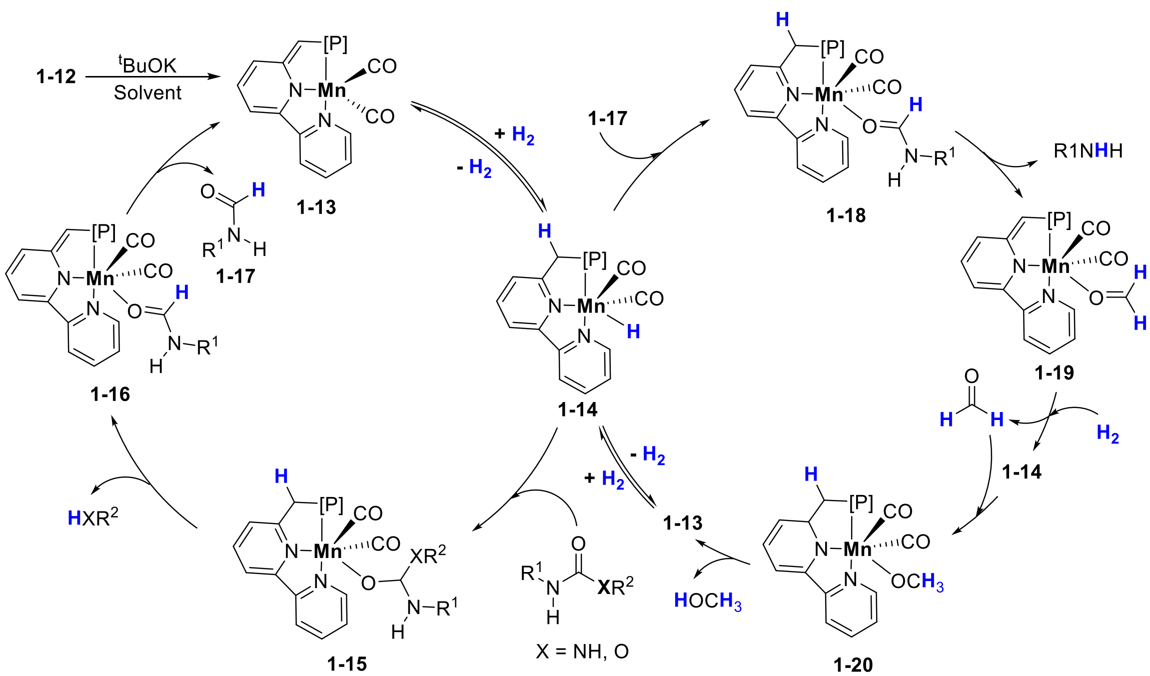

Scheme 1.6: Proposed Mechanism for the Catalytic Hydrogenolysis

1.3 Catalytic C–C Coupling Methods via C(sp^3)–N Bond Activation

Catalytic C-C coupling methods via C(sp^3)-N bond activation have emerged as an effective alkylation protocol, in which amine substrates are activated via deaminative hydrogen transfer or hydrogen borrowing processes. Both activated and non-activated amines have been successfully utilized as the substrates for the C-C bond forming reactions.

1.3.1 C(sp^3)–N Bond Activation by Oxidative Addition

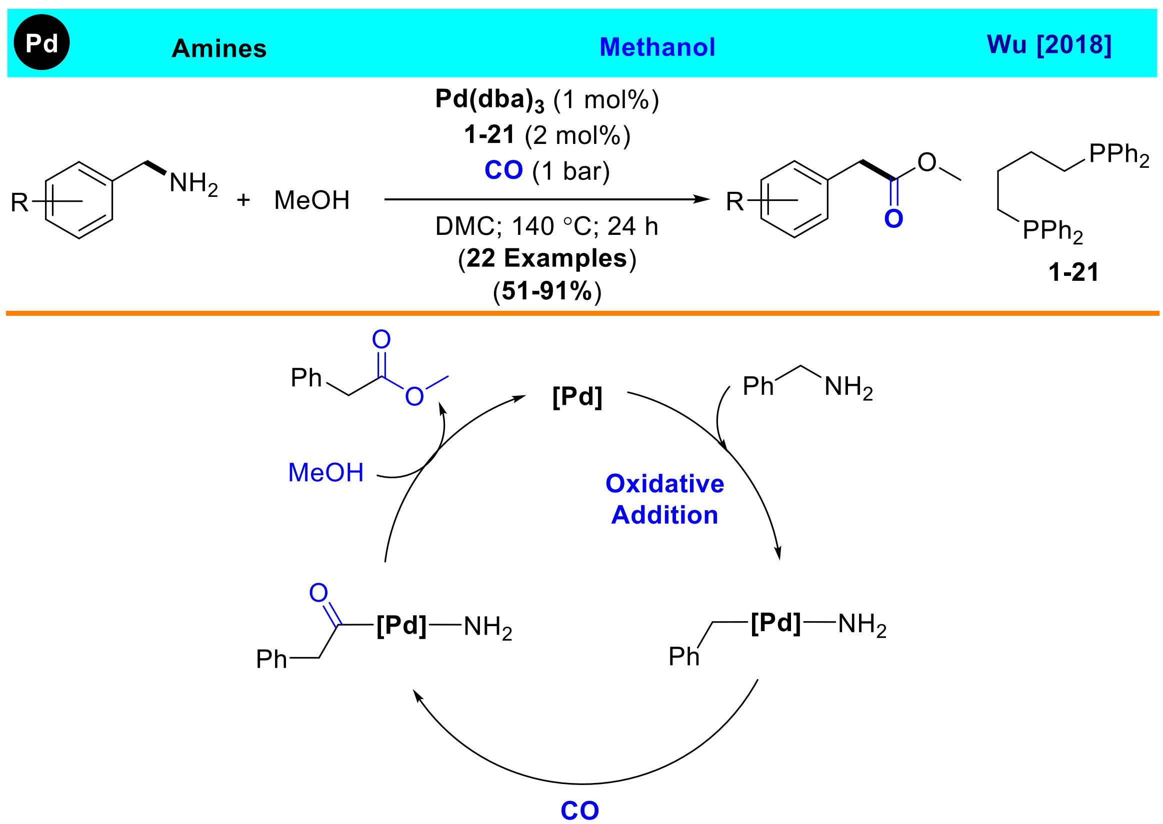

Scheme 1.7: Pd-Catalyzed Carbonylative C–N Cleavage of Benzyl Amines

Transition metal catalyzed C-N bond oxidative addition reactions have been successfully employed to form new C-C bonds. In 2018, Wu and coworkers reported palladium/DPPB (1,4-bis(diphenylphosphino)butane) **1-21** catalyzed direct carbonylative strategy on benzyl amines. They were able to synthesize 2-arylacetates by employing benzyl amines, methanol and CO and by using dimethyl carbonate (DMC) as a green solvent.[20] Organopalladium complex was formed by direct oxidative addition of benzylamine on palladium. Coordination and insertion of CO gave the acylpalladium intermediate, which was nucleophilically attacked by MeOH to give the desired ester product (**Scheme 1.7**).

1.3.1.1 C(sp^3)–N Bond Activation by Oxidative Addition of Ammonium Salt

In 2017, Huang group developed a novel Ni(0) catalyzed method by introducing amine−I_2 charge-transfer (C-T) complex **1-23**, which facilitates the C−N bond oxidative addition via the formation of Ni(I) complex **1-24**.

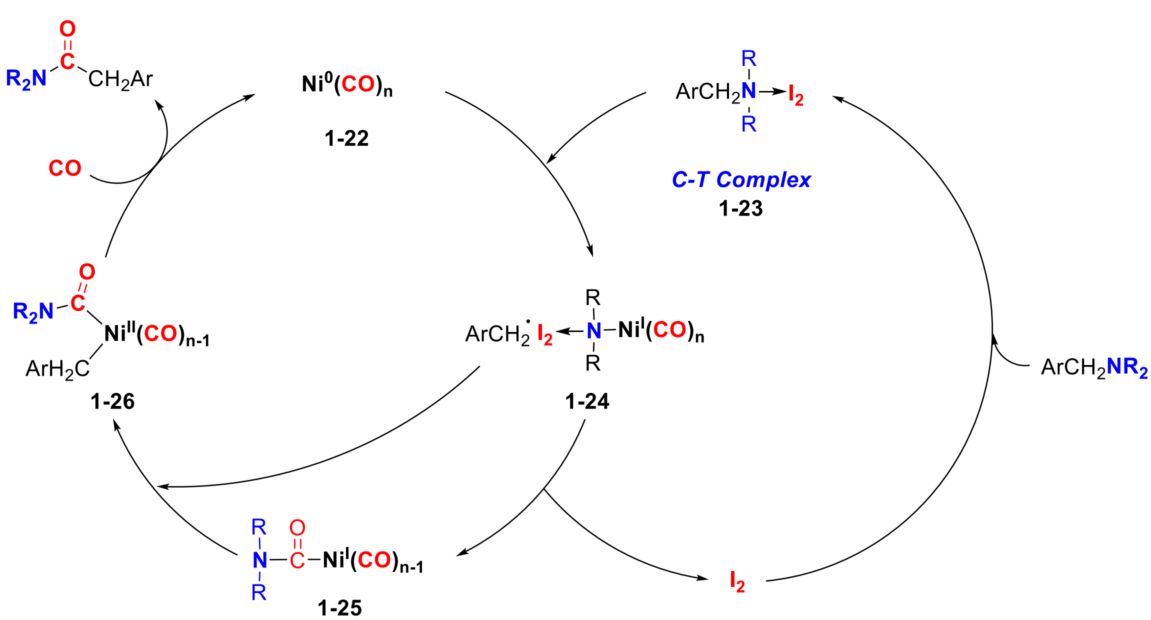

Scheme 1.8: Synthesis of Amides from Benzyl Amines

Migratory insertion of CO into the C−N bond gives a Ni(I) complex **1-25** along with the release of I_2, which could further react with benzyl amines to form C-T complex **1-23**. Subsequently, the benzylic radical would react with the active Ni(I) complex **1-25** by giving Ni(II) -amide complex **1-26** via outer-sphere electron-transfer process, which underwent reductive elimination to afford the desired product and Ni(0) species **1-22** (**Scheme 1.8**).[21]

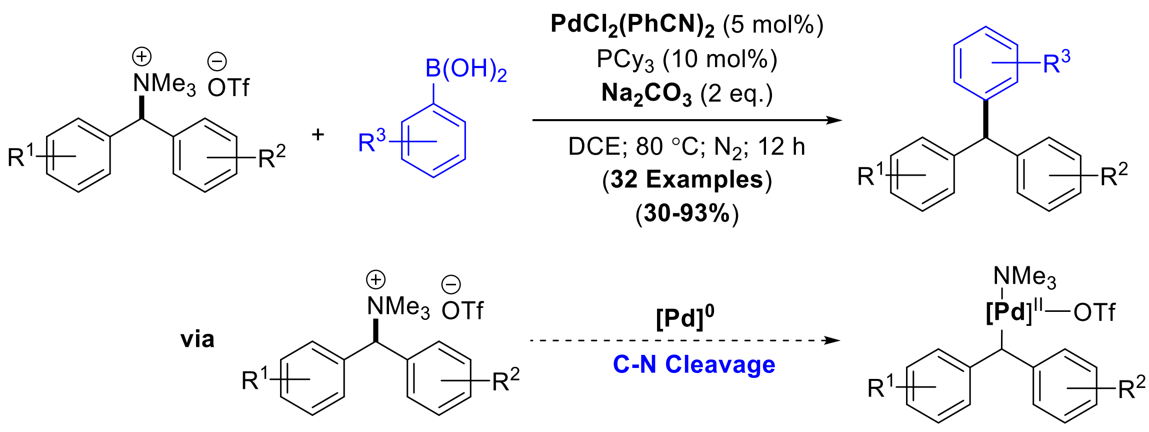

Scheme 1.9: Palladium Catalyzed Triarylmethane Compounds

Shao group in 2018 reported an efficient palladium-catalyzed Suzuki coupling of ammonium triflates with arylboronic acids (**Scheme 1.9**).[22] Many triarylmethane derivatives were synthesized by employing 1,1-diarylmethyl-trimethylammonium triflates with arylboronic acids via C−N bond oxidative addition as the key step. The authors claimed with the oxidative addition of ammonium triflate would form the formation of Pd(II) complex **1-27**, The oxidative addition step was supported by ESI-MS analysis, as they were able to detect corresponding mass for palladium complex **1-27**. In 2019, they further developed the coupling reaction to synthesize diarylmethanes and internal alkyne derivatives by adopting the similar strategy. Diarylmethanes were synthesized by employing arylsilanes with benzyltrimethylammonium salts under Hiyama cross coupling pathway[23] and internal alkyne derivatives by employing benzylic ammonium salts with terminal alkynes under Sonogashira coupling pathway.[24]

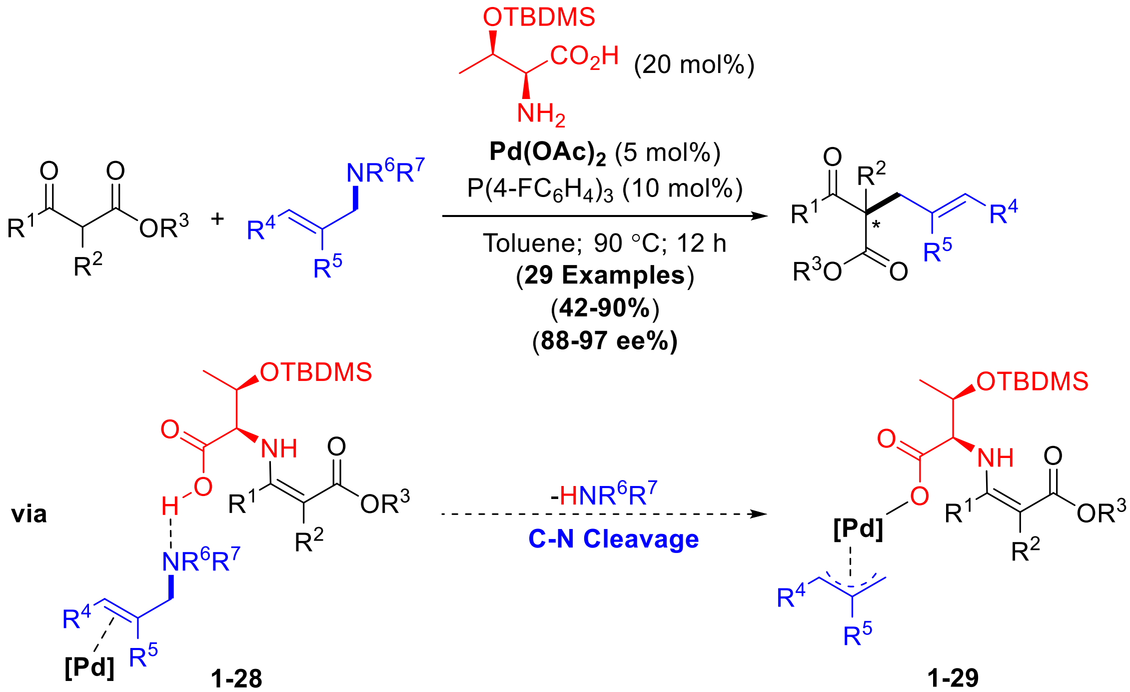

Scheme 1.10: Asymmetric Allylation of α-Branched β-Ketoesters

In 2019, Tian and coworkers introduced an asymmetric allylation of α-branched β-ketoesters, by utilizing O-TBDMS-L-threonine, $Pd(OAc)_2$, and $P(4\text{-}FC_6H_4)_3$ catalyzed system with allylic amines (**Scheme 1.10**).[25] Tien group extended the reaction to the asymmetric allylation of α-branched β-ketoesters via enamine/palladium catalysis with C−N bond cleavage. The chiral α-amino acid activates both α-branched β-ketoester and allylic amine by formation of enamine via the formation of complex **1-28**. The C−N bond activation would generate the π-allylpalladium complex **1-29** by releasing secondary amine, which then takes place intramolecular C−C bond formation between the enamine and the π-allylpalladium moiety to form the corresponding enantioenriched α,α-disubstituted β- ketoester products.

1.3.1.2 Catalytic C(sp^3)–N Bond Activation by Oxidative Addition of Strained Amines

In 2015, Doyle group reported Ni-catalyzed Negishi cross-coupling reaction to achieve quaternary carbon contained β-substituted phenethylamines.[26] They used different olefinic ligands to achieve Negishi cross-coupling type transformations. The cross-coupling reaction is believed to be occur by an intermediate **1-30**, which is generated from the aziridine and Ni catalyst via either a SET oxidative addition pathway or from an intermediate **1-31**, or a S_N2-type oxidative addition pathway. Subsequent cyclization would form nickelocycle **1-32**, and the reductive elimination via the transmetallated species **1-33** would afford the desired β-substituted phenethylamine products (**Scheme 1.11**).

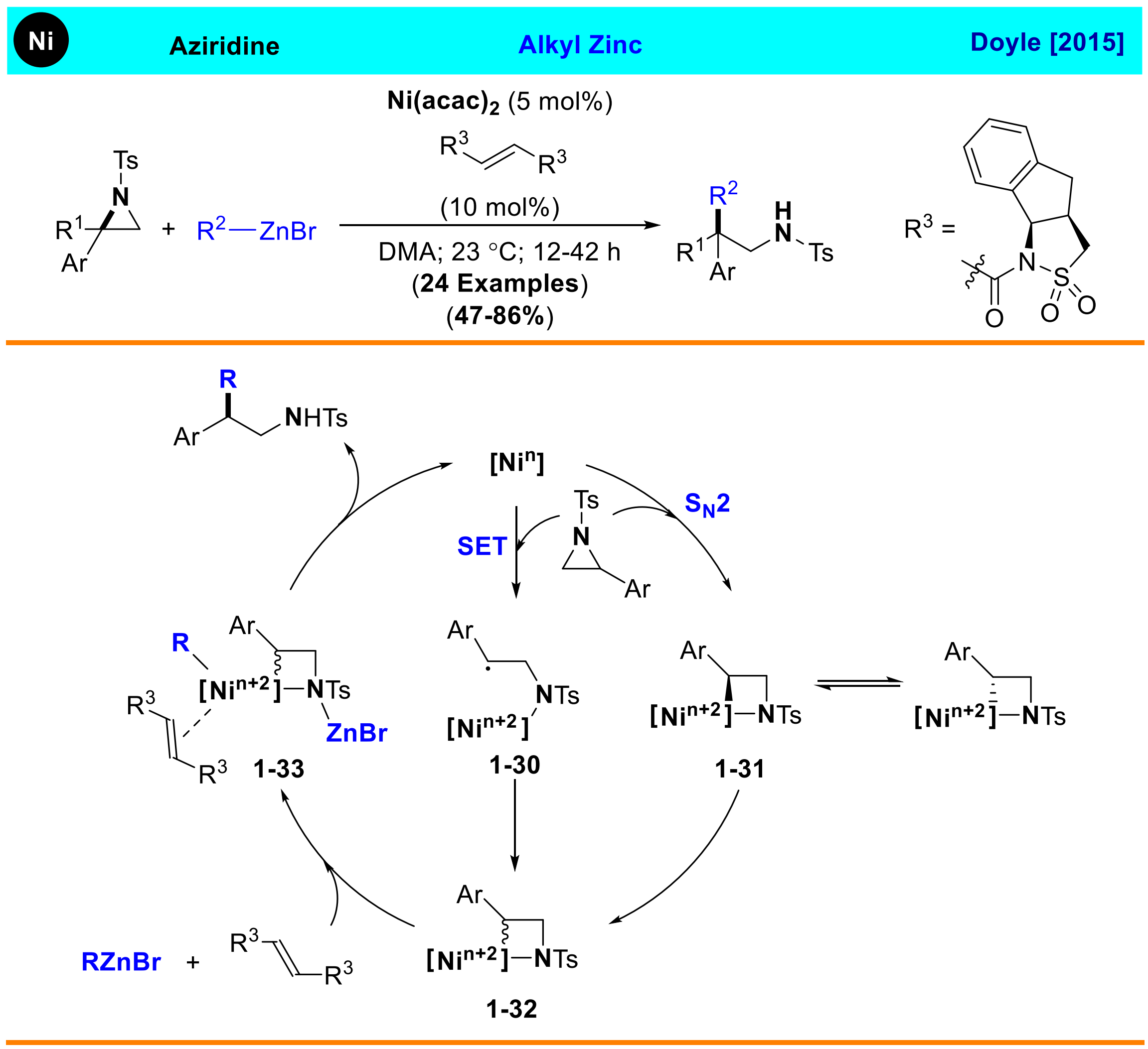

Scheme 1.11: Proposed Mechanistic Pathway for Ni-Catalyzed Negishi Cross-Coupling Reaction of Aziridines with RZnBr

In 2018, Xiao and coworkers reported similar dual visible light photoredox and nickel-catalyzed cross-coupling strategy to access β-substituted amines from the reaction of 2-arylaziridines and potassium benzyltrifluoroborates. The catalytic system provided an excellent regioselectivity for more hindered C−N bond cleavage of strained arylaziridine derivatives (**Eq. 1.7**).[27]

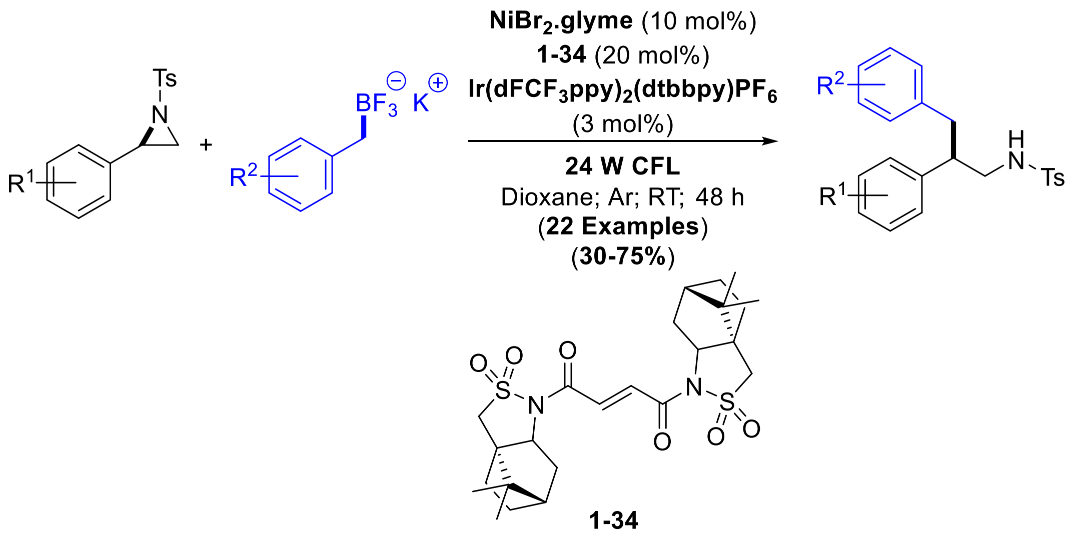

(Eq. 1.7)

The authors proposed a mechanism via in situ formed active Ni(0) **1-34**, which undergoes an oxidative addition into the more hindered C−N bond of aziridine to give the azanickelacyclobutane species **1-36**. Here, the electron deficient olefin ligand plays an important role in regioselectivity during oxidative addition step. Meanwhile, single electron transfer (SET) from potassium benzyltrifluoroborates on photoexcited state Ir(III)* would generate benzylic radical, which would be quickly captured by complex **1-36** by forming alkylnickel(III) intermediate species **1-37**. Reductive elimination of alkylnickel(III)cyclobutene species **1-37** furnishes the formation of Ni(I) amino complex **1-38**, which then undergoes another SET reduction mediated by the reduced photocatalyst Ir(II) to regenerate the active Ir(III) catalyst **1-35** and potassium salt of the product **1-39**. (**Scheme 1.12**).

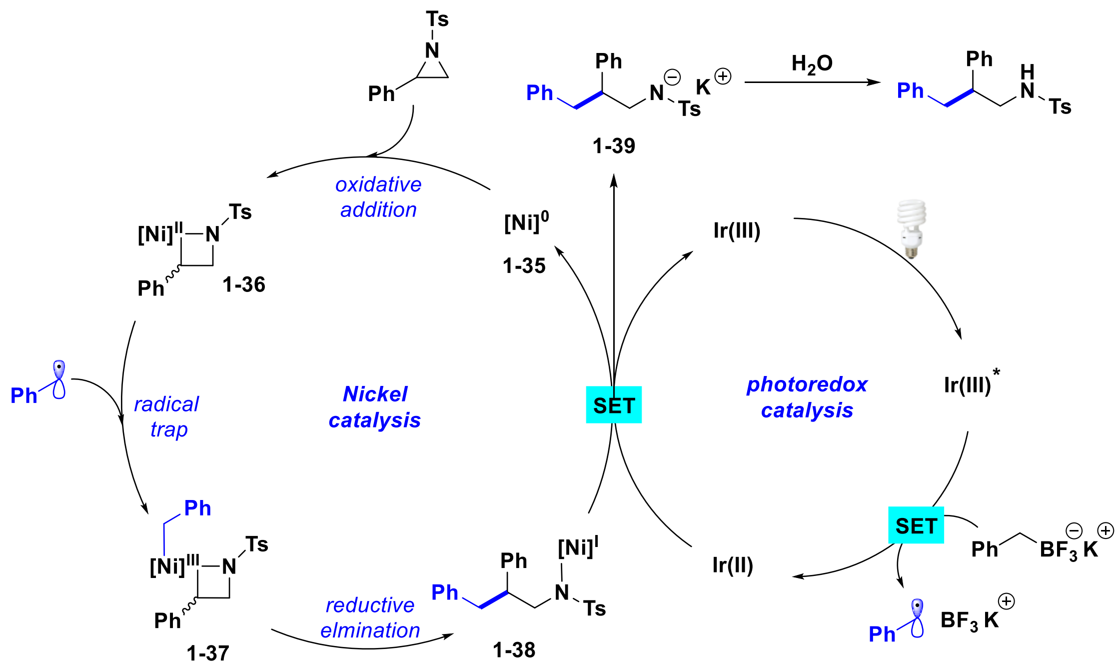

Scheme 1.12: Proposed Dual Nickel/Photoredox Catalyzed Pathway

1.3.2 Catalytic C(sp^3)–N Bond Activation via Imine Species

Lin and coworkers in 2017 achieved ring opening of N-acylaziridine via homolytic cleavage of a more substituted C−N bond. Zn dust (10-20 mol%) as the reductant was used generate the active Ti^{III} catalytic species.[28] The proposed mechanism involves the coordination to N-acylaziridine derivative **1-40** to the redox-active metal complex **1-42**, which promotes homolytic cleavage of the more substituted C−N bond via single-electron transfer from the metal center to the aziridine derivative to form carbon radical tethered **1-43**. This radical intermediate reacts with an alkene to afford intermediate radical species **1-44**. Subsequent cyclization yields the [3+2] cycloaddition pyrrolidine product **1-41** by regeneration of the active catalytic species (**Scheme 1.13**).

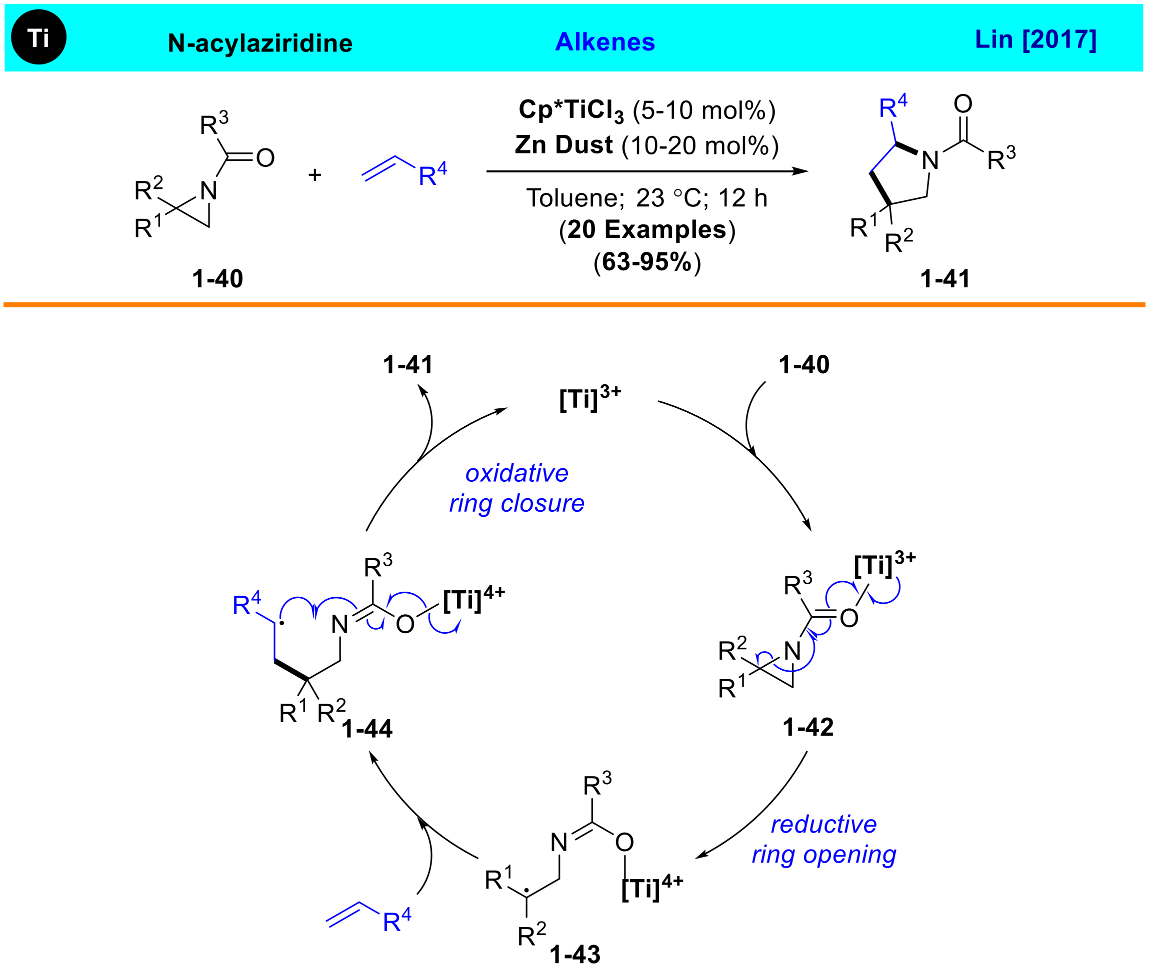

Scheme 1.13: Redox-Relay Catalytic Cycle for [3+2] Cycloaddition of N-Acylaziridine Derivative and an Alkene

The proposed redox-relay catalytic cycle, involving reductive aziridine ring opening and oxidative ring closure is believed to be turnover limiting step of the radical catalysis. In 2013, Yi group reported a Ru-catalyzed direct C−N bond activation strategy by employing biomass derived α- and β-amino acid derivatives to construct C−C bond with ketones to form 2-alkylketone products. The reaction showed a broad substrate scope and excellent diastereoselectivity, and the C−N bond activation step has been proposed to occur after the decarboxylation of the amino acid substrate (**Eq. 1.8**).[29]

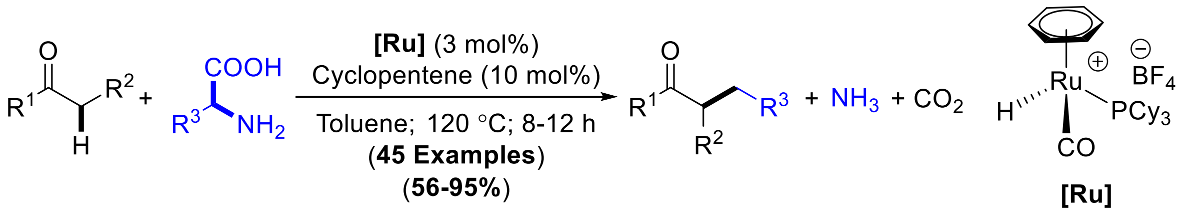

(Eq. 1.8)

1.3.3 Catalytic C(sp^3)–N Bond Activation via Iminium and Ammonium Species

Sarpong group reported a convenient synthesis of oxazaborinines **1-46** by using palladium catalyzed intramolecular coupling of vinylogous N-allylamide **1-45** via an iminium intermediate **1-47**.[30] Vinylogous amide species **1-45** was activated by alkyl boron to give the iminium intermediate **1-47**. Oxidative addition of iminium intermediate **1-47** onto the palladium in the presence of pyridinium p-toluenesulfonate (PPTS; Brønsted acid) would afford π-allyl complex **1-48** and enolate equivalent **1-49**.

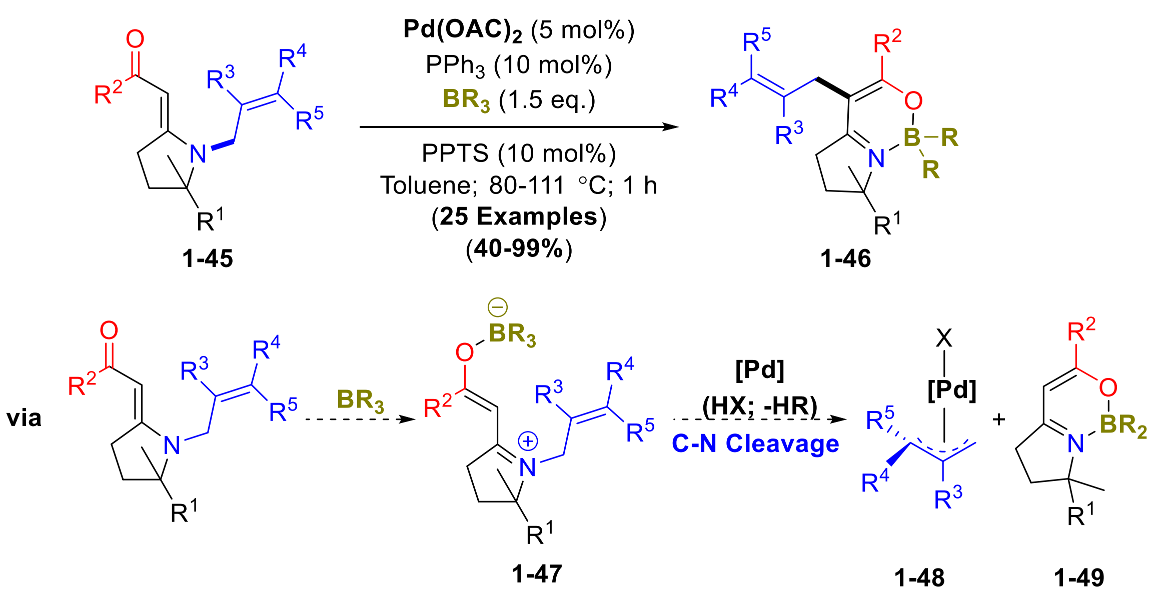

Scheme 1.14: Synthesis of Oxazaborinines by Intramolecular Rearrangement via Formation of Palladium π-Allyl Chemistry

Oxazaborinine **1-46** would be liberated by allylic alkylation of an intermediate **1-49** via formal [3,3] rearrangement (**Scheme 1.14**).

Quaternary ammonium salts are considered very useful substrates as leaving group, as illustrated by the pioneering work by Jenny et al. in 1988 on arylammonium salts for the cross-coupling reactions.[31] In 2015, Li and coworkers demonstrated catalytic C−N bond cleavage via elimination of ammonium salts for the C−H insertion reactions of arylketones with diazo compounds.[32]

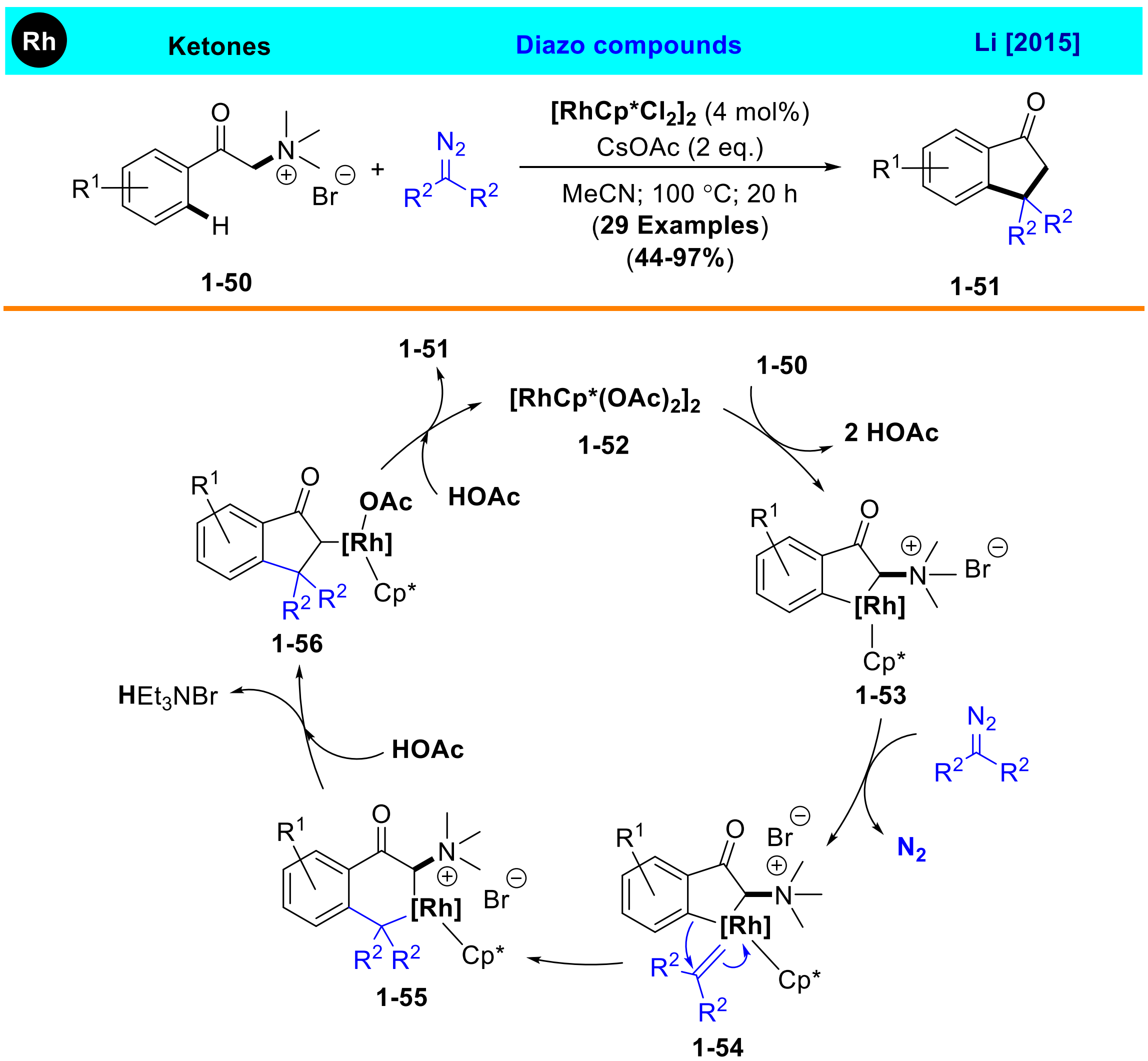

Scheme 1.15: Proposed Mechanism for the Rhodium-Catalyzed C−N Bond Cleavage of Phenacylammonium Salts

In this case, the ammonium group was employed as a directing group for the C−H activation of phenacylammonium salts **1-50** to synthesize benzocyclopentanones **1-51**. It is noteworthy that the one-pot reaction of α-bromoacetophenones and trimethylamine led to the desired products through the in-situ formed phenacylammonium salt **1-50**. On the basis of experimental and DFT calculations, the authors proposed a mechanism which involves an ortho C−H activation of the phenacylammonium enolate salt **1-50** followed by cyclometalation to afford a rhodacyclic intermediate **1-53**. Subsequent coordination and denitrogenation of a diazo ester would generate the Rh-carbene species **1-54**. Intramolecular insertion of the Rh−Aryl bond into a carbene species **1-54** generates a Rh(III) dialkyl intermediate **1-55**, which in the presence of HOAc would facilitate the C−N bond activation to result in liberation of HEt_3NBr. Finally, the protonolysis of **1-56** would release the benzocyclopentanone product **1-51** and regenerate the active Rh catalyst **1-52** (**Scheme 1.15**).

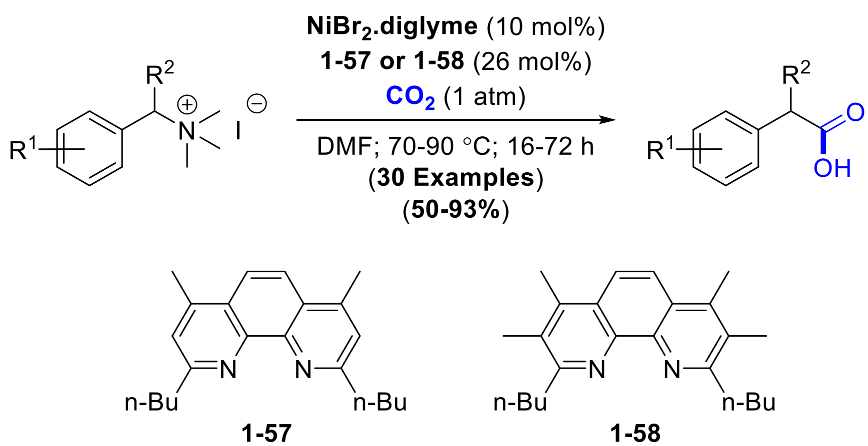

(Eq. 1.9)

In 2016, Martins group reported a nickel-catalyzed reductive carboxylation of benzylic C−N bonds with carbon dioxide elimination which is usually associated[33] with carboxylation of benzyl electrophiles.[34] The procedure is believed to proceed via a formation of benzyl electrophiles by C−N bond activation of bis(phen)-nickel complexes (**Eq. 1.9**). In 2017, Tortosa and coworkers presented enantioselective catalytic Kumada type coupling reaction of secondary propargylic ammonium salts with aryl Grignard reagents stereospecific alkynylation transformations. Interestingly, this catalytic system gave only the α-regioisomer via S_N2 type mechanism by quaternary C−N bond activation of the propargylic ammonium salts. (**Scheme 1.16**).[35]

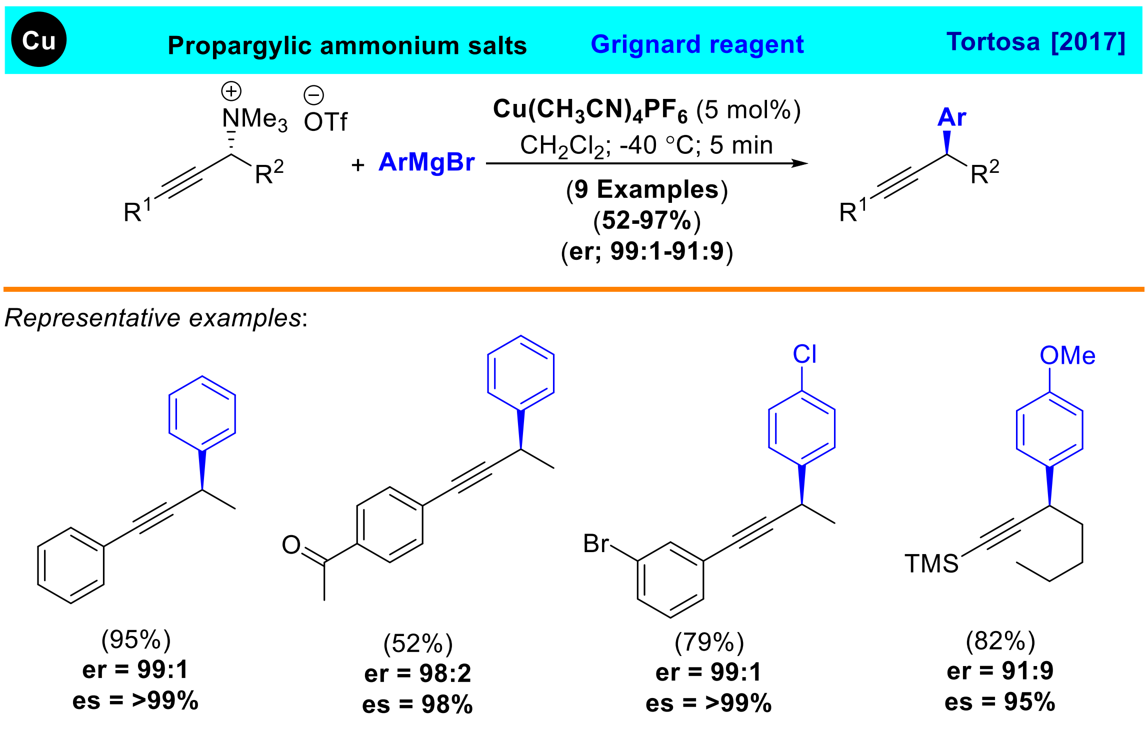

Scheme 1.16: Stereospecific Substitution Reactions of Propargylic Ammonium salt Derivatives

The amino group is amenable to late-stage functionalization and easily purify via acid/base extraction, and Watson group developed a new catalytic C−N bond activation strategy by converting amines into Katritzky pyridinium salts[36] (**Scheme 1.17**). They observed high chemoselectivity for the benzylic C−N bond activation on Suzuki−Miyaura type cross coupling reaction on $Ni^{I/III}$ catalytic system by employing alkylpyridinium salts with aryl boronic acids. The catalytic coupling method provided an easy access to alkyl arenes via C−N bond activation, which is amenable for a wide range of primary and secondary amines with high degree of functional group tolerance. The authors proposed a mechanism which is initiated by SET from a Ni(I) species to the pyridinium salt (Katritzky salts) **1-59**, triggering fragmentation of **1-60** to give the alkyl radical Ni(II) species **1-61**. Arylnickel(II) intermediate **1-61** would react with this alkyl radical to form arylalkylNi(III) species. Finally, reductive elimination gives desired arylated product and active Ni(I) species (**Scheme 1.17**).[37]

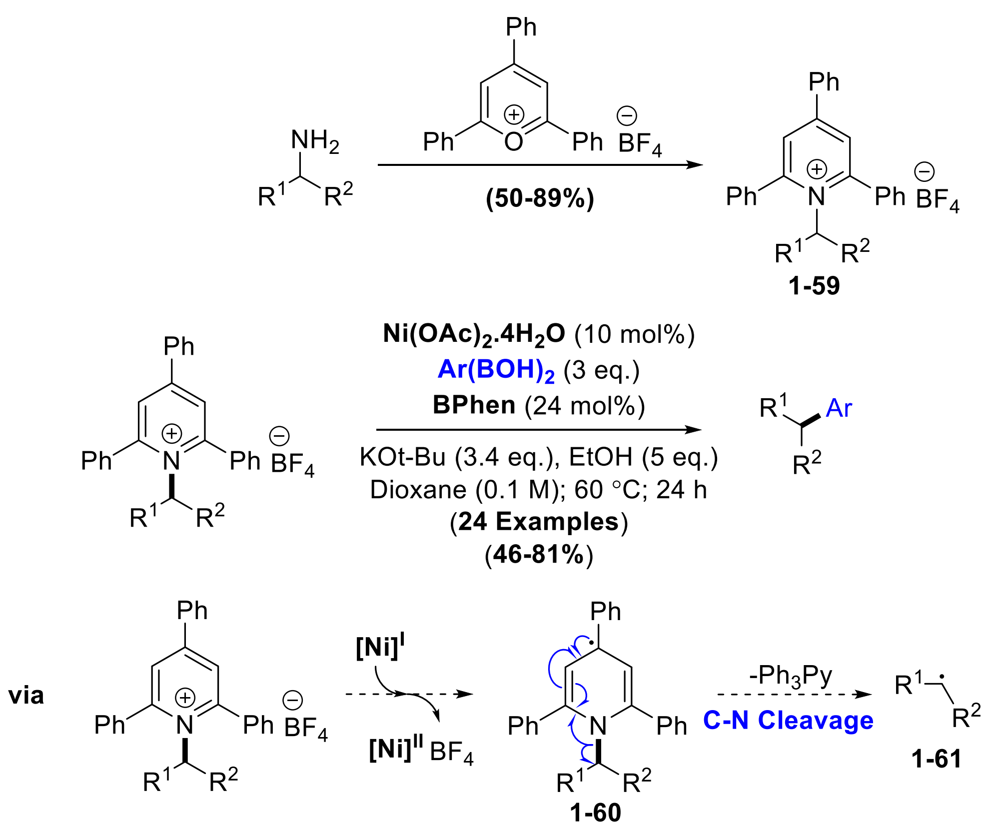

Scheme 1.17: Use of Alkyl Amines as Electrophiles for Nickel-Catalyzed Cross Couplings via C−N Bond Activation

In 2019, they extended same strategy to synthesize various alkyl−alkyl cross-coupling from alkyl amine derivatives with unactivated alkyl groups.[38] Martin group independently demonstrated the use of pyridinium salt by using nickel catalyzed C−N bond activation for cross-coupling reactions with aryl bromides to forge sp^3 C−C linkages.[39]

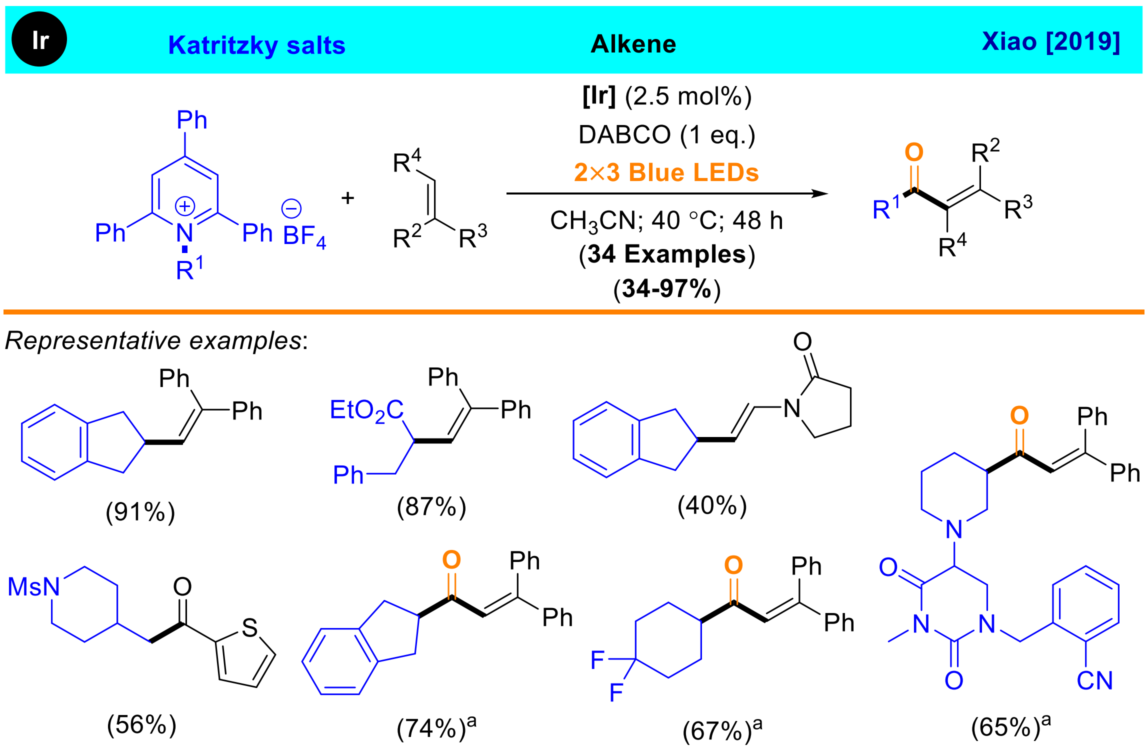

Scheme 1.18: Representative Examples of the Deaminative Heck Type Reaction Including Carbonylative Products. [a]CO (80 atm) has been used.

Xiao group developed visible-light photoredox catalytic strategy to effect the deaminative alkyl-Heck-type reaction to promote C−N bond activation via the pyridinium salt. A variety of aliphatic primary amines were effectively used as the starting materials to access corresponding alkene products in good yields. Moreover, this strategy was successfully applied to synthesize α,β-unsaturated carbonyl compounds flowing carbonyl insertion pathway (**Scheme 1.18**).[40] In 2019, Shu and coworkers developed the C−C coupling reaction between C−N electrophiles that demonstrates the C−N bond cleavage. By using nickel/Bphen catalytic system, both aryl- and benzyltrimethylammonium triflates were employed for the coupling with alkenes to construct substituted alkenes via C−N bond cleavage.[41] These transformations share a common mechanism involving single electron transfer pathways (SET) while tolerating a wide range of functionalities with good to excellent yields.

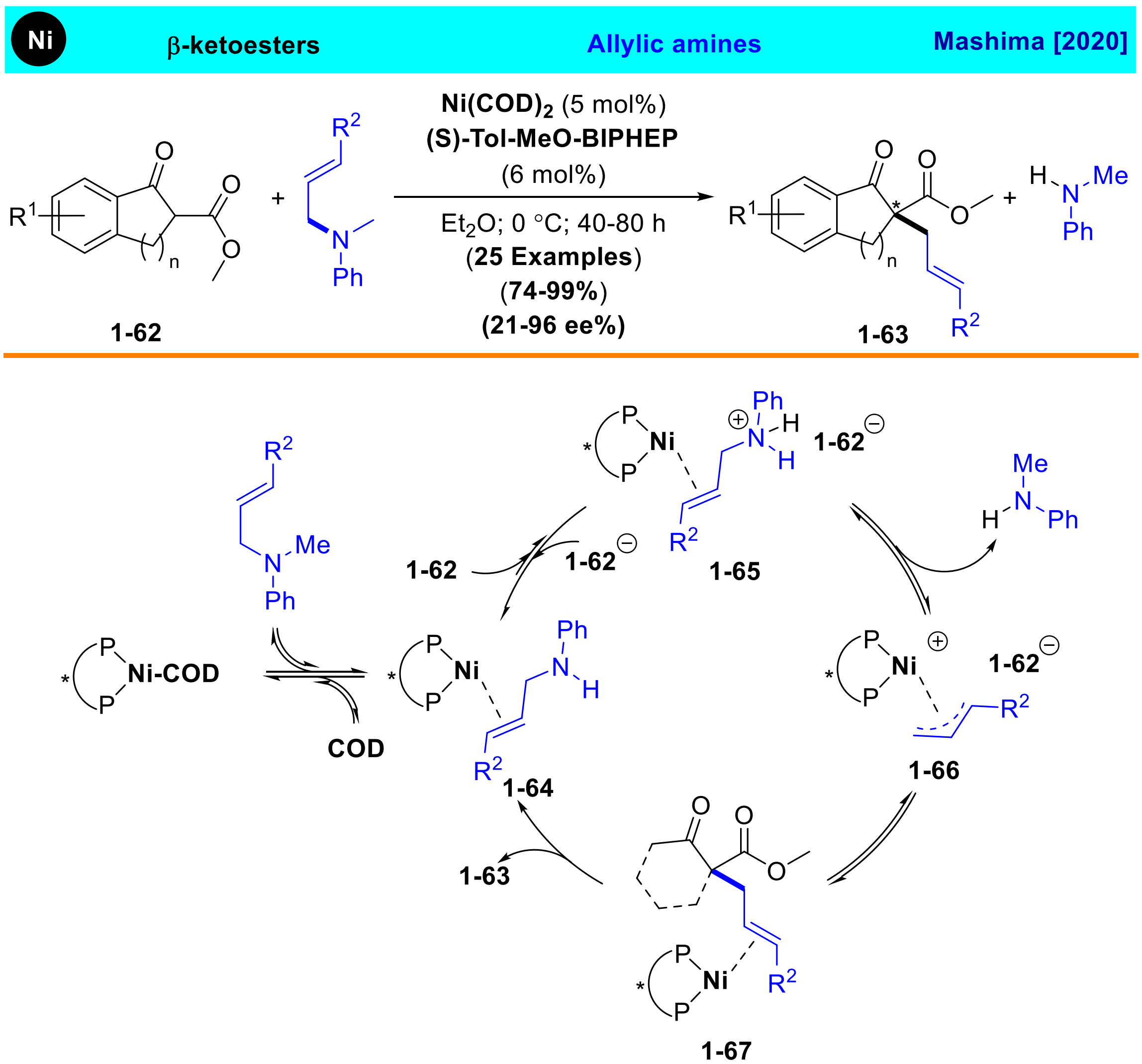

Scheme 1.19: Proposed Reaction Mechanism for the Asymmetric Allylic Alkylation

Very recently, Mashima and coworkers reported an asymmetric allylic alkylation of β-ketoesters **1-62** with allylic amines, where the C–N bond cleavage via ammonium species occurred from the protonation of amine moiety (**Scheme 1.19**).[42] A Ni(0) with a chiral diphosphine ligand has been found to be effective for the synthesis of alkylated products **1-63** with a high % e.e. The authors carried out DFT calculations to rationalize the mechanism, which is initiated by the coordination of allylic amine onto the Ni(0)-diphosphine complex in forming complex **1-64**. Protonation of the amine moiety by β-ketoester (endergonically; 22.9 kcal mol^{-1}) generates intermediate **1-65** and enolate **1-62** which are identified as the key species for the C−N bond cleavage step via formation of a nickel-allyl complex **1-66**. The complex **1-66** reacts with an outer-sphere enolate anion **1-62** to form product coordinated complex **1-67**. Lastly, an olefin exchange reaction between complex **1-67** and an allylamine proceeds to give the corresponding product **1-63** and the regeneration of active catalytic species **1-64**.

1.3.4 Catalytic C(sp^3)–N Bond Activation via *β*-N Elimination

Gooßen group developed ruthenium catalyzed regiospecific allylation of benzoic acids with allyl amines that proceeds via C−N bond activation. This ruthenium catalyzed reaction is believed to be proceed via β-amino elimination pathway without formation of metal allyl species. This directing group enabled protocol provided the formation of various allylarene motifs in reasonable yields under acidic conditions.[43]

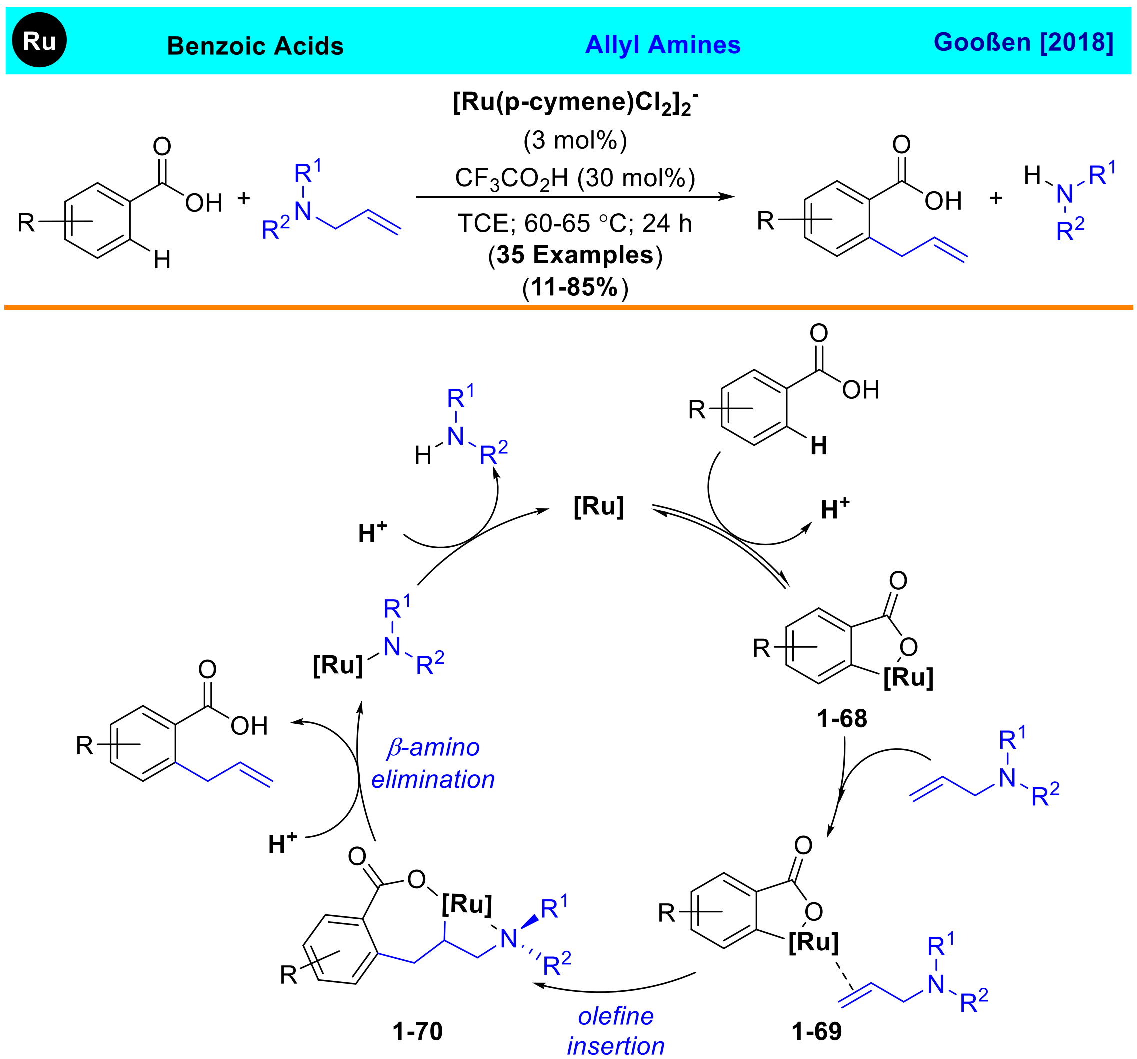

Scheme 1.20: Catalytic Cycle Represent C–N Activation via β-Amino Elimination

The observed KIEs under parallel experiments ($k_H/k_D = 2.8$) and under the competitive reaction conditions ($k_H/k_D = 4.5$) showed that the C−H activation is the rate-determining step. Experimentally determined bond strength of C−H (100 kcal/mol) and C−N (80 kcal/mol) were further made consistent with the C−H activation as the rate-determining step. Reactions were carried out with 1,1-dideuterio-allyl amine under standard conditions, which exclusively afforded the γ[D2] allylated product in 61% yield, in agreement with a β-amino elimination pathway. Base-assisted ortho C−H activation of the benzoic acid would be initiated by an allyl amine most likely acting as an auxiliary base by producing intermediate species **1-68**. The intermediate complex **1-70** is formed by coordination of an allyl amine followed by insertion of the olefinic group via intermediate **1-69**. The C–N bond cleavage via "β-amine elimination" pathway as a key step of the reaction would form the desired product along with ruthenium-amine intermediate. Finally, active catalytic species would be regenerated by protonation of the ruthenium-amine intermediate (**Scheme 1.20**).

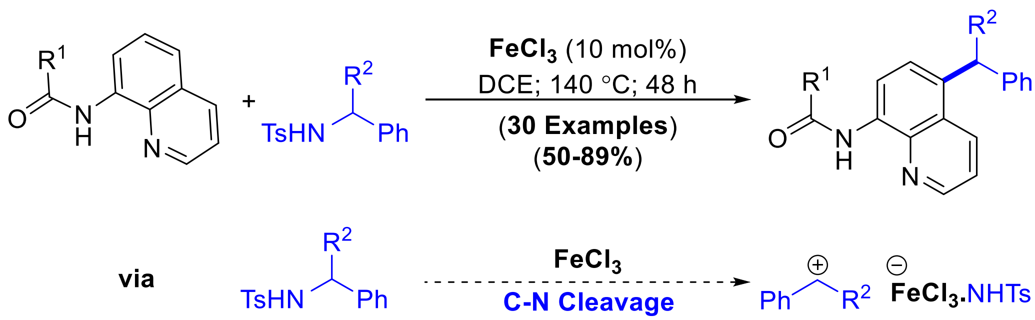

Scheme 1.21: Iron-mediated Remote C–H Bond Benzylation of 8-Aminoquinoline Amide Derivatives

Fu and coworkers in 2017 reported iron catalyzed C5-benzylation of quinoline frameworks. The reaction tolerated a wide range of N-benzylic sulfonamide derivatives with both aliphatic and aromatic amides (**Scheme 1.21**).[44] Electrophilic substitution reaction on electron-rich C5–H position of the chelated iron-aminoquinoline intermediate has been proposed for producing the desired benzylated products, in which an in-situ generated benzyl cation was generated from N-benzylic sulfonamide in the presence of ferric chloride as the catalyst. Active Fe catalyst was regenerated along with the desired benzylated products.

1.4 Catalytic C−C Coupling Methods via Arene C(sp^2)−N Bond Activation

Aryl C–N bonds are particularly inert, and more reactive intermediates such as aryldiazonium salts are needed to achieve arene C(sp^2)−N bond functionalization. Kakiuchi in 2007 first reported catalytic C-C coupling reaction of aryl compounds with pivalophenone derivatives and organoboronates via aryl C−N bond cleavage-by using $RuH_2(CO)(PPh_3)_3$ catalyst. The reaction was shown proceed via oxidative addition of aryl C−N bond to the ruthenium center.[45]

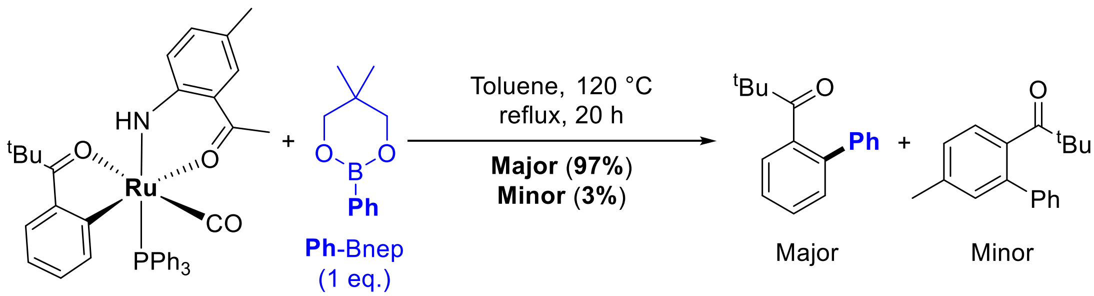

(Eq. 1.10)

In 2009, Kakiuchi group clearly demonstrated a direct C−N bond insertion into a Ru(0) complex.[46] The catalytically active Ru-aryl intermediates were synthesized, and the corresponding stoichiometric cross coupling products were obtained under standard reaction conditions, which was found to proceed via direct oxidative addition of the C(sp^2)–N Bond onto the ruthenium center (**Eq. 1.10**).

1.4.1 Arene C(sp^2)–N Bond Activation by Oxidative Addition

1.4.1.1 Catalytic Arene C(sp^2)–N Bond Activation via Direct Oxidative Addition

In 2017, Zeng and coworkers demonstrated an arene C(sp^2)–N bond cleavage reaction by adopting both experimental and theoretical study. Chromium(II) chloride precatalyst with an imino auxiliary directing group was used to achieve regio- and chemoselective Kumada type C−C coupling reactions.[47] Experimental evidences showed that the in-situ formed low-valent chromium species with Grignard reagent led to activation of the C(sp^2)–N bond. DFT calculations were consistent with the facile insertion of the C(sp^2)–N bond mediated by a high-spin chromium(0) complex (S = 2). Furthermore, theoretical model indicated that the donation of sole paired d electrons in the d^6 shell of high-spin chromium(0) complex to the antibonding orbital of the C(sp^2)–N bond and the nitrogen ligating interaction plays an important role in promoting the oxidative addition step of the reaction (**Scheme 1.22**). This external ligand-free reactivity from the low-spin state-controlled reactivity was found to be unusually sensitive to the supporting ligand environment.

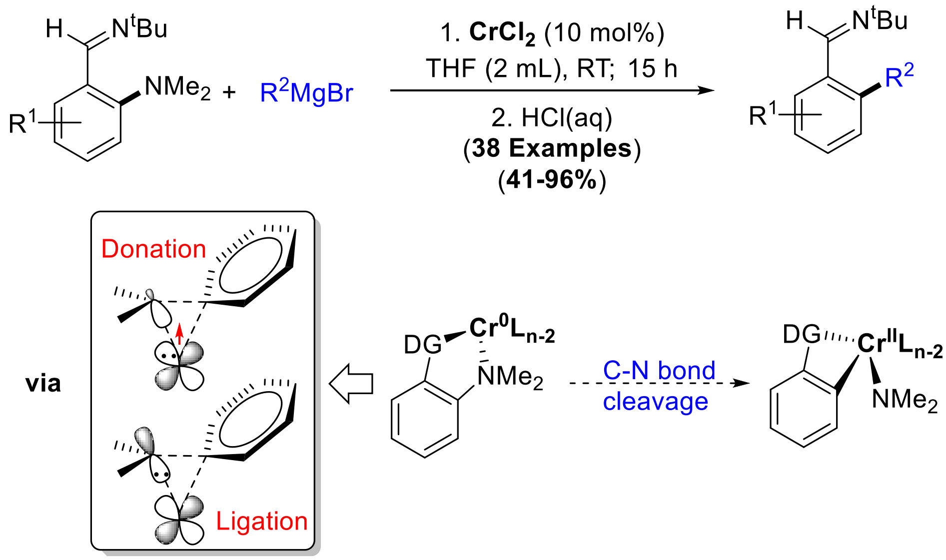

Scheme 1.22: Chromium-Catalyzed Cleavage of Aromatic Carbon−Nitrogen Bonds at Room Temperature

In 2017, Jiang and coworkers reported a on palladium catalyzed synthesis of aryl ketones via C−N bond cleavage by employing arylhydrazines and nitriles using molecular oxygen as an oxidant.[48] Notably, ^{18}O-labeling experiment indicated that the oxygen atom in the ketone molecule was derived from H_2O. The authors proposed a possible catalytic pathway by combining with the previous observations and mechanistic insights.

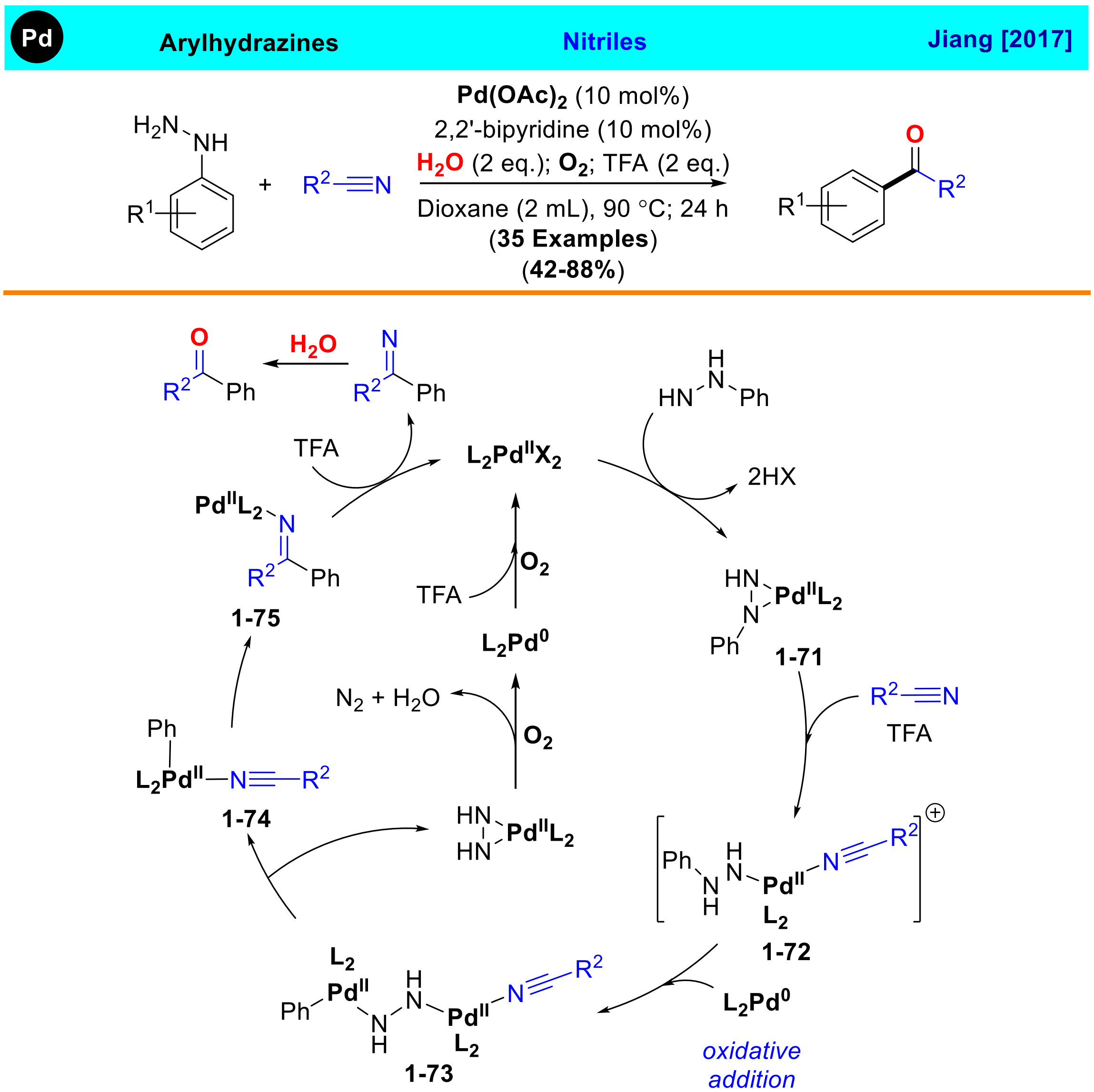

Scheme 1.23: Proposed Reaction Mechanism for Synthesis of Aryl Ketones

Initially, palladiaziridine intermediate **1-71** would form via the metathesis of phenyl hydrazide with a palladium catalyst (X=OAc). Subsequent nitrile group coordination **1-72** followed by oxidative addition would afford two palladium(II) centered intermediate

1-73 via C−N bond cleavage. Cleavage of the intermediate **1-73** would generate nitrile coordinated arylpalladium species **1-74** and palladiaziridine complex, which would be decomposed into active catalytic species via denitrogenative pathway. Palladium ketimine intermediate **1-75** would be formed via 1,2-addition of the aryl group to the coordinated nitrile moiety. The hydrolysis of the ketimine would release the desired aryl ketone products with the regeneration of active catalytic species (**Scheme 1.23**). Zhao and coworkers independently reported palladium catalyzed aerobic oxidative carbonylation reaction with aryl hydrazines. The oxidative carbonylation proceeded employing molecular oxygen as the terminal oxidant by releasing nitrogen gas and water.[49]

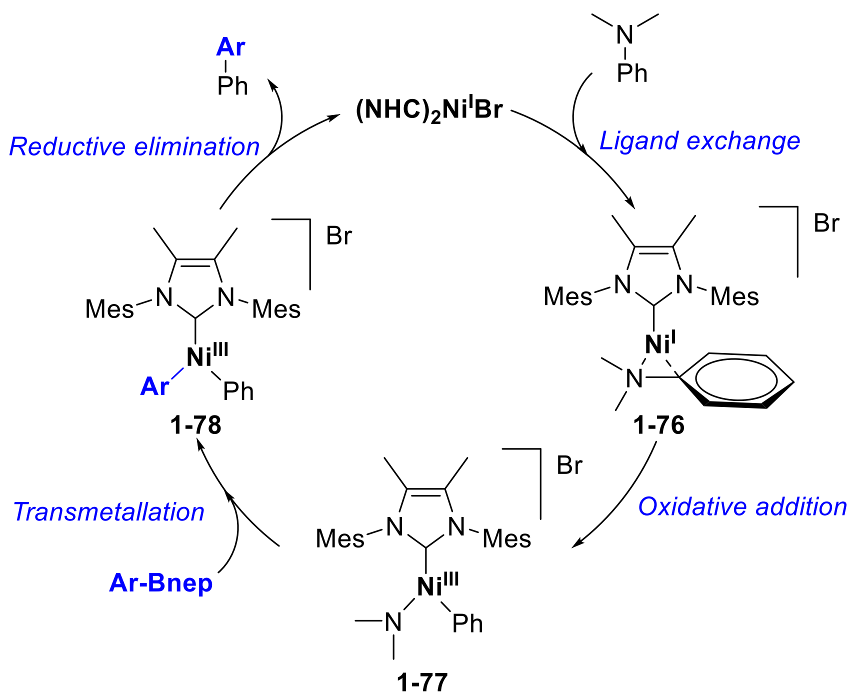

Scheme 1.24: Magnesium-Facilitated Ni(I)/Ni(III) Catalytic Cycle for Suzuki−Miyaura Coupling of Dimethyl Aryl Amines to Forge Biaryl Compounds

Later in 2018, Shi and coworkers reported the Ni-catalyzed Suzuki−Miyaura type cross-coupling of dimethyl aryl amines with arylboronic esters via C−N bond activation under reductive conditions.[50] The Ni(I)/Ni(III) catalytic system forged the desired biaryl products in the absence of directing groups and preactivation. Based on the EPR and DFT studies, the authors proposed a catalytic cycle, in which Ni(I) species **1-76**, initially generated from the ligand exchange of active catalyst with dimethyl aryl amine, led to oxidative addition of sp^2 C−N by producing Ni(III) species **1-77**. Transmetallation followed by reductive elimination on Ni(III) species **1-78** steps forged the desired biaryl products with the regeneration of active Ni(I) species (**Scheme 1.24**). Xia and coworkers reported a similar mechanistic insights for the nickel catalyzed Kumada coupling of aniline derivatives via selective cleavage of sp^2 C−N bond. DFT calculations revealed the insertion of nickel complex into sp^2 C−N bond as the rate-limiting step, and the Boc activation was found to be useful in C−N bond cleavage by weakening of the intrinsic bond strength.[51]

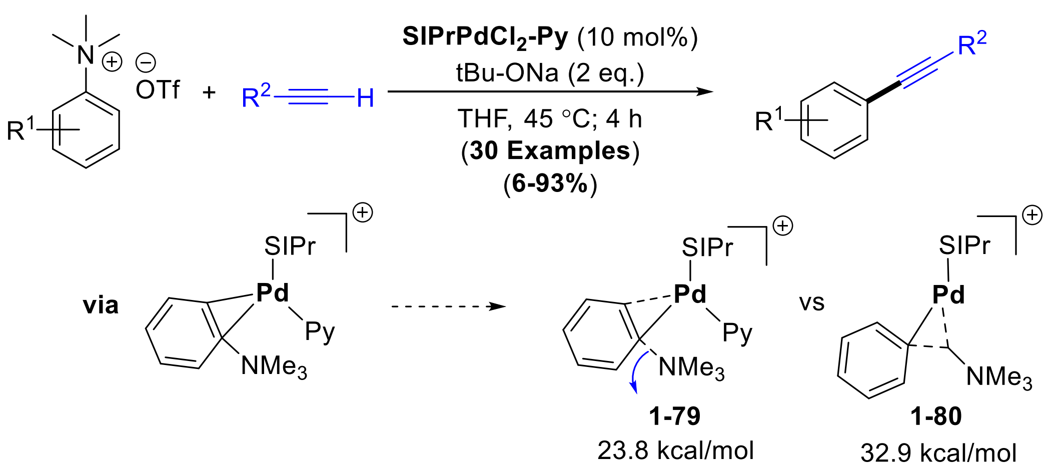

Scheme 1.25: Sonogashira Cross-Coupling of Terminal Alkyne with Aryltrimethylammonium Triflate

In 2019, Cao group reported Sonogashira cross-coupling reaction where aryltrimethylammonium salts were oxidatively added to the palladium-NHC catalytic system for releasing trimethylamine (**Scheme 1.25**).[52] DFT calculations showed that the oxidative addition step on releasing trimethylamine for the transition state **1-80** is 9.1 kcal/mol higher than that of the transition state **1-79**. Recently, You and coworkers reported a similar palladium catalyzed reaction with nitroarenes and terminal alkynes which was found to occur via direct oxidative addition of sp^2 $C{-}NO_2$ bond at elevated temperatures.[53] Very recently, Chelate assisted, $Ru_3(CO)_{12}$ catalyzed Suzuki-type carbonylative reaction with anilines and organoboranes via sp^2 C−N bond cleavage was reported by Wu and coworkers.[54] Later, they were able to further extend the scope of this reaction following the same strategy by employing alkenyl borates to generate 2-phenylolefin products.[55]

1.4.1.2 Arene C(sp^2)–N Bond Activation by Oxidative Addition of Ammonium Salt

In 2015, Wang group employed both activated and unactivated aryltrimethylammonium triflates to synthesize 2-aryl(benzo)oxazoles or 2-aryl(benzo)thiazoles with oxazoles with the demonstration of good compatibility of functional groups.[56] The authors proposed a mechanism based on the experimental data and prior reports on palladium chemistry. The Pd(0) species reacts with aryltrimethylammonium triflates to form an oxidative addition species **1-81** by releasing trimethylamine as a byproduct. Next, aryl(heteroaryl) palladium intermediate **1-82** would be generated via C−H palladation of azoles in the presence of a base. Finally, reductive elimination affords the cross-coupling product along with regeneration of the active Pd(0) species (**Scheme 1.26**).

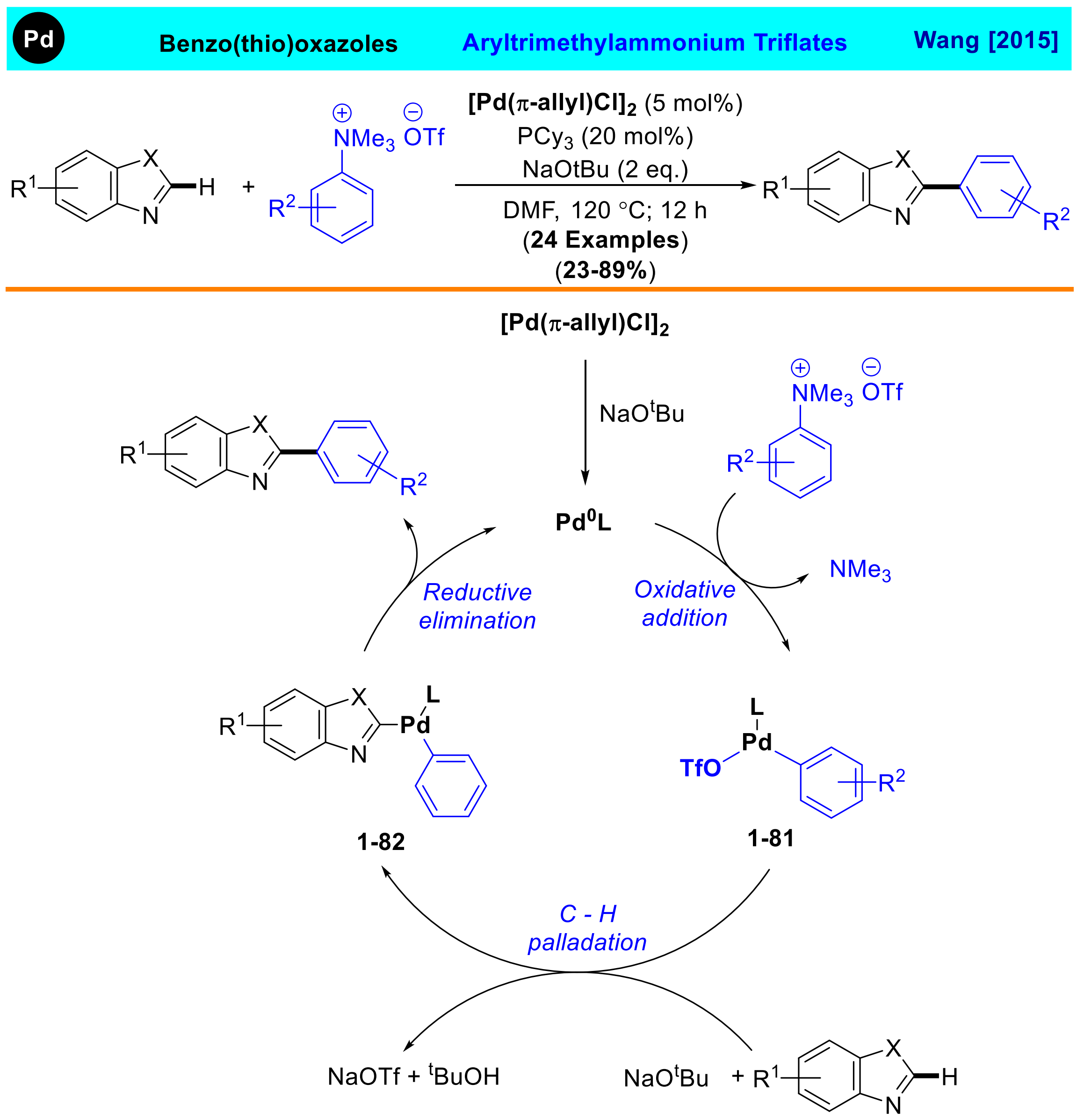

Scheme 1.26: Proposed Catalytic Cycle for Palladium Catalyzed Direct C−H Arylation of Oxazoles and Thiozaoles via C−N Bond Oxidative Addition

1.4.2 Arene C(sp^2) –N Bond Activation via Ammonium Salt

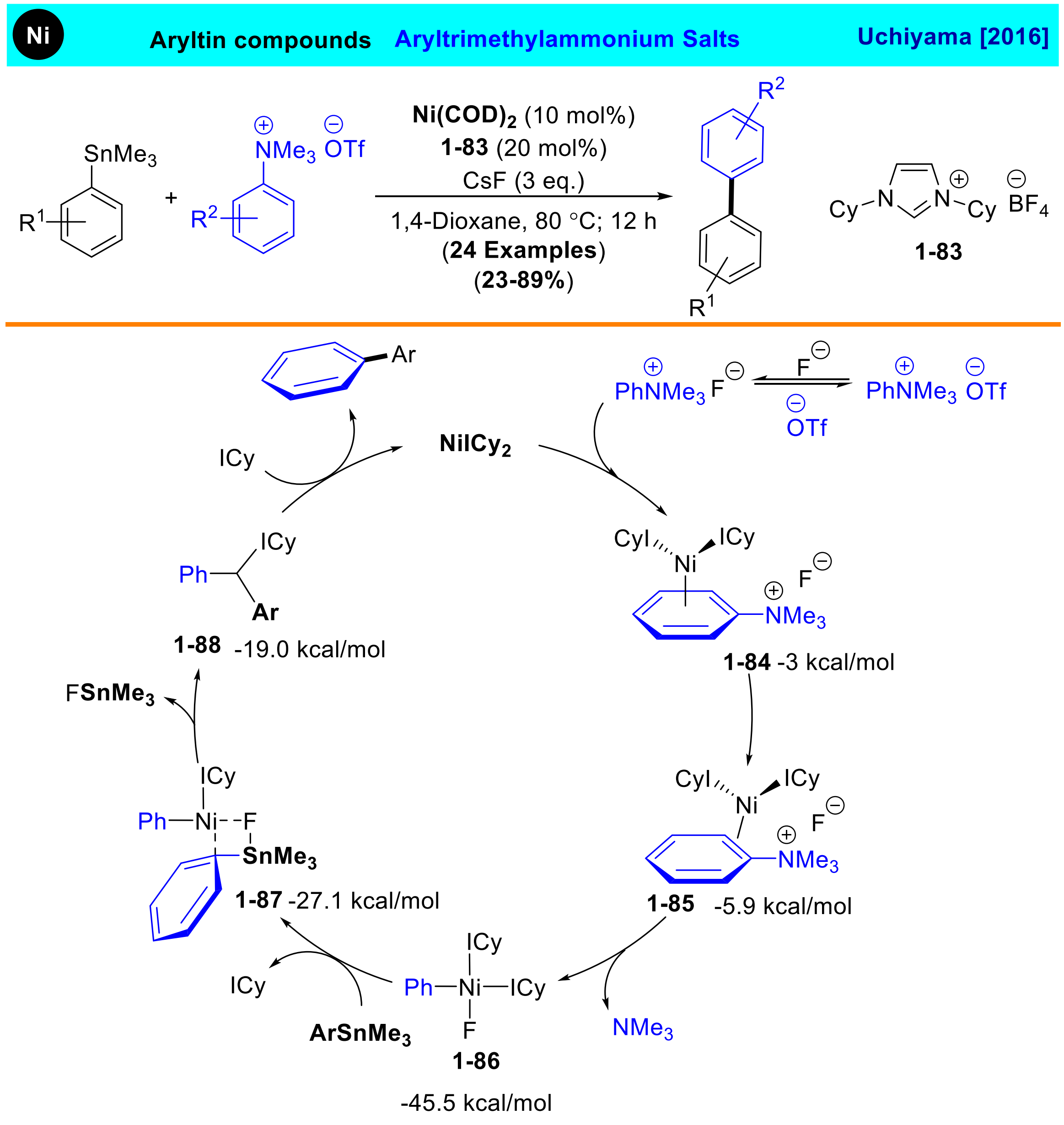

Scheme 1.27: Mechanistic Route Located by Means of DFT Calculations for the Stille Cross-Coupling Reactions of Aryltrimethylammonium Salts via C–N Bond Activation

In 2016, Uchiyama and coworkers reported Stille type cross-coupling with C–N electrophiles via cleavage of C(sp^2)–N bond, by employing a combination of experimental and computational methods.[57] DFT calculations revealed that the Ni(0)-π complex **1-84** is formed with -3.0 kcal/mol exothermicity from $Ni(ICy)_2$ and aryltrimethylammonium fluoride, which was generated via anion metathesis of aryltrimethylammonium triflate and CsF. Migration on the phenyl ring to the proximal position of the C–N bond only cost 10.2 kcal/mol to form the more stable complex **1-85**. The C–N bond cleavage takes place smoothly in a S_NAr process to afford intermediate **1-86** with release of trimethyl amine, in a highly exothermic fashion of -45.5 kcal/mol. The dissociation of ICy ligand and the coordination of aryltrimethylstannane to the Ni(II) complex **1-86** afford the complex **1-87** with an overall energy loss of 18.4 kcal/mol. The reductive elimination of $FSnMe_3$ affords the precursor complex **1-88**. Finally, the formation of desired biaryl compound takes place with the loss of only 2.3 kcal/mol along with regeneration of active catalytic species (**Scheme 1.27**).

1.4.3 Arene C(sp^2)–N Bond Activation by Free Radical Intermediate

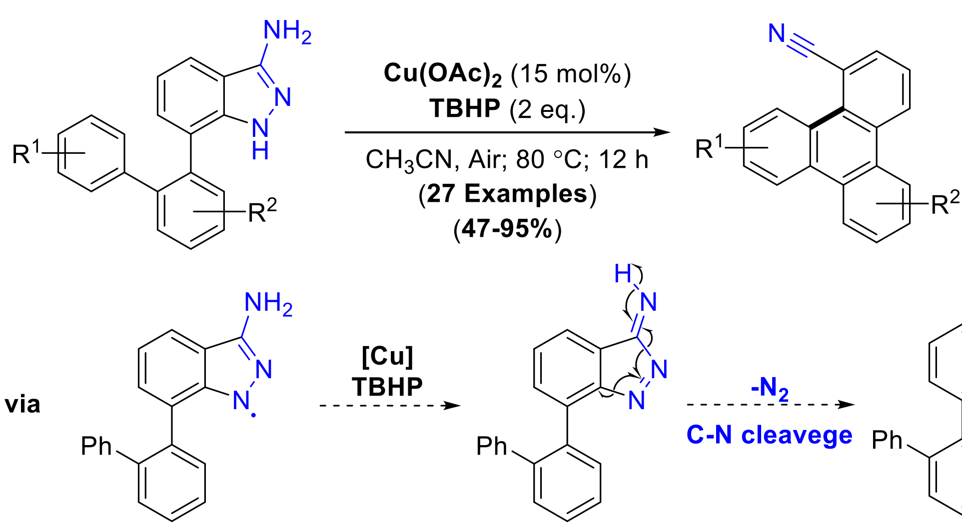

Scheme 1.28: Cu-Catalyzed Aromatic Metamorphosis of 3-Aminoindazoles

Song and coworkers presented an Cu-catalyzed aromatic metamorphosis via oxidative cleavage of two C−N bonds including arene C(sp^2)–N bond of 3-aminoindazoles.[58] DFT calculations and experimental observations indicated that this catalytic transformation involves oxidation, selective C−N bond activation, denitrogenation and radical cyclization steps. This unprecedented aromatic C–C bond formation would be useful for the construction of unsymmetrical nitrile containing triphenylenes (**Scheme 1.28**).

1.5 Catalytic C–C Coupling Methods via Olefinic C(sp^2)-N Bond Activation

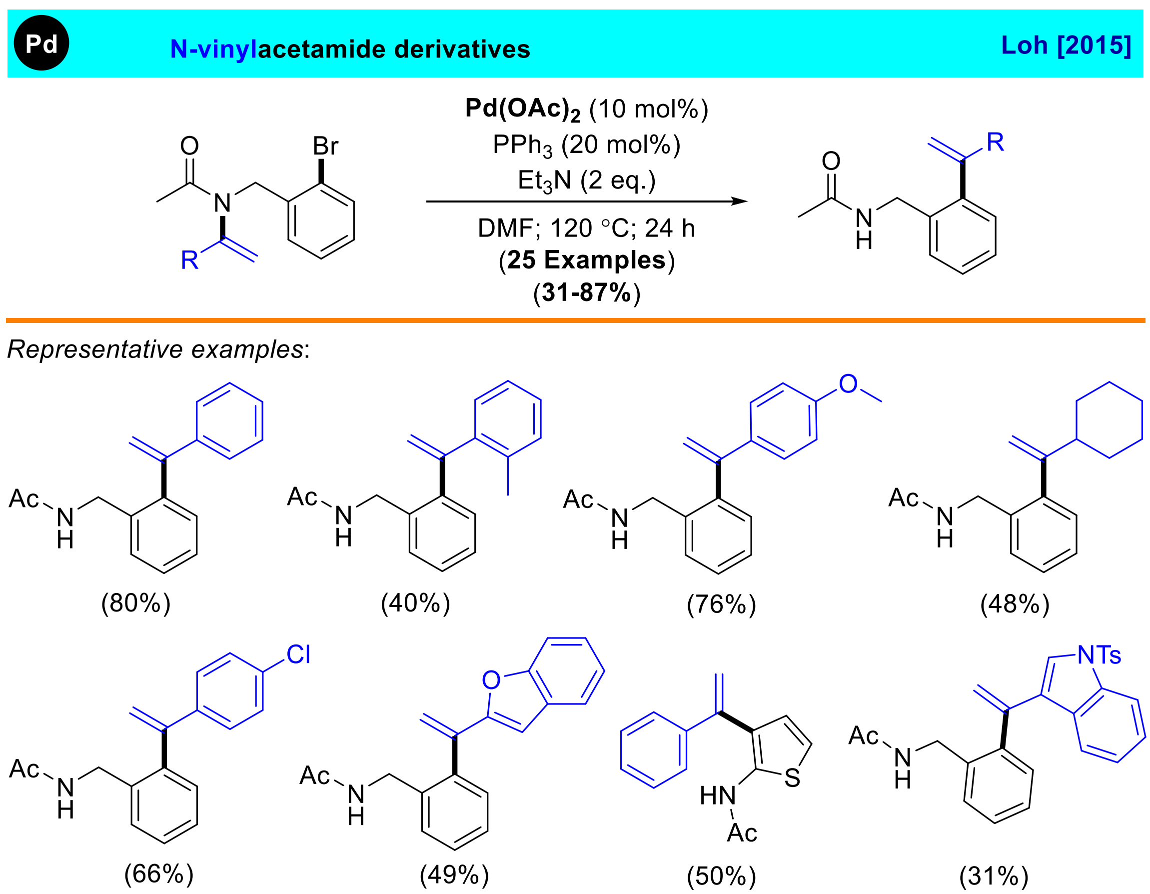

Scheme 1.29: Pd-Catalyzed Intramolecular C−N Bond Cleavage via Heck type coupling reaction of N-vinylacetamide derivatives

In 2015, Loh and coworkers developed a palladium-catalyzed intramolecular Heck coupling reaction by employing N-vinylacetamide derivatives via olefinic C(sp^2)–N bond cleavage (**Scheme 1.29**).[59] The reaction was shown to be compatible with both electron-rich and electron -poor substituted phenyl group, where the cleavage of C(sp^2)–N bond is believed to be occur via *β*-N elimination pathway. The oxidative addition of the C–Br bond to Pd(0) would form the palladium complex **1-89**, which is followed by intramolecular 5-exo-cyclization to produce a new five membered palladium complex **1-90**. The C–N bond activation through *β*–N elimination pathway would occur via the intermediate palladium species **1-91**. Finally, protonation and sequential reductive elimination would yield the desired product with regeneration of the active catalytic species (**Scheme 1.30**).

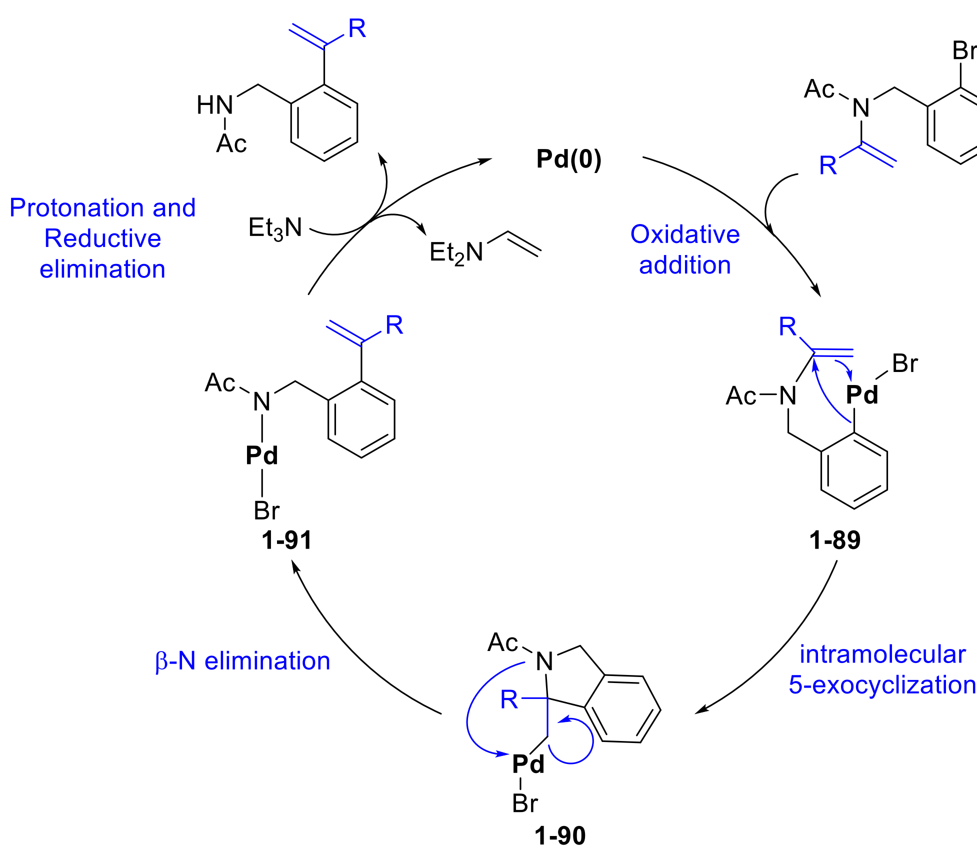

Scheme 1.30: Proposed Mechanism for Heck Reaction of N-Vinylacetamide Derivatives

1.6 Catalytic C–C Coupling Methods via C(sp)–N Bond Activation

Catalytic cyanation methods are a highly desired and user-friendly transformation compared to traditional cyanation methods using toxic reagents such as KCN, $Zn(CN)_2$, and CuCN. In 2013, Fu and coworkers reported a rhodium catalyzed C−H cyanation reaction via C(sp)–N bond activation by using N-cyano-N-phenyl- p-toluenesulfonamide (NCTS) as the cyanation agent.[60] Later, Glorius group reported a cobalt catalyzed protocol for the similar transformation.[61] In 2015, Li and Ackermann further developed the direct cyanation of arenes and heteroarenes by using cobalt chemistry where β-N elimination has been proposed for the C(sp)–N bond activation step (**Scheme 1.31**).[62] Reversible ortho-arene C–H metalation, followed by coordination and insertion of NCTS would generate the key intermediate species **1-93** and **1-94**. Finally, β-N elimination furnishes the corresponding cyanated product **1-92**.

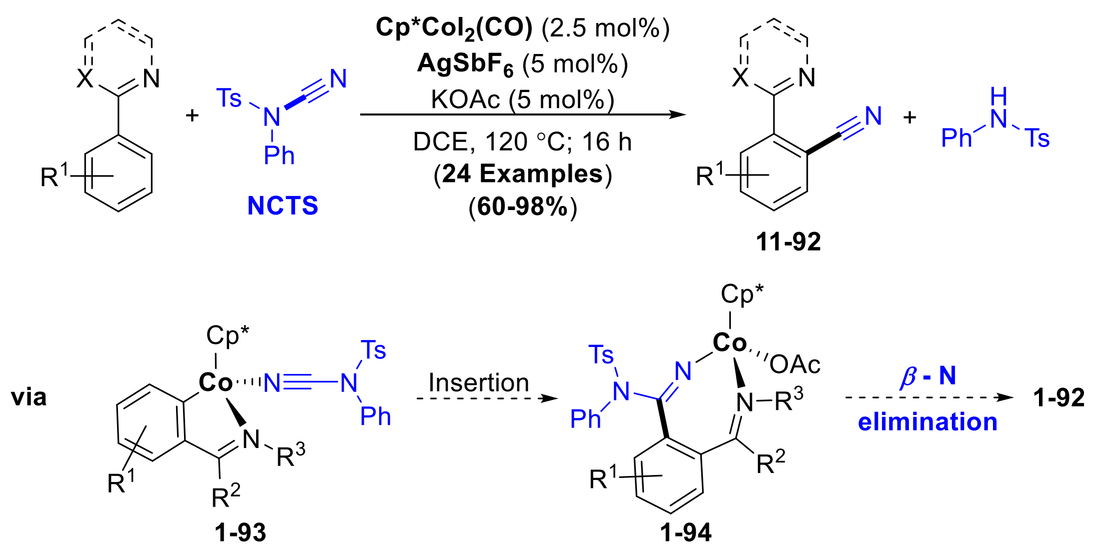

Scheme 1.31: Cobalt Catalyzed C–H Cyanation via C(sp)–N Bond Cleavage

1.7 Catalytic C–C Coupling Methods via Amide C(sp^2)–N Bond Activation

Suzuki–Miyaura cross coupling reaction has been found to be one of the most versatile C–C coupling reactions in both industrial and academic settings.[63] In this context, much attention has been devoted to transition metal catalyzed amide C(sp^2)–N bond activation reactions.[64] Recent studies revealed that the oxidative addition is an effective strategy for transition-metal-catalyzed activation of inert amide C(sp^2)–N bond due to $n_N \rightarrow \pi^*_{C=O}$ conjugation and partial double bond nature.[65] Due to partial double bond character, carbonyl amides have relatively short N−C(O) bonds with high rotational barrier for cis−trans isomerization (typically 15−20 kcal/mol), which have led to lower activity of the carbonyl group toward hydrolysis and nucleophilic addition. One approach is to look at the amide C(sp^2)–N bond activation is the making distorted amides, have been attracted the widespread attention, which include steric repulsion; conformational effects; anomeric amides; steric restriction (**Scheme 1.32**).

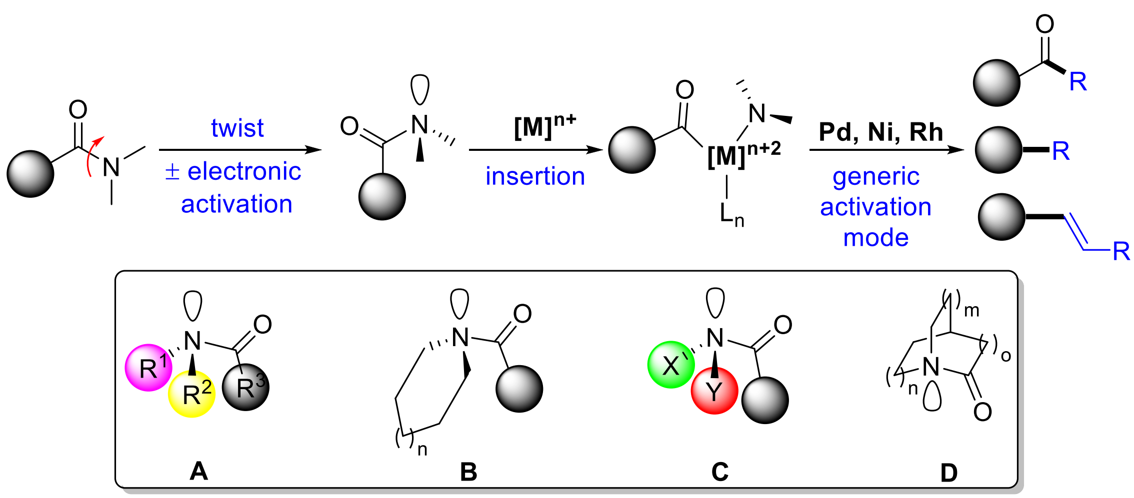

Scheme 1.32: Amide Bond Destabilization for Transition Metal Catalysis; **A.** Steric Repulsion **B**. Conformational Effects (ring or allylic strain) **C**. Anomeric or Electronic Delocalization (as manifested in amides of XXN−C(O) type, where X is an electronegative substituent) **D**. Steric Restriction

1.7.1 Amide C(sp^2)–N Bond Activation by Direct Oxidative Addition

Garg and coworkers reported an uncommon cleavage of the amide C–N bond from nickel-catalyzed Suzuki–Miyaura C–C coupling of amides (**Scheme 1.33**).[66] The methodology was well tolerated for a variety of carbonyl functional groups that bear acidic protons. Potential synthetic utility was also demonstrated by synthesizing pharmaceutically important glucagon receptor modulator.

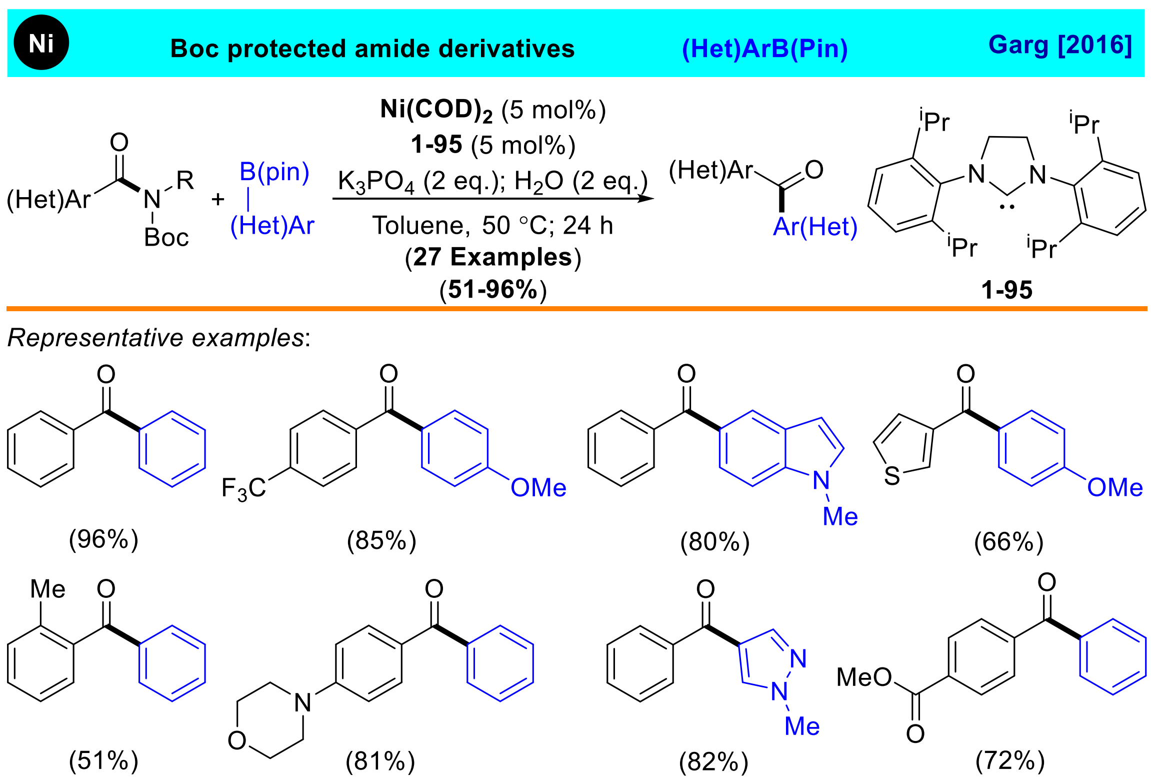

Scheme 1.33: Nickel-Catalyzed Suzuki–Miyaura Coupling of Amides

They further showed that the Ni/SIPr system is an effective catalyst for the formation of alkyl aryl ketones via Negishi type coupling of amides by utilizing both primary and sterically hindered secondary organozinc reagents as alkylating agents.[67] The nickel mediated C−C bond formation has been demonstrated by using aliphatic amide derivatives.[68] Zou[69] and Szostak[70] groups independently reported analogous palladium catalyzed acylative Suzuki coupling of arylboronic acids with carboxylic amides via amide C(sp^2)–N bond activation. In 2017, Szostak group reported a more generalized version of cross-coupling reaction which is promoted by a commercially available, air- and moisture-stable (NHC)Pd(R-allyl)Cl catalyst with several amide derivatives. This Pd-NHC system provided a significant improvement over other catalytic for amide C−N bond activation methods. Both Szostak and Gandhi group employed N-acylsaccharins **1-96** as a electrophilic acyl transfer reagent via acylmetal intermediates to synthesize a variety of functionalized ketones (**Scheme 1.34**).[71]

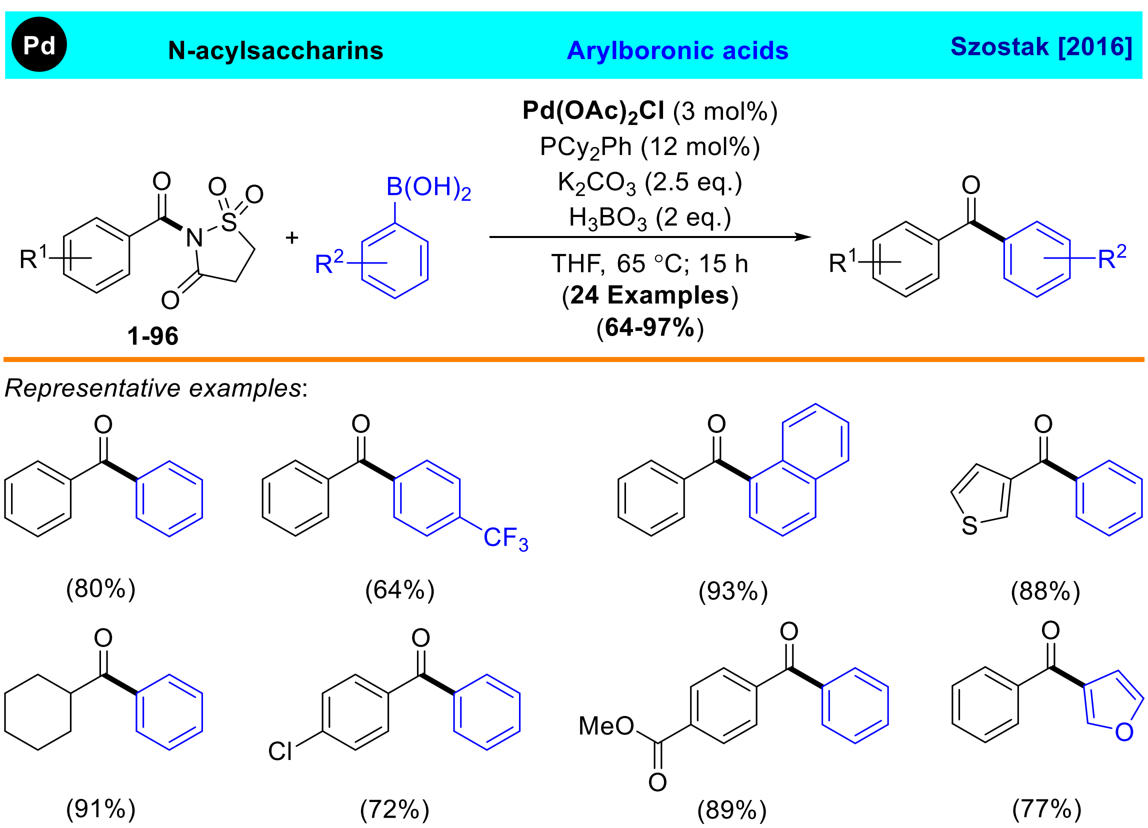

Scheme 1.34: Pd-Catalyzed Suzuki−Miyaura Cross-Coupling of N-Acylsaccharins by C−N Bond Cleavage[71a]

N-acylsaccharins served as amide-based electrophilic acyl transfer reagents via acylmetal intermediates. Mechanistic studies strongly support the amide C−N bond twist as the enabling feature for the C−N activation. The Szostak group has demonstrated a palladium catalyzed Suzuki−Miyaura cross-coupling with arylboronic acids by using N-acyl-5,5-dimethylhydantoins **1-97** as a mild acyl-transfer reagent via selective amides C−N bond cleavage (**Eq. 1.11**).[72]

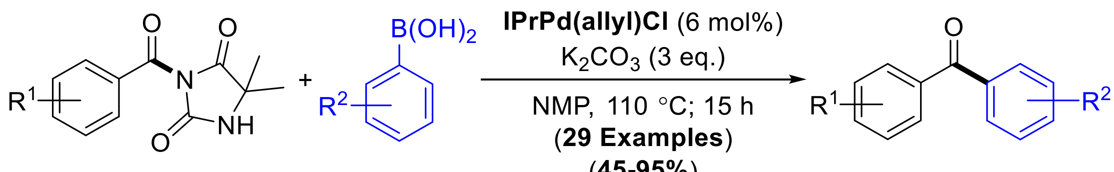

1-97

(Eq. 1.11)

In 2019, Stanley group used N-benzoyl-N-phenylbenzamides as acyl-transfer reagent triggered by nickel-catalyzed amide C−N bond activation, which is a intermolecular, three-component carboacylation reaction with norbornene derivatives.[73] Nickel-catalyzed alkylation of amides was reported by Rueping group by employing alkylboranes as nucleophilic partners under relatively mild reaction conditions.[74] Yu and Matsuo presented electrophile cross coupling reaction between alkylpyridinium salts (Katritzky salts) and amides via nickel catalyzed amide C−N bond activation. This reaction believed to be proceeded through SET mechanism.[75] Szostak group further looked in to more chemoselective amide C–N cleavage protocol to develop Heck type transformation and they were able to successfully obtain useful olefin derivatives by employing simple olefins under palladium chemistry (**Eq. 1.12**).[76]

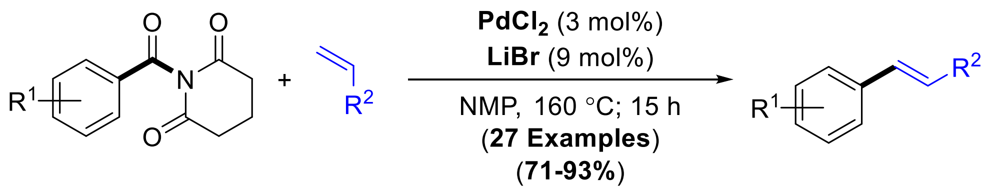

(Eq. 1.12)

Mechanistic investigations revealed that the reaction involves a cationic palladium complex with decarbonylation as the rate limiting step. Relative reactivities further suggested that oxidative addition is not the rate limiting step. Also, competitive experiments were indicated that the sterically demanding ortho aryl substrates play an important role in accelerating the reaction due to steric effects. In 2016, they carried out extensive study on nickel, palladium and rhodium to develop C–C cross coupling methods via amide C(sp^2)–N bond activation.

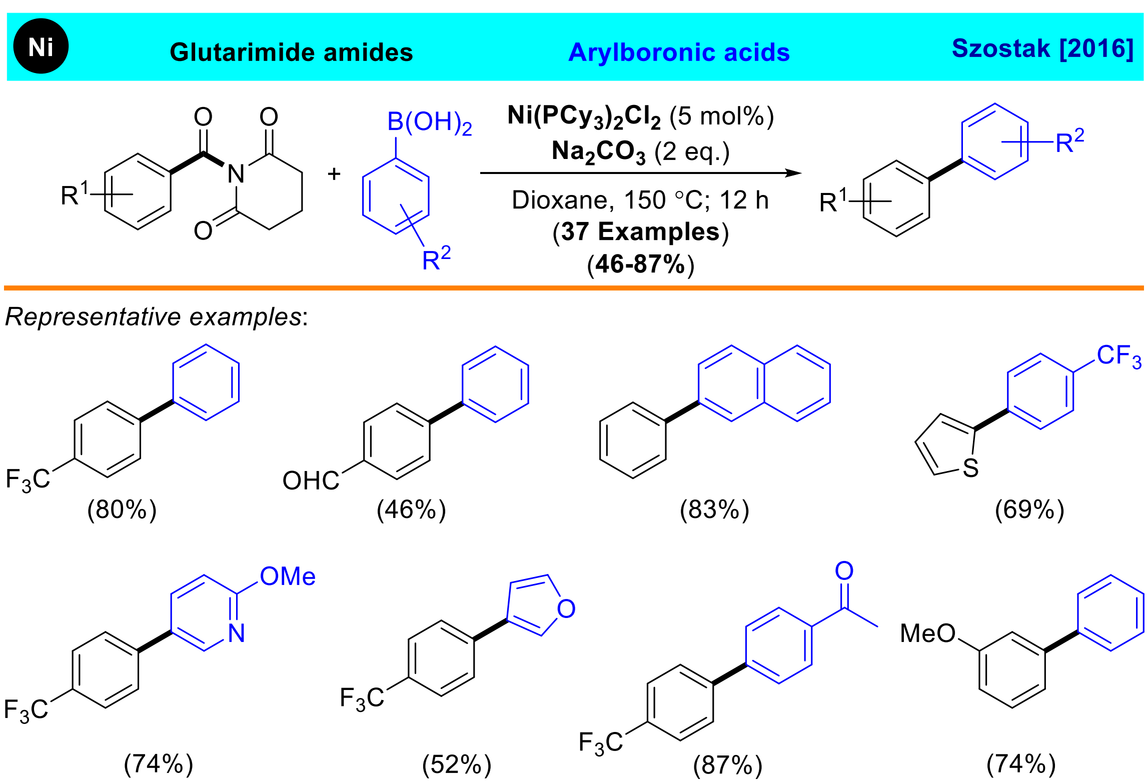

Scheme 1.35: Nickel-Catalyzed Suzuki Biaryl Synthesis Through Cross-Coupling of Amides with Boronic Acids via C–N Bond Activation

Suzuki–Miyaura biaryl coupling of amides with commercially available boronic acids were found to be effective with air-stable $Ni(PCy_3)_2Cl_2$ complex, without additional ligands or hygroscopic additives. Generation of aryl electrophiles on nickel at elevated temperatures from bench-stable amides were reported as first nickel catalyzed example on biaryl synthesis (**Scheme 1.35**).[77] Formation of an Ar-Ni-$CONR_2$ intermediate **1-98** by direct oxidative addition to the aryl–acyl bond might be operative for C–N bond activation. Transmetallation would form the intermediate complex **1-99**, which then decarbonylation occurred to form complex **1-100**. Finally, desired biaryl products will be afforded by reductive elimination step (**Scheme 1.36**).

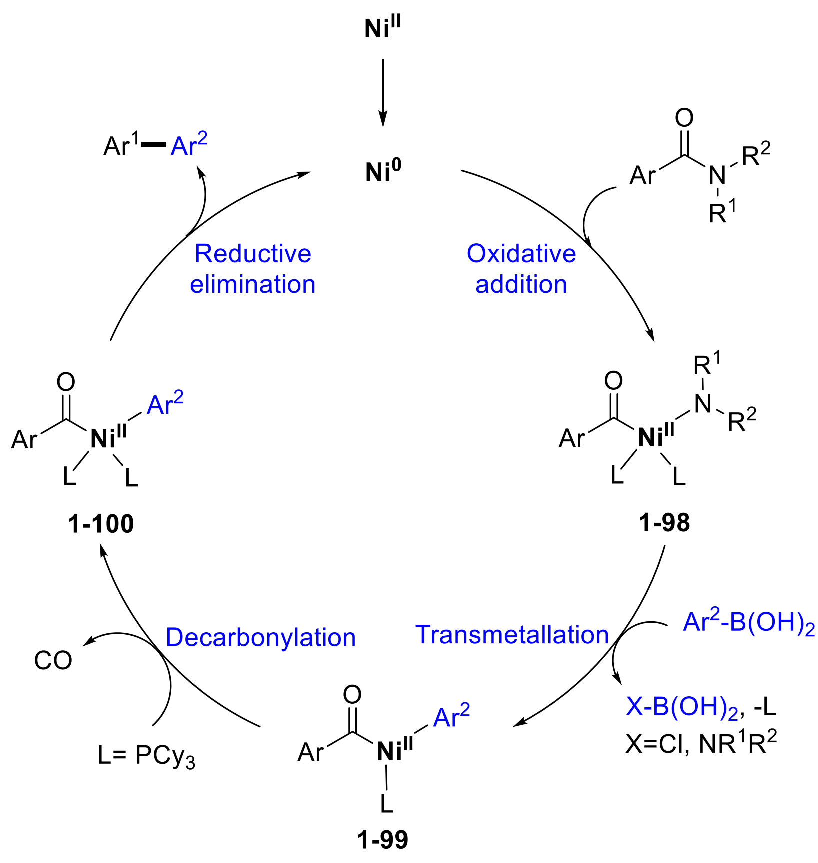

Scheme 1.36: Proposed Mechanism for Biaryl Synthesis via C–N Bond Oxidative Addition

They successfully developed a rhodium catalytic system via amide C–N bond activation protocol to generate biaryl products, along with arene C–H activation for the substrates with a directing group.[78] Rueping group reported a nickel catalyzed Sonogashira type cross coupling reaction by employing amides with protected terminal alkynes as coupling partners.

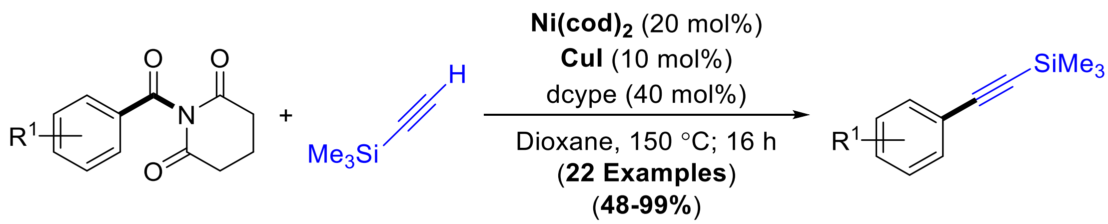

(Eq. 1.14)

This methodology enables a facile route for C(sp^2)−C(sp) bond formation via direct C(sp^2)−N activation followed by decarbonylation of amides (**Eq. 1.13**).[79] Very recently, Lee and coworkers reported nickel catalyzed Claisen condensation of two different amides to furnish the desired β-ketoamides in the presence of manganese and LiCl (**Eq. 1.15**).[80]

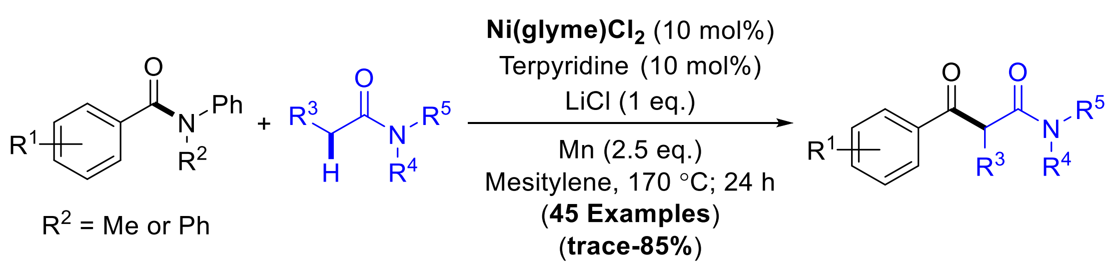

(Eq. 1.15)

DFT calculations and the experimental data uncovered the formation of the manganese enolate during the reaction and the reductive elimination of nickelacylalkyl species has been proposed as the rate-determining step. Altogether, these reactions share similar mechanistic features for transition metal catalyzed amide bond activation for the synthesis of pharmaceutically important products.

In 2015, Murakami's group reported palladium catalyzed intramolecular insertion of alkenes into the C−N bond of β-lactams to form the tricyclic nitrogen heterocycles.[81] The proposed mechanism involves via initial oxidative addition of C−N bond to form a five-membered palladacycle intermediate. Subsequent alkene insertion by forming seven membered palladacycle followed by reductive elimination furnishes the desired products (**Equation 1.15**).

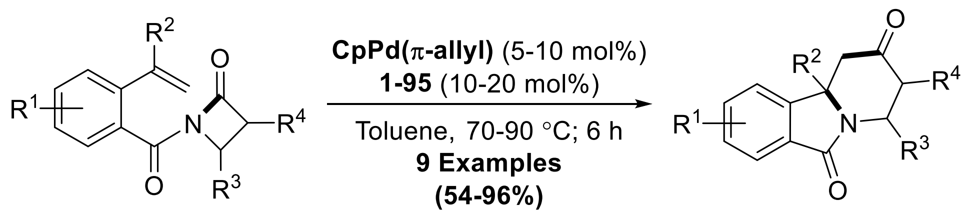

(Eq. 1.15)

In 2017, Garg group reported an intramolecular non-decarbonylative Mizoroki–Heck reaction of amide derivatives via amide C–N bond activation.[82] Diastereoselective polycyclic or spirocyclic products containing quaternary centers were obtained by using sterically hindered tri- and tetrasubstituted olefin derivatives. Moreover, an adduct bearing vicinal, highly substituted sp^3 carbon stereocenters was also obtained by using amide derivatives as building blocks for the assembly of complex scaffolds (**Scheme 1.37**). Catalytic conversion would proceed through a sequence akin to classical Mizoroki–Heck chemistry, via oxidative addition, subsequent olefin coordination, insertion and β-hydride elimination steps. Liu and coworkers presented theoretical insights for the mechanisms of intramolecular insertion of alkenes into the carbon-nitrogen bond of β-lactams. These theoretical investigations revealed that the oxidative addition, alkene insertion, and reductive elimination are the key steps governing the alkene insertion as the rate-determining step for the reaction.[83]

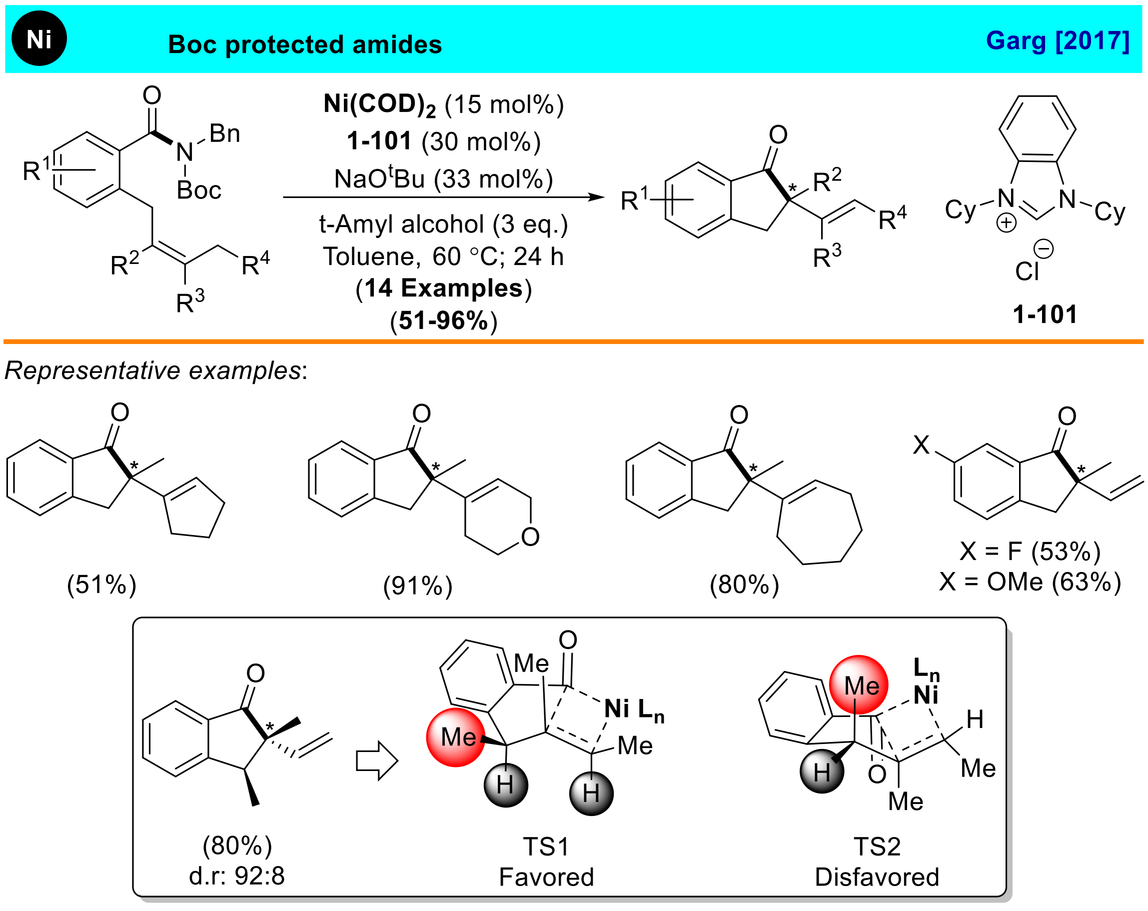

Scheme 1.37: Mizoroki–Heck Cyclization of a Variety of tri- and Tetrasubstituted Olefin Substrates

Very recently Dang group carried out DFT calculations which provided detailed mechanistic insights for Pd-catalyzed non-decarbonylative and Ni-catalyzed decarbonylative Suzuki−Miyaura cross coupling reactions of N-acetylamides.[84] Nickel catalyst is conducive to the d → π^* back donation from nickel to CO **1-102**, which stabilizes the decarbonylative transition state by promoting decarbonylation. On the other hand, palladium has a higher electronegativity which possesses weaker d → π^* back donation from palladium to CO **1-103**. Therefore, Pd-catalyzed reaction gives the ketones as the product via nondecarbonylative pathway. This origin of the chemoselectivity has been explained by back donation characteristics of the central metal atom. (**Scheme 1.38**).

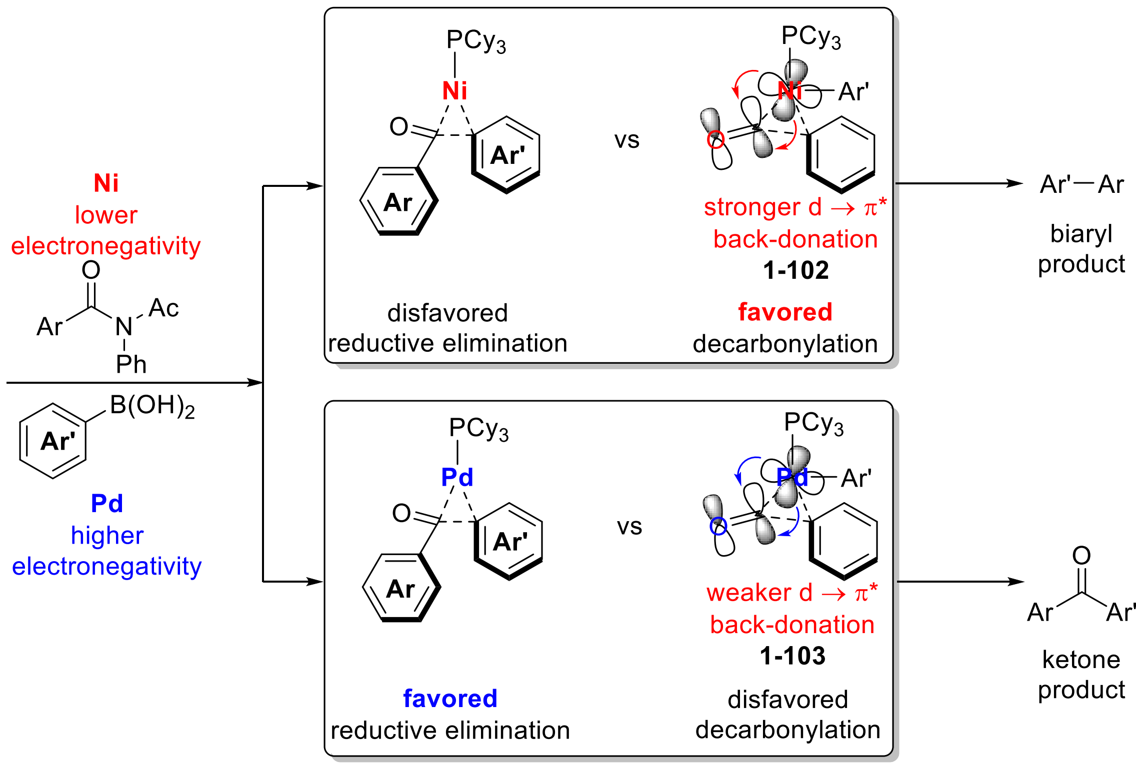

Scheme 1.38: Decarbonylation vs Reductive Elimination of Ni and Pd Catalyzed Suzuki−Miyaura Coupling Reactions

In 2017, Pan and coworkers reported a first example using amide as an electrophile to couple with another electrophile, via reductive cross-coupling of amides and aryl iodides, under nickel chemistry without using highly basic and pyrophoric nucleophiles (**Scheme 1.39**).[85] Initially, the active Ni(0) catalyst generates from reduction of Ni(II), which activates the C−N bond of glutarimide resulting in the Ni(II) intermediate species **1-105**. Iodobenzene reduced by reactive nickel(I) species **1-107** results in the phenyl radical, and which undergoes radical oxidative addition to Ni(II) species **1-105** to give the nickel(III) intermediate **1-106**.

1.7.2 Amide C(sp^2) –N Bond Activation by Single-electron Reduction

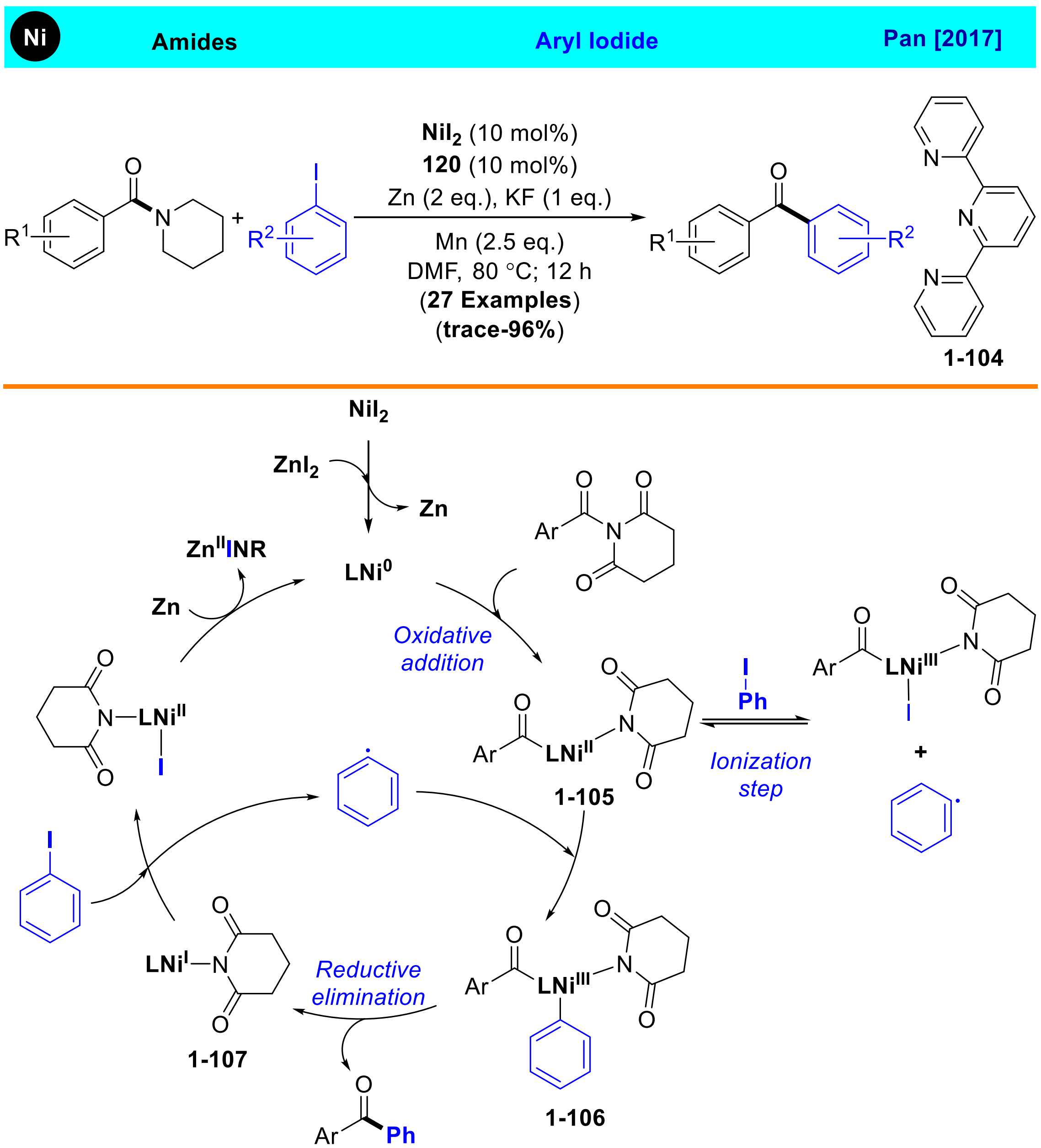

Scheme 1.39: Proposed Mechanism for Reductive Cross-Coupling of Amides

Desired cross-coupling ketone product would be afforded by reductive elimination of nickel(III) intermediate **1-106** along with reactive nickel(I) complex **1-107**. Reaction of nickel(I) complex **1-107** with iodobenzene followed by reduction will be regenerated the active Ni(0) catalytic species. According to the general mechanism found in atom-transfer radical addition reactions[86], aryl radicals would also be generated by the reaction between Ni(II) intermediate **1-105** and iodobenzene.

In 2020, Li and coworkers reported an acylation of aryl and alkyl bromides by employing acylimidazoles via C–N bond cleavage (**Scheme 1.40**).[87]

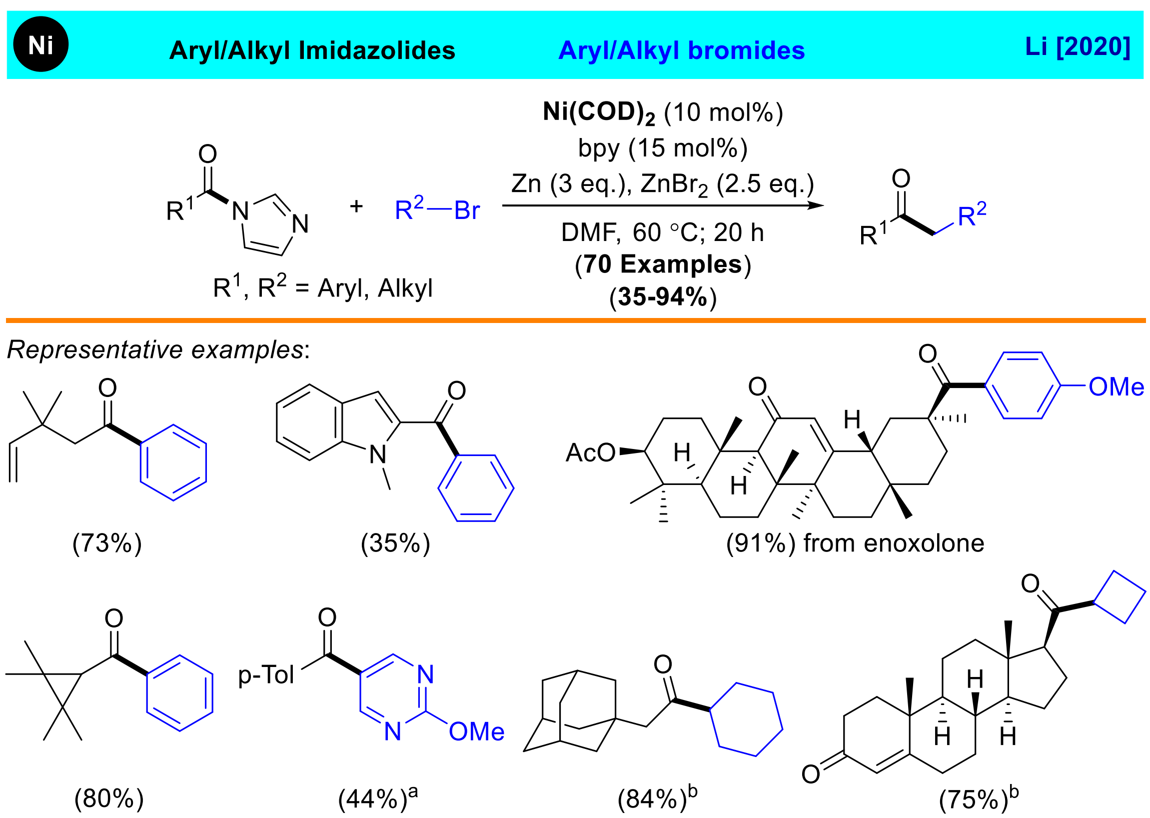

Scheme 1.40: Ni-Catalyzed Reductive Cross-Coupling of Alkyl/Aryl Imidazolides with Alkyl/Aryl Bromides; [a]10 mol % NiI_2, 20 mol % Terpyridine, $ZnCl_2$ (2.0 eq.), Zn (3.0 eq.), and 110 °C were Used; [b]10 mol % NiI_2, 15 mol % 4-4´-Dimethoxy-2-2´-bipyridine, $MgCl_2$ (2.0 eq.), Zn (3.0 eq.), THF/DMF at Room Temperature were Used

Notably, the homocoupling of aryl and alkyl bromides led to form symmetric ketones as the common byproduct. Radical clock experiments revealed that cross-coupling reactions of acylimidazoles are derived from primary and secondary acids, and a highly unusual carbon monoxide (CO)-extrusion-recombination pathway proceeds via radical intermediates. Interestingly, when (bromomethyl)cyclopropane was examined under standard conditions, a cyclopropane ring opened product obtained as the exclusive product, which indicated that the alkyl bromide had indeed proceeded via a radical pathway.

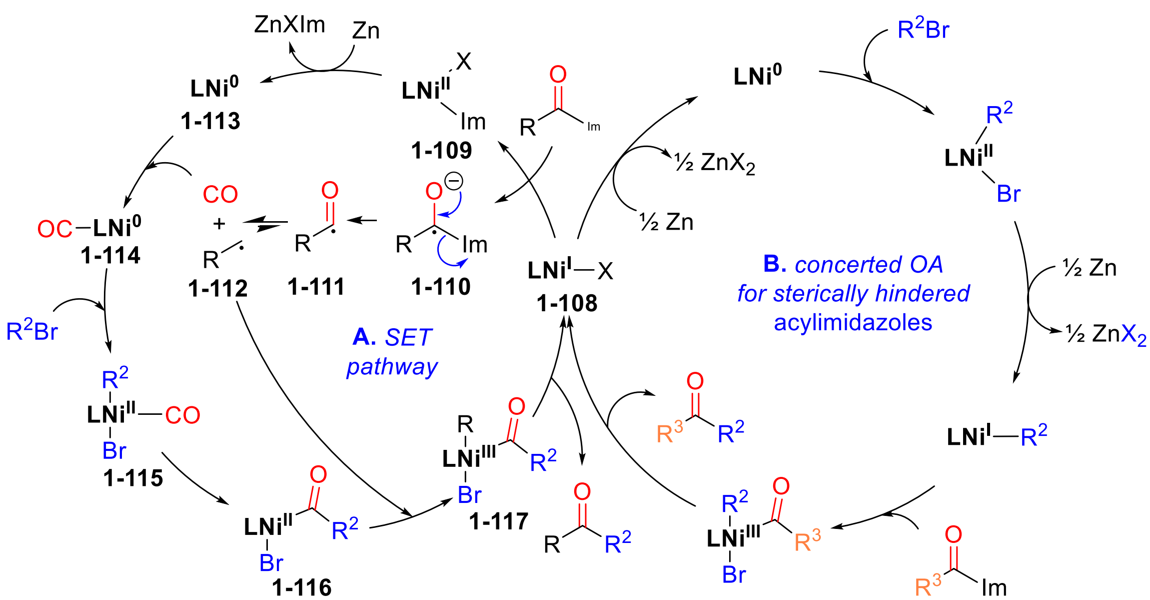

L = bpy, Terpyridine, 4´-Dimethoxy-2-2´-bipyridine
R^3 = sterically hindered alkyl; Im = Imidazole

Scheme 1.41: Proposed Mechanistic Pathways; A) Single Electron Transfer for Spatially Accessible Acylimidazoles; B) Concerted Oxidative Addition for Sterically hindered Acylimidazoles

As indicated in pathway **A**, Ni(I) complex **1-108**, acts as a reducing reagent that gives an electron to the less sterically hindered imidazolide via a single-electron transfer (SET), thus generating Ni(II) complex **1-109**. Subsequent fragmentation of the radical anion **1-110** gives rise to an acyl radical **1-111** that undergoes CO extrusion to form CO and an alkyl radical **1-112**. Further reduced imidazolide Ni(II) complex **1-113** by zinc, then traps a CO to form Ni(0) carbonyl complex **1-114**, which then subjected to oxidative addition of alkyl bromide via a radical process affording Ni(II) carbonyl complex **1-115**. CO insertion followed by combination of the alkyl radical species **1-116** results in formation of Ni(III) intermediate **1-117** via Ni(II)complex **1-116**. Desired ketone product and Ni(I) complex **1-108** will be regenerated after reductive elimination step (**Scheme 1.41**). Sterically hindered imidazolides such as the acylimidazoles believed to be occurred via two electron process via pathway **B**.

1.7.3 Lewis Base Promoted Amide C(sp^2)–N Bond Activation

In 2016, Szostak group reported the synergistic combination of Lewis base and palladium catalysis to activate C−N bond of N,N-di-Boc-activated amides. A number of structurally diverse biaryl ketone products were synthesized on palladium-catalyzed Suzuki−Miyaura cross-coupling by employing di-Boc-activated amides.[88]

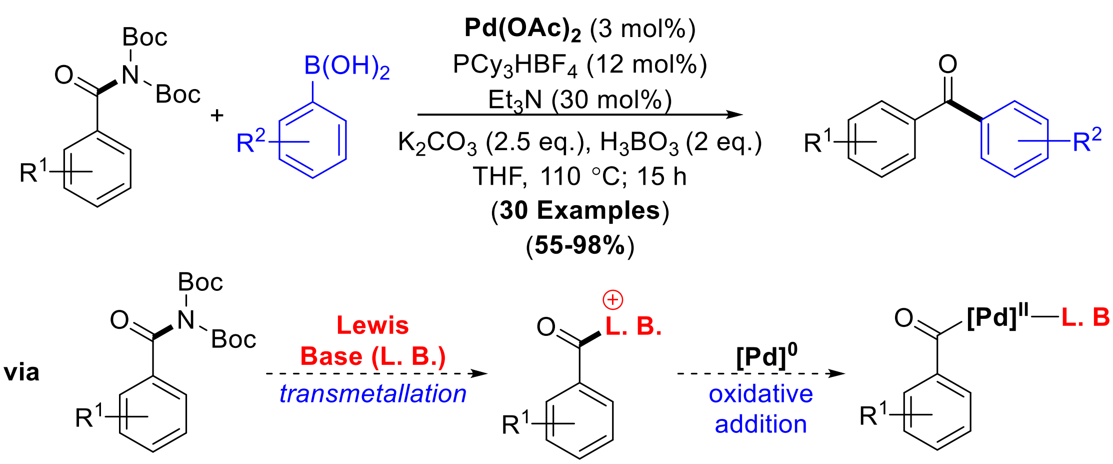

Scheme 1.42: Activation of N,N-di-Boc-activated Amide C−N Bond by the Aid of a Lewis Base

Synthetic utility was demonstrated by direct functionalization of pharmaceutically useful amide scaffolds in a gram scale synthesis. Synergistic mechanism was explained by invoking selective oxidative addition into the weak acylammonium bond to generate a highly reactive acyl-Pd(II) intermediate (**Scheme 1.42**).

1.8 Catalytic C-C Coupling Methods via C=N Bond Activation

2H-Azirines are highly reactive three-membered heterocyclic unsaturated compounds analogues to the saturated analogue aziridine which are highly important class of compounds found in natural products and biologically active compounds. Also, this class of compounds are used as valuable building blocks in organic synthesis due to their high ring strain. Number transition metal catalyzed C=N bond activation reactions has been developed by employing azirines. In 2018, Ding and coworkers used Zinc catalyzed [3 + 2] cycloaddition reaction by employing benzimidates and 2H-azirines to synthesize substituted imidazoles (**Scheme 1.43**). This protocol provided good functional group tolerance by having moderate to good yields.[89]

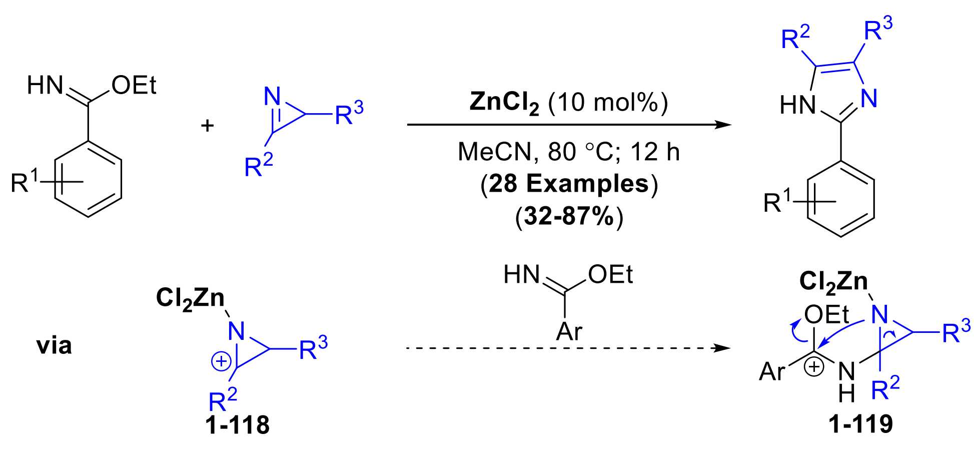

Scheme 1.43: $ZnCl_2$ Catalyzed [3 + 2] Cycloaddition of Benzimidates and 2H-Azirines

First, cationic azirine complex **1-118** would be formed in the presence of $ZnCl_2$. Which would undergo nucleophilic attack by benzimidate to generate intermediate complex **1-119**. Subsequent ring opening and intramolecular nucleophilic attack of the N to the carbocation and OEt as a leaving group form the five membered ring intermediate lead the formation of imidazole product. Very recently Song and coworkers reported a Cu-catalyzed C–H arylation of enamines via C–N bond activation of 3-aminoindazoles. This expedient approach yielded 3-aminoindazoles with good to excellent yields by concomitant in situ generation of a cyano group (**Scheme 1.44**).[90]

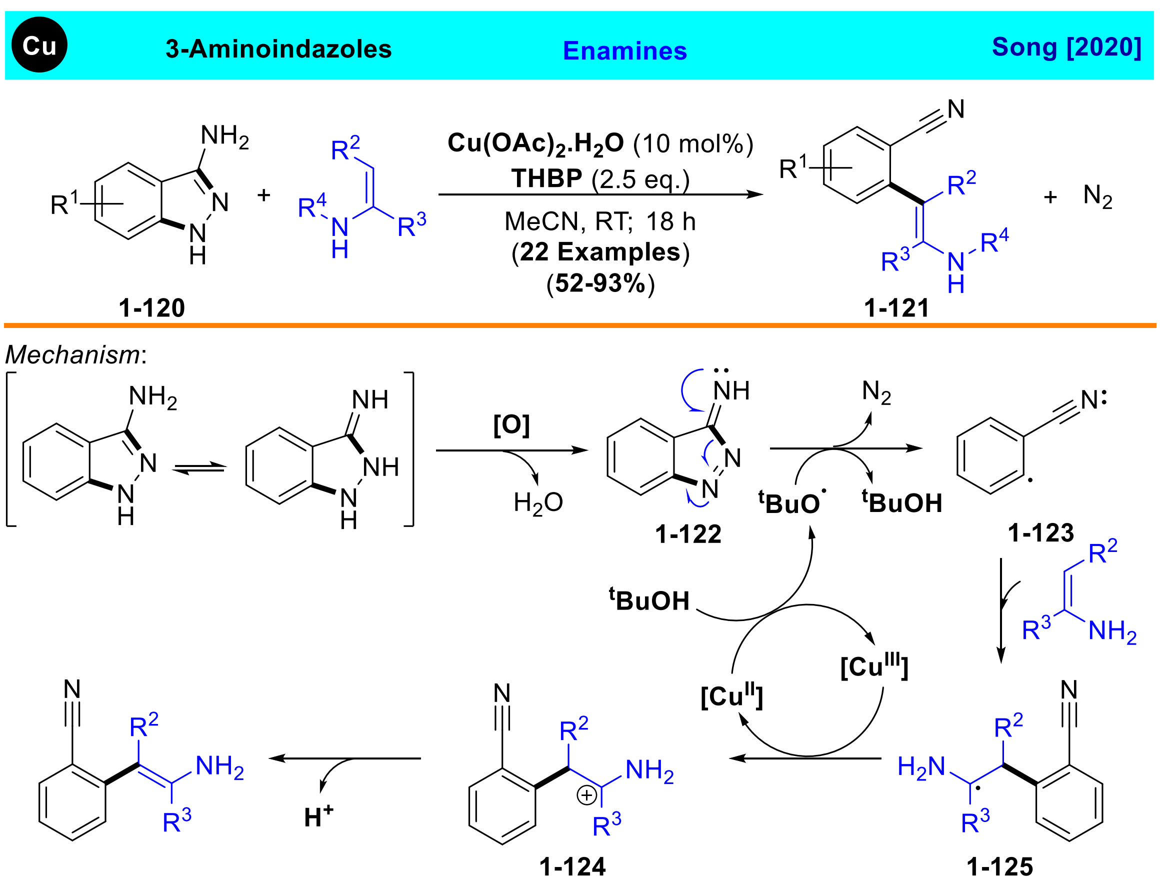

Scheme 1.44: Cu Catalyzed Denitrogenative C–H Arylation of Enamines

Catalytic cycle initiated by oxidation of 3-aminoindazole **1-120** by formation of compound **1-122**. Simultaneously, tert-butoxyl radical would be generated via single electron transferred from the Cu(II) species to TBHP to deliver the Cu(III) species. Subsequent abstraction of a proton from the compound **1-122** leads the formation of benzonitrile radical intermediate **1-123** with extruding molecular nitrogen. Radical addition of intermediate **1-123** with the enamine gives rise to the production of radical intermediate **1-124**, which is oxidized by the Cu(III) species to afford the carbocation intermediate **1-125** and Cu(II) species. Deprotonation of intermediate **1-125** furnishes the final product **1-121**.

1.9 Catalytic C–Heteroatom Coupling Methods via C–N Bond Activation

1.9.1 Catalytic C-N Coupling Methods via C(sp^3)-N Bond Activation

Chemical synthesis of carbon–heteroatom bond is very important transformation in the number of industrial and pharmaceutical processes. While various types of carbon–heteroatom bond formation reactions have been reported, herein we will discuss catalytic C-N coupling methods via C–N activation with special reference to the reports came out during last five years. Apart from other carbon–heteroatom bonds, C–N coupling methods is a ubiquitous motif in most of the natural and synthetic compounds. Transition-metal catalyzed C–N coupling methods via C−N bond cleavage by oxidative addition, iminium and ammonium species, formation of imine and radical pathways will be discussed in this section.

1.9.1.1 C(sp^3)-N Bond Activation by Oxidative Addition

Selective cleavage of the C−N bond of a primary amine is a challenging process because amine group is a poor leaving group and the N−H bonds have a relatively low tolerance for functional groups. However, protonation of the NH_2 group makes it a better leaving group by decreasing the C−N bond strength. Therefore, acid-catalyzed C−N bond activation through the ammonium ion provides one way of C−N bond cleavage of the primary amines. On the other hand, formation of "**C−[M]−N**" by an oxidative addition to the transition metals with or without the aid of the acid should be an effective and direct strategy to realize the cleavage of C−N bonds. In 2015, Huang group reported a method to generate α,β-diamino acid esters under mild conditions by palladium catalyzed

C(sp^3)−N bond activation.[91] The reaction proceeded through the efficient insertion of carbenoids into the C−N bond of aminals (**Scheme 1.45**).

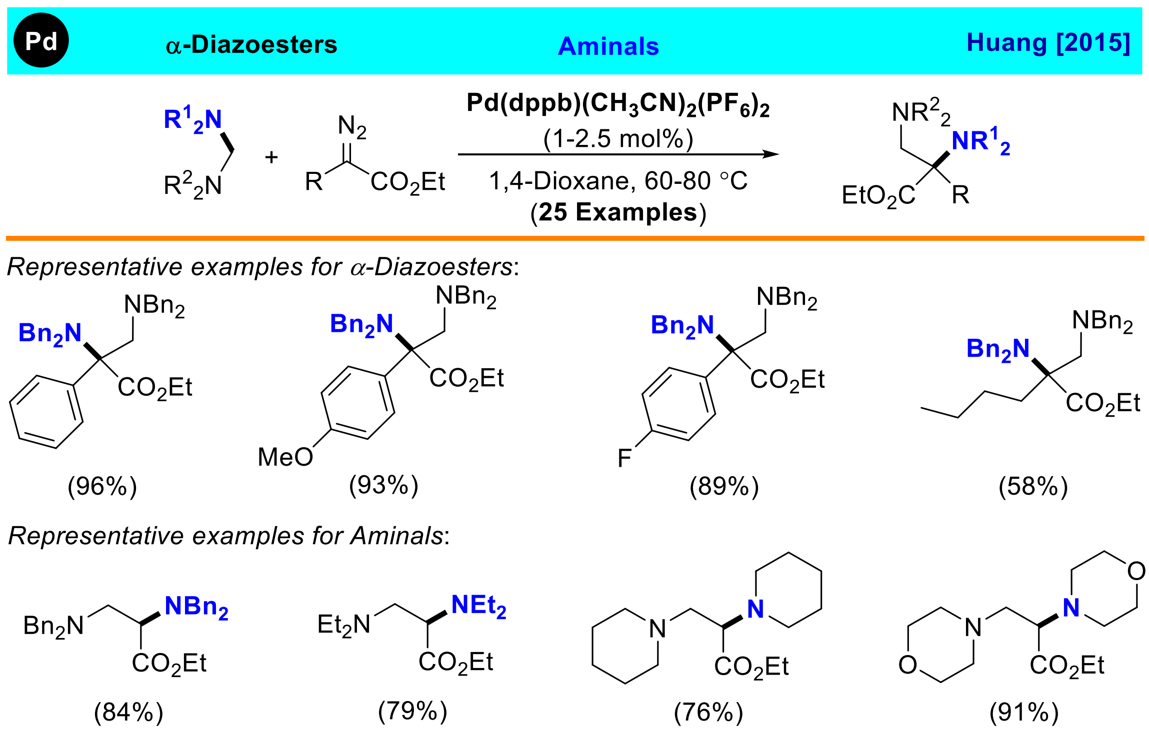

Scheme 1.45: Substrate Scope of α-Diazoesters and Aminals

The mechanistic studies revealed that the formation of three-membered palladocycle **1-126** was involved in the catalytic cycle. The cationic cyclopalladated species **1-126** reacts with a diazoester by giving palladium–carbenoid intermediate **1-127**. Subsequent migratory insertion of the aminomethyl moiety would generate the species **1-128** followed by nucleophilic attack release nucleophilic R_2N^- to form species **1-129**. Finally, reductive elimination released the desired α,β-diamino acid ester by regeneration of the active catalytic species.

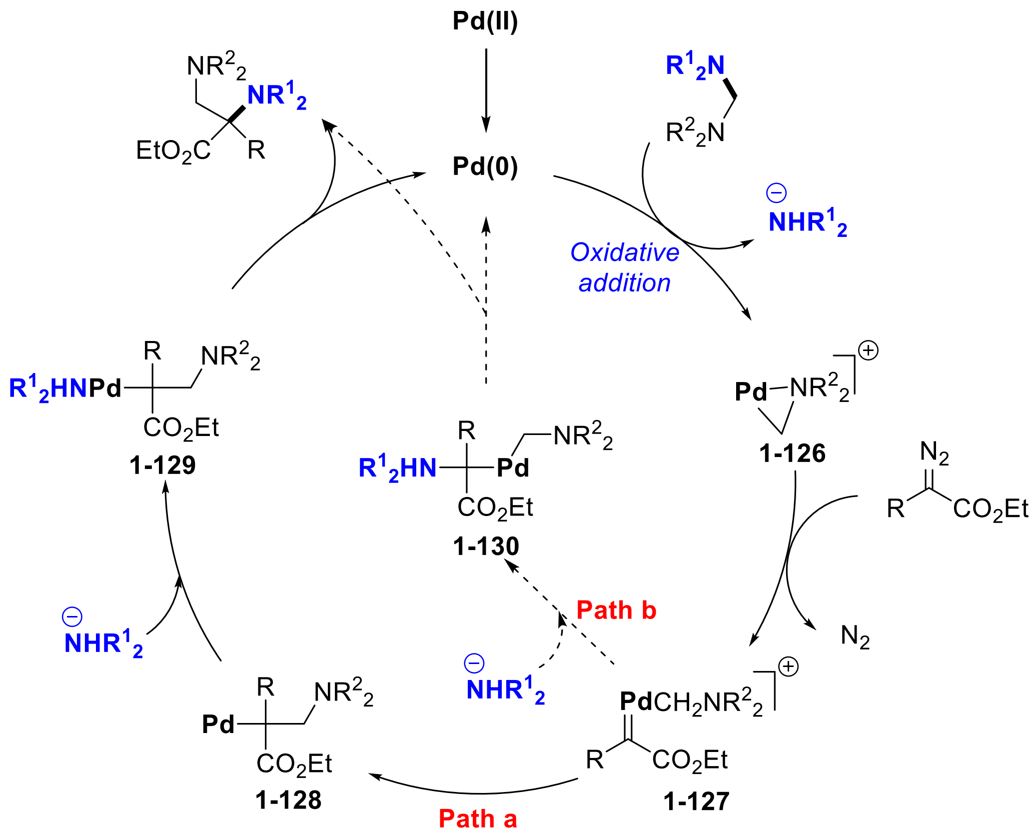

Scheme 1.46: Proposed Mechanism for the Synthesis of α,β-Diamino Acid Ester Derivatives

Alternatively, the intermediate species **1-130** would release nucleophilic R_2N^- from the intermediate **1-127**, which undergoes reductive elimination to give desired product under path b (**Scheme 1.46**). They were able to generate a number of pharmaceutically important tetracyclic N-[2-(methoxycarbonyl)-ethyl]indoloisoquinolinones **1-131** by using a Pd(II)-catalyzed double intramolecular cyclization of 1,2-diarylethynes **1-132** bearing an N- methyl-N-[2-(methoxycarbonyl)ethyl]amino with an aminocarbonyl compounds (**Scheme 1.47**).

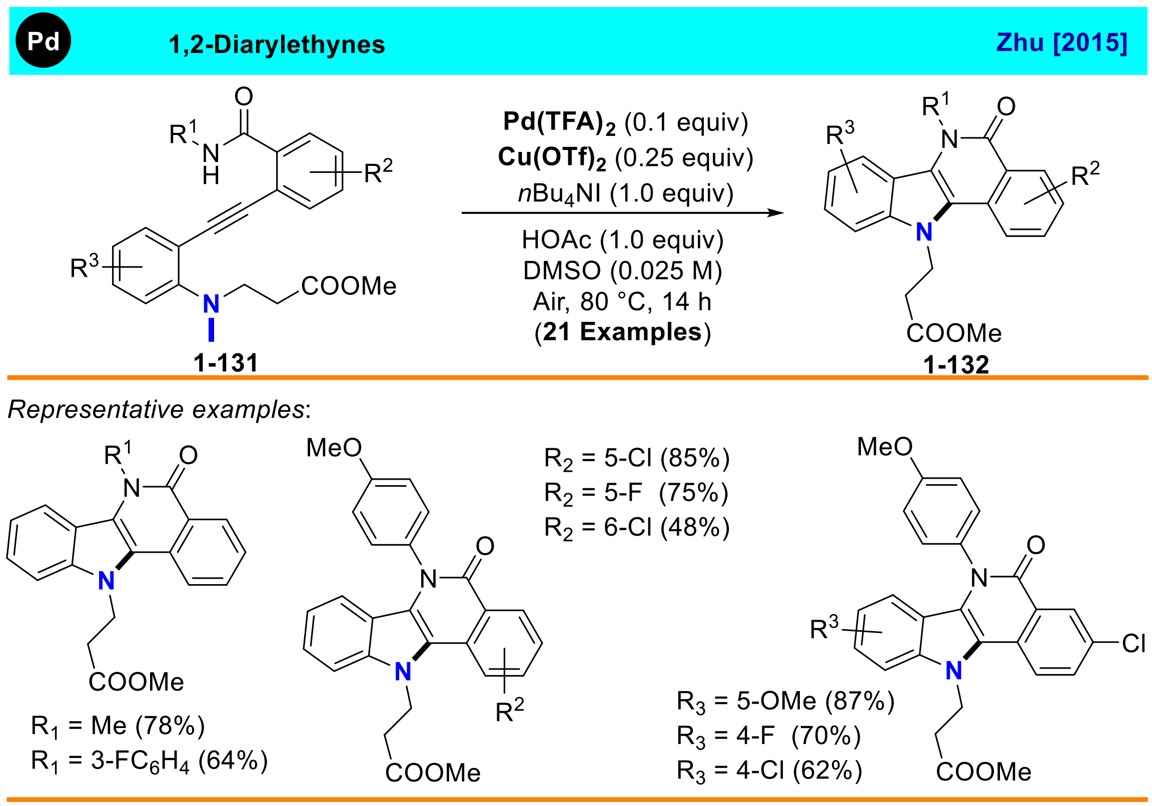

Scheme 1.47: Synthesis of Tetracycles by Oxidative Diamination of Alkynes

Synthetically useful ring expanded products were formed from transition metal catalyzed ring expansion of aziridines via oxidative addition of the C−N bond. In 2015, Zhang group reported a rhodium-catalyzed intramolecular formal hetero-[5 + 2] cycloaddition of vinyl alkyne aziridines **1-133** for the synthesis of fused azepine derivatives **1-134** (**Eq. 1.16**).[92] This novel catalytic method afforded the number of synthetically useful compounds with excellent functional-group compatibility up to >99% enantioselective products under relatively mild conditions.

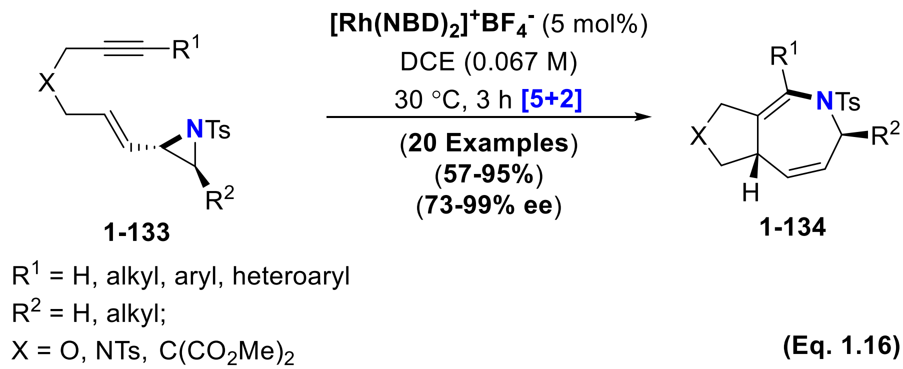

(Eq. 1.16)

1.9.1.2 C(sp^3)-N Bond Activation via Iminium Ion Species

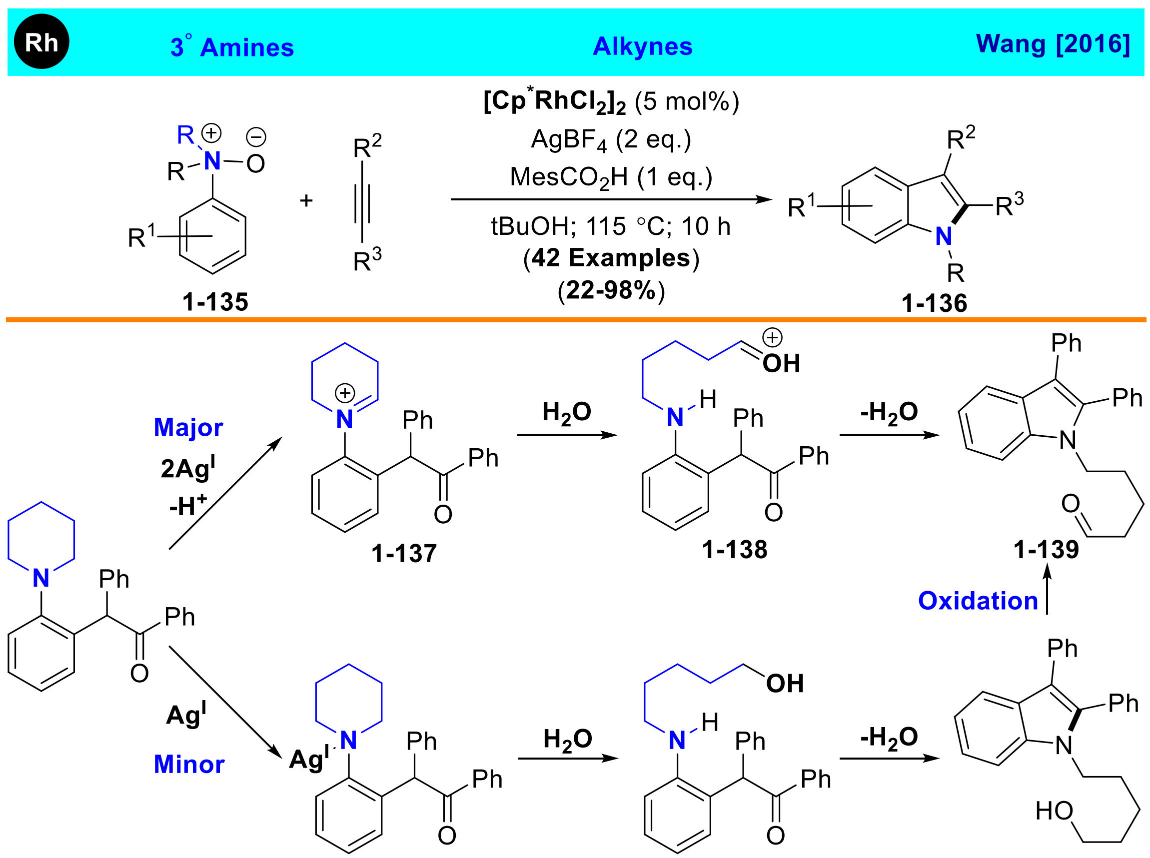

Scheme 1.48: Mechanistic Insights for C−N bond Cleavage Via Iminium Species

A number of transition metal catalyzed C−N bond cleavage via the formation of iminium ion species, have been demonstrated recently. In 2016, Wang and coworkers reported the oxidative coupling reaction of tertiary aniline N-oxides **1-135** with internal alkynes, to afford N-alkylindole derivatives **1-136**. More significantly, dealkylative cyclization reaction occurred via C−N bond cleavage through the iminium ion species (**Scheme 1.48**).[93] Iminium ion **1-137** was generated from single electron oxidation deprotonation, and another single electron oxidation by the use of silver as an oxidant, as indicated in the major pathway. Simple hydrolysis of **1-137** would generate an intermediate **1-138**, which then undergoes an intramolecular nucleophilic cyclization to afford indole derivatives **1-139**. This strategy has been successfully applied by Huang group in 2017 to synthesize α,β-unsaturated amides from alkynes with carbon monoxide and tertiary amines as amine source, catalyzed by palladium complex. They were able to develop the C−N bond cleavage of tertiary amines by using DTBP (di-tert-butyl peroxide) as an oxidant via formation of iminium ion intermediate, and the amine moiety was successfully incorporated to the enone products (**Scheme 1.49**).[94]

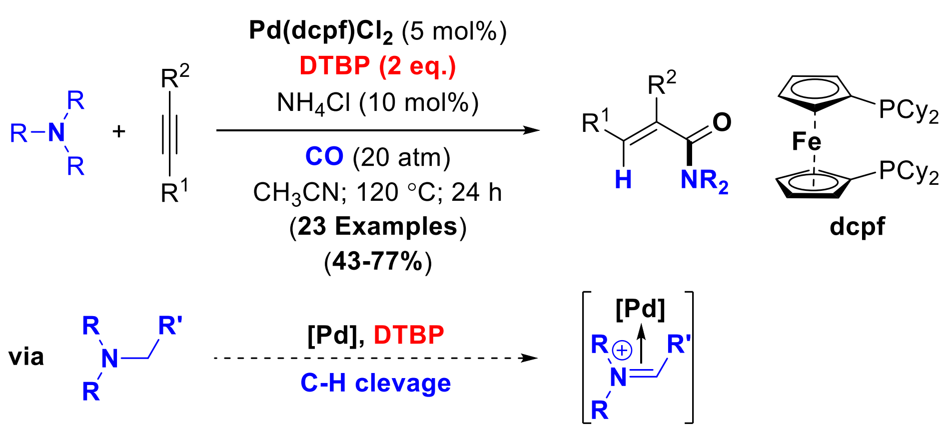

Scheme 1.49: Hydroaminocarbonylation of Alkynes with Amines

Similarly, catalytic C−N bond cleavage strategy was demonstrated by Song and coworkers by using tertiary amines to synthesize imidazo[1,2-a]pyrimidines **1-140**. Copper mediated oxidation of tertiary amines afforded the iminium species, which undergoes via two different pathways to render acetaldehyde as well as formaldehyde. In the presence of water iminium ion was hydrolyzed to yield a secondary amine and acetaldehyde products. On the other hand, deprotonation of tertiary amine would yield an enamine species, which would react with oxygen to render a dioxygencontaining four-membered heterocycle, to form corresponding formamide and formaldehyde. Acrolein **1-141** would be generated from the formaldehyde and acetaldehyde in-situ formed from the amine, which finally reacts with 2-aminobenzo[d]imidazoles to produce imidazo[1,2-a]pyrimidine derivatives **1-140** (**Scheme 1.50**).[95]

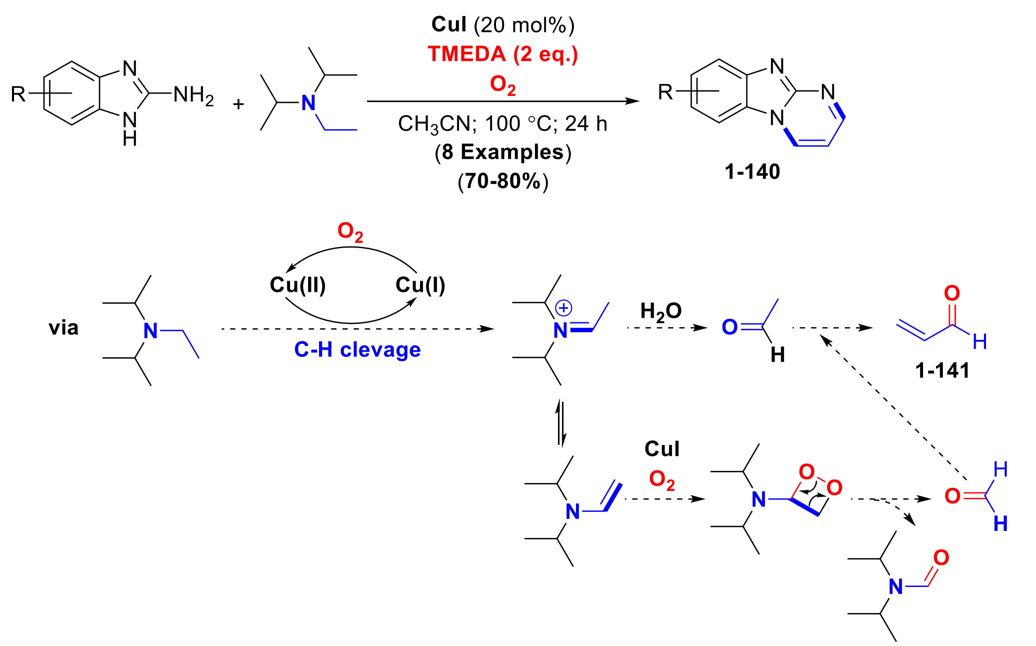

Scheme 1.50: Synthesis of Imidazo[1,2-A]Pyrimidines by In Situ Generated Acrolein via Iminium Ion Mediated C−N Bond Cleavage

In 2018, Chai group developed a method to form synthetically useful 2-(furan-3-yl)acetamides **1-143** following C−N bond cleavage on palladium via formation of iminium species by using cascade reactions of allenols **1-142** in the presence of tertiary amine.[96] Tertiary amine coordinates to the palladium alkyl species **1-144** by giving intermediate complex **1-145**. Subsequently, iminium ion coordinated intermediate species **1-146** is given through the elimination of HI from the C−H cleavage of **1-145**. The intermediate species **1-146** will be further transformed into a palladium amine species facilitated by the in situ formed water via C−N bond cleavage, with an elimination of acetaldehyde and hydrogen as byproducts (**Scheme 1.51**).

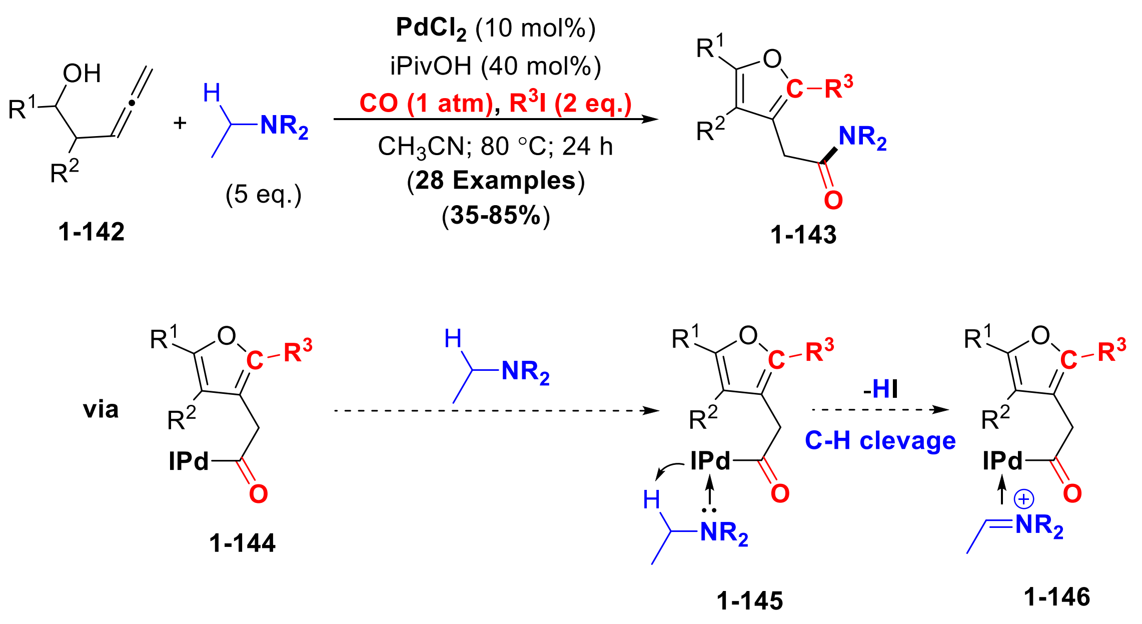

Scheme 1.51: Synthesis of 2-(Furan-3-yl)acetamides from Allenols

1.9.1.3 C(sp^3)-N Bond Activation via Ammonium Ion Species

An ammonium species considered as a good leaving group. Hence, converting the amine group to ammonium ions provides an effective way to cleavage of a C−N bond by a Lewis acid-assistance. Common strategy to activation of the Csp^3−N bond via ammonium ion species is the use of N-sulfonyl compounds, which are easily undergo C−N bond cleavage by yielding corresponding carbocations and primary sulfonamides as neutral byproducts with the aid of either a Lewis acid or a Brønsted acid conditions.[97] In 2019, Zeng and coworkers reported the substrate scope relevant to Buchwald−Hartwig amination reaction, utilizing quaternary ammonium salts via C−N bond cleavage pathway with a palladium t-BuXPhos catalytic system. Both N-aryl or N-arylmethyl heteroarenes were afforded in moderate to excellent yields via C−N bond cleavage (**Scheme 1.52**).[98]

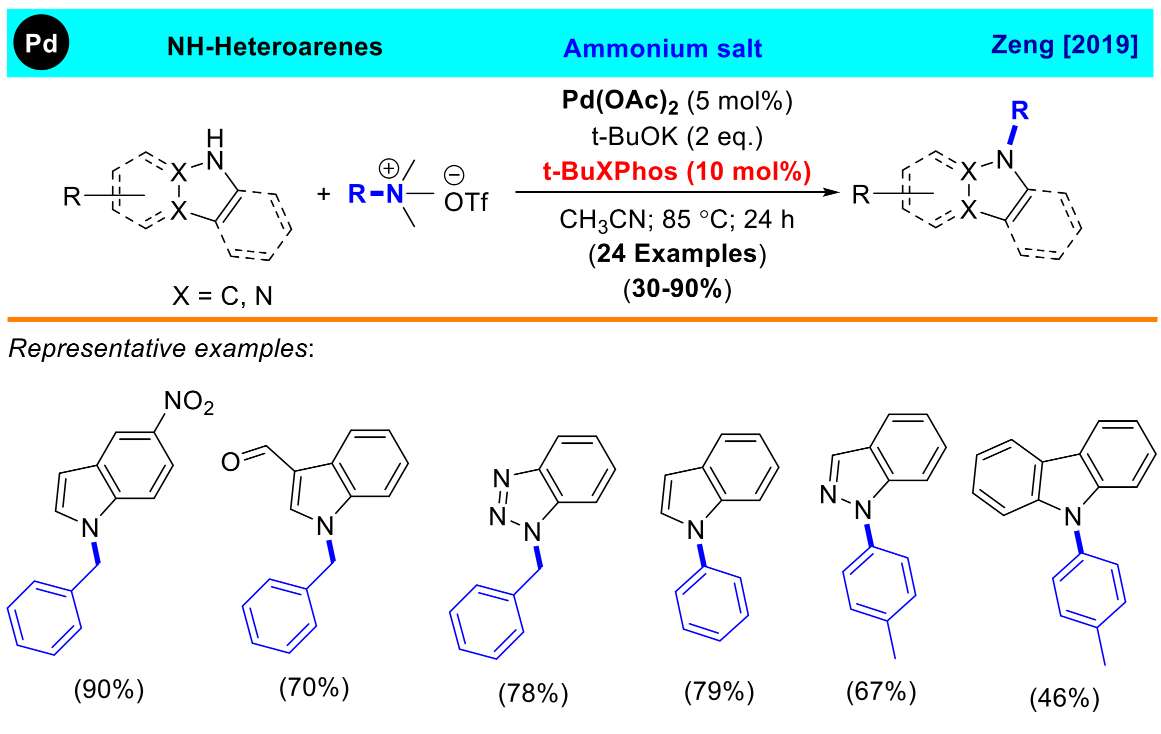

Scheme 1.52: Palladium-Catalyzed C−N Coupling of Quaternary Ammonium Salts with NH-Heteroarenes

Lu and coworkers in 2019 reported the use of 3-methyleneazetidines and diazo compounds to get 4-methyleneproline derivatives **1-149** via Rh-catalyzed [4 + 1] cycloaddition strategy with the ring expansion.[99] Mechanistic studies revealed the C−H insertion, O−H insertion[100], and olefin cyclopropanation, which are common transformations in Rh carbene chemistry, were diminished by predomination of [4+1] cycloaddition by indicating robustness of this method to generate 4-methyleneproline derivatives. Subsequently, number of tricyclic fused small to moderate N-heterocycles were synthesized by intramolecular reaction. Formation of rhodium carbene complexes are well established with the reaction of diazo compounds[101] **1-148**, which is being nucleophilic attack by the azetidine nitrogen **1-147** to form a ylide **1-150**. Subsequently, ylide **1-150** is transformed into desired product **1-149** via direct 1,2-migration or ring opening with zwitterionic species **1-151** followed by ring closure (**Scheme 1.53**).

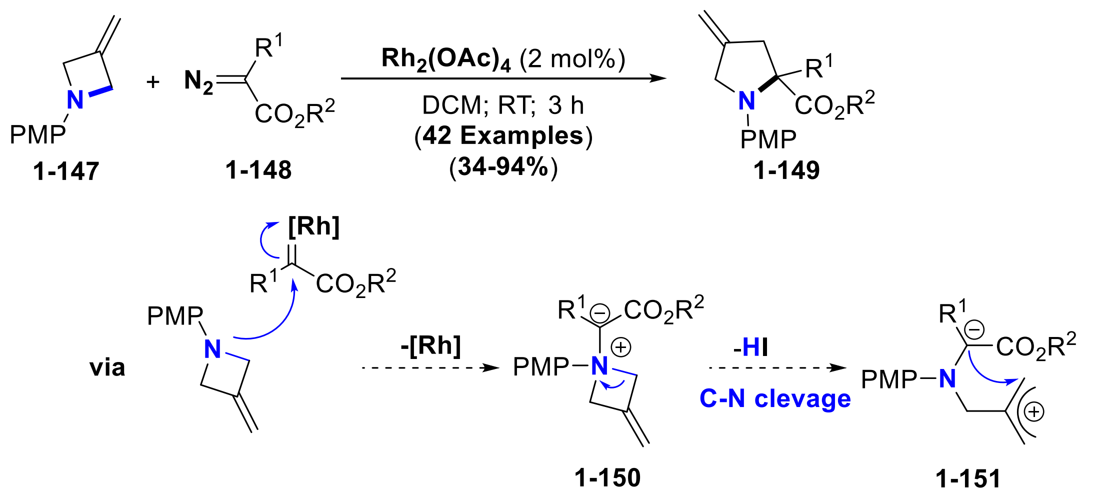

Scheme 1.53: Rhodium-Catalyzed Ring Expansion via C−N Activation and Coupling of In-Situ Generated Quaternary Ammonium Salts

1.9.2 Catalytic C-N Coupling Methods via Amide C(sp^2)-N Bond Activation

Amides are one of the most valuable functional groups as their presence in numerous molecules such as pharmaceutical agents, natural products, peptides etc. C–N coupling methods via amide C(sp^2)–N bond activation examples were reported in related with transamidation reactions; those involved the conversion of one amide to another. Development of the transamidation reaction, where cleavage of C(sp^2)–N bond of an amide is a long-standing challenge in synthetic chemistry, due to unfavorable kinetic and thermodynamic factors. Reported literature confirmed that the most effective way to activate amide C(sp^2)–N bond through oxidative addition to the transition metal ion.

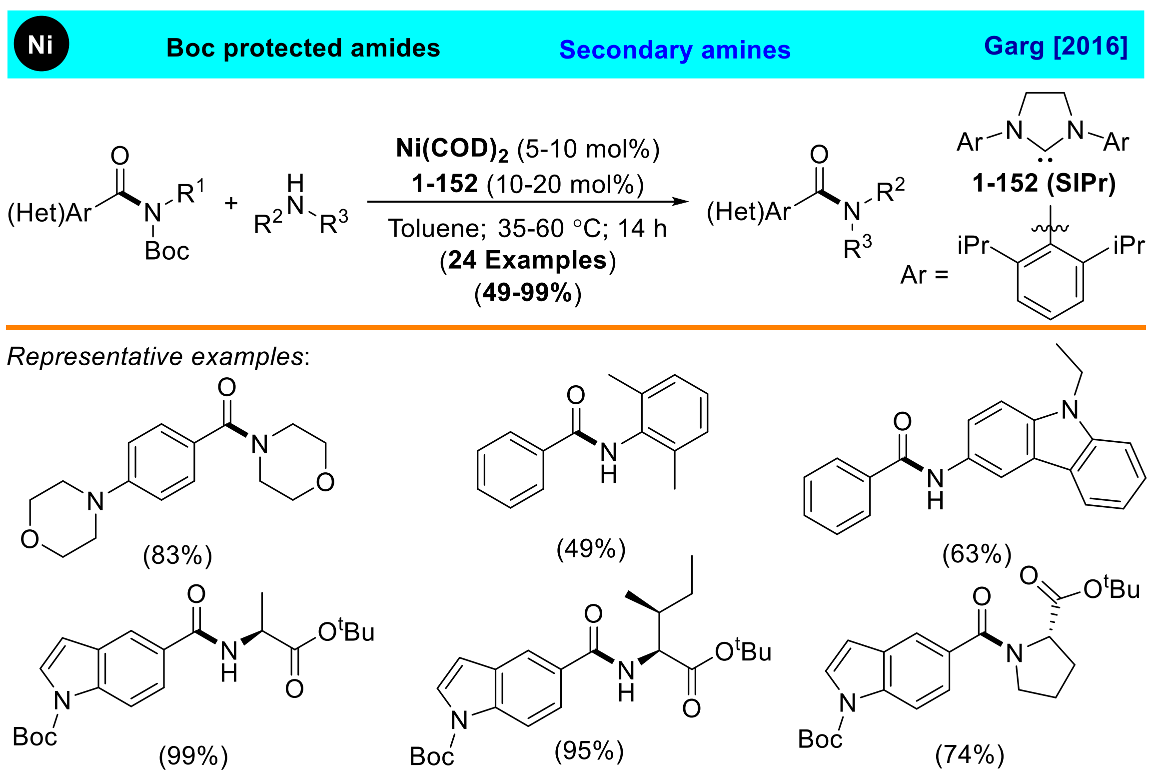

Scheme 1.54: Transamidation with Amine and Amino-acid Derivatives

In 2016, Garg and coworkers reported a two-step approach to effect the transamidation of secondary amides. Simple Boc-activation of the secondary amide followed by nickel-catalyzed oxidative addition of an acyl C–N bond afforded corresponding amides with excellent yields for number of amines including amino-acid derivatives (**Scheme 1.54**).[102] In 2017, Szostak group reported palladium NHC (NHC = N-heterocyclic carbene) catalyzed protocol for transamidation of secondary carboxamides. Wide range of N-Boc and N-Ts protected amides were effectively employed for the transamidation with commercially available, air- and moisture-stable (NHC)Pd(R-allyl)Cl complexes.[103] In 2018, Lee and coworkers reported nickel briphos ligand system catalyzed direct transamidation of secondary amides with amines. In this protocol secondary amides were directly used without preactivation by Boc protection, as TMSCl activates the amine derivatives by forming corresponding bis(trimethylsilyl)anilines.[104]

1.10 Summary and Conclusions

Recent studies on transition-metal-catalyzed C−N activation methods have been emerged as effective protocols for using readily available nitrogen containing compounds to construct synthetically important molecules. In this chapter we have reviewed new C−C and C−N bond formation reactions with special reference to mechanistic insights. Mechanistically interesting pathways have been discussed in detail which were supported by theoretical calculations. Some of the reactions discussed were achieved via atom-economical fashion which are expected to broad development by wide investigation in near future. We have reviewed number of recent amide C−N bond activation reactions including several new transformations, such as Suzuki−Miyaura, Negishi cross coupling reactions, esterification, and transamidation reactions. We have a great expectation that the area of C−N bond activation using nonprecious metals will continue to flourish and, in turn, will promote the growing use of simple primary amines and un-activated nitrogen containing molecules as synthons in organic synthesis.

Chapter 2

Efficient Synthesis of Secondary Amines from the Ruthenium-Catalyzed Deaminative Coupling Reaction of Amines

2.1 Introduction

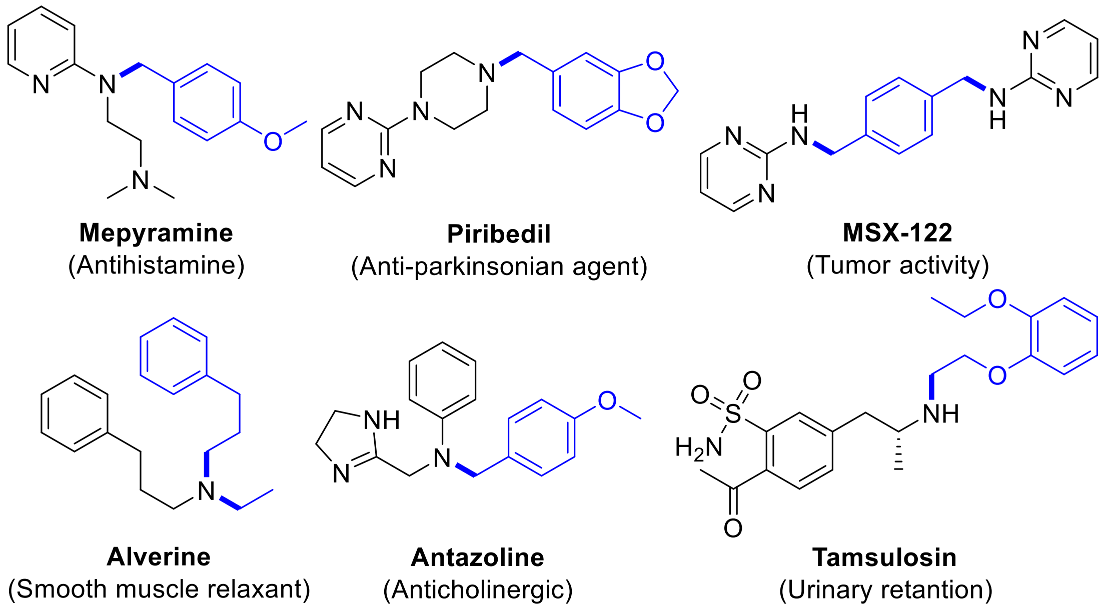

Figure 2.1: Selected Examples of Important Drug Molecules with Alkylated Amine Functionalities[105]

Selective carbon–nitrogen bond formation reactions represent a key step for the synthesis of a plethora of pharmaceutically active compounds, with the growing repertoire of biologically relevant nitrogen containing molecules.[106] Since amines are one of the prominent compounds present in pharmaceutical compounds, many synthetic methods have been developed over the years. Transition metal catalyzed C-N formation methods such as Buchwald–Hartwig[107], Ullmann reactions[108] and hydroaminations[109] have greatly advanced the synthetic versatility in forming nitrogen containing pharmaceutical agents.

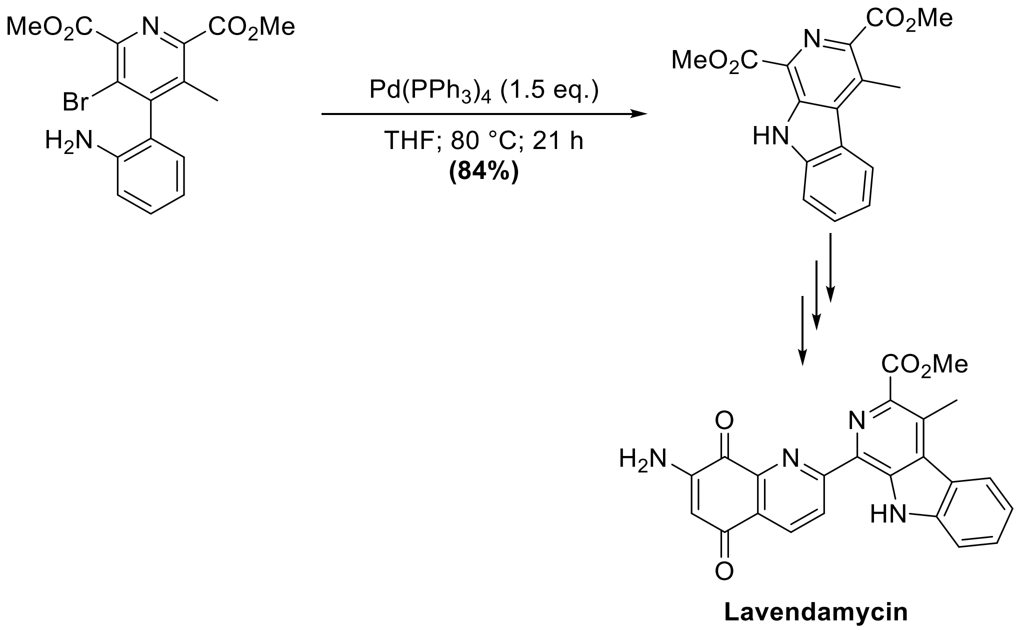

Scheme 2.1: Pd(0)-mediated Stochiometric Intramolecular Amination

In 1983, Migita and coworkers reported a palladium catalyzed C–N cross-coupling reaction of aryl bromides and N,N-diethylamino-tributyltin. They were able to demonstrate the limited reaction scope to only for few sterically unencumbered substrates.[110] Later in 1984, Boger and Panek employed Pd(0)-catalyzed C–N bond formation method for the synthesis of lavendamycin (**Scheme 2.1**)[111]. In 1994, Hartwig group reported a systematic study on Migita's work by using well-defined palladium compounds (**Scheme 2.2**).[112] In the same year, Buchwald group reported an extension of the Migita's work to obtain a variety of secondary amines by introducing transamination of Bu_3SnNEt_2. They were able to improve in both the product yields[113] as well as the substrate scope by using the Pd catalysts with bidentate phosphine ligands, diphenylphosphinobinapthyl (BINAP) and diphenylphosphinoferrocene (DPPF).[114] Due to chelation of diphosphine ligands, the Pd-catalyzed Buchwald–Hartwig amination has been shown to be highly effective for forming aryl C-N bond forming reactions.

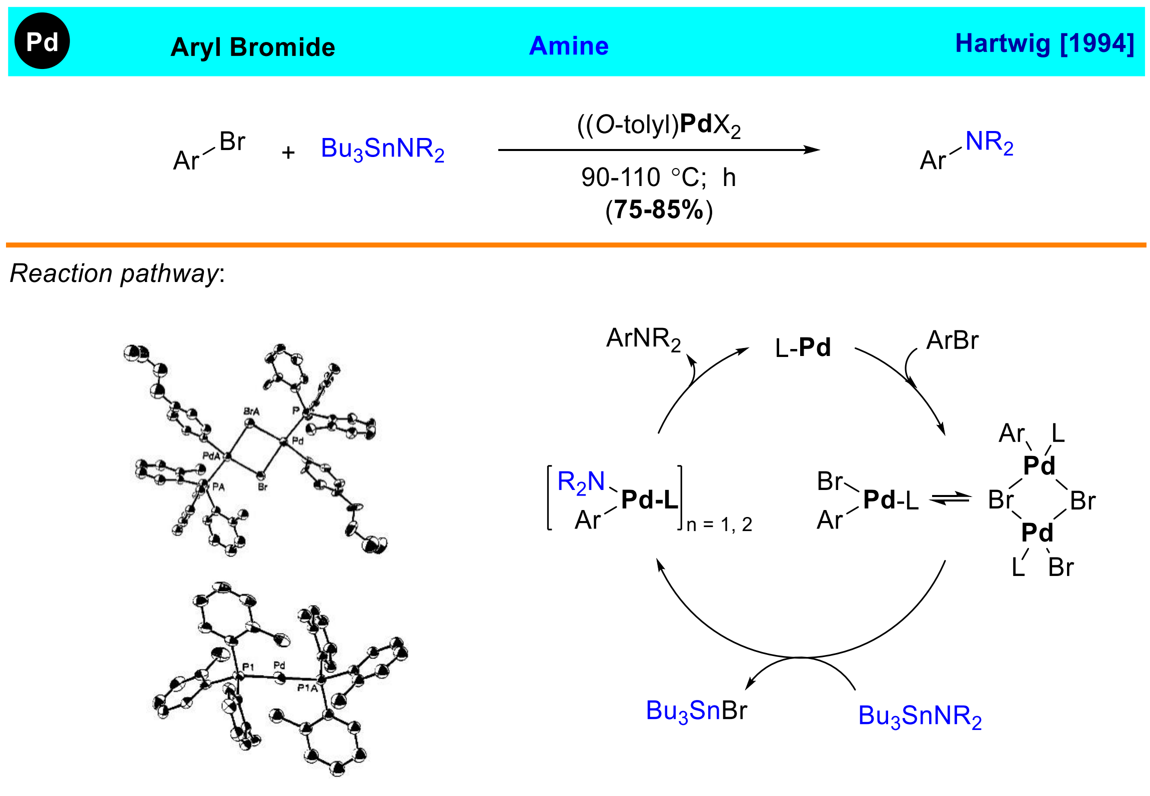

Scheme 2.2: Palladium Catalyzed Amination (Left: X-Ray Structures of Catalytically Relevant Palladium Intermediates; Right: Proposed Catalytic Cycle)

Ullmann and Goldberg initially discovered aromatic nucleophilic substitution reactions which required stoichiometric amounts of copper and high reaction temperatures. Subsequent improvements have led to the development into catalytic version of the coupling reaction. Eycken and co-workers in 2014 used copper-catalyzed intramolecular Ullmann coupling strategy to prepare 4H-benzo[f]imidazo[1,4]diazepin-6-ones (**Eq. 2.1**).[115]

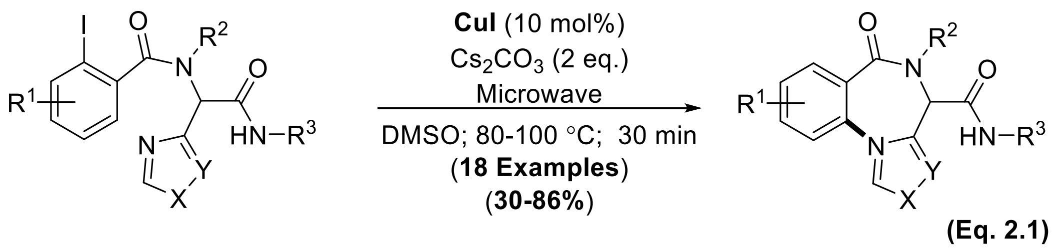

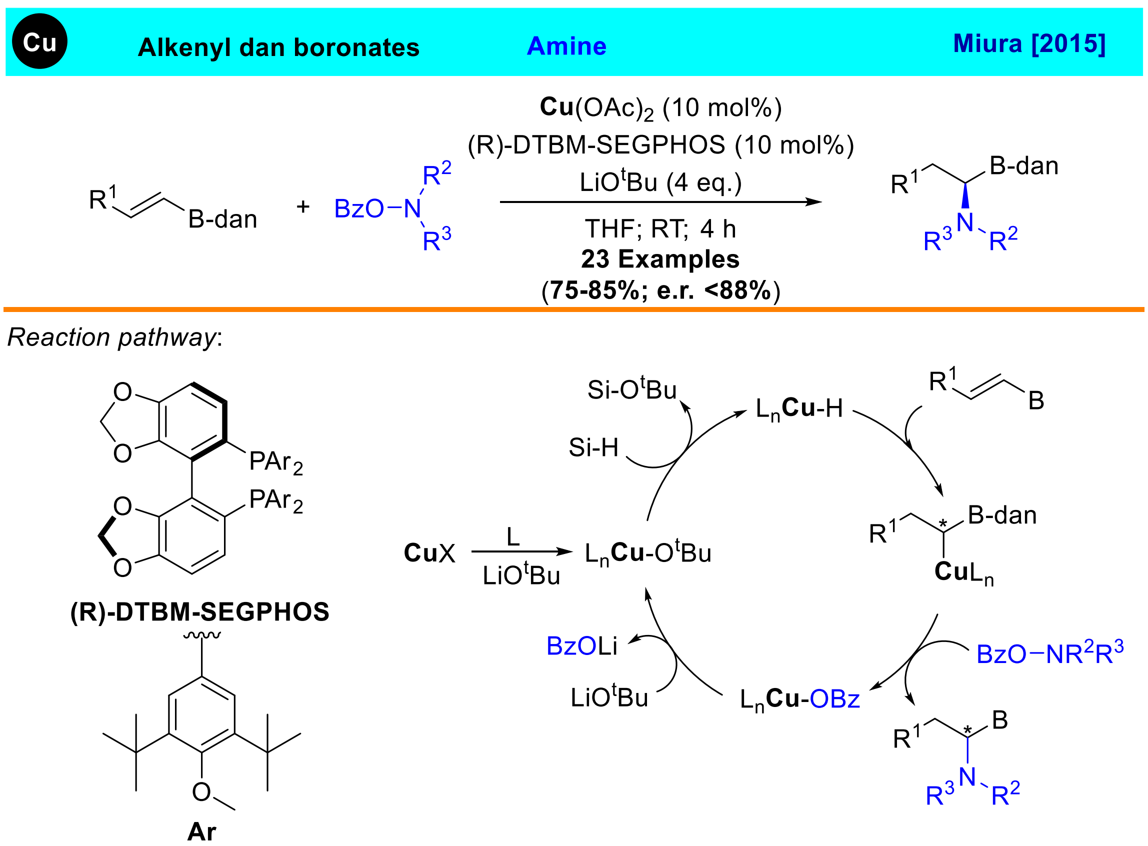

Scheme 2.3: Copper Catalyzed Enantioselective Hydroamination

Hydroamination reaction, an addition of N-H bond of amine or ammonia across a C−C multiple bonds, is an atom economical method to generate alkylamines. Amine nucleophilicity would be markedly reduced in the presence of electron-withdrawing substituents.[116] In 2015, Miura and co-workers reported a Cu-catalyzed asymmetric hydroamination of alkenyl boronates with hydrosilanes and hydroxylamines to synthesize optically active α-aminoboronic esters. The umpolung electrophilic amination strategy enables the construction of chiral centers with α-unactivated alkyl side chains (**Scheme 2.4**).[117] These procedures require specific metal complexes and often suffer from the co-production of considerable amounts of wasteful byproducts.

Borrowing hydrogen and hydrogen auto-transfer methodologies have been developed to overcome the drawbacks associated with these C-N bond formation methods. Borrowing hydrogen technique is well suited for catalytic reactions involving temporary transfer of protons and hydrides from the substrates. The strategy has been used for a variety of catalytic process, in which hydrogen-rich substrates are transformed into C−C bond forming reactions and products (**Scheme 2.5**).

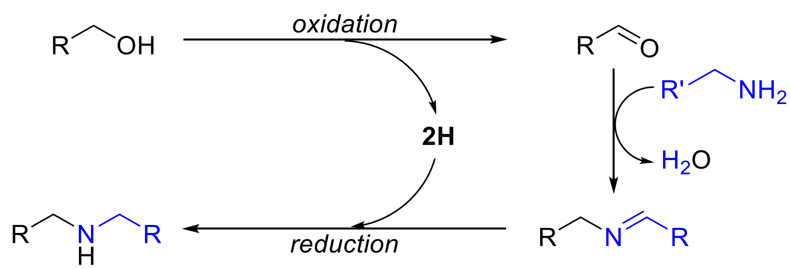

Scheme 2.4: Schematic Representation of the Borrowing Hydrogen Technique for the Alkylation of Amines by Primary Alcohols

Transition-metal-catalyzed dehydrogenative coupling methods have been shown to be highly effective way to utilize borrowing hydrogen strategy to activate amines and alcohols.[118] In particular, several late-transition-metal catalysts have been successfully employed to promote amine-alcohol coupling reactions via a borrowing hydrogen technique to synthesize secondary amines.[106, 119] The reaction sequence starts with the dehydrogenation of alcohol to the corresponding aldehyde via an iron complex **2-1**. One 'hydrogen equivalent' is temporarily stored at the bifunctional catalyst **2-2**, converted to the intermediate complex **2-3**, and the carbonyl intermediate reacts with amine to form an imine intermediate and water. The 'borrowed' hydrogen equivalent from alcohol is used for the reduction of the imine intermediate to afford the desired products (**Scheme 2.5**).

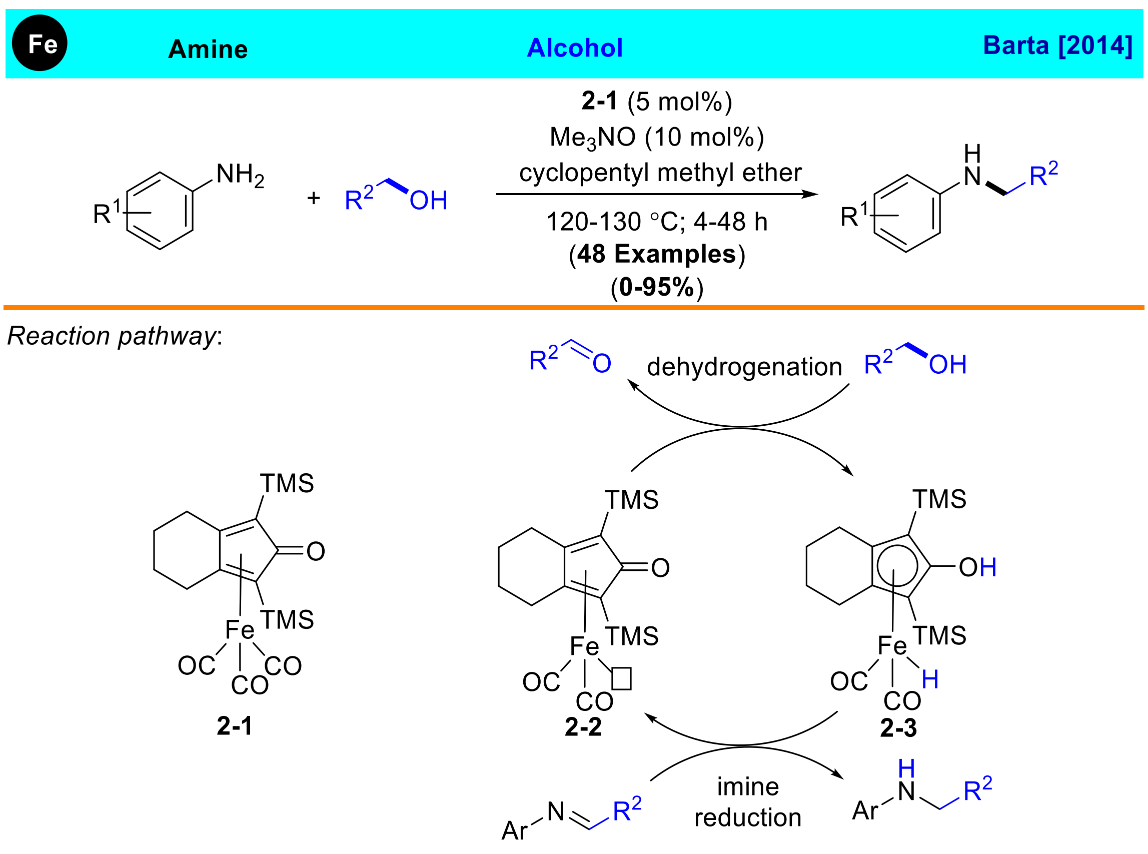

Scheme 2.5: Iron Catalyzed Selective Monoalkylation of Functionalized Anilines with Alcohols[119a]

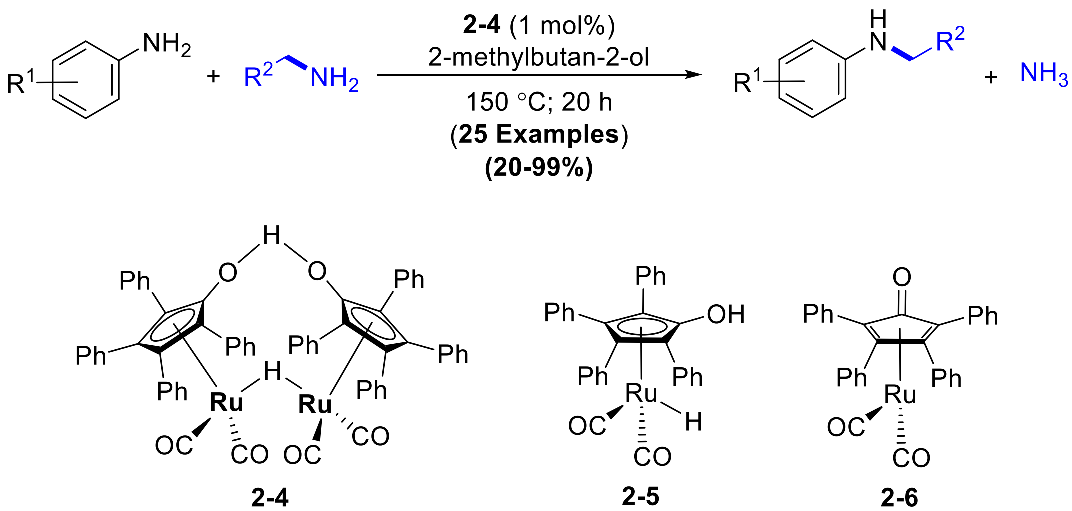

(Eq. 2.2)

Traditionally, the synthesis of secondary amines were commonly achieved by using the reductive amination methods.[120] Most of these traditional methods suffer from the formation of copious amounts of salt byproducts and require stoichiometric reducing agents and/or additives. Catalytic deaminative coupling methods have been emerged as an alternative protocol for the synthesis of secondary amines. In 2007, Beller group[121] used Shvo catalyst[121a] **2-4** for selective dealkylation reaction of amines. A variety of aliphatic amines with anilines react smoothly to give the corresponding aryl amines in excellent yields. The authors proposed that the reaction proceeds under transfer hydrogenation conditions via the formation of the active catalytic species **2-5** and **2-6**.[121a] (**Eq. 2.2**). The coupling reaction of aniline with primary amines by using soluble Co catalysts have been achieved for the synthesis of unsymmetric secondary amines.[122] More recently, a palladium-absorbed titanium dioxide (Pd/TiO_2) photocatalytic system has been used for the synthesis of symmetric secondary amines from the coupling of primary amines (**Eq. 2.3**).[123]

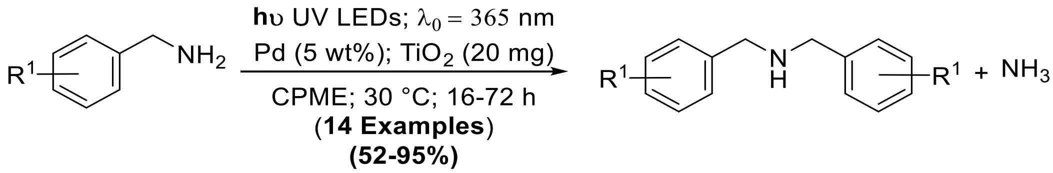

(Eq. 2.3)

Very recently, Peng and co-workers reported a CdSe/CdS core/shell quantum dots (QDs) system for visible light induced transfer hydrogenation reactions of imines to amines.[124] From both economic and environmental perspectives, the development of chemo-selective catalytic coupling methods via C−N bond cleavage of amines and related nitrogen compounds remains an important goal in the fields of homogeneous catalysis and organic synthesis.

2.2 Results and Discussion

2.2.1 Synthesis of Cationic Ruthenium Hydride Complex 2-10

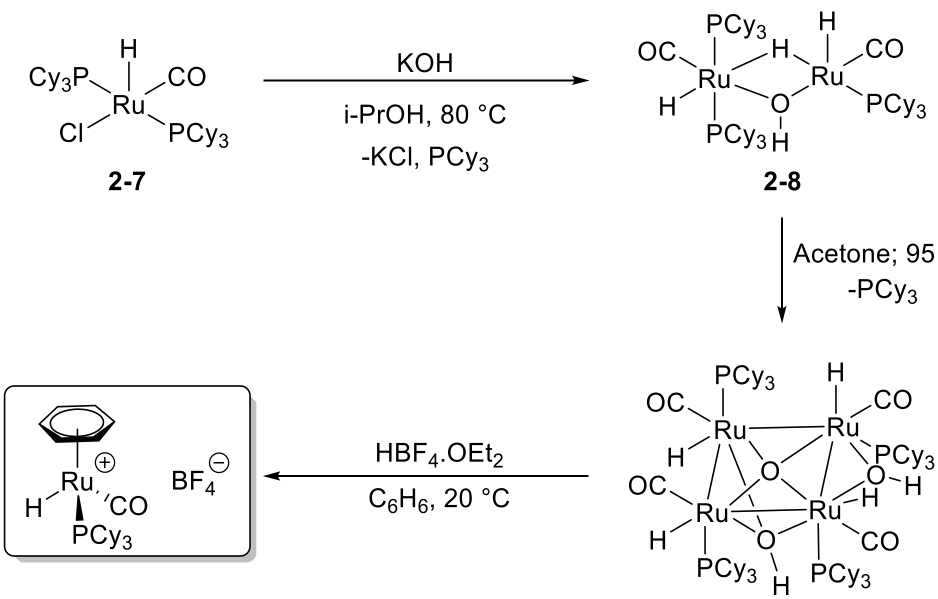

Scheme 2.6: Synthesis of Cationic Ruthenium Hydride Complex **2-10**

Recently, our research group developed a convenient method for the synthesis for a well-defined cationic ruthenium-hydride complex $[(\eta^6\text{-}C_6H_6)(PCy_3)(CO)RuH]^+BF_4^-$ (**2-10**) from the protonation reaction of tetranuclear ruthenium complex $\{[(PCy_3)(CO)RuH]_4(\mu\text{-}O)(\mu\text{-}OH)_2\}$ **2-9** with $HBF_4.OEt_2$. The cationic ruthenium hydride complex **2-10** was obtained by two step synthetic procedures from the dimeric ruthenium hydride complex $(PCy_3)_2(CO)RuHCl$ **2-7**.[125] Base hydrolysis reaction of **2-7** with potassium hydroxide in isopropyl alcohol produced the bimetallic ruthenium complex **2-8** in >90% yield. The complex **2-8** was purified by either recrystallization techniques (85%) or chromatographic method (90%). The subsequent treatment of **2-8**

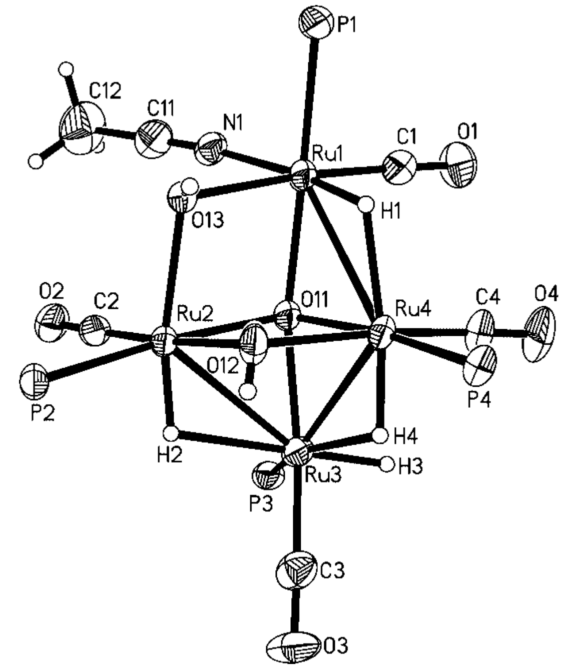

Figure 2.2: X-ray Crystal Structure Of **2-9** Drawn With 50% Thermal Ellipsoids. Cyclohexyl Groups Are Omitted For Clarity.

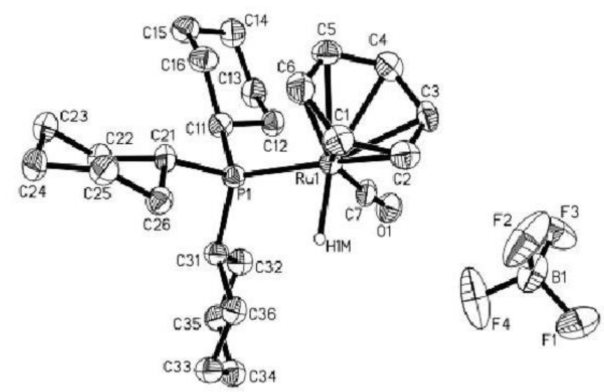

Figure 2.3: X-Ray Crystal Structure of Cationic Ruthenium Hydride Complex **2-10**

with wet acetone at 95 ºC yielded the tetranuclear Ru complex **2-9** in 84 % yield as brown-red powder. Thus, the treatment of **2-9** (200 mg, 0.12 mmol) with $HBF_4.OEt_2$ (64 μL) in C_6H_6 at room temperature cleanly afforded the cationic ruthenium hydride complex **2-10**, which was isolated in 90% yield as ivory-colored solid (**Scheme 2.9**). The characterization of the ruthenium-hydride complex was performed by NMR spectroscopic and X-ray crystallographic techniques. The ruthenium hydride signal of **2-10** was observed at δ -10.39 (d, J_{PH} = 25.9 Hz) in CD_2Cl_2, and phosphine signal was observed at δ 72.9 ppm by $^{31}P\{^1H\}$ NMR spectroscopy. The molecular structure of the ruthenium hydride **2-10** showed a three-legged piano-stool geometry, which is capped by a η^6-benzene moiety.

2.2.2 Synthesis of [Ru(3-,5-(^{t}Bu)$_2$(1-,2-(O)$_2$)C_6H_2)(PCy_3)$_2$(CO)] 2-11 and [Ru($C_{14}H_8$(1-,2-(O)$_2$))(PCy_3)$_2$(CO)] 2-13 Complexes

The complex **2-10** (117 mg, 0.20 mmol), 3,5-di-*tert*-butyl-o-benzoquinone **2-12b** (44 mg, 0.20 mmol), PCy_3 (56 mg, 0.20 mmol) were dissolved in CH_2Cl_2 (3 mL) in a 25 mL Schlenk tube equipped with a Teflon screw cap stopcock and a magnetic stirring bar under N_2 stream. After stirring for 24 h in a water bath set at 70 °C, the solvent was removed under vacuum, and the residue was washed with 2% hexanes/EtOAc under nitrogen atmosphere (**Eq. 2.4**). The resulting residue was dissolved in acetone (3 mL), layered with n-pentane (4 mL), and stored in a glove box for five days for crystallization.

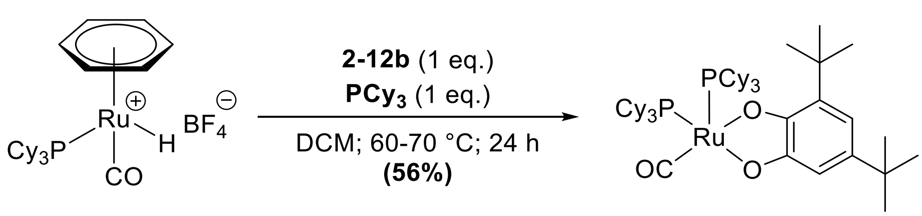

2-10 **2-11**

(Eq. 2.4)

The resulting solid was filtered through a fritted funnel to yield the complex **2-11** (102 mg, 56%) as a reddish crystalline solid. Single crystals of **2-11** were obtained by slow evaporation in EtOAc/pentanes, and its structure was determined by X-ray crystallography (**Figure 2.4**).

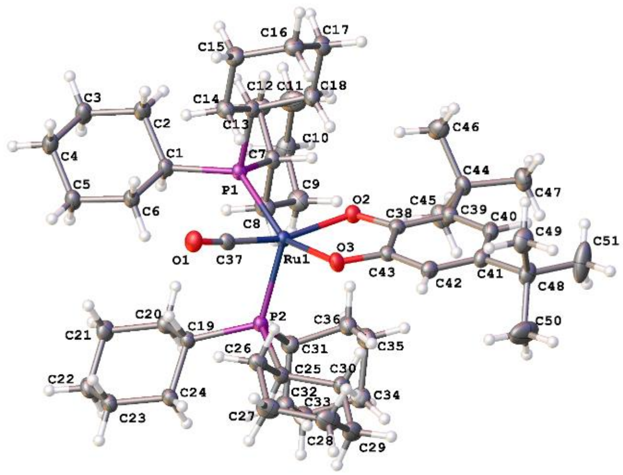

Figure 2.4: Molecular Structure of **2-11**

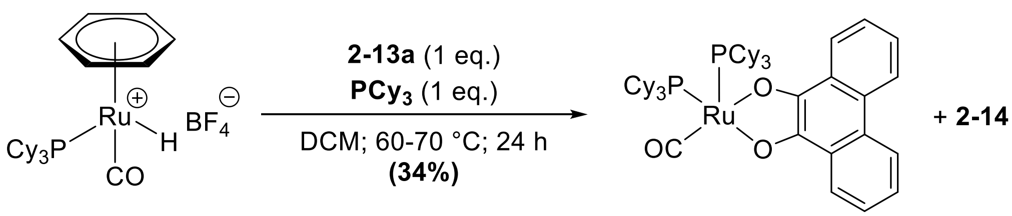

2-10 **2-13**

(Eq. 2.5)

Similar procedure was used to synthesize complex **2-13** from the reaction of **2-10** with 9,10-phenanthrenequinone **2-12a** as the ligand (**Eq. 2.5**). However, in this case, the ruthenium catecholate complex **2-13** was decomposed into the complex $[Ru(C_{14}H_8(1\text{-},2\text{-}(O)_2))(PCy_3)_2(CO)_2]$ **2-14**, which was completely identified by single X-ray crystallographic analysis (**Figure 2.5**). High resolution ESI/MS analysis indicated that the complex **2-13** was formed in the crude reaction mixture (34% yield) and the procedure described in section **6.2.4** afforded the complex **2-13** in 80% yield. High resolution ESI/MS data was used to characterize the complex **2-13**.

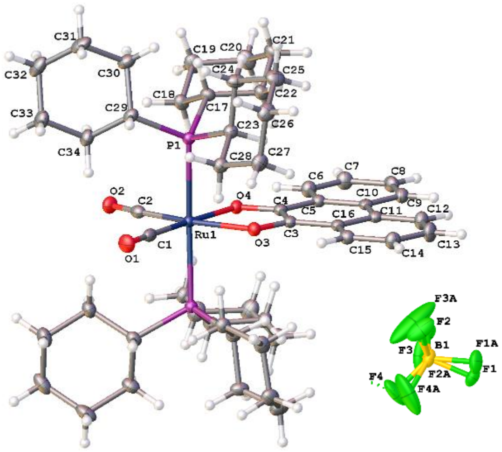

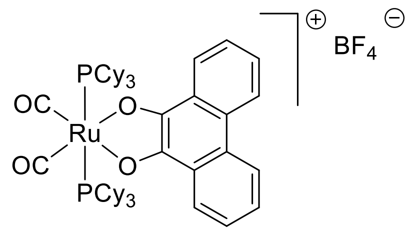

2-14

Figure 2.5: Molecular Structure of Side Product [Ru($C_{14}H_8$(1-,2-(O)$_2$))(PCy_3)$_2$(CO)$_2$] BF_4^- Complex **2-14**

2.2.3 Synthesis of [(PCy_3)$_2$(CO)RuH(OH_2)$_2$]BF_4^- Complex 2-15

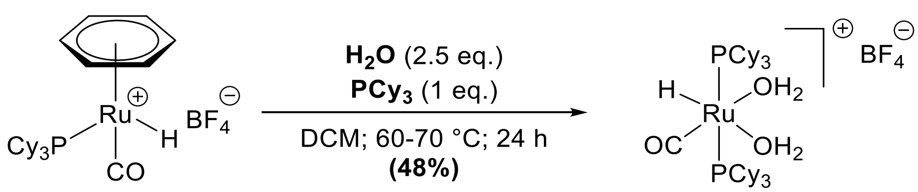

2-10 **2-15**

(Eq. 2.6)

Similar procedure as described in section **6.2.5** was used to synthesize the ruthenium hydride complex (**Eq. 2.6**). To our delight, the cationic ruthenium complex [(PCy_3)$_2$(CO)RuH(OH_2)$_2$]BF_4^- (**2-15**) was obtained in 48% yield. However, the water coordinated complex **2-15** did not show any activity for the C–N bond cleaved amine coupling reactions.

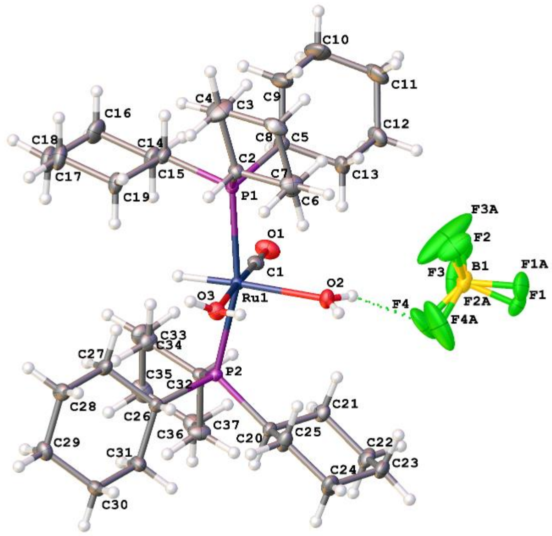

Figure 2.6: Molecular Structure of $[(PCy_3)_2(CO)RuH(OH_2)_2]BF_4^-$ Complex **2-15**

2.2.4. Synthesis of Symmetric and Unsymmetrical Secondary Amines via C–N Bond Activation

In an effort to develop novel catalytic coupling methods via C–N bond activation in which the liberation of ammonia is served as the driving force, we initially explored the promotional effect of the bidentate oxygen ligands for the ruthenium complex **2-9** by using the coupling reaction of primary amines.[126] The coupling reaction of benzylamine with cyclohexylamine in the presence of **2-9** and 4-(1,1-dimethylethyl)-1,2-benzenediol **2-16** afforded the selective formation of symmetric and unsymmetric secondary amines (**2-17**) via C–N bond cleavage (**Scheme 2.13**). From extensive screening efforts with the various oxygen and nitrogen containing ligands, the 1,2-catechol ligands were found to promote the one pot selective synthesis of symmetric secondary amines in nearly quantitative yields. Both symmetric **2-18** and unsymmetric **2-17** amines were selectively afforded from using the isolated ruthenium catecholate complex **2-11** in excellent yields (**Scheme 2.8** and **Table 2.2**).

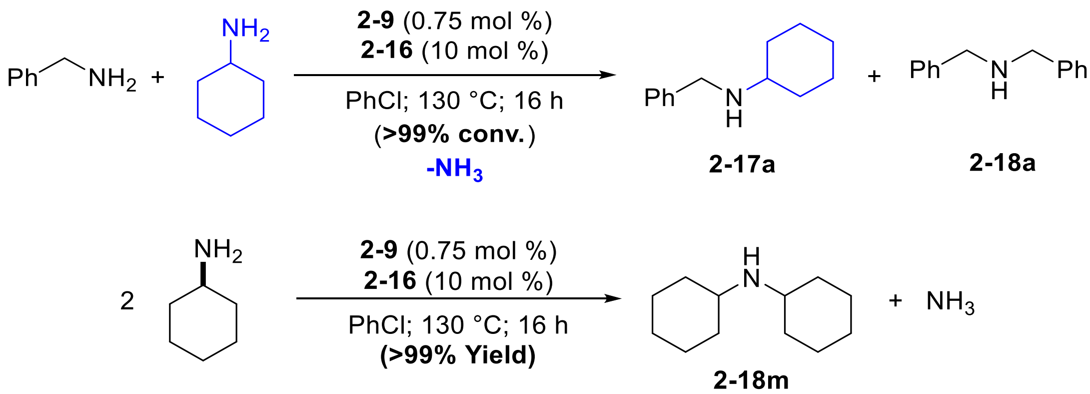

Scheme 2.7: Ru-Catechol Homogeneous System for the sp^3 C-N Bond Activation Strategy (99% conversion) with Primary Amines

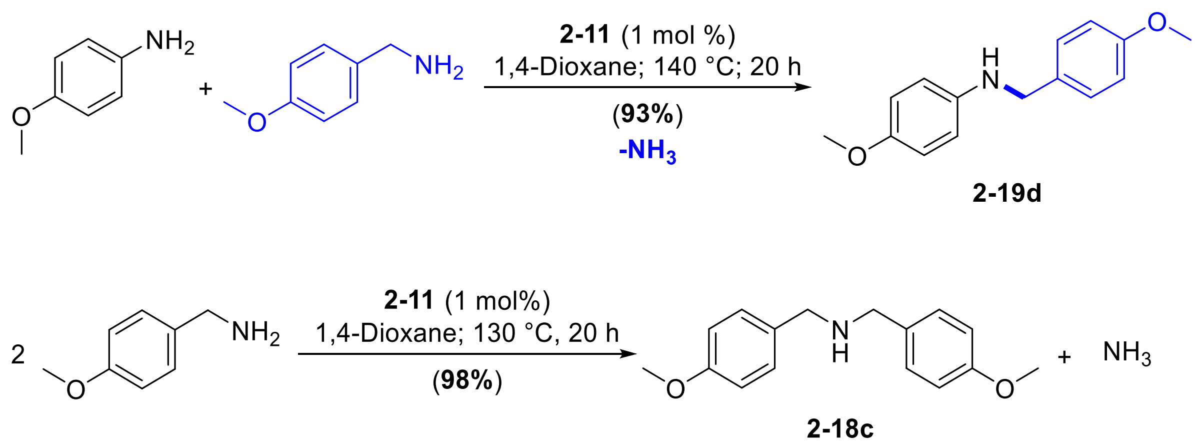

Scheme 2.8: Synthesis of Symmetric and Unsymmetric Secondary Amines from the Deaminative Coupling of Primary Amines via **2-11** as the Catalyst

2.2.5 Ligand Promoted Ruthenium Catalyzed Synthesis of Symmetric and Unsymmetrical Secondary Amines via C–N Bond Activation

2.2.6 Optimization Studies

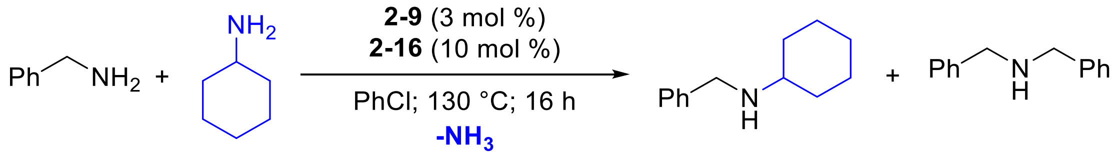

2-17a **2-18a**

(Eq. 2.7)

2.2.6.1 Catalyst and Solvent Screening

We initially screened soluble Ru catalysts with phenol and related oxygen and nitrogen ligands to promote the C−N bond activation reactions. We have chosen the coupling reaction of benzylamine with cyclohexylamine for screening of both ruthenium catalysts and the ligands (**Eq. 2.7**). Initially, both the tetranuclear Ru−H complex **2-9** and the cationic ruthenium complex **2-10** with a catechol ligand were found to exhibit the most promising activity for the coupling reaction among the screened Ru catalysts, as analyzed by both GC and NMR spectroscopic methods. To improve the yield and the selectivity for unsymmetric coupling products (**2-17**), a variety of parameters such as ligands, catalysts, solvents and the temperature were optimized, and the results are summarized in (**Table 2.1**).

Table 2.1: Catalyst and Solvent Screening for the Reaction of Benzylamine with Cyclohexylamine.[a]

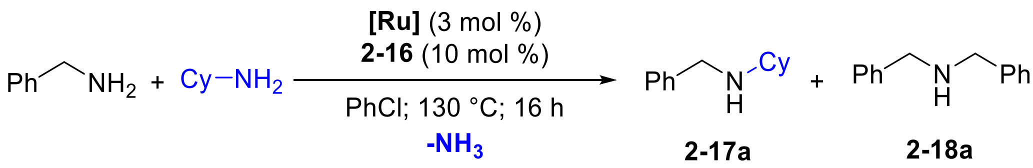

entry	catalyst	deviation from standard condition	yield (%)[b] **2-17a/2-18a**
1	$[RuH_2(CO)(PPh_3)_3]$		0
2	$RuHCl(p\text{-cymene})_2$		<1
3	$[RuCl_2(PPh_3)_3]$		5/3
4	$[RuCl_3{\cdot}3H_2O)]$	without **2-16**	<1
5	$[RuCl_3{\cdot}3H_2O)]$		0/31
6	$[Ru(COD)Cl_2]_x$		14/7
7	**2-7**		70/15
8	**2-10**	without **2-16**	<5
9	**2-10**		70/16
10	**2-9**		74/22
11	**2-9**	without 2-16/ $HBF_4{\cdot}OEt_2$	13/0
12	**2-9**	$HBF_4{\cdot}OEt_2$	65/1

[a]Reaction conditions: catalyst (3 mol % Ru), ligand (10 mol %), benzylamine (0.5 mmol), cyclohexylamine (0.7 mmol), chlorobenzene (2 mL), 130 °C, 16 h. [b]The product yield was determined by ^{1}H NMR using hexamethylbenzene as an internal standard.

We have chosen chlorobenzene as the solvent for the coupling reactions even though nonprotic polar solvents such as chlorobenzene and dioxane afforded the highest product yields and selectivity. The formation of the byproduct ammonia was detected in the crude mixture as analyzed by both NMR and GC−MS methods.

2.2.6.2 Ligand Screening

The 4-(1,1-dimethylethyl)-1,2-benzenediol ligand **2-16** was found to give the highest activity and selectivity in forming unsymmetric amine product **2-17a** over the symmetric product **2-18a** among the screened oxygen and nitrogen ligands as summarized in **Table 2.2**. A 3:1 ratio of catechol ligand to ruthenium catalyst was found to exhibit the optimum catalytic activity. Compared to other catechol ligands, **2-16** gave the best product yield under the reaction conditions (entry 6). Other catechol ligands such as **2-16a, 2-16b** and **2-16d** were found to be less effective (entries 7, 8 and 10). Interestingly, the electron-deficient catechol ligand **2-16c** gave better results (entry 9), and 2-hydroxybenzyl alcohol **2-21** was quite effective for the transformation (entry 11). Electron rich phenols and anilines gave lower reactivity and selectivity in forming the product **2-17a** (entry 12-14). In general, catechol ligands were found to be as effective as **2-17a** for this transformation.

The coupling reaction did not proceed at below 100 °C, while only a slightly improved product yield and the selectivity at an elevated temperature (entry 5, 15 and 16). To our delight, we recently found that the use of the benzoquinone ligand **2-12**, an oxidized analogue of catechol, significantly improved the yield of **2-17a** to 90% in 1,4-dioxane (entry 1). A higher coordinating ability of benzoquinone might be beneficial for promoting the catalytic activity of ruthenium catalyst. We also found that the isolated ruthenium catecholate complex **2-11** at a considerably lower catalyst loading (1 mol%) exhibited a substantially higher activity for the transformation (entry 4).

Table 2.2: Ligand Screening for the Reaction of Benzylamine with Cyclohexylamine.[a]

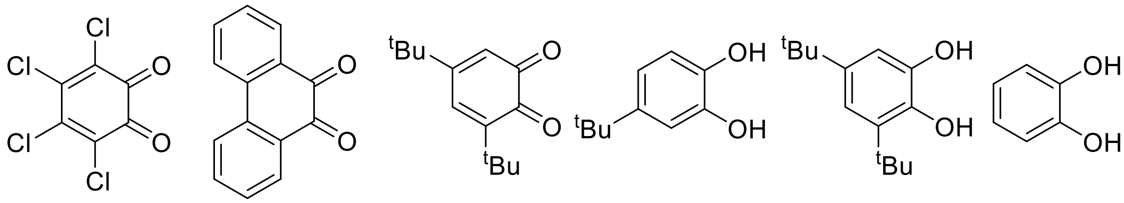

2-12 **2-12a** **2-12b** **2-16** **2-16a** **2-16b**

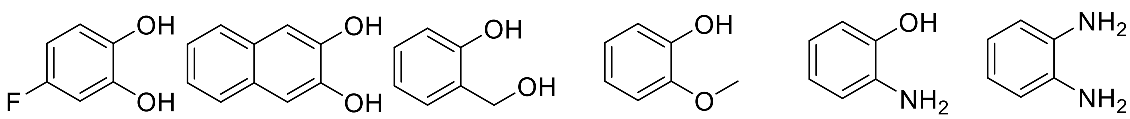

2-16c **2-16d** **2-21** **2-22** **2-23** **2-24**

entry	ligand	deviation from standard condition	yield (%)[d] **2-17a/2-18a**
1[b]	2-12		88/11
2[b]	2-12a		79/16
3[b]	2-12b		84/15
4[c]	-	Complex **2-11** (1 mol%)	90/9
5[c]	-	100 °C	<1
6	**2-16**		74/22
7	2-16a		67/6
8	2-16b		68/20
9	2-16c		80/15
10	2-16d		63/18
11	2-21		60/12
12	2-22		30/15
13	2-23		15/10
14	2-24		27/12
15	**2-16**	140 °C	76/23
16	**2-16**	100 °C	<1
17	-	without Ru-catalyst; NH_4PF_6	<1
18	-	without Ru-catalyst; BF_3	0
19	-	without Ru-catalyst; $HBF_4 \cdot OEt_2$	0
20	-	without Ru-catalyst	0

[a]Reaction conditions: catalyst **2-9** (3 mol % Ru), additive (7 mol %), benzylamine (0.5 mmol), cyclohexylamine (0.7 mmol), ligand (10 mol %), chlorobenzene (2 mL), 130 °C, 16 h. [b]Catalyst **2-10** in 1,4-dioxane (2 mL). [c]Ruthenium complex **2-11** (1 mol %) in 1,4-dioxane (2 mL). [d]The product yield of **2-17a** was determined by ^{1}H NMR using hexamethylbenzene as an internal standard.

2.2.7 Reaction Scope

After further ligand screening and optimization studies, we have established the standard reaction conditions at 1.0 mmol scale as: **2-9** (0.75 mol %, 3 Ru mol %)/**2-16** (10 mol %) in chlorobenzene (2 mL) at 130 °C. Although the initial results were obtained from the optimized catalyst system **2-9**/**2-16** under the standard conditions, we further tested selected substrates for the coupling reaction with ruthenium catecholate complex **2-11** in 1,4-dioxane. The optimized standard conditions were used for all these coupling reactions, unless otherwise noted as described in Tables **2.3**, **2.4** and **2.5** with slight modifications on the reaction time and temperature.

2.2.7.1 Synthesis of Unsymmetric Secondary Amines from the Deaminative Coupling

The substrate scope for the synthesis of unsymmetrical secondary amines from the deaminative coupling reaction of primary amines is summarized in **Table 2.3**. The coupling of benzylic amines with a variety of aliphatic and benzylic primary amines selectively formed the unsymmetric secondary amine products by affording moderate to good yields **2-17a−l**. An excess amount (1.4 eq.) of the second amine (usually more electron rich) was found to improve the product selectivity for the formation of unsymmetric amines **2-17**, and <20% of the symmetric amine products was formed in the crude mixture in most cases. Analytically pure unsymmetric amine products **2-17a−v** were readily isolated after column chromatographic separation technique by using silica gel and n-hexanes/EtOAc.

Table 2.3: Synthesis of Unsymmetric Secondary Amines from the Deaminative Coupling of Primary Amines

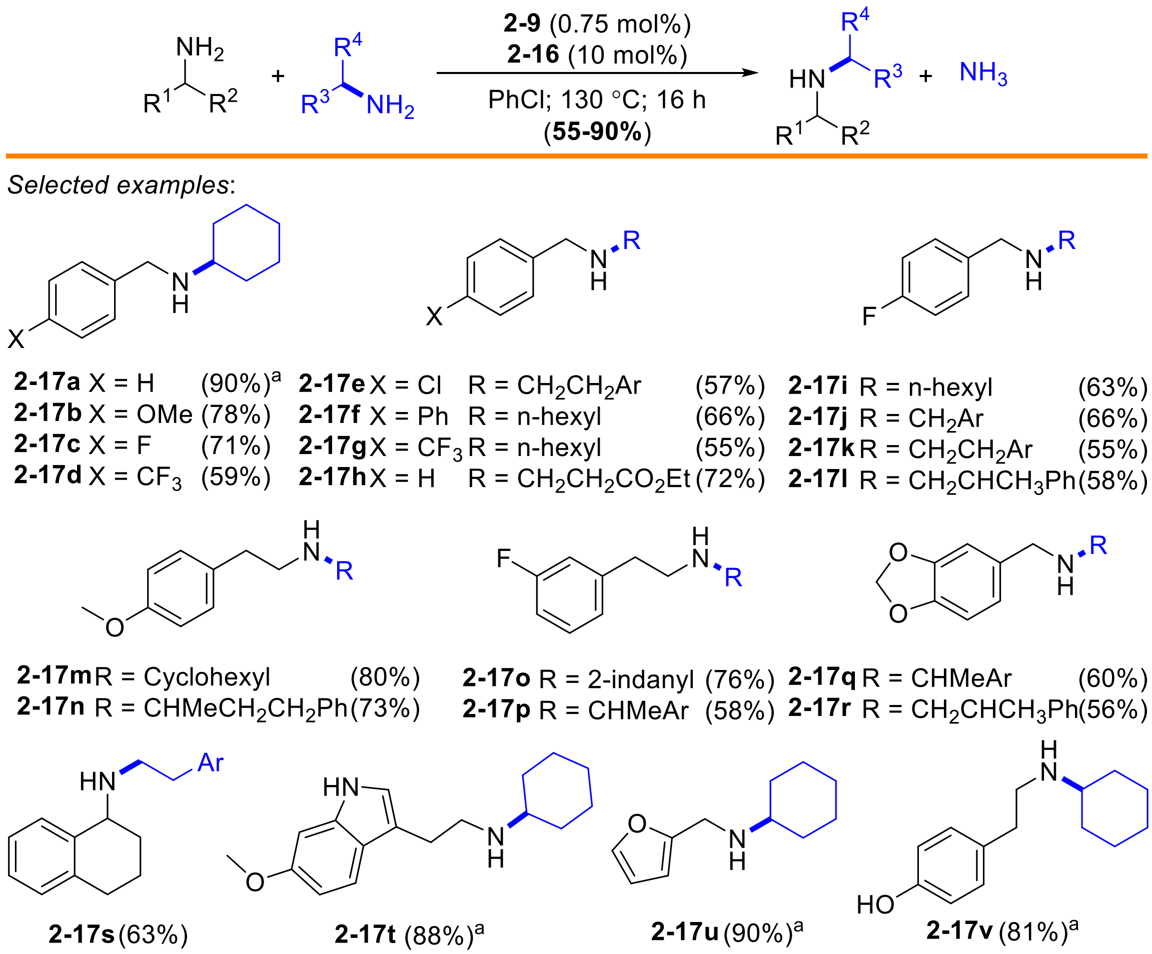

Reaction conditions: catalyst **2-9** (3 mol % Ru), amine (1 mmol), amine (1.4 mmol), ligand (10 mol %), chlorobenzene (2 mL), 130 °C, 16 h. [a]Ruthenium complex **2-11** (1 mol%) in 1,4-dioxane (2 mL) were used (^{1}H NMR yield using hexamethylbenzene as an internal standard); Ar = C_6H_4-4-OMe.

The coupling reaction with phenethyl amines was found to be more selective towards unsymmetric coupling reaction. The coupling of both electron rich and poor phenethyl amines with both benzylic and aliphatic amines also gave the selective formation of products **2-17m−p**. Piperonylamine and 1,2,3,4-tetrahydro-1-naphthylamine afforded the corresponding products in good yields **2-17q−s**. Under the standard reaction conditions' pharmaceutically important 5-methoxytryptamine, furfuryl amine and tyramine with cyclohexylamine selectively yielded the unsymmetric secondary amine products in 80%, 69% and 69% respectively **2-17t−v**.[126b] In sharp contrast, the reaction with 1 mol % of isolated ruthenium catecholate complex **2-11** gave enhanced product yields for the same set of substrates, 88%, 90% and 81%. For these cases, the coupling of benzylic and other aryl-substituted amines with electron-rich amines tends to favor the formation of unsymmetrical amines over the symmetrical amines. In contrast, the coupling of two different aliphatic amines with a sterically nondemanding group yielded a mixture of symmetric and unsymmetric amines. The coupling reaction with secondary and tertiary amines was found to be very sluggish and unselective, resulting in a complex mixture of products. The catalytic coupling method is operationally simple and exhibits high chemoselectivity toward the formation of unsymmetric secondary amines without resorting to employing any reactive reagents.

2.2.7.2 Synthesis of Symmetric Secondary Amines from the Deaminative Coupling

We next explored the substrate scope for the formation of symmetric secondary amines by using the catalyst system **2-9**/**2-16** (**Table 2.4**). Benzylic primary amines reacted smoothly to afford the secondary amine products **2-18a−g** without the formation of tertiary amines or other side products. The self-coupling reaction of 3-phenylpropylamine gave a more selective product formation of secondary amine **2-18k**, while having relatively lower amount of tertiary amine than standard condition.

Table 2.4: Synthesis of Symmetric Secondary Amines from the Deaminative Coupling of Primary Amines

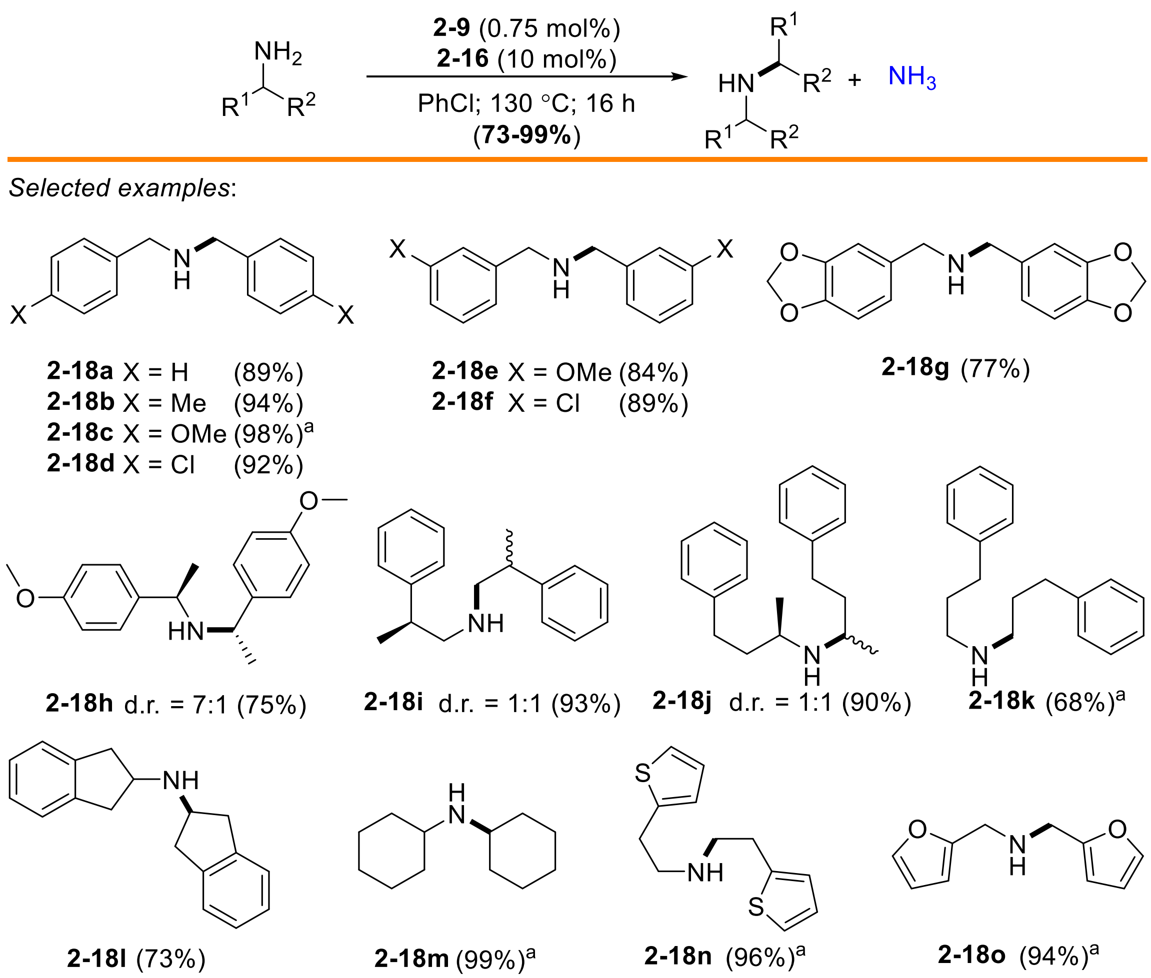

Reaction conditions: catalyst **2-9** (3 mol % Ru), amine (1 mmol), ligand (10 mol %), chlorobenzene (2 mL), 130 °C, 16 h. [a]Ruthenium complex **2-11** (1 mol%) in 1,4-dioxane (2 mL) were used (^{1}H NMR yield using hexamethylbenzene as an internal standard); Yields for isolated products.

The coupling of indanylamines formed the corresponding secondary amine products **2-18l**. Cyclohexyl, thiophene and furan substituted amines predictively yielded the corresponding secondary amine products **2-18m−o**. Generally, the coupling of chiral primary amines led to a 1:1 diastereomeric mixture of products as illustrated by the formation of **2-18i** and **2-18j**, but interestingly, a diastereoselective formation of the product **2-18h** was obtained in the case of (R)-4-methoxy-α-methylbenzenemethane amine (d.r. = 7:1). A mixture of secondary and tertiary amines (40-50% of tertiary amines) was formed for sterically nondemanding aliphatic amines such as n-hexylamine, while phenyl ethyl amines selectively formed the predicted products. Delightfully, isolated ruthenium catecholate complex **2-11** afforded the almost quantitate product formation without having tertiary amine byproduct for both **2-18c** and **2-18m−o** cases. The catalytic method delivers an operationally simple synthesis of symmetric secondary amines from readily available primary amines without using any reactive reagents via a deaminative coupling strategy.[120,122]

2.2.7.3 Synthesis of Unsymmetric Secondary Amines from the Deaminative Coupling of Anilines with Primary Amines

To further illustrate the synthetic versatility of the catalytic coupling method, we next explored the coupling reaction of aniline derivatives with primary amine substrates to synthesize drug candidates such as *Piribedil* and *Alverine*, as well as synthetically useful tridentate chelating agent *Di-(2-picolyl)amine*. The coupling of para-substituted anilines with benzylic amines led to the selective formation of unsymmetric amine products **2-19a−f** without any significant amount of the symmetric amine products. Similarly, the reaction of para-substituted anilines with 3,4,5-trimethoxybenzylamine afforded the coupling products **2-19g−i** in excellent yields.

Table 2.5: Synthesis of Unsymmetric Secondary Amines from the Deaminative Coupling of Anilines and Substrates of Biological Relevance with Amines

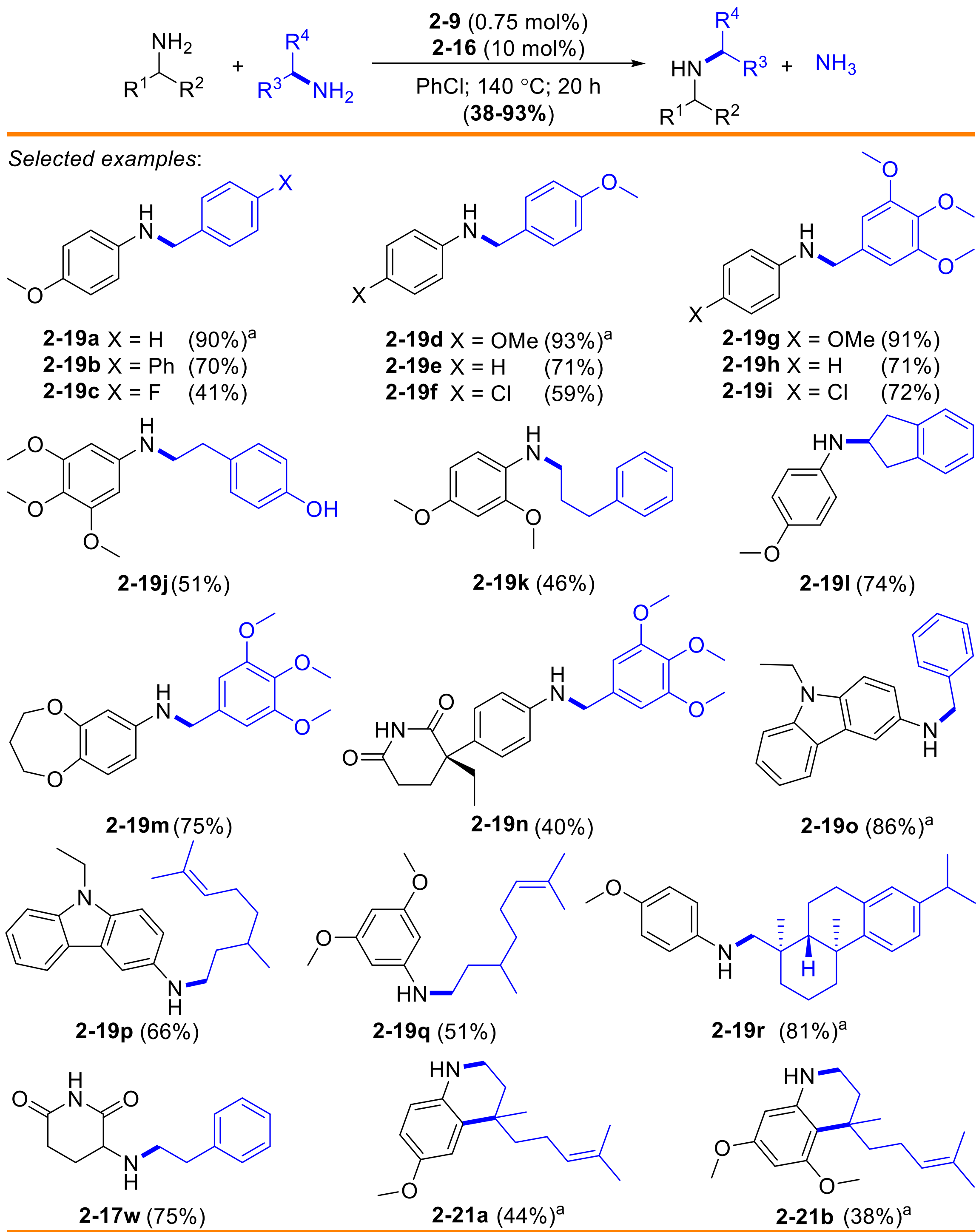

Reaction conditions: catalyst **2-9** (3 mol % Ru), amine 1 (1 mmol), amine 2 (1.4 mmol), ligand (10 mol %), chlorobenzene (2 mL), 140 °C, 20 h. [a]Ruthenium complex **2-11** (1 mol%) in 1,4-dioxane (2 mL) were used. [1]H NMR yield using hexamethylbenzene as an internal standard. isolated product yields.

The treatment of 3,4,5-trimethoxyaniline with tyramine yielded the product **2-15j** in 51% yield, and the reaction with ortho-substituted sterically demanding aniline compound with phenylpropylamine yielded the selective secondary amine product **2-15k** in 46% yield. The coupling reaction of 4-methoxyaniline with 2-aminoindane and 3,4-dihydro-2H-1,5-benzodioxepin-7-amine with 3,4,5-trimethoxybenzylamine yielded the corresponding coupling products **2-19l** and **2-19m** in 74% and 75% yields, respectively. The coupling of (R)-(+)-aminoglutathimide with 3,4,5-trimethoxybenzylamine led to the optically active coupling product (R)- **2-19n** without any detectable racemization.

Biologically relevant amines were formed in excellent yields when we used the isolated ruthenium catecholate complex **2-11** in 1,4-dioxane. The treatment of 3-amino-9-ethylcarbazole with benzylamine and geranylamine predictively yielded the product **2-19o–p** in 86% and 66% yield respectively. Also, the coupling reaction of 3,5-dimethoxyaniline with geranylamine afforded the corresponding dehydrogenated coupling product **2-19q** in 51% yield. The coupling reactions of 4-methoxyaniline with (+)-dehydroabietylamine also afforded the corresponding secondary amine product **2-19r** in 81% yield with >99% single diastereomer. The coupling reaction of L-glutamine with 3-phenylpropylamine led to the cyclized amine products **2-17w** in 75% yield. The formation of cyclized product **2-17w** can be rationalized by initial dehydrative cyclization of glutamine followed by the deaminative coupling with the primary amine substrate. The coupling reactions of electron donating aniline derivatives with geranylamine with the complex **2-11** gave the cyclized coupling product **2-21a-b** in 44% and 38% yields, indicating that the novel synthetic route to generate *1,2,3,4-tetrahydro-4,methylquinoline* derivatives. Di-(2-picolyl)amine **2-18p**, which is a chelating tridentate common ligand important in coordination chemistry were synthesized using **2-11** as the catalyst in 1,4-dixane by having 51% yield. Finally, the current protocol was extended to a one-pot synthesis of pharmaceutically useful drug candidates *Piribedil* and *Alverine*. *Piribedil* **2-20a** is an antiparkinsonian agent and piperazine derivative which acts as a D2 and D3 receptor agonist and known to have α-adrenergic antagonist properties.

Table 2.6: Synthesis of Drug Candidates and Synthetically useful ligands from the Deaminative Coupling of Amines

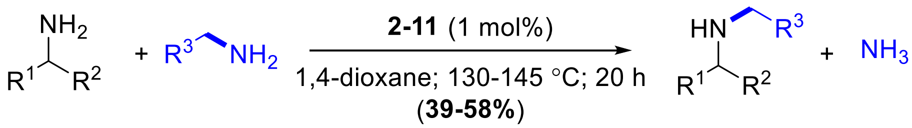

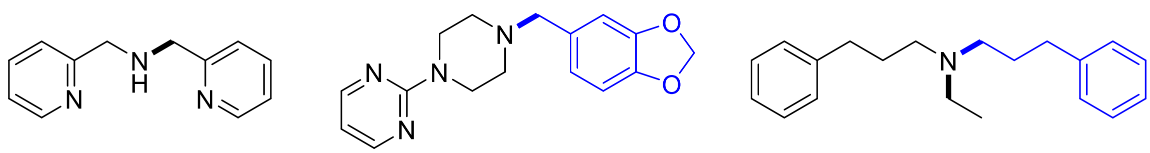

2-18p (51%)	**2-20a** (39%)	**2-20b** (58%)
Di-(2-picolyl)amine	**Piribedil**	**Alverine**
(Chealating Ligand)	(Anti-parkinsonian agent)	(Smooth muscle relaxant)

Reaction conditions: catalyst **2-11** (1 mol%), amine 1 (1 mmol) and/or amine 2 (1.4 mmol) in 1,4-dioxane (2 mL) were used. (^{1}H NMR yield using hexamethylbenzene as an internal standard).

The one-pot synthetic reaction of 1-(2-Pyrimidyl)piperazine with piperonylamine selectively formed the product *Piribedil* **2-20a** under ruthenium catalyst **2-11** in 1,4-diaxane as the solvent at 140 °C. *Alverine* **2-20b** is a drug used for irritable bowel syndrome, (functional gastrointestinal disorder), which is a known smooth muscle relaxant, was synthesized through sequential amine self-condensation of 3-phenylpropylamine, which yields the product **2-18k** followed by N-ethylation with ethyl amine under standard condition, affording product **2-20b** in 58% overall yield. The catalytic coupling method provides an environmentally benign, and operationally simple protocol to afford the symmetric and unsymmetric secondary amines in moderate to excellent yields without formation of wasteful byproducts.

2.2.8 Mechanistic Studies

2.2.8.1 Reaction Profile Study

The deaminative coupling reaction of 4-methoxybenzylamine was used to gain mechanistic insights. The self condensation of 4-methoxybenzylamine was monitored by NMR spectroscopy to probe the overall reaction profile. In a J-Young NMR tube equipped with Teflon stopcock, 4-methoxybenzylamine (34 mg, 0.25 mmol) and the catalyst system **2-9** (3 mg, 0.75 mol %)/**2-16** (4 mg, 10 mol %) were dissolved in toluene-d_8 (0.5 mL). The tube was immersed in an oil bath at 130 °C, and the reaction progress was monitored by ^{1}H NMR in 20 min intervals. As shown in **Figure 2.7**, the secondary amine product **2-18c** was formed steadily at the expense of the benzylamine substrate. Initially, the formation of a minor product was also observed (∼10%), which gradually disappeared within 200 min of the reaction time. The structure of minor product was subsequently determined to be imine *p*-OMe-$C_6H_4CH{=}NCH_2C_6H_4$(*p*-OMe) **2-22** by both NMR and GC/MS, which was obtained from a separate preparatory-scale experiment.

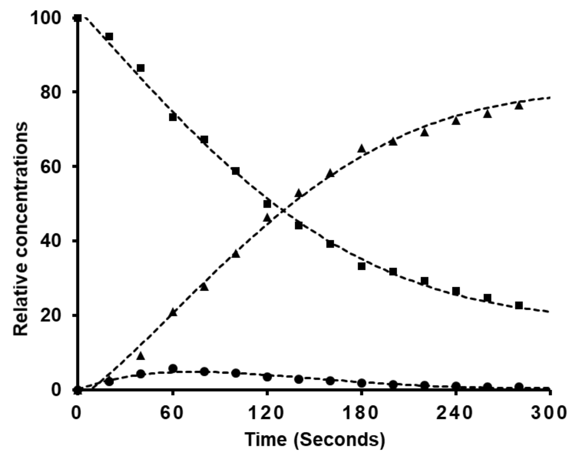

Figure 2.7: Reaction profile for the coupling of 4-methoxybenzylamine: 4-methoxy-benzylamine (■), (▲) **2-14c** and *p*-OMe-$C_6H_4CH{=}NCH_2C_6H_4$(*p*-OMe) **2-22** (●)

2.2.8.2 Deuterium Labeling Study

Deuterium-labeling pattern on the product from the reaction of aniline-d_7 with 4-methoxybenzylamine was also investigated. A reaction tube consisting of aniline-d_7 (50 mg, 0.5 mmol) with 4-methoxybenzylamine (69 mg, 0.5 mmol) in the presence of **2-9** (7 mg, 0.75 mol %)/**2-16** (8 mg, 10 mol %) in chlorobenzene (1 mL) was heated in an oil bath at 140 °C for 20 h. The product ***2-19e-d*** was isolated by silica gel column chromatography, and its deuterium content was analyzed by ^{1}H and ^{2}H NMR (**Eq. 2.8**). A significant amount of deuterium was incorporated into the methylene position of **2-19e**-*d* (18% D) without any deuterium exchange on the arene ortho C−H positions.

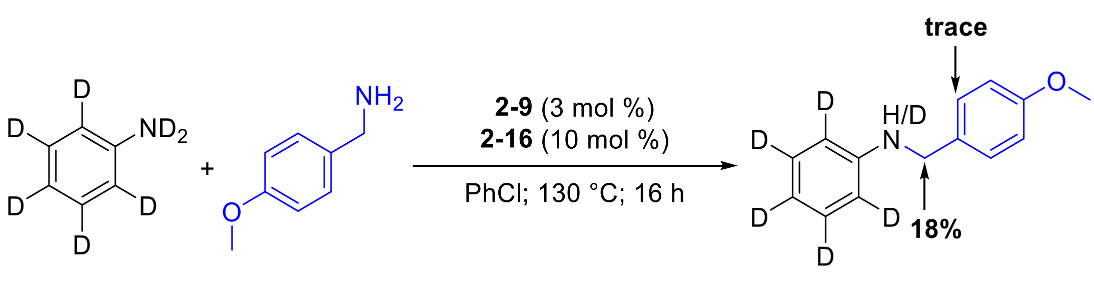

2-19e-*d*

(Eq. 2.8)

In a control experiment, the treatment of the isolated product **2-19e** with aniline-d_7 in the presence of **2-9** (0.75 mol %)/**2-16** (10 mol %) did not lead to any significant deuterium exchange into the benzyl position of **2-19e** under similar reaction conditions after 20 h. A significant amount of the deuterium incorporation suggests that a facile and reversible imine-to-amine hydrogenation-dehydrogenation process might have occurred during the product formation of **2-19e**.

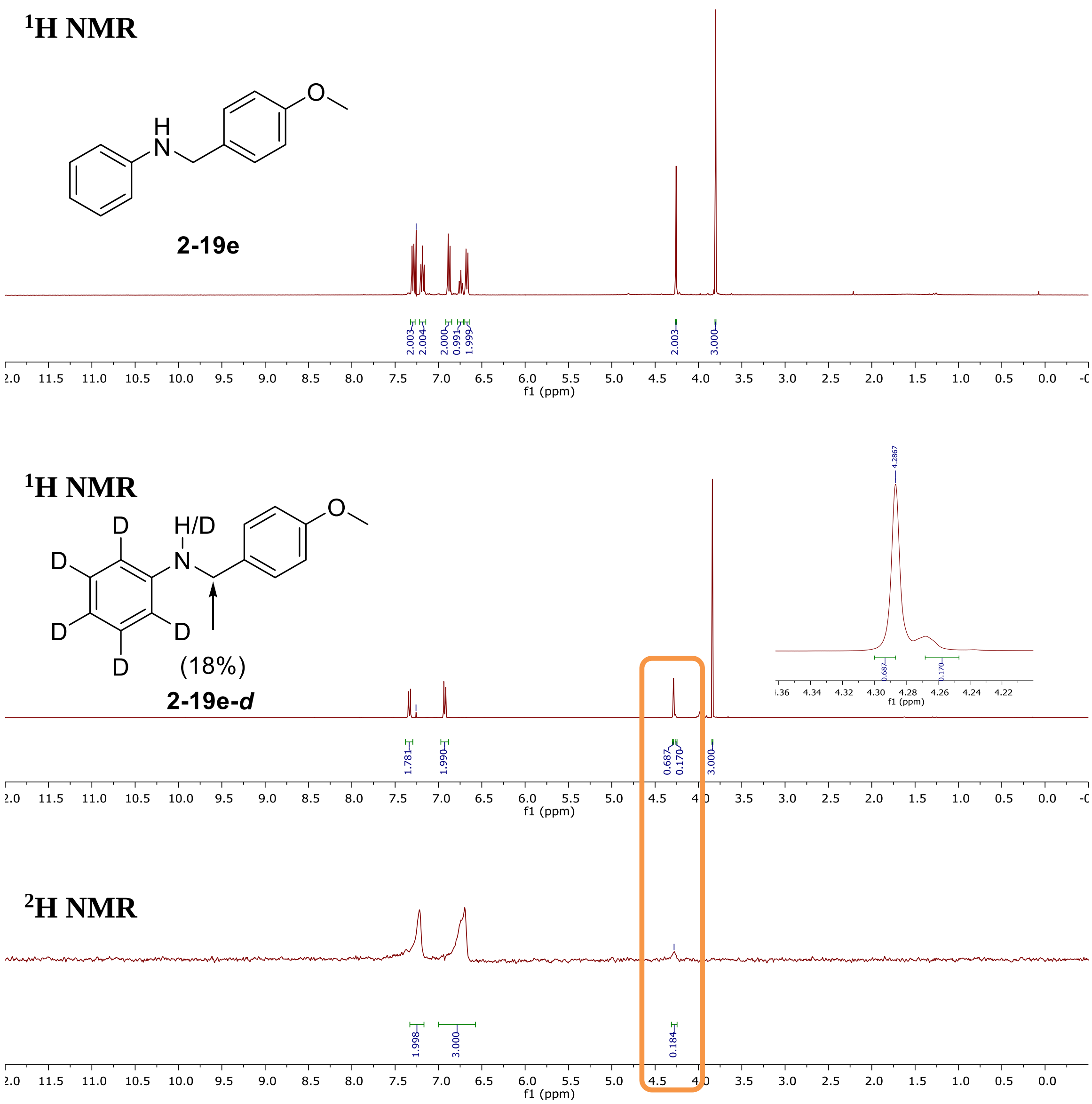

Figure 2.8: Top: ^{1}H NMR Spetrum for **2-19e**; Bottom: ^{1}H and ^{2}H NMR Spetra of H/D Exchange Pattern of the Reaction with 4-Methoxybenzylamine and Aniline -d_7

2.2.8.3 Carbon Isotope Effect Study

To discern the rate-limiting step of the catalytic reaction, we employed Singleton's high-precision NMR technique to measure the carbon isotope effect for the coupling reaction.[127] The reaction tube of 4-methoxybenzylamine (2 mmol) and **2-9** (0.75 mol %)/**2-16** (10 mol %) in chlorobenzene (4 mL) was heated at 130 °C for 16 h for high conversion product **2-18c** and low conversion sample was obtained after 2−3 h of the reaction time. The product **2-18c** was isolated by column chromatography on silica gel and was analyzed by ^{13}C NMR. The most pronounced carbon isotope effect was observed on the α-carbon of the product **2-18c** when the ^{13}C ratio of the product at three high conversions (86−89%) was compared with the sample obtained at low conversions (12−15%) [(average of ^{13}C at 87% conversion)/(average of ^{13}C at 13% conversion) at benzyl C_α = 1.015±0.001)] (**Eq. 2.9**). The significant carbon isotope effect on the α-CH_2 carbon is consistent with the C−N bond cleavage turnover-limiting step. In support of this notion, Singleton and co-workers showed that the observation of the most pronounced carbon isotope effect has been a definitive tool for establishing the rate-limiting step for both C−C and C−O bond-forming reactions.[127c]

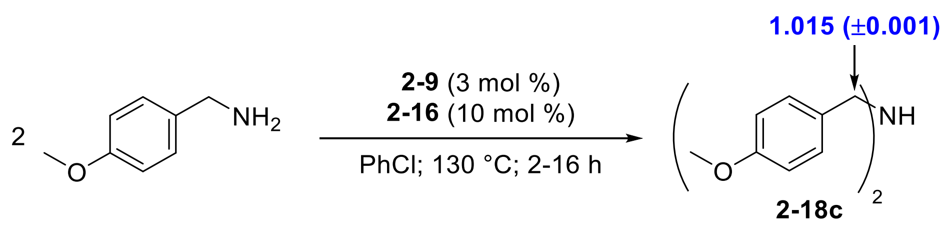

(Eq. 2.9)

While C−N bond cleavage has been found to be the turnover-limiting step for a number of chemical and biochemical coupling reactions,[128] very few carbon kinetic isotope effect measurements have been reported for the catalytic C-N cleavage reactions.

Fry and co-workers measured pronounced carbon isotope effects in the Hofmann elimination reaction of para -substituted (2-phenylethyl)- trimethylammonium bromides, which indicated an E2 mechanism involving C−N bond cleavage step.[129] In a urease catalyzed hydrolysis of hydroxyurea, Cleland and co-workers observed a significant carbon isotope effect on the carbonyl carbon but not on the nitrogen atom, which argues for the formation of a common intermediate prior to the C−N bond cleavage step.[130]

2.2.8.4 Hammett Study

The Hammett plot was constructed from measuring the rate of the coupling reaction of a series of para-substituted benzylamines 4-X-$C_6H_4CH_2NH_2$ (X = OMe, Me, H, Cl, F, CF_3) in the presence of **2-9** (0.75 mol %)/**2-16** (10 mol %) in toluene-d_8 (**Figure 2.9**). The rate of each substrate was obtained by measuring the appearance of the product peaks, which were normalized against an internal standard (hexamethyl benzene) as analyzed by ^{1}H NMR. The k_{obs} for each catalytic run was determined from a first order plot. The Hammett plot of $\log(k_X/k_H)$ vs σp showed a linearly correlated pattern with $\rho = -0.79 \pm 0.1$. A relatively high negative slope suggests a significant cationic character buildup on the amine substrate during the coupling reaction.

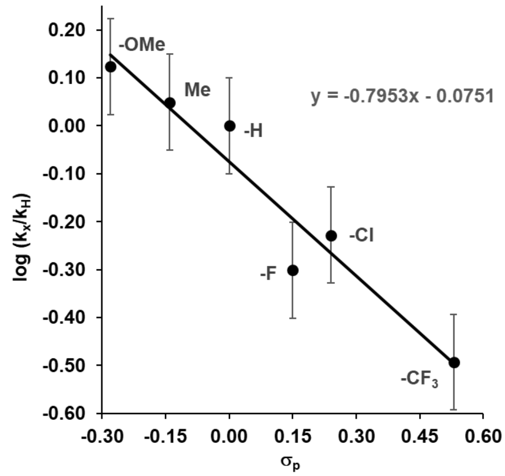

Figure 2.9: Hammett Plot of the Coupling of 4-Methoxyaniline with *p*-X-$C_6H_4CH_2NH_2$

2.2.9 Detection of an Active Catalytic Species by NMR Method

Cationic ruthenium hydride complex **2-10** and 4-fluorobenzene1,2-diol **2-16c** were reacted in a sealed J-Young tube as indicated in the **Eq. 2.10**, and the products were analyzed by ^{1}H and ^{31}P NMR. We tentatively assigned these novel ruthenium hydride species as π-coordinated species **2-23** and the chelated catecholate species **2-24**.

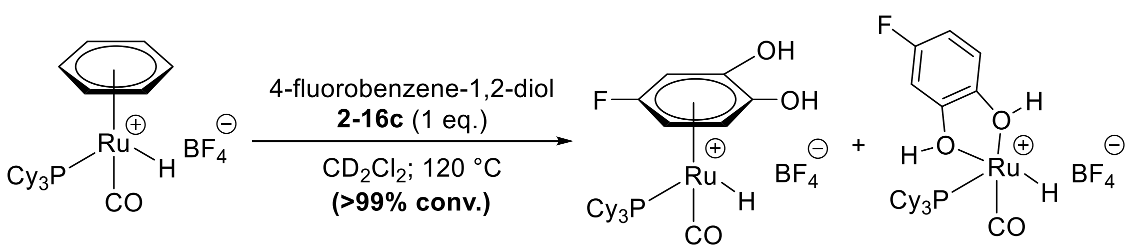

(Eq. 2.10)

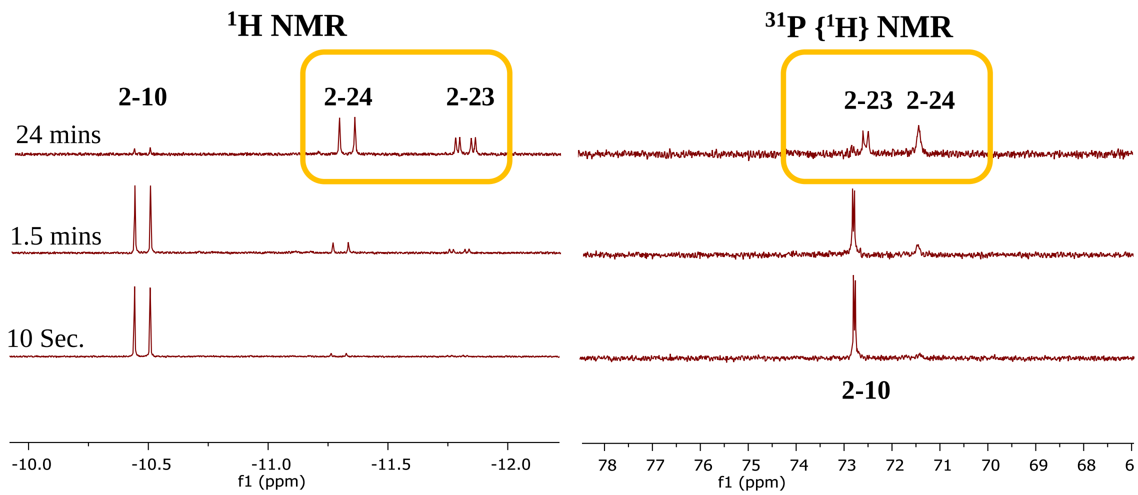

Figure 2.10: ^{1}H and ^{31}P {^{1}H} NMR of Active Catalytic Species (**2-23** and **2-24**) Detected by the Reaction of 4-Fluorobenzene-1,2-diol and the Complex **2-10**.

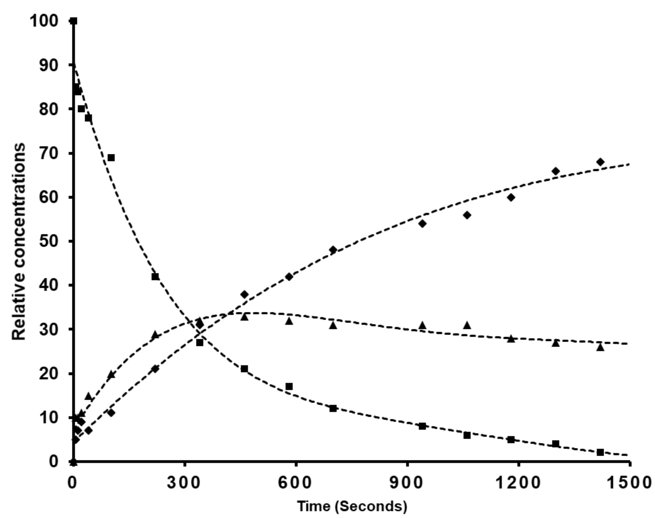

Figure 2.11: The Plot of Relative Concentration of The Ruthenium Hydride Species Generated from the Complex **2-10** (■) vs Time. Complex **2-23** (▲), Complex **2-24** (♦).

The ^{1}H NMR of active catalytic species **2-23** showed the Ru-H signals (^{1}H-NMR δ -11.76 (d, J_{PH} = 6.7 Hz), -11.83 (d, J_{PH} = 6.9 Hz); ^{31}P-NMR {^{1}H} δ 72.5, 72.6) and **2-24** (^{1}H-NMR δ -11.30 (d, J_{PH} = 25.5 Hz); ^{31}P-NMR {^{1}H} δ 71.4)). Free benzene molecule was detected from the reaction of 4-fluorobenzene-1,2-diol. The plot of relative concentration of the two major catalytic species vs time is shown in **Figure 2.11**.

2.2.10 Synthesis and X-Ray Crystallographic Determination of Ruthenium Catecholate Complexes

In an effort to develop novel deaminative C–C coupling reaction with the ketone substrates and primary amines, we were able to observe a higher activity and selectivity when the catechol ligand was replaced with the 1,2-benzoquinone ligand. Delightfully, the chelated ruthenium catecholate complexes were isolated and identified (**2-11**, **2-14** and **2-15**) as described in the section **2.2.2** and **2.2.3**. Synthetic protocol was established for the synthesis of complex **2-11** which exhibited a remarkable activity for the C–N bond activation coupling reactions including secondary amine synthesis.

2.3 Proposed Mechanism

We present a plausible mechanistic hypothesis for the deaminative coupling reaction based on these kinetic and spectroscopic results (**Scheme 2.9**). Considering the observation of imine product, we propose the formation of a Ru-imine species **2-24** as a catalytically active species, which would be initially generated from the dehydrogenation of amine substrate. From the observation of imine product **2-22**, we propose the formation of a Ru−imine species **2-25** as a catalytically active species, which would be initially generated from the dehydrogenation of amine substrate.

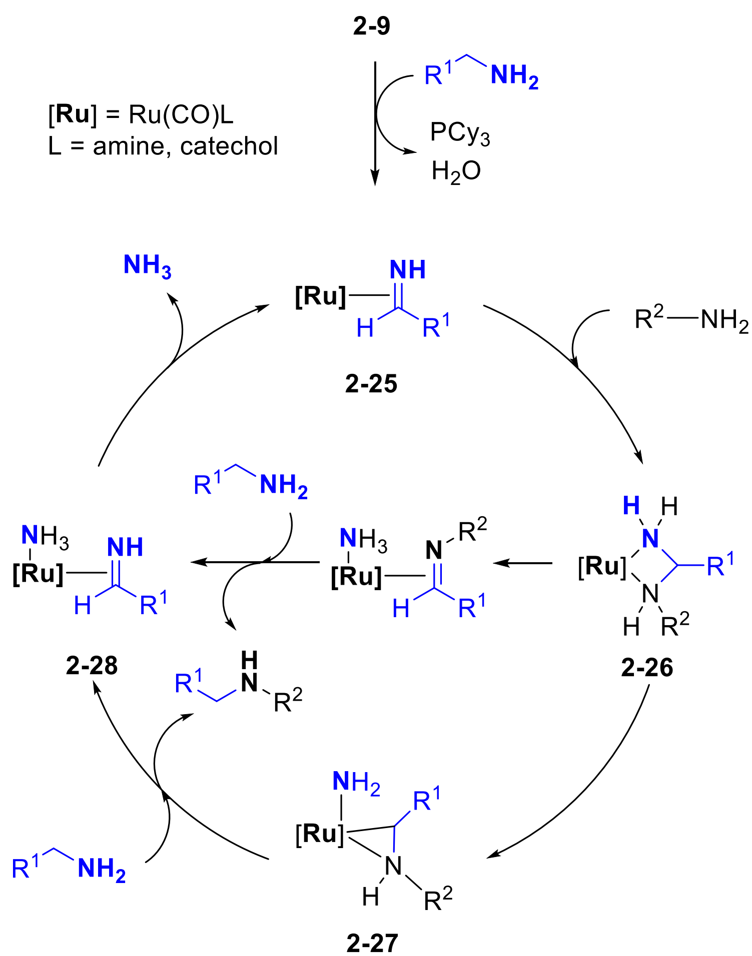

Scheme 2.9: Proposed Mechanism for the Deaminative Coupling of Primary Amines

To demonstrate the reversibility of the imine formation, we performed the reaction of PhN=CHPh (1.0 mmol) with cyclohexylamine (1.4 mmol) in the presence of **2-9**/**2-16** at 130 °C. The reaction produced a complex mixture of aniline and the crossover products. In support of this notion, some oxidative C−N bond cleavage reactions are known to proceed via the formation of an imine intermediate.[131] The coordination of imine substrate to the Ru center would increase the electrophilic nature of the imine carbon, and the nucleophilic addition of the second amine substrate would proceed to form the Ru intermediate di-amine species **2-26**. Many structurally similar transition metal−urea complexes have been synthesized, and their reactivity patterns have been well established.[132] The observation of carbon isotope effect provides an experimental support for the rate-limiting C−N cleavage step in forming the Ru-aminoalkyl species **2-27**. In support of this, we have observed the prominent ^{13}C isotope effect on the benzylic carbon of the symmetric coupling product **2-18** (C_α = 1.015±0.001). The dehydrogenation of second amine substrate in conjunction with the hydrogen transfer would form the coupling products **2-17/2-18** and **2-19** with the regeneration of imine species **2-28**. Both the detection of imine product and the selective deuterium incorporation on the α-CH_2 of **2-18e-*d*** suggest that the dehydrogenation and hydrogen transfer steps are likely facile and reversible under the reaction conditions.

2.4 Summary and Conclusion

In conclusion, we successfully devised a highly chemoselective synthesis of secondary amines from the deaminative coupling of primary amines. The catechol ligand promoted ruthenium catalytic system was found to exhibit a uniquely high activity and selectivity in forming both symmetric and unsymmetric secondary amines. The activity and selectivity were further enhanced by using the ruthenium catalyst **2-10** with benzoquinone ligands. The catalytic method is operationally simple, exhibits a broad substrate scope, tolerates common organic functional groups, and forms ammonia as the sole byproduct without employing any reactive reagents. The kinetic and spectroscopic studies indicate that the coupling reaction proceeds via the formation of imine species with the turnover limiting C−N bond cleavage step.

The isolated ruthenium catecholate complex **2-11** has been found to exhibit a higher activity for the deaminative coupling reaction illustrating the role of catechol additive as a chemo-selective ligand. We have successfully demonstrated synthetic utility of the coupling method via C–N activation for the synthesis of both symmetric and unsymmetric synthesis of amines, as well as the synthesis of drug candidates biologically active compounds. We used the catalytic deaminative method as a key step in the synthesis of the drug candidate *Piribedil* which is a dopamine antagonist for the treatment of Parkinson's disease.[133] The isolated ruthenium-catecholate catalyst was used for the synthesis of pharmaceutically active molecule *Alverine* by self-condensation and tertiary amine formation. We published an article in *J. Org. Chem.* **2018**, *83*, 4932–4947 (DOI: doi.org/10.1021/acs.joc.8b00649) on the basis of the part of work described in this Chapter. The article has been selected as a *Featured Article* for the issue and highlighted in *Organic Chemistry Portal* **2018** (https://www.organic-chemistry.org/abstracts/lit6/329.shtm).

Chapter 3

Scope and Mechanistic Study of the Redox-Active 1,2-Benzoquinone Enabled Ruthenium-Catalyzed Deaminative α-Alkylation of Ketones with Amines

3.1 Introduction

The α-alkylation of carbonyl compounds via the generation of enolates represents one of the most widely used carbon-carbon bond formation methods in organic synthesis.[134] The α-alkylation of carbonyl compounds have been extensively utilized in synthesis of natural products and pharmaceutically important drug molecules.[135] Since traditional alkylation methods using stoichiometric amounts of strong base and organic halide coupling partners lead to the formation of copious wasteful byproducts, concerted research efforts have been devoted to the development of selective catalytic alkylation protocols that would avoid the use of strong base and obviate the formation of wasteful byproducts.

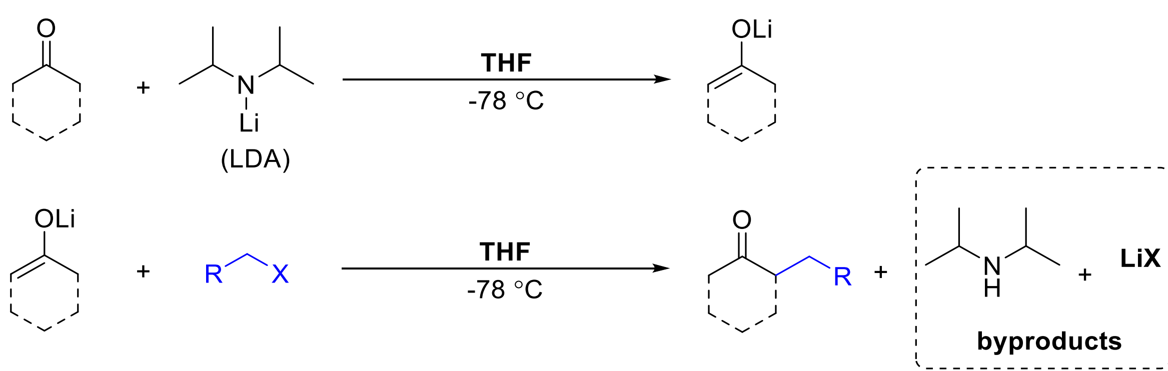

Scheme 3.1: Traditional Alpha Alkylation of Ketones by Lithium Enolates

The industrial processes heavily relies on enolates as pre-activated nucleophiles and alkyl halides as activated electrophiles for the formation of C−C bonds of ketones (**Scheme 3.1**). Stoichiometric amounts of strong base, such as lithium diisopropylamine, has been commonly used to generate metal-enolates, in which the alkylation reaction is performed typically under the cryogenic conditions. Moreover, the traditional alkylation methods employ alkyl halides, which are expensive and generate halide-containing salts.[136] The alkylation via Stork enamine provides an alternative strategy to obtain α-alkylated products from the direct coupling of nucleophilic enamine intermediate upon addition with an alkyl halide or Michael acceptor (**Scheme 3.2**).[137] However, the drawbacks of the alkylation method are that a stoichiometric amount of salt byproduct is produced and the reaction is favored to give a regioselective product at the less hindered side.

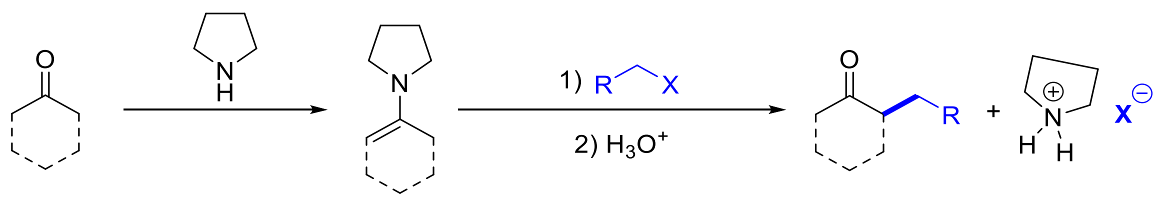

Scheme 3.2: General Stork Enamine Reaction

Transition metal-catalyzed "hydrogen borrowing" methodology, which involves the dehydrogenation of alcohols followed by aldol-type condensation with the ketone substrates, has been shown to be highly effective for promoting the alkylation of ketones with alcohols.[135a, 138] In a significant advance for sustainable synthesis, earth-abundant transition metal catalysts have been successfully employed for the catalytic alkylation method via hydrogen borrowing technology.[139] Very recently, Donohoe and co-workers achieved chemo- and regioselective synthesis of acyl-cyclohexenes by utilizing ketones with diols via a tandem acceptorless dehydrogenation-[1,5]-hydride shift cascade reaction (**Scheme 3.3**).[140]

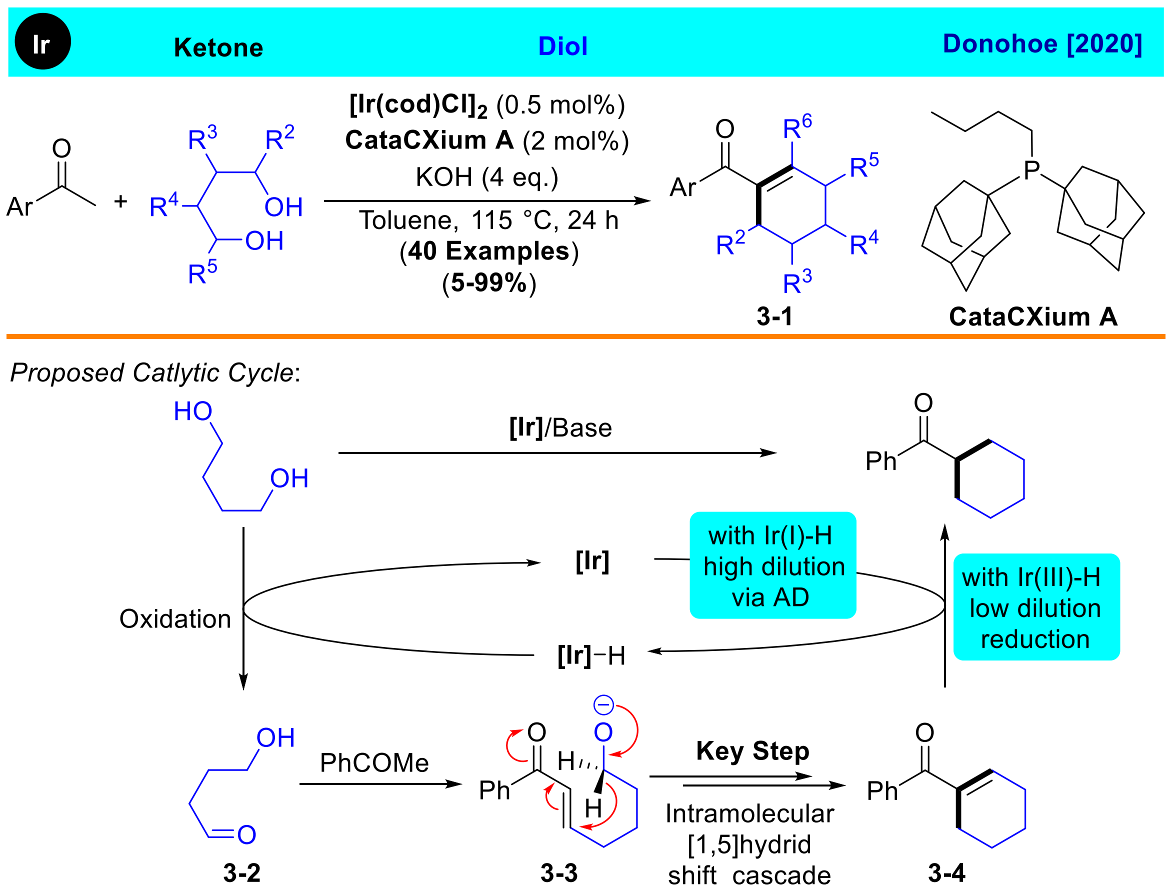

Scheme 3.3: Chemo- and Regioselective Synthesis of Acyl-Cyclohexenes from Diols; AD = Acceptorless Dehydrogenation

Upon oxidation of the diol substrate to the corresponding hydroxyaldehyde, aldol condensation with acetophenone would proceed to form an alkoxy enone **3-2**. The alkoxy enone **3-2** then undergoes a cascade involving an intramolecular [1,5]-hydride shift **3-3** followed by aldol condensation to form the corresponding cyclohexene **3-4**. The cyclohexene adduct **3-4** can further be reduced to the corresponding cyclohexane with the regeneration of the active iridium catalyst.

A number of novel catalytic C–H functionalization methods have been devised to promote direct alkylation and alkenylation of ketones with alkenes and alkynes.[141] In a seminal report, MacMillan and co-workers developed a direct β-arylation of cyclic ketones with electron-deficient arylnitriles by combining photocatalysis with organocatalytic enamine alkylation protocol.[142] Fagnoni and co-workers employed photoactive tungsten catalysts to achieve the direct coupling of cyclopentanones with electron-deficient alkenes to give β-alkylated products.[143] Widenhoefer and Che groups independently reported intramolecular C–H alkylation methods for γ,σ-enone substrates to form cyclic ketones by using Pd and Au catalysis.[144] Dong and co-workers recently reported a direct α-alkylation of ketones with simple alkenes by using a bifunctional Rh catalytic system, in which an aza-indoline moiety was found to promote the conversion of α-C–H bond of ketones into an enamine sp^2 C–H bond prior to the alkylation reaction.[145] The bifunctional ligand, 7-azaindoline, activates the ketone α-C-H bonds via enamine formation, **3-7** while the linked pyridyl moiety acted as a directing group, and the oxidative addition of a low-valent Rh(I) metal into the resulting enamine C-H bond affords the rhodium hydride species **3-8**. Olefin insertion followed by reductive elimination would generate the intermediate **3-9**, which undergoes hydrolysis to regenerate the active catalytic species and corresponding alkylated product **3-6**.

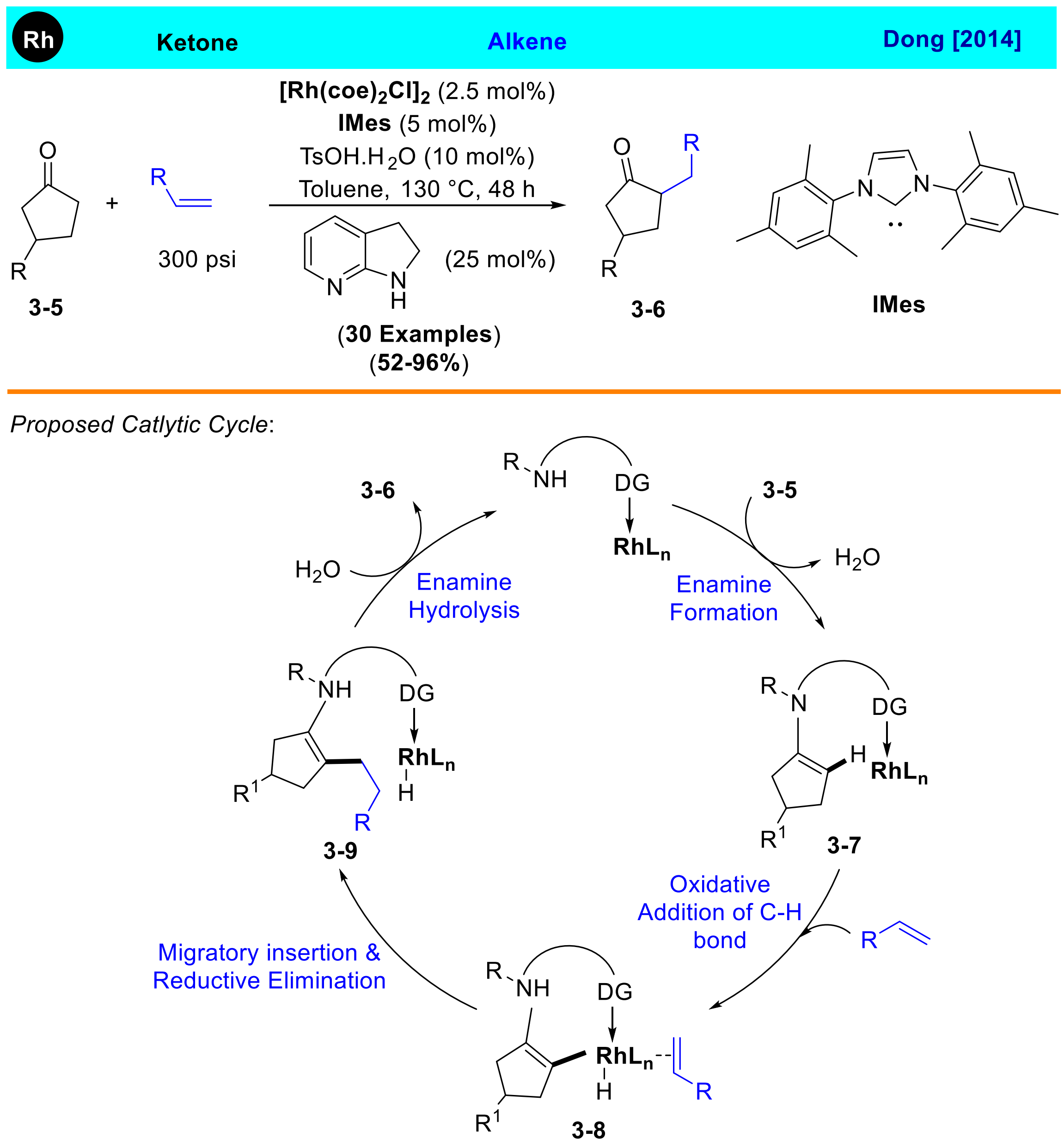

Scheme 3.4: Proposed Catalytic Cycle for Dong's Bifunctional Rh Catalytic System

In recent years, transition metal-catalyzed deaminative coupling methods have emerged as an effective tool for C–C bond coupling reactions.[3a] Glorius and co-workers devised an efficient deaminative alkylation of amines via the generation of pyridinium ions by employing visible-light photoredox catalysis.[146] Zhang group reported Pd-catalyzed allylic alkylation of carbonyl compounds with allylamines, which has been shown to involve a direct allylic C−N bond cleavage via the formation of Pd-allyl species.[122] Martin and co-workers recently reported a highly regioselective Ni-catalyzed deaminative alkylation of unactivated olefins by using pyridinium reagents.[147] Fu and co-workers reported an efficient photocatalytic deaminative and decarboxylative alkylation of silyl enol ethers with redox-active esters and *N*-alkylpyridinium salts.[148] From both synthetic and environmental points of view, catalytic C−C coupling methods via C−N cleavage by employing readily available amines as the substrates have been regarded as a highly attractive strategy for the synthesis of complex organic molecules as well as for reforming processes of nitrogen-containing biomass feedstocks.[3a, 3b, 64b]

3.2 Results and Discussion

We previously discovered that the cationic ruthenium hydride complex $[(\eta^6\text{-}C_6H_6)(PCy_3)(CO)RuH]^+BF_4^-$ **2-10** is a highly effective catalyst precursor for the deaminative and decarboxylative coupling reaction of ketones with amino acids.[29] We subsequently found that the ruthenium-hydride complex **2-10** with a 1,2-catechol ligand exhibits an exceptionally high chemoselectivity for promoting the deaminative coupling reactions of amines to form unsymmetric secondary amines and quinazolinone derivatives.[149] To extend the synthetic utility of ligand controlled catalysis, we have been exploring the promotional effects of various oxygen and nitrogen ligands on ruthenium catalysts for the deaminative coupling reactions of amines. Herein, we report the development and scope of a highly regioselective catalytic deaminative alkylation method of ketones with amines, which is mediated by a well-defined ruthenium catalyst containing a redox-active *ortho*-benzoquinone ligand. We also delineate comprehensive experimental and computational studies for establishing a detailed mechanism of the catalytic reaction. The salient features of the catalytic method are that the α-alkylation ketone products are formed in regio- and stereoselective fashion without employing any reactive reagents or forming any wasteful byproducts, while tolerating a number of common organic functional groups.

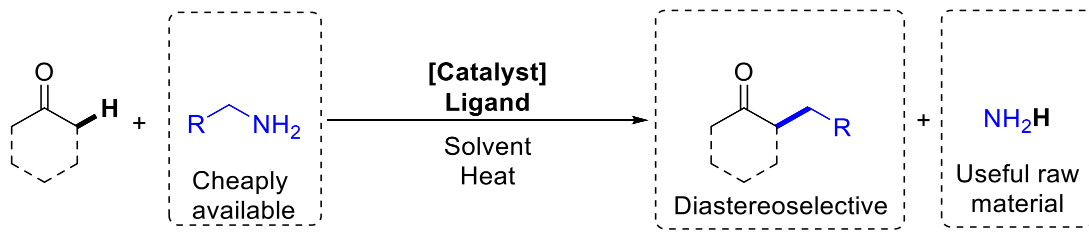

Scheme 3.5: General Scheme for the Alkylation Protocol for Ketones with Amines

3.2.1 Reaction Discovery and Optimization Studies

We initially discovered that the catalytic system consisted of the Ru–H complex **2-10** and a redox-active 1,2-benzoquinone ligand exhibited high catalytic activity for the deaminative coupling of acetophenone with 4-methoxybenzylamine to form the α-alkylated product **3-10a**. The coupling reaction shown in **Eq. 3.1** has been used as the standard example unless otherwise noted.

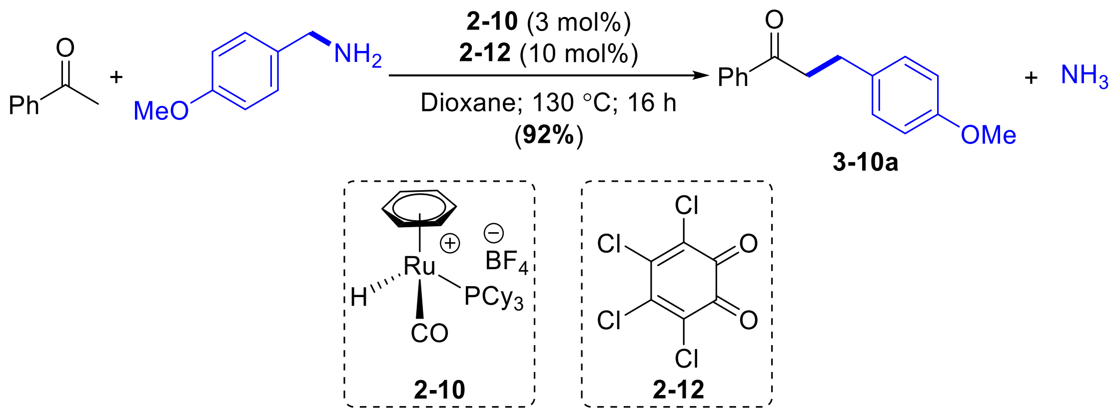

(Eq. 3.1)

3.2.2.1 Ligand Screening

We first evaluated the ligand effect for the reaction of acetophenone with 4-methoxybenzylamine. Without using any ligand, the **3-10a** product was formed in 28% yield along with the imine product (**Table 3.2**; entry 8). While using phenol ligands (**3-11a**) or 1-methoxyphenol (**3-11b**) ligands led to slight improved results compared to the ligand-free conditions, catechol ligands (**2-16**) gave the desired product **3-10a** in significantly increased yield. In accordance with the previous result in the ruthenium catalyzed C(sp^3)−N bond cleavage reaction, catechol ligand **2-16** was found to be effective and proved to be the optimal ligand for the selective synthesis of secondary amines.[126b] The catechol ligands with both electron donating and withdrawing group **2-16a-e** were shown to be effective for promoting the catalytic reaction by giving modest to good yields (65-78%), whereas 2,2´-biphenol ligand **2-12j** gave a slight improved yield for the coupling reaction. The nitrogen donor ligands **3-32d** and **3-33** and aliphatic diols **2-12k** were found to be ineffective for the reaction.

Table 3.1: Ligand Screening for the Coupling of Acetophenone with 4-Methoxybenzylamine[a]

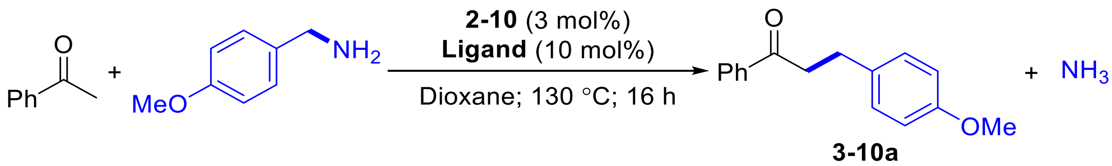

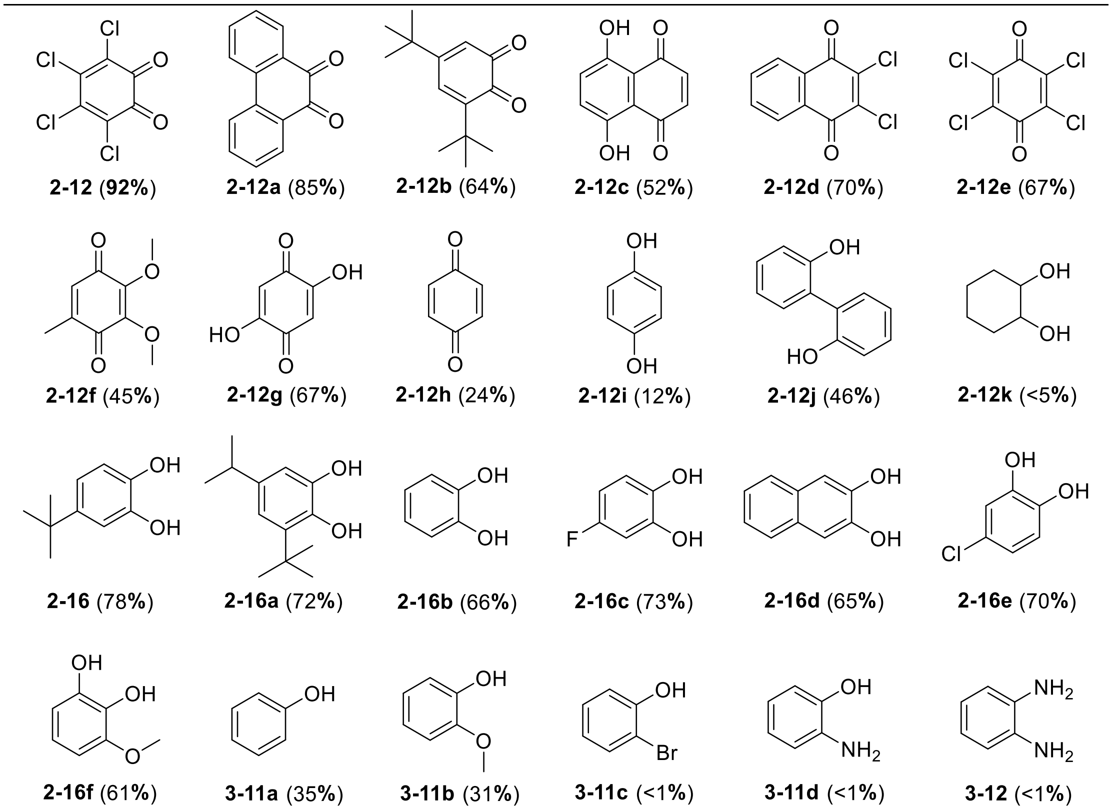

[a]Reaction conditions: acetophenone (0.5 mmol), 4-methoxybenzylamine (0.7 mmol), **2-10** (3 mol %), **ligand** (10 mol %), 1,4-dioxane (2 mL), 130 °C, 16 h. [b]The product yield of **3-10a** was determined by ^{1}H NMR by using hexamethylbenzene as an internal standard.

As shown in **Table 3.1**, the catalytic activity of **2-10** was found to be substantially enhanced by the addition of a 1,2-benzoquinone ligand with the efficient formation of product **3-10a**. In this case, secondary amine side product was observed as the minor product, indicating a high selectivity towards the desired alkylation product. The Ru-H complex **2-10** with 3,4,5,6-tetrachloro-1,2-benzoquinone **2-12** was found to exhibit the highest activity among screened benzoquinone ligands by affording 92% yield.

3.2.2.2 Catalyst and Solvent Screening

We found that 1,4-dioxane is the most suitable solvent for the coupling reaction (entry 2-7). The complex **2-10** was found to be most effective catalyst among the screened ruthenium catalysts (entry 1), where the reaction was tolerated the addition of 2 equivalents of water (entry 9). Lewis acids and PCy_3 did not show any activity for the coupling reaction (entry 19-22). A series of ligand screening and optimization efforts have led to the standard conditions for the coupling reaction: acetophenone (0.5 mmol), benzylamine (0.7 mmol), **2-10** (3 mol %) and **2-12** (10 mol %) in 1,4-dioxane (2 mL) at 130 °C for 16 h (**Table 3.2**). The ammonia byproduct, which was detected by GC-MS in a crude reaction mixture, was removed under vacuum along with the solvent, and the product **3-10a** was isolated by a column chromatographic separation on silica gel.

Table 3.2: Catalyst and Additive Screening for the Coupling of Acetophenone with 4-Methoxybenzylamine

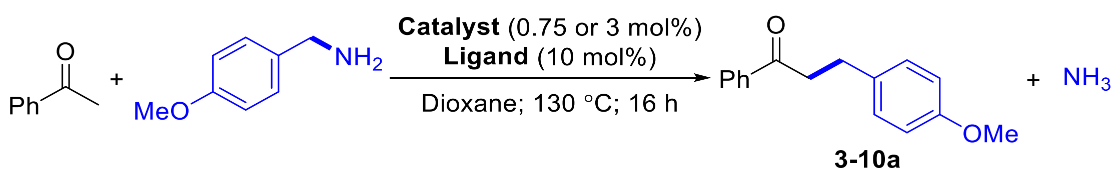

entry	catalyst	deviation from standard conditions	**3-10a** (%)[b]
1	**2-10**	none	**92**
2	**2-10**	t-butylethylene (1eq.)	84

3	**2-10**	cyclopentene (1eq.)	79
4	**2-10**	chlorobenzene (as a solvent)	46
5	**2-10**	1,2-DCE (as a solvent)	<10
6	**2-10**	xylene (as a solvent)	76
7	**2-10**	toluene (as a solvent)	83
8	**2-10**	without **2-12**	28
9	**2-10**	H_2O (2 eq.)	90
10	$[(PCy_3)(CO)RuH]_4(\mu\text{-}O)(\mu\text{-}OH)_2$	$HBF_4{\cdot}OEt_2$	79
11[c]	$[(PCy_3)(CO)Ru]_4(\mu\text{-}Cl)_4]^+BF_4^-$	-	54
12	$(PPh_3)_3(CO)RuH_2$	-	22
13	$(p\text{-cymene})_2RuHCl$	-	39
14	$RuCl_2(PPh_3)_3$	-	8
15	$RuCl_3{\cdot}3H_2O$	-	trace
16	$[Ru(COD)Cl_2]_x$	-	trace
17	$(PCy_3)_2(CO)RuHCl$	-	22
18	$[(PCy_3)(CH_3CN)(CO)RuH]^+BF_4^-$	-	56
19	-	none	0
20	-	$PCy_3/HBF_4{\cdot}OEt_2$	0
21	-	$HBF_4{\cdot}OEt_2$	0
22	-	$BF_3{\cdot}OEt_2$	0

[a]Standard conditions: acetophenone (0.5 mmol), 4-methoxybenzylamine (0.7 mmol), $[(C_6C_6)(PCy_3)(CO)RuH]^+ BF_4^-$ **2-10** (3 mol %), **2-12** (10 mol %), 1,4-dioxane (2 mL), 130 °C, 16 h. [b]The product yield of **3-10a** was determined by ^1H NMR using hexamethylbenzene as an internal standard. [c]0.75 mol% of the ruthenium catalyst has been used.

3.2.3 Reaction Scope

3.2.3.1 Deaminative α-C–H Alkylation of Ketones with Primary Amines

The substrate scope of the deaminative alkylation reaction was examined by using the *in-situ* generated catalyst system **2-10**/**2-12** under standard conditions. We initially examined the selective alkylation of methyl ketones with various amine substrates (**Table 3.3**). Benzylic amines with para-electron donating group were found to be most effective towards the product formation **3-10a-e**.

Table 3.3: Deaminative α-Alkylation of Methyl Ketones with Amines[a]

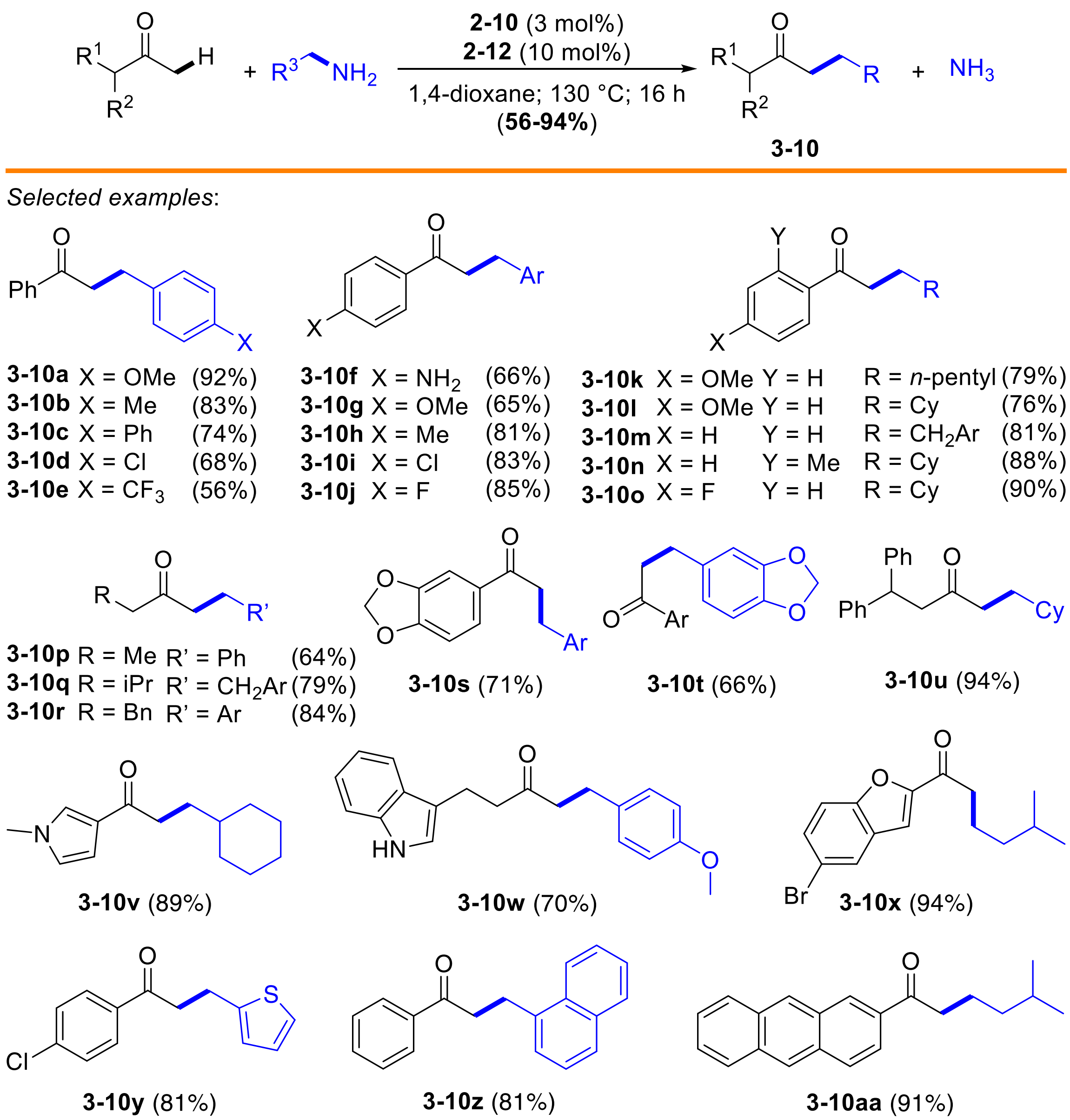

[a]Reaction conditions: ketone (0.5 mmol), amine (0.7 mmol), **2-10** (3 mol %), **2-12** (10 mol %), 1,4-dioxane (2 mL), 130 °C, 16 h. Ar = 4-methoxyphenyl

On the other hand, acetophenones with electron withdrawing group afforded the corresponding products in higher yields than the ones with electron donating group **3-10f-j**. Both benzylic and aliphatic primary amines were found to be suitable substrates for aryl-substituted ketones to form the α-alkylation products **3-10k-o**. The analogous coupling of aliphatic ketones with benzylic and aliphatic amines cleanly formed the α-alkylated ketone products **3-10p-r**. In these cases, methyl carbon was selectively alkylated over methylene carbon in good to excellent yields (64-84%). 3′,4′-(Methylenedioxy)acetophenone with 4-methoxybenzylamine also selectively formed the desired product in 71% yield **3-10s**. In contrast, analogous 1,3-benzodioxol-5-ylmethylamine afforded the corresponding product with an electron rich acetophenone substrate **3-10t** in 66% yield. Cyclohexylmethanamine was found to be a compatible amine substrate for the coupling reaction to form the products **3-10u**. A variety of heteroatom functional groups **3-10v-x** were tolerated in forming the desired α-alkylated ketone products. Amine substrates containing heterocycles (**3-10y**) as well as both polyaromatic substituted amines **3-10z** and ketones **3-10aa** were also found to be suitable substrates for the coupling reaction. These results demonstrated that the novel deaminative coupling method effectively leads to regioselective α- alkylation ketone substrates.

3.2.3.2 Deaminative α-Methylene C–H Alkylation of Ketones with Primary Amines

We next examined the scope of the coupling reaction of substituted ketone substrates (**Table 3.4**). The electron rich propiophenones with 4-methoxyphenylethylamine and benzylamine afforded the desired products **3-10ab** and **3-10ac** in 84% and 61% yields respectively. In general, the alkylation occurs regioselectively at the less substituted α-carbon of ketones, but the coupling of 1-phenyl-2-butanone with a benzylic amine formed the branched alkylated product **3-10ad-ae**, resulting from the regioselective alkylation on the phenyl-substituted carbon. The coupling reaction of cyclic ketones having different ring sizes with phenylethylamines and benzylic amines smoothly resulted in the alkylation products **3-10af-ak** in high yields. The coupling reaction of substituted cyclic ketones with benzylic amines resulted in a highly diastereoselective alkylation products **3-10al-an**. In contrast, the coupling with cyclohexanone with a chiral amine (*R*)-(+)-β-methylphenethylamine resulted in a 2.8:1 diastereomeric mixture of **3-10ao**.

Table 3.4: Deaminative α-Alkylation of Methylene Position of the Ketones with Amines[a]

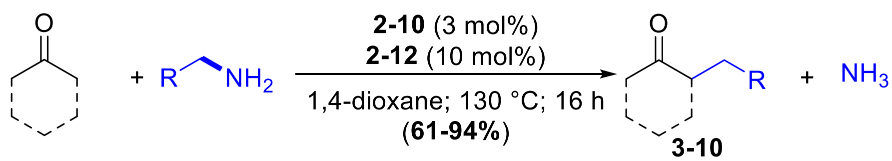

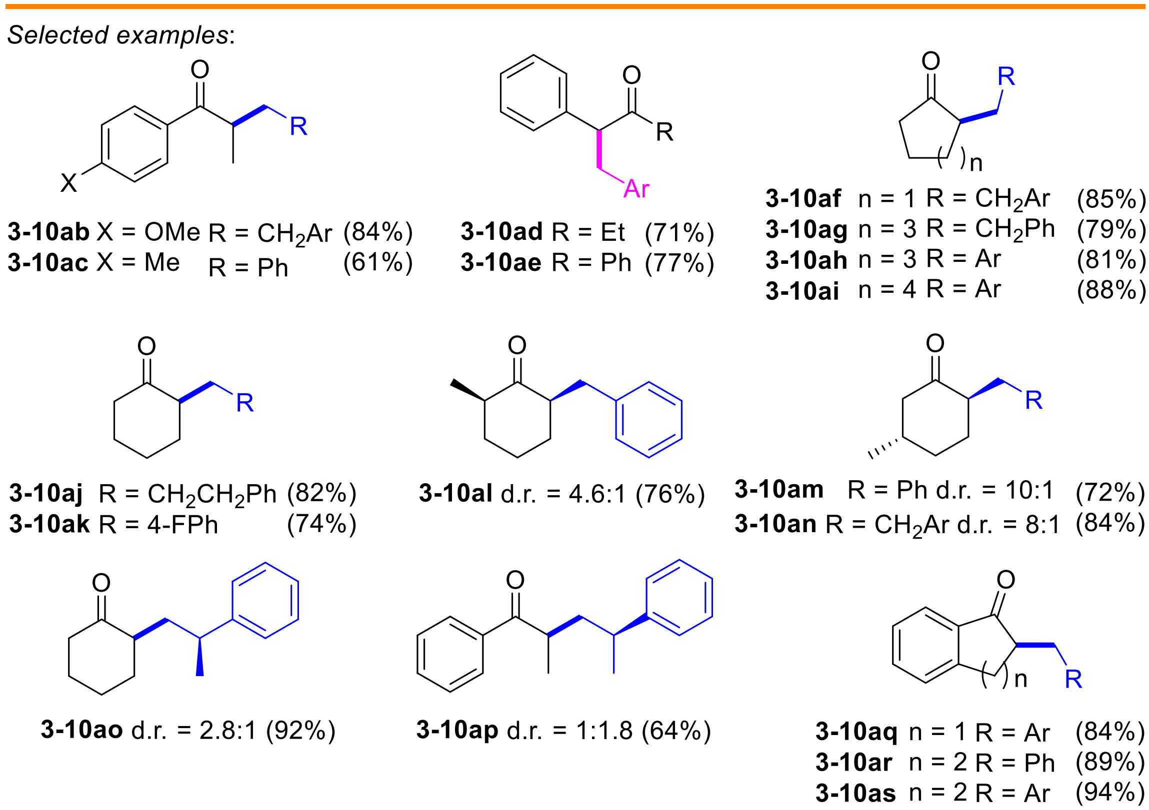

[a]Reaction conditions: ketone (0.5 mmol), amine (0.7 mmol), **2-10** (3 mol %), **2-12** (10 mol %), 1,4-dioxane (2 mL), 130 °C, 16 h. Ar = 4-methoxyphenyl

The coupling reaction of propiophenone with a chiral amine (*R*)-(+)-β -methylphenethylamine resulted in a decreased of both yield and diastereoselectivity. Sterically demanding primary or secondary amines with α-quaternary carbon did not give any alkylation products.

3.2.3.3 Deaminative α-Alkylation of Ketones with Biologically Active Primary Amines

We next explored the synthetic utility of the coupling method by employing several biologically active ketone and amine substrates (**Table 3.5**). The coupling of an indole-substituted ketone with (-)-*cis*-myrtanylamine yielded the coupling product **3-10at** without any detectable racemization on the chiral methyne position, the structure of which was determined by X-ray crystallography. The coupling of nabumetone with (-)-*cis*-myrtanylamine also shown the similar reactivity affording corresponding product **3-10au**. The treatment of 4-(1H-indol-3-yl)butan-2-one and nabumetone with geranylamine led to the coupling products **3-10av** and **3-10aw**, with the regioselective hydrogenation on the proximal double bond. The treatment of 4-morpholinylacetophenone with 4-methoxybenzylamine cleanly afforded the α-alkylated product **3-10ax** in 71% yield, the structure of which was also confirmed by X-ray crystallography. 4-Fluoroacetophenone and 4-morpholinobenzylamine smoothly formed the coupling product, as illustrated by the formation of **3-10ay**, and morpholinyl, furan-, and thiophene-substituted amines smoothly yielded the alkylation products **3-10az**, **3-10ba** and **3-10bb** respectively.

Table 3.5: Deaminative α-Alkylation of Ketones with Biologically Active Amines[a]

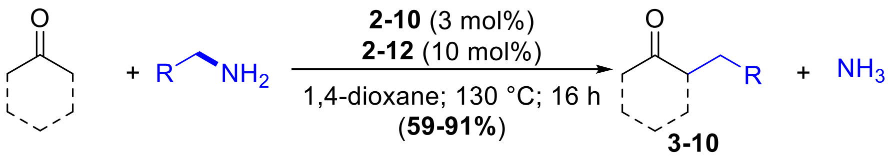

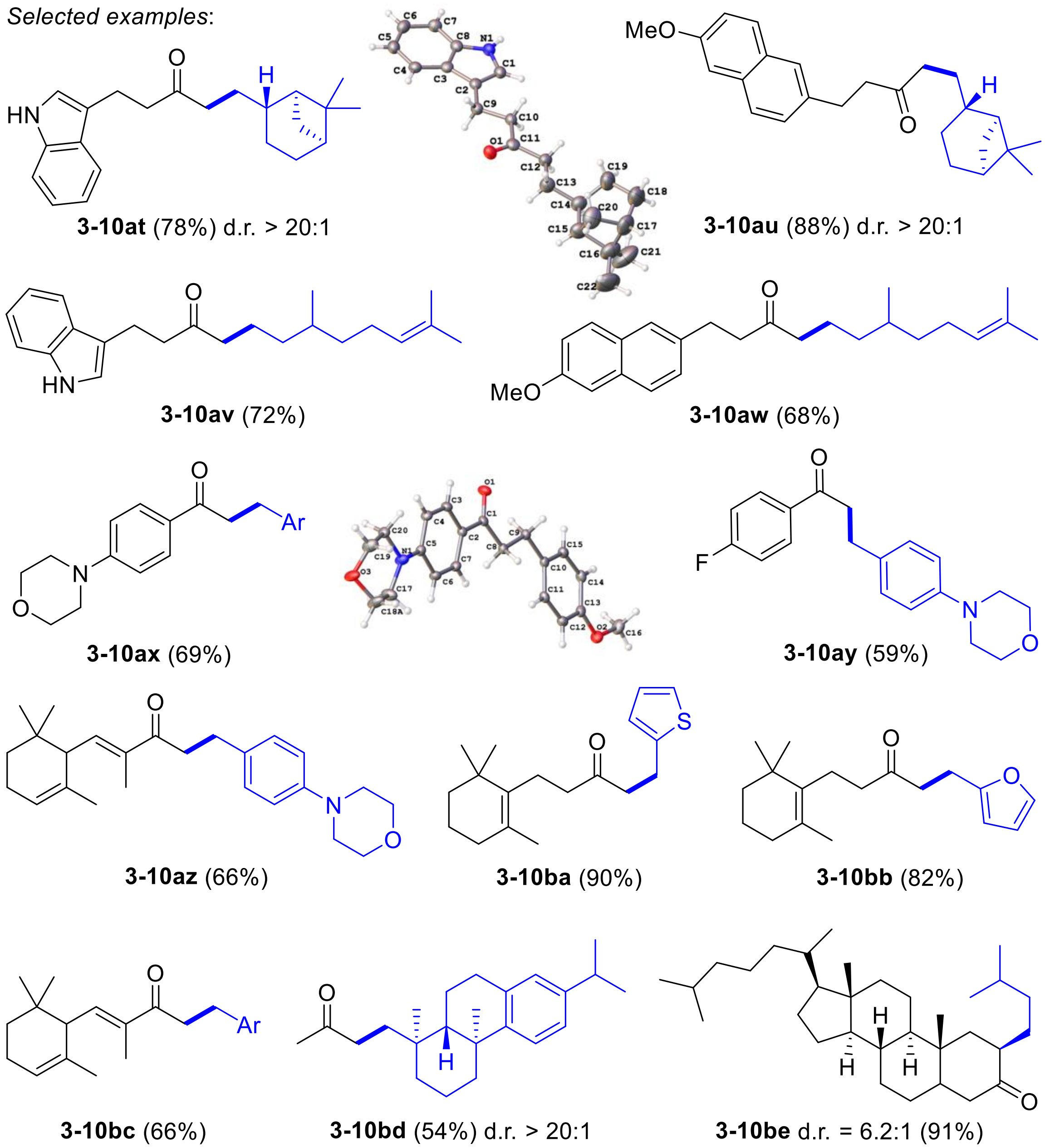

[a]Reaction conditions: ketone (0.5 mmol), amine (0.7 mmol), **2-10** (3 mol %), **2-12** (10 mol %), 1,4-dioxane (2 mL), 130 °C, 16 h. Ar = 4-methoxyphenyl

Unsaturated ketone substrates also well tolerated the reaction by giving good to excellent yields as shown in **3-10az-bc**. The coupling of acetone with (+)-dehydroabietylamine led to an essentially single diastereomer of the alkylation product **3-10bd**, while the coupling of 5-α-cholestan-3-one with *iso*-amylamine resulted in a 6:1 diastereomeric mixture of the product **3-10be**. These examples amply illustrate the synthetic utility as well as heteroatom functional group compatibility of the catalytic method in forming α-alkylated ketone products.

3.2.4 Mechanistic Studies

3.2.4.1 Reaction Profile Study

We have chosen the reaction of acetophenone with benzyl amines for probing the mechanism of alkylation reaction. First, we monitored the catalytic coupling reaction of acetophenone with 4-methoxybenzylamine by using the NMR method. Thus, the treatment of acetophenone (0.10 mmol) with 4-methoxybenzylamine (0.10 mmol) in the presence of complex **2-10** (3 mol %)/**2-12** (10 mol %) in toluene-d_8 (0.5 mL) in a J-Young NMR tube was immersed an oil bath set at 130 °C. The tube was taken out from the oil bath in 20 min intervals and was analyzed by ^{1}H NMR at ambient temperature. As shown in **Figure 3.1**, a rapid formation of the imine product $PhMeC{=}NCH_2C_6H_4$-4-OMe (**3-13a**) was initially observed, reaching at its maximum concentration within 40 min. After 1 h, the alkylation product **3-10a** was gradually appeared at the expense of **3-13a**, and the complete conversion to **3-10a** took about 3 h of the reaction time under these conditions. The formation of **3-10a** was found to exhibit the first order kinetics, as indicated by a linear plot of *ln*[**3-10a**] vs time (*vide infra*).

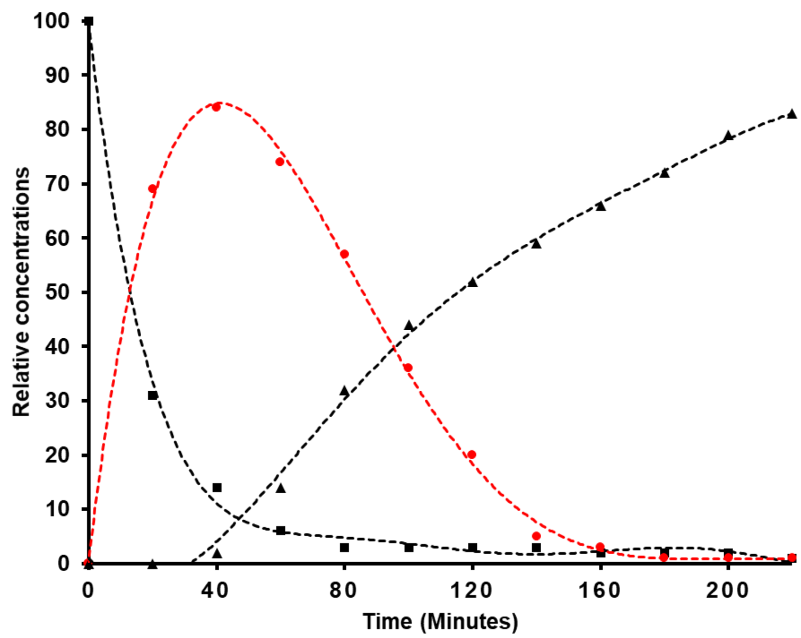

Figure 3.1: Reaction Profile for the Coupling Reaction of Acetophenone with 4-Methoxybenzylamine. Acetophenone (■), **3-10a** (▲), **3-13a** (●).

3.2.4.2 Reaction with Imine Substrate

In a separate preparatory-scale experiment, we have been able to isolate the imine product **3-13a** in 99% yield from the dehydrative coupling reaction of acetophenone with 4-methoxybenzylamine. The subsequent treatment of the isolated imine **3-13a** with **2-10** (3 mol %)/**2-12** (10 mol %) and water (2 eq.) under the standard conditions cleanly formed the product **3-10a** in >95% yield (**Scheme 3.6**).

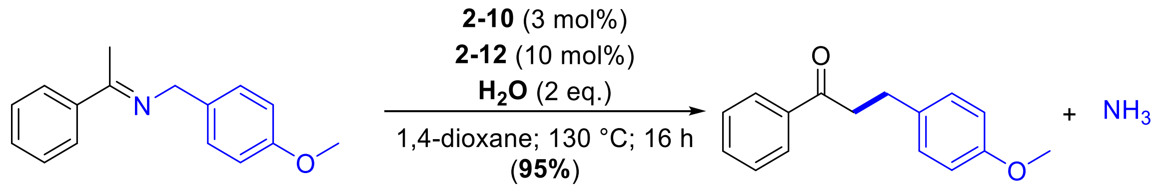

3-13a **3-10a**

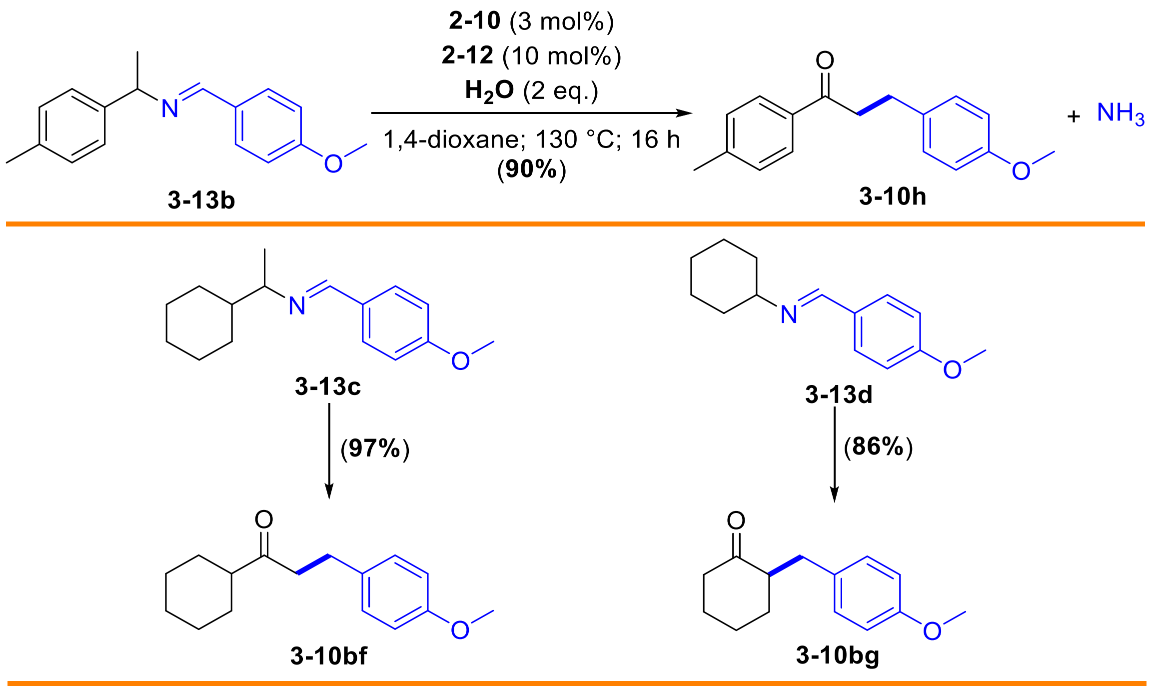

Scheme 3.6: Reaction of Imine Species **3-13a-d** Substrates Under Standard Reaction Conditions

In this case, the addition of water was found to be essential because a stoichiometric amount of water would be required for the hydrolysis of imine in forming the ketone product **3-10a**. Similar reactivity has been observed when the reaction was performed with the aldimine species **3-13b**, which was independently generated from the reaction of 1-(4-methylphenyl)ethylamine with 4-methoxybenzaldehyde. This observation suggested that the imine isomerization of 1-(4-methoxyphenyl)-N-(1-(p-tolyl)ethyl) methanimine **3-13b** to (4-Methoxyphenyl)-*N*-(1-phenylethylidene) methanamine **3-13a** is a possible pathway before the alkylation step. Also, independently synthesized aldimines **3-13c** and **3-13d** from the reaction of 4-methoxybenzaldehyde with cyclohexylamine and (S)-(+)-1-cyclohexylethylamine afforded the corresponding alkylated products **3-10bf** and **3-10bg** in 97% and 86% yields, respectively (**Scheme 3.6**).

3.2.4.3 Crossover Experiment

Both the reaction profile and the imine reaction experiments established that the imine **3-13a** is the requisite intermediate for the alkylation product **3-10a**. To probe whether **3-10a** is resulted from an intramolecular or an intermolecular disproportionation process, we next performed a set of crossover experiments by using the isolated imine substrates **3-13a** and **3-13c**. Thus, a 1:1 mixture of the independently generated **3-13a** (0.25 mmol) and *N*-cyclohexylidene-3-phenylpropan-1-amine (**3-13c**) (0.25 mmol) in 1,4-dioxane (2 mL) was treated with the catalytic system **2-10**/**2-12** and water (0.50 mmol) under otherwise the standard reaction conditions for 16 h (**Eq. 3.2**).

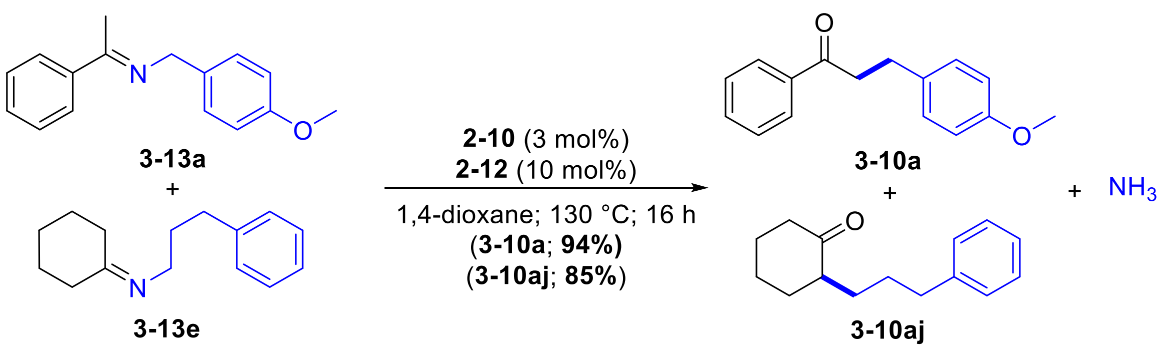

(Eq. 3.2)

The isolated product mixture contained a nearly 1:1 mixture of the products **3-10a** and **3-10aj** in 94% and 85% respectively, with only a small amount of the crossover products (<10%). The absence of crossover coupling products indicates that the conversion of initially formed Schiff base **3-13a** to the alkylation product **3-10a** predominantly proceeds via an intramolecular process.

3.2.4.4 Deuterium Labeling Study

We next examined the deuterium exchange pattern of the coupling reaction to probe the possible imine-to-enamine isomerization process. Thus, the treatment of perdeuterated acetophenone $C_6D_5COCD_3$ (0.50 mmol) with 4-methoxybenzylamine (0.70 mmol) in the presence of **2-10** (3 mol %)/**2-12** (10 mol %) under the standard conditions formed the coupling product **3-10a**-*d*, which was isolated by a column chromatography on silica gel (**Eq. 3.3**).

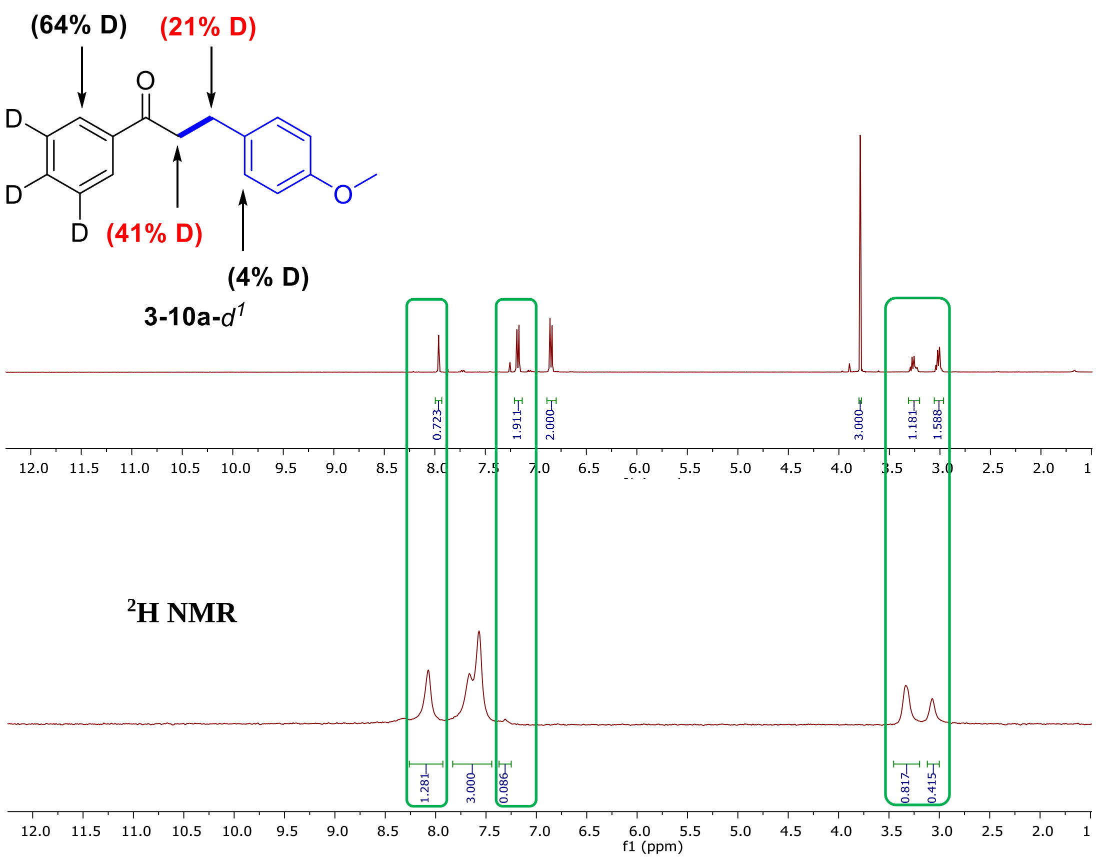

Figure 3.2: ^{1}H and ^{2}H NMR Spectra of the Product **3-10a**-*d*^{1}

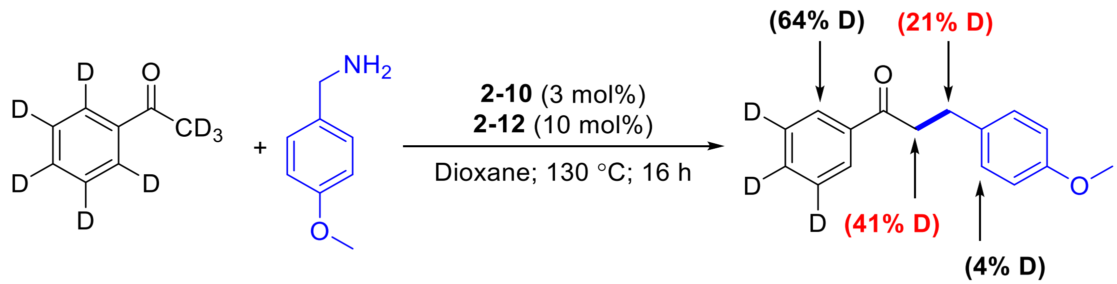

3-10a-*d*[1]

(Eq. 3.3)

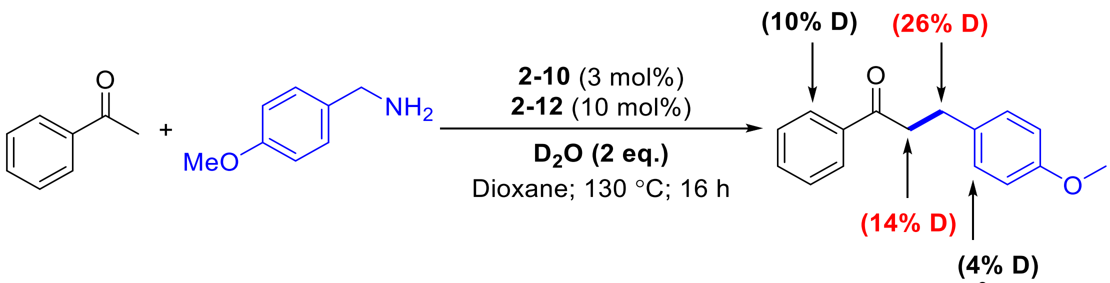

3-10a-*d*[2]

(Eq. 3.4)

The deuterium content of the isolated product **3-10a**-*d*[1] showed 41% on α-CH_2 and 21% on β-CH_2 positions as analyzed by ^{1}H and ^{2}H NMR (**Figure 3.2**). The analogous coupling reaction of acetophenone with 4-methoxybenzylamine and D_2O (2 eq.) resulted in 26% deuterium incorporation on the α-CH_2 and 14% on the β-CH_2 positions of the product **3-10a**-*d*[2] (**Eq. 3.4**). In a control experiment the treatment of **3-10a** with D_2O (2 eq.) under the standard reaction conditions were performed. However, significant deuterium exchange only to the α-CH_2 (30% D) without any measurable deuterium on β-CH_2 position of the product **3-10a** and in the **3-10a**-*d*[3] after the reaction (**Eq. 3.5**). A relatively high degree of H/D exchange on the α-CH_2 group of the isolated products **3-10a**-*d*[3] (30%) suggests a facile keto-enol tautomerization of the ketone product during and after the coupling reaction. In contrast, over 20% of deuterium incorporation on the β-CH_2 position of the product **3-10a**-*d*[1] (21%) and **3-10a**-*d*[3] (26%) supports the notion that a significant H/D exchange is resulted from the coupling reaction with amine substrate, and that the exchange process must have occurred during the coupling reaction, as noted by the absence of deuterium exchange under the control experiment conditions.

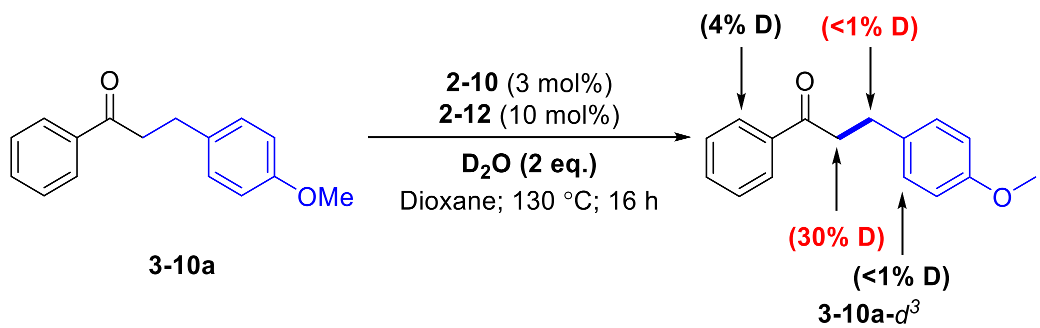

3-10a **3-10a**-*d*[3]

(Eq. 3.5)

The H/D exchange to α-CH_2 position can be readily explained by a facile and reversible imine-enamine tautomerization process, while the exchange to β-CH_2 position can be explained via an initial amine-imine dehydrogenation reaction (**Scheme 3.7**).

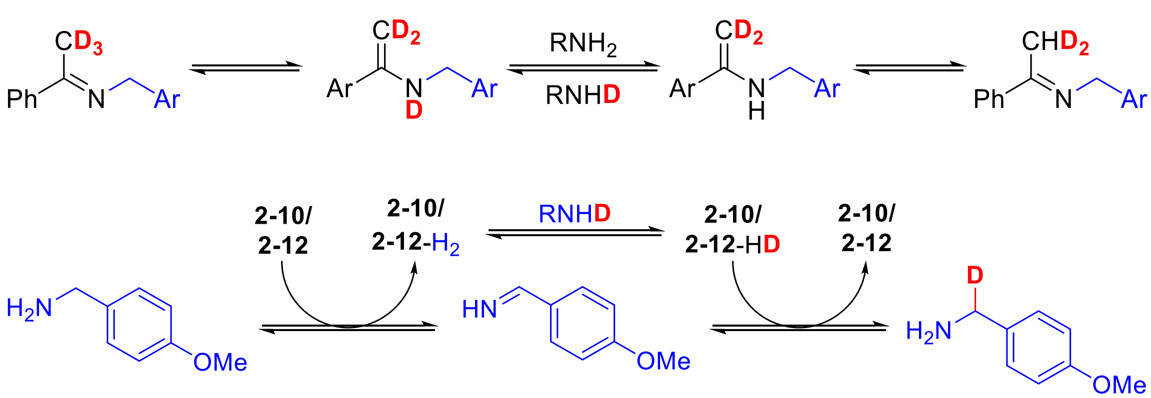

Scheme 3.7: H/D Exchange Mechanism via Imine-Enamine Tautomerization (top); and Amine-Imine Dehydrogenation Processes (bottom)

However, an alternate mechanism via the carbonyl-assisted 5-membered metallacyclic species cannot be ruled out at this point, in light of the recent development of carbonyl-directed catalytic sp^3 C–H functionalization methods.[17] In an unrelated process, an extensive H/D exchange on the *ortho*-arene position (64% of D) of the product **3-10-**d_1 can be explained via the chelate-assisted *ortho*-metalation and the reversible H/D exchange. This type of *ortho*-arene C–H/C–D exchange pattern has been commonly observed for chelate-assisted arene C–H insertion reactions.[150]

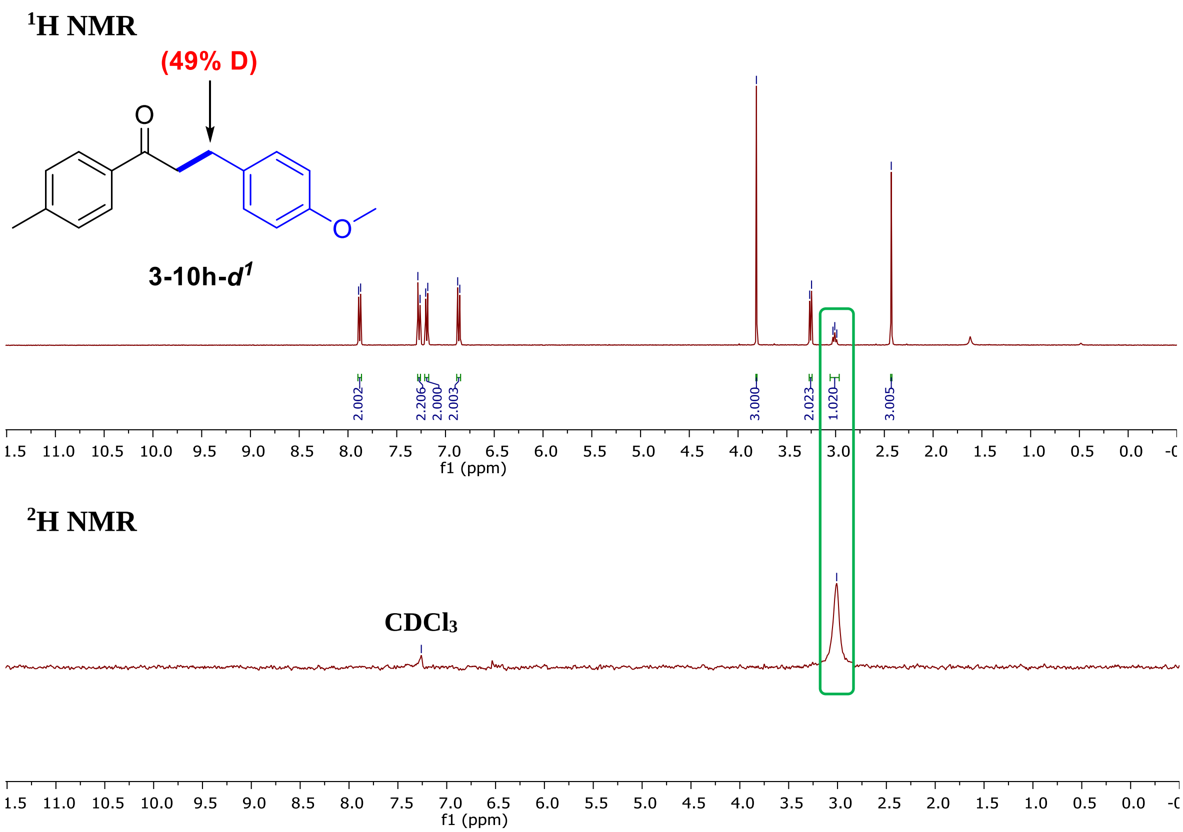

Figure 3.3: ^{1}H and ^{2}H NMR Spectra of **3-10h**-*d*^{1}

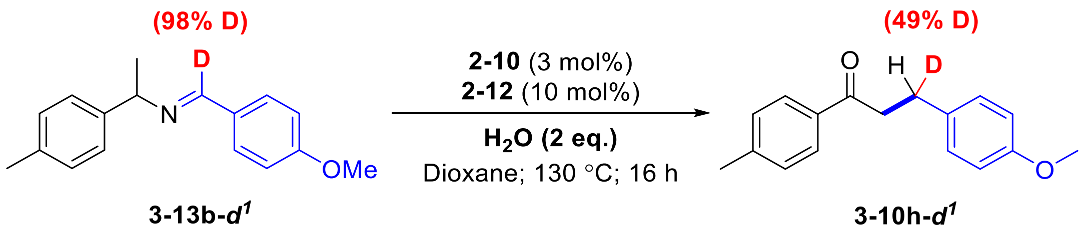

(Eq. 3.6)

Reversible H/D exchange process during the imine-enamine tautomerization was monitored by using the deuterium-labeled imine substrate **3-13b-**d^1, which was prepared from the reaction of 4-methoxybenzaldehyde-d^1 with 1-*p*-tolylethanamine. The treatment of **3-13b-**d^1 (98% D) with H_2O under the standard reaction conditions led to the formation of **3-10h-**d^1 with the exclusive deuterium on the β-CH_2 position (49% D), which amounts to >98% retention of the deuterium atom (**Eq. 3.6**). The absence of significant H/D exchange in the formation **3-10h-**d^1 is consistent with an irreversible C=N isomerization of an aldimine **3-13b-**d^1 to a more stable ketimine prior to the product formation. The similar imine-enamine tautomerization process has been observed in a number of metal-catalyzed C–C and C–N coupling reactions.[19]

3.2.4.5 Deuterium Isotope Effect Study

To probe electronic effects on the α-C–H bond activation, we measured the deuterium kinetic isotope effect for the α-alkylation reaction catalyzed by the complex **2-10**/**2-12** ligand with (4-Methoxyphenyl)-*N*-(1-phenylethylidene)methanamine **3-13a** (**Eq. 3.7**) and **3-13a**-*d* (**Eq. 3.8**). Thus, the rate of **3-13a** and **3-13a-***d* in the presence of **2-10** (3 mol %)/**2-12** (10 mol %) was measured by monitoring the appearance of the product signals on ^{1}H NMR, which were normalized against the peak of an internal standard (C_6Me_6). The k_{obs} was determined from a first-order plot of -ln[((**3-13a**$_0$) – (**3-13a**$_t$))/**3-**

13a$_0$] vs time (**Figure 3.4**). Deuterium kinetic isotope effect on the α-hydrogen of the **3-13a** intermediate was found to be k_H/k_D= 1.0±0.1, which indicates C–H activation of the reaction is not involving in the turnover limiting step.

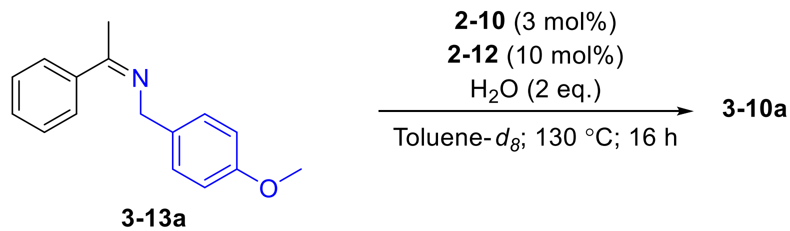

(Eq. 3.7)

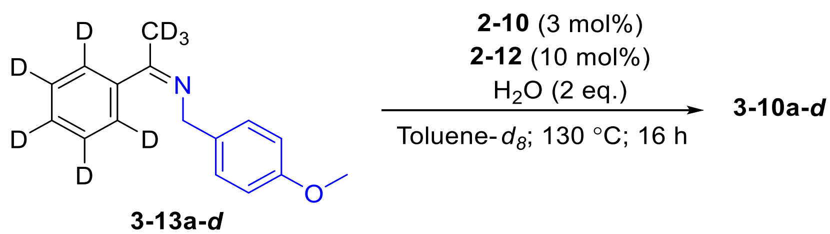

(Eq. 3.8)

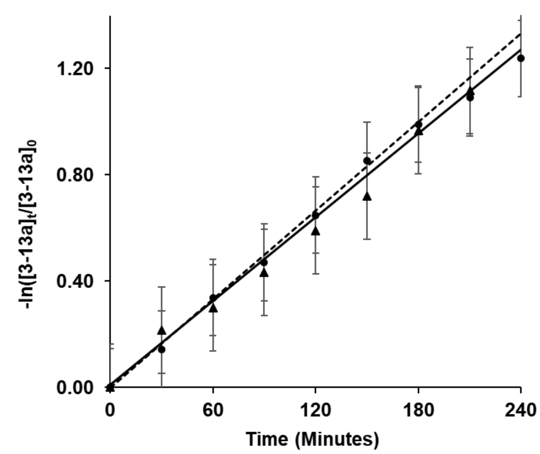

Figure 3.4: First Order Plot of the Catalytic α-Alkylation of (4-Methoxyphenyl)-N-(1-phenylethylidene)methanamine (▲) and Deuterated (4-Methoxyphenyl)-N-(1-phenylethylidene)methanamine (●)

3.2.4.6 Hammett Study

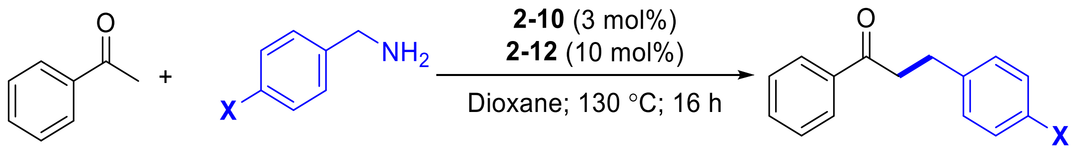

(Eq. 3.9)

Hammett equation describes a linear free-energy relationship of the reaction rates and equilibrium constants with respect to electronic nature of the substrates. We compared the electronic effects for the alkylation reaction by measuring the rates of the alkylation reaction of acetophenone with a series of *para*-substituted benzylamines *p*-X-$C_6H_4CH_2NH_2$ (X = OMe, Me, H, F, Cl, CF_3) (**Eq. 3.9**). The rate of the coupling reaction of acetophenone (0.20 mmol) with a *para*-substituted benzylamine (0.30 mmol) in the presence of **2-10** (3 mol %)/**2-12** (10 mol %) in toluene-d_8 was monitored by NMR.

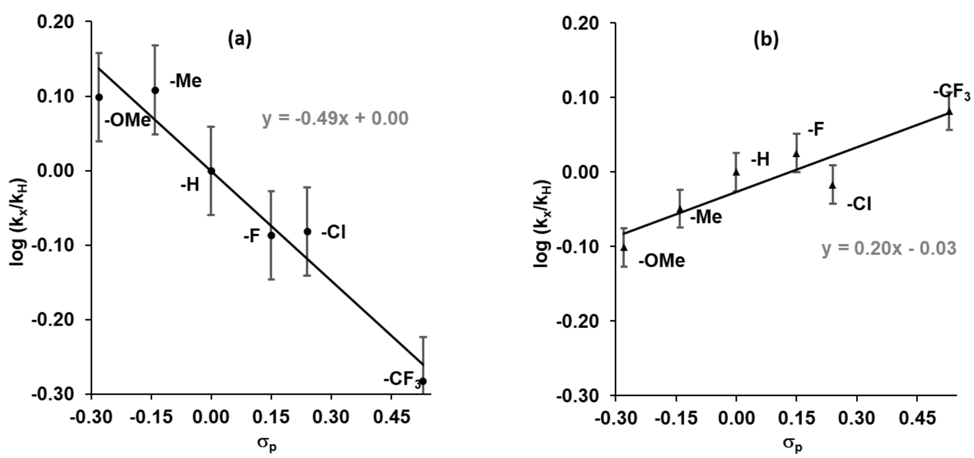

Figure 3.5: (a) Hammett Plot from the Coupling Reaction of Acetophenone with *p*-X-$C_6H_4CH_2NH_2$; (b) Hammett Plot from the Coupling Reaction of *p*-Y-$C_6H_4COCH_3$ with 4-Methoxybenzylamine

The appearance of the product peak **3-10** was normalized against an internal standard (C_6Me_6) in 30 min intervals, and the k_{obs} of each catalytic reaction was determined from a first-order plot of $ln[([C_6H_5COMe]_I - [C_6H_5COMe)]_t) /([C_6H_5COMe)]_i)_0]$ vs time. The Hammett plot of $\log(k_X/k_H)$ vs σ_p showed a linear correlation, in which the reaction is strongly promoted by an electron-releasing group of the amine substrate ($\rho = -0.49 \pm 0.1$) (**Figure 3.5a**). The analogous Hammett plot was also obtained from the alkylation reaction of a series of *para*-substituted acetophenones *p*-Y-C_6H_4COMe (Y = OMe, Me, H, F, Cl, CF_3) with 4-methoxybenzylamine (**Eq. 3.10**).

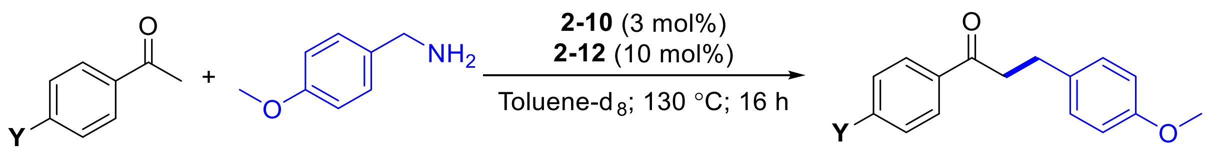

(Eq. 3.10)

The rate of the coupling reaction of a *para*-substituted acetophenone (0.20 mmol) with 4-methoxybenzylamine (0.30 mmol) in the presence of **2-10** (3 mol %)/**2-12** (10 mol %) in toluene-d_8 was measured by NMR, and the k_{obs} of each catalytic reaction was determined from a first-order plot of $ln[p\text{-OMe-}C_6H_4CH_2N{=}C(Me)\text{-}p\text{-Y-}C_6H_4]_i\text{-}[p\text{-OMe-}C_6H_4CH_2N{=}C(Me)\text{-}p\text{-Y-}C_6H_4]_t)/([p\text{-OMe-}C_6H_4CH_2N{=}C(Me)\text{-}p\text{-Y-}C_6H_4]_i)_0]$ vs time. In this case, the coupling reaction was moderately promoted by an electron-withdrawing group of the ketone substrate, as indicated by a relatively modest slope ($\rho = +0.20 \pm 0.1$) (**Figure 3.5b**). A strong promotional effect from *para*-electron-releasing group of the benzylamines suggests that the C–N bond cleavage step is strongly influenced by the nucleophilicity of the benzylic carbon. On the other hand, a moderate promotional effect from electron-deficient *para*-substituted acetophenones indicates that the electrophilic nature of the α-carbon of the ketone substrate is a significant factor for the C–C bond formation step.

With the observations of the Hammett correlation data in hand, we decided to perform a set of experiments to avoid the complex reaction kinetics by employing para substituted imines as the substrates (*p*-X-$C_6H_4CH_2N$=C(Me)C_6H_5; X = OMe, H, F, CF_3) and (*p*-OMe-$C_6H_4CH_2N$=C(Me)-*p*-Y-C_6H_4; Y = OMe, H, F, CF_3). The k_{obs} was determined from a first-order plot of -*ln*([*p*-X-$C_6H_4CH_2N$=C(Me)C_6H_5]$_t$/[*p*-X-$C_6H_4CH_2N$=C(Me)C_6H_5]$_0$) vs time (**Figure 3.6**).

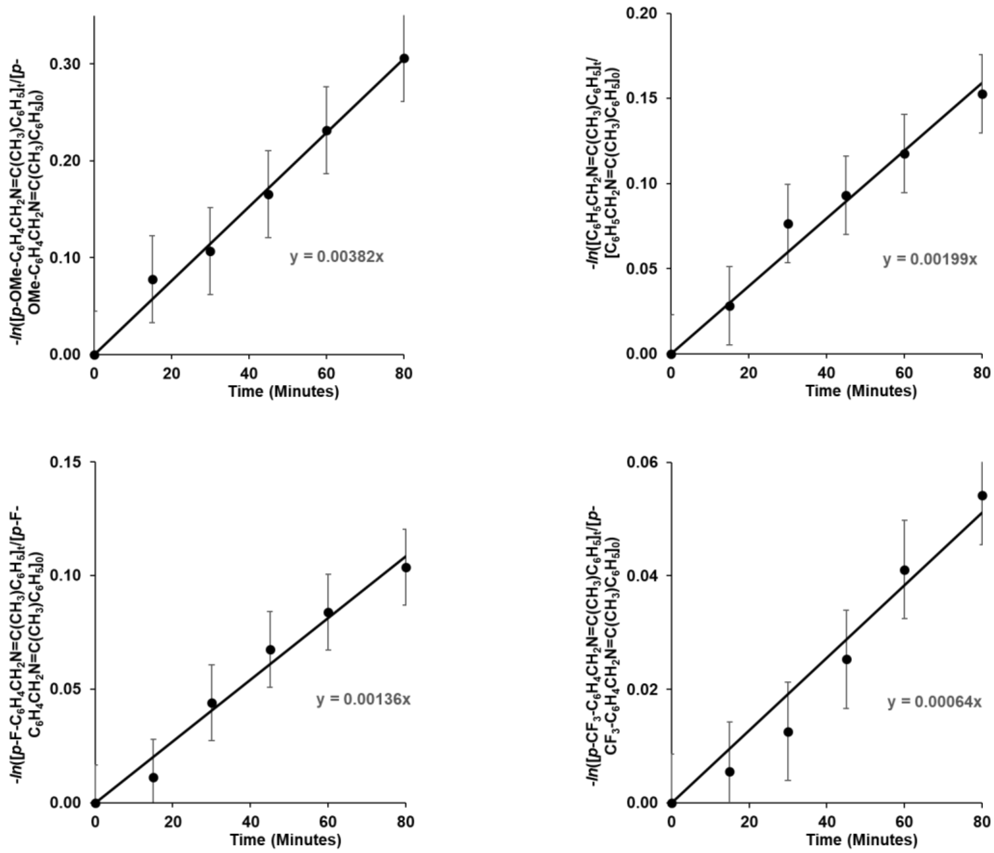

Figure 3.6: First-Order Plots of -*ln*([*p*-X-$C_6H_4CH_2N$=C(Me)C_6H_5]$_t$/[*p*-X-$C_6H_4CH_2N$=C(Me)C_6H_5]$_0$) vs time (X = OMe, H, F, CF_3)

Similarly, the k_{obs} of the analogous reaction was determined from a first-order plot of -*ln*([*p*-OMe-$C_6H_4CH_2N$=C(Me)-*p*-Y-C_6H_4]$_t$/[*p*-OMe-$C_6H_4CH_2N$=C(Me)-*p*-Y-C_6H_4]$_0$) (Y = OMe, H, F, CF_3) vs time (**Figure 3.7**). The Hammett plot of log(k_X/k_H) vs σ_p showed a linear correlation (**Figure 3.8**), suggesting that the initial formation and accumulation of the imine intermediate is not effectively involve in the overall kinetics for the coupling reaction of ketone and amine. This result is consistent with the electrophilic nature of the α-carbon of the imine intermediate is a significant factor for the C–C bond formation step.

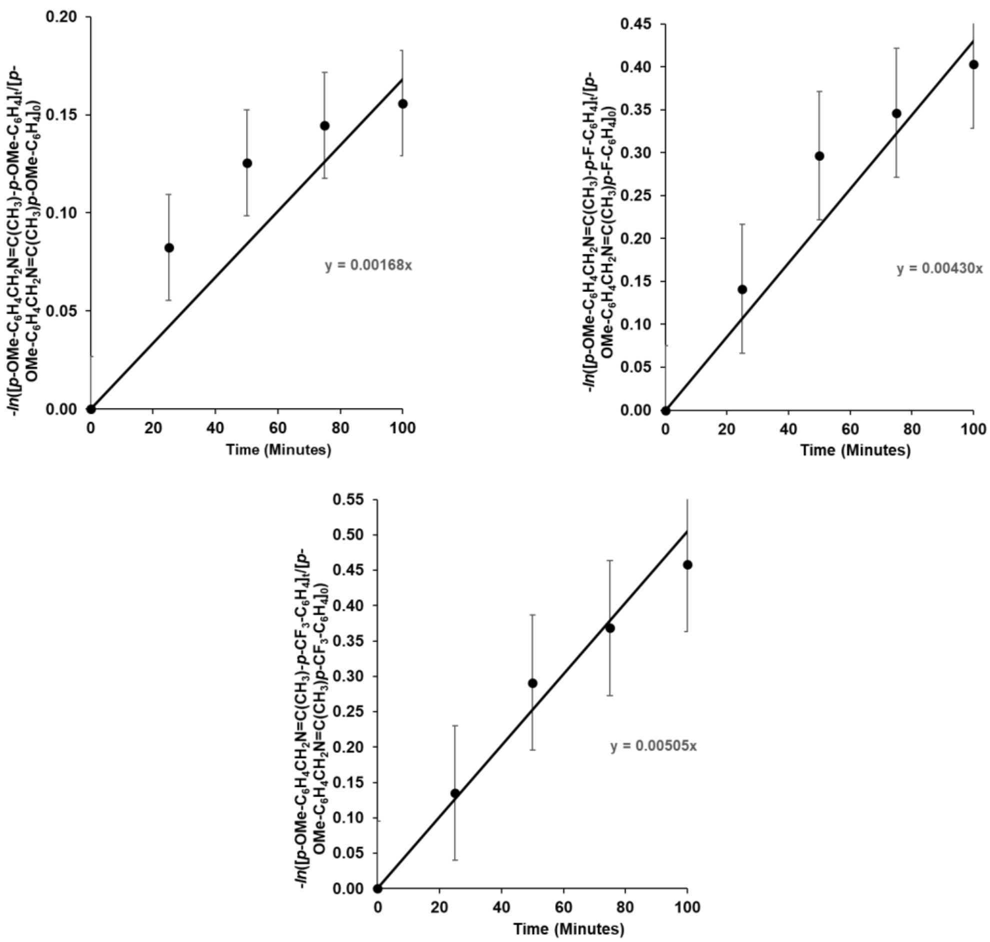

Figure 3.7: First-order Plots of -*ln*([*p*-OMe-$C_6H_4CH_2N$=C(CH_3)-*p*-Y-C_6H_4]$_t$/[*p*-OMe-$C_6H_4CH_2N$=C(CH_3)-*p*-Y-C_6H_4]$_0$) vs time (Y = OMe, F, CF_3)

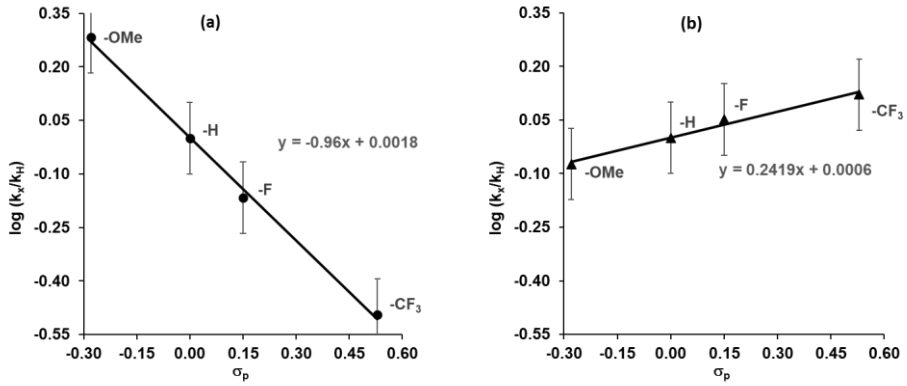

Figure 3.8: (a) Hammett Plot from the Rearrangement Reaction of *p*-X-$C_6H_4CH_2N=C(CH_3)C_6H_5$ (X = OMe, H, F, CF_3); (b) Hammett Plot from the Rearrangement Reaction of *p*-OMe-$C_6H_4CH_2N=C(CH_3)$-*p*-Y-C_6H_4 (Y = OMe, H, F, CF_3)

3.2.4.7 Carbon Isotope Effect Study

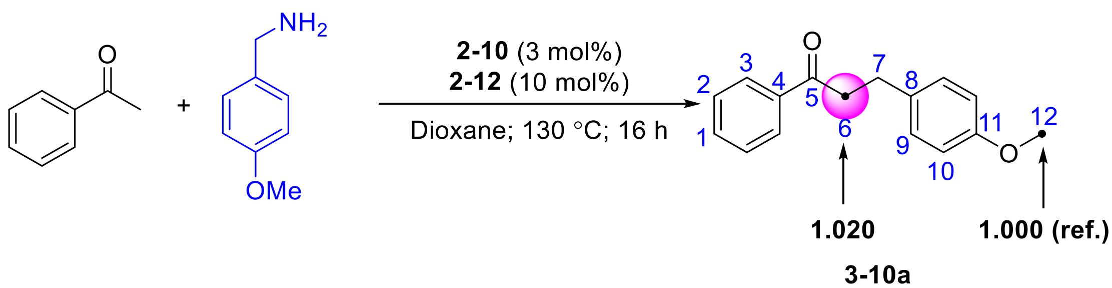

(Eq. 3.11)

The Hammett study implicates that either C–N bond cleavage or C–C bond formation is the most likely to be rate determining step for the catalytic alkylation reaction. To discern between these possible turnover limiting steps, we measured carbon kinetic isotope effect for the coupling reaction by employing Singleton's NMR technique at natural abundance.[127] Thus, the treatment of acetophenone (2.0 mmol) with 4-methoxybenzylamine (2.8 mmol) in the presence of **2-10** (3 mol %)/**2-12** (10 mol %) in 1,4-dioxane (8 mL) was heated at 130 °C for 20 h (**Eq. 3.11**). The product **3-10a** was isolated by a column chromatography on silica gel, and the procedure was repeated for three times to obtain a high product conversion sample of **3-10a**. The same experimental procedure was used for the isolation of a low product conversion sample of **3-10a**. The high precision ^{13}C NMR analysis showed the significant carbon isotope effect on the α-carbon of the product **3-10a** when the ^{13}C ratio of the product from a high conversion was compared with the sample obtained from a low conversion (^{13}C (avg 77% conversion)/^{13}C (avg 13% conversion) at C_α = 1.020±0.001; average of three runs), (**Table 3.6**). The observed carbon isotope effect on the α-carbon of the product **3-10a** can be rationalized via an asynchronous transition state on the C–C bond formation step.

Table 3.6: Average ^{13}C Integration of the Product **3-10a** Obtained from the Reaction of Acetophenone and 4-Methoxybenzylamine at High Conversion (Virgin, R_0; 78% conversion), at Low Conversion (R; avg 13% conversion) and the Calculated ^{13}C KIE (C12 = reference)

Carbon #	High Conversion (R_0)	Low Conversion (R)	R_0/R	KIE
1	1.1206	1.1213	0.9994	0.9994
2	2.1720	2.1728	0.9996	0.9996
3	2.1094	2.1207	0.9947	0.9947
4	1.1497	1.1475	1.0019	1.0019
5	1.1355	1.1351	1.0004	1.0004
6	**1.0694**	**1.0488**	**1.0196**	**1.0196**
7	1.0641	1.0668	0.9975	0.9975
8	1.1424	1.1481	0.9950	0.9950
9	2.0528	2.0552	0.9988	0.9988
10	2.0312	2.0392	0.9961	0.9961
11	1.1467	1.1504	0.9968	0.9968
12 (ref)	1.0000	1.0000	1.0000	1.0000

In support of this notion, Singleton and co-workers showed that the observation of most pronounced carbon isotope effect is a definitive evidence for establishing the rate-limiting step for both C–C and C–O bond forming reactions.[151] The C–N bond cleavage step has also been commonly considered as the turnover limiting step for catalytic reductive coupling reactions of amines and related organonitrogen compounds.[3b, 64b]

3.2.4.8 Determination of an Empirical Rate Law

Kinetics for the transformation of the isolated imine **3-13a** was measured as a function of [**2-10**], [**3-13a**] and [H_2O] under the standard reaction conditions unless otherwise noted (**Eq. 3.12**). Isolated imine **3-13a** has been used as the substrate to avoid induction period kinetics during the formation of **3-10a** or possible accumulation of intermediate species from the initial dehydration reaction.

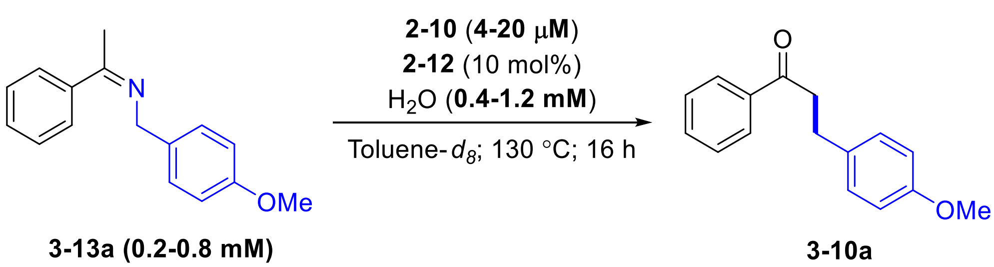

(Eq. 3.12)

The initial rate was measured from the appearance of the product of **3-10a** at four different catalyst concentrations (4-20 μM). The plot of **3-10a** vs time under four different catalyst concentrations clearly shows the concentration dependence with respect to **2-10** (**Figure 3.9a**). The plot of initial rate (v_0) as a function of [**2-10**] yielded a linear slope with the first order rate constant of 2.8×10^{-3} s^{-1} (**Figure 3.9b**).

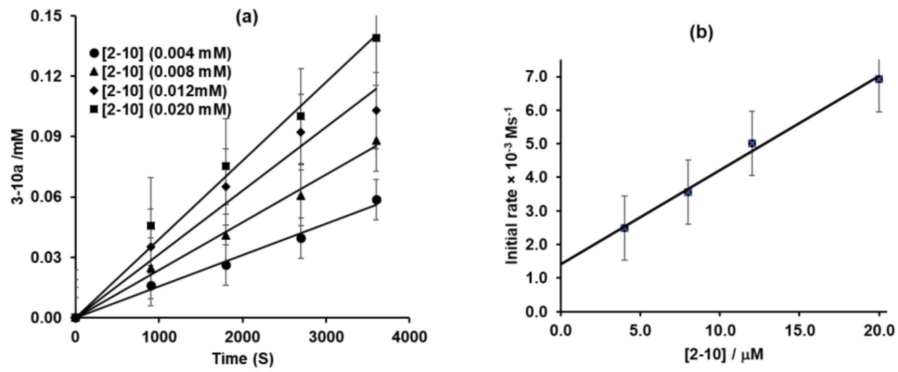

Figure 3.9: Plots for the (a) **3-10a** vs Time and (b) Initial Rate vs [**2-10**]

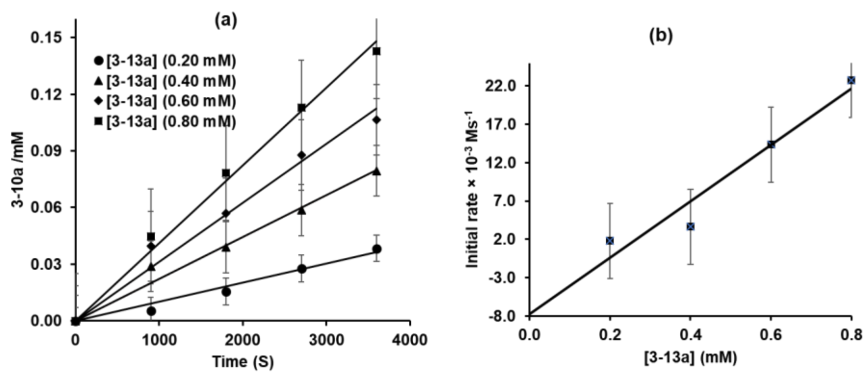

Figure 3.10: Plots for the (a) **3-10a** vs Time and (b) Initial Rate vs [**3-13a**]

As expected, the plot of **3-10a** vs time under four different imine concentrations of **3-13a** (0.2-0.8 mM) indicated the first order concentration dependence. The initial rate as a function of the substrate concentration [**3-13a**] (0.2-0.8 mM) also showed the first order rate dependence on **3-13a** in the range of the catalytically relevant concentrations (0.2-0.8 mM) (**Figure 3.10b**).

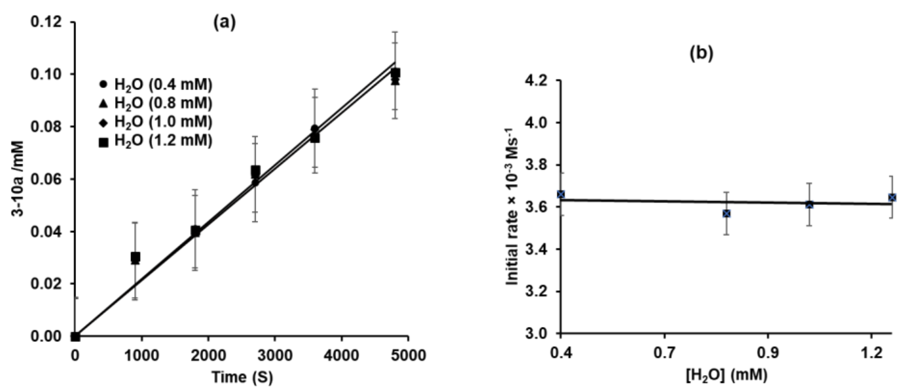

Figure 3.11: Plots for the (a) **3-10a** vs Time and (b) Initial Rate vs [**H_2O**]

On the other hand, no water concentration dependence was observed for the transformation (**Figure 3.11a**). The plot of initial rate vs [H_2O] showed a zero-order dependence in the range of 0.4-1.2 mM (**Figure 3.11b**). On the basis of these kinetic data, the empirical rate law for the reaction has been compiled as rate = k[**2-10**][**3-13a**]. The first order rate dependence on both [**3-13a**] and the catalyst [**2-10**] is consistent with an intramolecular process on the formation of **3-10a**, whereas the rate independence on [H_2O] indicates a facile imine hydrolysis step during the catalysis.

3.2.5 Detection of Catalytically Relevant Organic Products

We reasoned that the intramolecular alkyl migration mechanism would be the key step for the desired α-alkylated product formation, in which an enamine species would be a requisite intermediate for the coupling reaction. In an effort to detect the catalytically relevant enamine products, we were able to isolate and characterize the (Z)-1,1,1-trifluoro-4-(naphthalen-2-yl)-4-(3,4,5-trimethoxy benzylamino)but-3-en-2-one product **3-**

14 from the reaction of 4,4,4-trifluoro-1-(2-naphthyl)-1,3-butanedione and 3,4,5-trimethoxybenzylamine under standard reaction conditions (**Eq. 3.13**).

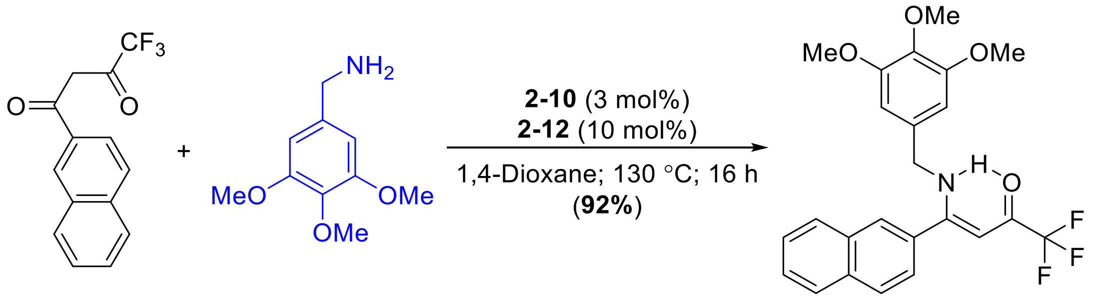

3-14

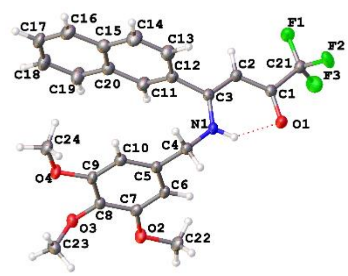

(Eq. 3.13)

The imine product **3-13** was established by both NMR and X-ray crystallographic methods, which clearly indicated that the formation of intramolecular hydrogen bonding stabilized the enamine intermediate. This observation indirectly supports the formation of enamine intermediate as the reaction did not yield the product **3-13** in the absence of the ruthenium catalyst **2-10**. When the isolated product **3-35** was subjected to the standard reaction conditions, it did not form the alkylation product, probably due to the stabilization of intramolecular hydrogen bonding and electronic reasons.

In a separate experiment, we tested the imine isomerization on ruthenium catalytic system by employing independently synthesized (E)-N-(4-methoxybenzylidene)-1,1-diphenylmethanamine **3-13f** under standard reaction conditions (**Eq. 3.14**). The aldimine product was completely isomerized into a stable ketoimine product *N*-(4-Methoxybenzyl)-1,1-diphenylmethanimine **3-13g**.

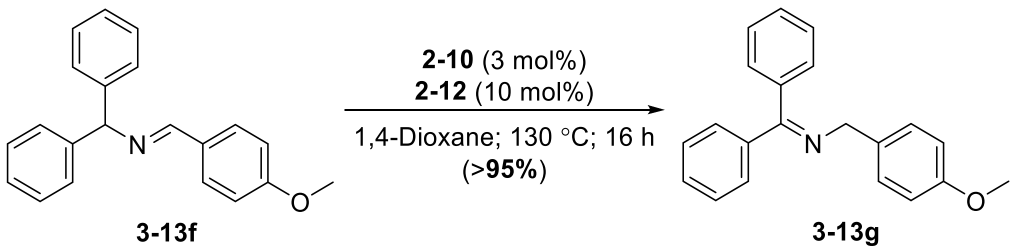

(Eq. 3.14)

When the catalytic system was tested for the reaction of electron rich ketone with 4-methoxybenzylamine under the standard reaction conditions, about 20% of unexpected byproduct **3-15** was formed along with 56% desired product **3-10g** (**Eq. 3.15**). In this case, the formation of trisubstituted pyridine byproduct **3-15** was difficult to rationalize due to symmetric nature of the product formation.

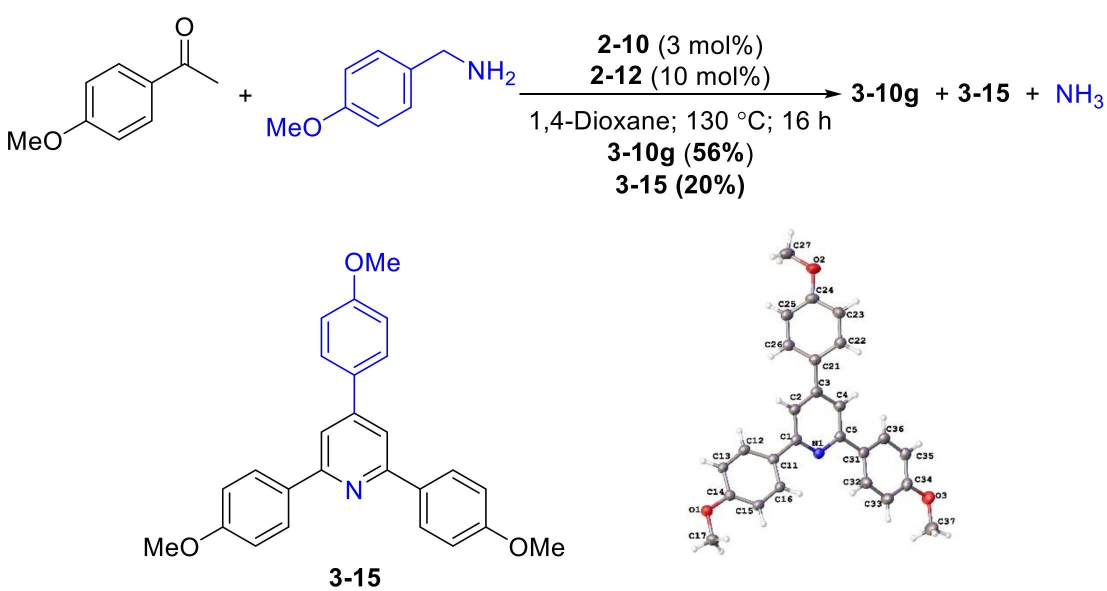

(Eq. 3.15)

In order to understand the reaction mechanism of the trisubstituted pyridine byproduct we decided to isolate and characterize the byproduct formed from the reaction of 7-bromo-1-tetralone with 2-thiophenemethylamine. To our delight we were able to obtain similar pyridine byproduct **3-16** from the 2:1 coupling of ketone and amine substrates (**Eq. 3.16**).

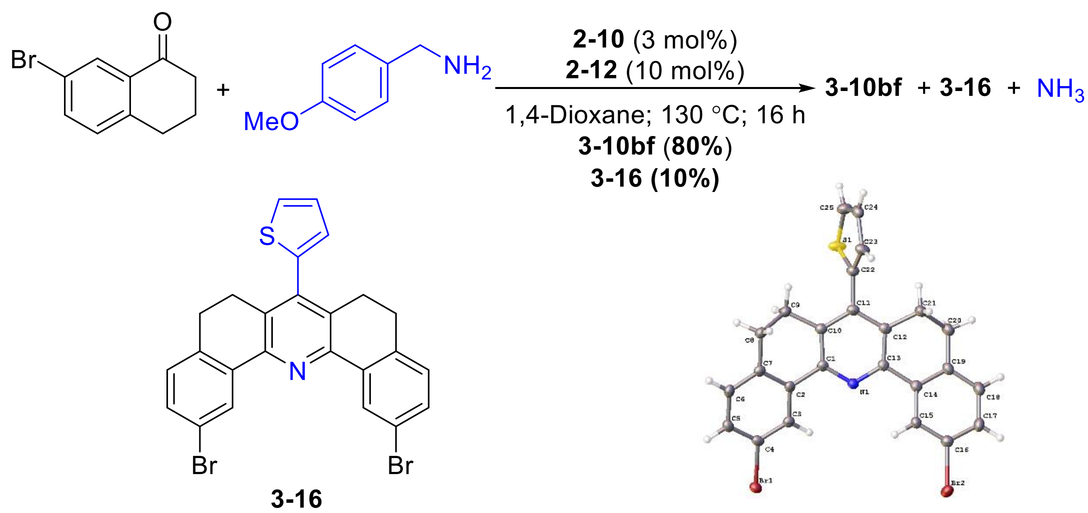

(Eq. 3.16)

This observation clearly suggested that the formation of the pyridine product **3-16** was resulted from the second enolate attack. As the imine intermediate proceeded the formation of desired alkylated product, the in-situ generated imine **3-16a**, from the initial dehydrative coupling of ketone and amine substrates, is the active substrate for the catalytic alkylation reaction. Coordination of the imine **3-16a** with the active ruthenium complex followed by imine-to-enamine isomerization and subsequent C-N bond activation would form intermediate ruthenium alkyl complex **3-16b**. An intramolecular [1,3]-alkyl migration would form the Ru-imine species **3-16c** and double bond isomerization would form the intermediate species **3-16d** and **3-16e**. Second enolate attack (2+2 addition) followed by dehydrative aromatization would generate the observed trisubstituted byproduct **3-16**. This observation provides an additional supportive evidence for the intra molecular 1,3-alkyl migration from the Ru-imine species.

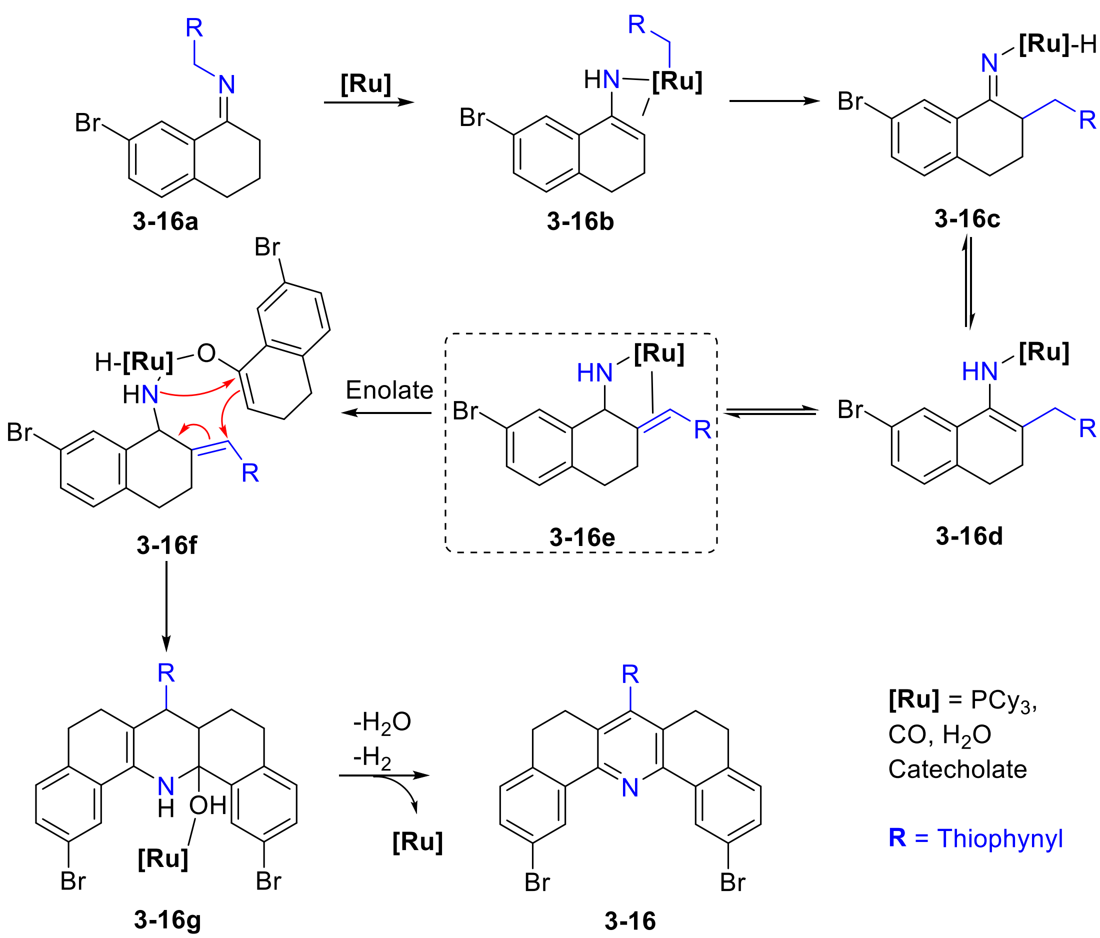

Scheme 3.8: Tentative Reaction Mechanism for the Formation of 2:1 Byproduct **3-16** from the Reaction of 7-bromo-1-tetralone with 2-thiophenemethylamine

3.2.6 Determination of Catalytic Activity of the Ru-Catecholate Complex 2-11

In an effort to detect/trap catalytically relevant species, we examined the reaction of **2-10** with a number of catechol and benzoquinone ligands. The complex **2-10** (117 mg, 0.20 mmol), 3,5-di-*tert*-butyl-o-benzoquinone **2-12b** (44 mg, 0.20 mmol), PCy_3 (56 mg, 0.20 mmol) were dissolved in CH_2Cl_2 (3 mL) in a 25 mL Schlenk tube equipped with a

Teflon screw cap stopcock and a magnetic stirring bar under N_2 stream. After stirring for 24 h in a water bath set at 70 °C, the solvent was removed under vacuum, and the residue was washed with 2% hexanes/EtOAc under nitrogen atmosphere. The resulting residue was dissolved in acetone (3 mL), layered with n-pentane (4 mL), and stored in a glove box for five days for crystallization. The resulting solid was filtered through a fritted funnel to yield the complex **2-11** (102 mg, 56%) as a reddish crystalline solid. Single crystals of **2-11** were obtained by slow evaporation in EtOAc/pentanes, and its structure was determined by X-ray crystallography (**Eq. 3.17**).

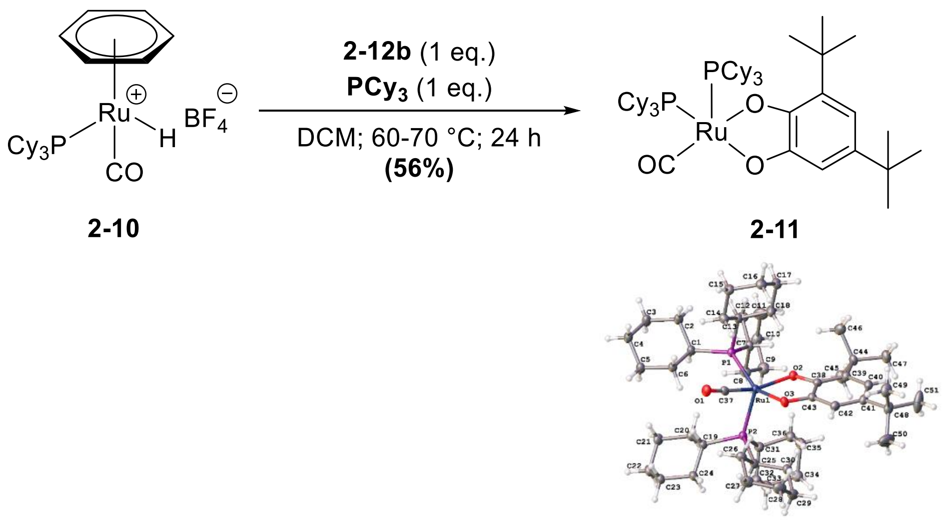

(Eq. 3.17)

The ruthenium catecholate complex **2-11** was found to exhibit a high catalytic activity for the alkylation reaction. For example, the treatment of acetophenone with 4-methoxybenzylamine in the presence of **2-11** (1 mol %) otherwise under the standard conditions efficiently afforded the alkylation product **3-10a** in 90% yield within 2 h (**Eq. 3.18**). It should be noted that the catalytic activity of **2-11** is substantially higher than the *in-situ* generated one, giving the desired product **3-10a** in a shorter reaction time at a lower catalyst loading.

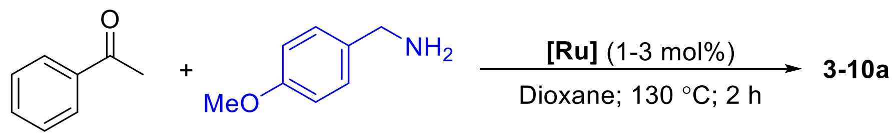

[Ru]	mol%	Yield of 3-10a
2-10/2-12b	3	(50%)
2-11	1	(90%)

(Eq. 3.18)

The rate of the transformation of imine **3-13a** to **3-10a** was quantitatively measured by using the catalyst **2-11** under the similar conditions as described in **Eq. 3.12**. The initial rate of the appearance of the product **3-10a** was measured at four different catalyst concentrations (4-12 mM), and the plot of initial rate (ν_0) as a function of [**2-11**] yielded the observed rate constant $k = 7.0 \times 10^{-3}$ s^{-1}, which is 2.5 times larger than the rate measured from *in-situ* generated catalyst **2-10**/**2-12** ($k = 2.8 \times 10^{-3}$ s^{-1}) (**Figure 3-12**).

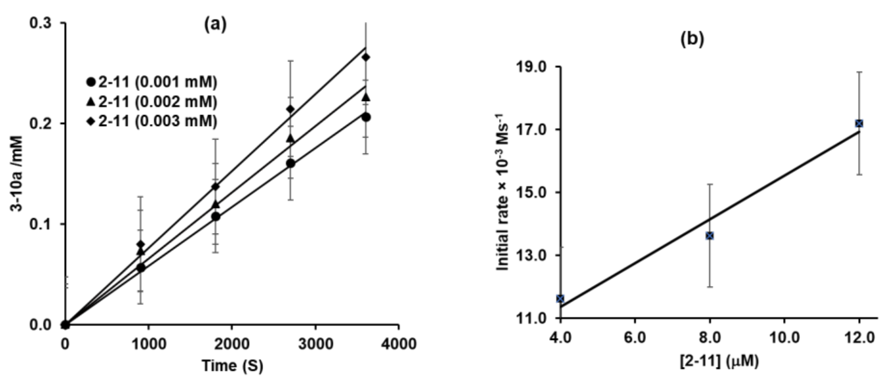

Figure 3.12: Plots for the Dependence of the Ruthenium Catecholate Complex **2-11** (a) **3-10a** vs Time and (b) Initial Rate vs [**2-11**]

Furthermore, to demonstrate its synthetic utility, a gram scale reaction was performed for the coupling reaction of acetophenone with 4-methoxybenzylamine by using the catalyst **2-11** (1 mol %), which yielded the product **3-10a** in 90% yield under the standard reaction conditions (**Eq. 3.19**). These results clearly demonstrate that the Ru-catecholate complex **2-11** is a catalytically relevant species for the alkylation reaction.

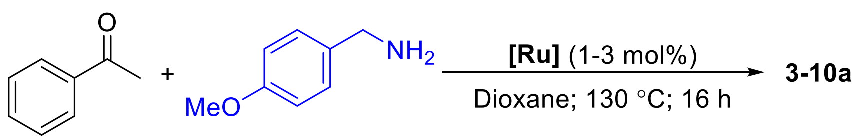

[Ru]	mol%	Yield of 3-10a
2-10/2-12b	3	(85%)
2-11	1	(90%)

(Eq. 3.19)

3.2.7 Computational Studies

3.2.7.1 Mechanistic Insights on Alkyl Migration Step

To gain detailed mechanistic insights on the requisite C–N bond cleavage step of the reaction, we performed density functional theory (DFT) computational analysis. Entire computational work was performed by our collaborator Marat R. Talipov, New Mexico State University. Initially, we carried out the calculations on a sigmatropic transformation of *N*,*N*-ethyl-2-propenylamine **3-18** into pentan-2-imine **3-19** in the absence of Ru catalyst by using a closed-shell M06L/def2-TZVPPD//M06L/def2-SV(P)+PCM(1,4-dioxane) method, which has successfully located the transition state for [1,3]-sigmatropic shift of ethyl group (**Figure 3.13**). However, in this case, the activation enthalpy exceeded the total enthalpy of separated ethyl and isopropenyl amino radicals (62.5 kcal/mol), which suggests that [1,3]-sigmatropic shift is not an energetically feasible pathway for this transformation ($\mathrm{D}H^{\ddagger}$ = 75.7 kcal/mol). Indeed, we found no viable transition state for the sigmatropic transformation by using an open-shell variation of the same computational method. The DFT analysis of non-catalyzed model system clearly suggested the efficacy of Ru-catalyzed enamine-to-imine transformation. We next performed the calculations for the same transformation in the presence of the Ru-catecholate complex **2-11** (without the *t*-Bu groups). Initial computational efforts to locate the transition state via a concerted sigmatropic rearrangement pathway were unsuccessful despite numerous attempts using either closed- or open-shell formalism.

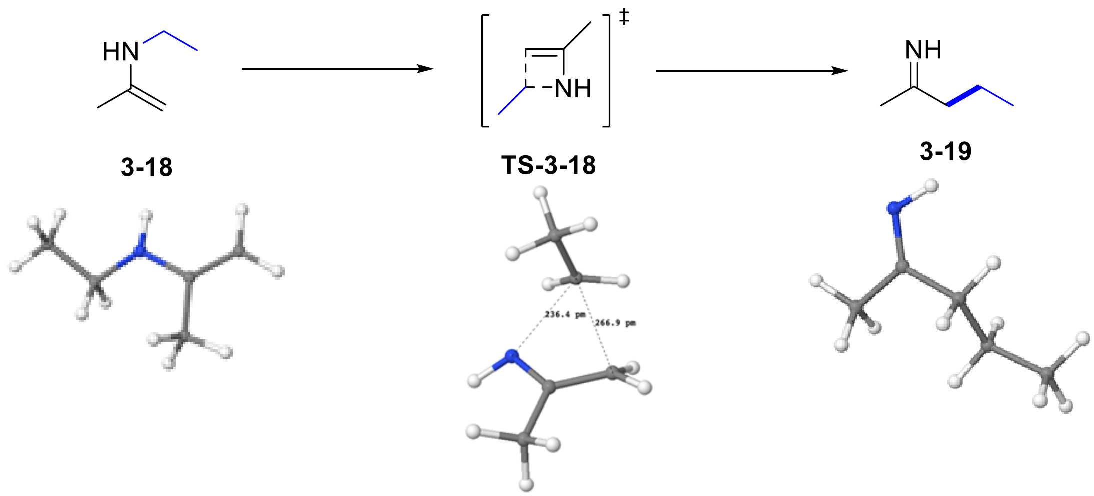

Figure 3.13: Schematic Representation of a Sigmatropic Transformation of *N*,*N*-Ethyl-2-Propenylamine to Pentan-2-Imine without Ruthenium Catalyst

The anticipated sigmatropic rearrangement pathway for **3-20a** to **3-22a** was eventually found by using the nudged elastic band (NEB) technique at the CASSCF(2,2)/def2-SV(P) level of theory, but the highest point of the pathway has 90 kcal/mol higher energy than **3-20a**, which is prohibitively high for this transformation under normal thermal conditions. Instead, our DFT calculations revealed an alternate stepwise mechanistic pathway via the formation of a Ru-alkyl intermediate **3-21a** (**Figure 3.14**).

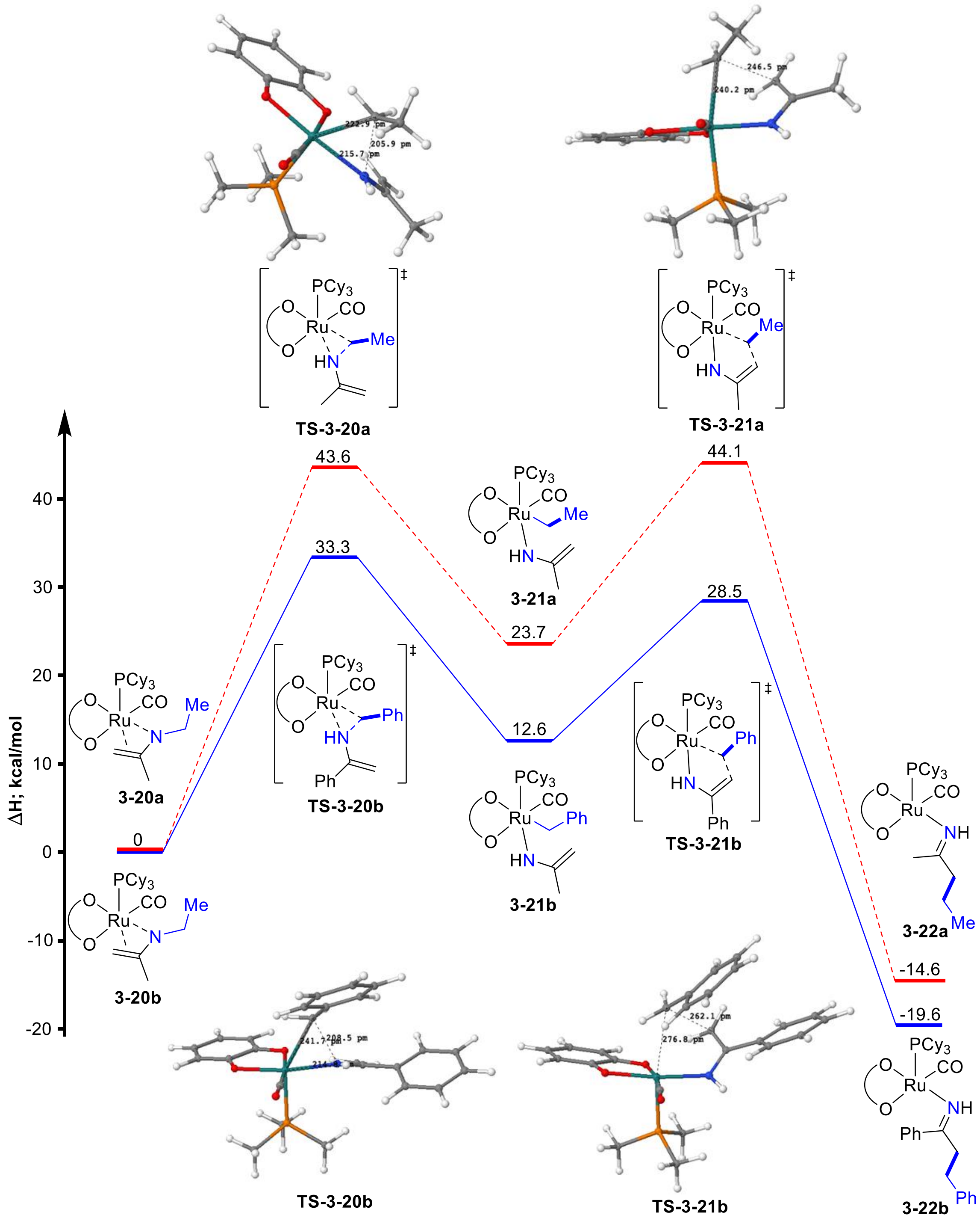

Figure 3.14: Enthalpy Profile for the Ru-mediated Transformation of **3-20a** to **3-22a** (Red Line) and **3-20b** to **3-22b** (Blue Line), Calculated at the M06L/def2-TZVPPD//M06L/def2-SV(P)+PCM(1,4-Dioxane) Level of Theory

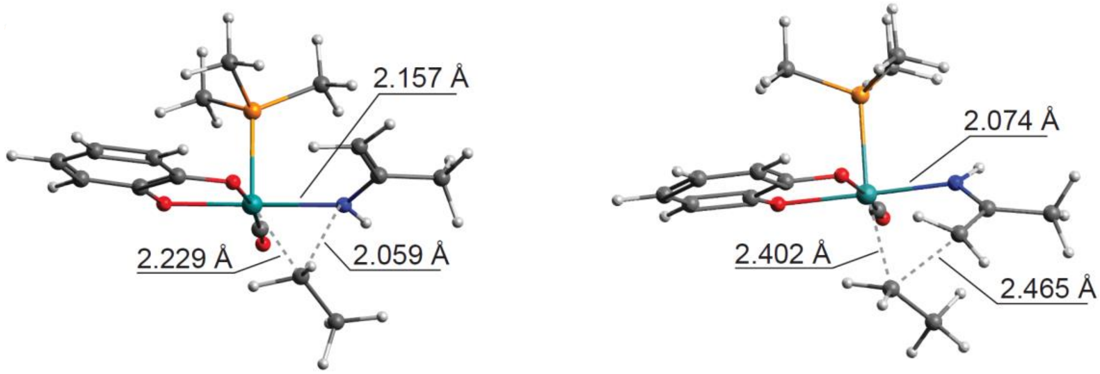

TS-3-20a **TS-3-21a**

Figure 3.15: Computed Structures of the Transition States **TS-3-20a** and **TS-3-21a**

The geometrically optimized structure of intermediate **3-21a** showed an octahedral Ru(IV) atom with a directly bound ethyl moiety. The activation enthalpies for both elementary steps were moderately low: for **3-20a** → **3-21a** via the transition state **TS-3-20a** has $DH^{\ddagger}$ = 43.6 kcal/mol, and for **3-21a** → **3-22a** via the **TS-3-21a** with $DH^{\ddagger}$ = 44.1 kcal/mol. Both activation enthalpy values are reasonable from the standpoint of experimental thermal conditions. The optimized structures of **TS-3-20a** and **TS-3-21a** (**Figure 3-15**) represent the transition of ethyl group from the nitrogen atom to ruthenium atom and from the ruthenium atom to the terminal carbon atom of the double bond, respectively. The visual analysis of the transition state structures was further supported by the intrinsic reaction coordinate (IRC) analysis. We observed that the reaction proceeds on the singlet potential energy surface with a formal Ru(IV) oxidation state, although the intermediate **3-21a** has a partial open-shell character ($\langle S^2 \rangle$ = 0.63/0.05 before/after the spin annihilation procedure, respectively) with a relatively low singlet-triplet gap of 13.4 kcal/mol. The analogous calculations for the benzyl-substituted enamine-to-imine rearrangement **3-20b** to **3-22b** showed a similar stepwise pathway via the Ru-benzyl intermediate **3-21b**, whose activation enthalpies were ~10 kcal/mol lower than the alkyl-substituted case ($\Delta H^{\ddagger}$ = 33.3 kcal/mol for **3-20b** → **3-21b**, $\Delta H^{\ddagger}$ = 28.5 kcal/mol for **3-21b** → **3-22b**) (**Figure 3.14**).

3.2.7.2 DFT Computational Study on Carbon Kinetic Isotope Effect

We also computed the carbon KIE by using the standard thermochemical analysis for the transformation of **3-20a** → **3-22a**. Specifically, we recalculated the activation enthalpy for the ^{13}C-modified **3-20a** and used the Eyring equation to evaluate the isotopic effect on the reaction rate. The computed carbon KIE value (C_α = 1.030) was in good agreement with the experimental KIE value (C_α = 1.020), which further corroborates a stepwise [1,3]-alkyl migration mechanism via the formation of Ru-alkyl intermediate **3-21**.

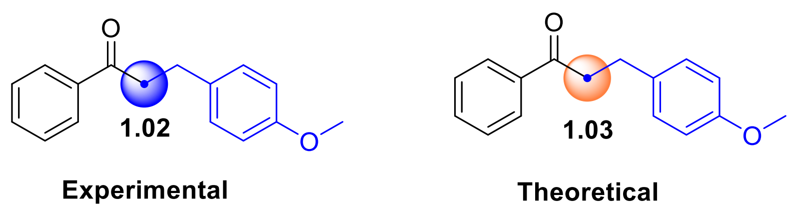

Figure 3.16: Experimental and Theoretical Carbon Kinetic Isotope Effects

3.2.7.3 DFT Computational Study on Hammett Study

Initial DFT calculations on the Hammett correlations by using the standard thermochemical analysis for the transformation of **3-20a → 3-21a** are consistent with the experimental data (**Figure 3.17a**). Also, the computed carbon enthalpy values for para substituted benzyl amine fragment of the enamine X = OMe, CF_3 found to be 32.4, 35.3 kcal/mol respectively and para substituted ketone fragment of the enamine X = CF_3, H, OMe found to be 32.3, 33.3, 33.6 kcal/mol respectively (**Figure 3.17b**; **3.18**). These data shown to be good agreement with the experimental Hammett correlations. These observations also further corroborates a stepwise [1,3]-alkyl migration mechanism via the formation of Ru-alkyl intermediate **3-41**.

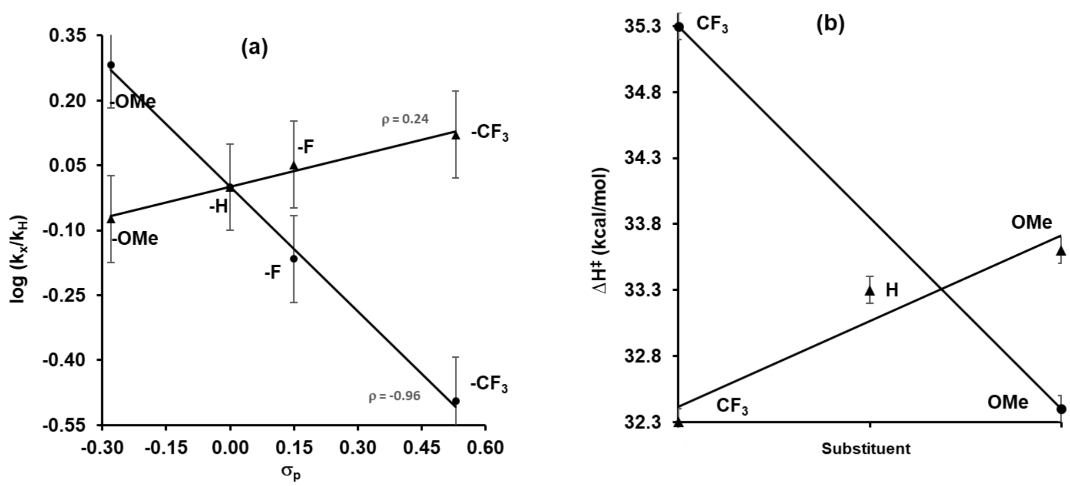

Figure 3.17: (a) Hammett Plot from the Reaction of *p*-X-$C_6H_4CH_2N$=C(CH_3)C_6H_5 (X = OMe, H, F, CF_3) (●) and *p*-OMe-$C_6H_4CH_2N$=C(CH_3)-*p*-Y-C_6H_4 (Y = OMe, H, F, CF_3) (▲); (b) Computed carbon enthalpy values for para substituted benzyl amine fragment of the enamine X = OMe, CF_3

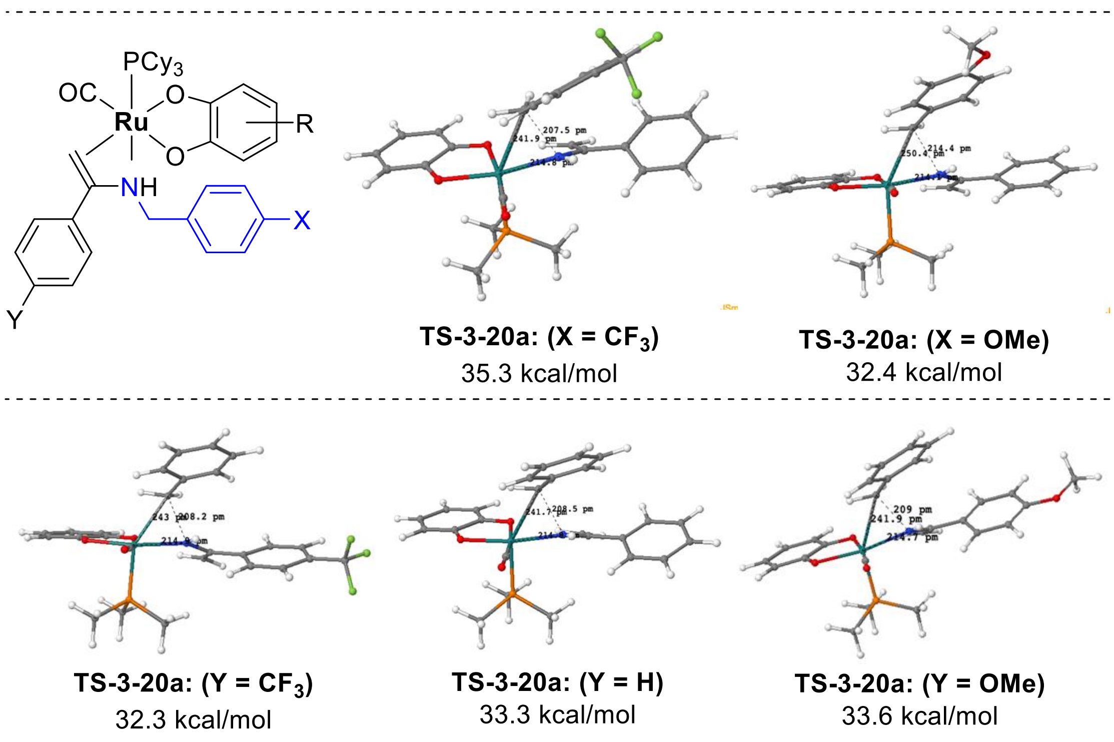

Figure 3.18: Transition States of the Standard Thermochemical Analysis for the Transformation of **3-20a** → **3-21a**

3.3 Proposed Mechanism of the Catalytic Reaction

We compiled a plausible mechanistic path for the alkylation reaction on the basis of these experimental and computational data (**Scheme 3.9**). The successful synthesis of the Ru-catecholate complex **2-11** and the demonstration of its high catalytic activity clearly support a coordinatively unsaturated Ru(II)-catecholate complex **3-23** as the catalytically active species. The coordinatively unsaturated Ru-catecholate complex **3-23** would be generated initially from the treatment of **2-10** with the reduced form of benzoquinone ligand via the ligand displacement, or directly from **2-11** via PCy_3 ligand dissociation.

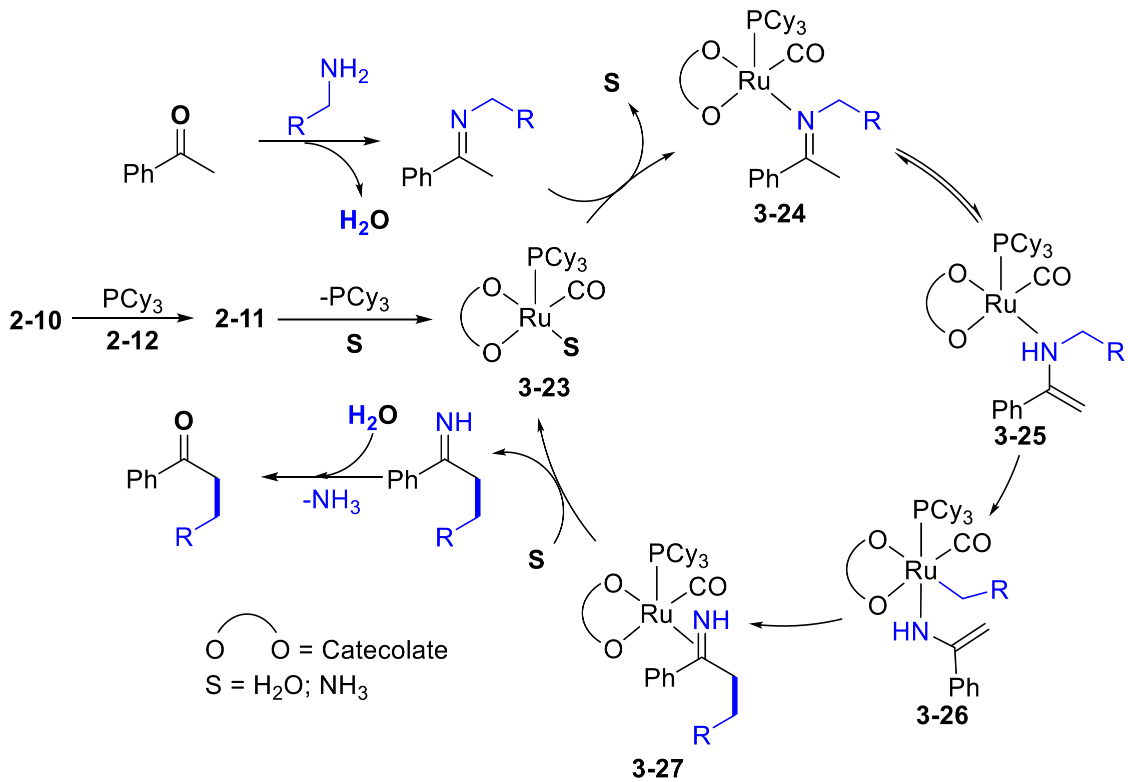

Scheme 3.9: Proposed Mechanism of the Deaminative α-Alkylation of Ketones with Amines

The ketimine **3-13**, which is formed form the initial dehydrative coupling of ketone and amine substrates, is the real substrate for the catalytic alkylation reaction. The coordination of imine substrate **3-13** and the subsequent imine-to-enamine isomerization should form the Ru-enamine species **3-25** via imine coordinated complex **3-24**. The deuterium labeling study supports a facile imine-to-enamine tautomerization step. The first-order kinetics on [**3-13a**] as well as the lack of imine crossover results provide experimental supports for an intramolecular alkyl migration mechanism in forming the Ru-imine species **3-27**. The observation of prominent carbon KIE on the α-carbon of the product **3-10a** is consistent with the C–C bond formation rate-determining step.

While the [1,3]-carbon migration step may occur either in stepwise or a concerted fashion, we could not find any specific literature examples on [1,3]-carbon shift on either enamine or imine compounds. On the other hand, the analogous thermally induced [1,3]-carbon shift reactions of vinylcycloalkanes have been well-known to occur in a concerted, suprafacial fashion, resulting in the inversion of stereochemistry on the migrating carbon atom.[152] A number of transition metal-catalyzed C–C coupling reactions of propargylic esters and related cycloisomerization reactions have been known to proceed via a [1,3]-carbon shift process,[153] and related Ag-catalyzed [1,3]-halogen shift reactions for vinyl and dienyl-containing compounds have also been reported recently.[154] In these sigmatropic [1,3]-carbon shift reactions, the orbital interactions between the σ-carbon and π-orbitals from unsaturated carbon atoms are essential for promoting the symmetry-allowed suprafacial carbon migration.

The DFT study revealed deeper mechanistic insights for the Ru-mediated [1,3]-alkyl migration step of the reaction. The DFT calculations showed that the direct enamine-to-imine rearrangement is a prohibitively high energy process in the absence of a Ru catalyst (**Figure 3-13**). The DFT calculations on the Ru-mediated enamine-to-imine rearrangement showed that the [1,3]-alkyl migration step proceeds in a stepwise fashion via the formation of the Ru(IV)-alkyl intermediate species **3-21**, apparently to avoid a high energy concerted pathway. The geometrical optimization of the Ru-catecholate complex **2-11** with the imine substrate led to a locally minimized structure of Ru(IV)-alkyl intermediate **3-21**, with a relatively moderate activation enthalpies ($DH^{\ddagger}$ = 43-44 kcal/mol). The DFT computational results as well as experimental Hammett and carbon KIE data clearly indicate that the [1,3]-alkyl migration is the turnover-limiting step of the catalytic reaction, in which the alkyl migration (C–N bond cleavage) step is promoted by the nucleophilicity of a-imine carbon. The rate independence on [H_2O] is consistent with a rapid hydrolysis of the resulting imine product to form the alkylation product **3-10** along with the regeneration of the Ru-catecholate complex **3-23**. Both experimental and DFT computational results provided new mechanistic insights that the Ru catalytic system (**2-10**/**2-12**) facilitates a normally energetically demanding and previously unexplored deaminative alkylation reaction by promoting a facile imine-to-enamine tautomerization and an intramolecular stepwise [1,3]-carbon migration process via the formation of Ru(IV)-alkyl intermediate species.

3.4 Summary and Conclusion

In summary, we have successfully developed a highly regioselective catalytic α-alkylation method of simple ketones from the deaminative coupling reaction with amines. The *in-situ* generated catalytic system consisted of the ruthenium-hydride complex and a redox-active 1,2-benzoquinone ligand (**2-10**/**2-12**) was found to exhibit a uniquely high activity and selectivity for promoting the deaminative coupling reaction. Kinetic and spectroscopic studies provide a detailed mechanistic picture for the catalytic reaction, which involves the initial formation of Schiff base from the dehydrative coupling of ketones with amine substrates, Ru-catalyzed imine-to-enamine isomerization and the turnover-limiting [1,3]-alkyl migration and hydrolysis steps. The DFT study revealed a low energy pathway for the [1,3]-alkyl migration step, which involves a stepwise mechanism via the formation of a Ru(IV)-alkyl species. In light of the successful synthesis of highly active Ru-catecholate complex **2-11**, we are continuing our efforts to search for new catalytic coupling methods that are enabled by transition metal catalysts with redox-active 1,2-benzoquinone ligands. We submitted a manuscript to *Journal of American Chemical Society,* and it is currently under revision. We are currently completing the DFT computational work to address the reviewer's comments.

Chapter 4

Synthesis of Quinazoline and Quinazolinone Derivatives via Ligand-Promoted Ruthenium-Catalyzed Dehydrogenative and Deaminative Coupling Reaction of 2-Aminophenyl Ketones and 2-Aminobenzamides with Amines

4.1 Introduction

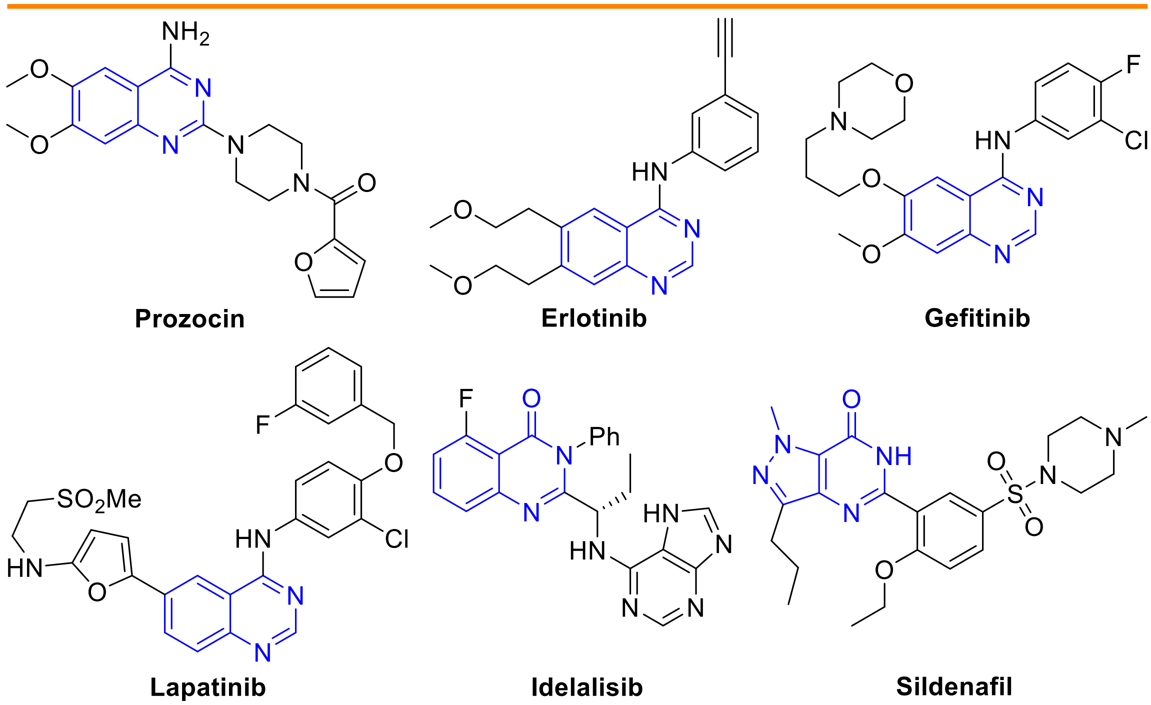

Figure 4.1: Selected Examples of Quinazoline and Quinazolinone Based Drugs

Quinazolines and quinazolinones are a privileged class of nitrogen heterocyclic scaffolds that have been found to exhibit a broad spectrum of pharmacological activities, including anti-inflammatory, antitubercular, and antiviral activities.[155] A number of quinazoline-based drugs such as prazocin and doxazosine have been approved to treat benign prostatic hyperplasia and post-traumatic stress disorder,[156] while both erlotinib and gefitinib have been used for the treatment of lung and pancreatic cancers (**Figure**

4.1).[157] Lapatinib, an inhibitor for epidermal growth factor, has been shown to be effective in combination therapy for breast cancer.[158] Several quinazolinone-based drugs including idelalisib have been shown to exhibit a broad spectrum of antimicrobial, antitumor, antifungal, and cytotoxic activities.[159] On the other hand, sildenafil is a potent and selective inhibitors of the type 5 cGMP phosphodiesterase from both rabbit platelets and human corpus cavernosum, which is currently used for the oral treatment of male erectile dysfunction.[160]

A number of different synthetic strategies for quinazolines and quinazolinones have been developed over the years, in part to meet the growing needs for screening of these pharmacologically important derivatives.[161] In 2013, Zhou and co-workers reported one-pot synthesis of 2-substituted quinazolines by using 2-aminobenzylamines and aldehydes via iridium-catalyzed hydrogen transfers with styrene as a hydrogen acceptor (**Eq. 4.1**).[162]

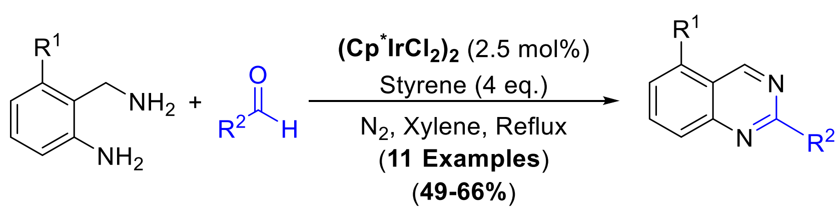

(Eq. 4.1)

In 2013, Wu and co-workers reported a palladium catalyzed three component coupling protocol for 2-iodoarylcarbodiimide **4-1**, phosphite and isocyanide to synthesize 4-imino-3,4-dihydroquinazolin-2-ylphosphonates **4-2**. A one-pot tandem procedure includes the nucleophilic isocyanide insertion, and the C-N coupling by reductive elimination through seven membered palladacycle (**Scheme 4.1**).[163] In these cases, more reactive reagents were utilized to generate a quinazoline core structure.

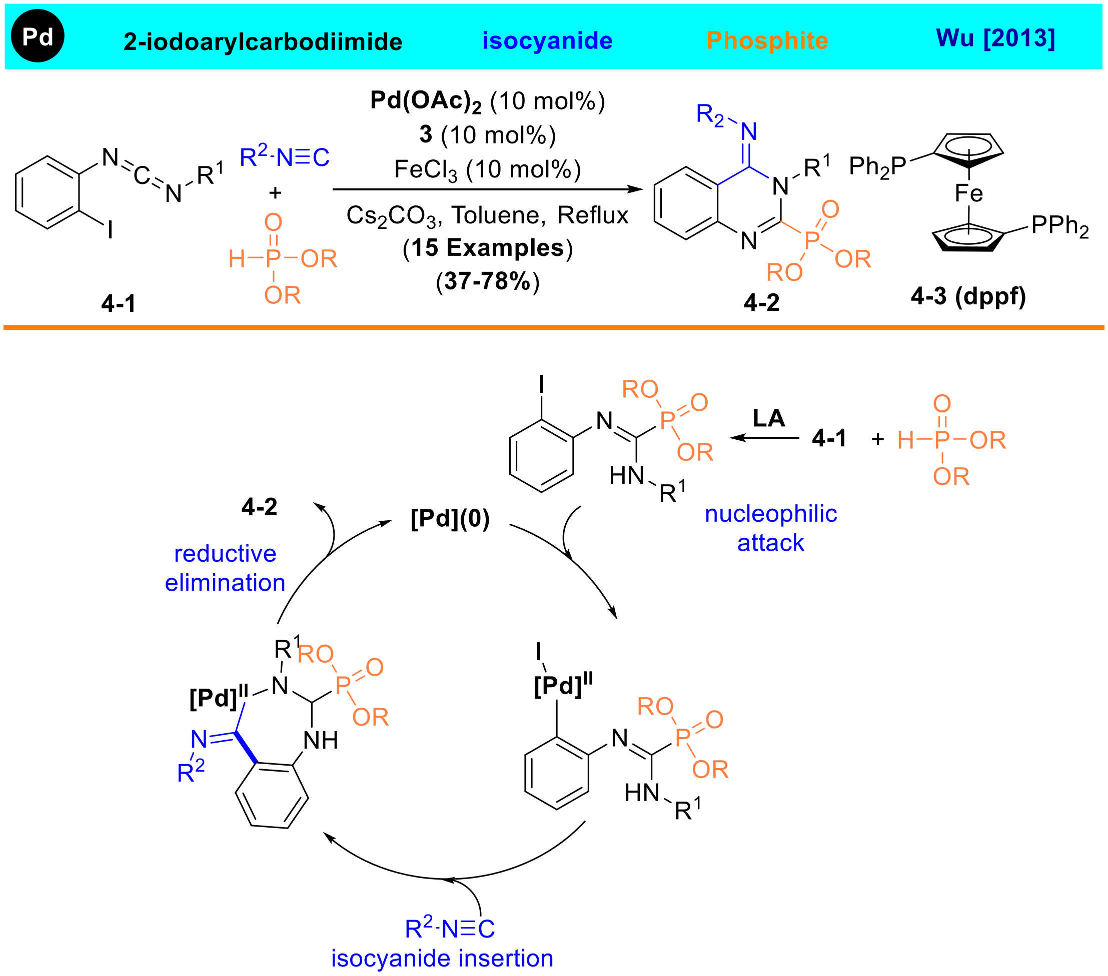

Scheme 4.1: A Proposed Synthetic Route to Phosphonylated Quinazolines

Several research groups have successfully utilized copper catalyzed Ullmann-type coupling methods of aryl bromides and benzamidines for the synthesis of quinazoline derivatives.[164] Similar Cu-catalyzed oxidative coupling methods of aniline derivatives with aldehydes and nitriles have also been developed for the construction of quinoline core structures.[165] Transition-metal-catalyzed oxidative C−H amination and alkylation methods have also been successfully employed to synthesize quinazoline and quinazolinone derivatives.[166] Fu and co-workers in 2009 achieved an efficient catalytic method for the synthesis of quinazolinone derivatives from the coupling reaction of 2-halobenzoic acid **4-4** derivatives with highly reactive amidines **4-5** (**Eq. 4.2**).[164a]

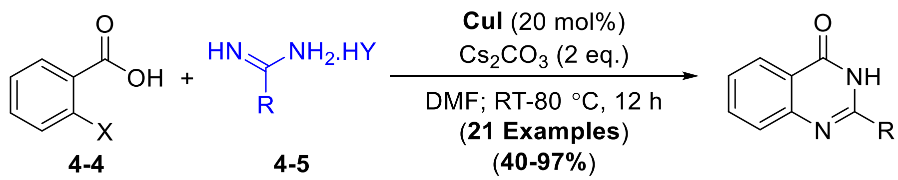

(Eq. 4.2)

In 2017 Molander and co-workers reported a Csp^3-centered alkyl radical cascade reaction via C−H alkylation of heterocycles (**Eq. 4.3**). The key step of this SET reaction involves the generation of Csp^3-centered radical which engages in the C−H alkylation of heterocyclic bases with 1,4-dihydropyridines (DHPs) **4-6**.[166d]

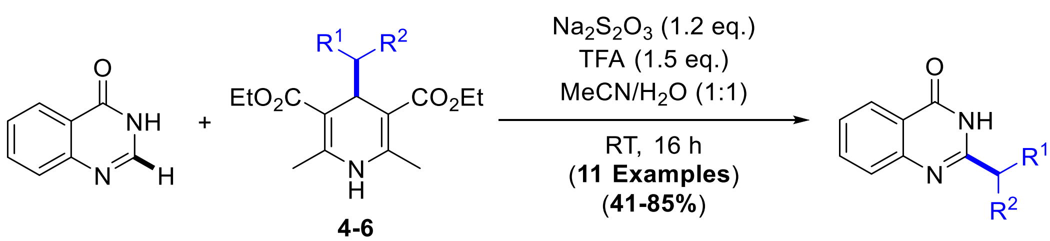

(Eq. 4.3)

Recently, Shang and co-workers has utilized an imine-protection strategy to synthesize quinazolinones via aerobic copper-catalyzed three component annulation reaction.[167] Initially, both aryl and alkyl amines were easily reacted with formaldehyde to form imines **4-7** and aliphatic imine. The [4 + 2] cycloaddition[168] between **4-7** and aliphatic imine followed by isomerization would result an aminal **4-10**. Alternatively, the addition of alkylamine to imine **4-7** followed by a condensation of aminal **4-8** with formaldehyde would generate an iminium ion **4-9**. Subsequent intramolecular Friedel–Crafts-type[169] of ortho-amino alkylation would form the aminal **4-10**. Single-electron oxidation-induced dehydrogenation[170] of **4-10** under oxidative copper catalysis followed by benzylic oxidation[171] would afford the desired N-substituted quinazolinone product via dihydroquinazoline 4-11 intermediate (**Scheme 4.2**).

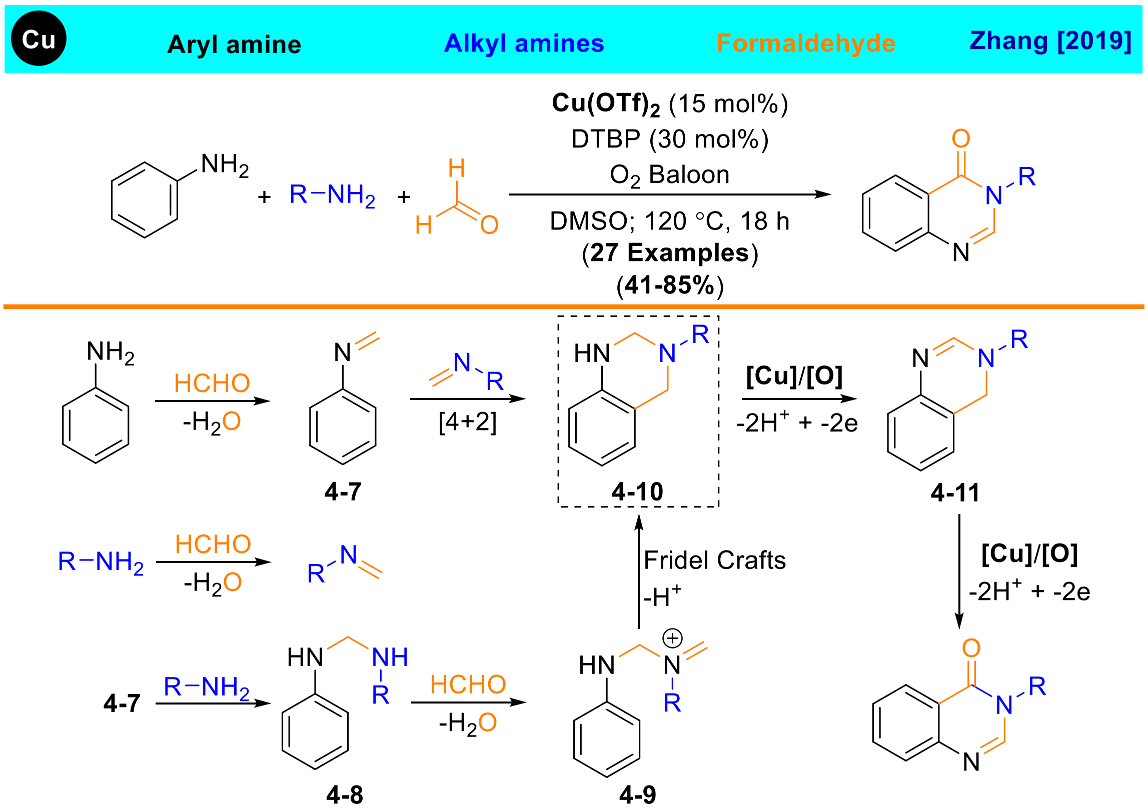

Scheme 4.2: Plausible Reaction Pathways for the Copper-Catalyzed Three Component Annulation Reaction

Cho and co-workers recently devised a practical synthesis of 2-arylquinazoline derivatives from the coupling of 2-aminobezylamines with halogenated toluene substrates.[172] Since the advent of the Niementowski condensation of anthranilic acids with amides,[173] a variety of sustainable synthetic methods have also been devised for the assembly of quinazolinone core structures.[174] Much research effort has been devoted to the development of catalytic coupling methods to increase efficiency and selectivity in constructing quinazolinone core structures. A number of transition-metal catalyzed direct coupling methods of aminobenzamides with alcohols and carbonyl compounds have been successfully exploited to synthesize quinazolinone derivatives.[175] Transition metal-catalyzed couplings of 2-aminobenzamides with alcohols and ketones[176], three-component couplings of 2-aminobenzamides, aryl halides or equivalents, isocyanides[177], and copper catalyzed,[167, 178] electrochemical,[179] are among the notable examples of catalytic synthesis of quinazolinones.

4.2 Results and Discussion

We previously discovered that the cationic ruthenium hydride complex **2-10** is a highly effective catalyst precursor for the deaminative and decarboxylative coupling reaction of ketones with amino acids.[29] We also reported that a phenol-coordinated cationic ruthenium−hydride complex is a highly effective catalyst for mediating the hydrogenolysis of aldehydes and ketones.[180] We subsequently found that the ruthenium-hydride complex **2-10** with a 1,2-catechol ligand exhibits an exceptionally high chemoselectivity for promoting the deaminative coupling reactions of amines to form unsymmetric secondary amines.[126b] To further extend the synthetic utility of ligand-promoted catalysis, we have been exploring the promotional effects of various oxygen and nitrogen ligands on ruthenium catalysts for the deaminative coupling reactions of amines.

In this Chapter, we disclose an efficient catalytic synthesis of quinazoline and quinazolinone derivatives from the dehydrogenative and deaminative coupling reactions of amino ketones and aminobenzamides with amines, which is mediated by a well-defined ruthenium catalyst containing a catechol ligand. The salient features of the catalytic method are that the regio- and diastereoselective fashion without employing any reactive reagents or forming any wasteful byproducts, while tolerating a number of common organic functional groups.

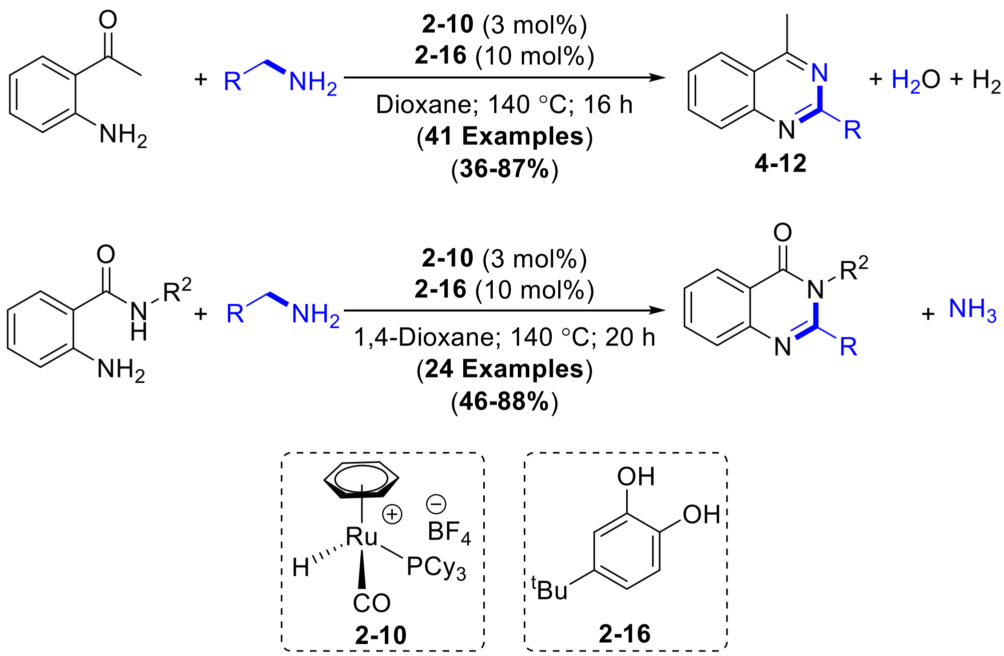

Scheme 4.3: Synthesis of Quinazoline and Quinazolinone Derivatives[149]

4.2.1 Optimization Studies

We initially explored the coupling reaction of 2-aminoketones with amines by employing the ligand promoted catalysis protocol in order to extend the scope and utility of deaminative coupling methods. Among the initially screened Ru catalysts and ligands, the in-situ generated catalytic system from the cationic ruthenium−hydride complex **2-10** with 4-(1,1-dimethylethyl)-1,2-benzenediol **2-16** was found to give the highest activity and selectivity for the coupling of 2-(aminophenyl)ethanone with 4-methoxybenzylamine in yielding the quinazoline product **4-12a** (**Table 4.1**). The coupling reaction conditions as described in **Eq. 4.4** have been used as the standard reaction conditions unless otherwise noted.

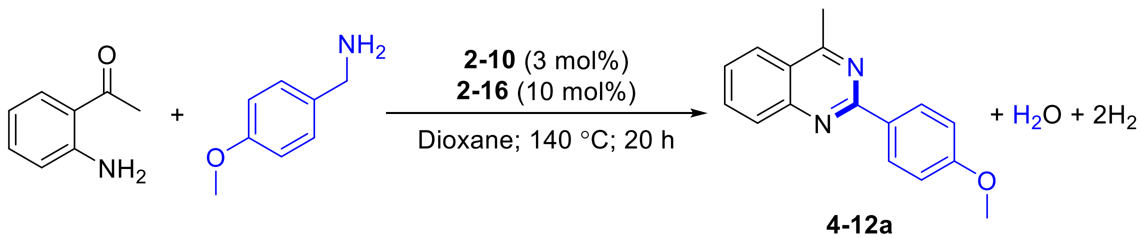

(Eq. 4.4)

4.2.1.1 Ligand Screening

We first evaluated the ligand effect for the reaction between 2-(aminophenyl)ethanone with 4-methoxybenzylamine. In the absence of any ligands, the reaction was found to be very sluggish as a trace amount of the product **4-12a** was obtained with both **2-9** and **2-10** catalysts (**Table 4.2**; entry 8). The addition of catechol ligands (**2-16, 2-16a-f**) significantly increased desired product **4-12a**. Binol **2-12j** or phenolic ligands (**3-11b-d**) was not effective for this noble transformation. In accordance with the previous results on the ruthenium catalyzed C(sp^3)−N bond cleavage reaction, the catechol ligand **2-16** was found to be the most effective for the selective synthesis of secondary amines.[126b] The catechol ligands **2-16a-e** with both electron donating and withdrawing group were shown to be effective for giving the products in giving modest to good yields (68-85%), whereas 2,2´-biphenol ligand **2-12j** gave only a trace amount of the product **4-12a** for the coupling reaction. As shown in **Table 4.1**, the catalytic activity of **2-10** was found to be substantially enhanced by the addition of a catechol ligand with the efficient formation of product **4-12a**. The nitrogen coordinating ligands **3-11d**, **3-12** and aliphatic diols were found to be completely ineffective for the catalytic reaction.

Table 4.1: Ligand Screening for the Coupling of 2-Aminophenylethanone with 4-Methoxybenzylamine[a]

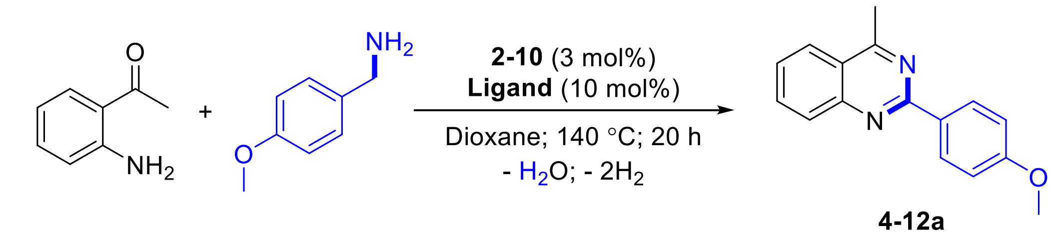

4-12a

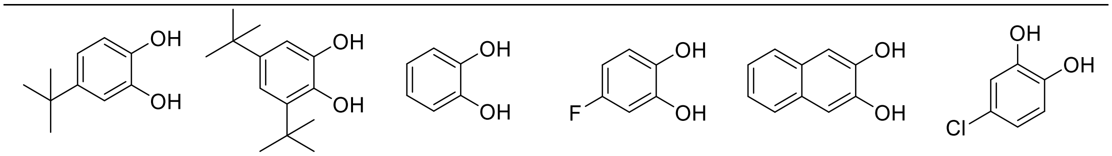

2-16 (85%) **2-16a** (79%) **2-16b** (77%) **2-16c** (83%) **2-16d** (81%) **2-16e** (76%)

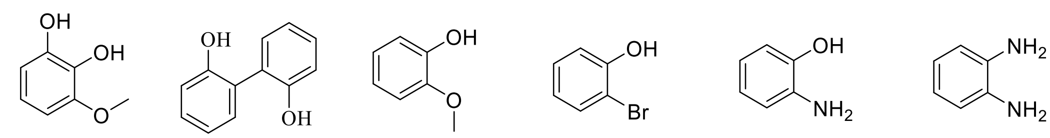

2-16f (68%) **2-12j** (<5%) **3-11b** (<5%) **3-11c** (<5%) **3-11d** (<10%) **3-12** (<10%)

[a]Reaction conditions: 2-aminophenylethanone (0.5 mmol), 4-methoxybenzylamine (0.7 mmol), **2-10** (3 mol %), ligand (10 mol %), 1,4-dioxane (2 mL), 140 °C, 20 h. [b]The product yield of **4-12a** was determined by ^{1}H NMR using hexamethylbenzene as an internal standard.

4.2.1.2 Catalyst and Solvent Screening

We screened the activity of commonly available ruthenium catalysts and acid catalysts, where 1,4-dioxane was found to be the most suitable solvent for the coupling reaction (entry 2-7). Among the screened ruthenium catalysts (entry 9-19), the Ru-H complex **2-10** was found to be the most effective catalyst (entry 1). Importantly, Lewis acids PCy_3 did not exhibit any activity for the coupling reaction (entry 22-24). These ligand screening and optimization efforts have led to the standard conditions for the coupling reaction: 2-aminophenylethanone (0.5 mmol), benzylamine (0.7 mmol), **2-10** (3 mol %) and **2-16** (10 mol %) in 1,4-dioxane (2 mL) at 140 °C for 40 h (**Table 4.2**). The water byproduct was detected by NMR in a crude reaction mixture, and hydrogen gas was removed under vacuum during the solvent evalopration. The product **4-12a** was isolated by a column chromatographic separation on silica gel.

Table 4.2: Catalyst and Additive Screening for the Coupling of 2-Aminophenylethanone with 4-Methoxybenzylamine[a]

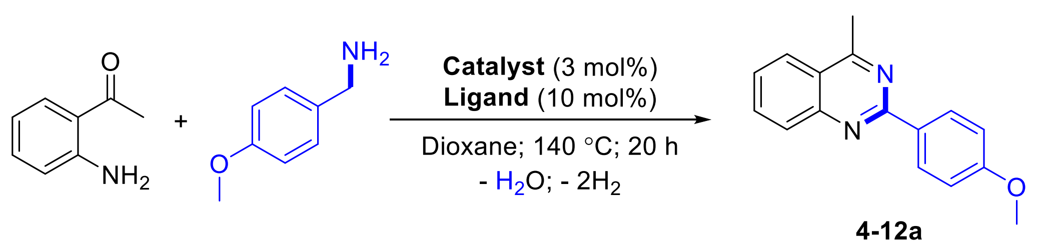

entry	catalyst	deviation from standard conditions	**4-12a** (%)[b]
1	$[(C_6H_6)(PCy_3)(CO)RuH]^+BF_4^-$ **2-10**	none	**85**
2	$[(C_6H_6)(PCy_3)(CO)RuH]^+BF_4^-$ **2-10**	t-butylethylene[c]	8
3	$[(C_6H_6)(PCy_3)(CO)RuH]^+BF_4^-$ **2-10**	chlorobenzene	52
4	$[(C_6H_6)(PCy_3)(CO)RuH]^+BF_4^-$ **2-10**	chlorobenzene/cyclopentene[c]	58
5	$[(C_6H_6)(PCy_3)(CO)RuH]^+BF_4^-$ **2-10**	1,2-DCE	0
6	$[(C_6H_6)(PCy_3)(CO)RuH]^+BF_4^-$ **2-10**	xylene	66

7	$[(C_6H_6)(PCy_3)(CO)RuH]^+BF_4^-$ **2-10**	t-amyl alcohol	15
8	$[(C_6H_6)(PCy_3)(CO)RuH]^+BF_4^-$ **2-10**	No ligand	trace
9	$[(PCy_3)(CO)RuH]_4(\mu\text{-}O)(\mu\text{-}OH)_2$ **2-9**	-	45
10	$[(PCy_3)(CO)RuH]_4(\mu\text{-}O)(\mu\text{-}OH)_2$ **2-9**	No ligand	9
11	$[(PCy_3)(CO)RuH]_4(\mu\text{-}O)(\mu\text{-}OH)_2$ **2-9**	chlorobenzene	6
12	$[(PCy_3)(CO)RuH]_4(\mu\text{-}O)(\mu\text{-}OH)_2$ **2-9**	chlorobenzene/cyclopentene[c]	trace
13	$[(PCy_3)(CO)RuH]_4(\mu\text{-}O)(\mu\text{-}OH)_2$ **2-9**	1,2-DCE	0
14	$(PPh_3)_3(CO)RuH_2$	-	25
15	$(p\text{-cymene})_2RuHCl$	-	18
16	$RuCl_2(PPh_3)_3$	-	12
17	$RuCl_3{\cdot}3H_2O$	-	0
18	$[Ru(COD)Cl_2]_x$	-	20
19	$(PCy_3)_2(CO)RuHCl$	-	18
20	$Ru_3(CO)_{12}$	-	30
21	$[(PCy_3)(CH_3CN)(CO)RuH]^+BF_4^-$	-	15
22	-	$HBF_4{\cdot}OEt_2$	0
23	BF_3OEt_2	-	0
24	PCy_3	-	0

[a]Standard conditions: 2-aminophenylethanone (0.5 mmol), 4-methoxybenzylamine (0.7 mmol), catalyst (3 mol %), ligand (10 mol %), 1,4-dioxane (2 mL), 140 °C, 20 h. [b] The product yield of **4-12a** was determined by ^{1}H NMR using hexamethylbenzene as an internal standard. [c]0.5 mmol of cyclopentene was added.

4.2.3 Reaction Scope for the Synthesis of Quinazolines and Quinazolinones

4.2.3.1 Synthesis of Quinazolines from the Coupling of 2-Aminophenyl Ketones with Primary Amines

With the optimized conditions in hand, we explored the substrate scope of the coupling reaction by using the *in-situ* generated catalyst system **2-10**/**2-16**. The coupling of 2-aminophenyl ketones with a variety of benzylic amines selectively formed the quinazoline products **4-12a−p** in 87-59% yields.

Table 4.3: Synthesis of Quinazolines from the Coupling of 2-Aminophenyl Ketones with Amines[a]

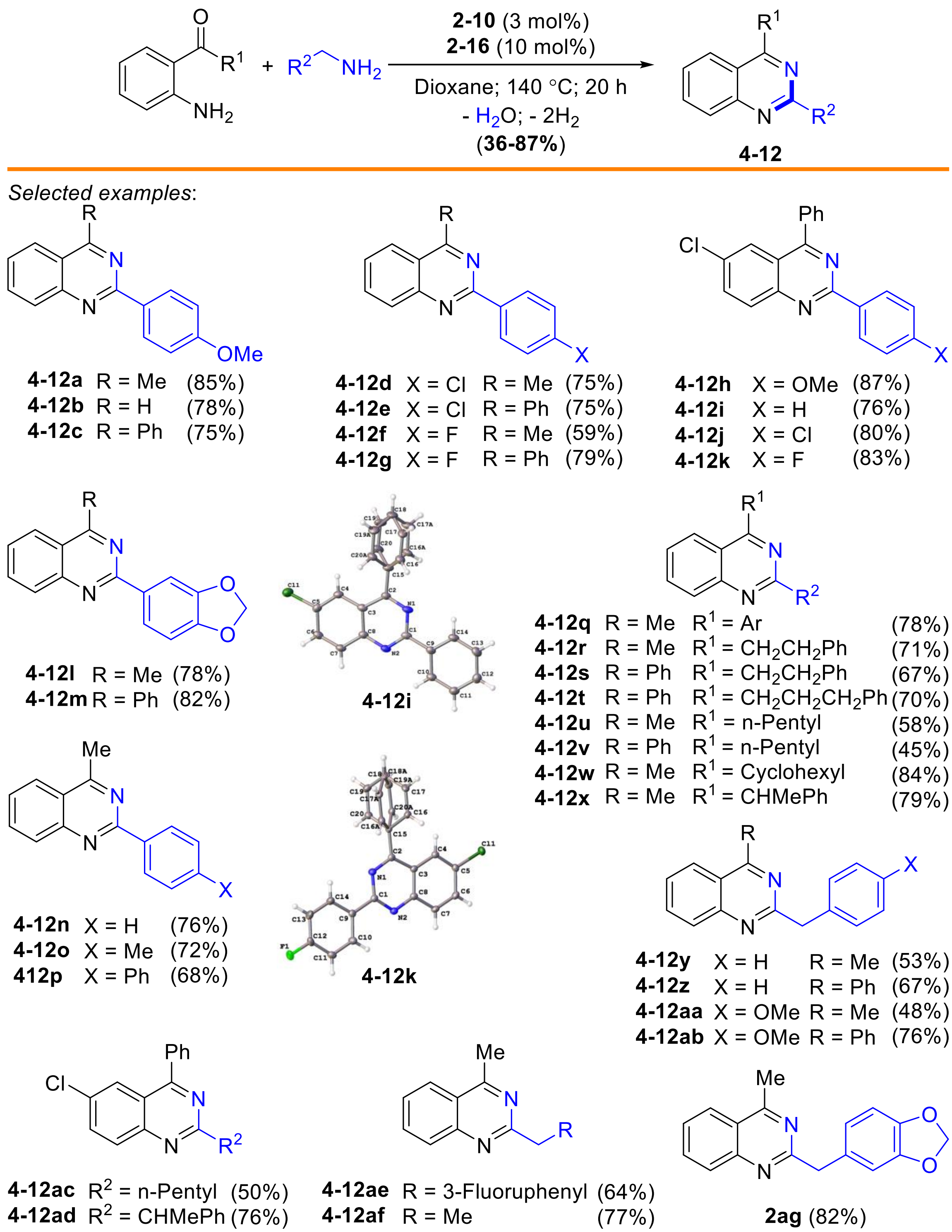

[a]Reaction conditions: aminoketone (0.5 mmol), amine (0.7 mmol), **2-10** (3 mol %), **2-16** (10 mol %), 1,4-dioxane (2 mL), 130 °C, 20 h. Ar = 3,4,5-trimethoxyphenyl

The coupling of 2-aminophenyl ketones with phenethylamines afforded the desired product **4-12q−t** (78-67%), **4-12y−ab** (48-76%), **4-12ae** (64%) and **4-12ag** (82%), demonstrating the versatility of phenethylamine substrate for the coupling reaction. The aliphatic amines also gave the selective formation of **4-12u−ac**, in 45-79% yields. While the coupling reaction of 2-aminphenyl ketone substrate with a branched amine smoothly yielded the coupling products **4-12x** and **4-12ad**, the coupling with sterically demanding secondary amines and branched amines generally yielded only a trace amount of the coupling products under the standard reaction conditions (**Table 4.3**). Interestingly, the reaction between 2-aminoacetophenone with allylamine yielded the quinazoline product **4-12af** with the selectively hydrogenated allylic double bond. Analytically pure quinazoline products were readily isolated after silica gel column chromatographic separation, and their structures were completely established by spectroscopic methods. The structure of **4-12i** and **4-12k** were also confirmed by X-ray crystallography. We also have been able to scale up the coupling reaction to a 2−3 mmol scale reaction to yield 0.5−0.7 g of **4-12b**, **4-12m** and **4-12ab**. The catalytic coupling method furnishes a direct synthesis of quinazoline products without using any reactive reagents and environmentally benign water and hydrogen as the byproducts.

4.2.3.2 Synthesis of Quinazolinones from the Coupling of 2-Aminobenzamides with Primary Amines

Adopting the previously developed deaminative coupling protocol,[126b] we next sought the catalytic coupling reaction of the 2-aminoarylamides with amines to form quinazolinone products (**Table 4.4**).

Table 4.4: Synthesis of Quinazolinones from the Coupling of 2-Aminobenzamides with Amines

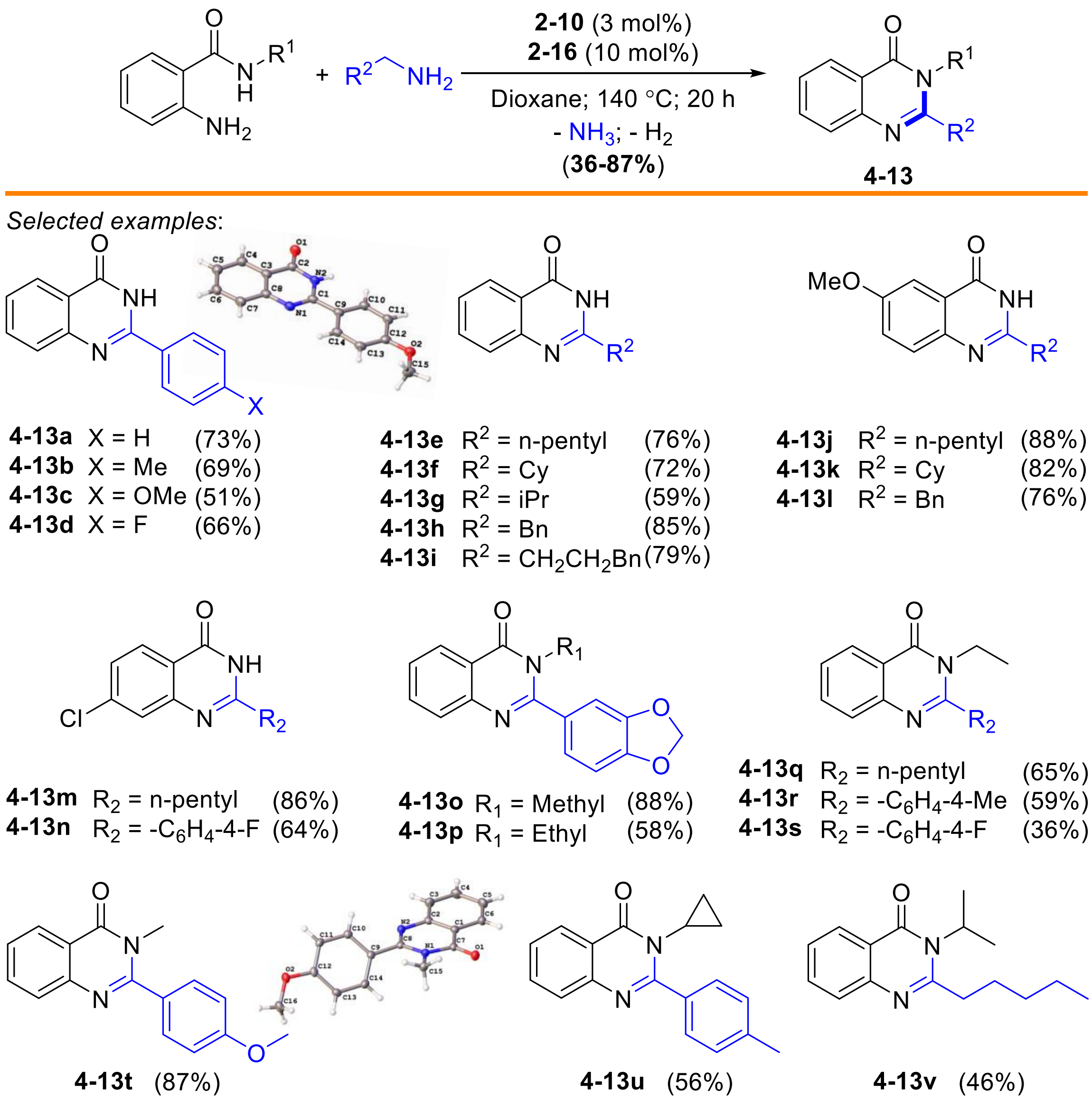

Thus, the treatment of 2-aminobenzamide (0.5 mmol) with benzylamine (0.7 mmol) in dioxane (2 mL) at 140 °C in the presence of the catalyst system **2-10** (3 mol %)/**2-16** (10 mol %) led to the selective formation of the quinazolinone product **4-13**, which was analyzed by both GC and NMR spectroscopic methods. The substrate scope of the coupling reaction was explored by using the catalyst system **2-10**/**2-16** under the standard conditions. The coupling of 2-aminobenzamides with both benzyl- and alkyl-substituted amines led to the selective formation of the quinazolinone products **4-13a−n** (88-51%) with no significant amount of the quinazoline or other side products. The analogous coupling reaction of N-alkyl-2- benzamides with both benzylamines and alkyl-substituted amines afforded the corresponding coupling products **4-13o−t** in moderate to high yields. Single crystals of **4-13c** and **4-13t** were obtained by slow evaporation in hexanes/EtOAc at room temperature, and its structure was determined by X-ray crystallography. The formation of quinazolinone product can be rationalized by initial deaminative coupling of amide and amine substrates followed by the cyclization dehydrogenation steps. The coupling reaction efficiently assembles synthetically valuable quinazolinone core structures by employing readily available amine and benzamide substrates.

4.2.3.3 Coupling Reaction of 2-Aminophenyl Ketones with Biologically Active Amines

To further demonstrate synthetic utility of the catalytic method, we next surveyed the substrate scope of the coupling method by employing several biologically active and functionalized 2-aminophenylketones and 2-aminobenzamides with a number of biologically active amine substrates (**Table 4.5**). The treatment of 2-aminophenylethanone with tryptamine led to the indole-substituted product **1-12ah** in moderate yield under the standard reaction conditions. The analogous coupling with (−)-cis-myrtanylamine formed the corresponding quinazoline products **4-12ai** and **4-12aj** in good yields (85, 70% respectively; d.r. = 10:1) with a minimal racemization on the β-carbon.

Table 4.5: Coupling Reaction of 2-Aminophenyl Ketones and 2-Aminobenzamides Biologically Active and Functionalized Amines[a]

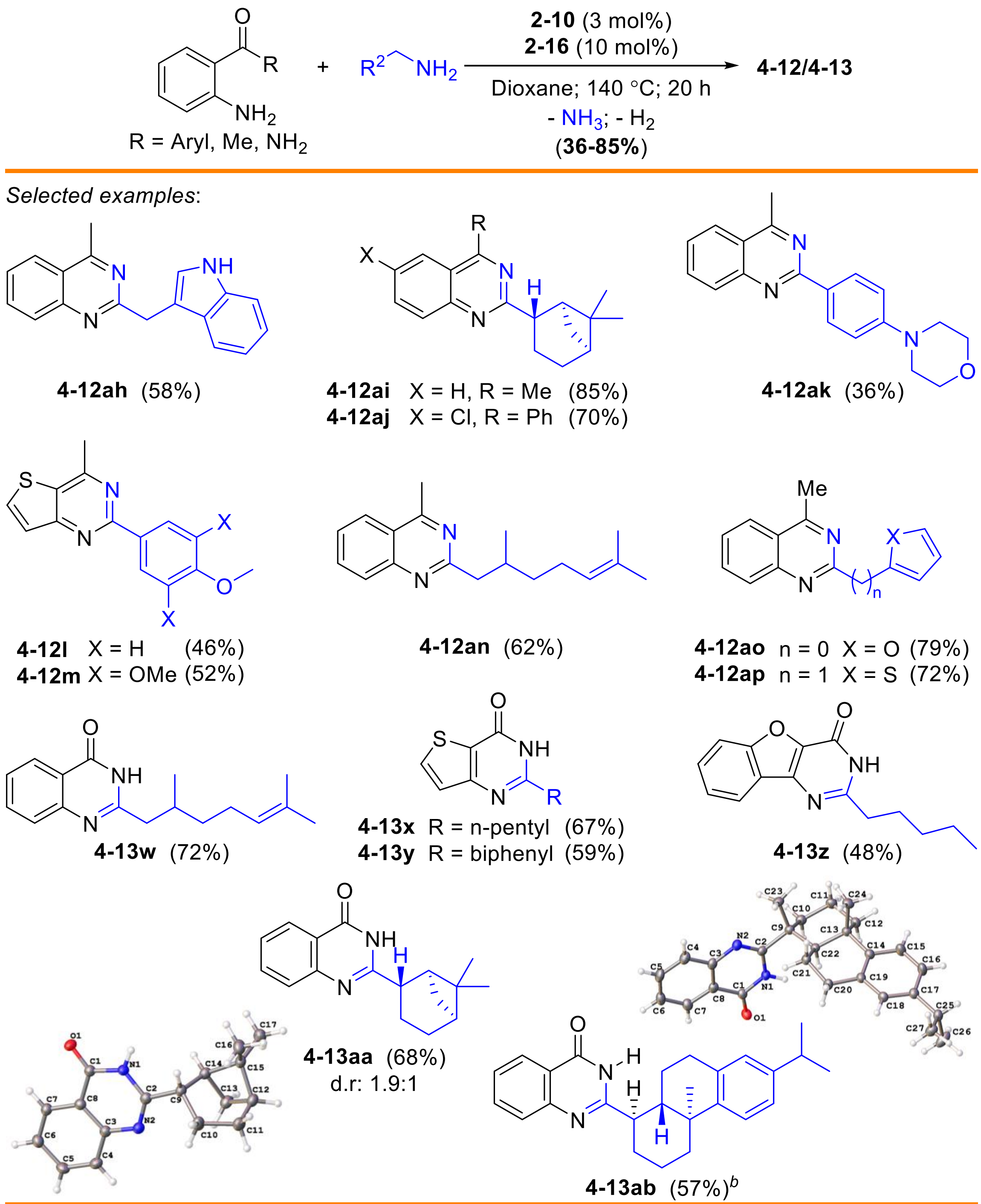

[a]Reaction conditions: amino ketone or benzamide (0.5 mmol), amine (0.7 mmol), **2-10** (3 mol %), **2-12** (10 mol %), 1,4-dioxane (2 mL), 140 °C, 20 h. [b]Benzamide (0.25 mmol), amine (0.35 mmol).

The coupling of 2-aminophenylethanone with a 4-morpholinyl-substituted amine predictively formed the desired product **4-12ak** in 36% yield. The coupling of a thiophene substituted amino ketone with electron rich benzyl amines yielded the desired products **4-12al** and **4-12am** in 46% and 52% yield respectively. The treatment of 2-aminoacetophenone with geranylamine formed the expected product **4-12an**, in 62% yield, with the selectively hydrogenated proximal olefinic group. The reaction of 2-aminoacetophenone with furfuryl amine and 2-thiopheneethanamine afforded the desired products **4-12o,p** in good yields. This extension clearly demonstrated the general applicability of the catalytic coupling method for the synthesis of quinazoline derivatives. The analogous treatment of 2-aminobenzamide with geranylamine formed the corresponding quinazolinone product **4-13w**, in which the neighboring olefinic group is selectively hydrogenated, confirming the unique catalytic activity as in the previous cases. The treatment of a thiophene-substituted amide with n-hexylamine and 4-phenylbenzylamine formed the corresponding quinazolinone products **4-13x,y** in moderate yield. The treatment of the catalytic system with 3-Aminobenzofuran-2-carboxamide with n-hexylamine afforded the desired product **4-13z** in modest yield (48%). The coupling of 2-aminobenzamide with (−)-cis-myrtanylamine formed the coupling product **4-13aa** with a modest diastereoselectivity (d.r. = 1.9:1). In sharp contrast, the analogous coupling with (+)-dehydroabietylamine resulted in the formation of the coupling product **4-13ab** without any detectable racemization. The structure and stereochemistry of both **4-13aa** (major diastereomer) and **4-13ab** quinazolinone products have been confirmed by X-ray crystallographic method.

4.2.4 Mechanistic Studies

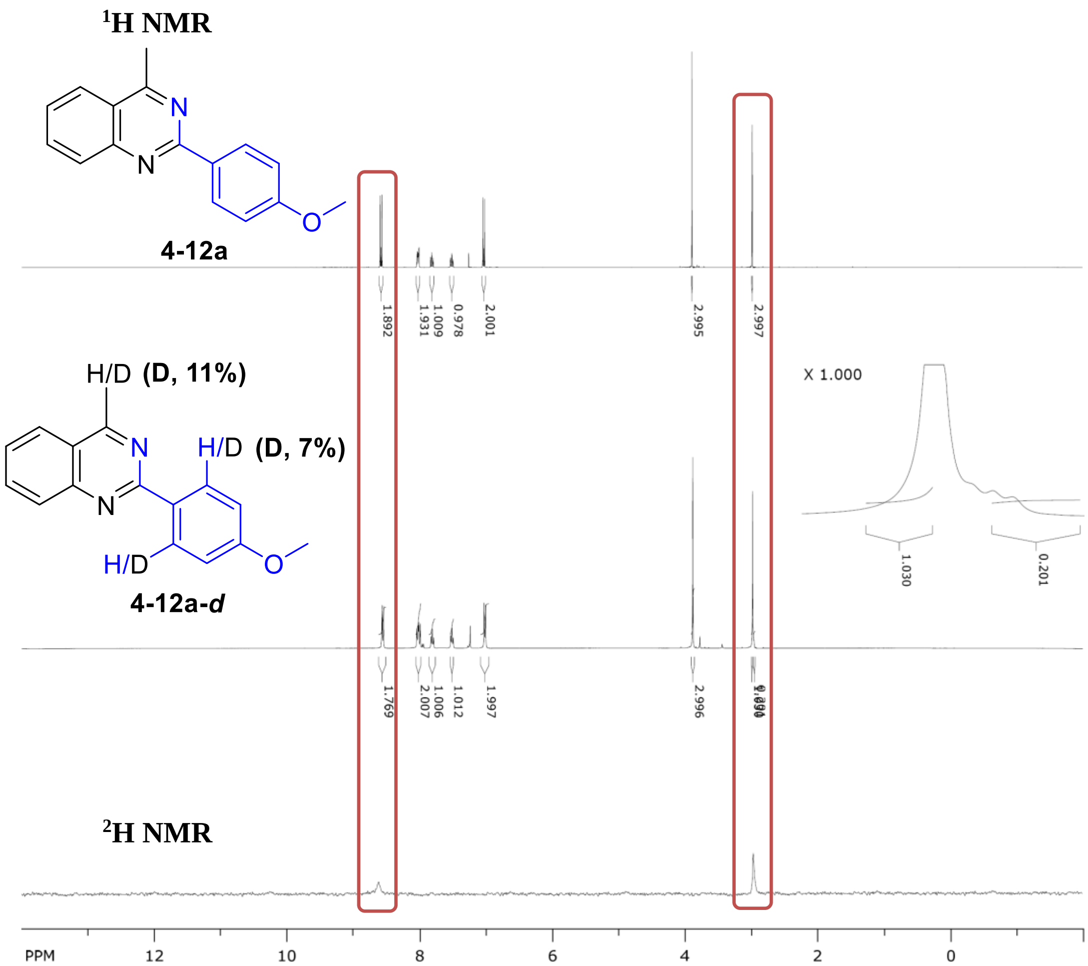

Figure 4.2: ^{1}H and ^{2}H NMR Spectra of **4-12a** and **4-12a**-*d*

4.2.4.1 Deuterium Labeling Study

We have chosen the reaction of 2-aminoacetophenone with 4-methoxybenzylamine for probing mechanistic insights for the coupling reaction. We examined the deuterium-labeling pattern from the reaction of 2-aminophenylethanone-d_3 (89% D) with 4-methoxybenzylamine (**Eq. 4.5**).

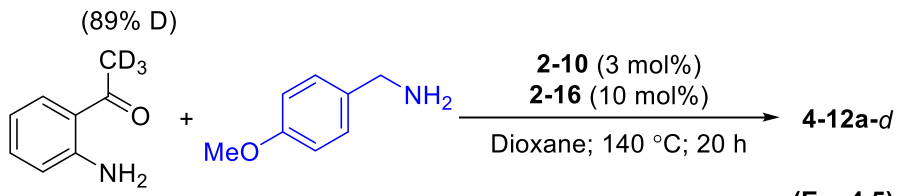

(Eq. 4.5)

Thus, the treatment of perdeuterated 2-aminophenylethanone-d_3 (0.50 mmol) with 4-methoxybenzylamine (0.70 mmol) in the presence of **2-10** (3 mol %)/**2-16** (10 mol %) under the standard reaction conditions formed the coupling product **4-12a**-*d*. The isolated product **4-12a**-*d* as analyzed by ^{1}H and ^{2}H NMR contained only 11% of the deuterium on the methyl group as most of the deuterium had been washed away (**Figure 4.2**). A relatively small amount of the deuterium on **4-12a**-*d* suggests an extensive keto−enol tautomerization under the reaction conditions.

4.2.4.2 Reaction Profile Study

To discern the nature of viable intermediate species, we monitored the reaction progress for the catalytic coupling reaction of 2-aminoacetophenone with 4-methoxybenzylamine by using NMR spectroscopic method. In a resealable NMR tube, a reaction mixture of 2-aminophenylethanone (0.25 mmol), 4-methoxybenzylamine (0.25 mmol), and in situ generated catalyst **2-10** (3 mol %)/**2-16** (10 mol %) in toluene-d_8 (0.5 mL) was immersed an oil bath set at 140 °C. The tube was taken out from the oil bath at 20 min intervals, and the reaction progress was recorded by ^{1}H NMR. The appearance of new set of peaks due to the imine product **4-14a** has been observed initially as both starting substrates are consumed. After about 100 min of reaction time, the peaks due to the quinazoline product **4-12a** began to appear as the imine peaks gradually disappeared. The plot of relative concentration vs time is shown in **Figure 4.3**.

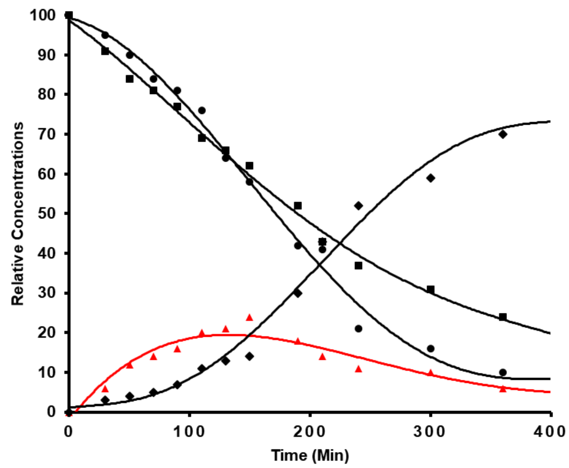

Figure 4.3: Reaction Profile for the Coupling Reaction of 2-Aminoacetophenone with 4-Methoxybenzylamine. 2-Aminophenylethanone (■), 4-Methoxybenzylamine (●) **4-12a** (♦), **4-14a** (▲).

4.2.4.3 Reaction with Imine Substrates

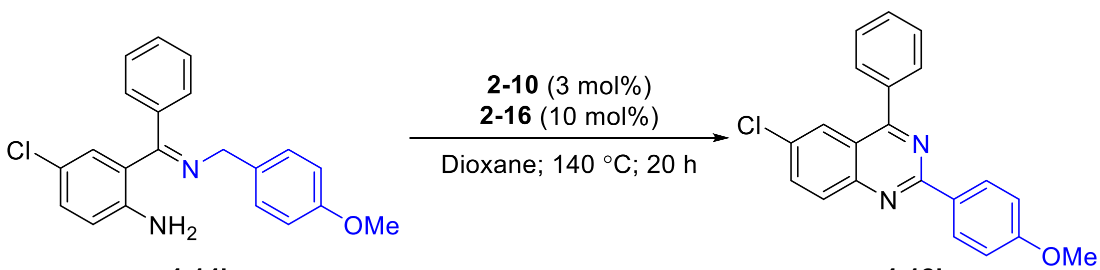

(Eq. 4.6)

To establish the imine as a requisite intermediate for the formation of quinazoline product, an independently synthesized **4-14b** was treated with in-situ generated catalytic system **2-10**/**2-16** under the standard reaction conditions, which proceeded smoothly to afford the quinazoline product **4-12h** in 87% yield (**Eq. 4.6**). In a control experiment, the analogous treatment of **4-14b** with p-toluenesulfonic acid (5 mol %) did not form the product **4-14h** under otherwise similar reaction conditions. The results showed that the ruthenium catalysis is essential for the cyclization and dehydrogenation steps of the product formation. Similarly, the reaction with the imine intermediate of the benzamide was performed under standard reaction conditions (**Eq. 4.7**). Interestingly, quantitative product formation was observed. When the reaction was performed under identical conditions without ruthenium catalyst did not give the desired product.

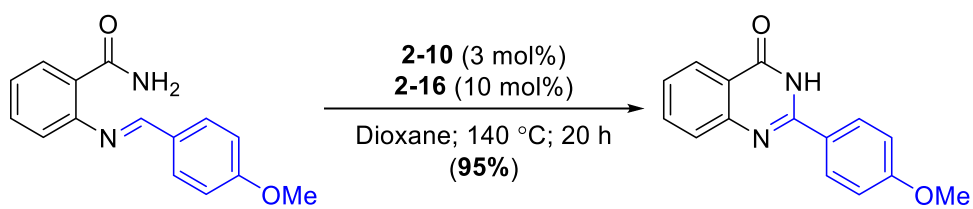

4-15 **4-13c**

(Eq. 4.7)

4.2.4.4 Reactivity of Ruthenium Catecholate Complex 2-11

To gain more insights for the catalytically relevant species, the catalytic activity of ruthenium catecholate complex **2-11** (1 mol%) was examined for the coupling reaction of 2-aminobenzamide and 4-methoxybenzylamine.

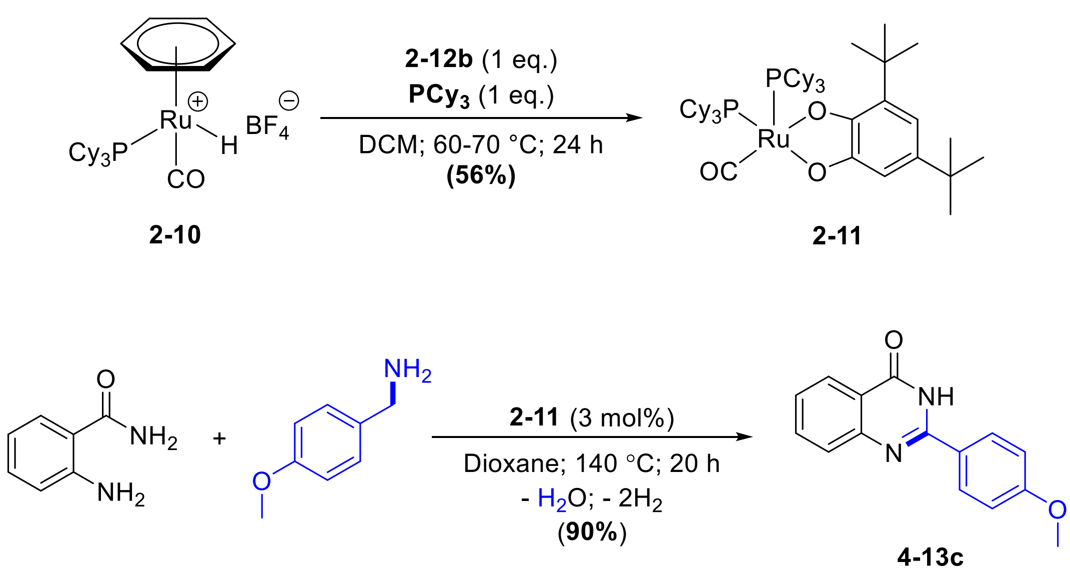

2-10 **2-11** **4-13c**

Scheme 4.4: Coupling Reaction of 2-Aminobenzamide and 4-Methoxybenzylamine with the Ruthenium Catecholate Complex **2-11**

To our delight, the reaction proceeds smoothly to give the product **4-13a** in 90% yield (**Scheme 4.4**). This result demonstrates that the ruthenium catecholate is a catalytically relevant species.

4.3 Proposed Mechanism of the Catalytic Synthesis of Quinazoline Derivatives

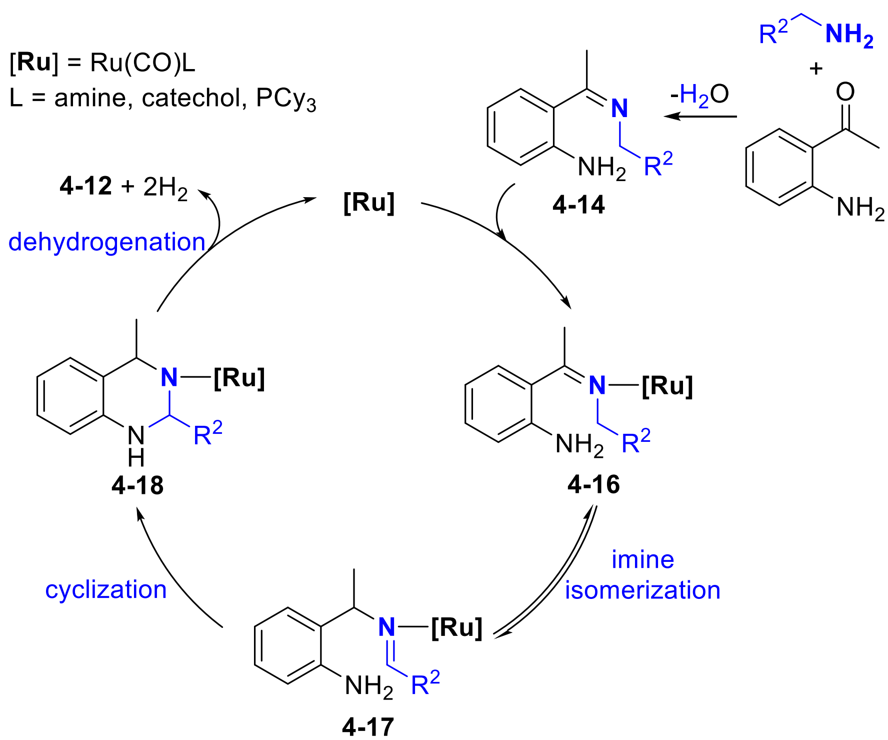

Scheme 4.5: Possible Mechanistic Sequence for the Formation of Quinazoline Products

We offer a plausible mechanistic sequence for the formation of the quinazoline products **4-12** on the basis of these preliminary results (**Scheme 4.5**). The reaction profile study clearly implicates that the imine intermediate **4-14** is generated from initial dehydrative coupling of amino ketone and amine substrates. The imine **4-14** would coordinate to the ruthenium by forming intermediate species **4-16**. We propose that the

Ru catalyst facilitates the imine isomerization to form the imine-coordinated species **4-17**. The subsequent cyclization **4-18** and dehydrogenation steps would yield the quinazoline product **4-12**. In support of this, we previously found that the ruthenium–hydride complexes are efficient catalysts for olefin isomerization reaction[125b] and dehydrogenation of saturated amines and carbonyl compounds.[181] While the exact role of catechol ligand is yet to be established, we believe that a redox-active catechol ligand may be essential for facilitating the dehydrogenation step on the catalysis.[182]

4.4 Summary and Conclusion

We have been able to devise a catalytic protocol for the synthesis of quinazoline and quinazolinone derivatives from the dehydrogenative and deaminative couplings of 2-aminophenyl ketones and 2-aminobenzamides with amines. The in-situ formed ruthenium–hydride complex with a catechol ligand (**2-10**/**2-16**) was found to exhibit uniquely high catalytic activity and selectivity in forming these products. The salient features of the catalytic method are that it employs readily available amine and aminoketone substrates, exhibits a broad substrate scope while tolerating common organic functional groups, and does not require any reactive reagents or forms any wasteful byproducts. We published an article on the basis of the work described in this Chapter: *Org. Lett.* **2019,** *21*, 3337-3341 (DOI: 10.1021/acs.orglett.9b01082). Also, the article has been highlighted in *Organic Chemistry Portal* **2019** (https://www.organic-chemistry.org/abstracts/lit6/835.shtm).

Chapter 5

Regioselective Synthesis of Quinoline and Dihydroquinazolin-4(1H)-one Derivatives via Deaminative and Decarboxylative Coupling Reactions of 2-Aminophenyl Ketones and 2-Aminobenzamides with β-Amino Acids and Branched Amines

5.1 Introduction

Concerted research efforts have been directed to devise transition metal catalyzed C−H coupling methods for the synthesis of biologically active nitrogen heterocyclic compounds **5-1–5-4** to promote synthetic efficiency and to reduce environmental impacts from the generation of harmful byproducts.[183] Quinolines are one of the most important class of nitrogen heterocyclic scaffolds, which have a wide range of medicinal applications in the treatment of various types of diseases as well as natural occurrence in plants and animals. Many quinoline derivatives have been shown to exhibit significant antimicrobial,[184] anticancer[185] and antimalarial[186] pharmacological activities (**Figure 5.2**). As such, the design of new versatile and efficient route for the synthesis of quinoline scaffolds remains an active area of research interest in both academia and industry.[187]

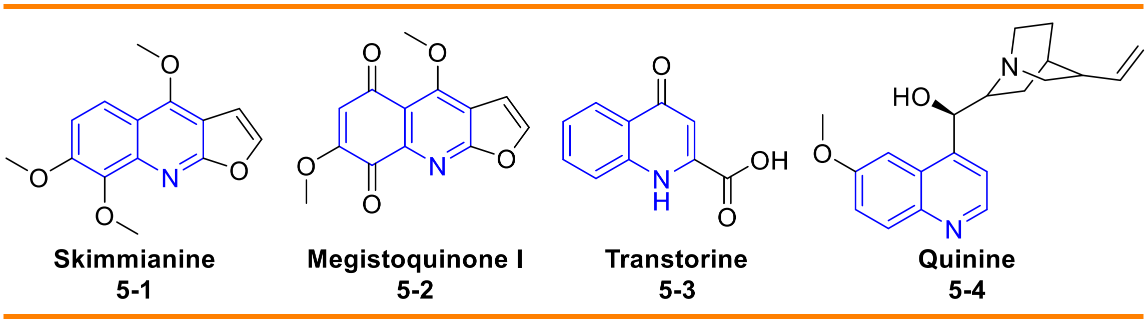

Figure 5.1: Quinoline Containing Natural Products

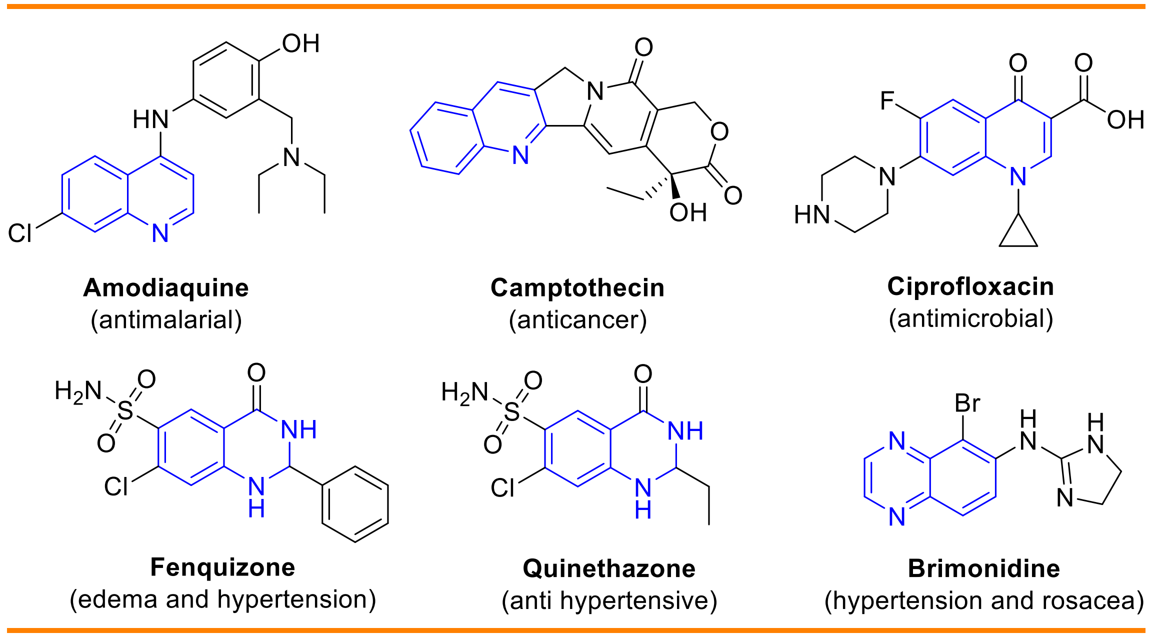

Figure 5.2: Selected Examples of Quinoline, Quinazolinone and Quinoxaline Based Drugs

Many transition-metal catalyzed synthetic methods for quinoline scaffolds have been reported in the last decades. A number of catalytic C−H coupling methods have been achieved by using earth-abundant Co and Ni catalysts.[188] Ruthenium complexes with trialkylammonium salts were utilized as catalysts to effect intermolecular C−C couplings of anilines with diols and glycols to synthesize quinoline derivatives.[189] Ir-BINAP catalytic system has been effectively applied to generate benzoquinoline derivatives from the coupling of naphthylamines with 1,3-diols.[190] Alami and co-workers devised a palladium catalytic system to promote direct decarboxylative coupling reaction to generate biheterocyclic quinoline derivatives **5-7** from quinolinone 3-carboxylic Acids **5-5** with substituted heterocyclic bromides **5-6** (**Eq. 5.1**). The extrusion of CO_2 from carboxylic acid derivative has been found to serve as the driving force for this reaction.[191]

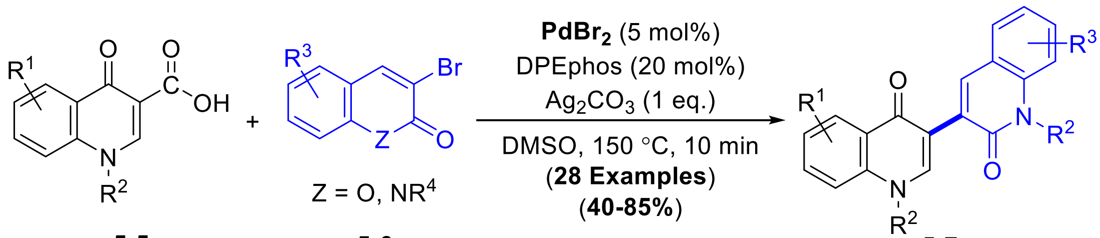

5-5 **5-6** **5-7**

(Eq. 5.1)

Amino acids are considered one of the fundamentally important building blocks in biochemistry[192] and in organic synthesis.[193] Amino acids are an attractive class of reagents for sustainable synthesis since they are readily available from biomass feedstock. While amino acids have been known used as chiral scaffolds and as organo-catalysts,[194] they have scarcely been used as the reagents for organic coupling reactions via C–N bond cleavage.[29] Natural biosynthetic pathways provide an ample inspiration for C–N bond cleavage reactions of amino acids by efficient deaminase, oxidase, and dehydrogenase enzymes.[195] Recently, Wu and co-workers developed a novel synthetic protocol for substituted quinoline syntheses from three component coupling reaction of aniline with two distinct α-amino acids under decarboxylative and deaminative pathway via the formation of imine and enamine intermediates.[196] In a seminal report, Wang and coworkers devised copper/DIPEA-catalytic system for aldehyde-induced intermolecular decarboxylative coupling reaction of natural α-amino acids and phosphites/phosphine oxides.[197] Allylic amination, alkylation, sulfonylation, and phosphinoylation products were also synthesized from the copper-catalyzed decarboxylative coupling reactions of conjugated β,γ-unsaturated carboxylic acids with corresponding coupling partners.[198] Iridium catalyzed visible-light-induced photoredox catalytic system has been established for easy access to β-aminohydroxylamines and vicinal diamines decarboxylative coupling of α-amino acids with nitrone substrates.[199] Photoredox decarboxylative coupling of α-amino acids with carbonyl compounds to access DNA-encoded 1,2-amino alcohols has also been reported.[200] Recently, Zhou and co-workers demonstrated a nickel catalyzed synthesis of 2,3-dihydroquinazolin-4(1H)-ones via decarboxylative pathway.[201] In 2017, Ogawa and coworkers devised cross-coupling and hydroamination to give 2,2-disubstituted quinazolinones via copper-catalyzed tandem reaction of vinyl halides **5-8** and 2-aminobenzamides (**Eq. 5.2**).[202] A number of late transition metal catalysts have been successfully utilized for the synthesis of 2,3-dihydroquinazolin-4(1H)-one derivatives.

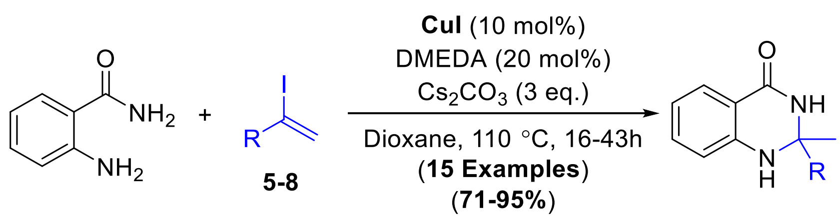

(Eq. 5.2)

5.2 Results and Discussion

We previously discovered that the cationic ruthenium hydride complex **2-10** is a highly effective catalyst precursor for the deaminative and decarboxylative coupling reaction of ketones with amino acids.[29] We also reported that a phenol-coordinated cationic ruthenium-hydride complex is a highly effective catalyst for mediating the hydrogenolysis of aldehydes and ketones.[180] We subsequently found that the ruthenium-hydride complex **2-10** with a 1,2-catechol ligand exhibits an exceptionally high chemo-selectivity for promoting the deaminative coupling reactions of amines to form unsymmetrical secondary amines[126b] and quinazolinone[149] derivatives. To further extend the synthetic utility of ligand-promoted C–N bond coupling reactions, we have been exploring the coupling reactions of 2-aminoketones with amines which led to the formation of quinoline byproduct **5-9** along with the expected quinazoline product **4-12aa** (**Eq. 5.3**).

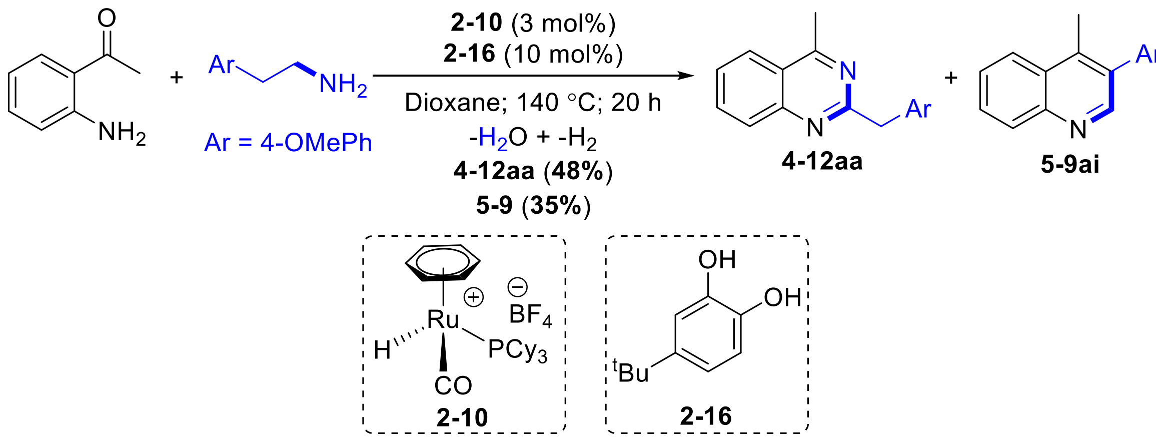

(Eq. 5.3)

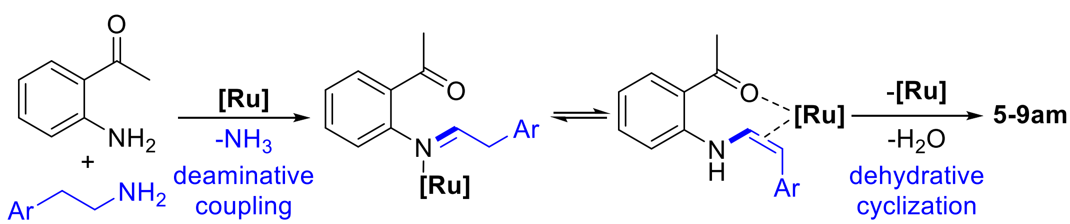

Scheme 5.1: Generation of Quinolines from the Reaction of 2-Aminoacetophenone with 2-(4-Methoxyphenyl)ethylamine

The regioselective formation of quinoline byproduct **5-9** can be rationalized by invoking the initial deaminative coupling[126b] followed by dehydrative cyclization steps via in-situ generated enamine intermediate. To generate quinolines with complete regioselectivity, we reasoned that the equilibrium between deaminative coupling vs initial imine formation should be the product determining step from the reaction of amine and aryl-ketone substrates. We tested the hypothesis by running the reaction with preformed imine generated from the 2-aminoacetophenone and phenylethylamine, which gave over

85% quinazoline with only a trace quinoline products (**Eq. 5.4**). While exploring suitable substrates in formation of quinoline products, we found that the β-amino acids are effective partners for the coupling reaction to afford 2-quinoline products (**Eq. 5.5**).

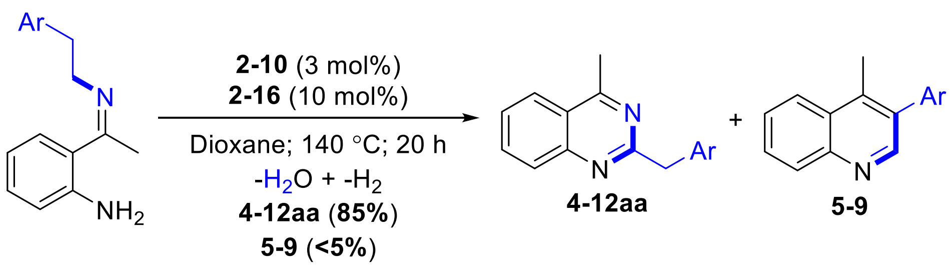

(Eq. 5.4)

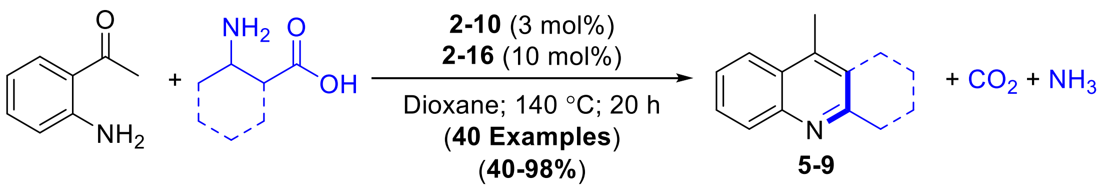

(Eq. 5.5)

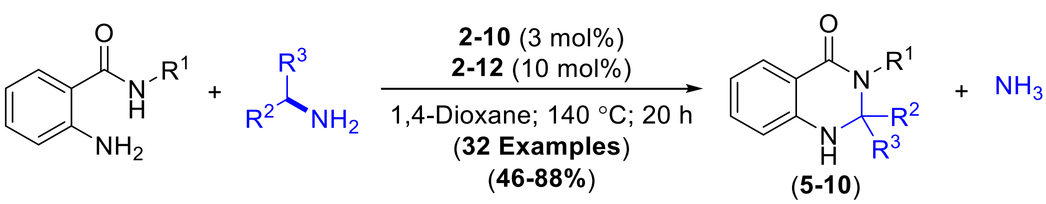

(Eq. 5.6)

In this Chapter, we disclose an efficient catalytic synthesis of quinoline and dihydroquinazolin-4(1H)-one derivatives from the dehydrogenative and deaminative coupling reactions of amino ketones and aminobenzamides with β-amino acids and branched amines (**Eq. 5.5 and 5.6**). The salient features of the catalytic method are that the synthetically useful nitrogen heterocyclic core structures are formed in regio- and diastereoselective fashion without employing any reactive reagents or forming any wasteful byproducts, while tolerating a number of common organic functional groups.

5.2.1 Optimization Studies

We initially explored the scope of coupling reaction of 2-aminoketones with β-amino acids by employing the ligand promoted catalysis protocol. Among the initially screened Ru catalysts and ligands, the in-situ generated catalytic system from the cationic ruthenium–hydride complex **2-10** with 4-(1,1-dimethylethyl)-1,2-benzenediol **2-16** was found to give the highest activity and selectivity for the coupling of 2-aminoacetaphenone with 3-aminobutanoic acid in yielding the quinoline product **5-9b** (**Table 5.1**). The coupling reaction conditions described in **Eq. 5.5** have been used as the standard reaction conditions unless otherwise noted.

5.2.1.1 Ligand Screening

We selected the coupling reaction of 2-aminoacetophenone with 3-aminobutanoic acid to evaluate the ligand effects. In the absence of any ligands, the reaction was found to be very sluggish as a trace amount of the product **5-9b** was obtained with the catalyst **2-10** (**Table 5.3**; entry 7). The addition of catechol ligands (**2-16, 2-16a-f**) significantly increased the formation of the desired product **5-9b**. In accordance with the previous results on the ruthenium catalyzed C(sp^3)–N bond cleavage reactions, binol, phenolic **3-11b,c** and amine containing ligands (**3-11b**, **3-12**) were not effective for the transformation, and the catechol ligand **2-16** was found to be the most effective for the selective synthesis of secondary amines.[126b] The catechol ligands with both electron donating and withdrawing group **2-16a-e** were found to be effective for the catalytic reaction in giving moderate to good yields (70-88%). As shown in **Table 5.1**, the catalytic activity of **2-10** was found to be substantially enhanced by the addition of a catechol ligand with the efficient formation of product **5-9b**.

Table 5.1: Ligand Screening for the Coupling of 2-Aminophenylethanone with 3-Aminobutanoic acid [a]

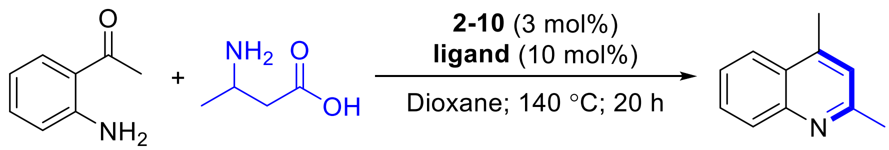

5-9b

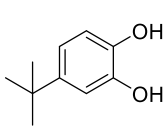	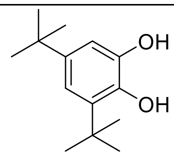	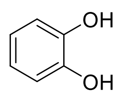	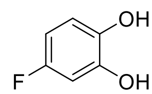	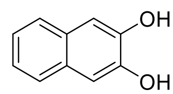	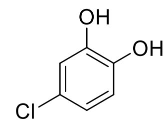
2-16 (88%)	**2-16a** (70%)	**2-16b** (72%)	**2-16c** (84%)	**2-16d** (79%)	**2-16e** (71%)
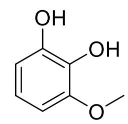	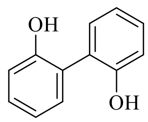	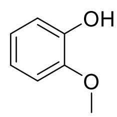	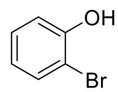	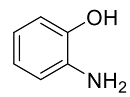	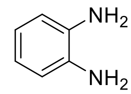
2-16f (60%)	**2-12j** (<10%)	**3-11b** (<10%)	**3-11c** (<10%)	**3-11d** (<10%)	**3-12** (<10%)

[a]Reaction conditions: 2-aminophenylethanone (0.5 mmol), 3-aminobutanoic acid (0.7 mmol), **2-10** (3 mol %), ligand (10 mol %), 1,4-dioxane (2 mL), 140 °C, 20 h. [b]The product yield of **5-9b** was determined by ^{1}H NMR using hexamethylbenzene as an internal standard.

We initially explored the coupling reaction of 2-aminobenzamide with β-amino acids in extending the synthetic utility of the coupling reaction. We screened the benzoquinone ligands, which gave the best result for branched amine substrates. As shown in the **Table 5.2**, the ligand **2-12** has resulted in the formation of desired product in 94% yield. In general, the benzoquinone ligands **2-12a,b,f-h** were shown to be more effective than the catechol ligands.

Table 5.2: Ligand Screening for the Coupling of 2-Aminobenzamide with 3-Aminobutanoic acid[a]

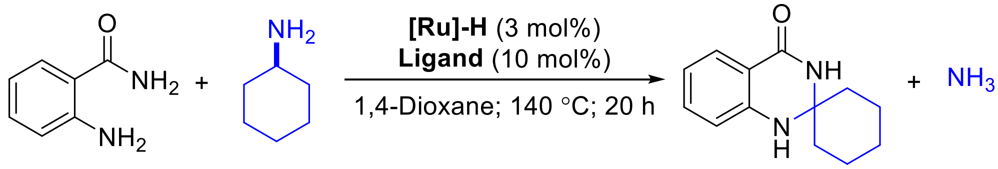

(**5-10m**)

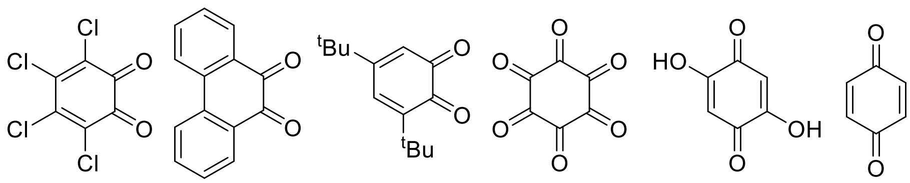

2-12 **2-12a** **2-12b** **2-12f** **2-12g** **2-12h**

entry	ligand	**5-10m** (%)[b]
1	**2-12**	94
2	**2-12a**	86
3	**2-12b**	85
4	**2-12f**	74
5	**2-12g**	81
6	**2-16b**	66
7	**2-16c**	72
8	**2-16d**	68
9	**2-12j**	30
10	**3-11b**	44
11	**3-11d**	trace
12	**3-12**	0

[a]Reaction conditions: 2-aminobenzamide (0.5 mmol), cyclohexylamine (0.7 mmol), **2-10** (3 mol %), ligand (10 mol %), 1,4-dioxane (2 mL), 140 °C, 20 h. [b]The product yield of **5-10m** was determined by ^{1}H NMR using hexamethylbenzene as an internal standard.

5.2.2.2 Catalyst and Solvent Screening

We compared the activity of commonly available ruthenium catalysts, where 1,4-dioxane was found to be the most suitable solvent for the coupling reaction (entry 2-6). Among the screened ruthenium catalysts, the Ru-H complex **2-10** was found to be the most effective catalyst (entry 1). Importantly, Lewis acids and PCy_3 did not exhibit any activity for the coupling reaction (entry 14-16).

Table 5.3: Catalyst and Additive Screening for the Coupling of 2-Aminophenylethanone with Aminobutanoic acid[a]

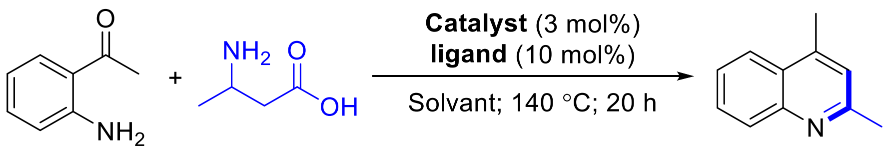

5-9b

entry	catalyst	deviation from standard conditions	**5-9b** (%)[b]
1	$[(C_6H_6)(PCy_3)(CO)RuH]^+BF_4^-$ **2-10**	none	**88**
2	$[(C_6H_6)(PCy_3)(CO)RuH]^+BF_4^-$ **2-10**	cyclopentene[c]	82
3	$[(C_6H_6)(PCy_3)(CO)RuH]^+BF_4^-$ **2-10**	chlorobenzene	54
4	$[(C_6H_6)(PCy_3)(CO)RuH]^+BF_4^-$ **2-10**	1,2-DCE	<10
5	$[(C_6H_6)(PCy_3)(CO)RuH]^+BF_4^-$ **2-10**	DME	<10
6	$[(C_6H_6)(PCy_3)(CO)RuH]^+BF_4^-$ **2-10**	Toluene	74
7	$[(C_6H_6)(PCy_3)(CO)RuH]^+BF_4^-$ **2-10**	No ligand	22
8	$[(PCy_3)(CO)RuH]_4(\mu\text{-}O)(\mu\text{-}OH)_2$ **2-9**	-	71
9	$(p\text{-cymene})_2RuHCl$	-	49
10	$RuCl_2(PPh_3)_3$	-	44
11	$RuCl_3{\cdot}3H_2O$	-	<10
12	$[Ru(COD)Cl_2]_x$	-	32
13	$(PCy_3)_2(CO)RuHCl$	-	55
14	-	$HBF_4{\cdot}OEt_2$	0
15	BF_3	-	0
16	PCy_3	-	0

[a]Standard conditions: 2-aminophenylethanone (0.5 mmol), aminobutanoic acid (0.7 mmol), catalyst (3 mol %), ligand (10 mol %), solvent (2 mL), 140 °C, 20 h. [b] The product yield of **5-9b** was determined by ^1H NMR using hexamethylbenzene as an internal standard. [c]0.5 mmol of cyclopentene was added.

These ligand screening and optimization efforts have led to the standard conditions for the coupling reaction: 2-aminophenylethanone (0.5 mmol), β-amino acid (0.7 mmol), **2-**

10 (3 mol %) and **2-16** (10 mol %) in 1,4-dioxane (2 mL) at 140 °C for 20 h (**Table 5.3**). The water byproduct was detected by NMR in a crude reaction mixture, and hydrogen gas was removed under vacuum along with the solvent. The product **5-9b** was isolated by a column chromatographic separation on silica gel.

Table 5.4: Catalyst and Additive Screening for the Coupling of 2-Aminobenzamide with Cyclohexylamine[a]

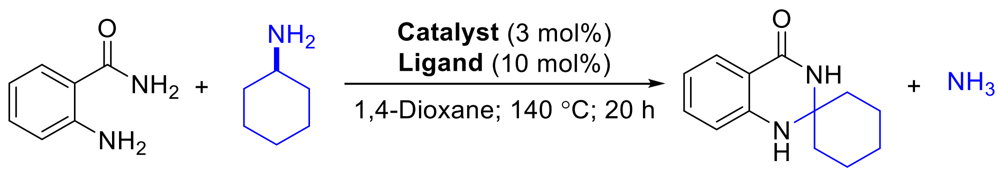

entry	catalyst	deviation from standard conditions	**5-10m** (%)[b]
1	$[(C_6H_6)(PCy_3)(CO)RuH]^+BF_4^-$ **2-10**	none	94
2	$[(C_6H_6)(PCy_3)(CO)RuH]^+BF_4^-$ **2-10**	chlorobenzene	61
3	$[(C_6H_6)(PCy_3)(CO)RuH]^+BF_4^-$ **2-10**	1,2-DCE	<10
4	$[(C_6H_6)(PCy_3)(CO)RuH]^+BF_4^-$ **2-10**	toluene	79
5	$[(C_6H_6)(PCy_3)(CO)RuH]^+BF_4^-$ **2-10**	chlorobenzene	74
6	$[(C_6H_6)(PCy_3)(CO)RuH]^+BF_4^-$ **2-10**	1,2-DCE	<10
7	$[(PCy_3)(CO)RuH]_4(\mu\text{-}O)(\mu\text{-}OH)_2$ **2-9**	-	74
8	$[(PCy_3)(CO)RuH]_4(\mu\text{-}O)(\mu\text{-}OH)_2$ **2-9**	$HBF_4{\cdot}OEt_2$	86
9	$[RuH_2(CO)(PPh_3)_3]$	-	41
10	$[(PCy_3)(CH_3CN)(CO)RuH]^+BF_4^-$	-	45
11	$RuHCl(p\text{-cymene})_2$	-	50
12	$[Ru(COD)Cl_2]_x$	-	trace
13	$[RuCl_3{\cdot}3H_2O)]$	-	trace
14	-	$HBF_4{\cdot}OEt_2$	0
15	-	BF_3	0
16	-	PCy_3	0

[a]Standard conditions: 2-aminophenylethanone (0.5 mmol), cyclohexylamine (0.7 mmol), catalyst (3 mol %), ligand (10 mol %), solvent (2 mL), 140 °C, 20 h. [b] The product yield of **5-10m** was determined by ^1H NMR using hexamethylbenzene as an internal standard. [c]0.5 mmol of cyclopentene was added.

Next, we screened the activity of both Ru catalysts and ligands for the coupling reaction of 2-aminobenzamide with branched amines. The screening and optimization efforts have led to the standard conditions for the coupling reaction: 2-aminoamide (0.5 mmol), branched amine (0.7 mmol), **2-10** (3 mol %) and **2-12** (10 mol %) in 1,4-dioxane (2 mL) at 140 °C for 20 h (**Table 5.4**). Among the screened ruthenium catalysts, the Ru-H complex **2-10** was found to be the most effective catalyst (entry 1), and Lewis acid or bases did not exhibit any activity, just as in the previous reaction. The product **5-10m** was isolated by a column chromatographic separation on silica gel.

5.2.2 Synthesis of Quinoline Derivatives from the Coupling of 2-Aminophenyl Ketones with β-Amino Acids

With the optimized conditions in hand, we explored the substrate scope of the coupling reaction by using the catalyst system **2-10**/**2-16** under the standard reaction conditions as described above. The coupling of 2-aminophenyl ketones with a variety of β-amino acids formed the quinoline products **5-9a–h** in a regioselective fashion in good to excellent yields (56-90%). The coupling of 2-aminophenyl ketones with cyclic β-amino acids also gave the selective formation of the desired products **5-9i–p** in excellent yields. Electron rich 3-amino-3-benzo[1,3]dioxol-5-yl-propionic acid reacted with a number of substituted 2-amino ketones to form the products in good to excellent yields **5-9q–t** (50-87%). Linear β-amino acids, such as β-homophenylalanine and 3-aminoheptanoic acid gave a mixture of 2,3-disubstituted quinoline products. This observation can be rationalized as a double bond isomerization on ruthenium in forming more thermodynamically favorable product. In this case, the coupling of 2-

aminobenzaldehyde with β-homophenylalanine afforded the desired 2-substituted quinoline product **5-9w-b** in only 34% yield along with the non-desired 2,3-disubstituted quinoline product **5-9w-a** in 65% yield. In contrast, 5-chloro-2-aminobenzophenone with β-homophenylalanine afforded the desired 2-substituted quinoline product **5-9y-b** in 12% yield and undesired 2,3-disubstituted quinoline product **5-9y-a** in 87% yield (**Scheme 5.2**).

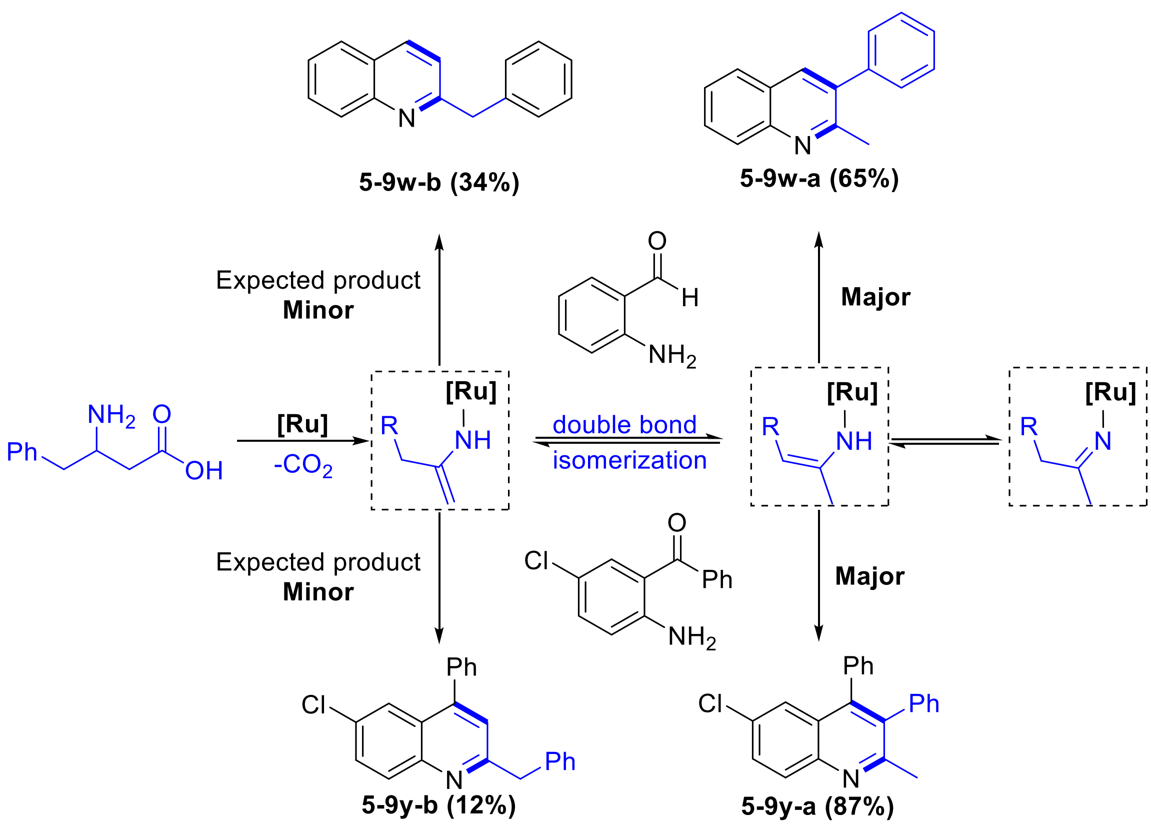

Scheme 5.2: Possible Explanation for the Product Selectivity

While the coupling reaction of 2-aminphenyl ketone substrate with a (±)-3-amino-5-methylhexanoic acid smoothly yielded regioselective coupling products **5-9aa-ac**, the coupling with sterically demanding (±)-β-leucine gave the desired product **5-9ad** in 51% yield.

Table 5.5: Synthesis of Quinoline Derivatives from the Coupling of 2- Aminophenyl Ketones with β-Amino Acids[a]

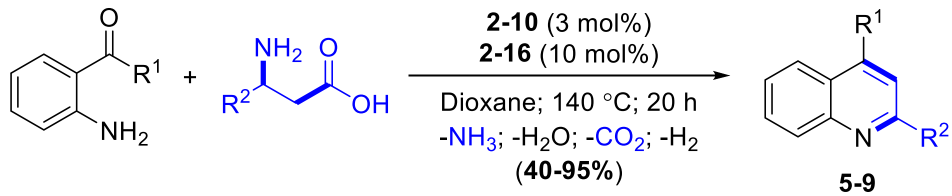

Selected examples:

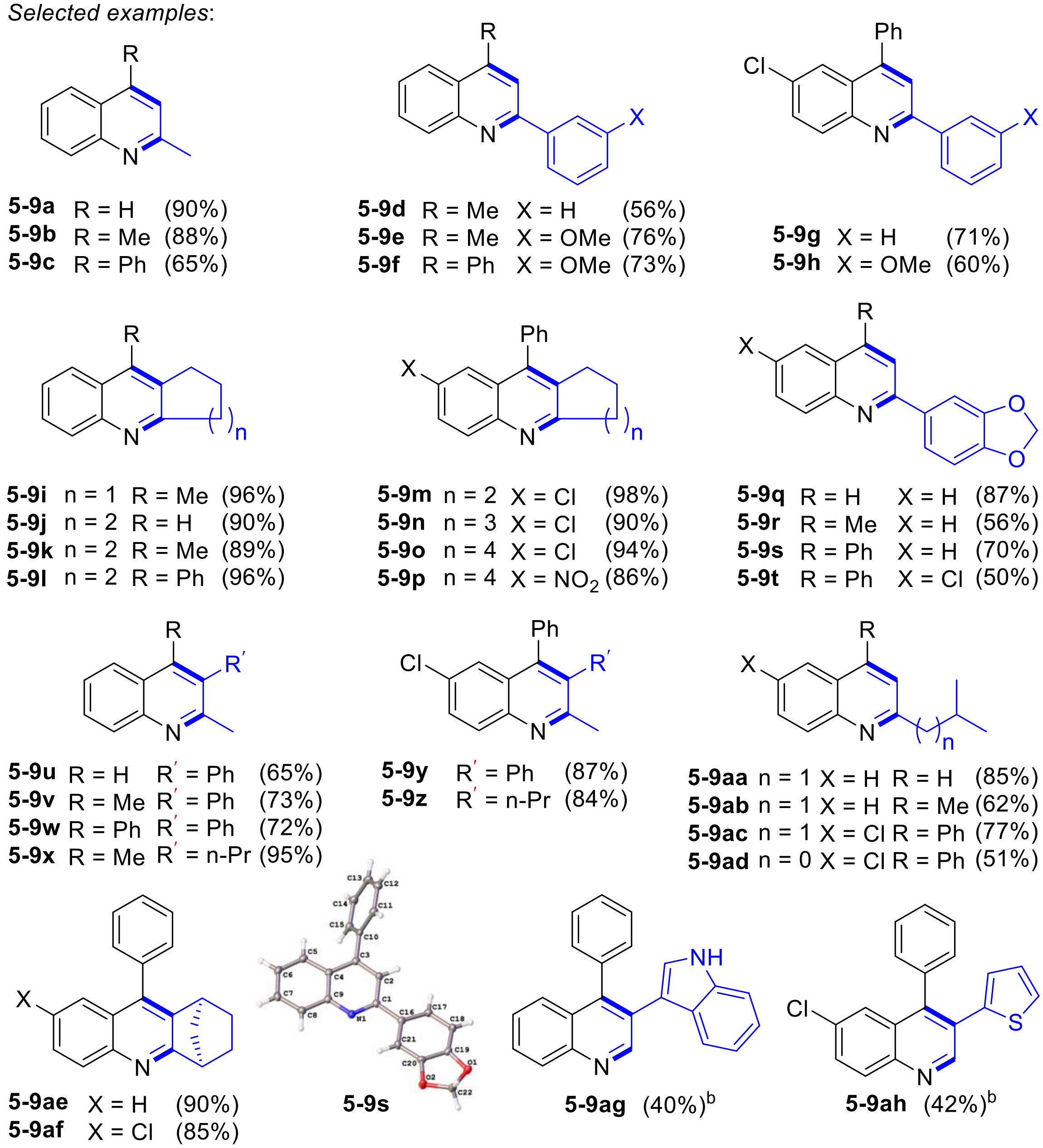

[a]Reaction conditions: aminoketone (0.5 mmol), amino acid (0.7 mmol), **2-10** (3 mol %), **2-16** (10 mol %), 1,4-dioxane (2 mL), 140 °C, 20 h. [b]Corresponding primary amine was used.

cis-endo-3-aminobicyclo[2.2.1]heptane-2-carboxylic acid was found to be a suitable substrate for the coupling reaction without giving any side products **5-9ae,af**. When the reaction was performed with tryptamine and 2-thiopheneethylamine, a mixture of quinazolinone and quinoline products **5-9ag** and **5-9ah** formed in 40% and 42% respectively under the standard reaction conditions. Single crystals of **5-9s** were obtained by slow evaporation in pentane/acetone at room temperature, and its structure was determined by X-ray crystallography.

5.2.3 Synthesis of Dihydroquinazolin-4(1H)-one from the Coupling of 2-Aminobenzamides with β-Amino Acids and Branched Primary Amines

Adopting the previously developed conditions, we next sought the catalytic coupling reaction of 2-aminobenzamide with β-amino acids which formed the desired dihydroquinazolin-4(1H)-one product in 80% yield. To further extend the synthetic utility, we next explored the coupling reaction of 2-aminobenzamide derivatives with branched primary amine substrates. In light of the previously developed deaminative coupling reaction of primary amines[126b], we sought to achieve a direct C–N bond cleavage via imine intermediate. Thus, the treatment of 2-aminobenzamide (0.5 mmol) with branched amine (0.70 mmol) in the presence of **2-10** (3 mol %) and **2-12** (10 mol %) in 1,4-dioxane (2 mL) at 140 °C smoothly formed the coupling products **5-10a–e** in good yields, which are analyzed by both GC and NMR spectroscopic methods. Single crystals of **5-10a** were obtained by slow evaporation in hexanes/EtOAc at room temperature, and its structure was determined by X-ray crystallography. The coupling of 2-aminobenzamides with both branched benzyl- and alkyl-substituted amines led to the selective formation of the dihydroquinazolin-4(1H)-one products **5-10f−k** (76-88%) without significant amount of the secondary amine or other side products.

Table 5.6: Synthesis of Dihydroquinazolin-4(1H)-one from the Coupling of 2-Aminobenzamides with Branched Amines

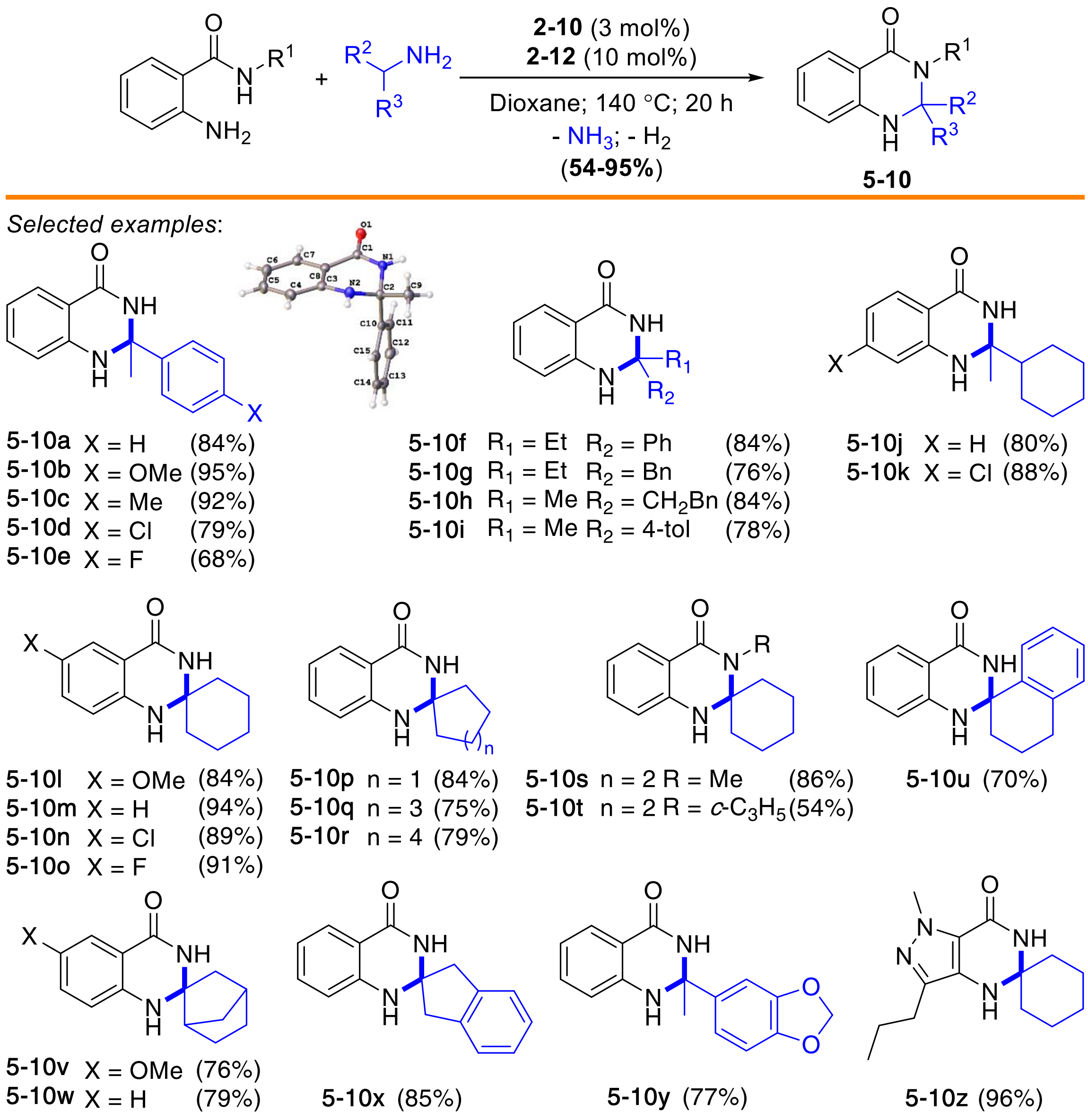

[a]Reaction conditions: aminoamide (0.5 mmol), branched amine (0.7 mmol), **2-10** (3 mol %), **2-12** (10 mol %), 1,4-dioxane (2 mL), 140 °C, 20 h.

The analogous coupling reaction of both 2-aminobenzamides and N-alkyl-2- benzamides with cyclic amines afforded the corresponding coupling products **5-10l−t** in moderate to high yields (54-91%). Benzocyclic and bicyclic amines also reacted smoothly to generate the desired dihydroquinazolin-4(1H)-one products **5-10u−x**. Interestingly, biologically relevant oxygen and nitrogen heterocyclic amines gave the desired product in excellent yields. The formation of dihydroquinazolin-4(1H)-one product can be rationalized by initial deaminative coupling of amide and amine substrates followed by the cyclization dehydrogenation steps. The coupling reaction efficiently assembles synthetically valuable dihydroquinazolin-4(1H)-one products core structures by employing readily available branched amine and benzamide substrates.

5.2.4 Coupling Reaction of 2-Aminophenylketones with Biologically Active Amines

To further demonstrate synthetic utility of the catalytic method, we next surveyed the substrate scope of the coupling method by employing several functionalized 2-aminophenyl ketones and 2-aminobenzamides with a number of biologically active amine substrates (**Table 5.7**). Treatment of (3-amino-6-nitrobenzofuran-2-yl)(phenyl)methanone with (1S,2R)-2-aminocyclohexanecarboxylic acid led to the nitro/chloro-substituted products **5-10i−j** in excellent yields under the standard reaction conditions. The analogous coupling reaction of 5-chloro-2-aminobenzophenone with in-situ generated 1-(4-(2,6,6-trimethylcyclohex-1-en-1-yl)but-2-en-2-yl)pyrrolidine and 1-(3-methyl-4-(2,6,6-trimethylcyclohex-2-en-1-yl)buta-1,3-dien-2-yl)pyrrolidine formed the corresponding quinoline products **5-9ak** and **5-9al** in good yields (59, 61% respectively) in a regioselective fashion.

Table 5.7: Coupling Reaction of 2-Aminophenyl Ketones and 2-Aminobenzamides Biologically Active and Functionalized Amines[a]

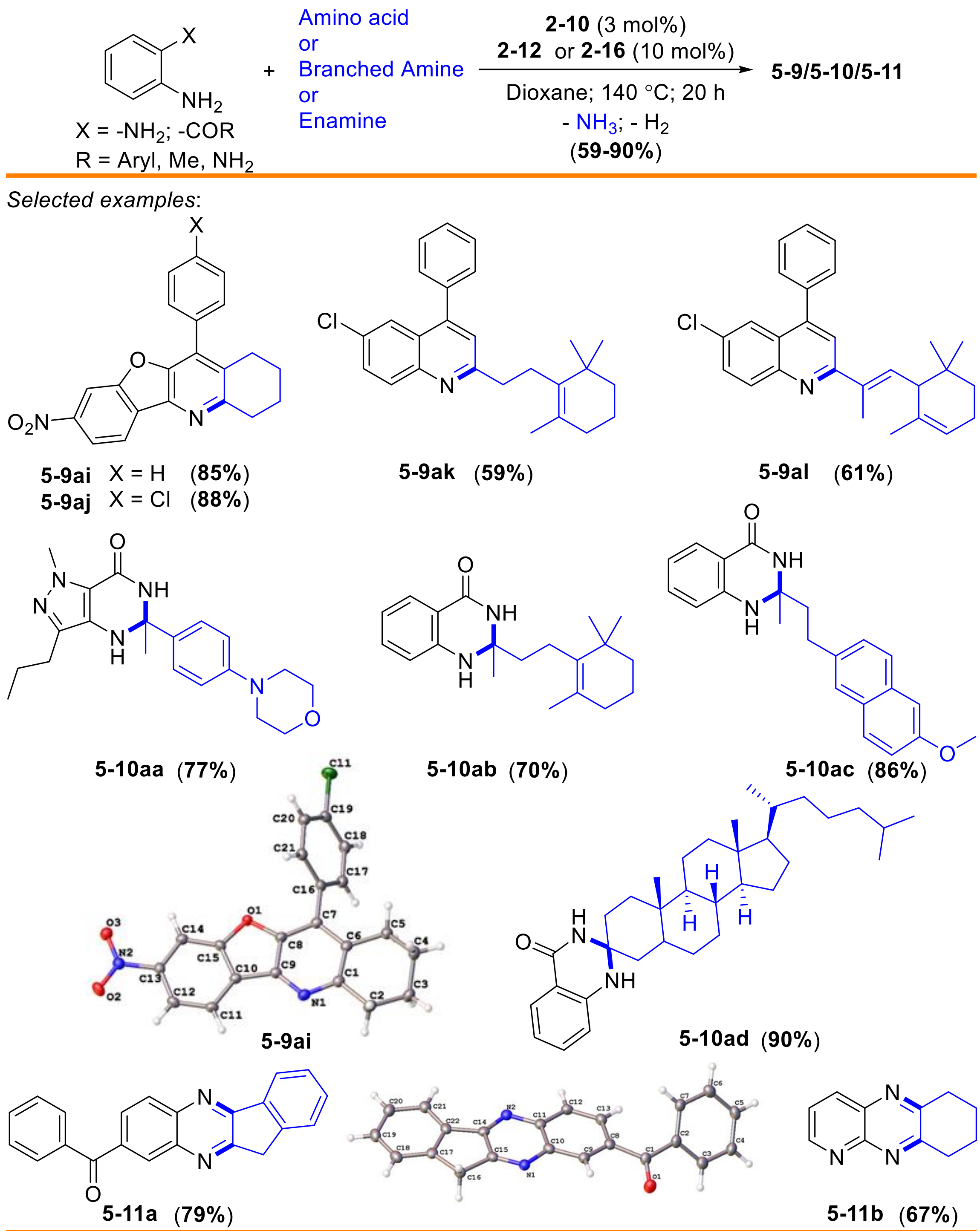

[a]Reaction conditions: 2-aminoketone or 2-aminobenzamide (0.5 mmol), amine/amino acid (0.7 mmol), **2-10** (3 mol %), **2-12** or **2/16** (10 mol %), 1,4-dioxane (2 mL), 140 °C, 20 h. [b]Benzene-1,2-diamine (0.5 mmol), enamine (0.5 mmol).

The coupling of 4-amino-1-methyl-3-n-propyl-5-pyrazolecarboxamide with a 4-morpholinyl-substituted amine predictively formed the desired product **5-10aa** in 96% yield. The coupling of 2-aminobenzamide with in-situ generated 1-(4-(2,6,6-trimethylcyclohex-1-en-1-yl)but-2-en-2-yl)pyrrolidine and 1-(4-(6-methoxynaphthalen-2-yl)but-2-en-2-yl)pyrrolidine yielded the desired dihydroquinazolin-4(1H)-one products **5-10ab** and **5-10ac** in 70% and 86% yields, respectively. Delightfully, the reaction of 2-aminobenzamide with 1-((8S,9R,10R,13S,14R,17S)-10,13-dimethyl-17-((S)-6-methylheptan-2-yl)-4,5,6,7,8,9,10,11,12,13,14,15,16,17-tetradecahydro-1H-cyclopenta[a]phenanthren-3-yl)pyrrolidine, afforded the desired cholesterol derivative **5-10ad** in an excellent yield (90%). The analogous treatment of 1,2-diamine with corresponding enamine also formed the quinoxaline product **5-11a-b**. The structures of both **5-9ai** and **5-11a** products have been confirmed by X-ray crystallographic method. These examples clearly demonstrated the general applicability of the catalytic coupling method in synthesizing biologically active dihydroquinazolin-4(1H)-one derivatives.

Synthetic utility of the catalytic method has been further tested by running a preparatory scale reaction of 2-amino-5-chlorobenzophenone (1.16 g, 5.0 mmol) with (1S,2R)-2-aminocyclohexanecarboxylic acid (1.0 g, 7 mmol) under standard reaction conditions. Analytically pure product **5-9m** was obtained by crystallization in dichloromethane and n-hexanes (1.17 g, 80%). Similarly, the reaction of 2-aminobenzamide (1.04 g, 7.5 mmol) and cyclohexylamine (1.04 g, 10.5 mmol) under standard reaction conditions afforded the product **5-10m** in 84% yield (1.36 g).

5.2.5 Mechanistic Studies

5.2.5.1 Deuterium Labeling Study

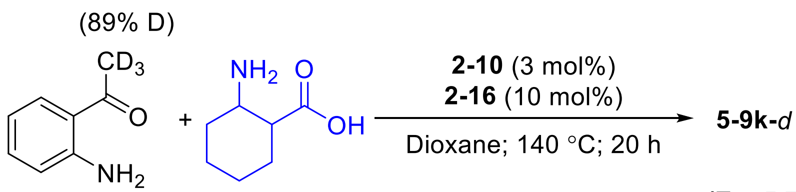

(Eq. 5.7)

We have chosen the coupling reaction of 2-aminoacetophenone with cyclohexylamine for probing mechanistic insights. First, we examined the deuterium-labeling pattern from the reaction of 2-aminophenylethanone-d_3 (89% D) with 4-methoxybenzylamine (**Eq. 5.7**).

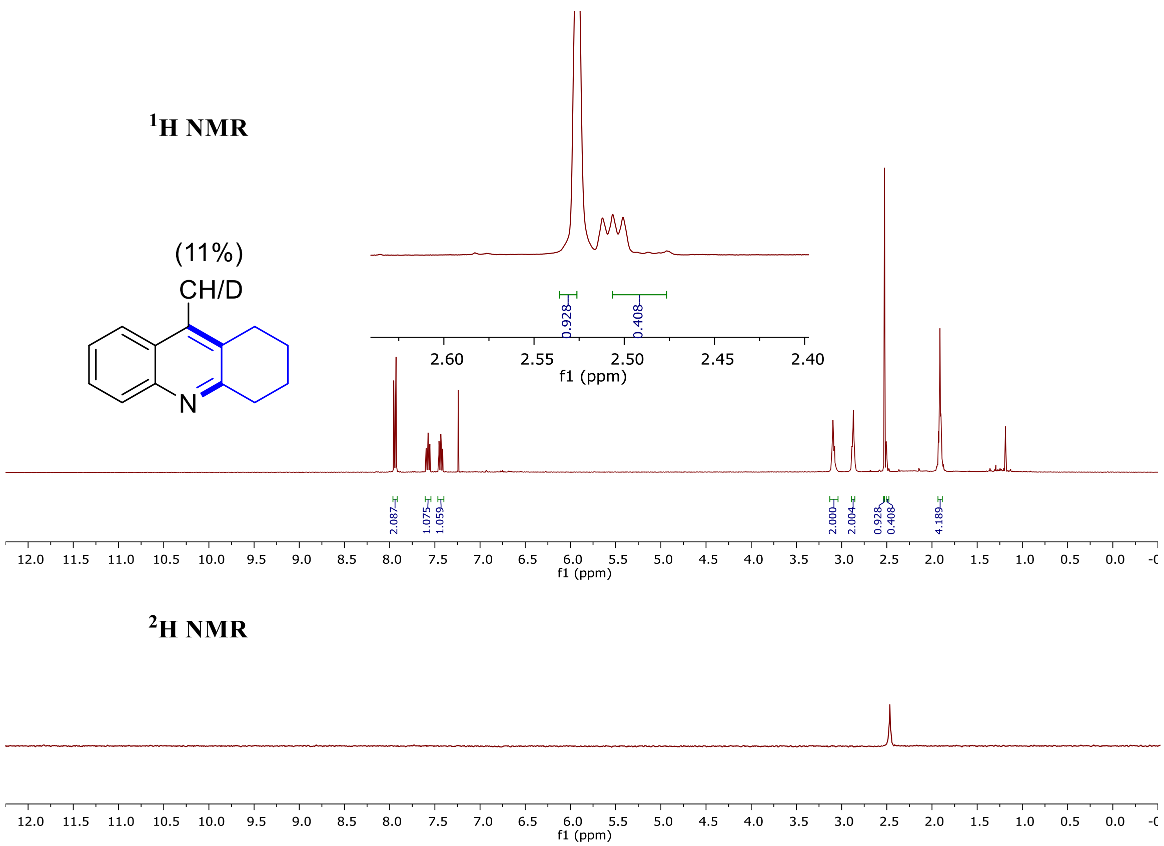

Figure 5.3: ^{1}H and ^{2}H NMR Spectra of **5-9k-*d*** Isolated from the Reaction of 2'-Aminoacetophenone-d_3 with (1S,2R)-2-Aminocyclohexanecarboxylic acid

Thus, the treatment of perdeuterated 2-aminophenylethanone-d_3 (0.50 mmol) with 2-aminocyclohexanecarboxylic acid (0.70 mmol) in the presence of **2-10** (3 mol %)/**2-16** (10 mol %) under the standard reaction conditions formed the coupling product **5-9k**-*d*. The isolated product **5-9k**-*d* as analyzed by ^{1}H and ^{2}H NMR contained only 11% of the deuterium on the methyl group as most of the deuterium had been washed away (**Figure 5.3**). A relatively small amount of the deuterium on **5-9k**-*d* suggests an extensive keto−enol tautomerization under the reaction conditions.

5.2.5.2 Carbon Isotope Effect Study

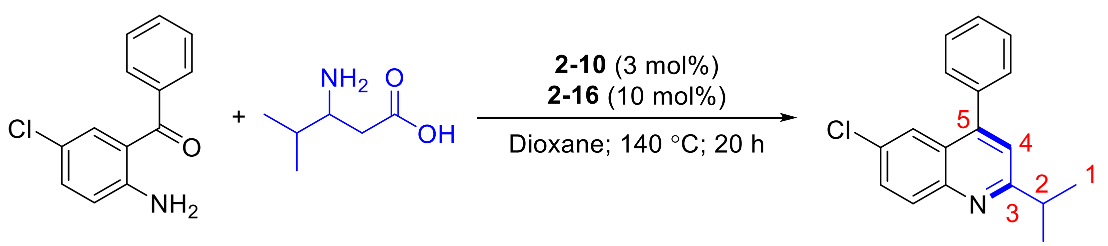

5-9ad

(Eq. 5.8)

To discern between the possible turnover limiting steps, Singleton's NMR technique[127] at natural abundance was used to measure the ^{12}C/^{13}C kinetic isotope effect (KIE) from the coupling reaction of 5-chloro-2-aminobenzophenone with β-leucine in the presence of **2-10** (3 mol %)/**2-16** (10 mol %) in 1,4-dioxane (8 mL) was heated at 130 °C for 20 h (**Eq. 5.8**). The high precision ^{13}C NMR analysis showed, most pronounced carbon KIE was observed on the β-carbon atom of the product **5-9ad**, when the ^{12}C/^{13}C ratio of the product at 92% conversion was compared to the product obtained at a low conversion (KIE on C3 = 1.018; average of 3 runs) The unique carbon KIE on the carbon atom of **5-9d** suggests that the C-N bond cleavage is intimately involved in the turnover limiting step of the coupling reaction. (**Table 5.8**).

Table 5.8: Average ^{13}C Integration of the Product 5-**9d** Obtained from the Reaction of 5-chloro-2-aminobenzophenone and β-Leucine at High Conversion (Virgin, R_0; 92% conversion), at Low Conversion (R; avg 15% conversion) and the Calculated ^{13}C KIE (C1 = reference)

Carbon #	High Conversion (R_0)	Low Conversion (R)	R_0/R	KIE
1 (ref)	1	1	1.0000	1.0000
2	2.1727	2.1722	1.0002	1.0002
3	**1.0749**	**1.0556**	**1.0181**	**1.0181**
4	1.0843	1.0799	1.0041	1.0041
5	1.4853	1.4899	0.9969	0.9969

5.2.5.3 Reaction with Enamine Substrates

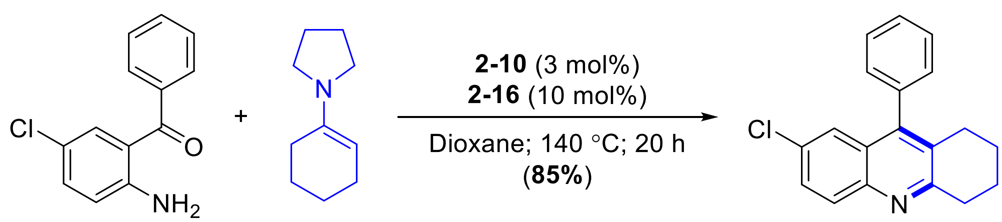

5-9m

(Eq. 5.9)

To establish the enamine as a requisite intermediate for the formation of quinoline product, the reaction of and 1-pyrrolidino-1-cyclohexene was tested under the standard reaction conditions, which proceeded smoothly to afford the quinoline product **5-9m** in 85% yield (**Eq. 5.9**). In a control experiment, analogous treatment of with p-toluenesulfonic acid (5 mol %) did not form the product **5-9m** under otherwise similar reaction conditions. Delightfully, the reaction with ruthenium catecholate **2-11** also afforded the desired product 85% yield indicating ruthenium catecholate is a viable catalytic species. The results showed that the ruthenium catalysis is essential for the cyclization and dehydrogenation steps of the product formation.

The reaction with the imine intermediate of the benzamide was performed under standard reaction conditions, which led to a quantitative product formation (**Eq. 5.10**). Interestingly, no desired product was formed when the reaction was performed under identical conditions without the ruthenium catalyst.

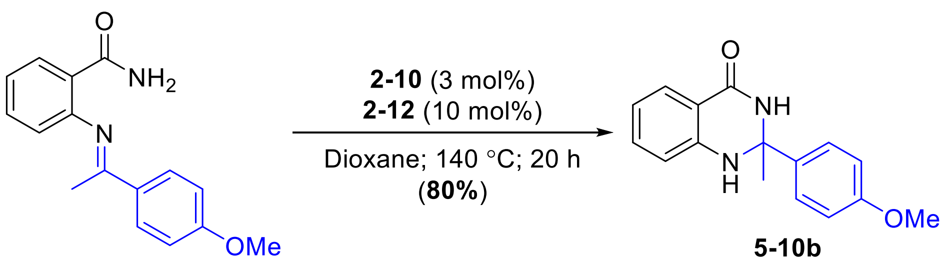

(Eq. 5.10)

5.2.5.4 Reaction with Dihydrocoumarin Substrates

To probe the deamination versus decarboxylation sequence, a number of different carbonyl substrates were tested with β-homoleucine substrate under standard reaction condition. The trapped amide product **5-12** was successfully obtained from the treatment of dihydrocoumarin with l-leucine (**Eq. 5.10**), and its structure was established by NMR and x-ray crystallography. The selective formation of the amide product **5-12** supports a preferential decarboxylation over the deamination step for the amino acid substrate. Transition metal catalyzed decarboxylative coupling methods have been successfully employed for the synthesis of complex organic molecules.[29]

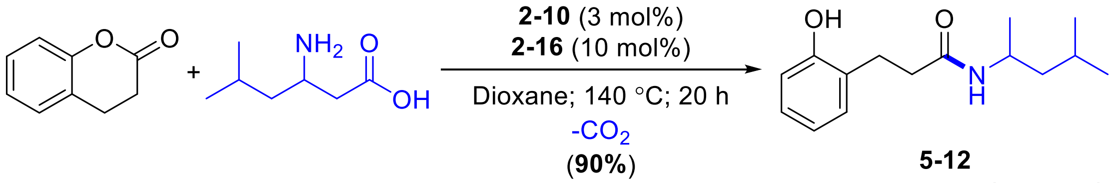

5-12

(Eq. 5.10)

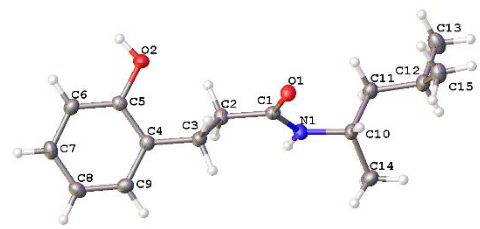

5.3 Proposed Mechanism of the Catalytic Synthesis of Quinoline Derivatives

We offer a plausible mechanistic sequence for the formation of the quinoline products **5-9** on the basis of these preliminary results (**Scheme 5.3**). The reaction with enamine provides an additional experimental support for the formation of enamine by initial decarboxylation of β-amino acid. In support of this hypothesis, we previously found that the ruthenium−hydride complexes are efficient catalysts for olefin isomerization reaction[125b] and dehydrogenation of saturated amines and carbonyl compounds.[181] We believe that a redox-active catechol ligand may be essential for facilitating the dehydrogenation step on the catalysis.[182] The coordination of 2-aminoacetophenone to the ruthenium intermediate species **5-13** would give an intermediate ruthenium complex **5-14**. Nucleophilic enolate attack followed by dehydrative coupling would afford the ruthenium coordinated imine species **5-8**. Final deaminative[126b] annulation steps would afford the corresponding regioselective quinoline product along with ammonia byproduct.

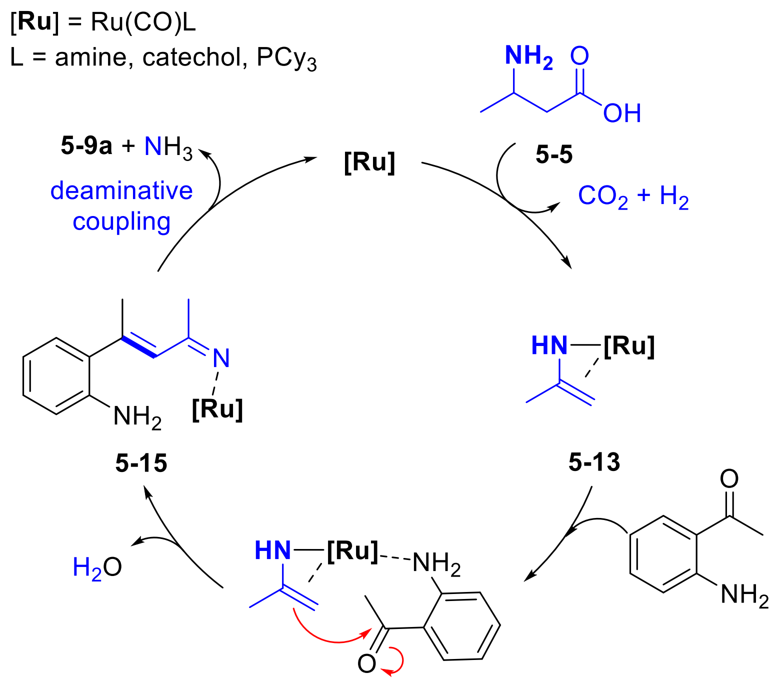

Scheme 5.3: Proposed Mechanistic Hypothesis for the Regio-selective synthesis of Quinolines from 2-Aminophenyl Ketones with β-Amino Acids

5.4 Conclusion

In summary, we have successfully developed a novel catalytic coupling method by using readily available β-amino acids and amines as substrates for the synthesis of nitrogen heterocycles. The salient features of the catalytic method are that it achieves direct C–N bond cleavage of biomass-derived β-amino acids, exhibits a broad range of substrate scope with high regioselectivity, and it does not require any reactive reagents or pre-functionalization of the substrates in forming the quinoline products. Synthetic utility of the catalytic system has been demonstrated by running a gram scale reaction and the reaction with biologically relevant substrates.

Chapter 6

Experimental Section

6.1 General Information

All operations were carried out in a nitrogen-filled glove box or by using standard high vacuum and Schlenk techniques unless otherwise noted. All the solvents used were freshly distilled over appropriate drying reagents. Chlorobenzene was distilled from purple solutions of sodium and benzophenone, and hexanes was dried over calcium hydride prior to use. All organic substrates were received from commercial sources and were used without further purification. The ^{1}H, ^{2}H, ^{13}C, and ^{31}P NMR spectra were recorded on a Varian 400 MHz FT-NMR spectrometer, and the data are reported as: s = singlet, d = doublet, t = triplet, q = quartet, m = multiplet, br = broad, app = apparent; coupling constant(s) in Hz; integration. In ^{1}H NMR, the chemical shifts were referenced to the residual hydrogen signal of the deuterated solvents. In $^{13}C\{1H\}$ NMR measurements, the signals of deuterated solvents were used as a reference. Reaction temperatures were reported as the temperatures of the oil bath. Mass spectra were recorded from Agilent 6850 GC-MS spectrometer by using a HP-5 (5% phenylmethylpolysiloxane) column (30 m, 0.32 mm, 0.25 μm) or from SHIMADZU GC-2010 Plus gas chromatography spectrometer coupled with GCMS-QP2010 SE mass spectrometer by using a SHIMADZU SH-Rxi-5SilMS (similar to 5% diphenyl/95%dimethyl polysiloxane) column (30 m, 0.25 mm, 0.25 μm). High resolution mass spectra were obtained at the Mass Spectrometry/ICP Lab, Department of Chemistry and Biochemistry, University of Wisconsin-Milwaukee, Milwaukee, WI and Analytical

Instrumentation Center, School of Pharmacy, University of Wisconsin-Madison, Madison, WI. Optical rotation was measured by using a 1 mL cell with 1 dm path length on a Perkin-Elmer 341 polarimeter with a sodium lamp, and are reported as [α_C^T] (c = g/100 mL, solvent). Elemental analyses were performed at the Midwest Microlab, Indianapolis, IN.

6.2 Experimental Procedures and Data for the Chapter 02

6.2.1 Synthesis of [$(PCy_3)(CO)RuH]_4(\mu^4$-O)(μ^3-OH)(μ^2-OH) Complex (2-9)

The tetranuclear Ruthenium complex **2-9** was synthesized in two steps from the 5- coordinated Ru-hydride complex $(PCy_3)_2$(CO)RuHCl **2-7** (**Scheme 2.9**). In a glovebox, a 500 mL Schlenk reactor equipped with a magnetic stirring bar and Teflon stopcock was charged with $(PCy_3)_2$(CO)RuHCl (726 mg, 1.0 mmol), KOH (6.5 mmol), and 2- propanol (5 mL). The reaction tube was brought out of the box and was stirred in an oil bath at 90 °C for 8 h. The solvent was removed under high vacuum, and the residue was washed with 2-propanol and benzene to obtain the binuclear Ru complex **2-8**. The binuclear Ru complex **2-8** can be purified by short column by benzene as the eluent. In the glove box, the obtained Ru binuclear complex **2-8** (500 mg, 0.46 mmol) and acetone (5 mL) were added to a 25 mL Schlenk tube equipped with a magnetic stirring bar and Teflon stopcock. The reaction tube was brought out of the glovebox and stirred in an oil bath at 100 °C for 4 h. After the tube was cooled to room temperature, the resulting red solid was filtered, washed with cold acetone (5 mL, 3 times), and recrystallized in dichloromethane to obtain product **2-9** in 90 % yield. Spectroscopic data for **2-9**: ^{1}H NMR (300 MHz, CD_2Cl_2) δ 2.25-1.15 (m, PCy_3), -2.50 and -2.60 (s, μ-OH), -

14.56 (d, J_{PH} = 19.2 Hz, Ru-H), -15.02 (d, J_{PH} = 18.0 Hz, Ru-H), -15.28 (d, J_{PH} = 34.8 Hz, Ru-H), -18.64 (dt, J_{PH} = 13.2, 4.8 Hz, Ru-H-Ru); ^{31}P{1H} NMR ($CDCl_3$, 121.6 MHz) δ 82.13 (s, PCy_3), 79.01 (d, J_{PP} = 14.0 Hz (PCy_3)), 71.96 (s, (PCy_3)), 68.89 (d, J_{PP} = 14.0 Hz, (PCy_3)); IR (CH_2Cl_2) νOH = 2926, 2849 cm^{-1}, νCO = 1925, 1912, 1894, 1868 cm^{-1}. Anal. Calcd for **2-9** $C_{76}H_{138}O_7P_4$-Ru_4: C 53.95; H 8.22. Found: C 55.03; H 8.14.[125a]

6.2.2 Synthesis of [(η^6-C_6H_6)RuH(CO)(PCy_3)]$^+$$BF_4^-$ Complex (2-10)

In a glove box, complex **2-9** (200 mg, 0.12 mmol) was dissolved in benzene (10 mL) in a 25 mL Schlenk tube equipped with a Teflon screw-cap stopcock and a magnetic stirring bar. The tube was brought out of the box, and $HBF_4 \cdot OEt_2$ (64 μL, 0.48 mmol) was added via syringe under N_2 stream. The color of the solution was changed from dark red to pale yellow immediately. After stirring for 1 h at room temperature, the solvent was removed under vacuum, and the residue was crashed by adding hexanes (20 mL). Filtering the resulting solid through a fritted funnel and recrystallization from CH_2Cl_2/hexanes yielded the product as a pale-yellow powder (262 mg, 95% yield). Single crystals of **2-10** suitable for X-ray crystallography were obtained from a slow evaporation of benzene and hexanes solution.

Data for **2-10**: ^{1}H NMR (CD_2Cl_2, 400 MHz) δ 6.53 (s, C_6H_6), 2.0-1.2 (m, PCy_3), -10.39 (d, J_{PH} = 25.9 Hz, Ru-H); ^{13}C{1H} NMR (CD_2Cl_2, 100 MHz), δ 196.4 (d, J_{CP} = 19.3 Hz, CO), 100.0 (C_6H_6), 38.4, 38.2, 30.2, 29.9, 27.4, 27.3 and 26.2 (PCy_3); ^{31}P{1H} NMR (CD_2Cl_2, 162 MHz) δ 72.9 (PCy_3); IR (KBr) νCO = 1991 cm^{-1}; Anal. Calcd for **2-10** $C_{25}H_{40}BF_4OPRu$: C, 52.18; H, 7.01. Found: C, 51.73; H, 6.91.[125b, 125c]

6.2.3 Synthesis of [Ru(PCy_3)$_2$(3-,5-(^{t}Bu)$_2$(1-,2-(O)$_2$)C_6H_2)CO] Complex 2-11

The complex **2-10** (117 mg, 0.20 mmol), 3,5-di-*tert*-butyl-o-benzoquinone **2-12b** (44 mg, 0.20 mmol), PCy_3 (56 mg, 0.20 mmol) were dissolved in CH_2Cl_2 (3 mL) in a 25 mL Schlenk tube equipped with a Teflon screw cap stopcock and a magnetic stirring bar under N_2 stream. After stirring for 24 h in a water bath set at 70 °C, the solvent was removed under vacuum, and the residue was washed with 2% hexanes/EtOAc under nitrogen atmosphere. The resulting residue was dissolved in acetone (3 mL), layered with n-pentane (4 mL), and stored in a glove box for five days for crystallization. The resulting solid was filtered through a fritted funnel to yield the complex **2-11** (102 mg, 56%) as a reddish crystalline solid. Single crystals of **2-11** were obtained by slow evaporation in EtOAc/pentanes, and its structure was determined by X-ray crystallography. Data for **2-11:** ^{1}H NMR (400 MHz, $CDCl_3$) δ 6.91 (s, 1H), 6.91 (s, 1H), 2.60–0.70 (m, 84H) ppm; ^{31}P{^{1}H} NMR (100 MHz, $CDCl_3$) δ 75.6, 75.4 ppm; HRMS (ESI-TOF) m/z: $[M + H]^+$ Calcd for $C_{51}H_{86}O_3P_2RuH$ 911.5183; Found 911.5146.

6.2.3.1 X-Ray Crystal Structure of Complex 2-11

Dark-red prism like single crystals of **2-11** were grown in pentanes/EtOAc at room temperature. A suitable crystal with the dimension of 0.748 × 0.105 × 0.04 mm^3 was selected and mounted on an Oxford SuperNova, Dual Cu at home/near, Atlas diffractometer, respectively. The crystal was kept at 100 K during data collection. Using Olex2,[203] the structure was solved with the olex2.solve[204] structure solution program using Charge Flipping and refined with the ShelXL[205] refinement package using Least Squares minimization. The molecular structure of **2-11** is shown in **Figure 6.1**.

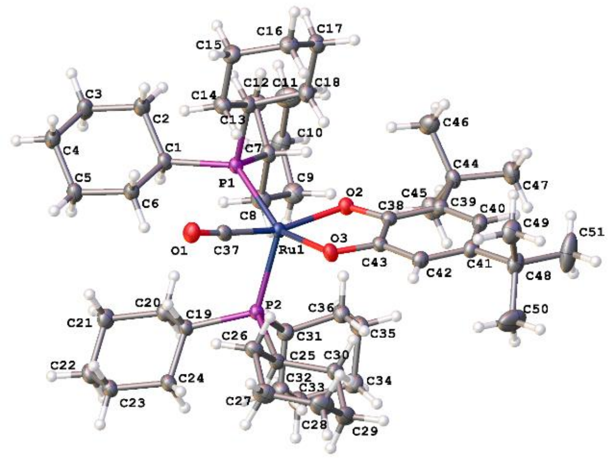

Figure 6.1: The Molecular Structure of Ruthenium Complex **2-11**

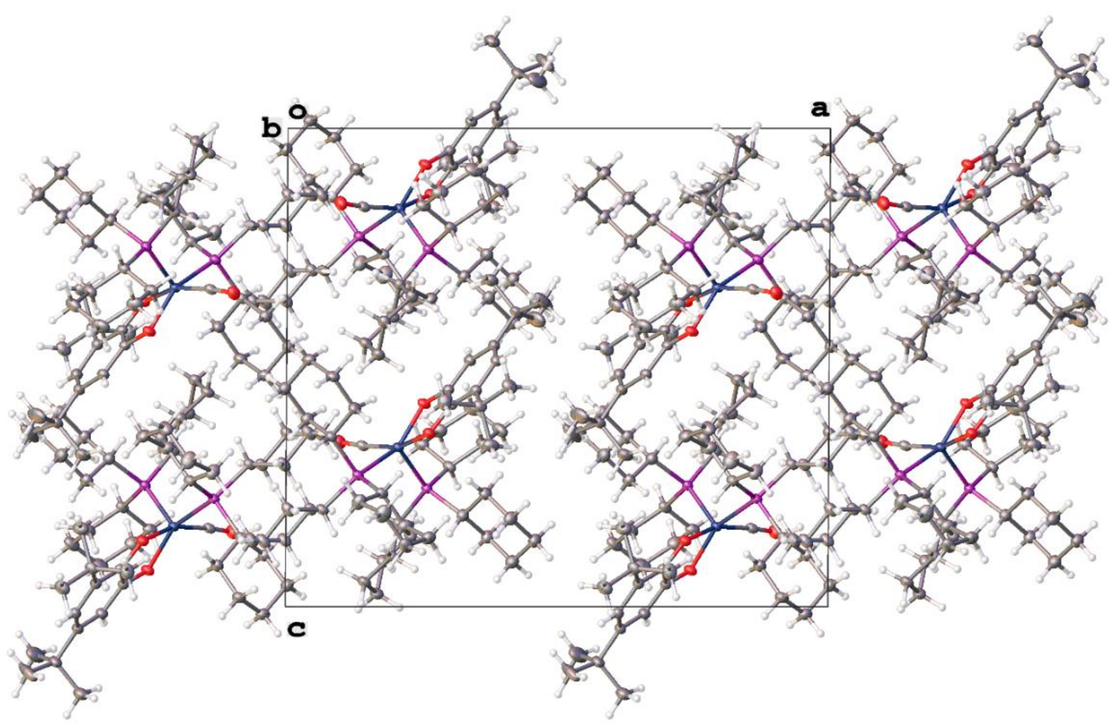

Figure 6.2: Crystal Packing of Ruthenium Complex **2-11**

6.2.3.2 X-ray Crystallographic Data for the Complex 2-11

Table 6.1: Crystal Data and Structure Refinement for Ruthenium Complex **2-11**

Identification code	yi4z
Empirical formula	$C_{51}H_{86}O_3P_2Ru$
Formula weight	910.20
Temperature/K	100.3(9)
Crystal system	monoclinic
Space group	$P2_1/c$
a/Å	20.07721(19)
b/Å	13.38539(14)
c/Å	17.77134(18)
α/°	90
β/°	90.3343(9)
γ/°	90
Volume/Å^3	4775.81(8)
Z	4
ρ_{calc}g/cm^3	1.266
μ/mm^{-1}	3.586
F(000)	1960.0
Crystal size/mm^3	0.215 × 0.183 × 0.116
Radiation	CuKα (λ = 1.54184)
2Θ range for data collection/°	7.938 to 141.126
Index ranges	$-24 \leq h \leq 22$, $-16 \leq k \leq 16$, $-20 \leq l \leq 21$
Reflections collected	44427
Independent reflections	9074 [R_{int} = 0.0418, R_{sigma} = 0.0273]
Data/restraints/parameters	9074/0/520
Goodness-of-fit on F^2	1.027
Final R indexes [I>=2σ (I)]	R_1 = 0.0319, wR_2 = 0.0821
Final R indexes [all data]	R_1 = 0.0358, wR_2 = 0.0856
Largest diff. peak/hole / e Å^{-3}	0.87/-0.55

6.2.4.1 X-ray Crystal Structure of Complex 2-14

Orange needles shaped single crystal of **2-14** were grown in pentanes/EtOAc at room temperature. A suitable crystal with the dimension of 0.603 × 0.112 × 0.024 mm^3 was selected and mounted on an Oxford SuperNova, Dual Cu at home/near, Atlas diffractometer, respectively. The crystal was kept at 100 K during data collection. Using Olex2,[203] the structure was solved with the olex2.solve[204] structure solution program using Charge Flipping and refined with the ShelXL[205] refinement package using Least Squares minimization.

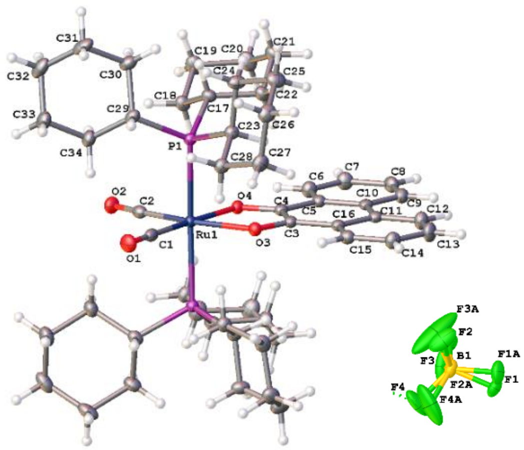

Figure 6.3: The Molecular Structure of Ruthenium Complex **2-14**

Data for **2-14:** ^{1}H NMR (400 MHz, $CDCl_3$) δ 7.95 (d, J = 7.6 Hz, 2H), 7.61 (d, J = 7.6 Hz, 2H), 7.21–7.10 (m, 4H), 2.71–0.62 (m, 78H) ppm; ^{31}P{^{1}H} NMR (100 MHz, $CDCl_3$) δ 75.0, 74.8 ppm; HRMS (ESI-TOF) m/z: $[M + H]^+$ Calcd for $C_{53}H_{76}O_3P_2RuH$ 911.5183; Found 911.5146.

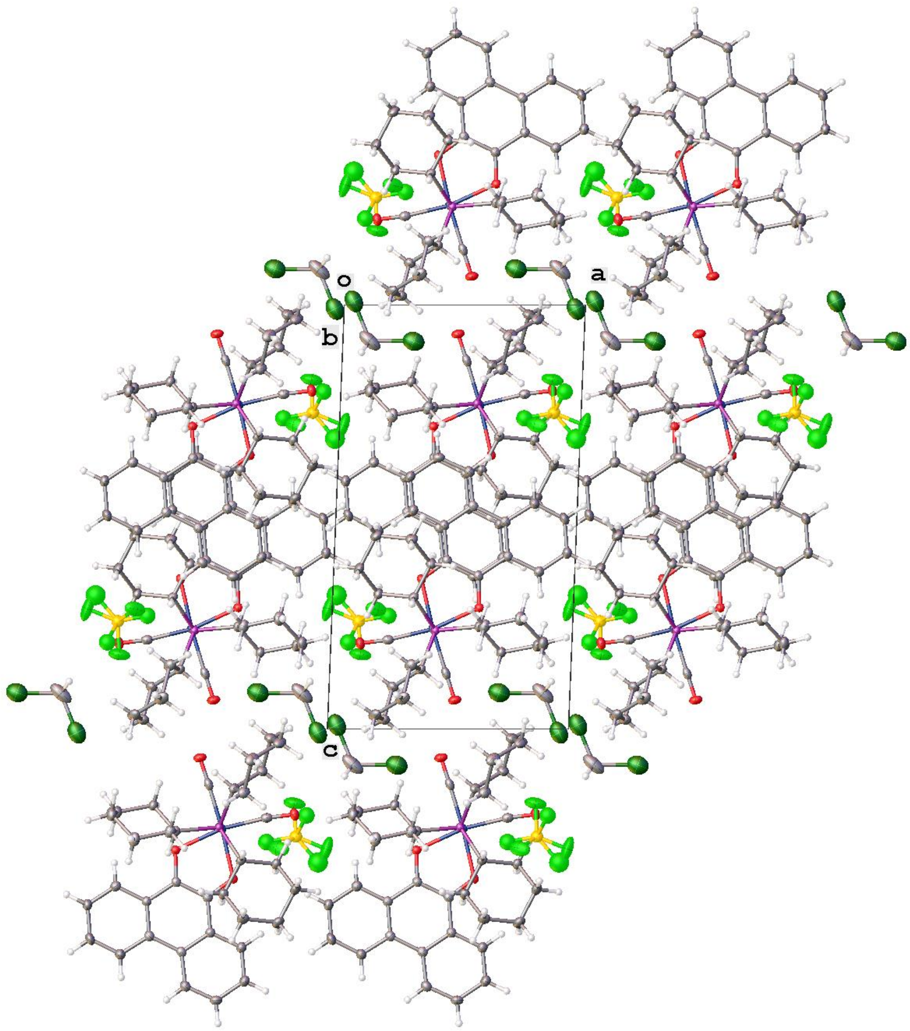

Figure 6.4: Crystal Packing of Ruthenium Complex **2-14**

6.2.4.2 X-ray Crystallography Data for the Complex 2-14

Table 6.2: Crystal Data and Structure Refinement for Ruthenium Complex **2-14**

Identification code	yi5b
Empirical formula	$C_{53}H_{76}BCl_2F_4O_4P_2Ru$
Formula weight	1097.85
Temperature/K	100.00(10)
Crystal system	monoclinic
Space group	$P2_1/m$
a/Å	9.83560(10)
b/Å	15.2197(2)
c/Å	17.2974(2)

α/°	90
β/°	92.2990(10)
γ/°	90
Volume/Å^3	2587.25(5)
Z	2
ρ_{calc}g/cm^3	1.409
μ/mm^{-1}	4.468
F(000)	1150.0
Crystal size/mm^3	0.603 × 0.112 × 0.024
Radiation	Cu Kα (λ = 1.54184)
2Θ range for data collection/°	7.74 to 141.174
Index ranges	-10 ≤ h ≤ 11, -18 ≤ k ≤ 18, -21 ≤ l ≤ 21
Reflections collected	24817
Independent reflections	5091 [R_{int} = 0.0364, R_{sigma} = 0.0251]
Data/restraints/parameters	5091/0/354
Goodness-of-fit on F^2	1.042
Final R indexes [I>=2σ (I)]	R_1 = 0.0325, wR_2 = 0.0840
Final R indexes [all data]	R_1 = 0.0368, wR_2 = 0.0868
Largest diff. peak/hole / e Å^{-3}	0.78/-1.07

6.2.5 Synthesis of [Ru(PCy_3)$_2$(CO)H(OH_2)$_2$) Complex 2-15

A 1,4-dioxane (2.0 mL) solution of complex **2-10** (117 mg, 0.2 mmol), water (9 mg, 0.5 mmol), tricyclohexylphosphine (56 mg, 0.2 mmol) were dissolved in CH_2Cl_2 (3 mL) in a 25 mL Schlenk tube equipped with a Teflon screw cap stopcock and a magnetic stirring bar under N_2 stream. After stirring for 24 h in a 50 °C water bath, the solvent was removed under vacuum, and the residue was washed with 2% hexanes/EtOAc in a nitrogen atmosphere. The resulting residue was dissolved in acetone (3 mL), layered with n-pentane (4 mL), and stored in a glove box for five days for crystallization. The resulting solid was filtered through a fritted funnel to yield the product as brownish crystalline solid, which was recrystallized by following similar procedure to obtain complex **2-15** (78 mg, 48%). Single crystals of **2-15** were obtained by slow evaporation in CH_2Cl_2/pentanes, and its structure was determined by X-ray crystallography. Data for **2-15:** Data for **2-14:** ^{1}H NMR (400 MHz, $CDCl_3$) δ 7.95 (d, J = 7.6 Hz, 2H), 7.61 (d, J = 7.6 Hz, 2H), 7.21–7.10 (m, 4H), 2.71–0.62 (m, 78H) ppm; ^{31}P{^{1}H} NMR (100 MHz, $CDCl_3$) δ 75.0, 74.8 ppm; HRMS (ESI-TOF) m/z: $[M + H]^+$ Calcd for $C_{37}H_{71}O_3P_2RuH$ 728.4005; Found 728.4005.

6.2.5.1 X-Ray Crystal Structure of Complex 2-15

Brownish needles shaped single crystal of **2-15** were grown in pentanes/EtOAc at room temperature. A suitable crystal with the dimension of 0.612 × 0.123 × 0.077 mm^3 was selected and mounted on an Oxford SuperNova, Dual Cu at home/near, Atlas diffractometer, respectively. The crystal was kept at 100 K during data collection. Using Olex2,[203] the structure was solved with the olex2.solve[204] structure solution program using Charge Flipping and refined with the ShelXL[205] refinement package using Least Squares minimization. The molecular structure of **2-15** is shown in **Figure 6.5**. The Ru(II) complex has an octahedral coordination. The hydride ligand was localized objectively and refined isotopically. The complex has trans-configuration in respect to phosphine ligands and cis-configuration in respect to aqua ligands. The tetrafluoroborate anion is disordered. The cations form H-bonds with bridging BF_4^- anions making 1-dimensional double chains along x axis.

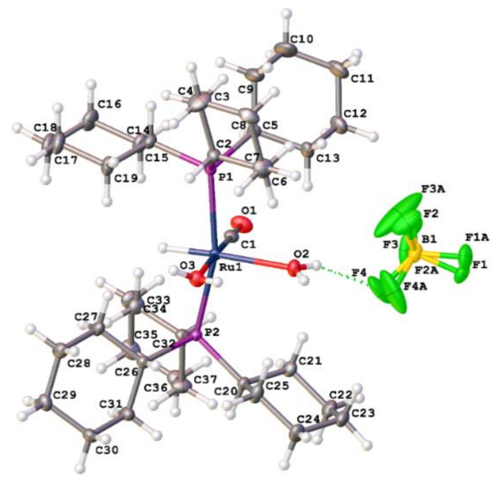

Figure 6.5: The Molecular Structure of Ruthenium Complex **2-15**

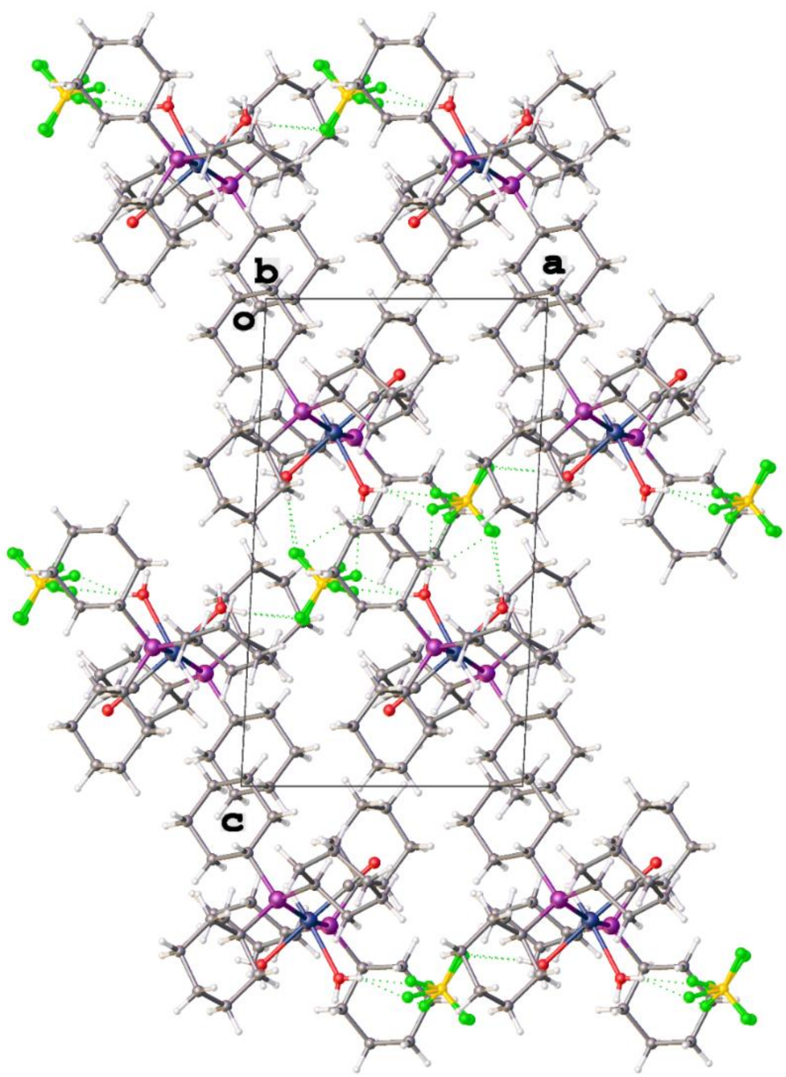

Figure 6.6: Crystal Packing of Ruthenium Complex **2-15**

6.2.5.2 X-ray Crystallographic Data for the Complex 2-15

Table 6.3: Crystal Data and Structure Refinement for Ruthenium Complex **2-15**

Identification code	yi4v
Empirical formula	$C_{37}H_{71}BF_4O_3P_2Ru$
Formula weight	813.75
Temperature/K	101(2)
Crystal system	triclinic
Space group	P-1
a/Å	9.84636(17)
b/Å	13.5122(3)
c/Å	17.1420(3)
α/°	71.3133(18)
β/°	86.8988(14)
γ/°	71.7993(17)
Volume/Å^3	2049.67(7)
Z	2
ρ_{calc}g/cm^3	1.319
μ/mm^{-1}	0.511
F(000)	864.0
Crystal size/mm^3	0.612 × 0.123 × 0.077
Radiation	MoKα (λ = 0.71073)
2Θ range for data collection/°	6.7 to 59.326
Index ranges	$-13 \le h \le 13$, $-17 \le k \le 17$, $-23 \le l \le 23$
Reflections collected	46281
Independent reflections	10496 [R_{int} = 0.0244, R_{sigma} = 0.0237]
Data/restraints/parameters	10496/20/490
Goodness-of-fit on F^2	1.060
Final R indexes [I>=2σ (I)]	R_1 = 0.0258, wR_2 = 0.0575
Final R indexes [all data]	R_1 = 0.0307, wR_2 = 0.0604
Largest diff. peak/hole / e Å^{-3}	0.87/-0.71

6.2.6 General Procedures for the Catalytic Synthesis of Secondary Amines

In a glove box, complex **2-9** (13 mg, 0.75 mol %) and 4-(1,1-dimethylethyl)-1,2-benzenediol **2-16**, (16 mg, 10 mol %) were dissolved in chlorobenzene (1 mL) in a 25 mL Schlenk tube equipped with a Teflon screw cap stopcock and a magnetic stirring bar. The resulting mixture was stirred for 5 to 10 minutes until the solution turned to a reddish green color. One (procedure for symmetric coupling reactions, 1.0 mmol of primary amine substrate) or two amines substrates (1.0 mmol and 1.4 mmol) in chlorobenzene (1 mL) were added to the reaction tube. After the tube was sealed, it was brought out of the glove box, and was stirred in an oil bath maintained at 130-140 °C for 16-20 h. The reaction tube was taken out of the oil bath and was cooled to room temperature. After the tube was open to air, the solution was filtered through a short silica gel column by eluting with CH_2Cl_2 (10 mL), and the filtrate was analyzed by GC-MS. Analytically pure product was isolated by a simple column chromatography on silica gel (280-400 mesh, hexanes/EtOAc).

In an alternative procedure, the complex **1-45** (17 mg, 3 mol %) and **1-46** (24 mg, 10 mol %) or complex **2-9** were dissolved in anhydrous 1,4-dioxane (1 mL) in a 25 mL Schlenk tube equipped with a Teflon screw cap stopcock and a magnetic stirring bar. After stirring for 5-10 min until the solution was turned light green color, both amine 1 (0.5 mmol) and an amine 2 (0.7 mmol) substrates, and dioxane (1 mL) was added to the tube. The tube was sealed, it was brought out of the glove box, and was stirred in an oil bath set at 130-140 °C for 16-20 h. Analytically pure product was isolated by flash chromatographic machine, Biotage Isolara™ One. Dry loading of a sample in to a 10g of silica gel Biotage® SNAP KPSil Cartridge has been used (**Figure 6.3.1.1**).

6.2.7.1 Reaction Profile Study

In a glove box, complex **2-9** (2 mg, 3 mol %) and **2-16** (2 mg, 10 mol %) were dissolved in toluene-d_8 (0.5 mL) in a 25 mL Schlenk tube equipped with a Teflon screw cap stopcock and a magnetic stirring bar. The resulting mixture was stirred for 10 minutes until the solution turned to a brownish green color. 4-methoxybenzylamine (14 mg, 0.10 mmol) were added to the reaction tube, and the solution was transferred into a J-Young NMR tube equipped with a Teflon screw cap stopcock. The tube was brought out of the glove box, and was immersed an oil bath set at 130 °C. The tube was taken out from the oil bath at 20 min intervals, was immediately cooled in ice-water bath, and was analyzed by ^{1}H NMR. The appearance of the product signal was normalized against an external standard peak (C_6Me_6).

6.2.7.2 Deuterium Labeling Study

In a glove box, complex **2-9** (7 mg, 0.75 mol %) and **2-16** (8 mg, 10 mol %) were dissolved in chlorobenzene (1 mL) in a 25 mL Schlenk tube equipped with a Teflon screw cap stopcock and a magnetic stirring bar. The resulting mixture was stirred for 5 to 10 minutes until the solution turned to a reddish green color. Aniline-d_7 (50 mg, 0.5 mmol) and 4-methoxybenzylamine (78 mg) in chlorobenzene (1 mL) were added to the reaction tube. After the tube was sealed, it was brought out of the glove box, and was stirred in an oil bath maintained at 140 °C for 20 h. Analytically pure product was isolated by a simple column chromatography on silica gel (280-400 mesh, *n*-hexanes/EtOAc). The ^{1}H and ^{2}H NMR spectra of the product **2-15e-*d*** are recorded (**Scheme 3.6.1**). Control experiment was conducted with the pure product **2-15e,** (107 mg, 0.5 mmol) with Aniline-d_7 (50 mg, 0.5 mmol) with the catalyst **2-9** (7 mg, 0.75 mol %) and **2-16** (8 mg, 10 mol %) which were dissolved in chlorobenzene (1 mL).

6.2.7.3 Carbon Isotope Effect Study

In a glove box, complex **2-9** (28 mg, 0.75 mol %) and **2-16** (32 mg, 10 mol %) were dissolved in chlorobenzene (2 mL) in a 25 mL Schlenk tube equipped with a Teflon screw cap stopcock and a magnetic stirring bar. The resulting mixture was stirred for 5 to 10 minutes until the solution turned to a reddish green color. 4-Methoxybenzylamine (274 mg, 2.0 mmol) and chlorobenzene (2 mL) were added to the reaction tube. After the tube was sealed, those were brought out of the box, and was stirred in an oil bath at 130 °C for 16 h. The tube was cooled to room temperature and filtered through a small silica column (CH_2Cl_2), and the product conversion was determined by GC (86%, 88% and 89% conversions). The product **2-14c** was isolated by a column chromatography on silica gel (hexanes/EtOAc). The procedure was repeated two more times. In a similar procedure, complex **2-9** (52 mg, 0.75 mol %) and **2-16** (80 mg, 10 mol %) were dissolved in chlorobenzene (5 mL) in a 100 mL Schlenk tube equipped with a Teflon screw cap stopcock and a magnetic stirring bar. 4-Methoxybenzylamine (685 mg, 5.0 mmol) and chlorobenzene (5 mL) were added to the reaction tube. After the tube was sealed, it was brought out of the box, and was stirred in an oil bath at 130 °C for 2 h. The tube was cooled to room temperature and filtered through a small silica column (CH_2Cl_2), and the product conversion was determined by GC (15%, 13% and 12% conversions). The product **2-14c** was isolated by a column chromatography on silica gel (hexanes/EtOAc). The NMR sample was prepared identically by dissolving **2-14c** (200 mg) in $CDCl_3$ (0.5 mL) in a 5 mm high precision NMR tube. The $^{13}C\{^{1}H\}$ NMR spectra were recorded with H-decoupling and 45-degree pulses. A 60 s delay between pulses was imposed to minimize T1 variations (d1 = 120 s, at = 5.0 s, np = 245098, nt = 512, dm = 'nny').

6.2.7.4 Hammett Study

In a glove box, complex **2-9** (20 mg, 0.75 mol %) and **2-16** (24 mg, 10 mol %) were dissolved in toluene-d_8 (1.5 mL) in a 25 mL Schlenk tube equipped with a Teflon screw cap stopcock and a magnetic stirring bar. The resulting mixture was stirred for 5 to 10 minutes until the solution turned to a reddish green color. 4-Methoxyaniline (185 mg, 1.5 mmol) was added to the reaction tube, and the solution was stirred for 5 min. The solution was divided into 6 equal portions, and *p*-X-$C_6H_4CH_2NH_2$ (0.3 mmol) (X = OMe, Me, H, F, Cl, CF_3) was added to each solution. The resulting mixture was transferred into six different J-Young NMR tubes each equipped with a Teflon screw cap stopcock. The tubes were brought out of the glove box, and were immersed an oil bath set at 140 °C. Each tube was taken out from the oil bath at 30 min time intervals, cooled in ice-water bath, and was analyzed by ^{1}H NMR. The reaction rate was measured by monitoring the appearance of the product signals on ^{1}H NMR, which was normalized against the internal standard peak (C_6Me_6). The k_{obs} was determined from a first-order plot of $-ln[(\text{4-methoxyaniline})_t/(\text{4-methoxyaniline})_0]$ vs time.

6.2.8.1 Characterization Data of the Novel Unsymmetric Secondary Amines Listed in Table 2.3

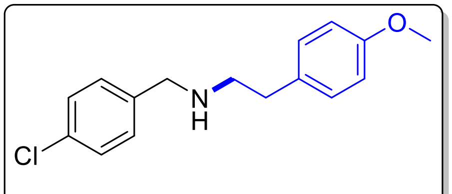

2-17e

***N*-(4-Chlorobenzyl)-2-(4-methoxyphenyl)ethanamine (2-17e).** A chlorobenzene (2.0 mL) solution of complex **2-9** (13 mg, 0.75 mol %), **2-16** (16 mg, 10 mol %), 4-chlorobenzylamine (141 mg, 1.0 mmol) and 4-methoxybenzeneethanamine (211 mg, 1.4 mmol) was stirred at 130 °C for 16 h. The product **2-17e** was isolated by a column chromatography on silica gel (*n*-hexane/EtOAc = 100:1 to 10:1; 158 mg, 57%). TLC; R_f = 0.4 (20% EtOAc in hexanes). Data for **2-17e**: ^{1}HNMR (400 MHz, $CDCl_3$) δ 7.30–7.25 (m, 2H), 7.24–7.19 (m, 2H), 7.15–7.09 (m, 2H), 6.87–6.82 (m, 2H), 3.79 (s, 3H), 3.76 (s, 2H), 2.87–2.82 (m, 2H), 2.80–2.74 (m, 2H), 1.73 (br s, 1H) ppm; ^{13}C{^{1}H} NMR (100 MHz, $CDCl_3$) δ 157.9, 138.6, 132.5, 131.7, 129.5, 129.3, 128.4, 113.8, 55.1, 53.0, 50.5, 35.2 ppm; GC-MS for $C_{16}H_{18}ClNO$, m/z = 275 (M^+). HRMS (ESI-TOF) m/z: $[M+H]^+$ Calcd for $C_{16}H_{18}ClNOH$ 276.1150; Found 276.1122.

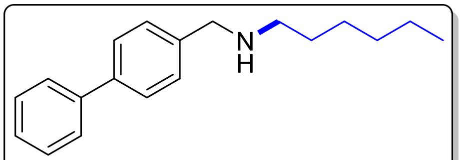

2-17f

***N*-(Biphenyl-4-ylmethyl)hexan-1-amine (2-17f).** A chlorobenzene (2.0 mL) solution of complex **2-9** (13 mg, 0.75 mol %), **2-16** (16 mg, 10 mol %), 4-pheylbenzylamine (183 mg, 1.0 mmol) and 1-hexamine (141 mg, 1.4 mmol) was stirred at 130 °C for 16 h. The product **2-17f** was isolated by a column chromatography on silica gel (*n*-hexane/EtOAc = 100:1 to 10:1; 176 mg, 66%). TLC; R_f = 0.3 (20% EtOAc in hexanes). Data for **2-17f**: ^{1}HNMR (400 MHz, $CDCl_3$) δ 7.61–7.54 (m, 4H), 7.46–7.37 (m, 4H), 7.36–7.31 (m, 1H), 3.83 (s, 2H), 2.66 (t, *J* = 7.3 Hz, 2H), 1.58–1.50 (m, 2H), 1.36–1.26 (m, 6H), 0.89 (t, *J* = 7.0 Hz, 3H) ppm; $^{13}C\{^1H\}$ NMR (100 MHz, $CDCl_3$) δ 141.0, 139.8, 139.6, 128.7, 128.5, 128.4, 127.1, 127.0, 53.7, 49.6, 31.8, 30.1, 27.0, 22.6, 14.1 ppm; GC-MS for $C_{19}H_{25}N$, m/z = 267 (M^+); HRMS (ESI-TOF) m/z: $[M+H]^+$ Calcd for $C_{19}H_{25}NH$ 268.2060; Found 268.2061.

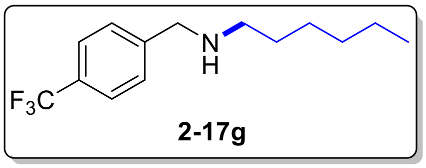

***N*-(4-(Trifluoromethyl)benzyl)hexan-1-amine (2-17g).** A chlorobenzene (2.0 mL) solution of complex **2-9** (13 mg, 0.75 mol %), **2-16** (16 mg, 10 mol %), 4-trifluromethylbenzylamine (175 mg, 1.0 mmol) and 1-hexamine (141 mg, 1.4 mmol) was stirred at 130 °C for 16 h. The product **2-17g** was isolated by a column chromatography on silica gel (*n*-hexanes/EtOAc = 100:1 to 10:1; 142 mg, 55%). TLC; R_f = 0.4 (20% EtOAc in hexanes). Data for **2-17g**: ^1H NMR (400 MHz, $CDCl_3$) δ 7.57 (d, *J* = 8.2 Hz, 2H), 7.44 (d, *J* = 8.2 Hz, 2H), 3.84 (s, 2H), 2.61 (t, *J* = 7.2 Hz, 2H), 1.58 (br s, 1H), 1.55–1.46 (m, 2H), 1.37–1.22 (m, 6H), 0.91–0.84 (m, 3H) ppm; $^{13}C\{^1H\}$ NMR (100 MHz, $CDCl_3$) δ 144.6, 129.1 (q, J_{CF} = 32.3 Hz), 128.3, 125.3 (q, J_{CF} = 3.8 Hz), 124.2 (q, J_{CF} = 272.0 Hz), 53.5, 49.5, 31.7, 30.0, 27.0, 22.6, 14.0; GC-MS for $C_{14}H_{20}F_3N$, m/z = 259 (M^+); HRMS (ESI-TOF) m/z: $[M+H]^+$ Calcd for $C_{14}H_{20}F_3NH$ 260.1621; Found 260.1627.

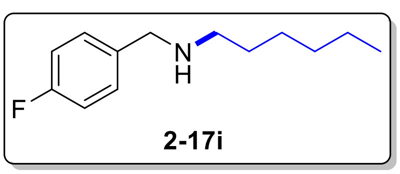

4-Fluoro-*N*-hexylbenzenemethanamine (2-17i). A chlorobenzene (2.0 mL) solution of complex **2-9** (13 mg, 0.75 mol %), **2-16** (16 mg, 10 mol %), 4-flurobenzylamine (125 mg, 1.0 mmol) and 1-hexamine (141 mg, 1.4 mmol) was stirred at 130 °C for 16 h. The product **2-17i** was isolated by a column chromatography on silica gel (*n*-hexane/EtOAc = 100:1 to 10:1; 132 mg, 63%). TLC; R_f = 0.3 (20% EtOAc in hexanes). Data for **2-17i**: ^{1}HNMR (400 MHz, $CDCl_3$) δ 7.30–7.24 (m, 2H), 7.02–6.95 (m, 2H), 3.74 (s, 2H), 2.59 (t, *J* = 7.3, 2H), 1.53–1.44 (m, 2H), 1.35–1.21 (m, 6H), 0.90–0.84 (m, 3H) ppm; $^{13}C\{^{1}H\}$ NMR (100 MHz, $CDCl_3$) δ 161.8 (d, J_{CF} = 244.6 Hz), 136.2 (d, J_{CF} = 3.1 Hz), 129.6 (d, J_{CF} = 7.9 Hz), 115.0 (d, J_{CF} = 21.2 Hz), 53.3, 49.4, 31.7, 30.0, 27.0, 22.6, 14.0 ppm; GC-MS for $C_{13}H_{20}FN$, m/z = 209 (M^+); HRMS (ESI-TOF) m/z: $[M+H]^+$ Calcd for $C_{13}H_{20}FNH$ 210.1653; Found 260.1654.

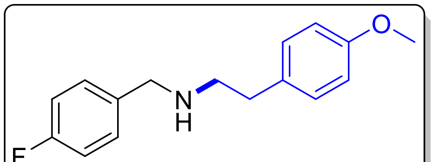

2-17k

***N*-[(4-fluorophenyl)methyl]-4-methoxy-benzeneethanamine (2-17k).** A chlorobenzene (2.0 mL) solution of complex **2-9** (13 mg, 0.75 mol %), **2-16** (16 mg, 10 mol %), 4-flurobenzylamine (125 mg, 1.0 mmol) and 4-methoxybenzeneethanamine (211 mg, 1.4 mmol) was stirred at 130 °C for 16 h. The product **2-17k** was isolated by a column chromatography on silica gel (*n*-hexane/EtOAc = 100:1 to 10:1; 142 mg, 55%). TLC; R_f = 0.3 (20% EtOAc in hexanes). Data for **2-17k**: ^{1}H NMR (400 MHz, $CDCl_3$) δ 7.27–7.21 (m, 2H), 7.15–7.10 (m, 2H), 7.03–6.96 (m, 2H), 6.87–6.82 (m, 2H), 3.79 (s, 3H), 3.76 (s, 2H), 2.88–2.83 (m, 2H), 2.80–2.74 (m, 2H), 1.69 (br s, 1H) ppm; $^{13}C\{^{1}H\}$ NMR (100 MHz, $CDCl_3$) δ 161.8 (d, J_{CF} = 244.6 Hz), 157.9, 135.8 (d, J_{CF} = 3.1 Hz), 131.8, 129.5, 129.5 (d, J_{CF} = 7.9 Hz), 115.0 (d, J_{CF} = 21.2 Hz), 113.8, 55.1, 53.0, 50.6, 35.2 ppm; GC-MS for $C_{16}H_{18}FNO$, m/z = 259 (M^+); HRMS (ESI-TOF) m/z: $[M+H]^+$ Calcd for $C_{16}H_{18}FNOH$ 260.1445; Found 260.1439.

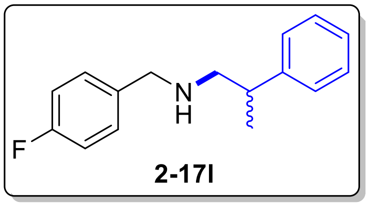

***N*-[(4-Fluorophenyl)methyl]-β-methylbenzeneethanamine (2-17l).** A chlorobenzene (2.0 mL) solution of complex **2-9** (13 mg, 0.75 mol %), **2-16** (16 mg, 10 mol %), 4-flurobenzylamine (125 mg, 1.0 mmol) and β-methylphenethylamine (189 mg, 1.4 mmol) was stirred at 130 °C for 16 h. The product **2-17l** was isolated by a column chromatography on silica gel (*n*-hexane/EtOAc = 100:1 to 10:1; 141 mg, 58%). TLC; R_f = 0.4 (20% EtOAc in hexanes). Data for **2-17l**: ^{1}H NMR (400 MHz, $CDCl_3$) δ 7.37–7.30 (m, 2H), 7.26–7.19 (m, 5H), 7.03–6.96 (m, 2H), 3.74 (ABq, *J* = 13.5 Hz, 2H), 2.99 (qt, *J* = 7.1, 7.0 Hz, 1H), 2.84–2.77 (m, 2H), 1.55 (br s, 1H), 1.28 (d, *J* = 7.0 Hz, 3H) ppm; ^{13}C{^{1}H} NMR (100 MHz, $CDCl_3$) δ 161.7 (d, J_{CF} = 244.2 Hz), 145.1, 135.8 (d, J_{CF} = 3.1 Hz), 129.4 (d, J_{CF} = 7.9 Hz), 128.5, 127.1, 126.3, 115.0 (d, J_{CF} = 21.2 Hz), 56.1, 52.9, 39.9, 20.0 ppm; GC-MS for $C_{16}H_{18}FN$, m/z = 243 (M^+); HRMS (ESI-TOF) m/z: $[M+H]^+$ Calcd for $C_{16}H_{18}FNH$ 244.1496; Found 244.1500.

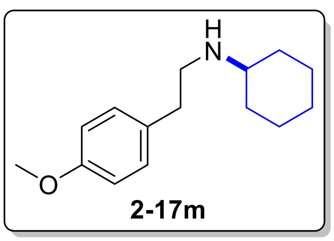

***N*-Cyclohexyl-4-methoxybenzeneethanamine (2-17m).** A chlorobenzene (2.0 mL) solution of complex **2-9** (13 mg, 0.75 mol %), **2-16** (16 mg, 10 mol %), 4-methoxybenzeneethanamine (151 mg, 1.0 mmol) and cyclohexylamine (139 mg, 1.4 mmol) was stirred at 130 °C for 16 h. The product **2-17m** was isolated by a column chromatography on silica gel (*n*-hexanes/EtOAc = 100:1 to 10:1; 187 mg, 80%). TLC; R_f = 0.3 (20% EtOAc in hexanes). Data for **2-17m**: ^{1}H NMR (400 MHz, $CDCl_3$) δ 7.10 (d, *J* = 8.7 Hz, 2H), 6.81 (d, *J* = 8.7 Hz, 2H), 3.75 (s, 3H), 2.86–2.81 (m, 2H), 2.74–2.68 (m, 2H), 2.39 (tt, *J* = 10.6, 3.8 Hz, 1H), 1.88–1.78 (m, 2H), 1.74–1.64 (m, 2H), 1.62–1.54 (m, 1H), 1.48 (br s, 1H), 1.29–0.95 (m, 5H) ppm;

$^{13}C\{^1H\}$ NMR (100 MHz, $CDCl_3$) δ 157.8, 132.0, 129.4, 113.7, 56.6, 55.0, 48.3, 35.5, 33.4, 26.0, 24.9 ppm; GC-MS for $C_{15}H_{23}NO$, m/z = 233 (M^+); HRMS (ESI-TOF) m/z: $[M+H]^+$ Calcd for $C_{15}H_{23}NOH$ 234.1852; Found 234.1854.

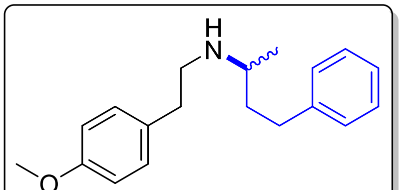

2-17n

***N*-(4-Methoxyphenethyl)-4-phenylbutan-2-amine (2-17n).** A chlorobenzene (2.0 mL) solution of complex **2-9** (13 mg, 0.75 mol %), **2-16** (16 mg, 10 mol %), 4-methoxybenzeneethanamine (151 mg, 1.0 mmol) and (±)1-methyl-3-phenyl-1-propanamine (209 mg, 1.4 mmol) was stirred at 130 °C for 16 h. The product **2-17n** was isolated by a column chromatography on silica gel (*n*-hexanes/EtOAc = 100:1 to 10:1; 208 mg, 73%. TLC; R_f = 0.3 (20% EtOAc in hexanes). Data for **2-17n**: ^1H NMR (400 MHz, $CDCl_3$) δ 7.30–7.25 (m, 2H), 7.21–7.11 (m, 5H), 6.88–6.83 (m, 2H), 3.79 (s, 3H), 2.94–2.84 (m, 1H), 2.82–2.70 (m, 3H), 2.70–2.52 (m, 3H), 1.82–1.72 (m, 1H), 1.66–1.56 (m, 1H), 1.54 (br s, 1H), 1.10 (d, *J* = 6.3 Hz, 3H) ppm; $^{13}C\{^1H\}$ NMR (100 MHz, $CDCl_3$) δ 157.9, 142.2, 132.0, 129.6, 128.3, 128.2, 125.6, 113.8, 55.2, 52.4, 48.5, 38.5, 35.5, 32.2, 20.2 ppm; GC-MS for $C_{19}H_{25}NO$, m/z = 283 (M^+); HRMS (ESI-TOF) m/z: $[M+H]^+$ Calcd for $C_{19}H_{25}NOH$ 284.2009; Found 284.2010.

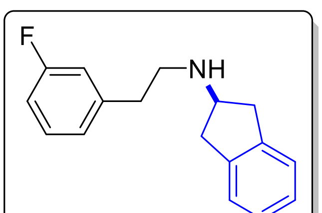

2-17o

***N*-(3-Fluorophenethyl)-2,3-dihydro-1*H*-inden-2-amine (2-17o).** A chlorobenzene (2.0 mL) solution of complex **2-9** (13 mg, 0.75 mol %), **2-16** (16 mg, 10 mol %), 2-(3-fluorophenyl)ethylamine (139 mg, 1.0 mmol) and 2-aminoindane (186 mg, 1.4 mmol) was stirred at 130 °C for 16 h. The product **2-17o** was isolated by a column chromatography on silica gel (*n*-hexane/EtOAc = 100:1 to 10:1; 193

mg, 76%). TLC; R_f = 0.4 (10% EtOAc in hexanes). Data for **2-17o**: ^{1}H NMR (400 MHz, $CDCl_3$) δ 7.3–7.24 (m, 1H), 7.24–7.12 (m, 4H), 7.06–7.00 (m, 1H), 6.99–6.89 (m, 2H), 3.67 (quintet, *J* = 6.9 Hz, 1H), 3.18 (dd, *J* = 15.5, 7.2 Hz, 2H), 3.01–2.92 (m, 2H), 2.89–2.81 (m, 2H), 2.75 (dd, *J* = 15.5, 6.6 Hz, 2H), 1.63 (br s, 1H) ppm; $^{13}C\{^1H\}$ NMR (100 MHz, $CDCl_3$) δ 162.8 (d, J_{CF} = 245.5 Hz), 142.5 (d, J_{CF} = 7.2 Hz), 141.5, 129.8 (d, J_{CF} = 8.3 Hz), 126.4, 124.6, 124.3 (d, J_{CF} = 2.7 Hz), 115.4 (d, J_{CF} = 20.8 Hz), 113.0 (d, J_{CF} = 21.0 Hz), 59.4, 49.2, 39.9, 36.2 (d, J_{CF} = 1.6 Hz) ppm; GC-MS for $C_{17}H_{18}FN$, m/z = 255 (M^+); HRMS (ESI-TOF) m/z: $[M+H]^+$ Calcd for $C_{17}H_{18}FNH$ 256.1496; Found 256.1501.

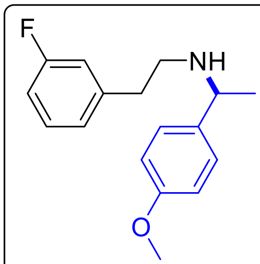

2-17p

***N*-(3-Fluorophenethyl)-1-(4-methoxyphenyl)ethanamine (2-17p).** A chlorobenzene (2.0 mL) solution of complex **2-9** (13 mg, 0.75 mol %), **2-16** (16 mg, 10 mol %), 2-(3-fluorophenyl)ethylamine (139 mg, 1.0 mmol) and (*R*)-(+)-1-(4-methoxyphenyl)ethylamine (211 mg, 1.4 mmol) was stirred at 130 °C for 16 h. The product **2-17p** was isolated by a column chromatography on silica gel (*n*-hexanes/EtOAc = 100:1 to 10:1; 157 mg, 58%). TLC; R_f = 0.3 (20% EtOAc in hexanes). Data for **2-17p**: ^{1}H NMR (400 MHz, $CDCl_3$) δ 7.27–7.16 (m, 3H), 6.98–6.80 (m, 5H), 3.80 (s, 3H), 3.73 (q, *J* = 6.6 Hz, 1H), 2.83–2.63 (m, 4H), 1.60 (br s, 1H), 1.32 (d, *J* = 6.6 Hz, 3H) ppm; $^{13}C\{^1H\}$ NMR (100 MHz, $CDCl_3$) δ 162.8 (d, J_{CF} = 245.4 Hz), 158.5, 142.6 (d, J_{CF} = 7.2 Hz), 137.3, 129.7 (d, J_{CF} = 8.3 Hz), 127.5, 124.3 (d, J_{CF} = 2.7 Hz), 115.4 (d, J_{CF} = 20.9 Hz), 113.7, 112.9 (d, J_{CF} = 21.0 Hz), 57.5, 55.2, 48.5, 36.1 (d, J_{CF} = 1.7 Hz), 24.2 ppm; GC-MS for $C_{17}H_{20}FNO$, m/z = 273 (M^+); HRMS (ESI-TOF) m/z: $[M+H]^+$ Calcd for $C_{17}H_{20}FNOH$ 274.1602; Found 274.1604.

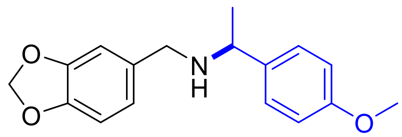

2-17q

***N*-(Benzo[d][1,3]dioxol-5-ylmethyl)-1-(4-methoxyphenyl)ethanamine (2-17q).** A chlorobenzene (2.0 mL) solution of complex **2-9** (13 mg, 0.75 mol %), **2-16** (16 mg, 10 mol %), 1-(1,3-benzodioxol-5-yl)methanamine (151 mg, 1.0 mmol) and (*R*)-(+)-1-(4-methoxyphenyl)ethylamine (211 mg, 1.4 mmol) was stirred at 130 °C for 16 h. The product **2-17q** was isolated by a column chromatography on silica gel (*n*-hexane/EtOAc = 100:1 to 10:1; 171 mg, 60%). TLC; R_f = 0.3 (20% EtOAc in hexanes). Data for **2-17q**: ^{1}H NMR (400 MHz, $CDCl_3$) δ 7.30–7.24 (m, 2H), 6.93–6.86 (m, 2H), 6.82–6.78 (m, 1H), 6.77–6.67 (m, 2H), 5.93 (s, 2H), 3.82 (s, 3H), 3.76 (q, *J* = 6.6 Hz, 1H), 3.52 (ABq, *J* = 13.2 Hz, 2H), 1.70 (br s, 1H), 1.34 (d, *J* = 6.6 Hz, 3H) ppm; ^{13}C{^{1}H} NMR (100 MHz, $CDCl_3$) δ 158.5, 147.6, 146.3, 137.4, 134.5, 127.7, 121.1, 113.8, 108.7, 108.0, 100.8, 56.5, 55.2, 51.3, 24.4 ppm; GC-MS for $C_{17}H_{19}NO_3$, m/z = 285 (M^+); HRMS (ESI-TOF) m/z: $[M+H]^+$ Calcd for $C_{17}H_{19}NO_3H$ 286.1438; Found 286.1427.

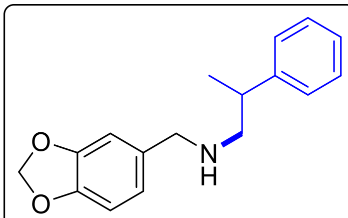

2-17r

N-(Benzo[d][1,3]dioxol-5-ylmethyl)-β-methylbenzeneethanamine (2-17r). A chlorobenzene (2.0 mL) solution of complex **2-9** (13 mg, 0.75 mol %), **2-16** (16 mg, 10 mol %), 1-(1,3-benzodioxol-5-yl)methanamine (151 mg, 1.0 mmol) and (±)-1-(4-methoxyphenyl)ethylamine (211 mg, 1.4 mmol) was stirred at 130 °C for 16 h. The product **2-17r** was isolated by a column chromatography on silica gel (n-hexanes/EtOAc = 100:1 to 10:1; 152 mg, 56%). TLC; Rf = 0.3 (20% EtOAc in hexanes). Data for **2-17r**: ^{1}H NMR (400 MHz, $CDCl_3$) δ 7.35–7.28 (m, 2H), 7.24–7.18 (m, 3H), 6.75 (d, J = 1.6 Hz, 2H), 6.73 (d, J = 7.9 Hz, 1H), 6.68 (dd, J

= 7.9, 1.6 Hz, 1H), 5.93 (s, 2H), 3.66 (ABq, J = 13.2 Hz, 2H), 2.96 (sextet, J = 7.1 Hz, 1H), 2.77 (d, J = 7.2 Hz, 2H), 1.66 (br s, 1H), 1.26 (d, J = 7.1 Hz, 3H) ppm; 13C{1H} NMR (100 MHz, $CDCl_3$) δ 147.6, 146.4, 145.2, 134.1, 128.5, 127.2, 126.4, 121.1, 108.6, 108.0, 100.8, 56.0, 53.5, 39.9, 20.1 ppm; GC-MS for $C_{17}H_{19}NO_2$, m/z = 269 (M+); HRMS (ESI-TOF) m/z: [M+H]+ Calcd for $C_{17}H_{19}NO_2H$ 270.1489; Found 270.1463.

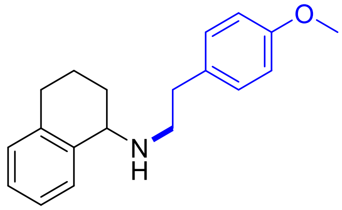

2-17s

***N*-[2-(4-Methoxyphenyl)ethyl]-1,2,3,4-tetrahydro-1-naphthalenamine (2-17s).** A chlorobenzene (2.0 mL) solution of complex **2-9** (13 mg, 0.75 mol %), **2-16** (16 mg, 10 mol %), 1,2,3,4-tetrahydro-1-naphthalenamine (147 mg, 1.0 mmol) and 4-methoxybenzeneethanamine (211 mg, 1.4 mmol) was stirred at 130 °C for 16 h. The product **2-17s** was isolated by a column chromatography on silica gel (*n*-hexanes/EtOAc = 100:1 to 10:1; 177 mg, 63%). TLC; R_f = 0.3 (10% EtOAc in hexanes). Data for **2-17s**: ^{1}H NMR (400 MHz, $CDCl_3$) δ 7.28–7.23 (m, 1H), 7.21–7.13 (m, 4H), 7.12–7.07 (m, 1H), 6.90–6.85 (m, 2H), 3.82 (s, 3H), 3.81 (t, *J* = 4.7 Hz, 1H), 3.05–2.89 (m, 2H), 2.87–2.69 (m, 4H), 2.01–1.86 (m, 3H), 1.80–1.70 (m, 1H), 1.63 (br s, 1H) ppm; ^{13}C{^{1}H} NMR (100 MHz, $CDCl_3$) δ 157.9, 139.0, 137.3, 132.1, 129.6, 129.0, 128.5, 126.5, 125.6, 113.7, 55.3, 55.2, 48.6, 35.7, 29.3, 28.2, 19.0 ppm; GC-MS for $C_{19}H_{23}NO$, m/z = 281 (M^+); HRMS (ESI-TOF) m/z: $[M+H]^+$ Calcd for $C_{19}H_{23}NOH$ 282.1852; Found 282.1843.

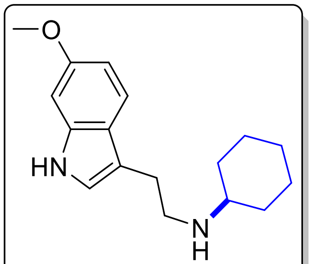

2-17t

***N*-Cyclohexyl-5-methoxytryptamine (2-17t).** A 1,4-dioxane (2.0 mL) solution of complex **2-11** (10 mg, 1 mol %), 5-methoxytryptamine (190 mg, 1.0 mmol) and cyclohexylamine (139 mg, 1.4 mmol) was stirred at 130 °C for 16 h. The product **2-17t** was isolated by a column chromatography on silica gel (*n*-hexane/EtOAc = 100:1 to 10:1; 88%). TLC; R_f = 0.2 (30% EtOAc in hexanes). Data for **2-17t**: ^{1}H NMR (400 MHz, $CDCl_3$) δ 8.21 (br s, 1H), 7.26–7.20 (m, 1H), 7.08–7.05 (m, 1H), 7.02–6.99 (m, 1H), 6.85 (dd, *J* = 8.8, 2.5 Hz, 1H), 3.86 (s, 3H), 3.07–2.90 (m, 4H), 2.45 (tt, *J* = 10.5, 3.7 Hz, 1H), 1.91–1.78 (m, 3H), 1.75–1.65 (m, 2H), 1.64–1.55 (m, 1H), 1.29–0.99 (m, 5H) ppm; $^{13}C\{^1H\}$ NMR (100 MHz, $CDCl_3$) δ 153.8, 131.5, 127.8, 122.8, 113.6, 112.1, 111.8, 100.6, 56.8, 55.9, 46.8, 33.5, 26.1, 25.9, 25.0 ppm; GC-MS for $C_{17}H_{24}N_2O$, m/z = 272 (M^+); HRMS (ESI-TOF) m/z: $[M+H]^+$ Calcd for $C_{17}H_{24}FN_2OH$ 273.1961; Found 273.1960.

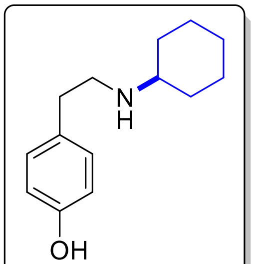

2-17v

4-[2-Cyclohexylaminoethyl]phenol (2-17v). A 1,4-dioxane (2.0 mL) solution of complex **2-11** (10 mg, 1 mol %), tyramine (136 mg, 1.0 mmol) and cyclohexylamine (139 mg, 1.4 mmol) was stirred at 130 °C for 16 h. The product **2-17v** was isolated by a column chromatography on silica gel (*n*-hexane/EtOAc = 100:1 to 10:1; 81%). TLC; R_f = 0.3 (20% EtOAc in hexanes). Data for **2-17v**: ^{1}H NMR (400 MHz, $CDCl_3$) δ 7.02 (d, *J* = 8.3 Hz, 2H), 6.72 (d, *J* = 8.3 Hz, 2H), 4.71 (br s, 1H), 2.93 (t, *J* = 6.9 Hz, 2H), 2.75 (t, *J* = 6.9 Hz, 2H), 2.47 (tt, *J* = 10.6, 3.6 Hz, 1H), 1.92–1.85 (m, 2H), 1.75–1.66 (m, 2H), 1.64–1.55 (m, 1H), 1.28–1.08 (m, 5H) ppm; $^{13}C\{^1H\}$ NMR (100 MHz, $CDCl_3$) δ 155.5, 130.0, 129.7, 115.9, 56.9, 47.6, 34.7, 32.9, 25.9, 25.0 ppm; GC-

MS for $C_{14}H_{21}NO$, m/z = 219 (M^+); Anal. Calcd for $C_{14}H_{21}NO$: C, 76.67; H, 9.65. Found: C, 76.78; H, 9.35; HRMS (ESI-TOF) m/z: $[M+H]^+$ Calcd for $C_{14}H_{21}NOH$ 220.1696; Found 220.1698.

6.2.8.2 Characterization Data of the Novel Symmetric Secondary Amines Listed in Table 2.4

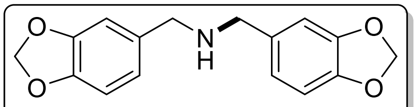

2-18g

Bis(3,4-methylenedioxybenzyl)amine (2-18g). A chlorobenzene (2.0 mL) solution of complex **2-9** (13 mg, 0.75 mol %), **2-16** (16 mg, 10 mol %) and 1-(1,3-benzodioxol-5-yl)methanamine (151 mg, 1.0 mmol) was stirred at 130 °C for 16 h. The product **2-18g** was isolated by a column chromatography on silica gel (*n*-hexanes/EtOAc = 100:1 to 10:1; 110 mg, 77%). TLC; R_f = 0.4 (40% EtOAc in hexanes). Data for **2-18g** ^{1}H NMR (400 MHz, $CDCl_3$) δ 6.85 (s, 2H), 6.77–6.75 (m, 4H), 5.94 (s, 4H), 3.69 (s, 4H), 1.59 (br s, 1H) ppm; $^{13}C\{^1H\}$ NMR (100 MHz, $CDCl_3$) δ 147.7, 146.5, 134.3, 121.2, 108.7, 108.0, 100.9, 52.7 ppm; GC-MS for $C_{16}H_{15}NO_4$, m/z = 285 (M^+); HRMS (ESI-TOF) m/z: $[M+H]^+$ Calcd for $C_{16}H_{15}NO_4H$ 286.1074; Found 286.1070.

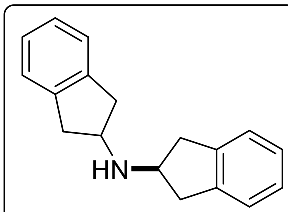

2-18l

Di-[2-aminoindane] (2-18l). A chlorobenzene (2.0 mL) solution of complex **2-9** (13 mg, 0.75 mol %), **2-16** (16 mg, 10 mol %) and 2-indanamine (133 mg, 1.0 mmol) was stirred at 130 °C for 16 h. The product **2-18l** was isolated by a column chromatography on silica gel (*n*-hexane/EtOAc = 100:1 to 10:1; 91 mg, 73%). TLC; R_f = 0.5 (20% EtOAc in hexanes). Data for **2-18l** ^{1}H NMR (400 MHz, $CDCl_3$) δ 7.30–7.24 (m, 4H), 7.24–7.18 (m, 4H), 3.83 (quintet, *J* = 7.2 Hz, 2H), 3.26 (dd, *J* = 15.4, 7.2 Hz, 4H), 2.85 (dd, *J* = 15.4, 7.2 Hz, 4H), 1.77 (br s, 1H) ppm; $^{13}C\{^1H\}$ NMR (100 MHz, $CDCl_3$) δ

141.5, 126.3, 124.5, 58.1, 40.2 ppm; GC-MS for $C_{18}H_{19}N$, m/z = 249 (M^+); HRMS (ESI-TOF) m/z: $[M+H]^+$ Calcd for $C_{18}H_{19}NH$ 250.1590; Found 250.1598.

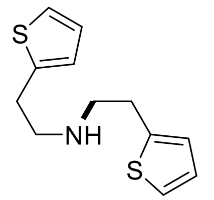

2-18n

***N*-(2-Thienylethyl)-2-thiopheneethanamine (2-18n).** A 1,4-dioxane (2.0 mL) solution of complex **2-11** (10 mg, 1 mol) and 2-thiopheneethanamine (127 mg, 1.0 mmol) was stirred at 130 °C for 16 h. The product **2-18n** was isolated by a column chromatography on silica gel (*n*-hexane/EtOAc = 100:1 to 10:1; 96%). TLC; R_f = 0.4 (30% EtOAc in hexanes). Data for **2-18n** ^{1}H NMR (400 MHz, $CDCl_3$) δ 7.22–7.04 (m, 2H), 6.96–6.87 (m, 2H), 6.85–6.75 (m, 2H), 3.06–2.99 (m, 4H), 2.98–2.90 (m, 4H), 2.45 (br s, 1H) ppm; $^{13}C\{^1H\}$ NMR (100 MHz, $CDCl_3$) δ 142.2, 126.8, 125.0, 123.5, 50.7, 30.2 ppm; GC-MS for $C_{12}H_{15}NS_2$, m/z = 237 (M^+); HRMS (ESI-TOF) m/z: $[M+H]^+$ Calcd for $C_{12}H_{15}NS_2H$ 238.0719; Found 238.0716.

6.2.8.3 Characterization Data of the of Novel Unsymmetric Secondary Listed in Table 2.5

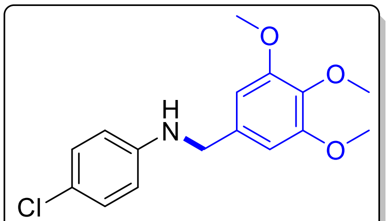

2-19i

3,4,5-Trimethoxy-*N*-(4-chlorophenyl)benzenemethanamine (2-19i). A chlorobenzene (2.0 mL) solution of complex **2-9** (7 mg, 0.75 mol %), **2-16** (8 mg, 10 mol %), 4-chloroaniline (64 mg, 0.5 mmol) and 3,4,5-trimethoxybenzylamine (138 mg, 0.7 mmol) was stirred at 140 °C for 20 h. The product **2-19i** was isolated by a column chromatography on silica gel (*n*-hexane/EtOAc = 150:1 to 40:1; 111 mg, 72%). TLC; R_f = 0.6 (50% EtOAc in hexanes). Data for **2-19i**: ^{1}H NMR (400 MHz, $CDCl_3$) δ 7.12 (d, *J* = 9.0 Hz, 2H), 6.58 (s, 2H), 6.57 (d, *J* = 9.0 Hz, 2H), 4.23 (s, 2H), 3.84 (s, 3H), 3.84 (s, 6H) ppm; $^{13}C\{^1H\}$ NMR

(100 MHz, $CDCl_3$) δ 153.4, 146.4, 137.0, 134.5, 129.0, 122.3, 114.0, 104.1, 60.8, 56.0, 48.8 ppm; GC-MS for $C_{16}H_{18}ClNO_3$, m/z = 307 (M^+). Anal. Calcd for $C_{16}H_{18}ClNO_3$: C, 62.44; H, 5.90. Found: C, 62.88; H, 6.05.

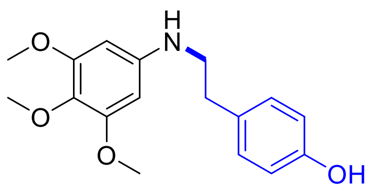

2-15j

4-(2-(3,4,5-Trimethoxyphenylamino)ethyl)phenol (2-19j). A chlorobenzene (2.0 mL) solution of complex **2-9** (7 mg, 0.75 mol %), **2-16** (8 mg, 10 mol %), 3,4,5-trimethoxyaniline (91 mg, 0.5 mmol) and 2-(4-hydroxyphenyl)ethanamine (96 mg, 0.7 mmol) was stirred at 140 °C for 20 h. The product **2-19j** was isolated by a column chromatography on silica gel (*n*-hexane/EtOAc = 150:1 to 40:1; 77 mg, 51%). TLC; R_f = 0.4 (50% EtOAc in hexanes). Data for **2-19j**: ^{1}H NMR (400 MHz, $CDCl_3$) δ 7.09–7.05 (m, 2H), 6.81–6.77 (m, 2H), 5.90 (s, 2H), 3.81 (s, 6H), 3.77 (s, 3H), 3.33 (t, *J* = 7.1 Hz, 2H), 2.86 (t, *J* = 7.1 Hz, 2H) ppm; $^{13}C\{^1H\}$ NMR (100 MHz, $CDCl_3$) δ 154.4, 153.9, 144.1, 130.7, 130.5, 129.8, 115.5, 91.1, 61.1, 55.9, 46.2, 34.4 ppm; GC-MS for $C_{17}H_{21}NO_4$, m/z = 303 (M^+); HRMS (ESI-TOF) m/z: $[M+H]^+$ Calcd for $C_{17}H_{21}NO_4H$ 304.1543; Found 304.1516.

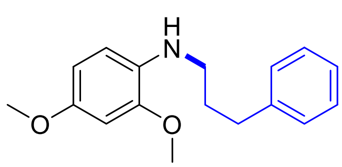

2-15k

2,4-dimethoxy-N-(3-phenylpropyl)aniline (2-19k). A chlorobenzene (2.0 mL) solution of complex **2-9** (7 mg, 0.75 mol %), **2-16** (8 mg, 10 mol %), 2,4-dimethoxyaniline (77 mg, 0.5 mmol) and 3-phenyl-1-propanamine (95 mg, 0.7 mmol) was stirred at 140 °C for 20 h. The product **2-19k** was isolated by a column chromatography on silica gel (*n*-hexane/EtOAc = 150:1 to 40:1; 97 mg, 46%). TLC; R_f = 0.6 (50% EtOAc in hexanes). Data for **2-19k**: ^{1}H NMR (400 MHz, $CDCl_3$) δ 7.36–7.28 (m, 2H), 7.27–7.19 (m, 3H), 6.56 (d, *J* = 8.5 Hz, 1H), 6.48 (d, *J* = 2.7

Hz, 1H), 6.43 (dd, J = 8.5, 2.7 Hz, 1H), 4.19 (br s, 1H), 3.84 (s, 3H), 3.78 (s, 3H), 3.15 (t, J = 7.1 Hz, 2H), 2.77 (t, J = 7.6 Hz, 2H), 2.06–1.96 (m, 2H) ppm; $^{13}C\{^1H\}$ NMR (100 MHz, $CDCl_3$) δ 152.0, 148.0, 141.7, 132.2, 128.4, 128.3, 125.8, 110.5, 103.7, 99.1, 55.7, 55.4, 44.1, 33.4, 31.0 ppm; GC-MS for $C_{17}H_{21}NO_2$, m/z = 271 (M^+). HRMS (ESI-TOF) m/z: $[M+H]^+$ Calcd for $C_{17}H_{21}NO_2H$ 272.1645; Found 272.1640.

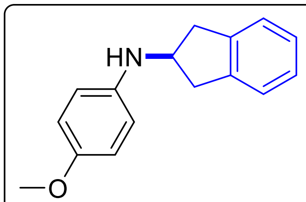

2-19l

***N*-(4-Methoxyphenyl)-2,3-dihydro-1H-inden-2-amine (2-19l).** A chlorobenzene (2.0 mL) solution of complex **2-9** (7 mg, 0.75 mol %), **2-16** (8 mg, 10 mol %), 4-methoxyaniline (62 mg, 0.5 mmol) and 2-aminoindan (93 mg, 0.7 mmol) was stirred at 140 °C for 20 h. The product **2-19l** was isolated by a column chromatography on silica gel (*n*-hexane/EtOAc = 150:1 to 40:1; 88 mg, 74%). TLC; R_f = 0.5 (30% EtOAc in hexanes). Data for **2-19l**: ^1H NMR (400 MHz, $CDCl_3$) δ 7.29–7.17 (m, 4H), 6.86–6.80 (m, 2H), 6.67–6.62 (m, 2H), 4.33 (tt, J = 6.8, 4.4 Hz,1H), 3.79 (s, 3H), 3.37 (dd, J = 16.0, 6.8 Hz, 2H), 2.90 (dd, J = 16.0, 4.4 Hz, 2H) ppm; $^{13}C\{^1H\}$ NMR (100 MHz, $CDCl_3$) δ 152.2, 141.4, 141.4, 126.5, 124.9, 114.9, 114.9, 55.7, 54.9, 40.1 ppm; GC-MS for $C_{16}H_{17}NO$, m/z = 239 (M^+); HRMS (ESI-TOF) m/z: $[M+H]^+$ Calcd for $C_{16}H_{17}NOH$ 240.1383; Found 240.1377.

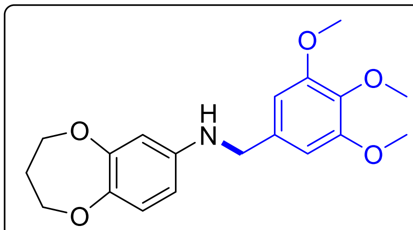

2-19m

***N*-(3,4,5-Trimethoxybenzyl)-3,4-dihydro-2*H*-benzo[b][1,4]dioxepin-7-amine (2-19m).** A chlorobenzene (2.0 mL) solution of complex **2-9** (7 mg, 0.75 mol %), **2-16** (8 mg, 10 mol %), 3,4-dihydro-2H-1,5-benzodioxepin-7-amine (83 mg, 0.5 mmol) and 3,4,5-trimethoxybenzylamine (138 mg, 0.7 mmol) was stirred at 140 °C for

20 h. The product **2-19m** was isolated by a column chromatography on silica gel (*n*-hexane/EtOAc = 150:1 to 40:1; 129 mg, 75%). TLC; R_f = 0.4 (50% EtOAc in hexanes). Data for **2-19m**: ^{1}H NMR (400 MHz, $CDCl_3$) δ 6.84 (d, *J* = 8.6 Hz, 1H), 6.59 (s, 2H), 6.38–6.34 (m, 1H), 6.31–6.26 (m, 1H), 4.19 (s, 2H), 4.15 (t, *J* = 5.4 Hz, 2H), 4.09 (t, *J* = 5.5 Hz, 2H), 3.84 (s, 6H), 3.83 (s, 3H), 2.14 (quintet, *J* = 5.5 Hz, 2H) ppm; $^{13}C\{^1H\}$ NMR (100 MHz, $CDCl_3$) δ 153.3, 152.1, 143.9, 143.6, 137.0, 134.4, 122.2, 108.7, 106.5, 104.5, 70.9, 70.8, 60.8, 56.1, 49.8, 32.4 ppm; GC-MS for $C_{19}H_{23}NO_5$, m/z = 345 (M^+); HRMS (ESI-TOF) m/z: $[M+H]^+$ Calcd for $C_{19}H_{23}FNO_5H$ 346.1649; Found 346.1618.

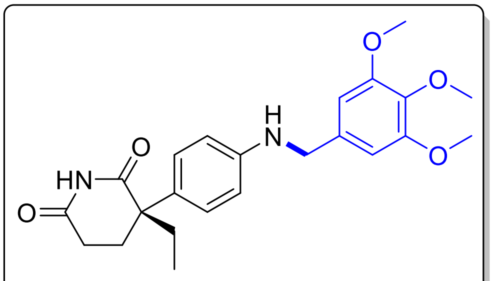

2-19n

(*R*)-3-Ethyl-3-(4-(3,4,5-trimethoxybenzylamino)phenyl)piperidine-2,6-dione (2-19n). A chlorobenzene (2.0 mL) solution of complex **2-9** (7 mg, 0.75 mol %), **2-16** (8 mg, 10 mol %), (*R*)-(+)-aminoglutethimide (116 mg, 0.5 mmol) and 3,4,5-trimethoxybenzylamine (138 mg, 0.7 mmol) was stirred at 140 °C for 20 h. The product **2-19n** was isolated by a column chromatography on silica gel (*n*-hexane/ethyl acetate = 100:1 to 1:1; 82 mg, 40%), $[\alpha]_D^{22}$ = +148.2 (c = 0.2 in CH_2Cl_2); TLC; R_f = 0.2 (50% EtOAc in hexanes). Data for **2-19n**: δ 7.98 (br s, 1H), 7.07 (d, *J* = 8.7 Hz, 2H), 6.64 (d, *J* = 8.7 Hz, 2H), 6.59 (s, 2H), 4.24 (s, 2H), 3.83 (s, 9H), 2.62–2.52 (m, 1H), 2.44 (dd, *J* = 13.2, 4.9 Hz, 1H), 2.31 (ddd, *J* = 14.2, 4.8, 2.7 Hz, 1H), 2.16 (dd, *J* = 13.8, 4.8 Hz, 1H), 1.99 (sext, *J* = 7.4 Hz, 1H), 1.87 (sextet, *J* = 7.4 Hz, 1H), 0.85 (t, *J* = 7.4 Hz, 3H) ppm; $^{13}C\{^1H\}$ NMR (100 MHz, $CDCl_3$) δ 175.5, 172.5, 153.4, 147.0, 137.1, 134.5, 127.1, 113.4, 113.4, 104.4, 60.8, 56.1, 50.2, 48.9, 32.9, 29.3, 26.9, 9.0 ppm; GC-MS for $C_{23}H_{28}N_2O_5$, m/z = 412 (M^+); HRMS (IT-TOF/ESI) Calcd for $C_{23}H_{28}N_2O_5$-H ($[M-H]^-$): 411.1925, Found: 411.1908.

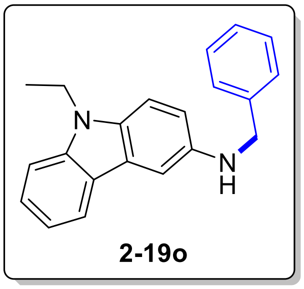

N-benzyl-9-ethyl-9H-carbazol-3-amine (2-19o). A 1,4-dioxane (2.0 mL) solution of complex **2-11** (10 mg, 1 mol %), 3-amino-9-ethylcarbazole (105 mg, 0.5 mmol) and benzylamine (75 mg, 0.7 mmol) was stirred at 140 °C for 20 h. The product **2-19o** was isolated by a column chromatography on silica gel (*n*-hexane/EtOAc = 150:1 to 40:1; 86%). TLC; R_f = 0.4 (50% EtOAc in hexanes). Data for **2-19o**: ^{1}H NMR (400 MHz, $CDCl_3$) δ 8.00 (dd, *J* = 7.8, 1.2 Hz, 1H), 7.48–7.39 (m, 4H), 7.39–7.32 (m, 3H), 7.31–7.28 (m, 1H), 7.24 (d, *J* = 8.7 Hz, 1H), 7.15 (dd, *J* = 7.8, 1.1 Hz, 1H), 6.94 (dd, *J* = 8.7–2.3 Hz, 1H), 4.45 (s, 2H), 4.29 (q, *J* = 7.2 Hz, 2H), 1.39 (t, *J* = 7.2 Hz, 3H) ppm; $^{13}C\{^1H\}$ NMR (100 MHz, $CDCl_3$) δ 140.8, 140.3, 139.3, 134.3, 128.6, 127.9, 127.3, 125.3, 123.5, 122.6, 120.4, 117.9, 114.7, 109.1, 108.3, 104.1, 50.2, 37.5, 13.8 ppm; GC-MS for $C_{21}H_{20}N_2$, m/z = 300 (M^+); HRMS (ESI-TOF) m/z: $[M+H]^+$ Calcd for $C_{21}H_{20}N_2H$ 301.1699; Found 301.1679.

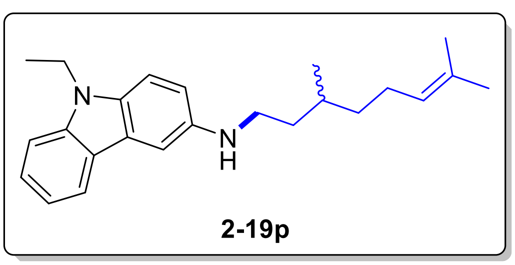

N-(3,7-dimethyloct-6-en-1-yl)-9-ethyl-9H-carbazol-3-amine (2-19p). A 1,4-dioxane (2.0 mL) solution of complex **2-9** (10 mg, 1 mol %), **2-16** (8 mg, 10 mol %), 3-amino-9-ethylcarbazole (105 mg, 0.5 mmol) and geranylamine (107 mg, 0.7 mmol) was stirred at 140 °C for 20 h. The product **2-19p** was isolated by a column chromatography on silica gel (*n*-hexane/EtOAc = 150:1 to 40:1; 66%). TLC; R_f = 0.4 (50% EtOAc in hexanes). Data for **2-19p**: ^{1}H NMR (400 MHz, $CDCl_3$) δ 8.06 (d, *J* = 7.8 Hz, 1H), 7.44 (td, *J* = 7.6, 1.1 Hz, 1H), 7.40–7.33 (m, 2H), 7.26 (d, *J* = 8.6 Hz, 1H), 7.19 (td, *J* = 7.5, 0.9 Hz, 1H), 6.90 (dd, *J* = 8.6, 2.3 Hz, 1H), 5.17 (tt, *J* = 7.1, 1.3 Hz, 1H), 4.32 (q, *J* = 7.2 Hz, 2H), 3.47 (brs, 1H), 3.34–3.20 (m, 2H), 2.13–2.00 (m, 2H), 1.81–1.62 (m, 2H), 1.74 (s, 3H), 1.66 (s, 3H), 1.59–1.46 (m, 2H), 1.42 (t, *J* = 7.2 Hz, 3H), 1.33–1.23 (m, 1H), 1.03 (d, *J* = 6.5 Hz, 3H) ppm; $^{13}C\{^1H\}$ NMR (100 MHz, $CDCl_3$) δ 142.1, 140.2, 133.8, 131.3, 125.2, 124.7, 123.6, 122.6, 120.3, 117.8, 114.5, 109.0, 108.2, 103.2, 43.5, 37.4, 37.1, 36.9, 30.5, 25.7, 25.5, 19.7, 17.7, 13.8 ppm; GC-MS for $C_{24}H_{32}N_2$, m/z = 348 (M^+).

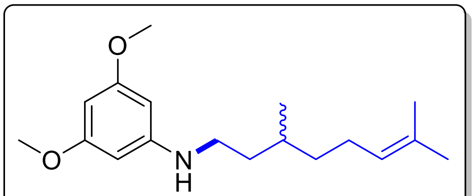

2-19q

N-(3,7-dimethyloct-6-en-1-yl)-3,5-dimethoxyaniline (2-19q). A 1,4-dioxane (2.0 mL) solution of complex **2-9** (10 mg, 1 mol %), **2-16** (8 mg, 10 mol %), 3,5-dimethoxyaniline (77 mg, 0.5 mmol) and geranylamine (107 mg, 0.7 mmol) was stirred at 140 °C for 20 h. The product **2-19q** was isolated by a column chromatography on silica gel (*n*-hexane/EtOAc = 150:1 to 40:1; 51%). TLC; R_f = 0.4 (50% EtOAc in hexanes). Data for **2-19q**: ^1H NMR (400 MHz, $CDCl_3$) δ 5.87 (t, *J* = 2.1 Hz, 1H), 5.79 (d, *J* = 2.1 Hz, 2H), 5.13–5.07 (m, 1H), 3.75 (s, 6H), 2.07–1.94 (m, 4H), 1.69 (s, 3H), 1.61 (s, 3H), 1.47–1.33 (m, 3H), 1.26–1.15 (m, 3H), 0.94 (t, *J* = 6.5 Hz, 3H) ppm; $^{13}C\{^1H\}$ NMR (100 MHz, $CDCl_3$) δ 161.7, 150.4, 131.3, 124.6, 91.4, 89.4, 55.1, 41.9, 37.0, 36.6, 30.4, 25.7, 25.4, 19.5, 17.6 ppm; GC-MS for $C_{18}H_{29}NO_2$, m/z = 291 (M^+).

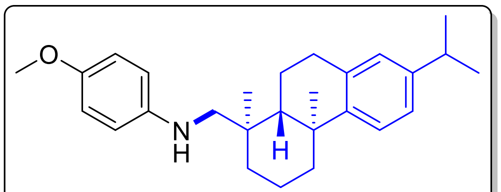

2-19r

N-(((1R,4aS,10aR)-7-isopropyl-1,4a-dimethyl-1,2,3,4,4a,9,10,10a-octahydrophenanthren-1-yl)methyl)-4-methoxyaniline (2-19r). A 1,4-dioxane (2.0

mL) solution of complex **2-9** (10 mg, 1 mol %), 4-methoxyaniline (62 mg, 0.5 mmol) and (+)-dehydroabietylamine (200 mg, 0.7 mmol) was stirred at 140 °C for 20 h. The product **2-19r** was isolated by a column chromatography on silica gel (*n*-hexane/EtOAc = 150:1 to 40:1; 88%). TLC; R_f = 0.7 (30% EtOAc in hexanes). Data for **2-19r**: ^{1}H NMR (400 MHz, $CDCl_3$) δ 7.54 (s, 1H), 7.22–7.19 (m, 1H), 7.05–7.02 (m, 1H), 7.00 (d, *J* = 8.8 Hz, 2H), 6.94–6.91 (m, 1H), 6.89 (d, *J* = 8.8 Hz, 2H), 3.82 (s, 3H), 2.90–2.85 (m, 2H), 2.39–2.34 (m, 1H), 2.04–1.93 (m, 2H), 1.86–1.73 (m, 6H), 1.55–1.47 (m, 4H), 1.33 (s, 3H), 1.29 (s, 3H), 1.24 (d, *J* = 6.9 Hz, 6H) ppm; ^{13}C{^{1}H} NMR (100 MHz, $CDCl_3$) δ 173.4, 157.5, 146.8, 134.7, 134.0, 127.0, 124.1, 123.9, 121.6, 114.1,55.4, 46.7, 46.1, 43.4, 42.8, 38.2, 36.1, 33.4, 30.0, 25.3, 24.0, 20.6, 18.4, 16.5, 14.0 ppm; GC-MS for $C_{27}H_{37}NO$, m/z = 391 (M^+); HRMS (ESI-TOF) m/z: $[M+H]^+$ Calcd for $C_{27}H_{37}NOH$ 392.2869; Found 392.2857.

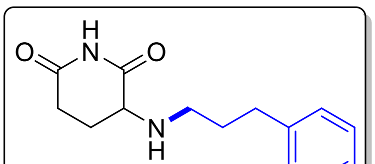

2-17w

3-(3-Phenylpropylamino)piperidine-2,6-dione (2-17w). A chlorobenzene (2.0 mL) solution of complex **2-9** (7 mg, 0.75 mol %), **2-16** (8 mg, 10 mol %), L-glutamine (73 mg, 0.5 mmol) and 3-phenyl-1-propanamine (95 mg, 0.7 mmol) was stirred at 140 °C for 20 h. The product **2-17w** was isolated by a column chromatography on silica gel (*n*-hexane/ethyl acetate = 50:1 to 1:1; 92 mg, 75%). TLC; R_f = 0.2 (50% EtOAc in hexanes). Data for **2-17w**: ^{1}H NMR (400 MHz, $CDCl_3$) δ 7.30–7.23 (m, 2H), 7.22–7.12 (m, 3H), 6.73 (br s, 1H), 4.08 (dd, *J* = 9.0, 4.8 Hz, 1H), 3.28 (dd, *J* = 8.9, 4.8 Hz, 1H), 2.63 (t, *J* = 7.5 Hz, 2H), 2.50–2.37 (m, 1H), 2.37–2.19 (m, 2H), 2.16–2.05 (m, 1H), 1.84 (quintet, *J* = 7.4 Hz, 2H) ppm; ^{13}C{^{1}H} NMR (100 MHz, $CDCl_3$) δ 179.5, 172.1, 141.4, 128.4, 128.3, 126.0, 57.1, 39.3, 33.2, 30.8, 29.4, 25.7 ppm;

GC-MS for $C_{14}H_{18}N_2O_2$, m/z = 246 (M^+); HRMS (ESI-TOF) m/z: $[M+H]^+$ Calcd for $C_{14}H_{18}N_2O_2H$ 247.1441; Found 247.1408.

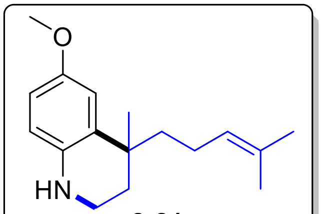
2-21a

(S)-6-methoxy-4-methyl-4-(4-methylpent-3-en-1-yl)-1,2,3,4-tetrahydroquinoline (2-21a). A 1,4-dioxane (2.0 mL) solution of complex **2-9** (10 mg, 1 mol %), 4-methoxyaniline (62 mg, 0.5 mmol) and geranylamine (107 mg, 0.7 mmol) was stirred at 140 °C for 20 h. The product **2-21a** was isolated by a column chromatography on silica gel (*n*-hexane/EtOAc = 150:1 to 40:1; 95%). TLC; R_f = 0.6 (30% EtOAc in hexanes). Data for **2-21a**: ^{1}H NMR (400 MHz, $CDCl_3$) δ 6.75 (d, *J* = 2.9 Hz, 1H), 6.58 (dd, *J* = 8.6, 2.9 Hz, 1H), 6.39 (d, *J* = 8.6 Hz, 1H), 5.2–4.98 (m, 1H), 3.73 (s, 3H), 1.72–1.52 (m, 8H), 1.30 (s, 3H), 1.23 (s, 3H), 0.88 (d, *J* = 6.5 Hz, 3H) ppm; $^{13}C\{^1H\}$ NMR (100 MHz, $CDCl_3$) δ 151.7, 137.2, 132.8, 124.6, 114.9, 114.6, 113.0, 112.1, 55.9, 50.6, 47.2, 43.3, 35.0, 30.9, 27.0, 24.8, 22.2 ppm; GC-MS for $C_{17}H_{25}NO$, m/z = 259 (M^+); HRMS (ESI-TOF) m/z: $[M+H]^+$ Calcd for $C_{17}H_{27}NOH$ 260.2014; Found 260.2014.

6.2.8.4 Characterization Data from the Compounds Listed in Table 2.6

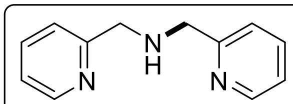
2-18p

Bis(2-pyridylmethyl)amine (2-18p). A 1,4-dioxane (2.0 mL) solution of complex **2-9** (10 mg, 1 mol %), 2-(aminomethyl)pyridine (108 mg, 1 mmol) was stirred at 130 °C for 16 h. The product **2-18p** was isolated by a column chromatography on silica gel (*n*-hexane/EtOAc = 150:1 to 40:1; 51%). TLC; R_f = 0.6 (30% EtOAc in hexanes). Data for **2-18p**: ^{1}H NMR (400 MHz, $CDCl_3$) δ 8.56–8.58 (m, 2H), 8.50–8.53 (m, 2H), 7.64–7.57 (m, 2H,), 7.26–7.20 (m, 2H), 3.99 (s, 4H), 3.05 (brs, 1H) ppm; $^{13}C\{^1H\}$ NMR (100 MHz, $CDCl_3$) δ 159.7, 148.8, 135.9, 122.4, 122.1, 54.5 ppm; GC-MS for $C_{12}H_{13}N_3$, m/z = 199 (M^+). ^1H and ^{13}C NMR spectral data were in good agreement with the literature values.[123]

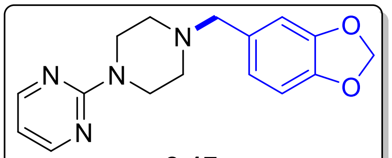
2-17a

Piribedil (2-20a). A 1,4-dioxane (2.0 mL) solution of complex **2-9** (10 mg, 1 mol %), 1-(2-Pyrimidyl)piperazine (82 mg, 0.5 mmol) and 1-(1,3-benzodioxol-5-yl)methanamine (151 mg, 1.0 mmol) was stirred at 140 °C for 20 h. The product **2-17a** was isolated by a column chromatography on silica gel (*n*-hexane/EtOAc = 30:1 to 1:1; 39%). Data for **2-17a**: ^1H NMR (400 MHz, $CDCl_3$) δ 8.29 (d, *J* = 4.6 Hz, 2H), 6.89 (s, 1H), 6.74 (s, 2H), 6.45 (t, *J* = 4.6 Hz, 1H), 5.95 (s, 2H), 3.82–3.79 (m, 4H), 3.46 (s, 2H), 2.50–2.47 (m, 4H) ppm; $^{13}C\{^1H\}$ NMR (100 MHz, $CDCl_3$) δ 161.6, 157.8, 147.5, 146.6, 132.0, 122.3, 109.7, 109.4, 107.8, 101.0, 62.8, 52.7, 43.6 ppm; GC-MS for $C_{16}H_{18}N_4O_2$, m/z = 298 (M^+). ^1H and ^{13}C NMR spectral data were in good agreement with the literature values.[206]

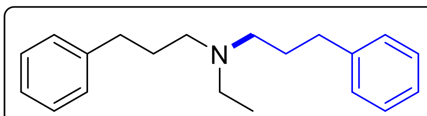
2-17b

Alverine (2-20b). A 1,4-dioxane (2.0 mL) solution of complex **2-9** (10 mg, 1 mol %), **2-14k** (127 mg, 0.5 mmol) and ethylamine (90 mg, 2.0 mmol) was stirred at 140 °C for 20 h. The product **2-17b** was isolated by a column chromatography on silica gel (*n*-hexane/EtOAc = 150:1 to 40:1; 58%). TLC; R_f = 0.7 (10% EtOAc in hexanes). Data for **2-17b**: ^1H NMR (400 MHz, $CDCl_3$) δ 7.25 (t, *J* = 7.8 Hz, 4H), 7.12−7.20 (m, 6H), 2.62−2.58 (m, 4H), 2.51 (q, *J* = 7.2 Hz, 2H), 2.45 (t, *J* = 7.3 Hz, 4H), 1.75 (tt, *J* = 8.0, 7.4 Hz, 4H), 0.97 (t, *J* = 7.2 Hz, 3H) ppm; $^{13}C\{^1H\}$ NMR (100 MHz,

$CDCl_3$) δ 142.2, 128.4, 128.3, 125.8, 52.9, 47.5, 33.7, 28.4, 11.4 ppm; GC-MS for $C_{20}H_{27}N$, m/z = 281 (M^+). ^1H and ^{13}C NMR spectral data were in good agreement with the literature values.[207]

6.3 Experimental Procedures and Data for the Chapter 3

6.3.1 General Procedure for the Catalytic Deaminative Coupling of Ketones with Amines

In a glove box, complex **2-10** (9 mg, 3 mol %), 3,4,5,6-tetrachloro-1,2-benzoquinone **2-12** (12 mg, 10 mol %) were dissolved in anhydrous 1,4-dioxane (1 mL) in a 25 mL Schlenk tube equipped with a Teflon screw cap stopcock and a magnetic stirring bar. After stirring for 5-10 min until the solution was turned light green color, both ketone (0.5 mmol) and an amine (0.7 mmol) substrates, and dioxane (1 mL) was added to the tube. The tube was sealed, it was brought out of the glove box, and was stirred in an oil bath set at 130 °C for 16-20 h. After the reaction tube was cooled to room temperature, the tube was open to air, the solution was filtered through a short silica gel column by eluting with CH_2Cl_2 (10 mL), and the filtrate was analyzed by GC-MS method. Analytically pure product **3-10** was isolated by a simple column chromatography on silica gel (280-400 mesh, hexanes/EtOAc).

6.3.2 General Procedure for the Catalyst and Ligand Screening Study

In a glove box, a Ru catalyst (3 mol % Ru atom) and a ligand (10 mol %) were dissolved in a solvent (1 mL) in a 25 mL Schlenk tube equipped with a Teflon screw cap stopcock and a magnetic stirring bar. The resulting mixture was stirred for 5-10 min. Phenylethanone (60 mg, 0.5 mmol), 4-methoxybenzylamine (69 mg, 0.7 mmol) and a solvent (1 mL) were added to the reaction tube. The tube was brought out of the glove box and was stirred in an oil bath at 130 °C for 16 h. The product yield was determined by ^{1}H NMR by using hexamethylbenzene as an internal standard. The results are summarized in **Table 3.1** and **3.2**.

6.3.3.1 Reaction Profile Study

In a glove box, complex **2-10** (2 mg, 3 mol %) and **2-12** (2 mg, 10 mol %) were dissolved in toluene-d_8 (0.5 mL) in a 25 mL Schlenk tube equipped with a Teflon screw cap stopcock and a magnetic stirring bar. The resulting mixture was stirred for 10 minutes until the solution turned to a brownish green color. Acetophenone (12 mg, 0.10 mmol) and 4-methoxybenzylamine (14 mg, 0.10 mmol) were added to the reaction tube, and the solution was transferred into a J-Young NMR tube equipped with a Teflon screw cap stopcock. The tube was brought out of the glove box, and was immersed an oil bath set at 130 °C. The tube was taken out from the oil bath at 20 min intervals, was immediately cooled in ice-water bath, and was analyzed by ^{1}H NMR. The appearance of the product signals were normalized against an external standard peak (C_6Me_6). The plot of the relative concentrations of substrates and products vs time is shown in **Figure 3.1**.

6.3.3.2 Reaction with Imine

In a glove box, complex **2-10** (2 mg, 3 mol %) and **2-12** (2 mg, 10 mol %) were dissolved in a 1,4-dioxane in a 25 mL Schlenk tube equipped with a Teflon screw cap stopcock and a magnetic stirring bar. After stirring for 5-10 min until the solution was turned light green color, (4-Methoxyphenyl)-*N*-(1-phenylethylidene)methanamine **3-13a** (120mg 0.5 mmol) and dioxane (1 mL) was added to the tube. The tube was sealed, it was brought out of the glove box, and was stirred in an oil bath set at 130 °C for 16-20 h. After the reaction tube was cooled to room temperature, the tube was open to air, the solution was filtered through a short silica gel column by eluting with CH_2Cl_2 (10 mL), and the filtrate was analyzed by GC-MS method. Analytically pure product 3-10 was isolated by a simple column chromatography on silica gel (280-400 mesh, hexanes/EtOAc).

6.3.3.3 Crossover Experiment

In a glove box, complex **2-10** (2 mg, 3 mol %) and **2-12** (2 mg, 10 mol %) were dissolved in a 1,4-dioxane in a 25 mL Schlenk tube equipped with a Teflon screw cap stopcock and a magnetic stirring bar. After stirring for 5-10 min until the solution was turned light green color, independently generated **3-13a** (60 mg, 0.25 mmol), *N*-cyclohexylidene-3-phenylpropan-1-amine (**3-13c**) (54 mg, 0.25 mmol) in 1,4-dioxane (2 mL) and dioxane (1 mL) was added to the tube. The tube was sealed, it was brought out of the glove box, and was stirred in an oil bath set at 130 °C for 16-20 h. After the reaction tube was cooled to room temperature, the tube was open to air, the solution was filtered through a short silica gel column by eluting with CH_2Cl_2 (10 mL), and the filtrate was analyzed by GC-MS method. Product yields were determined by NMR methods with hexamethylbenzene as the internal standard.

6.3.3.4 Deuterium Labeling Study

In a glove box, complex **2-10** (9 mg, 3 mol %), **2-12** (12 mg, 10 mol %), acetophenone-d_8 (64 mg, 0.5 mmol) and 4-methoxybenzylamine (96 mg, 0.7 mmol) were dissolved in 1,4-dioxane (2.0 mL) in a 25 mL Schlenk tube equipped with a Teflon screw cap stopcock and a stirring bar. The tube was brought out of the glove box, and stirred in an oil bath preset at 130 °C for 16 h. The reaction tube was taken out of the oil bath and was cooled to room temperature. After the tube was open to air, the solution was filtered through a short silica gel column by eluting with CH_2Cl_2 (10 mL), and the filtrate was analyzed by GC-MS. Analytically pure product was isolated by column chromatography on silica gel (230-460 mesh, hexanes/EtOAc = 80:1 to 10:1). The ^{1}H and ^{2}H NMR spectra of the product **2a**-*d* are shown in **Figure 3.2**.

6.3.3.5 Deuterium Isotope Effect Study

In a glove box, complex **2-10** (3 mg, 3 mol %), **2-12** (3 mg, 10 mol %), water (4 mg 2eq.) and (4-Methoxyphenyl)-*N*-(1-phenylethylidene)methanamine **3-13a** (24 mg, 0.2 mmol) were dissolved in toluene-d_8 (1 mL) in a 25 mL Schlenk tube equipped with a Teflon screw cap stopcock and a magnetic stirring bar. The resulting mixture was stirred for 5-10 min until the solid was completely dissolved and transferred into a J-Young NMR tube equipped with a Teflon screw cap stopcock. The tube was brought out of the glove box, and were immersed an oil bath set at 130 °C. The tube was taken out from the oil bath at 30 min time intervals, cooled in ice-water bath, and was analyzed by ^{1}H NMR. The reaction rate was measured by monitoring the appearance of the product signals on ^{1}H NMR, which was normalized against an internal standard peak (C_6Me_6). The k_{obs} was determined from a first-order plot of -ln[(**3-13a**$_0$) – (**3-13a**$_t$))/**3-13a**$_0$] vs time. Similar procedure was performed with the deuterated (4-Methoxyphenyl)-*N*-(1-phenylethylidene)methanamine-d_8. (**Figure 3.4**).

6.3.3.6 Hammett Study

In a glove box, complex **2-10** (21 mg, 3 mol %) and **2-12** (29 mg, 10 mol %) were dissolved in toluene-d_8 (1.5 mL) in a 25 mL Schlenk tube equipped with a Teflon screw cap stopcock and a magnetic stirring bar. The resulting mixture was stirred for 5-10 min until the solution was turned to a reddish green color. Acetophenone (144 mg, 1.2 mmol) was added to the reaction tube and was stirred for 5 min. The solution was divided into six equal portions, and *p*-X-$C_6H_4CH_2NH_2$ (0.30 mmol) (X = OMe, Me, H, F, Cl, CF_3)

was added to each solution. The resulting mixture was transferred into six different J-Young NMR tubes, each equipped with a Teflon screw cap stopcock. The tubes were brought out of the glove box, and were immersed an oil bath set at 130 °C. Each tube was taken out from the oil bath at 30 min time intervals, cooled in ice-water bath, and was analyzed by ^{1}H NMR. The reaction rate was measured by monitoring the appearance of the product signals on ^{1}H NMR, which was normalized against an internal standard peak (C_6Me_6). The k_{obs} was determined from a first-order plot of ln[([**3-10a**]$_i$-[**3-10a**]$_t$)/([**3-10a**]$_i$)$_0$] vs time. The Hammett plot of $\log(k_X/k_H)$ vs σ_p is shown in **Figure 3.5(a)** (ρ = -0.49 ± 0.1). The analogous procedure was used to obtain the Hammett correlation for ketones by using complex **2-10** (21 mg, 3 mol %)/**2-12** (29 mg, 10 mol %), 4-methoxybenzylamine (247 mg, 1.8 mmol) and *p*-Y-$C_6H_4COCH_3$ (0.2 mmol) (Y = OMe, Me, H, F, Cl, CF_3) in toluene-d_8 (1.5 mL). The Hammett plot of $\log(k_X/k_H)$ vs σ_p is shown in **Figure 3.5(b)** (ρ = +0.20 ± 0.1).

6.3.3.7 Carbon Isotope Effect Study

In a glove box, **2-10** (34 mg, 3 mol %) and **2-12** (48 mg, 10 mol %) were dissolved in 1,4-dioxane (2 mL) in a 25 mL Schlenk tube equipped with a Teflon screw cap stopcock and a magnetic stirring bar, and a resulting mixture was stirred for 5 to 10 min. Acetophenone (240 mg, 2.0 mmol), 4-methoxybenzylamine (384 mg, 2.8 mmol), and 1,4-dioxane (4 mL) were added to the reaction tube. After the tube was sealed, the tube was brought out of the box and was stirred in an oil bath at 130 °C for 20 h. The tube was cooled to room temperature and the solution was filtered through a small silica column and was eluted with CH_2Cl_2 (10 mL). The procedure was repeated for two more times, and the product conversion was determined by GC (92%, 89% and 90%

conversion). For low conversion samples, **2-10** (59 mg, 1 mol%) and **2-12** (96 mg, 4 mol %) were dissolved in 1,4-dioxane (8 mL) in a 100 mL Schlenk tube equipped with a Teflon screw cap stopcock and a magnetic stirring bar. Acetophenone (1.2 g, 10 mmol), 4-methoxybenzylamine (1.9 g, 14 mmol) and 1,4-dioxane (8 mL) were added to the reaction tube. The tube was brought out of the box and was stirred in an oil bath at 130 °C for 2 h. The procedure was repeated for two more times, and the product conversion was determined by GC (11%, 13% and 15% conversion). The product **3-10a** was isolated by a column chromatography on silica gel (hexanes/EtOAc) for the $^{13}C\{^{1}H\}$ NMR analysis.

The $^{13}C\{^{1}H\}$ NMR analysis was performed by following Singleton's ^{13}C NMR method[127]. The NMR sample was prepared identically by dissolving 3-(4-methoxyphenyl)-1-phenyl-1-propanone (**3-10a**) (280 mg) in $CDCl_3$ (0.5 mL) in a 5 mm high precision NMR tube. The $^{13}C\{^{1}H\}$ NMR spectra were recorded with H-decoupling and 45 degree pulses. A 60 s delay between pulses was imposed to minimize T_1 variations (d1 = 120 s, at = 5.0 s, np = 245098, nt = 512, dm = 'nny'). The data obtained were summarized in **Table 3.6**.

6.3.3.8 Determination of an Empirical Rate Law

In a glove box, **2-12** (19 mg, 10 mol %), water (29 mg, 2 eq.) and **3-13a** (191 mg, 0.8 mmol) were dissolved in toluene-d_8 (1.0 mL) in a 25 mL Schlenk tube equipped with a Teflon screw cap stopcock and a magnetic stirring bar. The resulting mixture was stirred for 5-10 min until the solution was turned to a reddish green color. The solution was divided into four equal portions, and each portion was transferred into four separate J-Young NMR tubes. A stock solution containing complex **2-10** (22 mg in 500 μL of toluene-d_8), were prepared and (52 μL, 4 mM), (78 μL, 8 mM), (105 μL, 12 mM), (131 μL, 20 mM) was added to the four different tubes respectively. The total volume of the reaction mixture was adjusted up to 500 μL by adding pure toluene-d_8 and each equipped with a Teflon screw cap stopcock. The tubes were brought out of the glove box, and were immersed an oil bath set at 130 °C. Each tube was taken out from the oil bath at 15 min time intervals, cooled in ice-water bath, and was analyzed by ^{1}H NMR. The reaction rate was measured by monitoring the appearance of the product signals on ^{1}H NMR, which was normalized against an internal standard peak (C_6Me_6). The initial rate of the reaction was determined from a first-order plot of **3-13a** vs time (**Figure 3.9(a), (b)**).

For Imine Dependence Study, complex **2-10** (14 mg, 3 mol %), **2-12** (19 mg, 10 mol %) and water (29 mg, 2eq.) in toluene-d_8 (1.0 mL) with **3-13a** (0.2, 0.4, 0.6 and 0.8 mM) was followed the same procedure. The initial rate of the reaction was determined from a first-order plot of **3-13a** vs time (**Figure 3.10 (a), (b)**).

For Water Dependence Study, complex **2-10** (14 mg, 3 mol %), **2-12** (19 mg, 10 mol %) and **3-13a** (191 mg, 0.8 mmol) in toluene-d_8 (1.0 mL) with water (0.4, 0.8, 1.0 and 1.2 mM) has been used by following above procedure (**Figure 3.11(a), (b)).**

6.3.3.9 Detection of Catalytically Relevant Organic Products

A 1,4-dioxane (2.0 mL) solution of complex **2-10** (9 mg, 3 mol %), **2-12** (12 mg, 10 mol %), 4,4,4-trifluoro-1-(2-naphthyl)-1,3-butanedione (133 mg, 0.5 mmol) and 3,4,5-trimethoxybenzylamine (99 mg, 0.5 mmol) was stirred at 130 °C for 16 h. The product **3-14** was isolated by column chromatography on silica gel (hexanes/EtOAc = 80:1–15:1; TLC: R_f = 0. (10% EtOAc in hexanes)). Yield = mg (92%). Compound **14** was completely characterized by both NMR and X-ray crystallographic techniques (**Eq. 3.13**). **3-15** and **3-16** compounds were obtained following standard procedure and completely characterized by both NMR and X-ray crystallographic techniques (**Eq. 3.14**, **Eq. 3.15**).

6.3.5 X-ray Crystallography Data for the Organic Products

6.3.5.1 X-ray Crystallography Data for 3-10at

Colorless plate like single crystals of **3-10at** were grown in pentanes/EtOAc at room temperature. A suitable crystal with the dimension of 0.36 × 0.305 × 0.043 mm^3 was selected and analyzed. Both symmetrically independent molecules have a planar extended conformation (with exception of bicyclic moiety). The molecules differ by orientation of the bicycle relative to the rest of the molecule – the dihedral angle C12-C13-C14-H is -56º in one of them and 45º and 174º in another one, which is disordered in a 2:1 population ratio. The compound seems to be enantiomerically pure; Flack parameter [0.2(2)]. The molecules form quasi-centrosymmetric dimers (which contributes into the uncertainty of Flack parameter), which are stacked along x axis. Also, the molecules form infinite chains along y axis through N-H…O hydrogen bonds. The aliphatic bicyclic moieties frame the resulting layers and form regions of lower order.

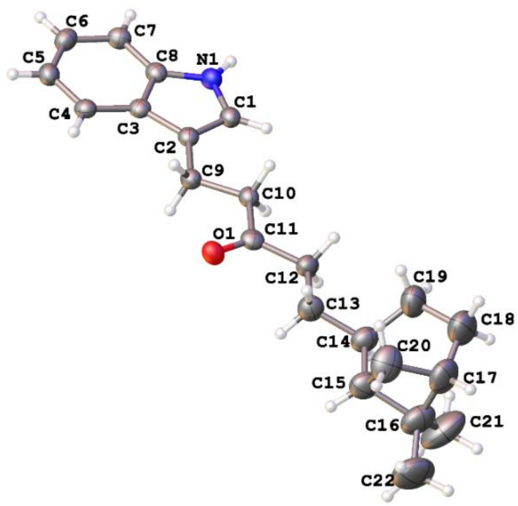

Figure 6.7: Molecular Structure of **3-10at**

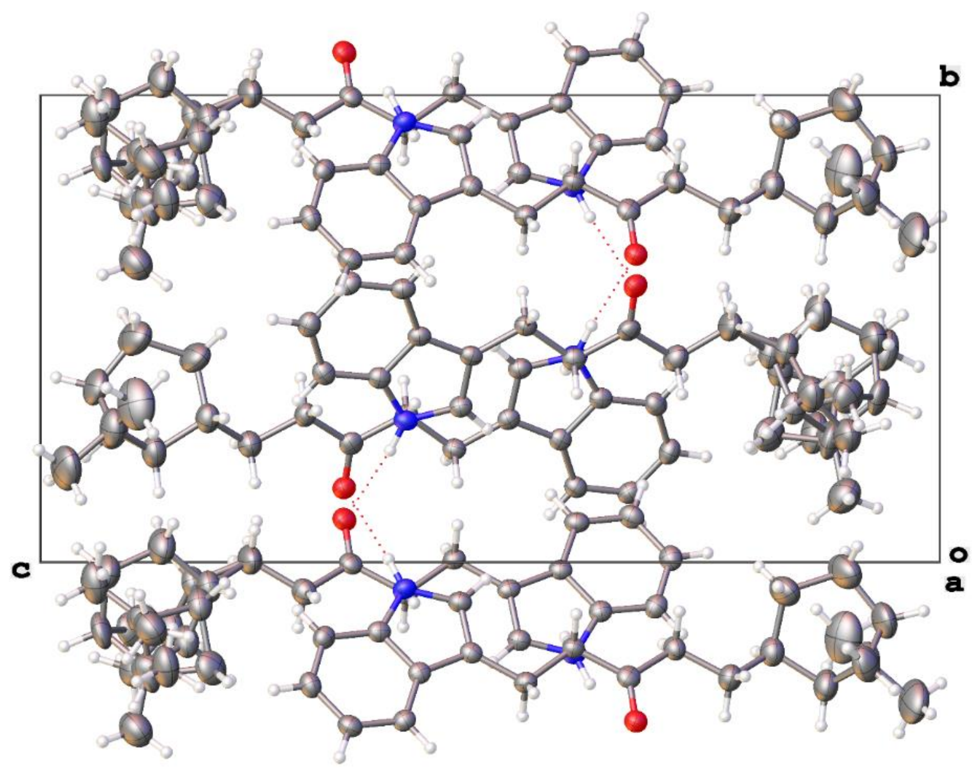

Figure 6.8: Crystal Packing of **3-10at**

Table 6.4: Crystal Data and Structure Refinement for **3-10at**

Identification code	yi4w
Empirical formula	$C_{22}H_{29}NO$

Formula weight	323.46
Temperature/K	100.00(14)
Crystal system	monoclinic
Space group	$P2_1$
a/Å	7.58070(12)
b/Å	11.25264(18)
c/Å	21.8958(5)
α/°	90
β/°	97.6552(19)
γ/°	90
Volume/Å^3	1851.13(6)
Z	4
ρ_{calc}g/cm^3	1.161
μ/mm^{-1}	0.535
F(000)	704.0
Crystal size/mm^3	0.36 × 0.305 × 0.043
Radiation	CuKα (λ = 1.54184)
2Θ range for data collection/°	8.148 to 141.094
Index ranges	$-9 \leq h \leq 7$, $-13 \leq k \leq 13$, $-26 \leq l \leq 25$
Reflections collected	15681
Independent reflections	6735 [R_{int} = 0.0327, R_{sigma} = 0.0337]
Data/restraints/parameters	6735/87/467
Goodness-of-fit on F^2	1.024
Final R indexes [I>=2σ (I)]	R_1 = 0.0527, wR_2 = 0.1420
Final R indexes [all data]	R_1 = 0.0599, wR_2 = 0.1509
Largest diff. peak/hole / e Å^{-3}	0.26/-0.21
Flack parameter	0.2(2)

6.3.5.2 X-ray Crystallography Data for 3-10ax

Colorless single crystals of **3-10ax** were grown in dichloromethane/*n*-pentane/EtOAc at room temperature. A suitable crystal with the dimension of 0.803 × 0.238 × 0.18 mm^3 was selected and analyzed. The molecule has an extended, almost planar conformation. Methoxy group and morpholine nitrogen are conjugated with the adjacent benzene rings. The morpholine group exhibits a multiple disorder, of which two components were identified. The main component (population ~70%) has a chair conformation.

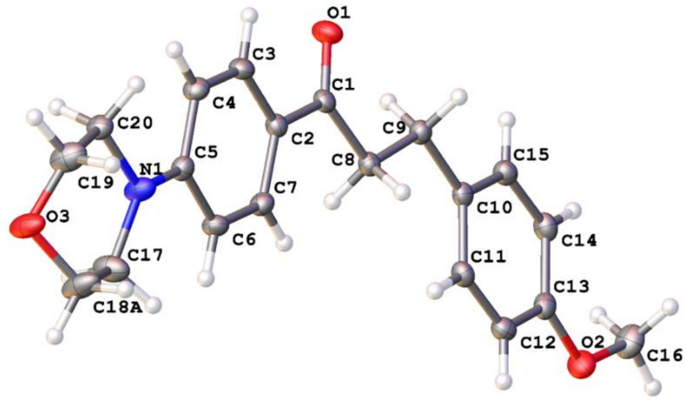

Figure 6.9: Molecular Structure of **3-10ax**

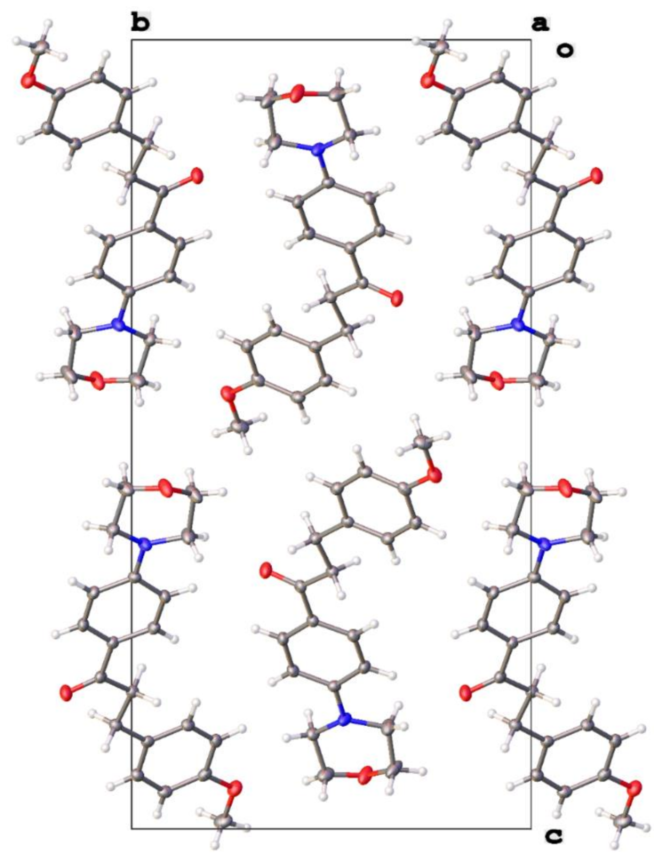

Figure 6.10: Crystal Packing of **3-10ax**; The Molecules form Translational Stacks along X Axis

Table 6.5: Crystal Data and Structure Refinement for **3-10ax**

Identification code	yi4t
Empirical formula	$C_{20}H_{23}NO_3$

Formula weight	325.39
Temperature/K	100.00(10)
Crystal system	monoclinic
Space group	$P2_1/n$
a/Å	5.16080(10)
b/Å	12.7726(4)
c/Å	25.3964(7)
α/°	90
β/°	93.866(2)
γ/°	90
Volume/$Å^3$	1670.24(8)
Z	4
ρ_{calc}g/cm^3	1.294
μ/mm^{-1}	0.087
F(000)	696.0
Crystal size/mm^3	0.803 × 0.238 × 0.18
Radiation	MoKα (λ = 0.71073)
2Θ range for data collection/°	6.58 to 59.448
Index ranges	$-7 \leq h \leq 7$, $-16 \leq k \leq 17$, $-35 \leq l \leq 34$
Reflections collected	19263
Independent reflections	4342 [R_{int} = 0.0321, R_{sigma} = 0.0337]
Data/restraints/parameters	4342/0/230
Goodness-of-fit on F^2	1.031
Final R indexes [I>=2σ (I)]	R_1 = 0.0513, wR_2 = 0.1156
Final R indexes [all data]	R_1 = 0.0746, wR_2 = 0.1295
Largest diff. peak/hole / e $Å^{-3}$	0.35/-0.33

6.3.5.3 X-ray Crystallography Data for 3-14

Colorless prisms like single crystals of **3-14** were grown in pentanes/EtOAc at room temperature. A suitable crystal with the dimension of 0.36 × 0.213 × 0.065 mm^3 was selected analyzed. The central moiety of the molecule has a π-conjugated planar structure enhanced by an intra-molecular H-bond N-H…O. The bond lengths C2-C1 [1.404(2) Å] and C2-C3 [1.391(2) Å] are practically equilibrated. The naphthyl and trimethoxybenzyl groups are rotated out of this plane to avoid steric hindrances. In the trimethoxybenzyl group, the central methoxy group is rotated by 73° out of conjugation because of this too.

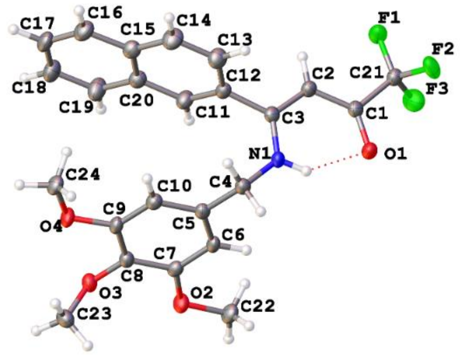

Figure 6.11: Molecular Structure of **3-14**

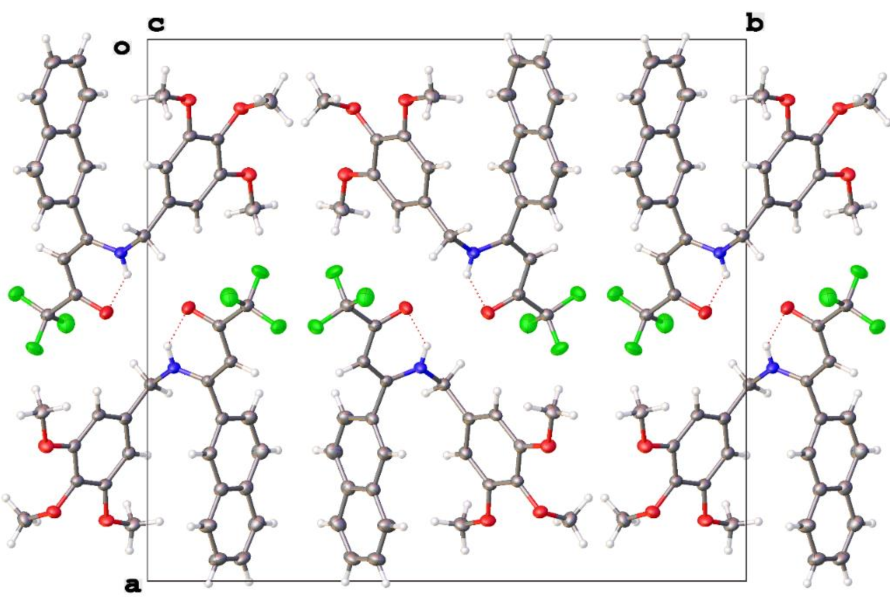

Figure 6.12: Crystal Packing of **3-14**

Table 6.6: Crystal Data and Structure Refinement for **3-14**

Identification code	yi4u
Empirical formula	$C_{24}H_{22}NO_4F_3$
Formula weight	445.42
Temperature/K	100(1)
Crystal system	monoclinic
Space group	$P2_1/c$

a/Å	18.7249(3)
b/Å	20.5703(4)
c/Å	5.47146(10)
α/°	90
β/°	96.3997(18)
γ/°	90
Volume/Å^3	2094.35(7)
Z	4
ρ_{calc}g/cm^3	1.413
μ/mm^{-1}	0.965
F(000)	928.0
Crystal size/mm^3	0.36 × 0.213 × 0.065
Radiation	CuKα (λ = 1.54184)
2Θ range for data collection/°	8.598 to 140.992
Index ranges	-21 ≤ h ≤ 22, -24 ≤ k ≤ 24, -6 ≤ l ≤ 6
Reflections collected	19580
Independent reflections	3961 [R_{int} = 0.0301, R_{sigma} = 0.0197]
Data/restraints/parameters	3961/0/296
Goodness-of-fit on F^2	1.037
Final R indexes [I>=2σ (I)]	R_1 = 0.0366, wR_2 = 0.0941
Final R indexes [all data]	R_1 = 0.0433, wR_2 = 0.0995
Largest diff. peak/hole / e Å^{-3}	0.30/-0.22

6.3.5.4 X-ray Crystallography Data for 3-15

Colorless needles like single crystals of **3-15** were grown in pentanes/EtOAc at room temperature. A suitable crystal with the dimension of 0.35 × 0.07 × 0.03 mm^3 was selected and analyzed. The structure contains four symmetrically independent molecules having a similar non-propeller conformation – the benzene rings adjacent to pyridine N-atom are rotated in opposite directions for all 4 molecules. In one of the molecules an anisyl group is disordered (180° rotation of OMe group with a corresponding parallel shift of the adjacent benzene ring).

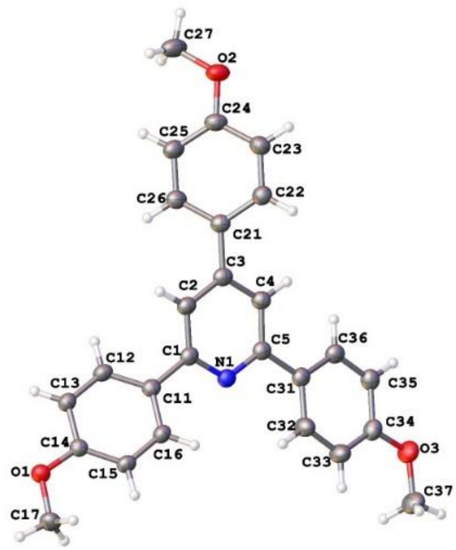

Figure 6.13: Molecular Structure of **3-15**

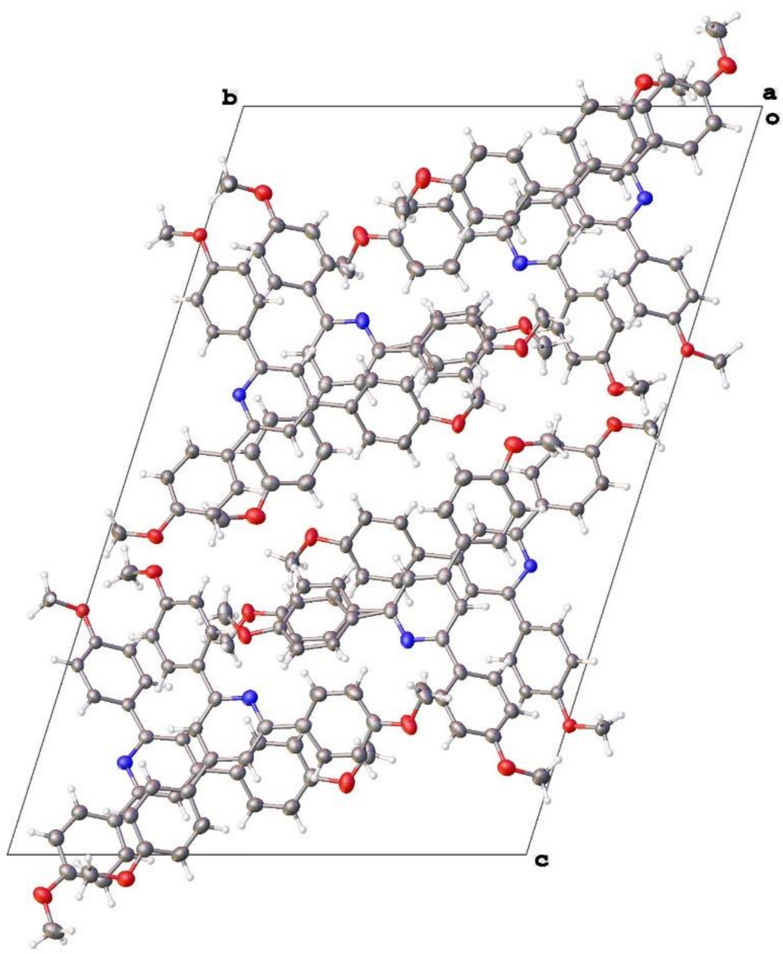

Figure 6.14: Crystal Packing of **3-15**

Table 6.7: Crystal Data and Structure Refinement for **3-15**

Identification code	yi3l
Empirical formula	$C_{26}H_{23}NO_3$
Formula weight	397.45
Temperature/K	100.15
Crystal system	triclinic
Space group	P-1
a/Å	7.42330(15)
b/Å	19.9021(4)
c/Å	29.7033(6)
α/°	72.3729(19)
β/°	87.8182(17)
γ/°	80.2040(17)
Volume/Å^3	4120.88(15)
Z	8
ρ_{calc}g/cm^3	1.281
μ/mm^{-1}	0.667
F(000)	1680.0
Crystal size/mm^3	0.35 × 0.07 × 0.03
Radiation	CuKα (λ = 1.54184)
2Θ range for data collection/°	8.9 to 141.88
Index ranges	$-9 \leq h \leq 8$, $-24 \leq k \leq 24$, $-36 \leq l \leq 36$
Reflections collected	74732
Independent reflections	15636 [R_{int} = 0.0498, R_{sigma} = 0.0326]
Data/restraints/parameters	15636/17/1161
Goodness-of-fit on F^2	1.026
Final R indexes [I>=2σ (I)]	R_1 = 0.0471, wR_2 = 0.1191
Final R indexes [all data]	R_1 = 0.0589, wR_2 = 0.1291
Largest diff. peak/hole / e Å^{-3}	0.27/-0.29

6.3.5.5 X-ray Crystallography Data for 3-16

Colorless plates like single crystals of **3-15** were grown in pentanes/EtOAc at room temperature. A suitable crystal with the dimension of 0.32 × 0.226 × 0.045 mm^3 was selected and analyzed. The molecule has a twisted shape (pseudo-torsion angle Br-C…C-Br is 26°). The thiophene moiety is rotationally disordered by 30%. The crystal structure is unremarkable. No stacking interactions found.

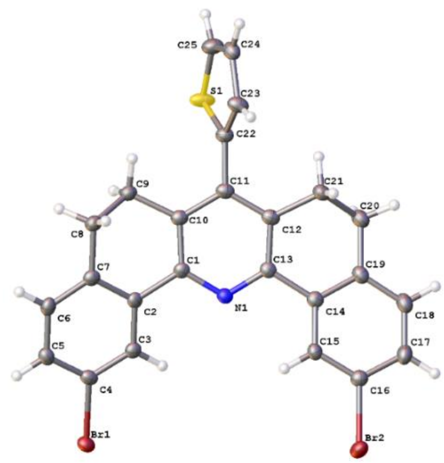

Figure 6.15: Molecular Structure of **3-16**

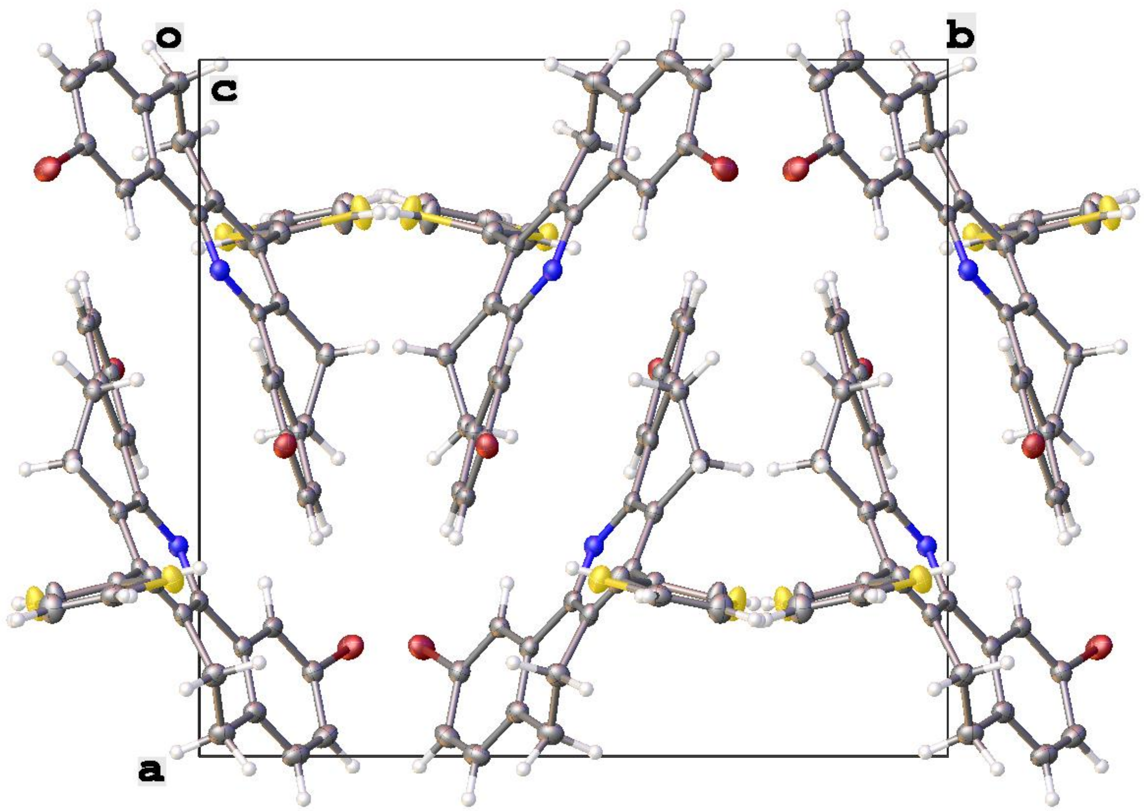

Figure 6.16: Crystal Packing of **3-16**

Table 6.8: Crystal Data and Structure Refinement for **3-16**

Identification code	yi5d

Empirical formula	$C_{25}H_{17}Br_2NS$
Formula weight	523.28
Temperature/K	100.00(10)
Crystal system	monoclinic
Space group	$P2_1/c$
a/Å	14.4965(3)
b/Å	14.9626(3)
c/Å	9.7254(2)
α/°	90
β/°	106.201(2)
γ/°	90
Volume/Å^3	2025.72(7)
Z	4
ρ_{calc}g/cm^3	1.716
μ/mm^{-1}	6.122
F(000)	1040.0
Crystal size/mm^3	0.32 × 0.226 × 0.045
Radiation	Cu Kα (λ = 1.54184)
2Θ range for data collection/°	8.676 to 141.036
Index ranges	$-17 \le h \le 17$, $-17 \le k \le 17$, $-11 \le l \le 11$
Reflections collected	18855
Independent reflections	3826 [R_{int} = 0.0377, R_{sigma} = 0.0235]
Data/restraints/parameters	3826/2/269
Goodness-of-fit on F^2	1.030
Final R indexes [I>=2σ (I)]	R_1 = 0.0255, wR_2 = 0.0654
Final R indexes [all data]	R_1 = 0.0293, wR_2 = 0.0675
Largest diff. peak/hole / e Å^{-3}	0.41/-0.42

6.3.6.1 Characterization Data of Organic Compounds Listed in Table 3.3

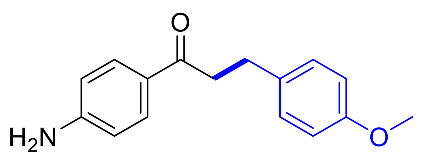

3-10f

1-(4-Aminophenyl)-3-(4-methoxyphenyl)propan-1-one (3-10f): A 1,4-dioxane (2.0 mL) solution of complex **2-10** (9 mg, 3 mol %), **2-12** (12 mg, 10 mol %), 4-acetylaniline (68 mg, 0.5 mmol) and 4-methoxybenzylamine (96 mg, 0.7 mmol) was stirred at 130 °C for 16 h. The product **3-10f** was isolated by column chromatography on silica gel (hexanes/EtOAc = 120:1–20:1; TLC: R_f = 0.4 (50% EtOAc in hexanes)). Yield = 84 mg (66%). Data for **3-10f:** ^{1}H NMR

(400 MHz, $CDCl_3$) δ 7.68 (d, *J* = 8.8 Hz, 2H), 7.15 (d, *J* = 8.7 Hz, 2H), 6.81 (d, *J* = 8.7 Hz, 2H), 6.56 (d, *J* = 8.8 Hz, 2H), 3.69 (s, 3H), 3.11–3.04 (m, 2H), 2.81 (t, *J* = 7.5 Hz, 2H) ppm; $^{13}C\{^1H\}$ NMR (100 MHz, DMSO) δ 196.7, 157.6, 153.5, 133.6, 130.5, 129.5, 124.8, 113.8, 112.9, 55.1, 29.4, 26.0 ppm; GC-MS for $C_{16}H_{17}NO_2$, m/z = 255 (M^+). HRMS (ESI-TOF) m/z: $[M + H]^+$ Calcd for $C_{16}H_{17}NO_2H$ 256.1332; Found 256.1302.

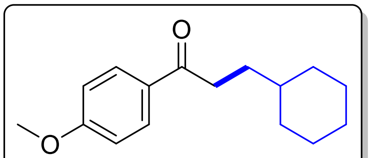

3-10l

3-Cyclohexyl-1-(4-methoxyphenyl)propan-1-one (3-10l): A 1,4-dioxane (2.0 mL) solution of complex **2-10** (9 mg, 3 mol %), **2-12** (12 mg, 10 mol %), 4′-methoxyacetophenone (75 mg, 0.5 mmol) and cyclohexylmethanamine (79 mg, 0.7 mmol) was stirred at 130 °C for 16 h. The product **3-10l** was isolated by column chromatography on silica gel (hexanes/EtOAc = 120:1–20:1; TLC: R_f = 0.6 (10% EtOAc in hexanes)). Yield = 94 mg (76%). Data for **3-10l:** ^1H NMR (400 MHz, $CDCl_3$) δ 7.93 (d, *J* = 8.9 Hz, 2H), 6.91 (d, *J* = 8.9 Hz, 2H), 3.83 (s, 3H), 2.97–2.85 (m, 2H), 1.79–1.56 (m, 7H), 1.32–1.09 (m, 4H), 0.99–0.85 (m, 2H) ppm; $^{13}C\{^1H\}$ NMR (100 MHz, $CDCl_3$) δ 199.4, 163.2, 130.2, 130.1, 113.6, 55.4, 37.4, 35.8, 33.1, 32.0, 26.5, 26.2 ppm; GC-MS for $C_{16}H_{22}O_2$, m/z = 246 (M^+). HRMS (ESI-TOF) m/z: $[M + H]^+$ Calcd for $C_{16}H_{22}O_2H$ 247.1693; Found 247.1663.

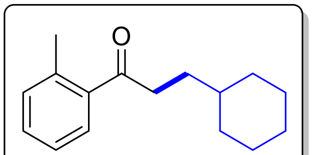

3-10n

3-Cyclohexyl-1-o-tolylpropan-1-one (3-10n). A 1,4-dioxane (2.0 mL) solution of complex **2-10** (9 mg, 3 mol %), **2-12** (12 mg, 10 mol %), 2′-methylacetophenone (75 mg, 0.5 mmol) and cyclohexylmethanamine (79 mg, 0.7 mmol) was stirred at 130 °C for 16 h. The product **3-10n** was isolated by column chromatography on silica gel (hexanes/EtOAc = 120:1–20:1; TLC: R_f = 0.8 (10% EtOAc in hexanes)). Yield = 101 mg

(88%). Data for **3-10n:** ^{1}H NMR (400 MHz, $CDCl_3$) δ 7.61 (d, J = 7.8 Hz, 1H), 7.38–7.32 (m, 1H), 7.26–7.22 (m, 2H), 2.89 (t, J = 7.7 Hz, 2H), 2.48 (s, 3H), 1.75–1.67 (m, 4H), 1.62–1.56 (m, 2H), 1.33–1.09 (m, 5H), 0.97–0.87 (m, 2H) ppm; ^{13}C{^{1}H} NMR (100 MHz, $CDCl_3$) δ 205.2, 138.3, 137.7, 131.8, 130.9, 128.2, 125.5, 39.2, 37.3, 33.1, 31.7, 26.5, 26.2, 21.2 ppm; GC-MS for $C_{16}H_{22}O$, m/z = 230 (M^+). HRMS (ESI-TOF) m/z: $[M + H]^+$ Calcd for $C_{16}H_{22}OH$ 231.1743; Found 231.1736.

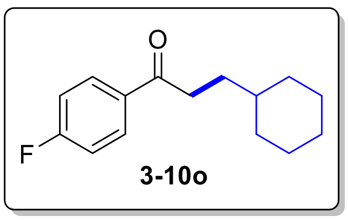

3-Cyclohexyl-1-o-tolylpropan-1-one (3-10o). A 1,4-dioxane (2.0 mL) solution of complex **2-10** (9 mg, 3 mol %), **2-12** (12 mg, 10 mol %), 2′-methoxyacetophenone (75 mg, 0.5 mmol) and cyclohexylmethanamine (79 mg, 0.7 mmol) was stirred at 130 °C for 16 h. The product **3-10o** was isolated by column chromatography on silica gel (hexanes/EtOAc = 120:1–20:1; TLC: R_f = 0.6 (10% EtOAc in hexanes)). Yield = 105 mg (90%). Data for **3-10o:** ^{1}H NMR (400 MHz, $CDCl_3$) δ 7.98 (dd, J = 8.6, 5.6 Hz, 2H), 7.14–7.07 (m, 2H), 2.93 (t, J = 7.7 Hz, 2H), 1.78–1.57 (m, 7H), 1.30–1.08 (m, 4H), 1.01–0.86 (m, 2H) ppm; ^{13}C{^{1}H} NMR (100 MHz, $CDCl_3$) δ 199.2, 165.6 (d, J_{CF} = 254.2 Hz), 133.4 (d, J_{CF} = 3.0 Hz), 130.6 (d, J_{CF} = 9.3 Hz), 115.5 (d, J_{CF} = 21.8 Hz), 37.3, 36.0, 33.1, 31.7, 26.5, 26.2 ppm; GC-MS for $C_{15}H_{19}FO$, m/z = 234 (M^+).

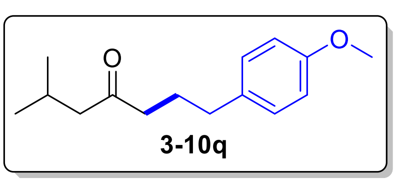

1-(4-Methoxyphenyl)-6-methylheptan-4-one (3-10q): A 1,4-dioxane (2.0 mL) solution of complex **2-10** (9 mg, 3 mol %), **2-12** (12 mg, 10 mol %), 4-methyl-2-pentanone (50 mg, 0.5 mmol) and 4-methoxybenzeneethanamine (106 mg, 0.7 mmol) was stirred at 130 °C for 16 h. The product **3-10q** was isolated by column chromatography on silica gel (hexanes/EtOAc = 120:1–20:1; TLC: R_f = 0.5 (10% EtOAc in hexanes). Yield = 93 mg (79%). Data for **3-10q:** ^{1}H NMR (400 MHz, $CDCl_3$) δ 7.08 (d, *J* = 8.6 Hz, 2H), 6.83 (d, *J* = 8.6 Hz, 2H), 3.79 (s, 3H), 2.55 (t, *J* = 7.5 Hz, 2H), 2.37 (t, *J* = 7.4 Hz, 2H), 2.25 (d, *J* = 6.7 Hz, 2H), 2.16–2.07 (m, 1H), 1.86 (pentet, *J* = 7.5 Hz, 2H), 0.89 (d, *J* = 6.7 Hz, 6H) ppm; ^{13}C{^{1}H} NMR (100 MHz, $CDCl_3$) δ 210.8, 157.8, 133.7, 129.3, 113.7, 55.2, 51.9, 42.4, 34.2, 25.4, 24.5, 22.6 ppm; GC-MS for $C_{15}H_{22}O_2$, m/z = 234 (M^+). HRMS (ESI-QTOF) m/z: $[M + Na]^+$ Calcd for $C_{15}H_{22}O_2H$ 257.1512; Found 257.1512.

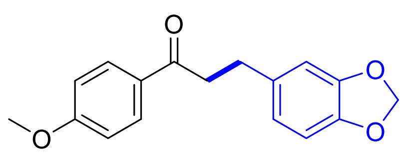

3-10t

3-(benzo[d][1,3]dioxol-5-yl)-1-(4-methoxyphenyl)propan-1-one (3-10t): A 1,4-dioxane (2.0 mL) solution of complex **2-10** (9 mg, 3 mol %), **2-12** (12 mg, 10 mol %), 4′-methoxyacetophenone (75 mg, 0.5 mmol) and 1,3-benzodioxol-5-ylmethylamine (106 mg, 0.7 mmol) was stirred at 130 °C for 16 h. The product **3-10t** was isolated by column chromatography on silica gel (hexanes/EtOAc = 120:1–20:1; TLC: R_f = 0.4 (10% EtOAc in hexanes)). Yield = 94 mg (66%). Data for **3-10t:** ^{1}H NMR (400 MHz, $CDCl_3$) δ 7.93 (d, *J* = 9.0 Hz, 2H), 6.92 (d, *J* = 9.0 Hz, 2H), 6.75–6.71 (m, 2H), 6.71–6.66 (m, 1H), 5.90 (s, 2H), 3.85 (s, 3H), 3.22–3.16 (m, 2H), 3.00–2.93 (m, 2H) ppm; ^{13}C{^{1}H} NMR (100 MHz, $CDCl_3$) δ 197.7, 163.4, 147.5, 145.7, 135.2, 130.2, 129.8, 121.1, 113.6, 108.8, 108.2, 100.7, 55.4, 40.2, 30.0 ppm; GC-MS for $C_{17}H_{16}O_4$, m/z = 284 (M^+). HRMS (ESI-TOF) m/z: $[M + H]^+$ Calcd for $C_{17}H_{16}O_4H$ 285.1121; Found 285.1090.

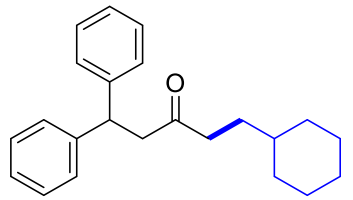

3-10u

5-Cyclohexyl-1,1-diphenylpentan-3-one (3-10u). A 1,4-dioxane (2.0 mL) solution of complex **2-10** (9 mg, 3 mol %), **2-12** (12 mg, 10 mol %), 4,4-diphenyl-2-butanone (112 mg, 0.5 mmol) and cyclohexylmethanamine (79 mg, 0.7 mmol) was stirred at 130 °C for 16 h. The product **3-10u** was isolated by column chromatography on silica gel (hexanes/EtOAc = 120:1–20:1; TLC: R_f = 0.8 (10% EtOAc in hexanes)). Yield = 150 mg (94%). Data for **3-10u:** ^{1}H NMR (400 MHz, $CDCl_3$) δ 7.48–7.01 (m, 10H), 4.64 (t, *J* = 7.6 Hz, 1H), 3.18 (d, *J* = 7.6 Hz, 2H), 2.39–2.31 (m, 2H), 1.71–1.57 (m, 5H), 1.42–1.35 (m, 2H), 1.22–1.03 (m, 4H), 0.88–0.76 (m, 2H) ppm; ^{13}C{^{1}H} NMR (100 MHz, $CDCl_3$) δ 209.2, 143.8, 128.4, 127.6, 126.2, 48.5, 45.9, 40.9, 36.8, 32.9, 30.6, 26.4, 26.1 ppm; GC-MS for $C_{23}H_{28}O$, m/z = 320 (M^+). HRMS (ESI-TOF) m/z: $[M + H]^+$ Calcd for $C_{23}H_{28}OH$ 321.2213; Found 321.2207.

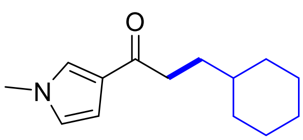

3-10v

3-Cyclohexyl-1-(1-methyl-1*H*-pyrrol-3-yl)propan-1-one (3-10v): A 1,4-dioxane (2.0 mL) solution of complex **2-10** (9 mg, 3 mol %), **2-12** (12 mg, 10 mol %), 3-Acetyl-1-methylpyrrole (62 mg, 0.5 mmol) and cyclohexylmethanamine (79 mg, 0.7 mmol) was stirred at 130 °C for 16 h. The product **3-10v** was isolated by column chromatography on silica gel (hexanes/EtOAc = 120:1–20:1; TLC: R_f = 0.3 (10% EtOAc in hexanes)). Yield = 98 mg (89%). Data for **3-10v:** ^{1}H NMR (400 MHz, $CDCl_3$) δ 7.21 (t, *J* = 1.9 Hz, 1H), 6.55 (d, *J* = 1.9 Hz, 2H), 3.67 (s, 3H), 2.72–2.66 (m, 2H), 1.77–1.63 (m, 5H), 1.59–1.54 (m, 2H), 1.27–1.10 (m, 4H), 0.95–0.86 (m, 2H) ppm; ^{13}C{^{1}H} NMR (100 MHz, $CDCl_3$) δ 196.5, 126.3, 125.7, 123.1, 109.3, 37.5, 37.1, 36.5, 33.1, 32.5, 30.9, 26.5, 26.2 ppm; GC-MS for $C_{14}H_{21}NO$, m/z = 219 (M^+). HRMS (ESI-TOF) m/z: $[M + H]^+$ Calcd for $C_{14}H_{21}NOH$ 220.1696; Found 220.1698.

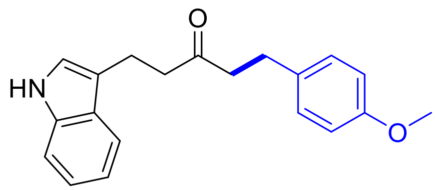

3-10w

1-(1*H*-Indol-3-yl)-5-(4-methoxyphenyl)pentan-3-one (3-10w): A 1,4-dioxane (2.0 mL) solution of complex **2-10** (9 mg, 3 mol %), **2-12** (12 mg, 10 mol %), 4-(1*H*-indol-3-yl)butan-2-one (94 mg, 0.5 mmol) and 4-methoxybenzylamine (96 mg, 0.7 mmol)was stirred at 130 °C for 16 h. The product **3-10w** was isolated by column chromatography on silica gel (hexanes/EtOAc = 120:1–20:1; TLC: R_f = 0.2 (10% EtOAc in hexanes)). Yield = 108 mg (70%). Data for **3-10w:** ^{1}H NMR (400 MHz, $CDCl_3$) δ 8.06 (brs, 1H), 7.59 (dd, *J* = 7.9, 0.6 Hz, 1H), 7.38–7.32 (m, 1H), 7.24–7.19 (m, 1H), 7.17–7.12 (m, 1H), 7.08 (d, *J* = 8.7 Hz, 2H), 6.93 (d, *J* = 2.2 Hz, 1H), 6.83 (d, *J* = 8.7 Hz, 2H), 3.80 (s, 3H), 3.10–3.02 (m, 2H), 2.90–2.76 (m, 4H), 2.70 (t, *J* = 7.6 Hz, 2H) ppm; $^{13}C\{^1H\}$ NMR (100 MHz, $CDCl_3$) δ 210.2, 157.8, 136.2, 133.0, 129.2, 127.0, 121.9, 121.5, 119.2, 118.6, 115.0, 113.8, 111.1, 55.2, 44.6, 43.4, 28.8, 19.2 ppm; GC-MS for $C_{20}H_{21}NO_2$, m/z = 307 (M^+). HRMS (ESI-TOF) m/z: $[M + H]^+$ Calcd for $C_{20}H_{21}NO_2H$ 308.1645; Found 308.1639.

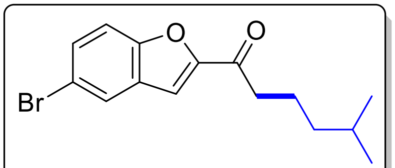

3-10x

1-(5-Bromobenzofuran-2-yl)-5-methylhexan-1-one (3-10x): A 1,4-dioxane (2.0 mL) solution of complex **2-10** (9 mg, 3 mol %), **2-12** (12 mg, 10 mol %), 1-(5-bromo-1-benzofuran-2-yl)ethan-1-one (119 mg, 0.5 mmol) and isoamylamine (61 mg, 0.7 mmol) was stirred at 130 °C for 16 h. The product **3-10x** was isolated by column chromatography on silica gel (hexanes/EtOAc = 120:1–

20:1; TLC: R_f = 0.8 (10% EtOAc in hexanes)). Yield = 103 mg (67%). Data for **3-10x:** ^{1}H NMR (400 MHz, $CDCl_3$) 7.83 (d, *J* = 1.9 Hz, 1H), 7.55 (dd, *J* = 8.9, 1.9 Hz, 1H), 7.45 (d, *J* = 8.9 Hz, 1H), 7.41 (s, 1H), 2.92 (t, *J* = 7.5 Hz, 2H), 1.80–1.72 (m, 2H), 1.59 (septet, *J* = 6.6 Hz, 1H), 1.30–1.24 (m, 2H), 0.90 (d, *J* = 6.6 Hz, 6H) ppm; $^{13}C\{^{1}H\}$ NMR (100 MHz, $CDCl_3$) δ 191.4, 154.1, 153.6, 131.0, 128.9, 125.7, 116.9, 113.9, 111.3, 39.2, 38.4, 30.9, 27.8, 22.5 ppm; GC-MS for $C_{15}H_{17}BrO_2$, m/z = 309 (M^+); HRMS (ESI-QTOF) m/z: $[M + H]^+$ Calcd for $C_{15}H_{17}BrO_2H$ 309.0485; Found 309.0476.

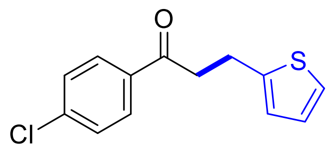

3-10y

1-(4-Chlorophenyl)-3-(thiophen-2-yl)propan-1-one (3-10y): A 1,4-dioxane (2.0 mL) solution of complex **2-10** (9 mg, 3 mol %), **2-12** (12 mg, 10 mol %), 4′-chloroacetophenone (77 mg, 0.5 mmol) and 2-thiophenemethylamine (79 mg, 0.7 mmol) was stirred at 130 °C for 16 h. The product **3-10y** was isolated by column chromatography on silica gel (hexanes/EtOAc = 120:1–20:1; TLC: R_f = 0.8 (10% EtOAc in hexanes)). Yield = 101 mg (81%). Data for **3-10y:** ^{1}H NMR (400 MHz, $CDCl_3$) δ 7.94–7.87 (m, 2H), 7.46–7.40 (m, 2H), 7.16–7.10 (m, 1H), 6.95–6.90 (m, 1H), 6.88–6.83 (m, 1H), 3.35–3.26 (m, 4H) ppm; $^{13}C\{^{1}H\}$ NMR (100 MHz, $CDCl_3$) δ 197.3, 143.5, 139.6, 134.9, 129.4, 128.9, 126.8, 124.7, 123.4, 40.5, 24.1 ppm; GC-MS for $C_{13}H_{11}ClOS$, m/z = 250 (M^+). HRMS (ESI-TOF) m/z: $[M + H]^+$ Calcd for $C_{13}H_{11}ClOSH$ 251.0292; Found 251.0262.

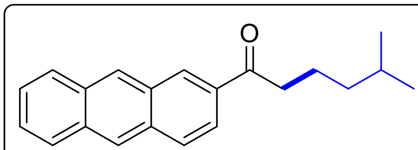

3-10aa

1-(Anthracen-2-yl)-6-methylheptan-1-one (3-10aa): A 1,4-dioxane (2.0 mL) solution of complex **2-10** (9 mg, 3 mol %), **2-12** (12 mg, 10 mol %), 2-acetylanthracene (110 mg, 0.5 mmol) and isoamylamine (61 mg, 0.7 mmol) was stirred at 130 °C for 16 h. The product **3-10aa** was isolated by column chromatography on silica gel (hexanes/EtOAc = 120:1–20:1; TLC: R_f = 0.7 (10% EtOAc in hexanes)). Yield = 132 mg (91%). Data for **3-10aa:** ^{1}H NMR (400 MHz, $CDCl_3$) δ 8.57 (s, 1H), 8.48 (s, 1H), 8.34 (s, 1H), 8.11–7.88 (m, 4H), 7.56–7.45 (m, 2H), 3.06 (t, J = 7.5 Hz, 2H), 1.89–1.77 (m, 2H), 1.66 (septet, J = 6.6 Hz, 1H), 1.40–1.27 (m, 2H), 0.96 (d, J = 6.6 Hz, 6H) ppm; $^{13}C\{^1H\}$ NMR (100 MHz, $CDCl_3$) δ 200.2, 133.7, 133.0, 132.5, 131.8, 130.8, 130.3, 128.8, 128.5, 128.3, 128.1, 126.5, 126.0, 125.8, 122.7, 38.6, 38.6, 27.9, 22.5, 22.3 ppm; GC-MS for $C_{21}H_{22}O$, m/z = 290 (M^+). HRMS (ESI-QTOF) m/z: $[M + H]^+$ Calcd for $C_{21}H_{22}OH$ 291.1743; Found 291.1734.

6.3.6.2 Characterization Data of the Compounds Listed in Table 3.4

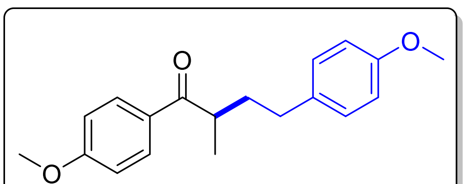
3-10ab

1,4-Bis(4-methoxyphenyl)-2-methylbutan-1-one (3-10ab): A 1,4-dioxane (2.0 mL) solution of complex **2-10** (9 mg, 3 mol %), **2-12** (12 mg, 10 mol %), 4′-methoxypropiophenone (82 mg, 0.5 mmol) and 4-methoxybenzeneethanamine (106 mg, 0.7 mmol) was stirred at 130 °C for 16 h. The product **3-10ab** was isolated by column chromatography on silica gel (hexanes/EtOAc = 120:1–20:1; TLC: R_f = 0.3 (10% EtOAc in hexanes)). Yield = 125 mg (84%). Data for **3-10ab:** 7.86 (d, J = 9.0 Hz, 2H), 7.06 (d, J = 8.8 Hz, 2H), 6.91 (d, J = 9.0 Hz, 2H), 6.81 (d, J = 8.8 Hz, 2H), 3.87 (s, 3H), 3.79 (s, 3H), 3.41 (sextet, J = 6.8 Hz, 1H), 2.63–2.51 (m, 2H), 2.17–2.08 (m, 1H), 1.74–1.65 (m, 1H), 1.21 (d, J = 6.8 Hz, 3H) ppm; $^{13}C\{^1H\}$ NMR (100 MHz, $CDCl_3$) δ 202.7, 163.3, 157.8, 133.9, 130.5, 129.5, 129.4, 113.7, 113.7, 55.4, 55.3, 39.2, 35.6, 32.6, 17.5 ppm; GC-MS for $C_{19}H_{22}O_3$, m/z =

298 (M^+). HRMS (ESI-TOF) m/z: $[M + H]^+$ Calcd for $C_{19}H_{22}O_3H$ 299.1642; Found 299.1631.

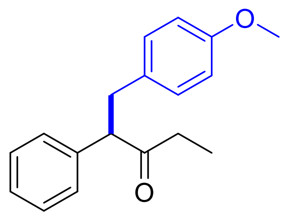

3-10ad

1-(4-Methoxyphenyl)-2-phenylpentan-3-one (3-10ad): A 1,4-dioxane (2.0 mL) solution of complex **2-10** (9 mg, 3 mol %), **2-12** (12 mg, 10 mol %), 1-phenyl-2-butanone (74 mg, 0.5 mmol) and 4-methoxybenzylamine (96 mg, 0.7 mmol) was stirred at 130 °C for 16 h. The product **3-10ad** was isolated by column chromatography on silica gel (hexanes/EtOAc = 120:1–20:1; TLC: R_f = 0.7 (10% EtOAc in hexanes)). Yield = 95 mg (71%). Data for **3-10ad:** ^{1}H NMR (400 MHz, $CDCl_3$) δ 7.30–7.21 (m, 3H), 7.19–7.14 (m, 2H), 6.94 (d, J = 8.1 Hz, 2H), 6.72 (d, J = 8.1 Hz, 2H), 3.87 (t, J = 7.4 Hz, 1H), 3.73 (s, 3H), 3.34 (dd, J = 13.9, 7.9 Hz, 1H), 2.83 (dd, J = 13.9, 6.9 Hz, 1H), 2.42–2.32 (m, 1H), 2.25–2.15 (m, 1H), 0.88 (t, J = 7.3 Hz, 3H) ppm; $^{13}C\{^1H\}$ NMR (100 MHz, $CDCl_3$) δ 210.6, 157.8, 138.8, 131.8, 129.9, 128.8, 128.3, 127.2, 113.6, 60.8, 55.2, 37.9, 35.7, 7.7 ppm; GC-MS for $C_{18}H_{20}O_2$, m/z = 268 (M^+). HRMS (ESI-QTOF) m/z: $[M + Na]^+$ Calcd for $C_{18}H_{20}O_2H$ 291.1356; Found 291.1346.

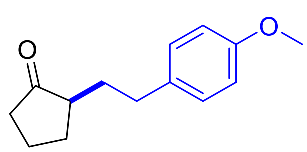

3-10af

2-(4-Methoxyphenethyl)cyclopentanone (3-10af): A 1,4-dioxane (2.0 mL) solution of complex **2-10** (9 mg, 3 mol %), **2-12** (12 mg, 10 mol %), cyclopentanone (42 mg, 0.5 mmol) and 4-methoxybenzeneethanamine (106 mg, 0.7 mmol) was stirred at 130 °C for 16 h. The product **3-10af** was isolated by column chromatography on silica gel (hexanes/EtOAc = 120:1–20:1; TLC: R_f = 0.5 (10% EtOAc in hexanes)). Yield = 93 mg (85%). Data for **3-10af:** ^{1}H NMR (400 MHz, $CDCl_3$) δ 7.11 (d, J = 8.7 Hz, 2H), 6.82 (d, J = 8.7 Hz, 2H), 3.78 (s, 3H), 2.71–2.55 (m, 2H), 2.33–2.19

(m, 2H), 2.16–1.97 (m, 4H), 1.81–1.71 (m, 1H), 1.59–1.47 (m, 2H) ppm; $^{13}C\{^{1}H\}$ NMR (100 MHz, $CDCl_3$) δ 221.4, 157.8, 133.6, 129.3, 113.7, 55.2, 48.3, 38.2, 32.6, 31.6, 29.7, 20.7 ppm; GC-MS for $C_{14}H_{18}O_2$, m/z = 218 (M^+); HRMS (ESI-QTOF) m/z: $[M + H]^+$ Calcd for $C_{14}H_{18}O_2H$ 219.1380; Found 219.1370.

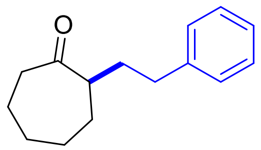

3-10ag

2-(4-Methoxyphenethyl)cycloheptanone (3-10ag): A 1,4-dioxane (2.0 mL) solution of complex **2-10** (9 mg, 3 mol %), **2-12** (12 mg, 10 mol %), cycloheptanone (56 mg, 0.5 mmol) and 2-phenylethylamine (85 mg, 0.7 mmol) was stirred at 130 °C for 16 h. The product **3-10ag** was isolated by column chromatography on silica gel (hexanes/EtOAc = 120:1–20:1; TLC: R_f = 0.7 (10% EtOAc in hexanes)). Yield = 85 mg (79%). Data for **3-10ag:** ^{1}H NMR (400 MHz, $CDCl_3$) δ 7.31–7.25 (m, 2H), 7.23–7.10 (m, 3H), 2.65–2.39 (m, 5H), 2.07–1.98 (m, 1H), 1.92–1.80 (m, 4H), 1.66–1.54 (m, 2H), 1.42–1.27 (m, 3H) ppm; $^{13}C\{^{1}H\}$ NMR (100 MHz, $CDCl_3$) δ 216.0, 142.0, 128.4, 128.3, 125.8, 51.4, 42.9, 33.9, 33.4, 31.4, 29.4, 28.5, 24.4 ppm; GC-MS for $C_{15}H_{20}O$, m/z = 216 (M^+); HRMS (ESI-TOF) m/z: $[M + H]^+$ Calcd for $C_{15}H_{20}OH$ 217.1587; Found 217.1557.

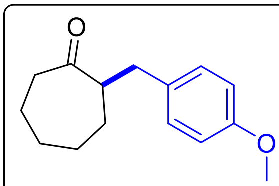

3-10ah

2-(4-Methoxybenzyl)cycloheptan-1-one (3-10ah): A 1,4-dioxane (2.0 mL) solution of complex **2-10** (9 mg, 3 mol %), **2-12** (12 mg, 10 mol %), cycloheptanone (56 mg, 0.5 mmol) and 4-methoxybenzylamine (96 mg, 0.7 mmol) was stirred at 130 °C for 16 h. The product **3-10ah** was isolated by column chromatography on silica gel (hexanes/EtOAc = 120:1–20:1; TLC: R_f = 0.6 (10% EtOAc in hexanes)). Yield = 94 mg (81%). Data for **3-10ah:** ^{1}H NMR (400 MHz, $CDCl_3$) δ 7.06 (d, J = 7.8 Hz, 2H), 6.80 (d, J = 7.8 Hz, 2H), 3.76 (s, 3H), 2.99 (dd, J = 13.4, 5.5 Hz, 2H), 2.80–2.71 (m, 1H), 2.50

(dd, J = 13.4, 8.5 Hz, 2H), 2.46–2.39 (m, 2H), 1.87–1.73 (m, 4H), 1.64–1.53 (m, 1H), 1.36–1.25 (m, 3H) ppm; $^{13}C\{^{1}H\}$ NMR (100 MHz, $CDCl_3$) δ 215.8, 157.8, 131.8, 130.0, 113.6, 55.1, 53.8, 43.1, 37.0, 30.2, 29.2, 28.5, 24.2 ppm; GC-MS for $C_{15}H_{20}O_2$, m/z = 232 (M^+); HRMS (ESI-TOF) m/z: $[M + H]^+$ Calcd for $C_{15}H_{20}O_2H$ 233.1536; Found 233.1505.

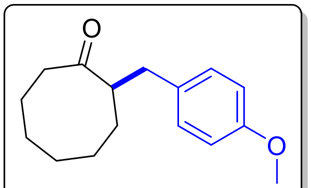

3-10ai

2-(4-Methoxybenzyl)cyclooctanone (3-10ai): A 1,4-dioxane (2.0 mL) solution of complex **2-10** (9 mg, 3 mol %), **2-12** (12 mg, 10 mol %), cyclooctanone (63 mg, 0.5 mmol) and 4-methoxybenzylamine (96 mg, 0.7 mmol) was stirred at 130 °C for 16 h. The product **3-10ai** was isolated by column chromatography on silica gel (hexanes/EtOAc = 120:1–20:1; TLC: R_f = 0.7 (10% EtOAc in hexanes)). Yield = 108 mg (88%). Data for **3-10ai:** ^{1}H NMR (400 MHz, $CDCl_3$) δ 7.03 (d, J = 8.6 Hz, 2H), 6.78 (d, J = 8.6 Hz, 2H), 3.75 (s, 3H), 2.95–2.84 (m, 2H), 2.56–2.46 (m, 1H), 2.33–2.25 (m, 1H), 2.15–2.08 (m, 1H), 2.02–1.92 (m, 1H), 1.84–1.45 (m, 7H), 1.38–1.28 (m, 1H), 1.24–1.15 ppm; $^{13}C\{^{1}H\}$ NMR (100 MHz, $CDCl_3$) δ 219.5, 157.8, 131.8, 129.8, 113.6, 55.1, 52.1, 43.0, 37.4, 32.7, 27.6, 25.3, 24.6, 24.5 ppm; GC-MS for $C_{16}H_{22}O_2$, m/z = 246 (M^+); HRMS (ESI-TOF) m/z: $[M + H]^+$ Calcd for $C_{16}H_{22}O_2H$ 247.1693; Found 247.1661.

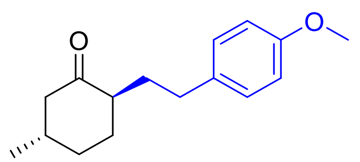

3-10an

(2R,5S)-2-(4-Methoxyphenethyl)-5-methylcyclohexanone (3-10an): A 1,4-dioxane (2.0 mL) solution of complex **2-10** (9 mg, 3 mol %), **2-12** (12 mg, 10 mol %), 3-methylcyclohexanone (56 mg, 0.5 mmol) and 4-methoxybenzeneethanamine (106 mg, 0.7 mmol) was stirred at 130 °C for 16 h. The product **3-10an** was isolated by column chromatography on silica gel (hexanes/EtOAc = 120:1–20:1; TLC: R_f = 0.7 (10% EtOAc in hexanes)). Yield = 103 mg

(84%). Data for **3-10an:** ^{1}H NMR (400 MHz, $CDCl_3$) δ 7.09 (d, *J* = 8.7 Hz, 2H), 6.82 (d, *J* = 8.7 Hz, 2H), 3.78 (s, 3H), 2.62–2.52 (m, 2H), 2.39–2.33 (m, 1H), 2.22–2.06 (m, 3H), 1.99 (td, *J* = 12.7, 1.1 Hz, 1H), 1.90–1.80 (m, 2H), 1.47–1.31 (m, 3H), 1.01 (d, *J* = 6.2 Hz, 3H) ppm; ^{13}C{^{1}H} NMR (100 MHz, $CDCl_3$) δ 212.6, 157.6, 134.3, 129.2, 113.7, 55.2, 50.6, 48.7, 35.7, 34.0, 33.0, 32.2, 30.9, 22.4 ppm; GC-MS for $C_{16}H_{22}O_2$, m/z = 246 (M^+). HRMS (ESI-TOF) m/z: $[M + H]^+$ Calcd for $C_{16}H_{22}O_2H$ 247.1693; Found 247.1668.

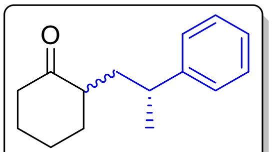

3-10ao

2-((*S*)-2-Phenylpropyl)cyclohexanone (3-10ao): A 1,4-dioxane (2.0 mL) solution of complex **2-10** (9 mg, 3 mol %), **2-12** (12 mg, 10 mol %), cyclohexanone (49 mg, 0.5 mmol) and (*R*)-(+)-β-methylphenethylamine (95 mg, 0.7 mmol) was stirred at 130 °C for 16 h. The product **3-10ao** was isolated by column chromatography on silica gel (hexanes/EtOAc = 120:1–20:1; TLC: R_f = 0.8 (10% EtOAc in hexanes)). Yield = 101 mg (94%). Data for **3-10ao:** ^{1}H NMR (400 MHz, $CDCl_3$) δ 7.33–7.26 (m, 2H), 7.24–7.09 (m, 3H), 2.88–2.72 (m, 1H), 2.41–2.29 (m, 1H), 2.25–2.09 (m, 3H), 2.04–1.89 (m, 2H), 1.83–1.74 (m, 1H), 1.66–1.52 (m, 2H), 1.42–1.29 (m, 2H), 1.25–1.21 (m, 3H) ppm; ^{13}C{^{1}H} NMR (100 MHz, $CDCl_3$) δ 213.5, 147.3, 128.4, 127.0, 125.9, 48.7, 42.3, 38.3, 37.6, 35.1, 28.3, 25.0, 22.9 ppm; GC-MS for $C_{15}H_{20}O$, m/z = 216 (M^+). HRMS (ESI-QTOF) m/z: $[M + Na]^+$ Calcd for $C_{15}H_{20}ONa$ 239.1406; Found 239.1413.

6.3.6.3 Characterization Data of the Compounds Listed in Table 3.5

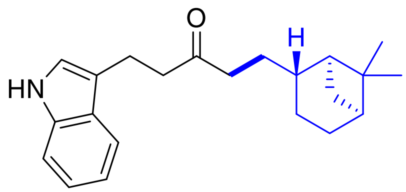

3-10at

1-((1*S*,2*R*,5*S*)-6,6-Dimethylbicyclo[3.1.1]heptan-2-yl)-5-(1H-indol-3-yl)pentan-3-one (3-10at). A 1,4-dioxane (2.0 mL) solution of complex **2-10** (9 mg, 3 mol %), **2-12** (12 mg, 10 mol %), 4-(1H-indol-3-yl)butan-2-one (94 mg, 0.5 mmol) and (−)-cis-myrtanylamine (107 mg, 0.7 mmol) was stirred at 130 °C for 16 h. The product **3-10at** was isolated by column chromatography on silica gel (hexanes/EtOAc = 120:1–20:1; TLC: R_f = 0.4 (10% EtOAc in hexanes)). Yield = 126 mg (78%). Data for **3-10at:** ^{1}H NMR (400 MHz, $CDCl_3$) δ 8.12 (brs, 1H), 7.61 (d, *J* = 7.6 Hz, 1H), 7.35 (d, *J* = 8.0 Hz, 1H), 7.24–7.18 (m, 1H), 7.16–7.11 (m, 1H), 6.96 (d, *J* = 2.3 Hz, 1H), 3.07 (t, *J* = 7.6 Hz, 2H), 2.83 (t, *J* = 7.6 Hz, 2H), 2.38 (t, *J* = 7.8 Hz, 2H), 2.07–1.99 (m, 1H), 1.91–1.82 (m, 2H), 1.79–1.57 (m, 2H), 1.79–1.57 (m, 4H), 1.54–1.42 (m, 2H), 1.37–1.24 (m, 2H), 1.20 (s, 3H), 0.81 (s, 3H) ppm; ^{13}C{^{1}H} NMR (100 MHz, $CDCl_3$) δ 211.6, 136.2, 127.1, 121.9, 121.5, 119.1, 118.6, 115.1, 111.1, 45.4, 43.1, 40.9, 40.8, 39.2, 34.3, 30.1, 26.7, 24.3, 23.3, 22.2, 20.0, 19.4 ppm; GC-MS for $C_{22}H_{29}NO$, m/z = 323 (M^+). HRMS (ESI-QTOF) m/z: $[M + Na]^+$ Calcd for $C_{22}H_{29}NONa$ 346.2141; Found 346.2145.

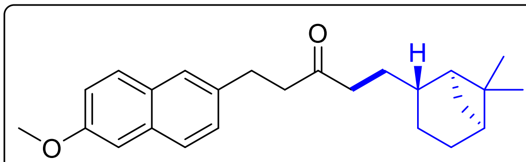

3-10au

1-((1S,2R,5S)-6,6-Dimethylbicyclo[3.1.1]heptan-2-yl)-5-(6-methoxynaphthalen-2-yl)pentan-3-one (3-10au): A 1,4-dioxane (2.0 mL) solution of complex **2-10** (9 mg, 3 mol %), **2-12** (12 mg, 10 mol %), nabumetone (114 mg, 0.5 mmol) and (−)-cis-myrtanylamine (107 mg, 0.7 mmol) was stirred at 130 °C for 16 h.

The product **3-10au** was isolated by column chromatography on silica gel (hexanes/EtOAc = 120:1–20:1; TLC: R_f = 0.6 (10% EtOAc in hexanes)). Yield = 160 mg (88%). Data for **3-10au:** ^{1}H NMR (400 MHz, $CDCl_3$) δ 7.67 (d, *J* = 8.4 Hz, 2H), 7.55 (s, 1H), 7.29 (dd, *J* = 8.4, 1.8 Hz, 1H), 7.14 (dd, *J* = 8.8, 2.5 Hz, 1H), 7.11 (d, *J* = 2.5 Hz, 1H), 3.90 (s, 3H), 3.03 (t, *J* = 7.6 Hz, 2H), 2.79 (t, *J* = 7.6 Hz, 2H), 2.40–2.31 (m, 2H), 2.05–1.97 (m, 1H), 1.88–1.79 (m, 2H), 1.77–1.56 (m, 4H), 1.51–1.41 (m, 2H), 1.30 (d, *J* = 10.0 Hz, 1H), 1.19 (s, 3H), 0.98–0.85 (m, 1H), 0.79 (s, 3H) ppm; $^{13}C\{^1H\}$ NMR (100 MHz, $CDCl_3$) δ 210.6, 157.1, 136.2, 133.0, 128.9, 128.8, 127.5, 126.8, 126.2, 118.7, 105.5, 55.1, 45.4, 44.2, 40.9, 40.8, 39.2, 34.2, 30.1, 29.7, 26.7, 24.3, 23.3, 22.2, 20.0 ppm; GC-MS for $C_{25}H_{32}O_2$, m/z = 364 (M^+). HRMS (ESI-TOF) m/z: $[M + H]^+$ Calcd for $C_{25}H_{32}O_2H$ 365.2475; Found 305.2457.

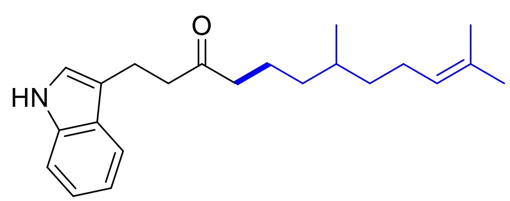

3-10av

1-(1H-Indol-3-yl)-7,11-dimethyldodec-10-en-3-one (3-10av). A 1,4-dioxane (2.0 mL) solution of complex **2-10** (9 mg, 3 mol %), **2-12** (12 mg, 10 mol %), 4-(1H-indol-3-yl)butan-2-one (94 mg, 0.5 mmol) and geranylamine (107 mg, 0.7 mmol) was stirred at 130 °C for 16 h. The product **3-10av** was isolated by column chromatography on silica gel (hexanes/EtOAc = 120:1–20:1; TLC: R_f = 0.5 (10% EtOAc in hexanes)). Yield = 117 mg (72%). Data for **3-10av:** ^{1}H NMR (400 MHz, $CDCl_3$) δ 8.14 (brs, 1H), 7.60 (d, *J* = 7.8 Hz, 1H), 7.35 (dt, *J* = 8.0, 1.0 Hz, 1H), 7.24–7.17 (m, 1H), 7.13 (td, *J* = 7.8, 1.0 Hz, 1H), 6.97 (s, 1H), 5.10 (tt, *J* = 7.1, 1.4 Hz, 1H), 3.12–3.01 (m, 2H), 2.89–2.76 (m, 2H), 2.42–2.32 (m, 2H), 2.02–1.90 (m, 2H), 1.70 (s, 3H), 1.61 (s, 3H), 1.57–1.50 (m, 1H), 1.50–1.17 (m, 4H), 1.17–1.02 (m, 2H), 0.86 (d, *J* = 6.6 Hz, 3H) ppm; $^{13}C\{^1H\}$ NMR (100

MHz, $CDCl_3$) δ 211.2, 136.2, 131.0, 127.1, 124.8, 121.9, 121.5, 119.1, 118.6, 115.1, 111.1, 43.3, 43.1, 36.9, 36.4, 32.2, 25.7, 25.4, 21.3, 19.3, 19.3, 17.6 ppm; GC-MS for $C_{22}H_{31}NO$, m/z = 325 (M^+). HRMS (ESI-TOF) m/z: $[M + H]^+$ Calcd for $C_{22}H_{31}NOH$ 326.2478; Found 326.2474.

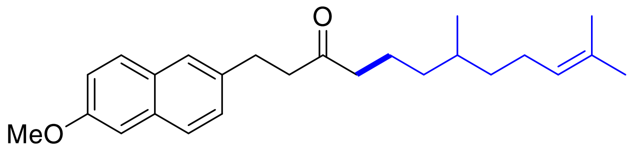

3-10aw

1-(6-Methoxynaphthalen-2-yl)-7,11-dimethyldodec-10-en-3-one (3-10aw). A 1,4-dioxane (2.0 mL) solution of complex **2-10** (9 mg, 3 mol %), **2-12** (12 mg, 10 mol %), nabumetone (114 mg, 0.5 mmol) and geranylamine (107 mg, 0.7 mmol) was stirred at 130 °C for 16 h. The product **3-10aw** was isolated by column chromatography on silica gel (hexanes/EtOAc = 120:1–20:1; TLC: R_f = 0.7 (10% EtOAc in hexanes)). Yield = 124 mg (68%). Data for **3-10aw:** ^{1}H NMR (400 MHz, $CDCl_3$) δ 7.67 (d, *J* = 8.6 Hz, 2H), 7.55 (s, 1H), 7.29 (dd, *J* = 8.4, 1.8 Hz, 1H), 7.13 (dd, *J* = 8.8, 2.5 Hz, 1H), 7.10 (d, *J* = 2.5 Hz, 1H), 5.09 (tt, *J* = 7.1, 1.4 Hz, 1H), 3.91 (s, 3H), 3.03 (t, *J* = 7.6 Hz, 2H), 2.84–2.74 (m, 2H), 2.37 (t, *J* = 7.4 Hz, 2H), 2.12–1.83 (m, 3H), 1.69 (s, 3H), 1.61 (s, 3H), 1.56–1.48 (m, 1H), 1.41–1.34 (m, 1H), 1.33–1.19 (m, 2H), 1.16–1.01 (m, 2H), 0.86 (d, *J* = 6.5 Hz, 3H) ppm; $^{13}C\{^1H\}$ NMR (100 MHz, $CDCl_3$) δ 210.4, 157.2, 136.2, 133.0, 131.0, 129.0, 128.8, 127.5, 126.9, 126.2, 124.8, 118.7, 105.5, 55.2, 44.2, 43.3, 36.9, 36.4, 32.2, 29.7, 25.7, 25.4, 21.2, 19.3, 17.6 ppm; GC-MS for $C_{25}H_{34}O_2$, m/z = 366 (M^+). HRMS (ESI-TOF) m/z: $[M + H]^+$ Calcd for $C_{25}H_{34}O_2H$ 367.2632; Found 367.2627.

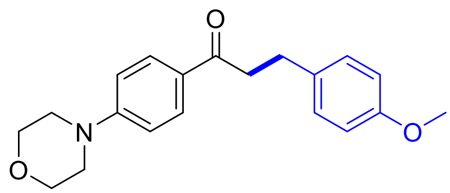

3-10ax

3-(4-Methoxyphenyl)-1-(4-morpholinophenyl)propan-1-one (3-10ax). A 1,4-dioxane (2.0 mL) solution of complex **2-10** (9 mg, 3 mol %), **2-12** (12 mg, 10 mol %), 4′-morpholinoacetophenone (102 mg, 0.5 mmol) and 4-methoxybenzylamine (96 mg, 0.7 mmol) was stirred at 130 °C for 16 h. The product **3-10ax** was isolated by column chromatography on silica gel (hexanes/EtOAc = 120:1–20:1; TLC: R_f = 0.1 (10% EtOAc in hexanes)). Yield = 116 mg (71%). Data for **3-10ax:** ^{1}H NMR (400 MHz, $CDCl_3$) δ 7.90 (d, *J* = 9.0 Hz, 2H), 7.17 (d, *J* = 8.6 Hz, 2H), 6.87 (d, *J* = 9.0 Hz, 2H), 6.84 (d, *J* = 8.6 Hz, 2H), 3.88–3.83 (m, 4H), 3.78 (s, 3H), 3.32–3.27 (m, 4H), 3.21–3.16 (m, 2H), 3.02–2.96 (m, 2H) ppm; ^{13}C{^{1}H} NMR (100 MHz, $CDCl_3$) δ 197.6, 157.8, 154.0, 133.5, 130.0, 129.2, 127.7, 113.8, 113.2, 66.4, 55.1, 47.4, 40.1, 29.5 ppm; GC-MS for $C_{20}H_{23}NO_3$, m/z = 325 (M^+). HRMS (ESI-TOF) m/z: $[M + H]^+$ Calcd for $C_{20}H_{23}NO_3H$ 326.1751; Found 326.1751.

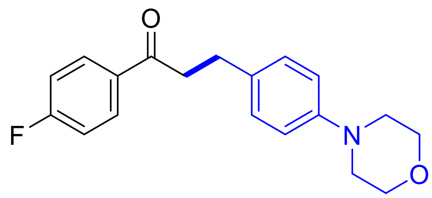

3-10ay

1-(4-Fluorophenyl)-3-(4-morpholinophenyl)propan-1-one (3-10ay): A 1,4-dioxane (2.0 mL) solution of complex **2-10** (9 mg, 3 mol %), **2-12** (12 mg, 10 mol %), 4′-fluoroacetophenone (69 mg, 0.5 mmol) and 4-morpholinobenzylamine (134 mg, 0.7 mmol) was stirred at 130 °C for 16 h. The product **3-10ay** was isolated by column chromatography on silica gel (hexanes/EtOAc = 120:1–20:1; TLC: R_f = 0.2 (10% EtOAc in hexanes)). Yield = 93 mg (59%). Data for **3-10ay:** ^{1}H NMR (400 MHz, $CDCl_3$) δ 8.01–7.94 (m, 2H), 7.17 (d, *J* = 8.7 Hz, 2H), 7.14–7.08 (m, 2H), 6.89 (d, *J* = 8.7 Hz, 2H), 3.91–3.84 (m, 4H), 3.27–3.21 (m, 2H), 3.13 (t, *J* = 4.8 Hz, 4H), 3.04–2.96 (m, 2H) ppm; $^{13}C\{^1H\}$ NMR (100 MHz, $CDCl_3$) δ 197.8, 165.6 (d, J_{CF} = 254.5 Hz), 133.2 (d, J_{CF} = 3.1 Hz), 130.6 (d, J_{CF} = 9.1 Hz), 129.1, 127.8, 117.1, 116.1, 115.6 (d, J_{CF} = 21.8 Hz), 66.8, 49.7, 40.4, 29.1 ppm; GC-MS for $C_{19}H_{20}FNO_2$, m/z = 313 (M^+). HRMS (ESI-TOF) m/z: $[M + H]^+$ Calcd for $C_{19}H_{20}FNO_2H$ 314.1527; Found 314.1517.

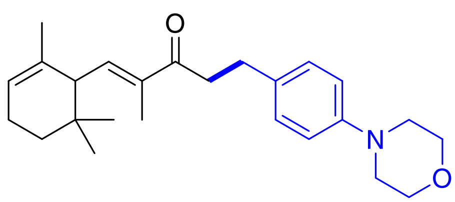

3-10az

(*E*)-2-Methyl-5-(4-morpholinophenyl)-1-(2,6,6-trimethylcyclohex-2-enyl)pent-1-en-3-one (3-10az). A 1,4-dioxane (2.0 mL) solution of complex **2-10** (9 mg, 3 mol %), **2-12** (12 mg, 10 mol %), α-cetone (103 mg, 0.5 mmol) and 4-morpholinobenzylamine (134 mg, 0.7 mmol) was stirred at 130 °C for 16 h. The product **3-10az** was isolated by column chromatography on silica gel (hexanes/EtOAc = 120:1–20:1; TLC: R_f = 0.4 (10% EtOAc in hexanes)). Yield = 126 mg (66%). Data for **3-10az:** ^1H NMR (400 MHz, $CDCl_3$) δ 7.12 (d, *J* = 8.5 Hz, 2H), 6.85 (d, *J* = 8.5 Hz, 2H), 6.38 (dd, *J* = 11.1, 1.5 Hz, 1H), 5.48–5.39 (m, 1H), 3.87–3.84 (m, 4H), 3.14–3.10 (m, 4H), 2.98–2.90 (m, 2H), 2.89–2.82 (m, 2H), 2.64 (d, *J* = 11.1 Hz, 1H), 2.09–2.00 (m, 2H), 1.86 (d, *J* = 1.1 Hz, 3H), 1.55–1.48 (m, 3H), 1.47–1.42 (m, 1H), 1.26–1.20 (m, 1H), 0.92 (s, 3H), 0.78 (s, 3H) ppm; $^{13}C\{^1H\}$ NMR (100 MHz, $CDCl_3$) δ 201.2, 149.6, 144.0, 139.8, 137.3, 133.2, 129.1, 121.9, 115.9, 66.9, 50.1, 49.6, 39.6, 32.8, 31.7, 30.0, 27.1, 27.1, 23.0, 22.8, 12.0 ppm; GC-MS for $C_{25}H_{35}NO_2$, m/z = 381 (M^+). HRMS (ESI-QTOF) m/z: $[M + H]^+$ Calcd for $C_{25}H_{35}NO_2H$ 382.2741; Found 382.2726.

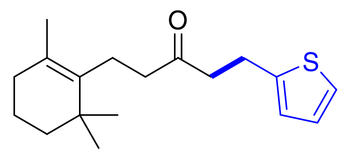

3-10ba

1-(Thiophen-2-yl)-5-(2,6,6-trimethylcyclohex-1-enyl)pentan-3-one (3-10ba): A 1,4-dioxane (2.0 mL) solution of complex **2-10** (9 mg, 3 mol %), **2-12** (12 mg, 10 mol %), dihydro-β-ionone (97 mg, 0.5 mmol) and 2-thiophenemethylamine (79 mg, 0.7 mmol) was stirred at 130 °C for 16 h. The product **3-10ba** was isolated by column chromatography on silica gel (hexanes/EtOAc = 120:1–20:1; TLC: R_f = 0.8 (10% EtOAc in hexanes)). Yield = 137 mg (94%). Data for **3-10ba:** ^{1}H NMR (400 MHz, $CDCl_3$) δ 7.11 (dd, J = 5.1, 1.1 Hz, 1H), 6.90 (dd, J = 5.1, 3.4 Hz, 1H), 6.80 (dd, J = 3.4, 1.1 Hz, 1H), 3.13 (t, J = 7.3 Hz, 2H), 2.79 (t, J = 7.4 Hz, 2H), 2.50–2.45 (m, 2H), 2.31–2.21 (m, 2H), 1.90 (t, J = 6.9 Hz, 2H), 1.58–1.56 (m, 1H), 1.55 (s, 3H), 1.43–1.39 (m, 2H), 1.09–1.07 (m, 1H), 0.97 (s, 6H) ppm; ^{13}C{^{1}H} NMR (100 MHz, $CDCl_3$) δ 209.4, 143.6, 135.8, 127.7, 126.7, 124.5, 123.2, 44.2, 43.7, 39.6, 34.9, 32.6, 28.3, 24.0, 22.1, 19.7, 19.4 ppm; GC-MS for $C_{18}H_{26}OS$, m/z = 290 (M^+). HRMS (ESI-QTOF) m/z: $[M + H]^+$ Calcd for $C_{18}H_{26}OSH$ 291.1777; Found 291.1771.

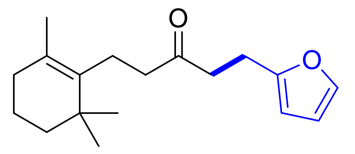

3-10bb

1-(Furan-2-yl)-5-(2,6,6-trimethylcyclohex-1-enyl)pentan-3-one (3-10bb): A 1,4-dioxane (2.0 mL) solution of complex **2-10** (9 mg, 3 mol %), **2-12** (12 mg, 10 mol %), dihydro-β-ionone (97 mg, 0.5 mmol) and furfurylamine (68 mg, 0.7 mmol) was stirred at 130 °C for 16 h. The product **3-10bb** was isolated by column chromatography on silica gel (hexanes/EtOAc = 120:1–20:1; TLC: R_f = 0.8 (10% EtOAc in hexanes)). Yield = 118 mg (86%). Data for **3-10bb:** ^{1}H NMR (400 MHz, $CDCl_3$) δ 7.28 (dd, J = 1.9, 0.9 Hz, 1H), 6.26 (dd, J = 3.2, 1.9 Hz, 1H), 5.98 (dd, J = 3.2, 0.9 Hz, 1H), 2.92 (t, J = 7.4 Hz, 2H), 2.77–2.71 (m, 2H), 2.50–2.45 (m, 2H), 2.28–

2.22 (m, 2H), 1.89 (t, *J* = 7.0 Hz, 2H), 1.57–1.56 (m, 1H), 1.55 (s, 3H), 1.42–1.38 (m, 2H), 1.07–1.06 (m, 1H), 0.96 (s, 6H) ppm; $^{13}C\{^1H\}$ NMR (100 MHz, $CDCl_3$) δ 209.5, 154.5, 141.0, 135.9, 127.8, 110.1, 105.1, 43.6, 40.6, 39.6, 35.0, 32.7, 28.4, 22.3, 22.2, 19.7, 19.4 ppm; GC-MS for $C_{18}H_{26}O_2$, m/z = 274 (M^+). HRMS (ESI-QTOF) m/z: $[M + H]^+$ Calcd for $C_{18}H_{26}O_2H$ 275.2006; Found 275.1994.

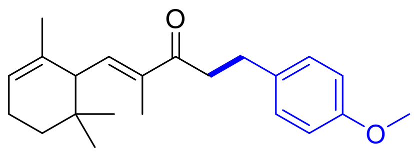

3-10bc

(*E*)-5-(4-Methoxyphenyl)-2-methyl-1-(2,6,6-trimethylcyclohex-2-enyl)pent-1-en-3-one (3-10bc): A 1,4-dioxane (2.0 mL) solution of complex **2-10** (9 mg, 3 mol %), **2-12** (12 mg, 10 mol %), α-cetone (103 mg, 0.5 mmol) and 4-methoxybenzylamine (96 mg, 0.7 mmol) was stirred at 130 °C for 16 h. The product **3-10bc** was isolated by column chromatography on silica gel (hexanes/EtOAc = 120:1–20:1; TLC: R_f = 0.7 (10% EtOAc in hexanes)). Yield = 155 mg (95%). Data for **3-10bc:** ^1H NMR (400 MHz, $CDCl_3$) δ 7.12 (d, *J* = 8.6 Hz, 2H), 6.83 (d, *J* = 8.6 Hz, 2H), 6.38 (dd, *J* = 11.1, 1.5 Hz, 1H), 5.48–5.39 (m, 1H), 3.78 (s, 3H), 2.99–2.91 (m, 2H), 2.91–2.83 (m, 2H), 2.65 (d, *J* = 11.1 Hz, 1H), 2.09–2.00 (m, 2H), 1.87 (d, *J* = 1.2 Hz, 3H), 1.52 (dd, *J* = 3.6, 1.7 Hz, 3H), 1.49–1.42 (m, 1H), 1.27–1.21 (m, 1H), 0.93 (s, 3H), 0.79 (s, 3H) ppm; $^{13}C\{^1H\}$ NMR (100 MHz, $CDCl_3$) δ 201.2, 157.8, 144.0, 137.3, 133.5, 133.1, 129.2, 121.9, 113.8, 55.1, 50.1, 39.6, 32.7, 31.7, 30.0, 27.1, 27.0, 22.9, 22.7, 11.9 ppm; GC-MS for $C_{22}H_{30}O_2$, m/z = 326 (M^+). HRMS (ESI-QTOF) m/z: $[M + H]^+$ Calcd for $C_{22}H_{30}O_2H$ 327.2319; Found 327.2308.

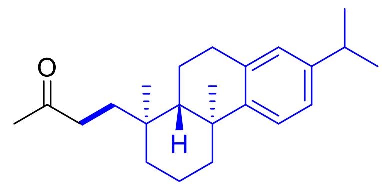

3-10bd

4-((1*S*,4a*S*,10a*S*)-7-Isopropyl-1,4a-dimethyl-1,2,3,4,4a,9,10,10a-octahydrophenanthren-1-yl)butan-2-one (3-10bd): A 1,4-dioxane (2.0 mL) solution of complex **2-10** (9 mg, 3 mol %), **2-12** (12 mg, 10 mol %), acetone (29 mg, 0.5 mmol) and (+)-dehydroabietylamine (200 mg, 0.7 mmol) was stirred at 130 °C for 16 h. The product **3-10bd** was isolated by column chromatography on silica gel (hexanes/EtOAc = 120:1–20:1; TLC: R_f = 0.9 (10% EtOAc in hexanes)). Yield = 88 mg (54%). Data for **3-10bd:** ^{1}H NMR (400 MHz, $CDCl_3$) δ 7.17 (d, *J* = 8.2 Hz, 1H), 6.99 (dd, *J* = 8.2, 1.9 Hz, 1H), 6.89 (d, *J* = 1.9 Hz, 1H), 2.95–2.78 (m, 3H), 2.38–2.29 (m, 2H), 2.14 (s, 3H), 1.88–1.49 (m, 10H), 1.44–1.30 (m, 4H), 1.22 (d, *J* = 6.9 Hz, 6H), 0.93 (s, 3H) ppm; $^{13}C\{^1H\}$ NMR (100 MHz, $CDCl_3$) δ 209.6, 147.5, 145.5, 134.7, 126.8, 124.2, 123.8, 47.7, 38.5, 38.2, 37.5, 37.2, 37.0, 35.3, 33.4, 30.2, 30.1, 29.7, 25.2, 24.0, 20.6, 18.9, 18.6 ppm; GC-MS for $C_{23}H_{34}O$, m/z = 326 (M^+). HRMS (ESI-TOF) m/z: $[M + H]^+$ Calcd for $C_{23}H_{34}OH$ 327.2682; Found 327.2684.

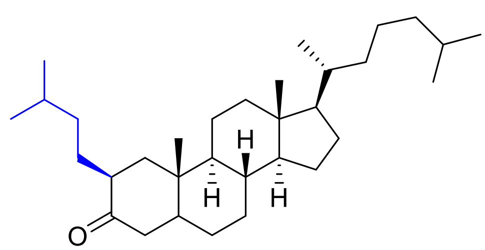

3-10be

(8*R*,9*S*,10*S*,13*R*,14*S*,17*R*)-2-Isopentyl-10,13-dimethyl-17-((*R*)-6-methylheptan-2-yl)-dodecahydro-2*H*-cyclopenta[a]phenanthren-3(4*H*,9*H*,14*H*)-one (3-10be): A 1,4-dioxane (2.0 mL) solution of complex **2-10** (5 mg, 3 mol %), **2-12** (6 mg, 10 mol %), 5α-cholestan-3-one (97 mg, 0.25 mmol) and isoamylamine (44 mg, 0.5 mmol) was stirred at 130 °C for 16 h. The product **3-10be** was isolated by column chromatography on silica gel (hexanes/EtOAc = 120:1–20:1; TLC: R_f = 0.8 (10% EtOAc in hexanes)). Yield = 104 mg

(91%). Data for **3-10be:** ^{1}H NMR (400 MHz, $CDCl_3$) δ 2.37–2.15 (m, 3H), 2.11–2.02 (m, 2H), 2.00–1.95 (m, 1H), 1.86–1.76 (m, 2H), 1.75–1.60 (m, 2H), 1.59–1.44 (m, 5H), 1.41–1.20 (m, 8H), 1.17–0.96 (m, 14H), 0.93–0.81 (m, 15H), 0.73–0.62 (m, 4H) ppm; ^{13}C{^{1}H} NMR (100 MHz, $CDCl_3$) δ 213.0, 56.2, 56.2, 53.9, 48.1, 46.6, 46.3, 45.1, 42.6, 39.9, 39.5, 36.5, 36.3, 36.1, 35.7, 35.2, 31.7, 28.7, 28.3, 28.2, 28.0, 26.9, 24.2, 23.8, 22.8, 22.7, 22.5, 22.5, 21.5, 18.6, 12.5, 12.1 ppm; GC-MS for $C_{32}H_{56}O$, m/z = 456 (M^+). HRMS (ESI-QTOF) m/z: $[M + Na]^+$ Calcd for $C_{32}H_{56}OH$ 479.4223; Found 479.4218.

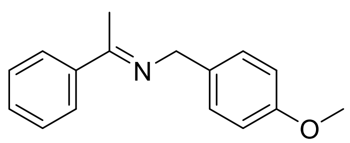

3-13a

(4-Methoxyphenyl)-*N*-(1-phenylethylidene)methanamine (3-13a): A mixture of acetophenone (240 mg, 2 mmol), 4-methoxybenzylamine (274 mg, 2 mmol), *p*-toluenesulfonic acid (2 mg, 0.4 mol %) and 4 Å molecular sieves (15 mg) in toluene (4 mL) was reacted for 5 h under refluxing conditions. After filtered through a celite bed, analytically pure product was isolated by column chromatography on silica gel (column was flushed with 20 mL of pure Et_3N before loading the sample; hexanes/Et_3N = 100:1–10:1; Yield = 458 mg (96%). Data for **3-13a:** ^{1}H NMR (400 MHz, $CDCl_3$) δ 7.95–7.87 (m, 2H), 7.45–7.42 (m, 3H), 7.40 (d, J = 8.7 Hz, 2H), 6.95 (d, J = 8.7 Hz, 2H), 4.72 (s, 2H), 3.83 (s, 3H), 2.35 (s, 2H) ppm; ^{13}C{^{1}H} NMR (100 MHz, $CDCl_3$) δ 165.5, 158.2, 140.9, 132.6, 129.4, 128.6, 128.0, 126.6, 113.7, 55.1, 55.0, 15.6 ppm; GC-MS for $C_{16}H_{17}NO$, m/z = 239 (M^+). HRMS (ESI-TOF) m/z: $[M + H]^+$ Calcd for $C_{16}H_{17}NOH$ 240.1383; Found 240.1383.

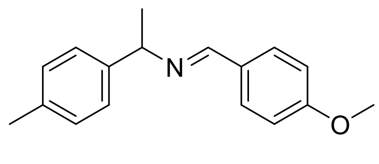

3-13b

***N*-(4-Methoxybenzylidene)-1-p-tolylethanamine (3-13b):** A mixture of 4-methoxybenzaldehyde (680 mg, 5 mmol), 1-*p*-tolylethanamine (676 mg, 5 mmol), *p*-toluenesulfonic acid (4 mg, 0.4 mol %) and 4 Å molecular sieves (30 mg) in anhydrous toluene (5 mL) was reacted for 2 h under reflux conditions. After filtered through a celite, analytically pure product was isolated by column chromatography on silica gel (column was flushed with 20 mL of pure Et_3N before loading the sample; hexanes/Et_3N = 100:1–10:1; Yield = 1.21 g (96%). Data for **3b:** ^{1}H NMR (400 MHz, $CDCl_3$) δ 8.35 (s, 1H), 7.79 (d, *J* = 8.8 Hz, 2H), 7.39 (d, *J* = 8.0 Hz, 2H), 7.21 (d, *J* = 8.0 Hz, 2H), 6.95 (d, *J* = 8.8 Hz, 2H), 4.57 (q, *J* = 6.3 Hz, 1H), 3.74 (s, 3H), 2.39 (s, 3H), 1.68 (d, *J* = 6.3 Hz, 3H) ppm; ^{13}C{^{1}H} NMR (100 MHz, $CDCl_3$) δ 161.5, 159.1, 141.7, 136.1, 129.8, 128.9, 128.7, 126.4, 113.7, 66.8, 55.0, 31.3, 20.8 ppm; GC-MS for $C_{17}H_{19}NO$, m/z = 253 (M^+). HRMS (ESI-TOF) m/z: $[M + H]^+$ Calcd for $C_{16}H_{17}NOH$ 254.1539; Found 254.1525.

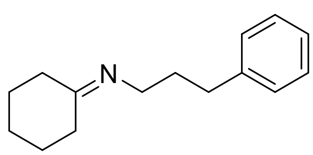

3-13e

***N*-Cyclohexylidene-3-phenylpropan-1-amine (3-13e):** A mixture of cyclohexanone (196 mg, 2 mmol), 3-phenyl-1-propylamine (270 mg, 2 mmol), *p*-toluenesulfonic acid (2 mg, 0.2 mol %), and 4 Å molecular sieves (15 mg) in anhydrous toluene (4 mL) was reacted for 5 h under reflux conditions. After filtered through a celite bed, analytically pure product was isolated by column chromatography on silica gel (column was flushed with 20 mL of pure Et_3N before loading the sample; hexanes/Et_3N = 100:1–10:1; Yield = 380 mg (88%). Data for **3-13e:** ^{1}H NMR (400 MHz, $CDCl_3$) δ 7.26–7.20 (m, 2H), 7.19–7.10 (m, 3H), 3.28 (d, *J* = 7.2 Hz, 1H), 2.79–2.46 (m, 4H), 2.36–2.11 (m, 3H), 1.96–1.55 (m, 8H) ppm; $^{13}C\{^{1}H\}$ NMR (100 MHz, $CDCl_3$) δ 172.7, 141.9, 128.0, 127.9, 125.4, 49.1, 41.6, 39.6, 33.4, 28.5, 25.7 ppm; GC-MS for $C_{15}H_{21}N$, m/z = 215 (M^+). HRMS (ESI-TOF) m/z: $[M + H]^+$ Calcd for $C_{15}H_{21}NH$; 216.1747 Found 216.1737.

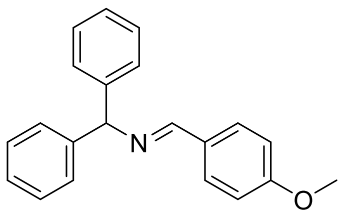

3-13f

(*E*)-*N*-(4-methoxybenzylidene)-1,1-diphenylmethanamine (3-13f): A mixture of α-aminodiphenylmethane (183 mg, 1 mmol), 4-methoxybenzaldehyde (136 mg, 1 mmol) and sodium sulfate (0.40 g) in CH_2Cl_2 (2.0 mL) was stirred at room temperature for 18 h. After filtered through celite, analytically pure product was isolated by recrystallization. Yield = 295 mg (98%). Data for **3-13f:** ^{1}H NMR (400 MHz, $CDCl_3$) δ 8.40 (s, 1H), 7.84 (d, *J* = 8.8 Hz, 2H), 7.55–7.49 (m, 1H), 7.47–7.45 (m, 3H), 7.41–7.32 (m, 4H), 7.31–7.34 (m, 2H), 6.97 (d, *J* = 8.8 Hz, 2H), 5.62 (s, 1H), 3.86 (s, 3H) ppm; $^{13}C\{^{1}H\}$ NMR (100 MHz, $CDCl_3$) δ 161.6, 160.0, 144.1, 130.0, 129.2, 128.3, 127.6, 126.8, 113.8, 77.7, 55.3 ppm; GC-MS for $C_{21}H_{19}NO$, m/z = 301 (M^+). ^{1}H and ^{13}C NMR spectral data are in good agreement with the literature values.[208]

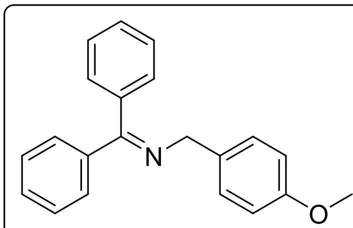

3-13g

***N*-(4-Methoxybenzyl)-1,1-diphenylmethanimine (3g):** A 1,4-dioxane (2.0 mL) solution of complex **2-10** (9 mg, 3 mol %), **2-12** (12 mg, 10 mol %), (*E*)-N-(4-methoxybenzylidene)-1,1-diphenylmethanamine **(3-10g)** (151 mg, 0.5 mmol) was stirred at 130 °C for 2 h. The product **3-10e** was isolated by column chromatography on silica gel (hexanes/EtOAc = 80:1–15:1; TLC: R_f = 0.6 (10% EtOAc in hexanes)). Yield = 123 mg (82%). Data for **3-**

10e: ^{1}H NMR (400 MHz, $CDCl_3$) δ 7.70 (d, *J* = 8.1 Hz, 2H), 7.52–7.47 (m, 2H), 7.46–7.30 (m, 4H), 7.30–7.17 (m, 4H), 6.88 (d, *J* = 8.6 Hz, 2H), 4.58 (s, 2H), 3.80 (s, 3H) ppm; ^{13}C{^{1}H} NMR (100 MHz, $CDCl_3$) δ 168.6, 158.3, 139.6, 136.6, 132.6, 130.1, 128.7, 128.6, 128.5, 128.2, 128.0, 127.8, 113.7, 56.7, 55.2 ppm; GC-MS for $C_{21}H_{19}NO$, m/z = 301 (M^+). ^{1}H and ^{13}C NMR spectral data are in good agreement with the literature values.[209]

6.3.7 DFT Computational Study

Electronic structure calculations were performed with the Gaussian 16 package, revision C01.[210] For the density functional theory (DFT) calculations we used M06L functional[211] in combination with def2-SV(P) basis set.[212] After geometry optimization, the SCF energies were refined by single-point calculations with triple-zeta def2-TZVPPD basis set.[212] For Ru, the 28 core electrons were treated using the effective core approach[213] for both double-zeta and triple-zeta basis sets. Solvent effects were included using the implicit integral equation formalism polarizable continuum model (IEF-PCM, also referred as PCM)[214] with the solvent parameters characteristic for 1,4-dioxane (e = 2.2099). For all DFT calculations, ultrafine Lebedev's grid was used with 99 radial shells per atom and 590 angular points in each shell. The wave function stability tests were performed to ensure that the closed-shell singlet states were the lowest-energy solution (for **6'**, the SCF solution was found to have a partial open-shell character).[215] Tight cutoff convergence criteria on atomic forces (2E-6 and 1E-6 au for maximum/RMS forces, respectively) and displacements (6E-6 and 4E-6 au for maximum/RMS displacements, respectively) were used in geometry optimization procedure. Hessian matrices were calculated for the optimized structures to identify their nature (that is, zero imaginary frequencies for minima and one for transition states). Intrinsic reaction coordinate (IRC)[216] was followed for the pentan-2-imine to pentan-2-imine (both for the uncatalyzed reaction and for the reaction in presence of the Ru-catecholate complex **4** with removed *t*-Bu groups) to validate the assignment of transition states to the corresponding elementary steps. Thermodynamic functions were calculated using the ideal gas approximation based on the particle-in-the-box, rigid rotor, and quantum harmonic oscillator models for the translational, rotational, and vibrational degrees of freedom, respectively.

6.4 Experimental Procedures and Characterization Data for Chapter 4

6.4.1.1 General Procedure for the Catalytic Synthesis of Quinazolines

In a glove box, complex **2-10** (9 mg, 3 mol %), 4-(1,1-dimethylethyl)-1,2-benzenediol (**2-16**) (8 mg, 10 mol %) were dissolved in anhydrous 1,4-dioxane (1 mL) in a 25 mL Schlenk tube equipped with a Teflon screw cap stopcock and a magnetic stirring bar. After stirring for 5-10 min until the solution was turned light green color, both a 2-aminophenylketone (0.5 mmol) and an amine (0.7 mmol) substrates, and dioxane (1 mL) was added to the tube. The tube was sealed, it was brought out of the glove box, and was stirred in an oil bath set at 140 °C for 20 h. After the reaction tube was cooled to room temperature, the tube was open to air, the solution was filtered through a short silica gel column by eluting with CH_2Cl_2 (10 mL), and the filtrate was analyzed by GC-MS method. Analytically pure product **4-12** was isolated by a simple column chromatography on silica gel (280-400 mesh, hexanes/EtOAc).

6.4.1.2 General Procedure for the Catalytic Synthesis of Quinazolinones

In a glove box, complex **2-10** (9 mg, 3 mol %), **2-16** (8 mg, 10 mol %), were dissolved in 1,4-dioxane (1 mL) in a 25 mL Schlenk tube equipped with a Teflon screw cap stopcock and a magnetic stirring bar. The resulting mixture was stirred for 5-10 min until the solution was turned to light green color. Both 2-aminobenzamide (0.5 mmol) and an amine (0.7 mmol) substrates were dissolved in dioxane (1 mL), and the solution was added to the reaction tube. The tube was brought out of the glove box and was stirred in an oil bath set at 140 °C for 20 h. The reaction tube was taken out of the oil bath, and it was cooled to room temperature. The resulting solution was filtered through a short silica gel column by eluting with CH_2Cl_2 (10 mL), and the filtrate was analyzed by GC-MS.

Analytically pure product **4-13** was isolated by a simple column chromatography on silica gel (280-400 mesh, hexanes/EtOAc).

6.4.2 Catalyst and Ligand Screening Study

In a glove box, a Ru catalyst (3 mol % Ru atom) and a ligand (10 mol %) were dissolved in a solvent (1 mL) in a 25 mL Schlenk tube equipped with a Teflon screw cap stopcock and a magnetic stirring bar. The resulting mixture was stirred for 5-10 min. 2-Aminophenylethanone (68 mg, 0.5 mmol), 4-methoxybenzylamine (69 mg, 0.7 mmol) and a solvent (1 mL) were added to the reaction tube. The tube was brought out of the glove box and was stirred in an oil bath at 140 °C for 20 h. The product yield was determined by ^{1}H NMR by using hexamethylbenzene as an internal standard. The results are summarized in **Table 4.1** and **Table 4.2**.

6.4.3 General Procedures for the Mechanistic Studies

We have chosen the reaction of 2-aminoacetophenone with 4-methoxybenzylamine for probing mechanistic insights for the coupling reaction.

6.4.3.1 Deuterium Labeling Study

In a glove box, 2-aminophenylethanone-d_3 (89 % D, 69 mg, 0.5 mmol), 4-methoxybenzylamine (96 mg, 0.7 mmol) and complex **2-10** (3 mol %) were dissolved in 1,4-dioxane (2 mL) in a 25 mL Schlenk tube equipped with a Teflon screw cap stopcock and a stirring bar. The tube was brought out of the box, and stirred in an oil bath preset at 140 °C for 20 h. The reaction tube was taken out of the oil bath, and was cooled to room temperature. After the tube was open to air, the solution was filtered through a short silica gel column by eluting with CH_2Cl_2 (10 mL), and the filtrate was analyzed by GC-MS. Analytically pure product was isolated by column chromatography on silica gel (230-460 mesh, hexanes/EtOAc = 100:1 to 10:1). The ^1H and ^2H NMR spectra of the product **4-12a** and **4-12a**-*d* are shown in **Figure 4.2**.

6.4.3.2 Reaction Profile Experiment

In a glove box, complex **2-10** (5 mg, 3 mol %) and **2-16** (4 mg, 10 mol %) were dissolved in toluene-d_8 (0.5 mL) in a 25 mL Schlenk tube equipped with a Teflon screw cap stopcock and a magnetic stirring bar. The resulting mixture was stirred for 5 to 10 minutes until the solution turned to a blueish green color. 2-aminophenylethanone (34 mg, 0.25 mmol) and 4-methoxybenzylamine (35 mg, 0.25 mmol) were added to the reaction tube, and the solution was transferred into a J-Young NMR tube equipped with a Teflon screw cap stopcock. The tube was brought out of the glove box, and was immersed an oil bath set at 130 °C. The tube was taken out from the oil bath at 20 min intervals, was immediately cooled in ice-water bath, and was analyzed by ^1H NMR. The appearance of the product signals were normalized against the internal standard peak (C_6Me_6). The plot of relative concentration vs time is shown in **Figure 4.3**.

6.4.3.3 Reaction with Imines

Following the standard procedure, a reaction tube containing 4-chloro-2-(((4-methoxybenzyl)imino)(phenyl)methyl)aniline **4-14b** and complex **2-10** (3 mol %) in 1,4-dioxane (2 mL) was stirred at 140 °C for 20 h. The column chromatography on silica gel (hexanes/EtOAc = 100:1 to 10:1) led to the isolation of the product **4-12h** in 87% yield.

Following the standard procedure, a reaction tube containing (E)-2-((4-methoxybenzylidene)amino)benzamide **4-15** and complex **2-10** (3 mol %) in 1,4-dioxane (2 mL) was stirred at 140 °C for 20 h. The column chromatography on silica gel (hexanes/EtOAc = 40:1 to 10:1) led to the isolation of the product **4-13c** in 87% yield.

6.4.3.3 Reaction with Ruthenium Catecholate Complex 2-11

In a glove box, complex **2-11** (9 mg, 1 mol %) was dissolved in 1,4-dioxane (1 mL) in a 25 mL Schlenk tube equipped with a Teflon screw cap stopcock and a magnetic stirring bar. The resulting mixture was stirred for 5-10 min until the solution was turned to light green color. Both 2-aminobenzamide (68 mg, 0.5 mmol) and 4-methoxybenzylamine (96 mg, 0.7 mmol) substrates were dissolved in dioxane (1 mL), and the solution was added to the reaction tube. The tube was brought out of the glove box and was stirred in an oil bath set at 140 °C for 20 h. The reaction tube was taken out of the oil bath, and it was cooled to room temperature. The resulting solution was filtered through a short silica gel column by eluting with CH_2Cl_2 (10 mL), and the filtrate was analyzed by GC-MS. Analytically pure product **4-13c** was isolated by a simple column chromatography on silica gel (280-400 mesh, hexanes/EtOAc).

6.4.4.1 X-ray Crystallography Data for 4-12i

Colorless single crystals of **4-12i** were grown in dichloromethane/*n*-hexane/Ethylacetate at room temperature. A suitable crystal with the dimension of 0.643 × 0.052 × 0.02 mm^3 was selected and analyzed. The 2-phenylquinazoline moiety has a planar conjugated structure. The 4-phenyl group is rotated out of its plane and is disordered over 2 equally populated positions. The disorder of the 4-phenyl groups within the stacks is apparently caused by two possible equivalent alternated patterns of their edge-to-face arrangement both within the stacks and between them.

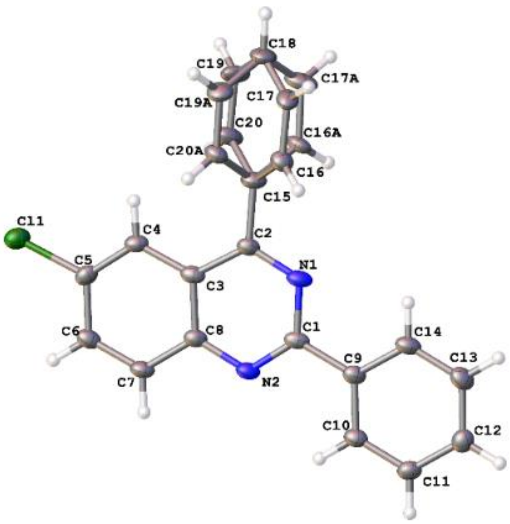

Figure 6.17: Molecular Structure of **4-12i**

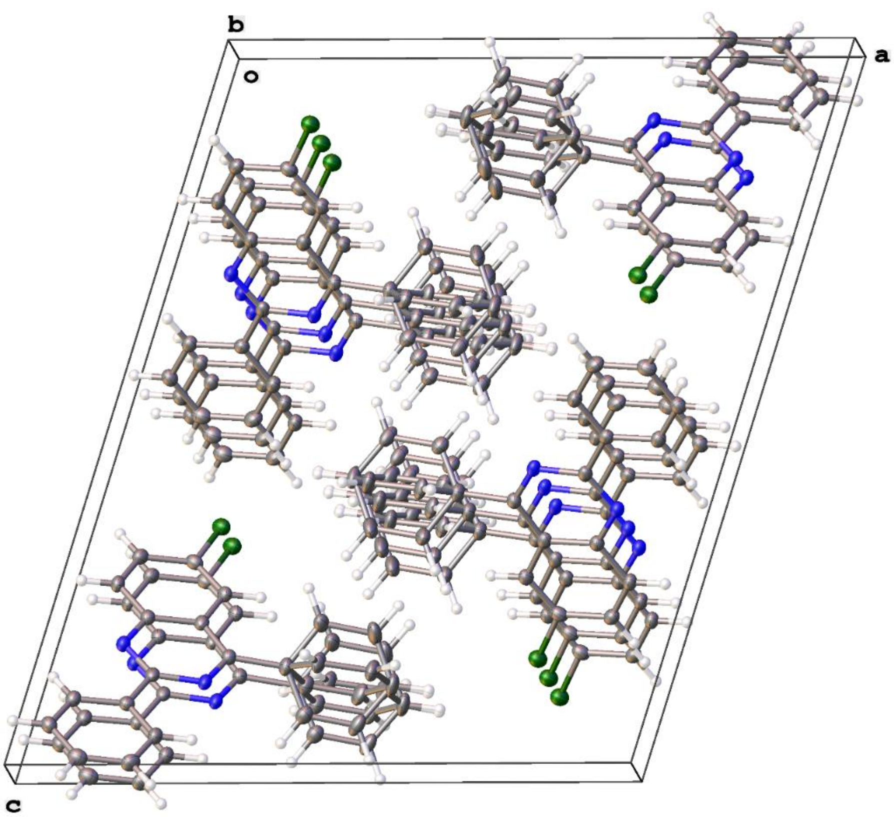

Figure 6.18: Crystal Packing of **4-12i**

Table 6.9: Crystal Data and Structure Refinement for **4-12i**

Identification code	yi3p
Empirical formula	$C_{20}H_{13}ClN_2$
Formula weight	316.77
Temperature/K	100.15
Crystal system	monoclinic
Space group	$P2_1/c$
a/Å	16.1612(10)
b/Å	4.9257(4)
c/Å	19.6178(17)
α/°	90
β/°	106.980(8)
γ/°	90
Volume/Å^3	1493.6(2)
Z	4
ρ_{calc}g/cm^3	1.409
μ/mm^{-1}	2.248
F(000)	656.0
Crystal size/mm^3	0.643 × 0.052 × 0.02
Radiation	CuKα (λ = 1.54184)
2Θ range for data collection/°	9.428 to 141.218
Index ranges	$-19 \le h \le 19$, $-6 \le k \le 5$, $-23 \le l \le 23$
Reflections collected	12968
Independent reflections	2793 [R_{int} = 0.0568, R_{sigma} = 0.0355]
Data/restraints/parameters	2793/0/244
Goodness-of-fit on F^2	1.050
Final R indexes [I>=2σ (I)]	R_1 = 0.0619, wR_2 = 0.1462
Final R indexes [all data]	R_1 = 0.0716, wR_2 = 0.1545
Largest diff. peak/hole / e Å^{-3}	0.43/-0.97

6.4.4.2 X-ray Crystallographic Data for 4-12k

Colorless single crystals of **4-12k** were grown in dichloromethane/*n*-hexane/EtOAc at room temperature. A suitable crystal with the dimension of 0.61 × 0.03 × 0.02 mm^3 was selected and analyzed. The 2-phenylquinazoline moiety has a planar conjugated structure. The 4-phenyl group is rotated out of its plane and is disordered over

2 equally populated positions. The molecules form translational stacks along y axis. The disorder of the 4-phenyl groups within the stacks is apparently caused by two possible equivalent alternated patterns of their edge-to-face arrangement both within the stacks and between them.

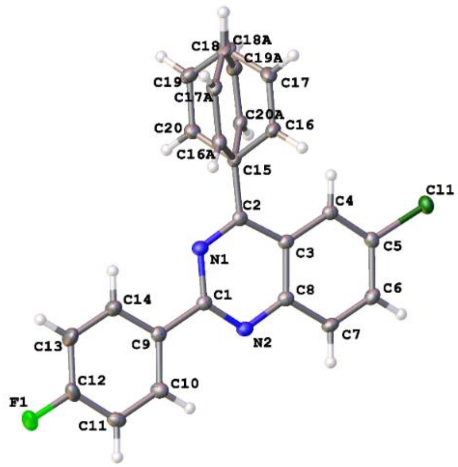

Figure 6.19: Molecular Structure of **4-12k**

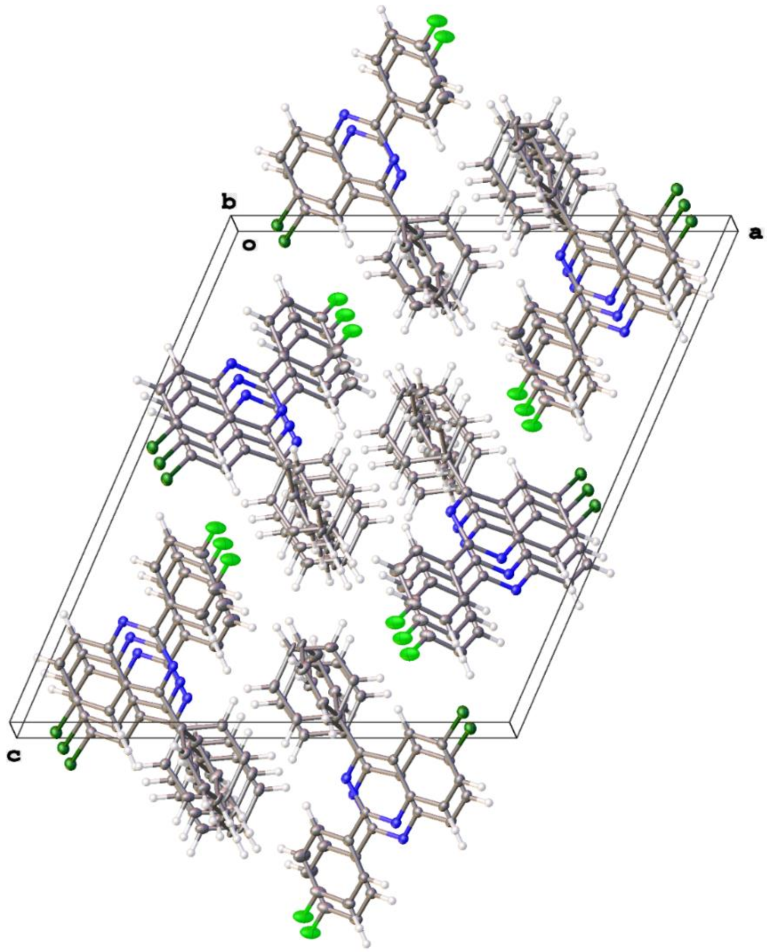

Figure 6.20: Crystal Packing of **4-12k**

Table 6.10: Crystal Data and Structure Refinement for **4-12k**

Identification code	yi3n
Empirical formula	$C_{20}H_{12}ClFN_2$
Formula weight	334.77
Temperature/K	446.15
Crystal system	monoclinic
Space group	$P2_1/c$
a/Å	17.3595(3)
b/Å	4.85966(9)
c/Å	19.2750(4)
α/°	90
β/°	113.162(2)
γ/°	90
Volume/Å^3	1494.99(6)
Z	4

ρ_{calc}g/cm^3	1.487
μ/mm^{-1}	2.379
F(000)	688.0
Crystal size/mm^3	0.61 × 0.03 × 0.02
Radiation	CuKα (λ = 1.54184)
2Θ range for data collection/°	9.318 to 141.362
Index ranges	$-20 \leq h \leq 21$, $-5 \leq k \leq 5$, $-23 \leq l \leq 23$
Reflections collected	14159
Independent reflections	2832 [R_{int} = 0.0454, R_{sigma} = 0.0320]
Data/restraints/parameters	2832/24/262
Goodness-of-fit on F^2	1.052
Final R indexes [I>=2σ (I)]	R_1 = 0.0346, wR_2 = 0.0895
Final R indexes [all data]	R_1 = 0.0429, wR_2 = 0.0957
Largest diff. peak/hole / e Å^{-3}	0.28/-0.31

6.4.4.3 X-ray Crystallographic Data for 4-13c

Colorless single crystals of **4-13c** were grown in hexanes/EtOAc at room temperature. A suitable crystal with the dimension of 0.37 × 0.081 × 0.049 mm^3 was selected and analyzed. The molecule has an overall planar shape with the OMe group conjugated with the adjacent benzene ring. The molecules form centrosymmetric H-bonded dimers packed into translational stacks along y axis.

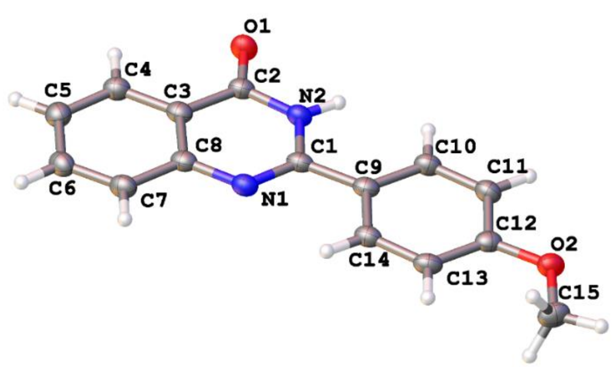

Figure 6.21: Molecular Structure of **4-13c**

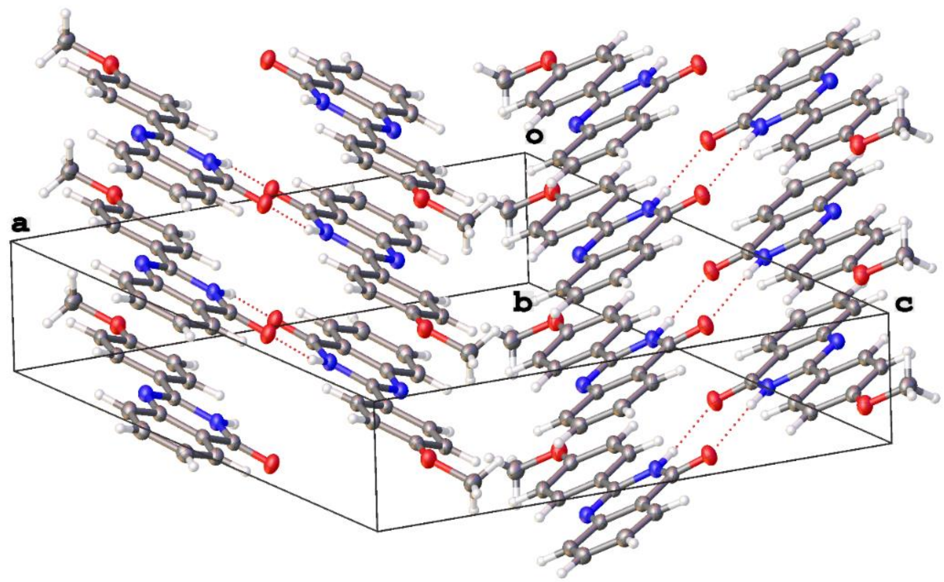

Figure 6.22: Crystal Packing of **4-13c**

Table 6.11: Crystal Data and Structure Refinement for **4-13c**

Identification code	yi3t
Empirical formula	$C_{15}H_{12}N_2O_2$
Formula weight	252.27
Temperature/K	100.15
Crystal system	monoclinic
Space group	$P2_1/n$
a/Å	16.2243(8)
b/Å	3.8498(2)
c/Å	19.0475(13)
α/°	90
β/°	96.405(5)
γ/°	90
Volume/Å^3	1182.30(12)
Z	4
ρ_{calc}g/cm^3	1.417
μ/mm^{-1}	0.782
F(000)	528.0
Crystal size/mm^3	0.37 × 0.081 × 0.049
Radiation	CuKα (λ = 1.54184)
2Θ range for data collection/°	7.588 to 141.582
Index ranges	$-19 \leq h \leq 19$, $-3 \leq k \leq 4$, $-22 \leq l \leq 22$

Reflections collected	10343
Independent reflections	2252 [R_{int} = 0.0330, R_{sigma} = 0.0182]
Data/restraints/parameters	2252/0/174
Goodness-of-fit on F^2	1.074
Final R indexes [I>=2σ (I)]	R_1 = 0.0435, wR_2 = 0.1259
Final R indexes [all data]	R_1 = 0.0458, wR_2 = 0.1301
Largest diff. peak/hole / e Å^{-3}	0.25/-0.23

6.4.4.4 X-ray Crystallography Data for 4-13t

Colorless single crystals of **4-13t** were grown in Ethylacetate/n-hexanes at room temperature. A suitable crystal with the dimension of 0.12 × 0.07 × 0.05 mm^3 was selected and analyzed. The structure has two symmetrically independent molecules. They have practically identical dihedral angle between their cyclic moieties – 44.6 and 45.0° but the difference in planarity of methoxy group is more perceptible – 5.1 vs. 12.3°. In the crystals the molecules form stacks along x axis where both independent molecules alternate in a head-to-head fashion. There are no pi-pi interactions in the stacks, rather some C-H…pi contacts.

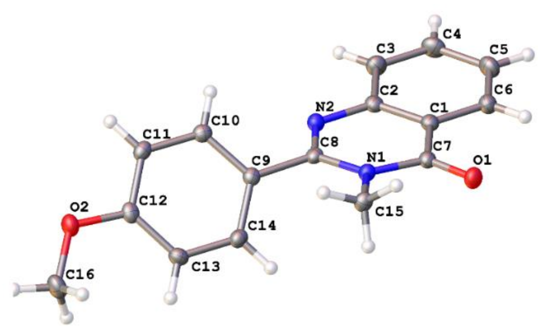

Figure 6.23: Molecular Structure of **4-13t**

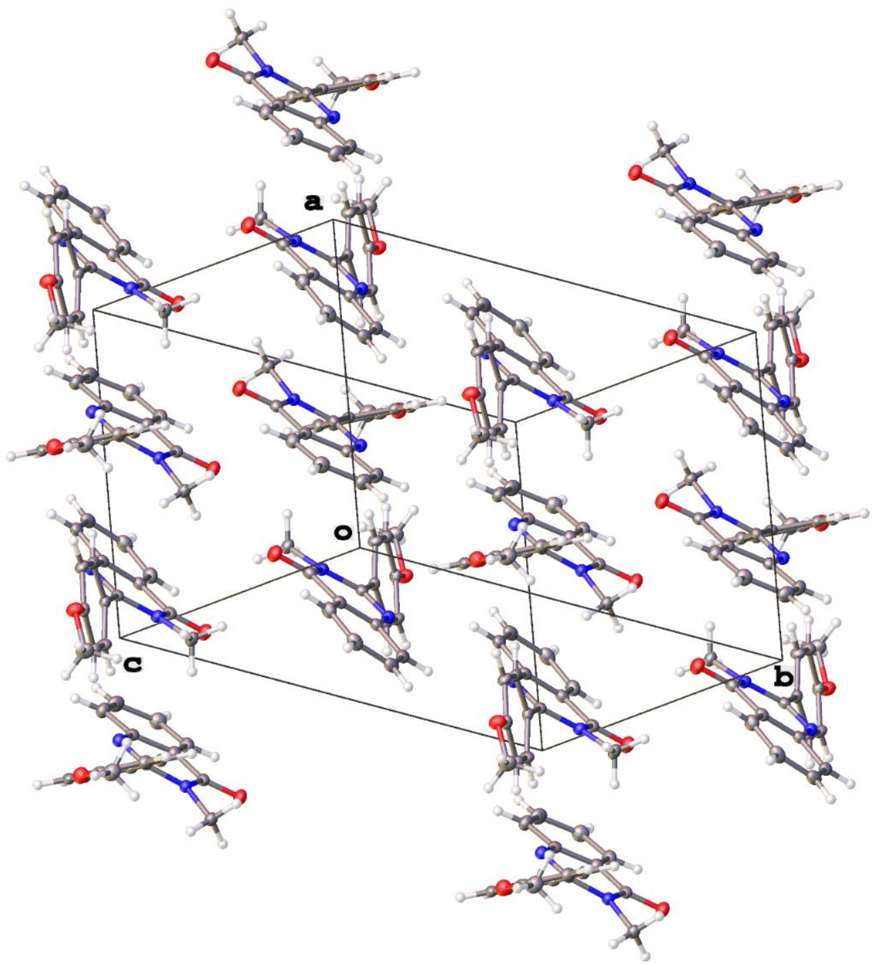

Figure 6.24: Crystal Packing of **4-13t**

Table 6.12: Crystal Data and Structure Refinement for **4-13t**

Identification code	yi4h
Empirical formula	$C_{16}H_{14}N_2O_2$
Formula weight	266.29
Temperature/K	101(1)
Crystal system	triclinic
Space group	P-1
a/Å	9.6896(4)
b/Å	12.6773(6)
c/Å	12.8491(4)
α/°	118.075(4)
β/°	91.014(3)
γ/°	109.265(4)
Volume/Å^3	1285.98(10)
Z	4

ρ_{calc}g/cm^3	1.375
μ/mm^{-1}	0.092
F(000)	560.0
Crystal size/mm^3	0.12 × 0.07 × 0.05
Radiation	MoKα (λ = 0.71073)
2Θ range for data collection/°	6.48 to 59.482
Index ranges	$-13 \leq h \leq 13$, $-17 \leq k \leq 17$, $-17 \leq l \leq 16$
Reflections collected	28972
Independent reflections	6544 [R_{int} = 0.0354, R_{sigma} = 0.0349]
Data/restraints/parameters	6544/0/365
Goodness-of-fit on F^2	1.057
Final R indexes [I>=2σ (I)]	R_1 = 0.0458, wR_2 = 0.1087
Final R indexes [all data]	R_1 = 0.0640, wR_2 = 0.1213
Largest diff. peak/hole / e Å^{-3}	0.29/-0.26

6.4.4.5 X-ray Crystallography Data for 4-13aa

Colorless single crystals of **4-13aa** were grown in EtOAc/n-hexanes at room temperature. A suitable crystal with the dimension of 0.646 × 0.171 × 0.065 mm^3 was selected and analyzed. The structure contains 2 symmetrically independent molecules differing by conformation along C2-C9 bond – the dihedral angle N1-C2-C9-C14 is -84.4(2)° in one molecule and -68.1(2)° in another one. Both molecules represent the same S,S,S-enantiomer. The absolute configuration was established beyond doubts [Flack parameter is 0.01(5)]. The molecules form H-bonded quasi-centrosymmetric dimers through N-H…O interactions. The molecules are also stacked along x axis with quasi-centrosymmetric overlap of quinazolone moieties.

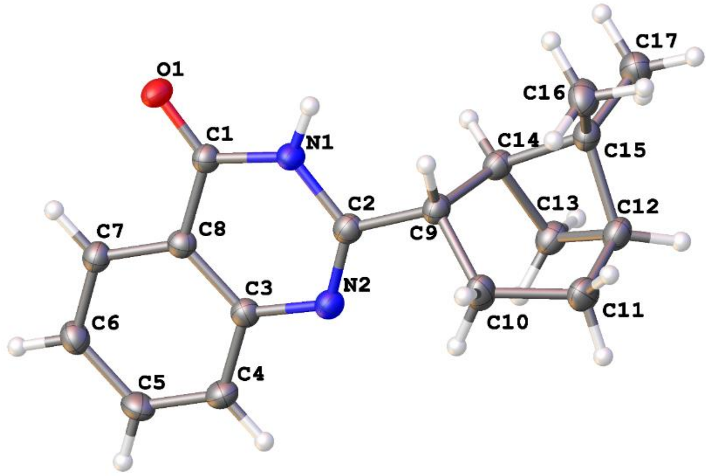

Figure 6.25: Molecular Structure of **4-13aa**

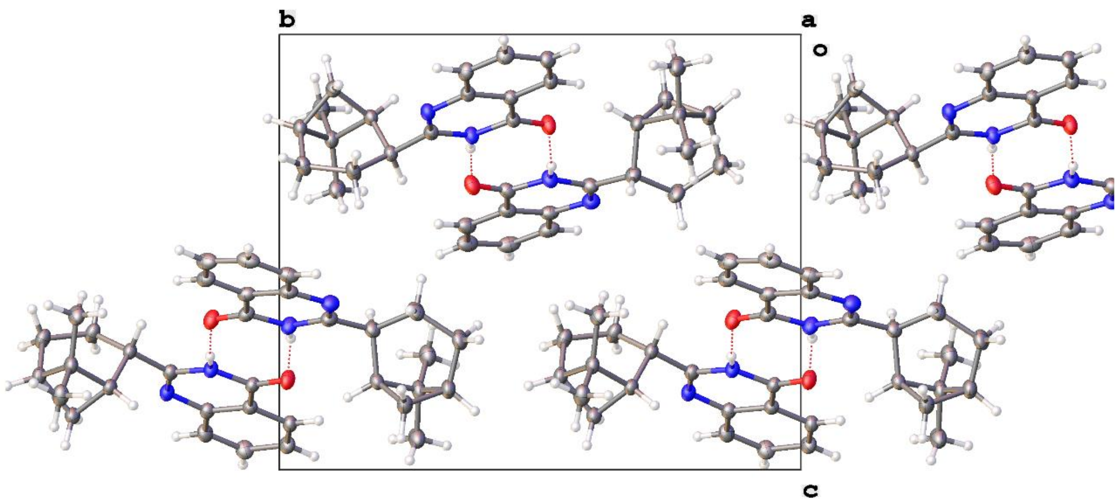

Figure 6.26: Crystal Packing of **4-13aa**

Table 6.13: Crystal Data and Structure Refinement for **4-13aa**

Identification code	yi3z
Empirical formula	$C_{17}H_{20}N_2O$
Formula weight	268.35
Temperature/K	101.3(10)
Crystal system	monoclinic
Space group	$P2_1$
a/Å	7.33998(9)
b/Å	15.20169(11)

c/Å	13.16998(13)
α/°	90
β/°	105.9526(11)
γ/°	90
Volume/Å^3	1412.92(2)
Z	4
ρ_{calc}g/cm^3	1.262
μ/mm^{-1}	0.620
F(000)	576.0
Crystal size/mm^3	0.646 × 0.171 × 0.065
Radiation	CuKα (λ = 1.54184)
2Θ range for data collection/°	6.98 to 141.282
Index ranges	$-8 \leq h \leq 8$, $-18 \leq k \leq 18$, $-15 \leq l \leq 16$
Reflections collected	25935
Independent reflections	5350 [R_{int} = 0.0201, R_{sigma} = 0.0127]
Data/restraints/parameters	5350/1/366
Goodness-of-fit on F^2	1.029
Final R indexes [I>=2σ (I)]	R_1 = 0.0303, wR_2 = 0.0814
Final R indexes [all data]	R_1 = 0.0308, wR_2 = 0.0820
Largest diff. peak/hole / e Å^{-3}	0.20/-0.17
Flack parameter	0.01(5)

6.4.4.6 X-ray Crystallography Data for 4-13ab

Colorless single crystals of **4-13ab** were grown in EtOAc/Dichloromethane/n-pentanes at room temperature. A suitable crystal with the dimension of 0.528 × 0.083 × 0.016 mm^3 was selected and analyzed. The molecule represents a C9(**R**), C13(**S**)-enantiomer established objectively with a good probability [Flack parameter 0.18(8)]. The saturated 6-membered rings are trans-fused that corresponds to **R**-configuration of chiral center at C22. The Me-groups occupy axial positions and quinazolinone group – an equatorial one (the ring C9…C13, C22 has a chair conformation). The ring annealed with benzene moiety has C22-sofa conformation. In the crystal, the molecules form H-bonded dimers over crystallographic 2-fold axes through N-H…O interactions. The dimers are loosely stacked (at 3.65 Å and 169°).

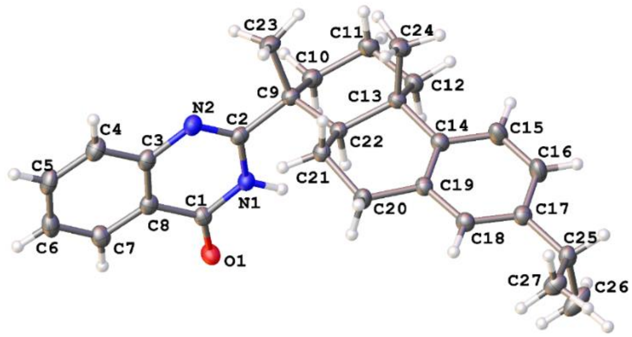

Figure 6.27: Molecular Structure of **4-13ab**

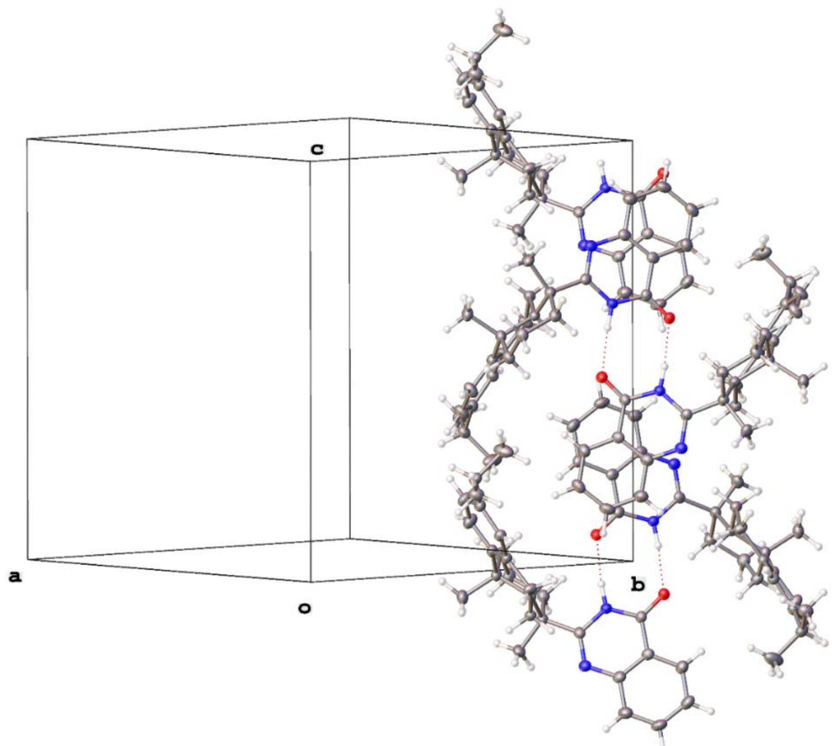

Figure 6.28: Crystal Packing of **4-13ab**

Table 6.14: Crystal Data and Structure Refinement for **4-13ab**

Identification code	yi4n
Empirical formula	$C_{27}H_{32}N_2O$
Formula weight	400.54
Temperature/K	100.00(10)
Crystal system	tetragonal
Space group	$P4_12_12$
a/Å	16.41058(8)

b/Å	16.41058(8)
c/Å	16.10936(19)
α/°	90
β/°	90
γ/°	90
Volume/Å^3	4338.37(7)
Z	8
ρ_{calc}g/cm^3	1.226
μ/mm^{-1}	0.571
F(000)	1728.0
Crystal size/mm^3	0.528 × 0.083 × 0.016
Radiation	CuKα (λ = 1.54184)
2Θ range for data collection/°	7.618 to 141.342
Index ranges	$-20 \leq h \leq 20$, $-15 \leq k \leq 19$, $-17 \leq l \leq 19$
Reflections collected	38387
Independent reflections	4137 [R_{int} = 0.0280, R_{sigma} = 0.0132]
Data/restraints/parameters	4137/0/280
Goodness-of-fit on F^2	1.056
Final R indexes [I>=2σ (I)]	R_1 = 0.0283, wR_2 = 0.0713
Final R indexes [all data]	R_1 = 0.0297, wR_2 = 0.0724
Largest diff. peak/hole / e Å^{-3}	0.16/-0.12
Flack parameter	0.13(8)

6.4.5.1 Characterization Data of the Quinazolin Compounds Listed in Table 4.3

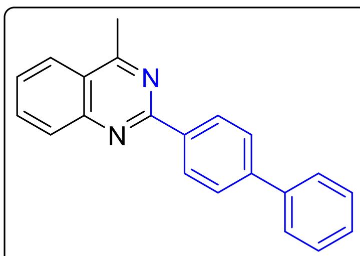

4-12p

2-([1,1'-Biphenyl]-4-yl)-4-methylquinazoline (4-12p): A 1,4-dioxane (2.0 mL) solution of complex **2-10** (9 mg, 3 mol %), **2-16** (8 mg, 10 mol %), 2-aminophenylethanone (68 mg, 0.5 mmol), and 4-phenylbenzylamine (128 mg, 0.7 mmol) was stirred at 140 °C for 20 h. The product **4-12p** was isolated by column chromatography on silica gel (hexanes/EtOAc = 100:1–10:1; TLC: R_f = 0.5 (10% EtOAc in hexanes)). Yield = 101 mg (68%). Data for **4-12p:** ^{1}H NMR (400 MHz, $CDCl_3$) δ 8.71 (d, *J* = 8.4 Hz, 2H), 8.11 (t, *J* = 8.8 Hz, 2H), 7.93–7.83 (m, 1H), 7.78 (d, *J* = 8.4 Hz, 2H), 7.74–7.67 (m, 2H), 7.59 (t, *J* = 7.6 Hz, 1H), 7.52–7.45

(m, 2H), 7.43–7.35 (m, 1H), 3.04 (s, 3H) ppm; $^{13}C\{^1H\}$ NMR (100 MHz, $CDCl_3$) δ 168.4, 159.8, 150.2, 143.1, 140.7, 137.0, 133.6, 129.0, 128.8, 127.6, 127.3, 127.2, 126.9, 125.0, 123.0, 22.1 ppm; GC-MS for $C_{21}H_{16}N_2$, m/z = 296 (M^+). HRMS (ESI-TOF) m/z: $[M + H]^+$ Calcd for $C_{21}H_{16}N_2H$ 297.1386; Found 297.1399.

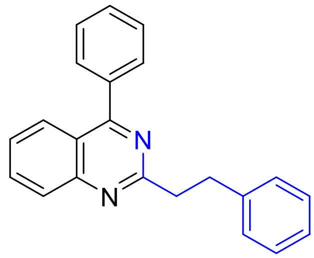

4-12s

2-Phenethyl-4-phenylquinazoline (4-12s): A 1,4-dioxane (2.0 mL) solution of complex **2-10** (9 mg, 3 mol %), **2-16** (8 mg, 10 mol %), 2-aminobenzophenone (99 mg, 0.5 mmol), and 3-phenyl-1-propanamine (95 mg, 0.7 mmol) was stirred at 140 °C for 20 h. The product **4-12s** was isolated by column chromatography on silica gel (hexanes/EtOAc = 80:1–10:1; TLC: R_f = 0.3 (10% EtOAc in hexanes)). Yield = 104 mg, (67%). Data for **4-12s:** ^1H NMR (400 MHz, $CDCl_3$) δ 8.06 (d, J = 8.9 Hz, 2H), 7.86 (t, J = 7.8 Hz, 1H), 7.78–7.71 (m, 2H), 7.59–7.48 (m, 4H), 7.35–7.23 (m, 4H), 7.22–7.15 (m, 1H), 3.54–3.46 (m, 2H), 3.35–3.27 (m, 2H) ppm; $^{13}C\{^1H\}$ NMR (100 MHz, $CDCl_3$) δ 168.6, 166.0, 151.3, 141.6, 137.3, 133.6, 129.9, 129.9, 128.6, 128.5, 128.3, 128.3, 127.0, 126.8, 125.9, 121.2, 41.5, 34.8 ppm; GC-MS for $C_{22}H_{18}N_2$ m/z = 310 (M^+). HRMS (ESI-TOF) m/z: $[M + H]^+$ Calcd for $C_{22}H_{18}N_2H$ 311.1543; Found 311.1563.

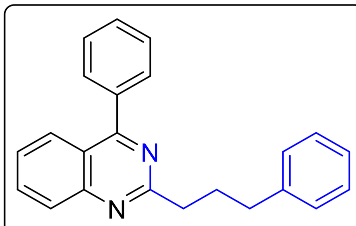

4-12t

2-Phenethyl-4-phenylquinazoline (4-12t): A 1,4-dioxane (2.0 mL) solution of complex **2-10** (9 mg, 3 mol %), **2-16** (8 mg, 10 mol %), 2-aminobenzophenone (99 mg, 0.5 mmol), and 4-benzenebutanamine (104 mg, 0.7 mmol) was stirred at 140 °C for 20 h. The product **4-12t** was isolated by column chromatography on silica gel (hexanes/EtOAc = 80:1–10:1; TLC:

R_f = 0.3 (10% EtOAc in hexanes)). Yield = 114 mg, (70%). Data for **4-12t:** ^{1}H NMR (400 MHz, $CDCl_3$) δ 8.04 (d, *J* = 8.5 Hz, 2H), 7.85 (t, *J* = 8.6 Hz, 1H), 7.78–7.70 (m, 2H), 7.60–7.53 (m, 3H), 7.51 (t, *J* = 8.6 Hz, 1H), 7.29–7.20 (m, 4H), 7.17–7.11 (m, 1H), 3.23 (t, *J* = 7.7 Hz, 2H), 2.79 (t, *J* = 7.8 Hz, 2H), 2.30 (pentet, *J* = 7.7 Hz, 2H) ppm; ^{13}C{^{1}H} NMR (100 MHz, $CDCl_3$) δ 168.6, 166.7, 151.3, 142.2, 137.3, 133.5, 129.9, 129.8, 128.6, 128.5, 128.2, 127.0, 126.7, 125.7, 121.2, 39.6, 35.8, 30.6 ppm; GC-MS for $C_{23}H_{20}N_2$ m/z = 324 (M^+). HRMS (ESI-TOF) m/z: $[M + H]^+$ Calcd for $C_{22}H_{18}N_2H$ 325.1656; Found 325.1640.

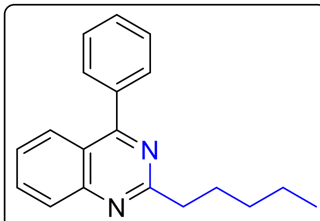

4-12v

2-Pentyl-4-phenylquinazoline (4-12v): A 1,4-dioxane (2.0 mL) solution of complex **2-10** (9 mg, 3 mol %), **2-16** (8 mg, 10 mol %), 2-aminobenzophenone (99 mg, 0.5 mmol), and 1-hexylamine (71 mg, 0.7 mmol) was stirred at 140 °C for 20 h. The product **4-12v** was isolated by column chromatography on silica gel (hexanes/EtOAc = 100:1–10:1; TLC: R_f = 0.5 (10% EtOAc in hexanes)). Yield = 62 mg (45%). Data for **4-12v:** ^{1}H NMR (400 MHz, $CDCl_3$) δ 8.12–8.00 (m, 2H), 7.86 (td, *J* = 7.6, 1.2 Hz, 1H), 7.80–7.71 (m, 2H), 7.61–7.54 (m, 3H), 7.52 (t, *J* = 7.9 Hz, 1H), 3.17 (t, *J* = 7.9 Hz, 2H), 2.0–1.91 (m, 2H), 1.50–1.34 (m, 4H), 0.91 (t, *J* = 7.1 Hz, 3H) ppm; ^{13}C{^{1}H} NMR (100 MHz, $CDCl_3$) δ 168.6, 167.2, 151.1, 137.3, 133.6, 129.9, 129.8, 128.6, 128.1, 127.0, 126.7, 121.2, 40.0, 31.8, 28.8, 22.6, 14.1 ppm; GC-MS for $C_{19}H_{20}N_2$ m/z = 276 (M^+); HRMS (ESI-TOF) m/z: $[M + H]^+$ Calcd for $C_{19}H_{20}N_2H$ 277.1699; Found 277.1665.

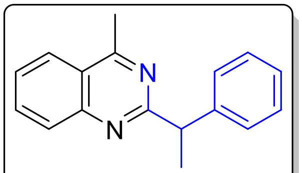

4-12x

4-Methyl-2-(1-phenylethyl)quinazoline (4-12x): A 1,4-dioxane (2.0 mL) solution of complex **2-10** (9 mg, 3 mol %), **2-16** (8 mg, 10 mol %), 2-aminophenylethanone (68 mg, 0.5 mmol), and (*R*)-(+)-β-methylphenethylamine (95 mg, 0.7 mmol) was stirred at 140 °C for 20 h. The product **4-12x** was isolated by column chromatography on silica gel (hexanes/EtOAc = 100:1–10:1; TLC: R_f = 0.5 (20% EtOAc in hexanes)). Yield = 98 mg (79%). Data for **4-12x:** ^{1}H NMR (400 MHz, $CDCl_3$) δ 8.05–7.97 (m, 2H), 7.82 (ddd, *J* = 8.4, 6.9, 1.4 Hz, 1H), 7.55 (ddd, *J* = 8.3, 6.9, 1.3 Hz, 1H), 7.52–7.47 (m, 2H), 7.31–7.26 (m, 2H), 7.20–7.15 (m, 1H), 4.53 (q, *J* = 7.2 Hz, 1H), 2.89 (s, 3H), 1.82 (d, *J* = 7.2 Hz, 3H) ppm; ^{13}C{^{1}H} NMR (100 MHz, $CDCl_3$) δ 171.6, 168.3, 149.9, 144.5, 133.2, 128.8, 128.2, 127.9, 126.6, 126.3, 124.8, 122.7, 49.1, 21.9, 20.8 ppm; GC-MS for $C_{17}H_{16}N_2$ m/z = 248 (M^+); HRMS (ESI-TOF) m/z: $[M + H]^+$ Calcd for $C_{17}H_{16}N_2H$ 249.1386, Found 249.1353; $[\alpha]_D^{22}$ = +5.2 (c = 0.1 g/100 mL in CH_2Cl_2).

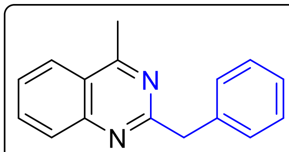

4-12y

2-Benzyl-4-methyl-quinazoline (4-12y): A 1,4-dioxane (2.0 mL) solution of complex **2-10** (9 mg, 3 mol %), **2-16** (8 mg, 10 mol %), 2-aminophenylethanone (68 mg, 0.5 mmol), and 1-amino-2-phenylethane (85 mg, 0.7 mmol) was stirred at 140 °C for 20 h. The product **4-12y** was isolated by column chromatography on silica gel (hexanes/EtOAc = 80:1–20:1; TLC: R_f = 0.4 (20% EtOAc in hexanes)). Yield = 62 mg, (53%). Data for **4-12y:** ^{1}H NMR (400 MHz, $CDCl_3$) δ 8.03 (d, *J* = 8.5 Hz, 1H), 7.98 (d, *J* = 8.6 Hz, 1H), 7.86–7.79 (m, 1H), 7.59–7.52 (m, 1H), 7.48–7.42 (m, 2H), 7.32–7.26 (m, 2H), 7.23–7.17 (m, 1H), 4.41 (s, 2H), 2.90 (s, 3H) ppm; ^{13}C{^{1}H} NMR (100 MHz, $CDCl_3$) δ 168.5, 165.1, 150.0, 138.6, 133.4, 129.2, 128.6, 128.3, 126.8, 126.3, 124.8, 122.5, 46.3, 21.8 ppm; GC-MS for $C_{16}H_{14}N_2$ m/z = 234 (M^+); HRMS (ESI-TOF) m/z: $[M + H]^+$ Calcd for $C_{16}H_{14}N_2H$ 235.1230, Found 235.1203.

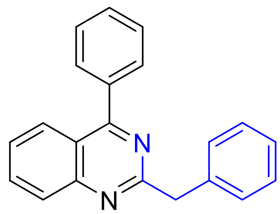

4-12z

2-Benzyl-4-phenylquinazoline (4-12z): A 1,4-dioxane (2.0 mL) solution of complex **2-10** (9 mg, 3 mol %), **2-16** (8 mg, 10 mol %), 2-aminobenzophenone (99 mg, 0.5 mmol), and 1-amino-2-phenylethane (85 mg, 0.7 mmol) was stirred at 140 °C for 20 h. The product **4-12z** was isolated by column chromatography on silica gel (hexanes/EtOAc = 80:1–10:1; TLC: R_f = 0.6 (20% EtOAc in hexanes). Yield = 99 mg (67%). Data for **4-12z:** ^{1}H NMR (400 MHz, $CDCl_3$) δ 8.12–7.99 (m, 2H), 7.83 (t, J = 7.7 Hz, 1H), 7.79–7.69 (m, 2H), 7.56–7.49 (m, 5H), 7.37–7.14 (m, 4H), 4.52 (s, 2H) ppm; $^{13}C\{^1H\}$ NMR (100 MHz, $CDCl_3$) δ 168.6, 165.2, 151.5, 138.6, 137.2, 133.4, 130.0, 129.8, 129.2, 128.7, 128.5, 128.5, 128.3, 126.9, 126.3, 121.2, 46.3 ppm; GC-MS for $C_{21}H_{16}N_2$ m/z = 296 (M^+); HRMS (ESI-TOF) m/z: $[M + H]^+$ Calcd for $C_{21}H_{16}N_2H$ 297.1386, Found 297.1352.

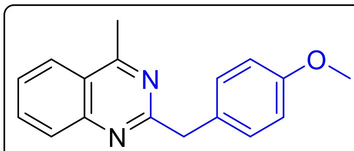

4-12aa

2-(4-Methoxybenzyl)-4-methylquinazoline (4-12aa): A 1,4-dioxane (2.0 mL) solution of complex **2-10** (9 mg, 3 mol %), **2-16** (8 mg, 10 mol %), 2-aminophenylethanone (68 mg, 0.5 mmol), and 2-(4-methoxyphenyl)ethanamine (106 mg, 0.7 mmol) was stirred at 140 °C for 20 h. The product **4-12aa** was isolated by column chromatography on silica gel (hexanes/EtOAc = 80:1–20:1; TLC: R_f = 0.3 (20% EtOAc in hexanes)). Yield = 63 mg (48%). Data for **4-12aa:** ^{1}H NMR (400 MHz, $CDCl_3$) δ 8.03 (d, J = 8.3 Hz, 1H), 7.98 (d, J = 8.5 Hz, 1H), 7.83 (dd, J = 8.5, 1.6 Hz, 1H), 7.55 (dd, J = 8.3, 1.6 Hz, 1H), 7.37 (d, J = 8.6 Hz, 2H), 6.83 (d, J = 8.6 Hz, 2H), 4.34 (s, 2H), 3.76 (s, 3H), 2.90 (s, 3H) ppm;

$^{13}C\{^1H\}$ NMR (100 MHz, $CDCl_3$) δ 168.6, 165.3, 158.2, 149.9, 133.5, 130.7, 130.1, 128.6, 126.8, 124.9, 122.5, 113.8, 55.2, 45.3, 21.8 ppm; GC-MS for $C_{17}H_{16}N_2O$ m/z = 264 (M^+); HRMS (ESI-TOF) m/z: $[M + H]^+$ Calcd for $C_{17}H_{16}N_2OH$ 265.1335, Found 265.1305.

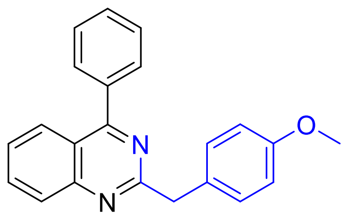

4-12ab

2-(4-Methoxybenzyl)-4-phenylquinazoline (4-12ab): A 1,4-dioxane (2.0 mL) solution of complex **2-10** (9 mg, 3 mol %), **2-16** (8 mg, 10 mol %), 2-aminobenzophenone (99 mg, 0.5 mmol), and 2-(4-methoxyphenyl)ethanamine (106 mg, 0.7 mmol) was stirred at 140 °C for 20 h. The product **4-12ab** was isolated by column chromatography on silica gel (hexanes/EtOAc = 80:1–20:1; TLC: R_f = 0.3 (20% EtOAc in hexanes). Yield = 124 mg, (76%). Data for **4-12ab:** ^1H NMR (400 MHz, $CDCl_3$) δ 8.11 (d, J = 8.5 Hz, 1H), 8.07 (d, J = 8.5 Hz, 1H), 7.87 (td, J = 7.6, 1.1 Hz, 1H), 7.79–7.71 (m, 2H), 7.59–7.55 (m, 3H), 7.54 (td, J = 7.6, 0.9 Hz, 1H), 7.45 (d, J = 8.6 Hz, 2H), 6.85 (d, J = 8.6 Hz, 2H), 4.46 (s, 2H), 3.77 (s, 3H) ppm; $^{13}C\{^1H\}$ NMR (100 MHz, $CDCl_3$) δ 168.7, 165.5, 158.2, 151.5, 137.3, 133.5, 130.8, 130.2, 130.0, 129.9, 128.5, 128.4, 126.9, 126.9, 121.2, 113.7, 55.2, 45.4 ppm; GC-MS for $C_{22}H_{18}N_2O$ m/z = 326 (M^+); HRMS (ESI-TOF) m/z: $[M + H]^+$ Calcd for $C_{22}H_{18}N_2OH$ 327.1492, Found 327.1467.

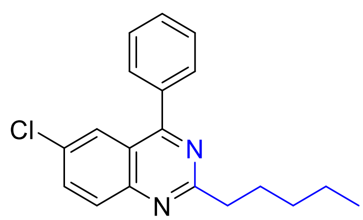

4-12ac

6-Chloro-2-pentyl-4-phenylquinazoline (4-12ac): A 1,4-dioxane (2.0 mL) solution of complex **2-10** (9 mg, 3 mol %), **2-16** (8 mg, 10 mol %), 2-amino-5-chlorobenzylphenone (116 mg, 0.5 mmol), and 1-hexylamine (71 mg, 0.7 mmol) was stirred at 140 °C for

20 h. The product **4-12ac** was isolated by column chromatography on silica gel (hexanes/EtOAc = 100:1–10:1; TLC: R_f = 0.8 (20% EtOAc in hexanes)). Yield = 78 mg (50%). Data for **4-12ac:** ^{1}H NMR (400 MHz, $CDCl_3$) δ 8.03 (d, *J* = 2.3 Hz, 1H), 8.02 (s, 1H), 7.80 (dd, *J* = 9.1, 2.3 Hz, 1H), 7.78–7.68 (m, 2H), 7.64–7.53 (m, 3H), 3.16 (t, *J* = 7.9 Hz, 2H), 2.01–1.90 (m, 2H), 1.50–1.33 (m, 4H), 0.91 (t, *J* = 7.1 Hz, 3H) ppm; ^{13}C{^{1}H} NMR (100 MHz, $CDCl_3$) δ 167.8, 167.5, 149.7, 136.8, 134.5, 132.3, 130.1, 129.9, 129.8, 128.8, 125.7, 121.7, 39.9, 31.8, 28.6, 22.5, 14.0 ppm; GC-MS for $C_{19}H_{19}ClN_2$ m/z = 310 (M^+); HRMS (ESI-TOF) m/z: $[M + H]^+$ Calcd for $C_{19}H_{19}ClN_2H$ 311.1310, Found 311.1300.

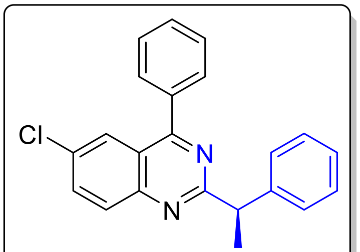

4-12ad

(*R*)-6-Chloro-4-phenyl-2-(1-phenylethyl)quinazoline (4-12ad): A 1,4-dioxane (2.0 mL) solution of complex **2-10** (9 mg, 3 mol %), **2-16** (8 mg, 10 mol %), 2-amino-5-chlorobenzylphenone (116 mg, 0.5 mmol), and (*R*)-(+)-β-methylphenethylamine (95 mg, 0.7 mmol) was stirred at 140 °C for 20 h. The product **4-12ad** was isolated by column chromatography on silica gel (hexanes/EtOAc = 100:1–10:1; TLC: R_f = 0.8 (20% EtOAc in hexanes)). Yield = 131 mg (76%). Data for **4-12ad:** ^{1}H NMR (400 MHz, $CDCl_3$) δ 8.14–7.98 (m, 2H), 7.85–7.71 (m, 3H), 7.66–7.51 (m, 5H), 7.31 (t, *J* = 7.5 Hz, 2H), 7.21 (t, *J* = 7.2 Hz, 1H), 4.67 (q, *J* = 7.1 Hz, 1H), 1.88 (d, *J* = 7.1 Hz, 3H) ppm; ^{13}C{^{1}H} NMR (100 MHz, $CDCl_3$) δ 168.7, 167.7, 149.7, 144.1, 136.9, 134.3, 132.5, 130.3, 130.2, 130.0, 128.7, 128.3, 128.0, 126.5, 125.6, 121.9, 49.0, 20.7 ppm; GC-MS for $C_{22}H_{17}ClN_2$ m/z = 344 (M^+); HRMS (ESI-TOF) m/z: $[M + H]^+$ Calcd for $C_{22}H_{17}ClN_2H$ 345.1153, Found 345.1118; $[\alpha]_D^{22}$ = +6.0 (c = 0.20 g/100 mL in CH_2Cl_2).

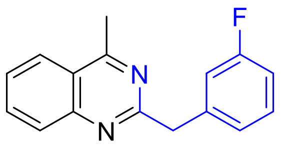

2-(3-fluorobenzyl)-4-methylquinazoline (4-12ae): A 1,4-dioxane (2.0 mL) solution of complex **2-10** (9 mg, 3 mol %), **2-16** (8 mg, 10 mol %), 2'-aminoacetophenone (68 mg, 0.5 mmol), and 3-fluorobenzeneethanamine (97 mg, 0.7 mmol) was stirred at 140 °C for 20 h. The product **4-12ae** was isolated by column chromatography on silica gel (hexanes/EtOAc = 100:1–10:1; TLC: R_f = 0.5 (10% EtOAc in hexanes). Yield = 81 mg, (64%). Data for **4-12ae:** ^{1}H NMR (400 MHz, $CDCl_3$) δ 8.06 (dd, *J* = 8.4, 0.7 Hz, 1H), 7.98 (dd, *J* = 8.4, 0.7 Hz, 1H), 7.85 (dd, *J* = 8.4, 1.4 Hz, 1H), 7.58 (dd, *J* = 8.3, 1.2 Hz, 1H), 7.26–7.12 (m, 3H), 6.92–6.86 (m, 1H), 4.38 (s, 2H), 2.92 (s, 3H) ppm; ^{13}C{^{1}H} NMR (100 MHz, $CDCl_3$) δ 168.7, 164.4, 162.8 (d, J_{CF} = 245.1 Hz), 150.0, 141.0 (d, J_{CF} = 7.6 Hz), 133.6, 129.7 (d, J_{CF} = 8.3 Hz), 128.6, 127.0, 124.9, 124.8 (d, J_{CF} = 2.8 Hz), 122.5, 116.1 (d, J_{CF} = 21.5 Hz), 113.3 (d, J_{CF} = 21.1 Hz), 45.9 (d, J_{CF} = 1.7 Hz), 21.8 ppm; GC-MS for $C_{16}H_{13}FN_2$ m/z = 252 (M^+). HRMS (ESI-TOF) m/z: $[M + H]^+$ Calcd for $C_{16}H_{13}FN_2H$ 253.1136; Found 253.1128.

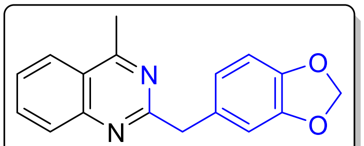

2-(Benzo[d][1,3]dioxol-5-ylmethyl)-4-methylquinazoline (4-12ag): A 1,4-dioxane (2.0 mL) solution of complex **2-10** (9 mg, 3 mol %), **2-16** (8 mg, 10 mol %), 2-aminophenylethanone (68 mg, 0.5 mmol), and 2-benzo[1,3]dioxol-5-yl-ethylamine (116 mg, 0.7 mmol) was stirred at 140 °C for 20 h. The product **4-12ag** was isolated by column chromatography on silica gel (hexanes/EtOAc = 80:1–20:1; TLC: R_f = 0.3 (20% EtOAc in hexanes)). Yield = 114 mg (82%). Data for **4-12ag:** ^{1}H NMR (400 MHz, $CDCl_3$) δ 8.02 (d, *J* = 8.3 Hz, 1H), 7.97 (d, *J* = 8.5 Hz, 1H), 7.82 (t, *J* = 7.7 Hz, 1H), 7.54 (t, *J* = 7.6 Hz, 1H), 6.96 (s, 1H), 6.89 (d, *J* = 8.0 Hz, 1H), 6.73 (d, *J* = 8.0 Hz, 1H), 5.88 (s, 2H), 4.30 (s, 2H), 2.90 (s, 3H) ppm; $^{13}C\{^{1}H\}$ NMR (100 MHz, $CDCl_3$) δ 168.6, 165.0, 149.9, 147.4, 146.0, 133.5, 132.3, 128.6, 126.8, 124.8, 122.4, 122.1, 109.6, 108.1, 100.7, 45.8, 21.8 ppm; GC-MS for $C_{17}H_{14}N_2O_2$ m/z = 278 (M^+). HRMS (ESI-TOF) m/z: $[M + H]^+$ Calcd for $C_{17}H_{14}N_2O_2H$ 279.1128; Found 279.1099.

6.4.5.2 Synthesis and Characterization of the Novel Quinazolinone Compounds Listed in Table 4.4

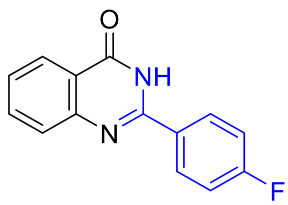

4-13d

2-(4-Fluorophenyl)quinazolin-4(3H)-one (4-13d): A 1,4-dioxane (2.0 mL) solution of complex **2-10** (9 mg, 3 mol %), **2-16** (8 mg, 10 mol %), anthranilamide (68 mg, 0.5 mmol), and 4-fluorobenzylamine (88 mg, 0.7 mmol) was stirred at 140 °C for 20 h. The product **4-13d** was isolated by column chromatography on silica gel (hexanes/EtOAc = 20:1–1:1; TLC: R_f = 0.3 (50% EtOAc in hexanes)). Yield = 79 mg, (66%). Data for **4-13d:** ^{1}H NMR (400 MHz, DMSO-d_6) δ 12.54 (br s, 1H), 8.28–8.19 (m, 2H), 8.15 (d, J = 7.9 Hz, 1H), 7.83 (t, J = 7.7 Hz, 1H), 7.73 (d, J = 8.1 Hz, 1H), 7.52 (t, J = 7.5 Hz, 1H), 7.44–7.34 (m, 2H) ppm; $^{13}C\{^{1}H\}$ NMR (100 MHz, DMSO-d_6) δ 164.1 (d, J_{CF} = 249.2 Hz), 162.3, 151.5, 148.7, 134.7, 130.4 (d, J_{CF} = 8.9 Hz), 129.3 (d, J_{CF} = 1.7 Hz), 127.5, 126.7, 125.9, 120.9, 115.7 (d, J_{CF} = 22.0 Hz) ppm; GC-MS for $C_{14}H_9FN_2O$, m/z = 240 (M^+); HRMS (ESI-TOF) m/z: $[M + H]^+$ Calcd for $C_{14}H_9FN_2OH$ 241.0772, Found 241.0744.

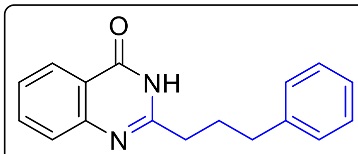

4-13i

2-(3-Phenylpropyl)quinazolin-4(3H)-one (4-13i): A 1,4-dioxane (2.0 mL) solution of complex **2-10** (9 mg, 3 mol %), **2-16** (8 mg, 10 mol %), anthranilamide (68 mg, 0.5 mmol), and 4-phenylbutylamine (104 mg, 0.7 mmol) was stirred at 140 °C for 20 h. The product **4-13i** was isolated by column chromatography on silica gel (hexanes/EtOAc = 20:1–1:1; TLC: R_f = 0.2 (50% EtOAc in hexanes)). Yield = 104 mg (79%). Data for **4-13i:** ^{1}H NMR (400 MHz, $CDCl_3$) δ 12.32 (br s, 1H), 8.26 (d, *J* = 7.9 Hz, 1H), 7.77 (t, *J* = 7.6 Hz, 1H), 7.70 (d, *J* = 8.1 Hz, 1H), 7.47 (t, *J* = 7.4 Hz, 1H), 7.28–7.13 (m, 5H), 2.96–2.71 (m, 4H), 2.25 (pentet, *J* = 7.6 Hz, 2H) ppm; ^{13}C{^{1}H} NMR (100 MHz, $CDCl_3$) δ 164.5, 156.6, 149.4, 141.3, 134.7, 128.4, 128.3, 127.1, 126.3, 126.1, 125.9, 120.4, 35.3, 35.3, 28.9 ppm; GC-MS for $C_{17}H_{16}N_2O$, m/z = 264 (M^+). HRMS (ESI-TOF) m/z: $[M + H]^+$ Calcd for $C_{17}H_{16}N_2OH$ 265.1335, Found 265.1309.

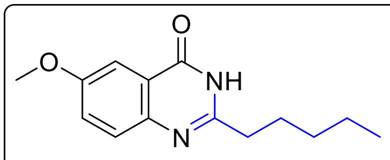

4-13j

6-Methoxy-2-pentylquinazolin-4(3H)-one (4-13j): A 1,4-dioxane (2.0 mL) solution of complex **2-10** (9 mg, 3 mol %), **2-16** (8 mg, 10 mol %), 2-amino-5-methoxybenzamide (83 mg, 0.5 mmol), and 1-hexylamine (71 mg, 0.7 mmol) was stirred at 140 °C for 20 h. The product **4-13j** was isolated by column chromatography on silica gel (hexanes/EtOAc = 40:1–1:1; TLC: R_f = 0.6 (50% EtOAc in hexanes)). Yield = 108 mg (88%). Data for **4-13j:** ^{1}H NMR (400 MHz, $CDCl_3$) δ 12.21 (br s, 1H), 7.64 (d, *J* = 9.0 Hz, 1H), 7.61 (d, *J* = 2.9 Hz, 1H), 7.35 (dd, *J* = 9.0, 2.9 Hz, 1H), 3.92 (s, 3H), 2.79 (t, *J* = 7.9 Hz, 2H), 1.93–1.84 (m, 2H), 1.46–1.36 (m, 4H), 0.91 (t, *J* = 7.0 Hz, 3H) ppm; ^{13}C{^{1}H} NMR (100 MHz, $CDCl_3$) δ 164.2, 158.0, 154.9, 143.9, 128.6, 124.9, 121.0, 105.5, 55.7, 35.6, 31.4, 27.3, 22.2, 13.9 ppm; GC-MS for $C_{14}H_{18}N_2O_2$, m/z = 246 (M^+); HRMS (ESI-TOF) m/z: $[M + H]^+$ Calcd for $C_{14}H_{18}N_2O_2H$ 247.1441, Found 247.1414.

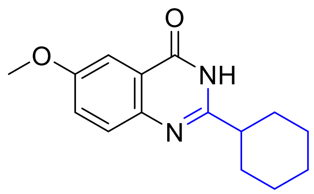

4-13k

2-Cyclohexyl-6-methoxyquinazolin-4(3H)-one (4-13k): A 1,4-dioxane (2.0 mL) solution of complex **2-10** (9 mg, 3 mol %), **2-16** (8 mg, 10 mol %), 2-amino-5-methoxybenzamide (83 mg, 0.5 mmol), and cyclohexylmethanamine (79 mg, 0.7 mmol) was stirred at 140 °C for 20 h. The product **4-13k** was isolated by column chromatography on silica gel (hexanes/EtOAc = 20:1–1:1; TLC: R_f = 0.6 (50% EtOAc in hexanes)). Yield = 106 mg (82%). Data for **4-13k:** ^{1}H NMR (400 MHz, $CDCl_3$) δ 11.22 (br s, 1H), 7.72–7.59 (m, 2H), 7.36 (dd, *J* = 9.0, 2.9 Hz, 1H), 3.92 (s, 3H), 2.67 (tt, *J* = 12.1, 3.3 Hz, 1H), 2.08–2.01 (m, 2H), 1.95–1.87 (m, 2H), 1.80–1.64 (m, 3H), 1.50–1.33 (m, 3H) ppm; $^{13}C\{^{1}H\}$ NMR (100 MHz, $CDCl_3$) δ 163.7, 158.0, 157.7, 144.1, 128.9, 124.8, 121.4, 105.6, 55.7, 44.6, 30.6, 26.0, 25.7 ppm; GC-MS for $C_{15}H_{18}N_2O_2$, m/z = 258 (M^+); HRMS (ESI-TOF) m/z: $[M + H]^+$ Calcd for $C_{15}H_{18}N_2O_2H$ 259.1441, Found 259.1413.

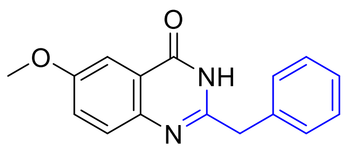

4-13l

2-Benzyl-6-methoxyquinazolin-4(3H)-one (4-13l): A 1,4-dioxane (2.0 mL) solution of complex **2-10** (9 mg, 3 mol %), **2-16** (8 mg, 10 mol %), 2-amino-5-methoxybenzamide (83 mg, 0.5 mmol), and 1-amino-2-phenylethane (85 mg, 0.7 mmol) was stirred at 140 °C for 20 h. The product **4-13l** was isolated by column chromatography on silica gel (hexanes/EtOAc = 20:1–1:1; TLC: R_f = 0.4 (50% EtOAc in hexanes)). Yield = 101 mg (76%). Data for **4-13l:** ^{1}H NMR (400 MHz, DMSO-d_6) δ 12.36 (br s, 1H), 7.56 (d, *J* = 8.9 Hz, 1H), 7.46 (d, *J* = 2.3 Hz, 1H), 7.42–7.34 (m, 3H), 7.34–7.27 (m, 2H), 7.27–7.19 (m, 1H), 3.91 (s, 2H), 3.84 (s, 3H) ppm; $^{13}C\{^{1}H\}$ NMR (100 MHz, DMSO-d_6) δ 161.8, 157.4, 153.6, 143.4, 136.8, 128.9, 128.6, 128.5, 126.8, 123.9, 121.5, 105.7, 55.6, 40.6 ppm; GC-MS for $C_{16}H_{14}N_2O_2$, m/z = 266 (M^+); HRMS (ESI-TOF) m/z: $[M + H]^+$ Calcd for $C_{16}H_{14}N_2O_2H$ 267.1128, Found 267.1096.

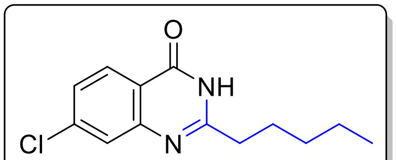

4-13m

7-Chloro-2-pentylquinazolin-4(3H)-one (4-13m): A 1,4-dioxane (2.0 mL) solution of complex **2-10** (9 mg, 3 mol %), **2-16** (8 mg, 10 mol %), 2-amino-4-chlorobenzamide (85 mg, 0.5 mmol), and 1-hexylamine (71 mg, 0.7 mmol) was stirred at 140 °C for 20 h. The product **4-13m** was isolated by column chromatography on silica gel (hexanes/EtOAc = 40:1–1:1; TLC: R_f = 0.8 (50% EtOAc in hexanes)). Yield = 107 mg (86%). Data for **4-13m:** ^{1}H NMR (400 MHz, $CDCl_3$) δ 12.42 (br s, 1H), 8.16 (d, *J* = 8.6 Hz, 1H), 7.68 (d, *J* = 1.7 Hz, 1H), 7.38 (dd, *J* = 8.6, 1.7 Hz, 1H), 2.78 (t, *J* = 7.9 Hz, 2H), 1.93–1.83 (m, 2H), 1.47–1.35 (m, 4H), 0.91 (t, *J* = 7.0 Hz, 3H) ppm; $^{13}C\{^1H\}$ NMR (100 MHz, $CDCl_3$) δ 164.0, 158.5, 150.4, 141.0, 127.5, 126.9, 126.8, 118.8, 35.7, 31.3, 27.0, 22.3, 13.9 ppm; GC-MS for $C_{13}H_{15}ClN_2O$, m/z = 250 (M^+); HRMS (ESI-TOF) m/z: $[M + H]^+$ Calcd for $C_{13}H_{15}ClN_2OH$ 251.0946, Found 251.0912.

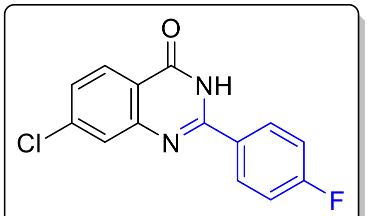

4-13n

7-Chloro-2-(4-fluorophenyl)quinazolin-4(3H)-one (4-13n): A 1,4-dioxane (2.0 mL) solution of complex **2-10** (9 mg, 3 mol %), **2-16** (8 mg, 10 mol %), 2-amino-4-chlorobenzamide (85 mg, 0.5 mmol), and 4-fluorobenzylamine (88 mg, 0.7 mmol) was stirred at 140 °C for 20 h. The product 4-1**3n** was isolated by column chromatography on silica gel (hexanes/EtOAc = 40:1–1:1; TLC: R_f = 0.8 (50% EtOAc in hexanes)). Yield = 88 mg (64%). Data for 4-1**3n:** ^{1}H NMR (400

MHz, DMSO-d_6) δ 12.70 (br s, 1H), 8.27–8.21 (m, 2H), 8.14 (d, *J* = 8.5 Hz, 1H), 7.78 (s, 1H), 7.55 (d, *J* = 8.5 Hz, 1H), 7.41 (t, *J* = 8.6 Hz, 2H) ppm; $^{13}C\{^1H\}$ NMR (100 MHz, DMSO-d_6) δ 164.2 (d, J_{CF} = 249.9 Hz), 161.8, 153.0, 149.8, 139.2, 130.6 (d, J_{CF} = 9.1 Hz), 129.0 (d, J_{CF} = 1.7 Hz), 128.0, 126.8, 126.5, 119.7, 115.7 (d, J_{CF} = 22.0 Hz) ppm; GC-MS for $C_{14}H_8ClFN_2O$, m/z = 274 (M^+); HRMS (ESI-TOF) m/z: $[M + H]^+$ Calcd for $C_{14}H_8ClFN_2OH$ 275.0382, Found 275.0351.

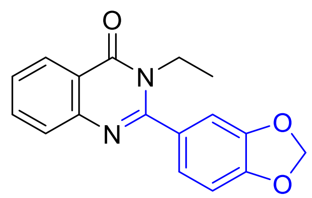

4-13p

2-(benzo[d][1,3]dioxol-5-yl)-3-ethylquinazolin-4(3H)-one (4-13p): A 1,4-dioxane (2.0 mL) solution of complex **2-10** (9 mg, 3 mol %), **2-16** (8 mg, 10 mol %), 2-amino-N-ethylbenzamide (82 mg, 0.5 mmol), and 1,3-benzodioxol-5-ylmethylamine (106 mg, 0.7 mmol) was stirred at 140 °C for 20 h. The product **4-13p** was isolated by column chromatography on silica gel (hexanes/EtOAc = 80:1–5:1; TLC: R_f = 0.3 (50% EtOAc in hexanes)). Yield = 85 mg, (58%). Data for **4-13p:** ^1H NMR (400 MHz, $CDCl_3$) δ 8.31 (d, *J* = 8.0 Hz, 1H), 7.85–7.66 (m, 2H), 7.59–7.43 (m, 1H), 7.03 (d, *J* = 8.0 Hz, 1H), 7.00 (s, 1H), 6.93 (d, *J* = 8.0 Hz, 1H), 6.05 (s, 2H), 4.08 (q, *J* = 7.0 Hz, 2H), 1.23 (t, *J* = 7.0 Hz, 3H) ppm; $^{13}C\{^1H\}$ NMR (100 MHz, $CDCl_3$) δ 161.9, 155.7, 148.8, 147.8, 146.8, 134.2, 128.8, 127.1, 126.9, 126.6, 121.9, 120.8, 108.5, 108.3, 101.6, 41.2, 14.1 ppm; GC-MS for $C_{17}H_{14}N_2O_3$, m/z = 294 (M^+). HRMS (ESI-TOF) m/z: $[M + H]^+$ Calcd for $C_{17}H_{14}N_2O_3H$ 295.1077; Found 295.1050.

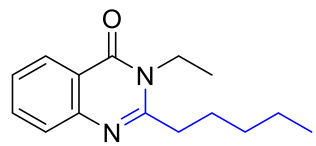

4-13q

3-Ethyl-2-pentylquinazolin-4(3H)-one (4-13q): A 1,4-dioxane (2.0 mL) solution of complex **2-10** (9 mg, 3 mol %), **2-16** (8 mg, 10 mol %), 2-amino-N-ethylbenzamide (82 mg, 0.5 mmol), and 1-hexylamine (71 mg, 0.7 mmol) was stirred at 140 °C for 20 h. The product **4-13q** was isolated by column chromatography on silica gel (hexanes/EtOAc = 80:1–5:1; TLC: R_f = 0.7 (50% EtOAc in hexanes)). Yield = 79 mg (65%). Data for **4-13q:** ^{1}H NMR (400 MHz, $CDCl_3$) δ 8.24 (d, *J* = 7.9 Hz, 1H), 7.69 (t, *J* = 7.6 Hz, 1H), 7.62 (d, *J* = 8.1 Hz, 1H), 7.41 (t, *J* = 7.4 Hz, 1H), 4.17 (q, *J* = 7.0 Hz, 2H), 2.81 (t, *J* = 7.8 Hz, 2H), 1.90–1.80 (m, 2H), 1.50–1.38 (m, 4H), 1.36 (t, *J* = 7.0 Hz, 3H) ppm; ^{13}C{^{1}H} NMR (100 MHz, $CDCl_3$) δ 162.0, 157.0, 134.0, 126.7, 126.6, 126.2, 120.4, 38.9, 35.0, 31.6, 27.4, 22.4, 14.1, 14.0 ppm; GC-MS for $C_{15}H_{20}N_2O$, m/z = 244 (M^+); HRMS (ESI-TOF) m/z: $[M + H]^+$ Calcd for $C_{15}H_{20}N_2OH$ 245.1648, Found 245.1622.

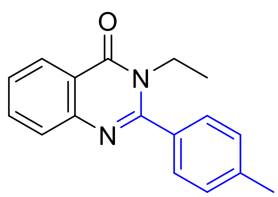
4-13r

3-Ethyl-2-(p-tolyl)quinazolin-4(3H)-one (4-13r): A 1,4-dioxane (2.0 mL) solution of complex **2-10** (9 mg, 3 mol %), **2-16** (8 mg, 10 mol %), 2-amino-N-ethylbenzamide (82 mg, 0.5 mmol), and 4-methylbenzylamine (85 mg, 0.7 mmol) was stirred at 140 °C for 20 h. The product **4-13r** was isolated by column chromatography on silica gel (hexanes/EtOAc = 80:1–5:1; TLC: R_f = 0.8 (50% EtOAc in hexanes)). Yield = 78 mg (59%). Data for **4-13r:** ^{1}H NMR (400 MHz, $CDCl_3$) δ 8.31 (d, *J* = 8.1 Hz, 1H), 7.76–7.69 (m, 2H), 7.50–7.45 (m, 1H), 7.42 (d, *J* = 7.6 Hz, 2H), 7.30 (d, *J* = 7.6 Hz, 2H), 4.04 (q, *J* = 7.0 Hz, 2H), 2.42 (s, 3H), 1.20 (t, *J* = 7.0 Hz, 3H) ppm; ^{13}C{^{1}H} NMR (100 MHz, $CDCl_3$) δ 161.9, 156.4, 146.8, 139.9, 134.2, 132.3, 129.3, 127.5, 127.1, 126.8, 126.6, 120.7, 41.1, 21.3, 14.0 ppm; GC-MS for $C_{17}H_{16}N_2O$, m/z = 264 (M^+); HRMS (ESI-TOF) m/z: $[M + H]^+$ Calcd for $C_{17}H_{16}N_2OH$ 265.1335, Found 265.1301.

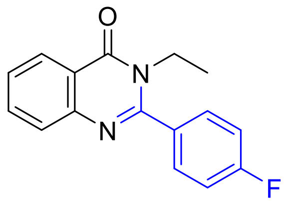

4-13s

3-ethyl-2-(4-fluorophenyl)quinazolin-4(3H)-one (4-13s): A 1,4-dioxane (2.0 mL) solution of complex **2-10** (9 mg, 3 mol %), **2-16** (8 mg, 10 mol %), 2-amino-N-ethylbenzamide (82 mg, 0.5 mmol), and 4-fluorobenzylamine (88 mg, 0.7 mmol) was stirred at 140 °C for 20 h. The product **4-13s** was isolated by column chromatography on silica gel (hexanes/EtOAc = 80:1–5:1; TLC: R_f = 0.4 (50% EtOAc in hexanes)). Yield = 48 mg, (36%). Data for **4-13s:** ^{1}H NMR (400 MHz, $CDCl_3$) δ 8.33 (d, J = 8.0 Hz, 1H), 7.91–7.70 (m, 2H), 7.66–7.45 (m, 3H), 7.28–7.19 (m, 2H), 4.05 (q, J = 7.0 Hz, 2H), 1.22 (t, J = 7.0 Hz, 3H) ppm; ^{13}C{^{1}H} NMR (100 MHz, $CDCl_3$) δ 163.6 (d, J_{CF} = 251.3 Hz), 161.6, 155.6, 146.1, 134.6, 130.7 (d, J_{CF} = 2.6 Hz), 130.0 (d, J_{CF} = 8.8 Hz), 127.4, 126.8, 123.8, 120.7, 116.1 (d, J_{CF} = 22.0 Hz), 41.3, 14.1 ppm; GC-MS for $C_{16}H_{13}FN_2O$, m/z = 268 (M^+). HRMS (ESI-TOF) m/z: $[M + H]^+$ Calcd for $C_{16}H_{13}FN_2OH$ 269.1085; Found 269.1058.

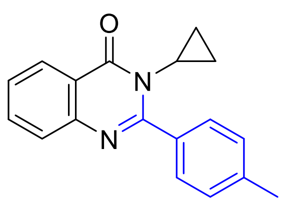

4-13u

3-Cyclopropyl-2-(p-tolyl)quinazolin-4(3H)-one (4-13u): A 1,4-dioxane (2.0 mL) solution of complex **2-10** (9 mg, 3 mol %), **2-16** (8 mg, 10 mol %), 2-amino-N-cyclopropylbenzamide (88 mg, 0.5 mmol), and 4-methylbenzylamine (85 mg, 0.7 mmol) was stirred at 140 °C for 20 h. The product **4-13u** was isolated by column chromatography on silica gel (hexanes/EtOAc = 80:1–5:1; TLC: R_f = 0.8 (50% EtOAc in hexanes)). Yield = 77 mg (56%). Data for **4-13u:** ^{1}H NMR (400 MHz, $CDCl_3$) δ 8.26 (d, J = 7.8 Hz, 1H), 7.80–7.64 (m, 2H), 7.58 (d, J = 7.6 Hz, 2H), 7.49–7.39 (m, 1H), 7.27 (d, J = 7.6 Hz, 2H), 3.24–3.00 (m, 1H), 2.41 (s, 3H), 0.98–0.85 (m, 2H), 0.56–0.37 (m, 2H) ppm; ^{13}C{^{1}H} NMR (100 MHz, $CDCl_3$) δ 164.0, 157.1, 146.9, 140.1, 134.2, 133.1, 129.3, 129.0,128.2, 127.2, 126.7, 126.5, 120.7, 30.3, 21.4, 11.3 ppm; GC-MS for $C_{18}H_{16}N_2O$, m/z = 276 (M^+); HRMS (ESI-TOF) m/z: $[M + H]^+$ Calcd for $C_{18}H_{16}N_2OH$ 277.1335, Found 277.1317.

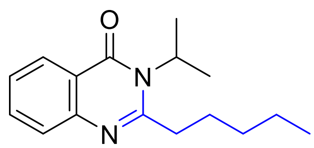

4-13v

3-Isopropyl-2-pentylquinazolin-4(3H)-one (4-13v): A 1,4-dioxane (2.0 mL) solution of complex **2-10** (9 mg, 3 mol %), **2-16** (8 mg, 10 mol %), 2-amino-N-(propan-2-yl)benzamide (89 mg, 0.5 mmol), and 1-hexylamine (71 mg, 0.7 mmol) was stirred at 140 °C for 20 h. The product **4-13v** was isolated by column chromatography on silica gel (hexanes/EtOAc = 80:1–10:1; TLC: R_f = 0.9 (50% EtOAc in hexanes)). Yield = 59 mg (46%). Data for **4-13v:** ^{1}H NMR (400 MHz, $CDCl_3$) δ 8.21 (d, J = 8.0 Hz, 1H), 7.69 (t, J = 7.5 Hz, 1H), 7.62 (d, J = 8.0 Hz, 1H), 7.41 (t, J = 7.5 Hz, 1H), 4.56 (m, 1H), 2.86 (t, J = 7.9 Hz, 2H), 1.85–1.77 (m, 2H), 1.68 (d, J = 6.8 Hz, 6H), 1.48–1.37 (m, 4H), 0.93 (t, J = 7.0 Hz, 3H) ppm; $^{13}C\{^1H\}$ NMR (100 MHz, $CDCl_3$) δ 162.6, 157.3, 146.7, 133.8, 126.3, 126.2, 126.1, 121.7, 36.4, 31.4, 31.2, 27.4, 22.3, 19.6, 13.8 ppm; GC-MS for $C_{16}H_{22}N_2O$, m/z = 258 (M^+); HRMS (ESI-TOF) m/z: $[M + H]^+$ Calcd for $C_{16}H_{22}N_2OH$ 259.1805, Found 259.1774.

6.4.5.3 Characterization of the Novel Quinazolin and Quinazolinone Compounds Listed in Table 4.5

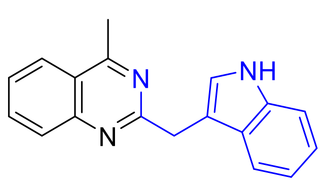

4-12ah

2-((1H-Indol-3-yl)methyl)-4-methylquinazoline (4-12ah): A 1,4-dioxane (2.0 mL) solution of complex **2-10** (9 mg, 3 mol %), **2-16** (8 mg, 10 mol %), 2-aminophenylethanone (68 mg, 0.5 mmol), and tryptamine (112 mg, 0.7 mmol) was stirred at 140 °C for 20 h. The product **4-12ah** was isolated by column chromatography on silica gel (hexanes/EtOAc = 60:1–5:1; TLC: R_f = 0.1 (20% EtOAc in hexanes)). Yield = 79 mg (58%). Data for **4-12ah:** ^{1}H NMR (400 MHz, $CDCl_3$) δ 8.45 (br s, 1H), 8.04–7.97 (m, 2H), 7.84–7.78 (m, 2H), 7.54 (ddd, *J* = 8.3, 6.9, 1.2 Hz, 1H), 7.27–7.24 (m, 1H), 7.14–7.09 (m, 2H), 7.06 (ddd, *J* = 7.8, 7.1, 1.2 Hz, 1H), 4.56 (s, 2H), 2.90 (s, 3H) ppm; ^{13}C{^{1}H} NMR (100 MHz, $CDCl_3$) δ 168.6, 165.5, 150.0, 136.3, 133.5, 128.5, 127.6, 126.7, 124.9, 122.9, 122.5, 121.8, 119.7, 119.2, 112.9, 111.0, 36.7, 21.8 ppm; GC-MS for $C_{18}H_{15}N_3$ m/z = 273 (M^+); HRMS (ESI-TOF) m/z: $[M + H]^+$ Calcd for $C_{18}H_{15}N_3H$ 274.1339, Found 274.1333.

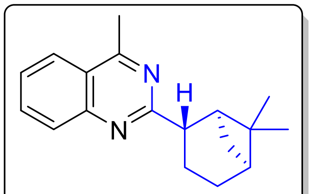

4-12ai

2-((1S,2S,5S)-6,6-Dimethylbicyclo[3.1.1]heptan-2-yl)-4-methylquinazoline (4-12ai): A 1,4-dioxane (2.0 mL) solution of complex **2-10** (9 mg, 3 mol %), **2-16** (8 mg, 10 mol %), 2-aminophenylethanone (68 mg, 0.5 mmol), and (−)-*cis*-myrtanylamine (107 mg, 0.7 mmol) was stirred at 140 °C for 20 h. The product **4-12ai** was isolated by column chromatography on silica gel (hexanes/EtOAc = 60:1–10:1; TLC: R_f = 0.8 (20% EtOAc in hexanes)). Yield = 113 mg (85%), d.r. = 10:1. Data for **4-12ai:** ^{1}H NMR (400 MHz, $CDCl_3$) δ 8.02 (d, *J* = 8.3 Hz, 1H), 7.95 (d, *J* = 8.4 Hz, 1H), 7.80 (t, *J* = 7.7 Hz, 1H), 7.52 (t, *J* = 7.6 Hz, 1H), 3.70–3.59 (m, 1H), 2.90 (s, 3H), 2.62–2.48 (m, 1H), 2.31–2.23 (m, 1H), 2.16–2.09 (m, 1H), 2.00–1.90 (m, 5H), 1.27 (s, 3H), 1.03 (s, 3H) ppm; ^{13}C{^{1}H} NMR (100 MHz, $CDCl_3$) δ 170.0, 167.9, 149.9, 133.1, 128.7, 126.3, 124.7, 122.6, 46.2, 44.8, 40.1, 39.8, 26.6, 24.6, 23.9, 21.8, 20.4, 19.3 ppm; GC-MS for $C_{18}H_{22}N_2$, m/z = 266 (M^+); HRMS (ESI-TOF) m/z: $[M + H]^+$ Calcd for $C_{18}H_{22}N_2H$ 267.1856, Found 267.1837; $[\alpha]_D^{22}$ = -29.1 (c = 0.1 g/100 mL in CH_2Cl_2).

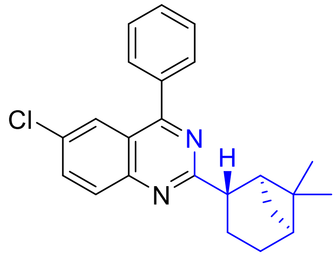

4-12aj

6-Chloro-2-((1S,2S,5S)-6,6-dimethylbicyclo[3.1.1]heptan-2-yl)-4-phenylquinazoline (4-12aj): A 1,4-dioxane (2.0 mL) solution of complex **2-10** (9 mg, 3 mol %), **2-16** (8 mg, 10 mol %), 5-chloro-2-aminobenzophenone (116 mg, 0.5 mmol), and (−)-*cis*-myrtanylamine (107 mg, 0.7 mmol) was stirred at 140 °C for 20 h. The product **4-12aj** was isolated by column chromatography on silica gel (hexanes/EtOAc = 60:1–10:1; TLC: R_f = 0.8 (20% EtOAc in hexanes)). Yield = 126 mg (70%), d.r. = 30:1. Data for **4-12aj:** ^{1}H NMR (400 MHz, $CDCl_3$) δ 8.03 (s, 1H), 7.99 (d, J = 9.0 Hz, 1H), 7.79–7.73 (m, 3H), 7.61–7.56 (m, 3H), 3.82–3.68 (m, 1H), 2.66–2.52 (m, 1H), 2.35–2.29 (m, 1H), 2.17–2.12 (m, 1H), 2.02–1.94 (m, 5H), 1.28 (s, 3H), 1.04 (s, 3H) ppm; $^{13}C\{^1H\}$ NMR (100 MHz, $CDCl_3$) δ 170.6, 167.4, 150.0, 137.1, 134.1, 132.0, 130.4, 130.0, 129.9, 128.7, 125.5, 121.9, 46.3, 44.9, 40.1, 26.7, 24.5, 23.9, 20.4, 19.4 ppm; GC-MS for $C_{23}H_{23}ClN_2$, m/z = 362 (M^+); HRMS (ESI-TOF) m/z: $[M + H]^+$ Calcd for $C_{23}H_{23}ClN_2H$ 363.1623, Found 363.1599; $[\alpha]_D^{22}$ = -34.5 (c = 0.2 g/100 mL in CH_2Cl_2).

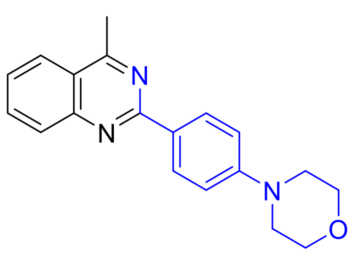

4-12ak

4-(4-(4-Methylquinazolin-2-yl)phenyl)morpholine (4-12ak): A 1,4-dioxane (2.0 mL) solution of complex **2-10** (9 mg, 3 mol %), **2-16** (8 mg, 10 mol %), 2-aminophenylethanone (68 mg, 0.5 mmol), and 4-morpholinobenzylamine (135 mg, 0.7 mmol) was stirred at 140 °C for 20 h. The product **4-12ak** was isolated by column chromatography on silica gel (hexanes/EtOAc = 80:1–10:1; TLC: R_f = 0.9 (20% EtOAc in hexanes)). Yield = 55 mg (36%). Data for **4-12ak:** ^{1}H NMR (400 MHz, $CDCl_3$) δ 8.54 (d, J = 8.4

Hz, 2H), 8.09–7.94 (m, 2H), 7.82 (t, *J* = 7.6 Hz, 1H), 7.51 (t, *J* = 7.6 Hz, 1H), 7.01 (d, *J* = 8.4 Hz, 2H), 3.92–3.87 (m, 4H), 3.32–3.27 (m, 4H), 2.98 (s, 3H) ppm; $^{13}C\{^1H\}$ NMR (100 MHz, $CDCl_3$) δ 167.9, 160.1, 152.8, 150.5, 133.3, 129.7, 129.4, 128.9, 126.1, 125.0, 122.6, 114.6, 66.8, 48.4, 22.0 ppm; GC-MS for $C_{19}H_{19}N_3O$, m/z = 305 (M^+); HRMS (ESI-TOF) m/z: $[M + H]^+$ Calcd for $C_{19}H_{19}N_3OH$ 306.1601, Found 306.1578.

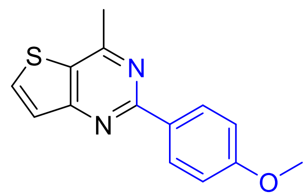

4-12al

2-(4-methoxyphenyl)-4-methylthieno[3,2-d]pyrimidine (4-12al): A 1,4-dioxane (2.0 mL) solution of complex **2-10** (9 mg, 3 mol %), **2-16** (8 mg, 10 mol %), 2-acetyl-3-aminothiophene (71 mg, 0.5 mmol), and 4-methoylbenzylamine (96 mg, 0.7 mmol) was stirred at 140 °C for 20 h. The product **4-12al** was isolated by column chromatography on silica gel (hexanes/EtOAc = 100:1–10:1; TLC: R_f = 0.4 (10% EtOAc in hexanes)). Yield = 50 mg (39%). Data for **4-12al:** ^1H NMR (400 MHz, $CDCl_3$) δ 8.49 (d, *J* = 8.7 Hz, 2H), 7.90 (d, *J* = 5.4 Hz, 1H), 7.55 (d, *J* = 5.4 Hz, 1H), 7.01 (d, *J* = 8.7 Hz, 2H), 3.88 (s, 3H), 2.83 (s, 3H) ppm; $^{13}C\{^1H\}$ NMR (100 MHz, $CDCl_3$) δ 161.4, 161.4, 161.2, 161.2, 134.5, 130.9, 129.8, 127.8, 125.0, 113.8, 55.3, 23.5 ppm; GC-MS for $C_{14}H_{12}N_2OS$, m/z = 256 (M^+). HRMS (ESI-TOF) m/z: $[M + H]^+$ Calcd for $C_{14}H_{12}N_2OSH$ 257.0743; Found 257.0710.

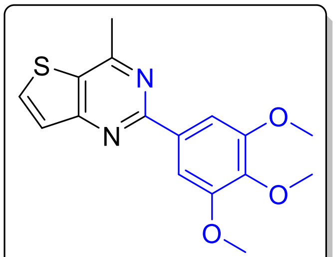

4-12am

4-Methyl-2-(3,4,5-trimethoxyphenyl)thieno[3,2-d]pyrimidine (4-12am): A 1,4-dioxane (2.0 mL) solution of complex **2-10** (9 mg, 3 mol %), **2-16** (8 mg, 10 mol %), 2-acetyl-3-aminothiophene (71 mg, 0.5 mmol), and 3,4,5-trimethoxybenzylamine (138 mg, 0.7 mmol) was stirred at 140 °C for 20 h. The product **4-12am** was isolated by column chromatography on silica gel (hexanes/EtOAc = 80:1–10:1; TLC: R_f = 0.4 (20% EtOAc in hexanes)). Yield = 82 mg (52%). Data for **4-12am:** ^{1}H NMR (400 MHz, $CDCl_3$) δ 7.92 (d, *J* = 5.4 Hz, 1H), 7.84 (s, 2H), 7.57 (d, *J* = 5.4 Hz, 1H), 4.02 (s, 6H), 3.92 (s, 3H), 2.85 (s, 3H) ppm; ^{13}C{^{1}H} NMR (100 MHz, $CDCl_3$) δ 161.4, 161.2, 160.8, 153.3, 140.0, 134.7, 133.6, 128.3, 125.0, 105.4, 60.9, 56.2, 23.5 ppm; GC-MS for $C_{16}H_{16}N_2O_3S$, m/z = 316 (M^+); HRMS (ESI-TOF) m/z: $[M + H]^+$ Calcd for $C_{16}H_{16}N_2O_3SH$ 317.0954, Found 317.0936.

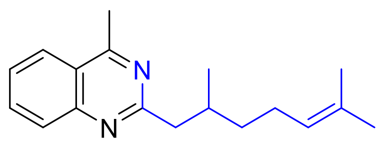

4-12an

2-(2,6-dimethylhept-5-en-1-yl)-4-methylquinazoline (4-12an): A 1,4-dioxane (2.0 mL) solution of complex **2-10** (9 mg, 3 mol %), **2-16** (8 mg, 10 mol %), 2'-aminoacetophenone (68 mg, 0.5 mmol), and geranylamine (107 mg, 0.7 mmol) was stirred at 140 °C for 20 h. The product **4-12an** was isolated by column chromatography on silica gel (hexanes/EtOAc = 80:1–10:1; TLC: R_f = 0.4 (10% EtOAc in hexanes)). Yield = 83 mg 62%). Data for **4-12an:** ^{1}H NMR (400 MHz, $CDCl_3$) δ 8.06 (d, *J* = 8.3 Hz, 1H), 7.96 (d, *J* = 8.4 Hz, 1H), 7.83 (dd, *J* = 7.6, 7.6 Hz, 1H), 7.56 (dd, *J* = 7.6, 7.6 Hz, 1H), 5.09 (t, *J* = 6.9 Hz, 1H), 3.07 (dd, *J* = 13.3, 6.4 Hz, 1H), 2.93 (s, 3H), 2.90–2.82 (m, 1H), 2.34–2.23 (m, 1H), 2.12–1.94 (m, 2H), 1.66 (s, 3H), 1.58 (s, 3H), 1.51–1.39 (m, 1H), 1.35–1.24 (m, 1H), 0.94 (d, *J* = 6.7 Hz, 3H) ppm; ^{13}C{^{1}H} NMR (100 MHz, $CDCl_3$) δ 167.9, 166.2, 149.8, 133.4, 131.1, 128.5, 126.5, 124.9, 124.8, 122.4, 47.3, 37.1, 33.0, 25.7, 25.5, 21.7, 19.3, 17.6 ppm; GC-MS for $C_{18}H_{24}N_2$, m/z = 268 (M^+). HRMS (ESI-TOF) m/z: $[M + H]^+$ Calcd for $C_{18}H_{24}N_2H$ 269.2012; Found 269.1988.

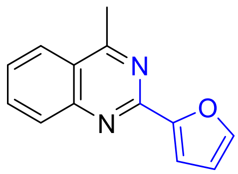

4-12ao

2-(2-Furanyl)-4-methylquinazoline (4-12ao): A 1,4-dioxane (2.0 mL) solution of complex **2-16** (9 mg, 3 mol %), **2-16** (8 mg, 10 mol %), 2'-aminoacetophenone (68 mg, 0.5 mmol), and furfurylamine (68 mg, 0.7 mmol) was stirred at 140 °C for 20 h. The product **4-12ao** was isolated by column chromatography on silica gel (hexanes/EtOAc = 100:1–10:1; TLC: R_f = 0.6 (10% EtOAc in hexanes)). Yield = 83 mg (79%). Data for **4-12ao:** ^{1}H NMR (400 MHz, $CDCl_3$) δ 8.09–8.04 (m, 2H), 7.85 (ddd, J = 8.5, 6.9, 1.2 Hz, 1H), 7.69–7.66 (m, 1H), 7.56 (ddd, J = 8.5, 6.9, 1.2 Hz, 1H), 7.45 (dd, J = 3.4, 0.8 Hz, 1H), 6.60 (dd, J = 3.4, 1.8 Hz, 1H), 2.98 (s, 3H) ppm; ^{13}C{^{1}H} NMR (100 MHz, $CDCl_3$) δ 168.7, 153.3, 150.0, 145.1, 142.0, 133.9, 129.0, 126.9, 125.1, 122.8, 113.8, 112.2, 21.9 ppm; GC-MS for $C_{13}H_{10}N_2O$ m/z = 210 (M^+). ^{1}H and ^{13}C NMR spectral data are in good agreement with the literature values.[217]

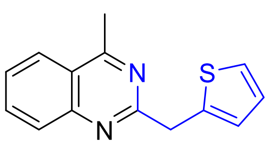

4-12ap

4-Methyl-2-(thiophen-2-ylmethyl)quinazoline (4-12ap): A 1,4-dioxane (2.0 mL) solution of complex **2-10** (9 mg, 3 mol %), **2-16** (8 mg, 10 mol %), 2-aminophenylethanone (68 mg, 0.5 mmol), and 2-thiopheneethanamine (89 mg, 0.7 mmol) was stirred at 140 °C for 20 h. The product **4-12ap** was isolated by column chromatography on silica gel (hexanes/EtOAc = 80:1–20:1; TLC: R_f = 0.2 (20% EtOAc in hexanes)). Yield = 86 mg (72%). Data for **4-12ap:** ^{1}H NMR (400 MHz, $CDCl_3$) δ 8.06 (ddd, J = 8.3, 1.3, 0.6 Hz, 1H), 7.98 (ddd, J = 8.3, 1.2, 0.6 Hz, 1H), 7.85 (dd, J = 8.3, 1.3 Hz, 1H), 7.58 (dd, J = 8.3, 0.9 Hz, 1H), 7.18–7.15 (m, 1H), 7.04–7.01 (m, 1H), 6.93 (dd, J = 5.1, 3.4 Hz, 1H), 4.59 (s, 2H), 2.94 (s, 3H) ppm; ^{13}C{^{1}H} NMR (100 MHz, $CDCl_3$) δ 168.8, 164.0, 149.9, 140.5, 133.6, 128.6, 127.0, 126.6, 125.8, 124.9, 124.4, 122.6, 40.6, 21.8

ppm; GC-MS for $C_{14}H_{12}N_2S$ m/z = 240 (M^+); HRMS (ESI-TOF) m/z: $[M + H]^+$ Calcd for $C_{14}H_{12}N_2SH$ 241.0794, Found 241.0765.

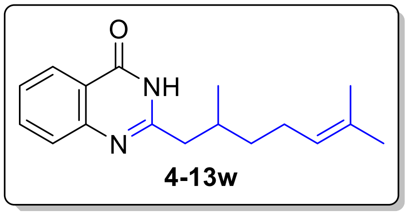

(±)-2-(2,6-Dimethylhept-5-en-1-yl)quinazolin-4(3H)-one (4-13w): A 1,4-dioxane (2.0 mL) solution of complex **2-10** (9 mg, 3 mol %), **2-16** (8 mg, 10 mol %), anthranilamide (68 mg, 0.5 mmol), and geranylamine (107 mg, 0.7 mmol) was stirred at 140 °C for 20 h. The product **4-13w** was isolated by column chromatography on silica gel (hexanes/EtOAc = 40:1–1:1; TLC: R_f = 0.3 (20% EtOAc in hexanes)). Yield = 97 mg (72%). Data for **4-13w:** ^{1}H NMR (400 MHz, $CDCl_3$) δ 12.29 (br s, 1H), 8.28 (d, *J* = 7.9 Hz, 1H), 7.77 (t, *J* = 7.6 Hz, 1H), 7.71 (d, *J* = 8.0 Hz, 1H), 7.46 (t, *J* = 7.6 Hz, 1H), 5.11 (t, *J* = 6.5 Hz, 1H), 2.85 (dd, *J* = 13.7, 6.0 Hz, 1H), 2.59 (dd, *J* = 13.7, 8.6 Hz, 1H), 2.27–2.19 (m, 1H), 2.17–1.97 (m, 2H), 1.64 (s, 3H), 1.59 (s, 3H), 1.52–1.42 (m, 1H), 1.41–1.31 (m, 1H), 1.02 (d, *J* = 6.8 Hz, 3H) ppm; $^{13}C\{^1H\}$ NMR (100 MHz, $CDCl_3$) δ 164.5, 156.4, 149.5, 134.7, 131.5, 127.2, 126.2, 126.2, 124.3, 120.4, 43.3, 36.9, 32.3, 25.6, 25.4, 19.2, 17.6 ppm; GC-MS for $C_{17}H_{22}N_2O$, m/z = 270 (M^+); HRMS (ESI-TOF) m/z: $[M + H]^+$ Calcd for $C_{17}H_{22}N_2OH$ 271.1805, Found 271.1770.

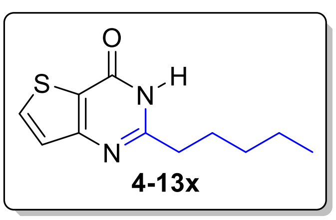

2-Pentylthieno[3,2-d]pyrimidin-4(3H)-one (4-13x): A 1,4-dioxane (2.0 mL) solution of complex **2-10** (9 mg, 3 mol %), **2-16** (8 mg, 10 mol %), 3-aminothiophene-2-carboxamide (71 mg, 0.5 mmol), and 1-hexylamine (71 mg, 0.7 mmol) was stirred at 140 °C for 20 h. The product **4-13x** was isolated by column chromatography on silica gel (hexanes/EtOAc = 80:1–5:1; TLC: R_f = 0.4 (30% EtOAc in hexanes)). Yield = 50 mg (60%). Data for **4-13x:** ^{1}H NMR (400 MHz, $CDCl_3$) δ 12.68 (brs, 1H), 7.81 (d, J = 5.2 Hz, 1H), 7.33 (d, J = 5.2 Hz, 1H), 2.82 (t, J = 7.8 Hz, 2H), 1.93–1.80 (m, 2H), 1.48–1.32 (m, 4H), 0.91 (t, J = 7.0 Hz, 3H); $^{13}C\{^1H\}$ NMR (100 MHz, $CDCl_3$) δ 160.9, 159.2, 159.0, 134.7, 125.1, 120.6, 35.3, 31.3, 27.5, 22.3, 13.9 HRMS (ESI-TOF) m/z: $[M + H]^+$ Calcd for $C_{11}H_{14}N_2OSH$ 223.0900; Found 223.0899.

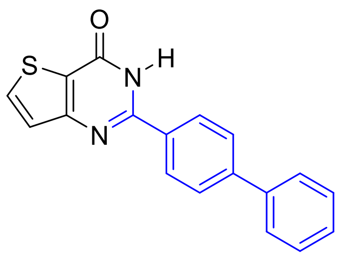

4-13y

2-([1,1'-Biphenyl]-4-yl)thieno[3,2-d]pyrimidin-4(3H)-one (4-13y): A 1,4-dioxane (2.0 mL) solution of complex **2-10** (9 mg, 3 mol %), **2-16** (8 mg, 10 mol %), 3-aminothiophene-2-carboxamide (71 mg, 0.5 mmol), and 4-phenylbenzylamine (128 mg, 0.7 mmol) was stirred at 140 °C for 20 h. The product **4-13y** was isolated by crystallization. Yield = 89 mg (59%). Data for **4-13y:** ^{1}H NMR (400 MHz, DMSO-d_6) δ 12.72 (br s, 1H), 8.29–8.19 (m, 3H), 7.84 (d, J = 8.2 Hz, 2H), 7.76 (d, J = 7.6 Hz, 2H), 7.54–7.46 (m, 3H), 7.44–7.39 (m, 1H) ppm; $^{13}C\{^1H\}$ NMR (100 MHz, DMSO-d_6) δ 158.6, 158.6, 154.0, 142.8, 139.0, 135.5, 131.4, 129.1, 128.5, 128.2, 126.9, 126.8, 125.5, 121.3 ppm; GC-MS for $C_{18}H_{12}N_2OS$, m/z = 304 (M^+); HRMS (ESI-TOF) m/z: $[M + H]^+$ Calcd for $C_{18}H_{12}N_2OSH$ 305.0743, Found 305.0718.

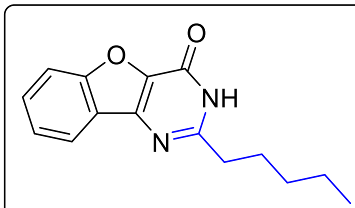

4-13z

2-Pentylbenzofuro[3,2-d]pyrimidin-4(3H)-one (4-13z): A 1,4-dioxane (2.0 mL) solution of complex **2-10** (9 mg, 3 mol %), **2-16** (8 mg, 10 mol %), 3-aminobenzofuran-2-carboxamide (88 mg, 0.5 mmol), and 1-hexylamine (71 mg, 0.7 mmol) was stirred at 140 °C for 20 h. The product **4-13z** was isolated by column chromatography on silica gel (hexanes/EtOAc = 50:1–1:4; TLC: R_f = 0.2 (80% EtOAc in hexanes)). Yield = 61 mg (48%). Data for **4-13z:** ^{1}H NMR (400 MHz, DMSO) δ 12.69 (brs, 1H), 8.00 (d, *J* = 7.7 Hz, 1H), 7.76 (d, *J* = 8.4 Hz, 1H), 7.69–7.57 (m, 1H), 7.45 (t, *J* = 7.4 Hz, 1H), 2.67 (t, *J* = 7.6 Hz, 2H), 1.82–1.64 (m, 2H), 1.37–1.24 (m, 4H), 0.95–0.77 (m, 3H) ppm; ^{13}C{^{1}H} NMR (100 MHz, DMSO) δ 159.8, 156.2, 153.4, 143.8, 137.6, 129.9, 124.3, 122.4, 121.5, 113.0, 34.3, 30.8, 27.2, 21.9, 13.9 ppm; GC-MS for $C_{15}H_{16}N_2O_2$, m/z = 256 (M^+). HRMS (ESI-TOF) m/z: $[M + H]^+$ Calcd for $C_{15}H_{16}N_2O_2H$ 257.1285; Found 257.1262.

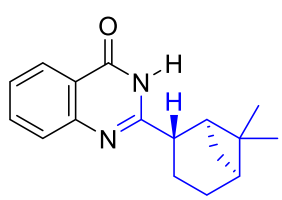

4-13aa

2-((1S,2S,5S)-6,6-Dimethylbicyclo[3.1.1]heptan-2-yl)quinazolin-4(3H)-one (4-13aa): A 1,4-dioxane (2.0 mL) solution of complex **2-10** (9 mg, 3 mol %), **2-16** (8 mg, 10 mol %), anthranilamide (68 mg, 0.5 mmol), and (−)-*cis*-myrtanylamine (107 mg, 0.7 mmol) was stirred at 140 °C for 20 h. The product **4-13aa** was isolated by column chromatography on silica gel (hexanes/EtOAc = 80:1–5:1; TLC: R_f = 0.4 (20% EtOAc in hexanes)). Yield = 91 mg (68%), d.r. = 99:1. Data for **4-13aa:** ^{1}H NMR (400 MHz, $CDCl_3$) δ 11.69 (br s, 1H), 8.25 (d, *J* = 7.9 Hz, 1H), 7.82–7.65 (m, 2H), 7.45 (t, *J* = 7.1 Hz, 1H), 3.46–3.32 (m, 1H), 2.63–2.47 (m, 1H), 2.31–2.21 (m, 1H), 2.21–2.12 (m, 1H), 2.02–1.84 (m, 4H), 1.75 (d, *J* = 10.3 Hz, 1H), 1.28 (s, 3H), 1.09 (s, 3H) ppm; ^{13}C{^{1}H} NMR (100 MHz, $CDCl_3$) δ 164.4, 159.6, 149.5, 134.5, 127.6, 126.1, 126.0, 120.8, 45.4, 41.2, 40.0, 39.8, 26.6, 23.9, 23.7, 20.3, 17.3 ppm; GC-MS for $C_{17}H_{20}N_2O$, m/z = 268 (M^+); HRMS (ESI-TOF) m/z: $[M + H]^+$ Calcd for $C_{17}H_{20}N_2OH$ 269.1648; Found 269.1614)); $[\alpha]_D^{22}$ = -28.0 (c = 0.79 g/100 mL in CH_2Cl_2).

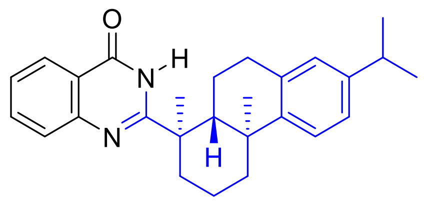

4-13ab

2-((1R,4aS,10aR)-7-Isopropyl-1,4a-dimethyl-1,2,3,4,4a,9,10,10a-octahydrophenanthren-1-yl)quinazolin-4(3H)-one (4-13ab): A 1,4-dioxane (2.0 mL) solution of complex **2-10** (9 mg, 3 mol %), **2-16** (8 mg, 10 mol %), anthranilamide (34 mg, 0.25 mmol), and (+)-((1R,4aS,10aR)-7-isopropyl-1,4a-dimethyl-1,2,3,4,4a,9,10,10a-octahydrophenanthren-1-yl)methanamine (100 mg, 0.35 mmol) was stirred at 140 °C for 20 h. The product **4-13ab** was isolated by column chromatography on silica gel (hexanes/EtOAc = 100:1–10:1; TLC: R_f = 0.7 (20% EtOAc in hexanes)). Yield = 57 mg (57%), d.r. > 99:1. Data for **4-13ab:** ^{1}H NMR (400 MHz, $CDCl_3$) δ 11.60 (br s, 1H), 7.80 (d, J = 7.9 Hz, 1H), 7.75–7.63 (m, 2H), 7.31 (d, J = 7.9 Hz, 2H), 7.09 (d, J = 8.1 Hz, 1H), 6.82 (s, 1H), 2.91–2.77 (m, 3H), 2.73 (d, J = 12.3 Hz, 1H), 2.46 (d, J = 10.6 Hz, 1H), 2.08 (t, J = 11.9 Hz, 1H), 1.97 (d, J = 13.6 Hz, 1H), 1.92–1.77 (m, 4H), 1.62 (s, 3H), 1.47–1.40 (m, 1H), 1.38 (s, 3H), 1.22 (t, J = 7.0 Hz, 6H) ppm; $^{13}C\{^1H\}$ NMR (100 MHz, $CDCl_3$) δ 163.9, 162.4, 148.8, 147.0, 145.5, 134.7, 134.2, 127.5, 126.8, 126.3, 126.0, 124.0, 123.8, 120.4, 45.6, 45.1, 38.1, 37.6, 37.4, 33.3, 29.9, 25.4, 24.0, 23.9, 20.8, 19.1, 17.1 ppm; GC-MS for $C_{27}H_{32}N_2O$, m/z = 400 (M^+); HRMS (ESI-TOF) m/z: $[M + H]^+$ Calcd for $C_{27}H_{32}N_2OH$ 401.2587, Found 401.2561; $[\alpha]_D^{22}$ = +15.3 (c = 0.19 g/100 mL in CH_2Cl_2).

6.5 Experimental Procedures and Characterization Data for Chapter 5

6.5.1.1 General Procedure for the Catalytic Synthesis of Quinolines

In a glove box, complex **2-10** (9 mg, 3 mol %), **2-16** (8 mg, 10 mol %), were dissolved in 1,4-dioxane (1 mL) in a 25 mL Schlenk tube equipped with a Teflon screw cap stopcock and a magnetic stirring bar. The resulting mixture was stirred for 5-10 min until the solution was turned blueish green color. 2'-Aminoacetophenone (68 mg, 0.5 mmol) and a β-amino acid (0.7 mmol) were dissolved in dioxane (1 mL), and the solution was added to the reaction tube. The tube was brought out of the glove box, and was stirred in an oil bath maintained at 140 °C for 20 h. The reaction tube was taken out of the oil bath, and was cooled to room temperature. The resulting solution was filtered through a short silica gel column by eluting with CH_2Cl_2 (10 mL), and the filtrate was analyzed by GC-MS. Analytically pure product **5-9** was isolated by a simple column chromatography on silica gel (280-400 mesh, hexanes/EtOAc).

6.5.1.2 General Procedure for the Catalytic Synthesis of 2,3-Dihydroquinazolin-4(1H)-one Products

In a glove box, complex **2-10** (9 mg, 3 mol %), **2-16** (12 mg, 10 mol %), were dissolved in 1,4-dioxane (1 mL) in a 25 mL Schlenk tube equipped with a Teflon screw cap stopcock and a magnetic stirring bar. The resulting mixture was stirred for 5-10 min until the solution was turned reddish green color. 2-Aminobenzamide (68 mg, 0.5 mmol) and a β-amino acid (0.7 mmol) were dissolved in 1,4-dioxane (1 mL), and the solution was added to the reaction tube. The tube was brought out of the glove box, and was stirred in an oil bath maintained at 140 °C for 20 h. The reaction tube was taken out of the oil bath, and was cooled to room temperature. The resulting solution was filtered through a short silica gel column by eluting with CH_2Cl_2 (10 mL), and the filtrate was analyzed by GC-MS. Analytically pure product **5-10** was isolated by a simple column chromatography on silica gel (280-400 mesh, hexanes/EtOAc) or crystallization technique.

Alternatively, In a glove box, complex **2-10** (9 mg, 3 mol %), **2-12** (12 mg, 10 mol %), were dissolved in 1,4-dioxane (1 mL) in a 25 mL Schlenk tube equipped with a Teflon screw cap stopcock and a magnetic stirring bar. The resulting mixture was stirred for 5-10 min until the solution was turned reddish green color. 2-Aminobenzamide (68 mg, 0.5 mmol) and a branched amine (0.7 mmol) were dissolved in 1,4-dioxane (1 mL), and the solution was added to the reaction tube. The tube was brought out of the glove box, and was stirred in an oil bath maintained at 140 °C for 20 h. The reaction tube was taken out of the oil bath, and was cooled to room temperature. The resulting solution was filtered through a short silica gel column by eluting with CH_2Cl_2 (10 mL), and the filtrate was analyzed by GC-MS. Analytically pure product **5-10** was isolated by a simple column chromatography on silica gel (280-400 mesh, hexanes/EtOAc) or crystallization technique.

6.5.2 Catalyst and Ligand Screening Study

In a glove box, a catalyst (3 mol % Ru) and a ligand (10 mol %) were dissolved in a solvent (1 mL) in a 25 mL Schlenk tube equipped with a Teflon screw cap stopcock and a magnetic stirring bar. The resulting mixture was stirred for 5-10 min until the solution was turned reddish green color. 2-Aminobenzamide (68 mg, 0.5 mmol) and cyclohexylamine (69 mg, 0.7 mmol) were dissolved in solvent (1 mL), and the solution was added to the reaction tube. The tube was brought out of the glove box, and was stirred in an oil bath at 140 °C for 20 h. The product yield was determined by ^{1}H NMR by using hexamethylbenzene as an internal standard. The results are summarized in **Tables 5.1** and **5.2**.

6.5.3.1 Deuterium Labeling Study

In a glove box, 2'-aminoacetophenone Me-D3 (90 % D, 68 mg, 0.5 mmol), (1S,2R)-2-aminocyclohexanecarboxylic acid (100 mg, 0.7 mmol), **2-10** (3 mol %), **2-16** (10 mol %), were dissolved in 1,4-dioxane (2 mL) in a 25 mL Schlenk tube equipped with a Teflon screw cap stopcock and a stirring bar. The tube was brought out of the box and immersed in an oil bath preset at 140 °C for 20 h. The reaction tube was taken out of the oil bath and was cooled to room temperature. After the tube was open to air, the solution was filtered through a short silica gel column by eluting with CH_2Cl_2 (10 mL), and the filtrate was analyzed by GC-MS. Analytically pure product was isolated by column chromatography on silica gel (230-460 mesh, hexanes/EtOAc = 50:1 to 10:1), and it was completely characterized by ^{1}H, ^{2}H NMR and GC-MS spectroscopic methods. The ^{1}H and ^{2}H NMR spectra of the product **5-9-*d*** are shown in **Figure 5.3**.

In a glove box, 2-aminobenzamide (68 mg, 0.5 mmol), cyclohexylamine (70 mg, 0.7 mmol), complex 1 (3 mol %) (20mg, 1 mmol) were dissolved in 1,4-dioxane (2 mL) in a 25 mL Schlenk tube equipped with a Teflon screw cap stopcock and a stirring bar. The tube was brought out of the box and immersed in an oil bath preset at 140 °C for 20 h. The reaction tube was taken out of the oil bath and was cooled to room temperature. After the tube was open to air, the solution was filtered through a short silica gel column by eluting with CH_2Cl_2 (10 mL), and the filtrate was analyzed by GC-MS. Analytically pure product was isolated by column chromatography on silica gel (230-460 mesh, hexanes/EtOAc = 30:1 to 5:1), and it was completely characterized by ^{1}H, ^{2}H NMR and GC-MS spectroscopic methods. The ^{1}H and ^{2}H NMR spectra of the product **5-10-*d*^{1}** are shown in **Figure 5.4**.

6.5.3.2 Reaction with Dihydrocoumarin with *β*-Amino Acids

In a glove box, dihydrocoumarin (74 mg, 0.5 mmol), DL-β-Homoleucine (102 mg, 0.7 mmol), **2-10** (3 mol %), **2-16** (10 mol %), were dissolved in 1,4-dioxane (2 mL) in a 25 mL Schlenk tube equipped with a Teflon screw cap stopcock and a stirring bar. The tube was brought out of the box and immersed in an oil bath preset at 140 °C for 20 h. The reaction tube was taken out of the oil bath and was cooled to room temperature. After the tube was open to air, the solution was filtered through a short silica gel column by eluting with CH_2Cl_2 (10 mL), and the filtrate was analyzed by GC-MS. Analytically pure product **5-12** was isolated by column chromatography on silica gel (230-460 mesh, hexanes/EtOAc = 50:1 to 10:1), and it was completely characterized by ^{1}H, ^{2}H NMR and GC-MS spectroscopic methods. **5-12** are shown in **Figure 5.6**.

6.5.3.3 Reaction with Enamine Substrate

A 1,4-dioxane (2.0 mL) solution of complex **2-10** (9 mg, 3 mol %), **2-16** (8 mg, 10 mol %), 5-chloro-2-aminobenzophenone (116 mg, 0.5 mmol) and 1-pyrrolidino-1-cyclohexene (91 mg, 0.6 mmol) was stirred at 140 °C for 20 h. The product **5-9m** was isolated by column chromatography on silica gel in 90% yield.

6.5.3.4 Preparatory Scale Reaction for the Synthesis of 5-9n and 5-10m

Synthesis of 5-9n: In a glove box, complex 1 (85 mg, 3 mol %) and **2-16** (80 mg, 10 mol %) were dissolved in 1,4-dioxane (5 mL) in a 125 mL Schlenk tube equipped with a Teflon screw cap stopcock and a magnetic stirring bar. The resulting mixture was stirred for 5 to 10 minutes until the solution turned to a blueish green color. 2-Amino-5-chlorobenzophenone (1.16 g, 5.0 mmol) and (1S,2R)-2-aminocyclohexanecarboxylic acid (1.0 g, 7 mmol) 1,4-dioxane (5 mL) were added to the reaction tube. After the tube was sealed, those were brought out of the box, and was stirred in an oil bath at 140 °C for 20 h. The tube was cooled to room temperature and filtered through a small silica column (CH_2Cl_2), and the product conversion was determined by GC (90%). Analytically pure product **5-9n** was obtained by crystallization in dichloromethane and n-hexanes (1.17 g, 80%).

Synthesis of 5-10: In a glove box, complex **2-10** (128 mg, 3 mol %) and **2-12** (180 mg, 10 mol %) were dissolved in 1,4-dioxane (5 mL) in a 125 mL Schlenk tube equipped with a Teflon screw cap stopcock and a magnetic stirring bar. The resulting mixture was stirred for 5 to 10 minutes until the solution turned to a blueish green color. 2-aminobenzamide (1.04 g, 7.5 mmol) and cyclohexylamine (1.04 g, 10.5 mmol) 1,4-dioxane (5 mL) were added to the reaction tube. After the tube was sealed, those were brought out of the box, and was stirred in an oil bath at 140 °C for 20 h. The tube was cooled to room temperature and filtered through a small silica column (CH_2Cl_2), and the product conversion was determined by GC (92%). Analytically pure product **5-10m** was obtained by crystallization in a mixture of 1:2 dichloromethane and ethyl acetate layered with n-hexanes (1.36 g, 84%).

6.5.4.1 X-ray Crystallography Data for 5-9s

Colorless needle shape single crystals of **5-10s** were grown in dichloromethane/*n*-hexane/Ethylacetate at room temperature. A suitable crystal with the dimension of 0.628

× 0.266 × 0.105 mm^3 was selected and analyzed. The Ph substituent is rotated by ~60° relative to the quinoline nucleus. The benzodioxolane group is more co-planar with quinoline moiety being rotated only by ~10°. The dioxolane ring is slightly non-planar – it has an envelope conformation with atom C22 bent out of plane of other atoms of the ring by 17.4°.

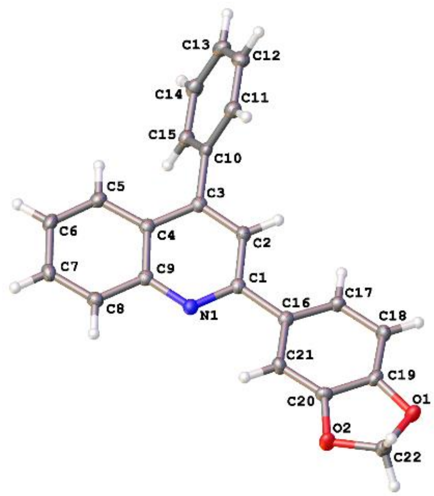

Figure 6.29: Molecular Structure of **5-9s**.

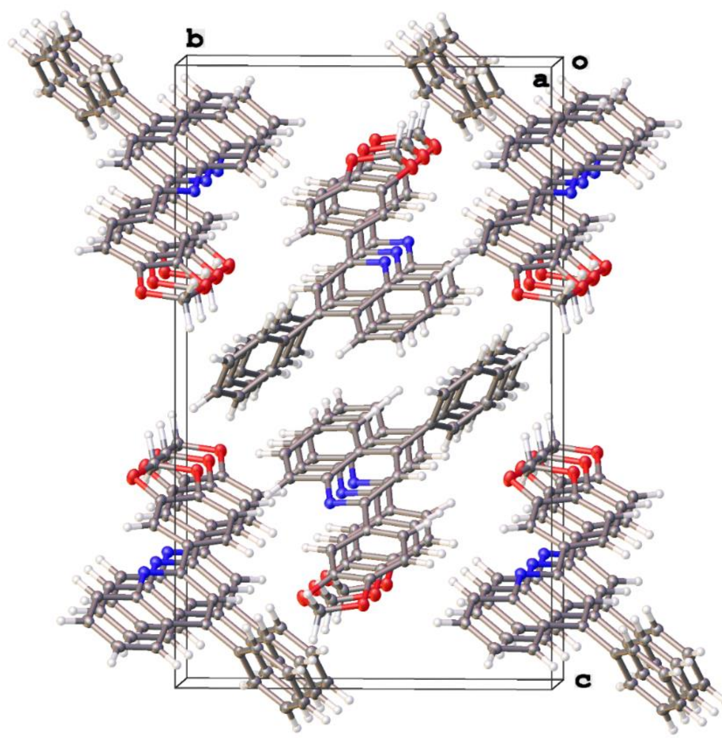

Figure 6.30: Crystal Packing of **5-9s**

Table 6.15: Crystal Data and Structure Refinement for **5-9s**

Identification code	yi3q
Empirical formula	$C_{22}H_{15}NO_2$
Formula weight	325.35
Temperature/K	100.15
Crystal system	monoclinic
Space group	$P2_1/c$
a/Å	6.28303(7)
b/Å	12.33805(16)
c/Å	20.3928(2)
α/°	90
β/°	91.5260(11)
γ/°	90
Volume/Å^3	1580.30(3)
Z	4
ρ_{calc}g/cm^3	1.367
μ/mm^{-1}	0.701
F(000)	680.0
Crystal size/mm^3	0.628 × 0.266 × 0.105
Radiation	CuKα (λ = 1.54184)
2Θ range for data collection/°	8.376 to 141.314
Index ranges	$-5 \leq h \leq 7$, $-15 \leq k \leq 15$, $-24 \leq l \leq 24$
Reflections collected	14591
Independent reflections	3000 [R_{int} = 0.0236, R_{sigma} = 0.0171]
Data/restraints/parameters	3000/0/226
Goodness-of-fit on F^2	1.049
Final R indexes [I>=2σ (I)]	R_1 = 0.0362, wR_2 = 0.0902
Final R indexes [all data]	R_1 = 0.0415, wR_2 = 0.0946
Largest diff. peak/hole / e Å^{-3}	0.20/-0.22

6.5.4.2 X-ray Crystallography Data for 5-9aj

Colorless needle like single crystals of **5-9aj** were grown in *n*-hexane/Ethylacetate at room temperature. A suitable crystal with the dimension of 0.35 × 0.03 × 0.02 mm^3 was selected and analyzed. The molecule has an overall planar shape with the p-chlorophenyl group rotated by 55° relative to the main framework. The cyclohexene moiety has C3, C4-half-chair conformation somewhat distorted to C4-sofa. The molecules form stacks along screw axes in y direction.

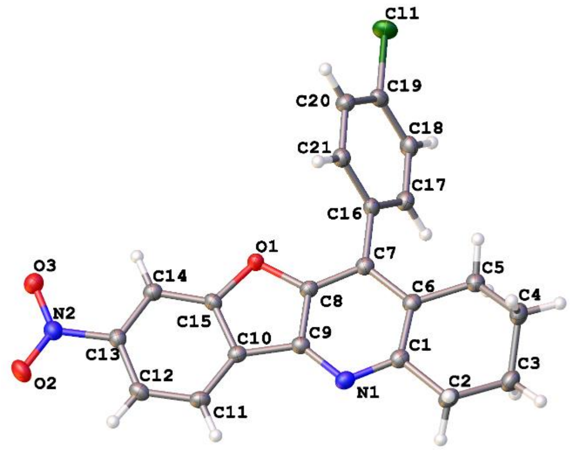

Figure 6.31: Molecular Structure of **5-9aj**

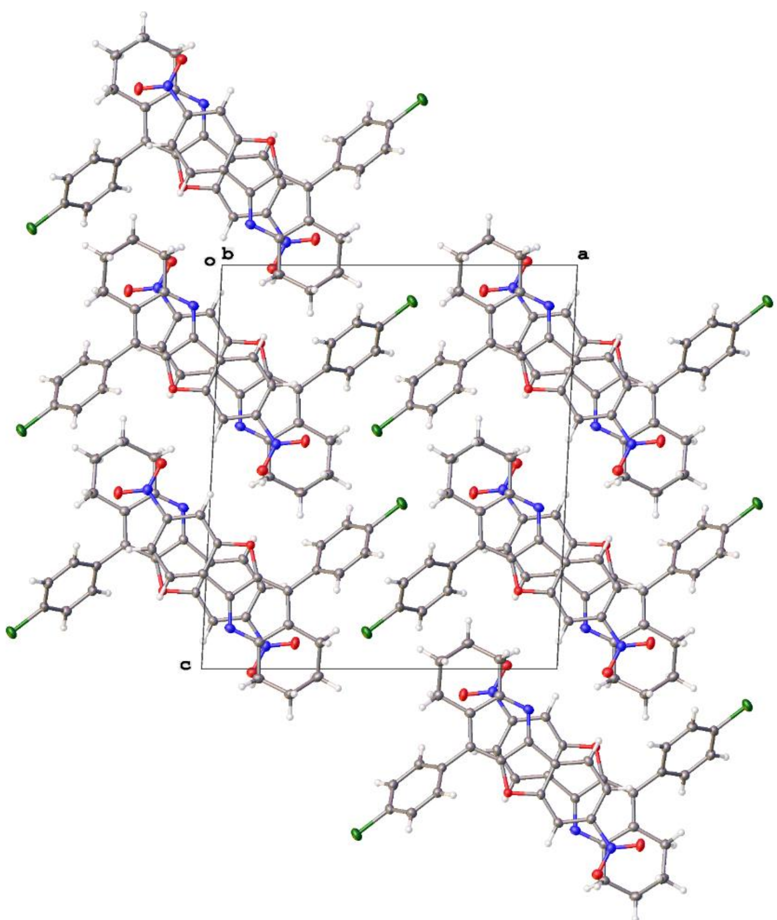

Figure 6.32: Crystal Packing of **5-9aj**

Table 6.16: Crystal Data and Structure Refinement for **5-9aj**

Identification code	yi3v
Empirical formula	$C_{21}H_{15}ClN_2O_3$
Formula weight	378.80
Temperature/K	100.15
Crystal system	monoclinic
Space group	$P2_1/c$
a/Å	14.8261(6)
b/Å	6.7994(3)
c/Å	16.8509(7)
α/°	90
β/°	92.899(4)
γ/°	90
Volume/Å^3	1696.55(12)
Z	4
ρ_{calc}g/cm^3	1.483
μ/mm^{-1}	2.215
F(000)	784.0
Crystal size/mm^3	0.35 × 0.03 × 0.02
Radiation	CuKα (λ = 1.54184)
2Θ range for data collection/°	10.514 to 141.458
Index ranges	$-18 \leq h \leq 17$, $-8 \leq k \leq 8$, $-19 \leq l \leq 20$
Reflections collected	15963
Independent reflections	3232 [R_{int} = 0.0442, R_{sigma} = 0.0290]
Data/restraints/parameters	3232/0/245
Goodness-of-fit on F^2	1.037
Final R indexes [I>=2σ (I)]	R_1 = 0.0338, wR_2 = 0.0861
Final R indexes [all data]	R_1 = 0.0414, wR_2 = 0.0931
Largest diff. peak/hole / e Å^{-3}	0.28/-0.26

6.5.4.3 X-ray Crystallography Data for 5-10a

Colorless prism shaped single crystals of **5-10a** (regular twins, 57° rotation around x axis) were grown in *n*-hexane/Ethylacetate at room temperature. A suitable crystal with the dimension of 0.16 × 0.11 × 0.05 mm^3 was selected and analyzed. The heterocycle of 2,3-dihydro-2-methyl-2-phenyl-4(1H)-quinazolinone moiety has a C2-sofa conformation with Ph group in an axial and Me group in an equatorial position. Imino group has a pyramidal configuration, despite the adjacent pi-conjugated benzene ring (its H atom deviates by 16° from NCC plane). The crystal is centrosymmetric, and the compound represents a racemic mixture of both enantiomers. The molecules form centrosymmetric dimers through H-bonds formed by their amido groups. Imido hydrogen does not have an acceptor for H-bond formation but It forms a close N-H…C contact with one of C atoms of Ph group of a neighboring molecule.

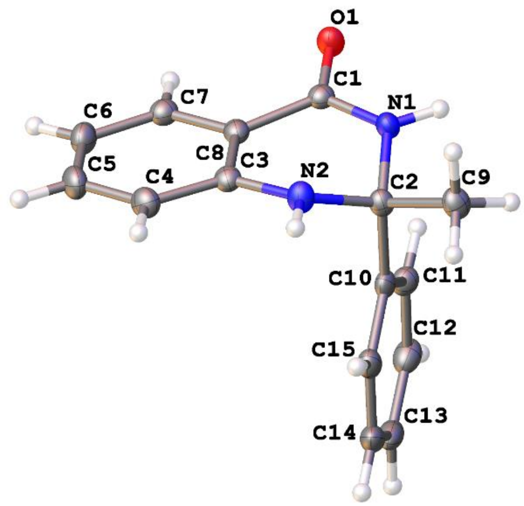

Figure 6.33: Molecular Structure of **5-10a**

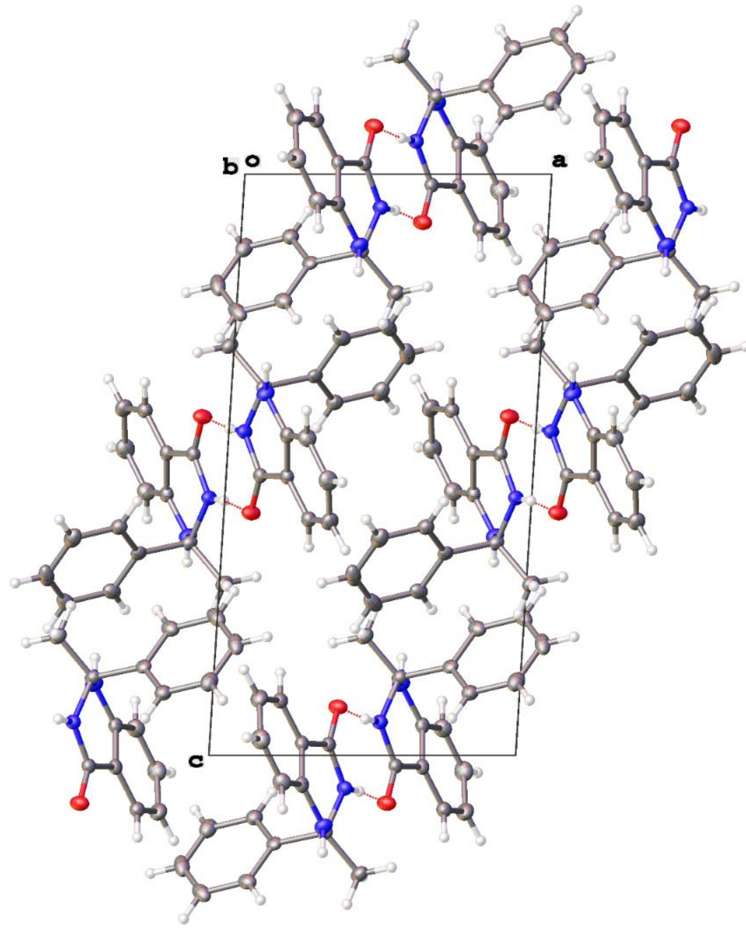

Figure 6.34: Crystal Packing of **5-10a**

Table 6.17: Crystal Data and Structure Refinement for **5-10a**

Identification code	yi4l5
Empirical formula	$C_{15}H_{14}N_2O$
Formula weight	238.28
Temperature/K	100.00(10)
Crystal system	monoclinic
Space group	$P2_1/n$
a/Å	8.46693(16)
b/Å	8.7469(2)
c/Å	16.0808(3)
α/°	90
β/°	93.5464(19)
γ/°	90
Volume/Å^3	1188.65(5)

Z	4
ρ_{calc}g/cm^3	1.332
μ/mm^{-1}	0.676
F(000)	504.0
Crystal size/mm^3	0.16 × 0.11 × 0.05
Radiation	CuKα (λ = 1.54184)
2Θ range for data collection/°	11.026 to 141.018
Index ranges	-10 ≤ h ≤ 10, -10 ≤ k ≤ 10, -19 ≤ l ≤ 19
Reflections collected	5192
Independent reflections	5192 [R_{int} = ?, R_{sigma} = 0.0110]
Data/restraints/parameters	5192/0/173
Goodness-of-fit on F^2	1.067
Final R indexes [I>=2σ (I)]	R_1 = 0.0331, wR_2 = 0.0888
Final R indexes [all data]	R_1 = 0.0366, wR_2 = 0.0913
Largest diff. peak/hole / e Å^{-3}	0.26/-0.23

6.5.4.4 X-ray Crystallography Data for 5-11n

Colorless needle like single crystals of **5-11n** (Regular twins, rotation 180° over reciprocal x*) were grown in *n*-pentane/Ethylacetate at room temperature. A suitable crystal with the dimension of 0.2 × 0.1 × 0.07 mm^3 was selected and analyzed. The structure contains two symmetrically independent molecules. The planar heterocyclic part makes dihedral angles of 20.8 and 15.7° with keto group. The phenyl group is rotated relative the keto group by 26.6 and 35.5°. The molecules form infinite stacks along y axis.

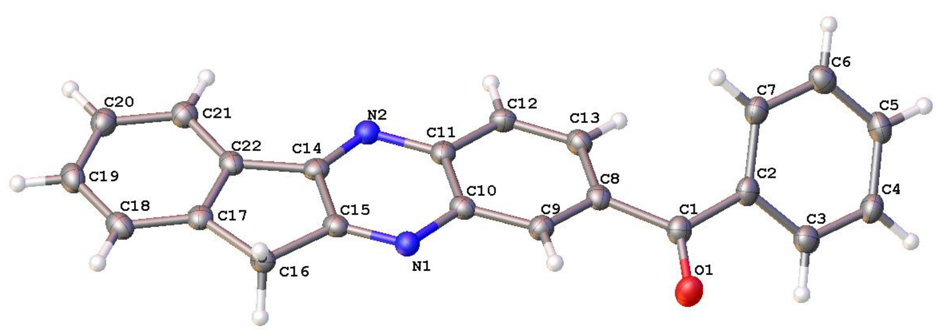

Figure 6.35: Molecular Structure of **5-11n**

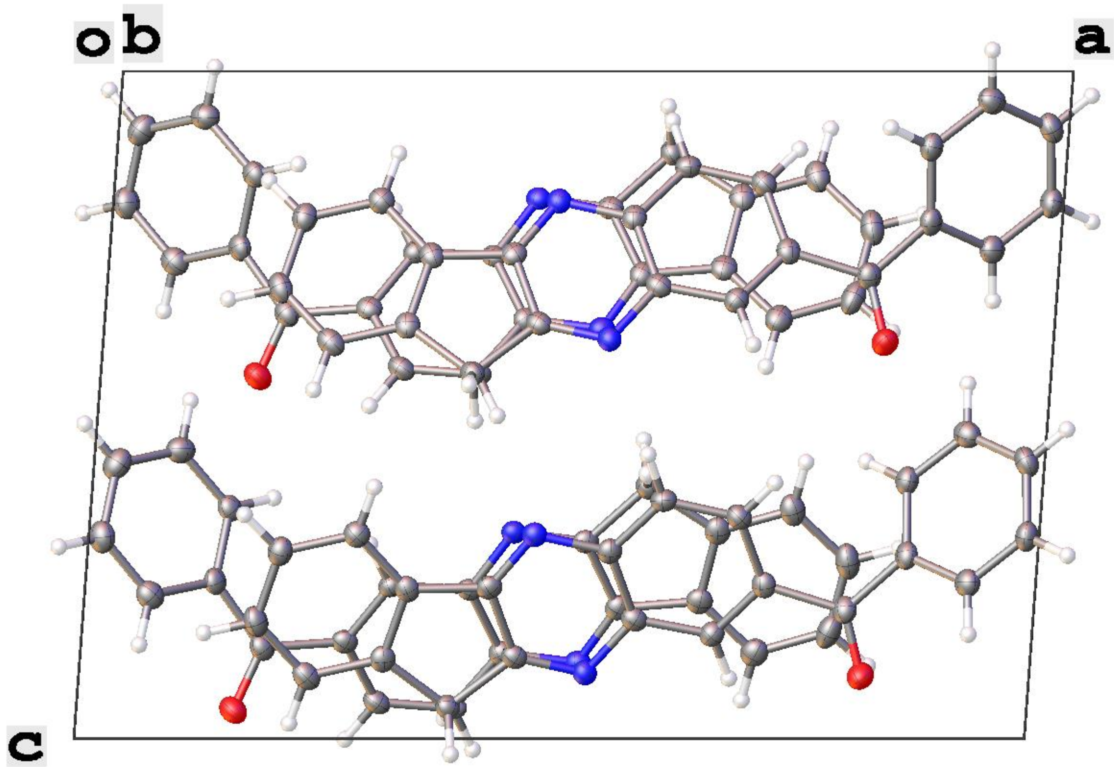

Figure 6.36: Crystal Packing of **5-11n**

Table 6.18: Crystal Data and Structure Refinement for **5-11n**

Identification code	yi5p5
Empirical formula	$C_{22}H_{14}N_2O$
Formula weight	322.35
Temperature/K	99.90(14)
Crystal system	monoclinic
Space group	Pc
a/Å	16.9135(5)
b/Å	7.6839(3)
c/Å	11.9057(3)
α/°	90
β/°	94.233(2)
γ/°	90
Volume/Å^3	1543.06(9)
Z	4
ρ_{calc}g/cm^3	1.388
μ/mm^{-1}	0.684
F(000)	672.0

Crystal size/mm^3	0.2 × 0.1 × 0.07
Radiation	Cu Kα (λ = 1.54184)
2Θ range for data collection/°	10.49 to 141.264
Index ranges	$-20 \le h \le 20$, $-9 \le k \le 9$, $-14 \le l \le 12$
Reflections collected	5515
Independent reflections	5515 [R_{int} = ?, R_{sigma} = 0.0192]
Data/restraints/parameters	5515/2/452
Goodness-of-fit on F^2	1.053
Final R indexes [I>=2σ (I)]	R_1 = 0.0338, wR_2 = 0.0882
Final R indexes [all data]	R_1 = 0.0366, wR_2 = 0.0901
Largest diff. peak/hole / e $Å^{-3}$	0.17/-0.19
Flack parameter	0.39(17)

6.5.4.5 X-ray Crystallography Data for 5-12

Colorless prism shaped of **5-12** were grown in *n*-pentane/Acetone at room temperature. A suitable single crystal with the dimension of 0.704 × 0.399 × 0.171 mm^3 was selected and analyzed. The molecule has an extended conformation. The trans-amide group is planar. The molecule contains a chiral center but the compound represents a racemate. In the centrosymmetric crystals, the molecules form layers along bc plane being connected through hydrogen bonds N-H…O and O-H…O.

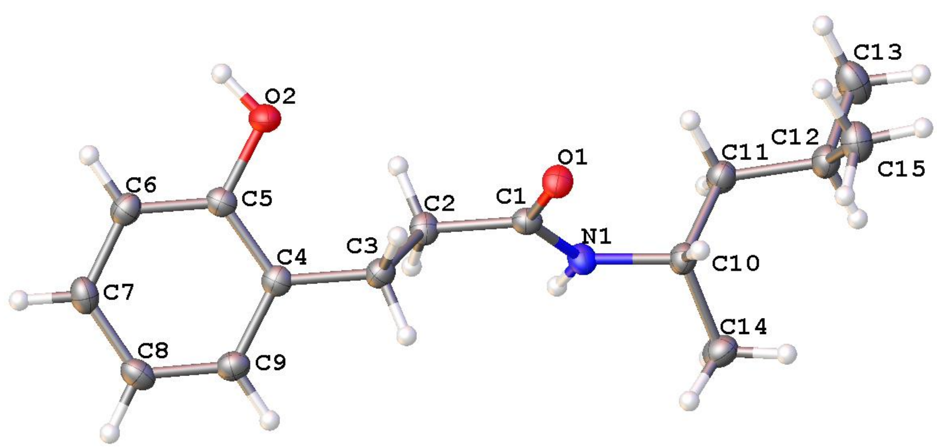

Figure 6.37: Molecular Structure of **5-12**

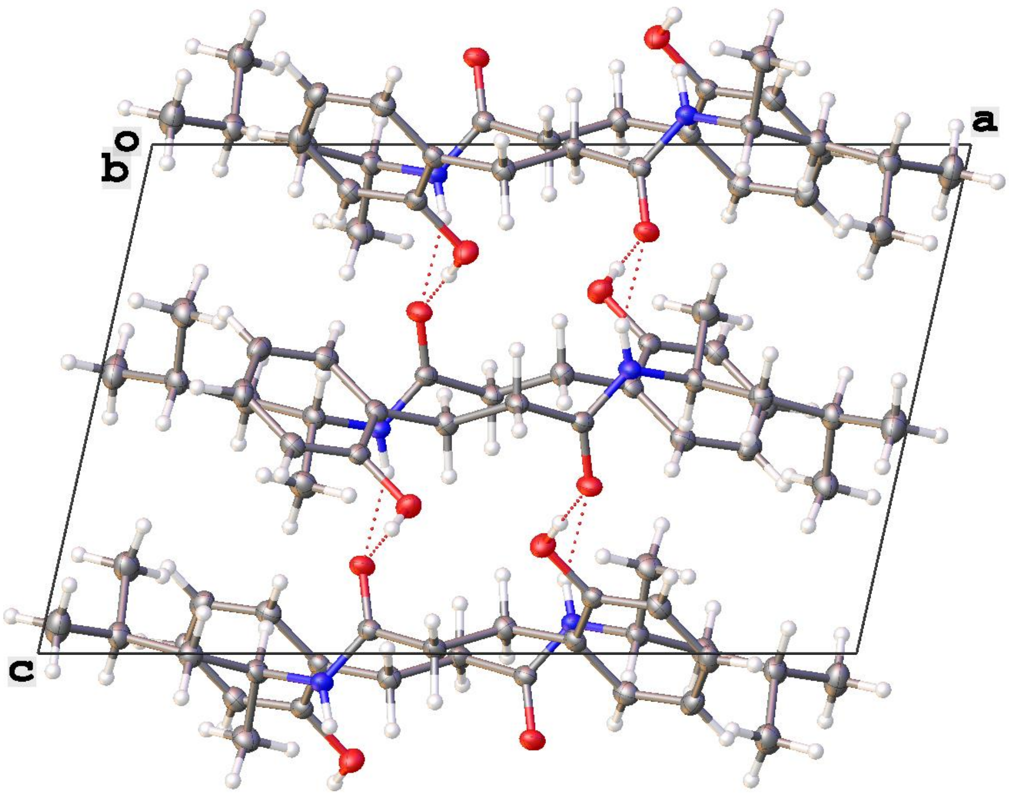

Figure 6.38: Crystal Packing of **5-12**

Table 6.19: Crystal Data and Structure Refinement for **5-12**

Identification code	yi5o
Empirical formula	$C_{15}H_{23}NO_2$
Formula weight	249.34
Temperature/K	100.2(5)
Crystal system	monoclinic
Space group	$P2_1/c$
a/Å	14.9237(2)
b/Å	10.35610(14)
c/Å	9.50085(16)
α/°	90
β/°	102.6627(17)
γ/°	90
Volume/Å^3	1432.65(4)
Z	4

ρ_{calc}g/cm^3	1.156
μ/mm^{-1}	0.599
F(000)	544.0
Crystal size/mm^3	0.704 × 0.399 × 0.171
Radiation	Cu Kα (λ = 1.54184)
2Θ range for data collection/°	10.482 to 141.238
Index ranges	-18 ≤ h ≤ 18, -12 ≤ k ≤ 12, -11 ≤ l ≤ 11
Reflections collected	25622
Independent reflections	2736 [R_{int} = 0.0355, R_{sigma} = 0.0148]
Data/restraints/parameters	2736/0/171
Goodness-of-fit on F^2	1.035
Final R indexes [I>=2σ (I)]	R_1 = 0.0337, wR_2 = 0.0834
Final R indexes [all data]	R_1 = 0.0389, wR_2 = 0.0876
Largest diff. peak/hole / e Å^{-3}	0.20/-0.19

6.5.3 Characterization of the Organic Products

6.5.5.1 Characterization of the Quinoline Compounds Listed in Table 5.5

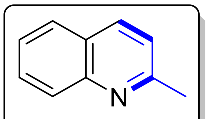

5-9a

2-Methylquinoline (**5-9a**): A 1,4-dioxane (2.0 mL) solution of complex **2-10** (9 mg, 3 mol %), **2-16** (8 mg, 10 mol %) 2-aminobenzaldehyde (61 mg, 0.5 mmol), and (±)-3-aminobutyric acid (72 mg, 0.7 mmol) was stirred at 140 °C for 20 h. The product **5-9a** was isolated by column chromatography on silica gel (hexanes/EtOAc = 110:1–5:1; TLC: R_f = 0.4 (20% EtOAc in hexanes)). Yield = 64 mg (90%). Data for **5-9a**: ^{1}H NMR (400 MHz, $CDCl_3$) δ 7.91 (d, *J* = 8.5 Hz, 1H), 7.76 (d, *J* = 8.5 Hz, 1H), 7.60–7.41 (m, 2H), 7.27 (t, *J* = 7.3 Hz, 1H), 7.00 (d, *J* = 8.5 Hz, 1H), 2.56 (s, 3H) ppm; ^{13}C{^{1}H} NMR (100 MHz, $CDCl_3$) δ 158.4, 147.4, 135.6, 128.9, 128.1, 127.1, 126.0, 125.2, 121.5, 24.9 ppm; GC-MS for $C_{10}H_9N$, m/z = 143 (M^+). ^{1}H and ^{13}C NMR spectral data are in good agreement with the literature values.[218]

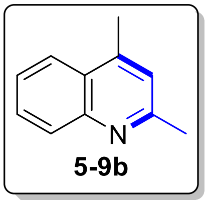

2,4-Dimethylquinoline (5-9b): A 1,4-dioxane (2.0 mL) solution of complex **2-10** (9 mg, 3 mol %), **2-16** (8 mg, 10 mol %) 2'-aminoacetophenone (68 mg, 0.5 mmol), and (±)-3-aminobutyric acid (72 mg, 0.7 mmol) was stirred at 140 °C for 20 h. The product **5-9b** was isolated by column chromatography on silica gel (hexanes/EtOAc = 110:1–5:1; TLC: R_f = 0.5 (20% EtOAc in hexanes)). Yield = 69 mg (88%). Data for **5-9b**: ^{1}H NMR (400 MHz, $CDCl_3$) δ 8.02 (d, *J* = 8.4 Hz, 1H), 7.92 (d, *J* = 8.3 Hz, 1H), 7.65 (dd, *J* = 8.4, 1.4 Hz, 1H), 7.48 (d, *J* = 8.3, 1.4 Hz, 1H), 7.10 (s, 1H), 2.68 (s, 3H), 2.63 (s, 3H) ppm; ^{13}C{^{1}H} NMR (100 MHz, $CDCl_3$) δ 158.5, 147.5, 144.2, 129.0, 129.0, 126.5, 125.3, 123.5, 122.6, 25.1, 18.5 ppm; GC-MS for $C_{11}H_{11}N$, m/z = 157 (M^+). ^{1}H and ^{13}C NMR spectral data are in good agreement with the literature values.[219]

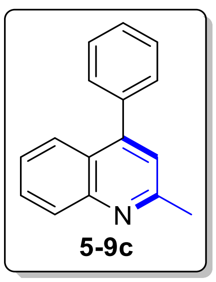

2-Methyl-4-phenylquinoline (5-9c): A 1,4-dioxane (2.0 mL) solution of complex **2-10** (9 mg, 3 mol %), **2-16** (8 mg, 10 mol %), 2-aminobenzophenone (99 mg, 0.5 mmol), and (±)-3-aminobutyric acid (72 mg, 0.7 mmol) was stirred at 140 °C for 20 h. The product **5-9c** was isolated by column chromatography on silica gel (hexanes/EtOAc = 100:1–5:1; TLC: R_f = 0.3 (20% EtOAc in hexanes)). Yield = 71 mg, (65%). Data for **5-9c** ^{1}H NMR (400 MHz, $CDCl_3$) δ 8.09 (d, *J* = 8.4 Hz, 1H), 7.86 (d, *J* = 8.4 Hz, 1H), 7.69 (t, *J* = 7.6 Hz, 1H), 7.55–7.45 (m, 5H), 7.43 (t, *J* = 7.6 Hz, 1H), 7.23 (s, 1H), 2.78 (s, 3H) ppm; ^{13}C{^{1}H} NMR (100 MHz, $CDCl_3$) δ 158.4, 148.4, 148.3, 138.1, 129.4, 129.2, 129.0, 128.5, 128.3, 125.7, 125.6, 125.0, 122.2, 25.3 ppm; GC-MS for $C_{16}H_{13}N$, m/z = 219 (M^+). ^{1}H and ^{13}C NMR spectral data are in good agreement with the literature values.[220]

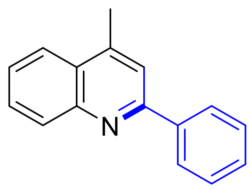

5-9d

4-Methyl-2-phenylquinoline (5-9d): A 1,4-dioxane (2.0 mL) solution of complex **2-10** (9 mg, 3 mol %), **2-16** (8 mg, 10 mol %), 2'-aminoacetophenone (68 mg, 0.5 mmol), and (±)-β-phenyl-β-alanine (116 mg, 0.7 mmol) was stirred at 140 °C for 20 h. The product **5-9d** was isolated by column chromatography on silica gel (hexanes/EtOAc = 100:1–5:1; TLC: R_f = 0.4 (20% EtOAc in hexanes)). Yield = 61 mg (56%). Data for **5-9d:** ^{1}H NMR (400 MHz, $CDCl_3$) δ 8.20 (d, *J* = 8.4 Hz, 1H), 8.18–8.13 (m, 2H), 8.00 (d, *J* = 8.4 Hz, 1H), 7.77–7.69 (m, 2H), 7.59–7.49 (m, 3H), 7.49–7.43 (m, 1H), 2.77 (s, 3H) ppm; ^{13}C{^{1}H} NMR (100 MHz, $CDCl_3$) δ 157.1, 148.1, 144.8, 139.8, 130.2, 129.3, 129.1, 128.7, 127.5, 127.2, 126.0, 123.6, 119.8, 19.0 ppm; GC-MS for $C_{16}H_{13}N$, m/z = 219 (M^+). ^{1}H and ^{13}C NMR spectral data are in good agreement with the literature values.[221]

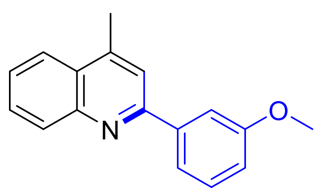

5-9e

2-(3-Methoxyphenyl)-4-methylquinoline (5-9e): A 1,4-dioxane (2.0 mL) solution of complex **2-10** (9 mg, 3 mol %), **2-16** (8 mg, 10 mol %), 2'-aminoacetophenone (68 mg, 0.5 mmol), and (±)-β-amino-3-methoxybenzenepropanoic acid (137 mg, 0.7 mmol) was stirred at 140 °C for 20 h. The product **5-9e** was isolated by column chromatography on silica gel (hexanes/EtOAc = 100:1–5:1; TLC: R_f = 0.4 (20% EtOAc in hexanes)). Yield = 94 mg (76%). Data for **5-9e:** ^{1}H NMR (400 MHz, $CDCl_3$) δ 8.19 (d, *J* = 8.5 Hz, 1H), 7.99 (d, *J* = 8.3 Hz, 1H), 7.77 (s, 1H), 7.75–7.68 (m, 3H), 7.54 (t, *J* = 7.6 Hz, 1H), 7.43 (t, *J* = 7.9 Hz, 1H), 7.02 (dd, *J* = 8.2, 1.9 Hz, 1H), 3.94 (s, 3H), 2.75 (s, 3H) ppm; ^{13}C{^{1}H} NMR (100 MHz, $CDCl_3$) δ 160.0, 156.8, 148.0, 144.7, 141.2, 130.2, 129.7, 129.3, 127.3, 126.0, 123.5, 119.9, 119.8, 115.2, 112.5, 55.3, 19.0 ppm; GC-

MS for $C_{17}H_{15}NO$, m/z = 249 (M^+). ^1H and ^{13}C NMR spectral data are in good agreement with the literature values.[222]

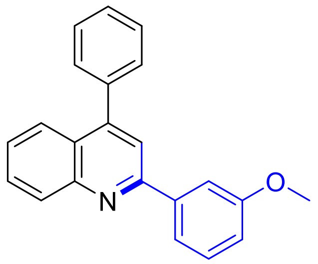

5-9f

2-(3-Methoxyphenyl)-4-phenylquinoline (5-9f): A 1,4-dioxane (2.0 mL) solution of complex **2-10** (9 mg, 3 mol %), **2-16** (8 mg, 10 mol %), 2-aminobenzophenone (99 mg, 0.5 mmol), and (±)-β-amino-3-methoxybenzenepropanoic acid (137 mg, 0.7 mmol) was stirred at 140 °C for 20 h. The product **5-9f** was isolated by column chromatography on silica gel (hexanes/EtOAc = 100:1–10:1; TLC: R_f = 0.6 (20% EtOAc in hexanes)). Yield = 113 mg (73%). Data for **5-9f:** ^1H NMR (400 MHz, $CDCl_3$) δ 8.27 (d, J = 8.5 Hz, 1H), 7.93 (d, J = 8.5 Hz, 1H), 7.83 (s, 1H), 7.82–7.71 (m, 3H), 7.62–7.41 (m, 7H), 7.04 (dd, J = 8.2, 2.2 Hz, 1H), 3.94 (s, 3H) ppm; $^{13}C\{^1H\}$ NMR (100 MHz, $CDCl_3$) δ 160.1, 156.6, 149.1, 148.7, 141.1, 138.3, 130.1, 129.8, 129.5, 129.5, 128.6, 128.4, 126.3, 125.8, 125.6, 120.0, 119.4, 115.4, 112.6, 55.4 ppm; GC-MS for $C_{22}H_{17}NO$, m/z = 311 (M^+). ^1H and ^{13}C NMR spectral data are in good agreement with the literature values.[223]

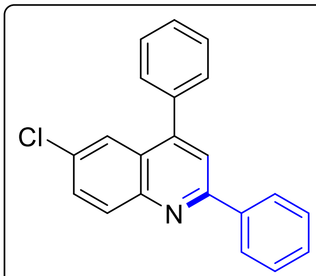

5-9g

6-Chloro-2,4-diphenylquinoline (5-9g): A 1,4-dioxane (2.0 mL) solution of complex **2-10** (9 mg, 3 mol %), **2-16** (8 mg, 10 mol %), 5-chloro-2-aminobenzophenone (116 mg, 0.5 mmol), and (±)-3-amino-3-phenylpropionic acid (116 mg, 0.7 mmol) was stirred at 140 °C for 20 h. The product **5-9g** was isolated by column chromatography on silica gel (hexanes/EtOAc = 100:1–5:1; TLC: R_f = 0.9 (20% EtOAc in hexanes)). Yield = 112 mg (71%). Data for **5-9g:** ^1H NMR (400 MHz, $CDCl_3$) δ 8.28–8.13 (m, 3H), 7.90 (s, 1H), 7.85 (s, 1H), 7.67 (d, *J* = 9.0 Hz, 1H),7.61–7.46 (m, 8H) ppm; $^{13}C\{^1H\}$ NMR (100 MHz, $CDCl_3$) δ 156.9, 148.3, 147.1, 139.0, 137.6, 132.1, 131.6, 130.3, 129.5, 129.3, 128.8, 128.7, 128.6, 127.4, 126.3, 124.4, 119.9 ppm; GC-MS for $C_{21}H_{14}ClN$, m/z = 315 (M^+). ^1H and ^{13}C NMR spectral data are in good agreement with the literature values.[224]

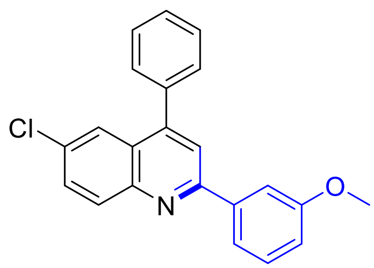

5-9h

6-Chloro-2-(3-methoxyphenyl)-4-phenylquinoline (5-9h): A 1,4-dioxane (2.0 mL) solution of complex **2-10** (9 mg, 3 mol %), **2-16** (8 mg, 10 mol %), 5-chloro-2-aminobenzophenone (116 mg, 0.5 mmol), and (±)-β-amino-3-methoxybenzenepropanoic acid (137 mg, 0.7 mmol) was stirred at 140 °C for 20 h. The product **5-9h** was isolated by column chromatography on silica gel (hexanes/EtOAc = 100:1–5:1; TLC: R_f = 0.5 (20% EtOAc in hexanes)). Yield = 104 mg (60%). Data for **5-9h:** ^1H NMR (400 MHz, $CDCl_3$) δ 8.18 (d, *J* = 9.0 Hz, 1H), 7.87 (d, *J* = 2.2 Hz, 1H), 7.83 (s, 1H), 7.81–7.77 (m, 1H), 7.73 (d, *J* = 7.7 Hz, 1H), 7.67 (dd, *J* = 9.0, 2.2 Hz, 1H), 7.61–7.51 (m, 5H), 7.43 (t, *J* = 7.9 Hz, 1H), 7.03 (dd, *J* = 8.2, 2.2 Hz, 1H) ppm; $^{13}C\{^1H\}$ NMR (100 MHz, $CDCl_3$) δ 160.1, 156.8, 148.4, 147.1, 140.6, 137.7, 132.2, 131.7, 130.4, 129.8, 129.4, 128.8, 128.7, 126.5, 124.4, 120.1, 119.9, 115.6, 112.6, 55.4 ppm; GC-MS for $C_{22}H_{16}ClNO$, m/z = 345 (M^+). ^1H and ^{13}C NMR spectral data are in good agreement with the literature values.[225]

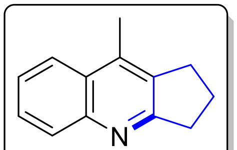

5-9i

2,3-Dihydro-9-methyl-1H-cyclopenta[b]quinoline (5-9i): A 1,4-dioxane (1.0 mL) solution of complex **2-10** (5 mg, 3 mol %), **2-16** (4 mg, 10 mol %), 2'-aminoacetophenone (34 mg, 0.25 mmol), and (±)-2-amino-cyclopentanecarboxylic acid (45 mg, 0.35 mmol) was stirred at 140 °C for 20 h. The product **5-9i** was isolated by column chromatography on silica gel (hexanes/EtOAc =

100:1–5:1; TLC: R_f = 0.2 (20% EtOAc in hexanes)). 88 mg (96%). Data for **5-9i:** ^{1}H NMR (400 MHz, $CDCl_3$) δ 7.99 (d, *J* = 8.4 Hz, 1H), 7.89 (d, *J* = 8.4 Hz, 1H), 7.59 (dd, *J* = 7.7, 1.4 Hz, 1H), 7.45 (dd, *J* = 7.7, 1.4 Hz, 1H), 3.14 (t, *J* = 7.6 Hz, 2H), 3.01 (t, *J* = 7.4 Hz, 2H), 2.53 (s, 2H), 2.16 (pentet, *J* = 7.6 Hz, 2H) ppm; ^{13}C{^{1}H} NMR (100 MHz, $CDCl_3$) δ 166.9, 147.3, 138.0, 133.9, 129.0, 127.9, 126.9, 125.1, 123.2, 35.0, 29.5, 22.9, 14.8 ppm; GC-MS for $C_{13}H_{13}N$, m/z = 183 (M^+). ^{1}H and ^{13}C NMR spectral data are in good agreement with the literature values.[226]

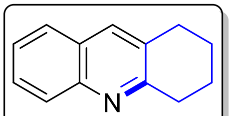
5-9j

1,2,3,4-Tetrahydroacridine (5-9j): A 1,4-dioxane (2.0 mL) solution of complex **2-10** (9 mg, 3 mol %), **2-16** (8 mg, 10 mol %), 2-aminobenzaldehyde (61 mg, 0.5 mmol), and (1S,2R)-2-aminocyclohexanecarboxylic acid (100 mg, 0.7 mmol) was stirred at 140 °C for 20 h. The product **5-9j** was isolated by column chromatography on silica gel (hexanes/EtOAc = 100:1–5:1; TLC: R_f = 0.3 (20% EtOAc in hexanes)). Yield = 82 mg (90%). Data for **5-9j:** ^{1}H NMR (400 MHz, $CDCl_3$) δ 7.96 (d, *J* = 8.5 Hz, 1H), 7.73 (s, 1H), 7.64 (d, *J* = 8.2 Hz, 1H), 7.57 (td, *J* = 7.6, 0.9 Hz, 1H), 7.39 (t, *J* = 7.5 Hz, 1H), 3.10 (t, *J* = 6.5 Hz, 2H), 2.92 (t, *J* = 6.4 Hz, 2H), 1.99–1.91 (m, 2H), 1.89–1.80 (m, 2H) ppm; ^{13}C{^{1}H} NMR (100 MHz, $CDCl_3$) δ 159.1, 146.5, 134.8, 130.8, 128.3, 128.1, 127.1, 126.8, 125.4, 33.5, 29.1, 23.1, 22.8 ppm; GC-MS for $C_{13}H_{13}N$, m/z = 183. ^{1}H and ^{13}C NMR spectral data are in good agreement with the literature values.[227]

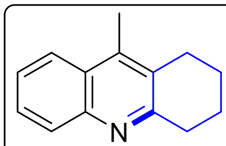
5-9k

9-Methyl-1,2,3,4-tetrahydroacridine (5-9k): A 1,4-dioxane (2.0 mL) solution of complex **2-10** (9 mg, 3 mol %), **2-16** (8 mg, 10 mol %), 2'-aminoacetophenone (68 mg, 0.5 mmol), and (1S,2R)-2-aminocyclohexanecarboxylic acid (100 mg, 0.7 mmol) was stirred at 140 °C for 20 h.

The product **5-9k** was isolated by column chromatography on silica gel (hexanes/EtOAc = 100:1–10:1; TLC: R_f = 0.3 (20% EtOAc in hexanes)). Yield = 88 mg (89%). Data for **5-9k:** ^{1}H NMR (400 MHz, $CDCl_3$) δ 7.94 (d, J = 8.4 Hz, 1H), 7.89 (d, J = 8.4 Hz, 1H), 7.56 (t, J = 7.6 Hz, 1H), 7.40 (t, J = 7.6 Hz, 1H), 3.12–3.03 (m, 2H), 2.83–2.76 (m, 2H) 2.45 (s, 3H), 1.92–1.82 (m, 4H) ppm; ^{13}C{^{1}H} NMR (100 MHz, $CDCl_3$) δ 158.3, 145.7, 141.0, 128.8, 128.4, 127.9, 126.7, 125.0, 123.1, 34.3, 26.9, 23.0, 22.6, 13.3 ppm; GC-MS for $C_{14}H_{15}N$, m/z = 197 (M^+). ^{1}H and ^{13}C NMR spectral data are in good agreement with the literature values.[228]

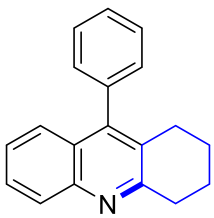
5-9l

9-Phenyl-1,2,3,4-tetrahydroacridine (5-9l): A 1,4-dioxane (2.0 mL) solution of complex **2-10** (9 mg, 3 mol %), **2-16** (8 mg, 10 mol %), 2-aminobenzophenone (99 mg, 0.5 mmol), and (1S,2R)-2-aminocyclohexanecarboxylic acid (100 mg, 0.7 mmol) was stirred at 140 °C for 20 h. The product **5-9l** was isolated by column chromatography on silica gel (hexanes/EtOAc = 100:1–5:1; TLC: R_f = 0.3 (20% EtOAc in hexanes)). Yield = 124 mg (96%). Data for **5-9l:** ^{1}H NMR (400 MHz, $CDCl_3$) δ 8.02 (d, J = 8.5 Hz, 1H), 7.56 (ddd, J = 7.4, 7.4, 1.2 Hz, 1H), 7.51–7.39 (m, 3H), 7.32–7.24 (m, 2H), 7.23–7.17 (m, 2H), 3.18 (t, J = 6.6 Hz, 2H), 2.57 (t, J = 6.5 Hz, 2H), 2.02–1.97 (m, 2H), 1.79–1.70 (m, 2H) ppm; ^{13}C{^{1}H} NMR (100 MHz, $CDCl_3$) δ 158.9, 146.3, 146.1, 137.0, 128.9, 128.4, 128.2, 127.6, 126.5, 125.6, 125.2, 34.1, 27.9, 22.9, 22.8 ppm (two carbon signals were obscured or overlapping); GC-MS for $C_{19}H_{17}N$, m/z = 259 (M^+). ^{1}H and ^{13}C NMR spectral data are in good agreement with the literature values.[229]

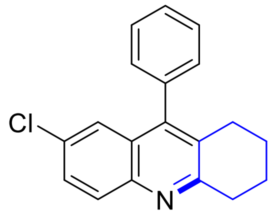

5-9m

7-Chloro-9-phenyl-1,2,3,4-tetrahydroacridine (5-9m): A 1,4-dioxane (2.0 mL) solution of complex **2-10** (9 mg, 3 mol %), **2-16** (8 mg, 10 mol %), 5-chloro-2-aminobenzophenone (116 mg, 0.5 mmol), and (1S,2R)-2-aminocyclohexanecarboxylic acid (100 mg, 0.7 mmol) was stirred at 140 °C for 20 h. The product **5-9m** was isolated by column chromatography on silica gel (hexanes/EtOAc = 100:1–10:1; TLC: R_f = 0.3 (20% EtOAc in hexanes). Yield = 144 mg (98%). Data for **5-9m:** ^{1}H NMR (400 MHz, $CDCl_3$) δ 7.90 (d, *J* = 9.0 Hz, 1H), 7.51–7.38 (m, 4H), 7.25 (d, *J* = 1.9 Hz, 1H), 7.19–7.12 (m, 2H), 3.13 (t, *J* = 6.6 Hz, 2H), 2.54 (t, *J* = 6.5 Hz, 2H), 1.94–1.86 (m, 2H), 1.75–1.68 (m, 2H) ppm; ^{13}C{^{1}H} NMR (100 MHz, $CDCl_3$) δ 159.3, 145.5, 144.5, 136.2, 130.9, 129.9, 129.2, 129.0, 128.8, 128.6, 127.9, 127.2, 124.3, 34.0, 27.9, 22.7, 22.6 ppm; GC-MS for $C_{19}H_{16}ClN$, m/z = 293 (M^+). ^{1}H and ^{13}C NMR spectral data are in good agreement with the literature values.[230]

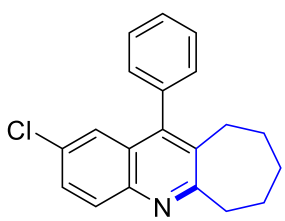

5-9n

2-Chloro-7,8,9,10-tetrahydro-11-phenyl-6H-cyclohepta[b]quinoline (5-9n): A 1,4-dioxane (2.0 mL) solution of complex **2-10** (9 mg, 3 mol %), **2-16** (8 mg, 10 mol %), 5-chloro-2-aminobenzophenone (116 mg, 0.5 mmol), and cis-2-aminocycloheptanecarboxylic acid (110 mg, 0.7 mmol) was stirred at 140 °C for 20 h. The product **5-9n** was isolated by column chromatography on silica gel (hexanes/EtOAc = 100:1–10:1; TLC: R_f = 0.5 (20% EtOAc in hexanes)). Yield = 138 mg (90%). Data for **5-9n:** ^{1}H NMR (400 MHz, $CDCl_3$) δ 7.95 (d, *J* = 8.9 Hz, 1H), 7.58–7.42 (m, 4H), 7.24 (d, *J* = 1.8 Hz, 1H), 7.22–7.14 (m, 2H), 3.28–3.22 (m, 2H), 2.70–2.64 (m, 2H), 1.87–1.80 (m, 4H), 1.63–1.55 (m, 2H) ppm; ^{13}C{^{1}H} NMR (100

MHz, $CDCl_3$) δ 165.0, 144.6, 144.1, 136.8, 134.8, 131.3, 130.1, 129.2, 128.9, 128.6, 127.9, 127.6, 125.1, 40.0, 31.8, 30.6, 28.3, 26.9 ppm; GC-MS for $C_{20}H_{18}ClN$, m/z = 307 (M^+). ^{1}H and ^{13}C NMR spectral data are in good agreement with the literature values.[231]

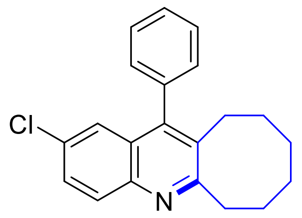

5-9o

2-Chloro-12-phenyl-6,7,8,9,10,11-hexahydrocycloocta[b]quinoline (5-9o): A 1,4-dioxane (2.0 mL) solution of complex **2-10** (9 mg, 3 mol %), **2-16** (8 mg, 10 mol %), 5-chloro-2-aminobenzophenone (116 mg, 0.5 mmol), and *cis*-2-amino-cyclooctanecarboxylic acid (120 mg, 0.7 mmol) was stirred at 140 °C for 20 h. The product **5-9o** was isolated by column chromatography on silica gel (hexanes/EtOAc = 100:1–10:1; TLC: R_f = 0.4 (20% EtOAc in hexanes)). Yield = 151 mg (94%). Data for **5-9o:** ^{1}HNMR (400 MHz, $CDCl_3$) δ 7.98 (d, *J* = 8.9 Hz, 1H), 7.65–7.37 (m, 4H), 7.21 (d, *J* = 6.5 Hz, 2H), 7.17 (d, *J* = 1.7 Hz, 1H), 3.21 (t, *J* = 6.1 Hz, 2H), 2.74 (t, *J* = 6.2 Hz, 2H), 2.01–1.86 (m, 2H), 1.56–1.42 (m, 4H), 1.40–1.27 (m, 2H) ppm; ^{13}C{^{1}H} NMR (100 MHz, $CDCl_3$) δ 163.8, 145.7, 144.7, 136.8, 132.9, 131.1, 130.1, 129.2, 129.0, 128.5, 127.9, 127.9, 124.8, 36.3, 31.1, 31.1, 28.1, 26.6, 25.7 ppm; GC-MS for $C_{21}H_{20}ClN$, m/z = 321 (M^+). HRMS (ESI-TOF) m/z: $[M + H]^+$ Calcd for $C_{21}H_{20}ClNH$; 322.1357 Found 322.1327.

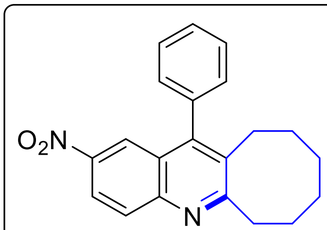

5-9p

2-Nitro-12-phenyl-6,7,8,9,10,11-hexahydrocycloocta[b]quinoline (5-9p): A 1,4-dioxane (2.0 mL) solution of complex **2-10** (9 mg, 3 mol %), **2-16** (8 mg, 10 mol %), 5-chloro-2-aminobenzophenone (116 mg, 0.5 mmol), and cis-2-amino-cyclooctanecarboxylic acid (120 mg, 0.7 mmol) was stirred at 140 °C for 20 h. The product **5-9p** was isolated by column chromatography on silica gel (hexanes/EtOAc = 100:1–10:1; TLC: R_f = 0.4 (20% EtOAc in hexanes)). Yield = 142 mg (86%). Data for **5-9p:** ^{1}H NMR (400 MHz, $CDCl_3$) δ 8.33 (dd, *J* = 9.2, 1.7 Hz, 1H), 8.15 (d, *J* = 1.7 Hz, 1H), 8.11 (d, *J* = 9.2 Hz, 1H), 7.66–7.45 (m, 3H), 7.27–7.18 (m, 2H), 3.24 (t, *J* = 6.1 Hz, 2H), 2.78 (t, *J* = 6.1 Hz, 2H), 1.99–1.90 (m, 2H), 1.55–1.42 (m, 4H), 1.40–1.29 (m, 2H) ppm; ^{13}C{^{1}H} NMR (100 MHz, $CDCl_3$) δ 167.8, 148.5, 148.2, 144.8, 135.8, 134.2, 130.2, 129.1, 128.7, 128.5, 126.3, 123.2, 121.8, 36.6, 31.1, 31.1, 28.2, 26.5, 25.7 ppm; GC-MS for $C_{21}H_{20}N_2O_2$, m/z = 332 (M^+); HRMS (ESI-TOF) m/z: $[M + H]^+$ Calcd for $C_{21}H_{20}N_2O_2H$, 333.1598 Found 333.1566.

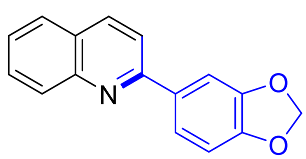

5-9q

2-(1,3-Benzodioxol-5-yl)quinoline (5-9q): A 1,4-dioxane (2.0 mL) solution of complex **2-10** (9 mg, 3 mol %), **2-16** (8 mg, 10 mol %), 2-aminobenzaldehyde (61 mg, 0.5 mmol), and (±)-3-amino-3-benzo[1,3]dioxol-5-yl-propionic acid (146 mg, 0.7 mmol) was stirred at 140 °C for 20 h. The product **5-9q** was isolated by column chromatography on silica gel (hexanes/EtOAc = 100:1–5:1; TLC: R_f = 0.5 (20% EtOAc in hexanes)). Yield = 108 mg (87%). Data for **5-9q:** ^{1}H NMR (400 MHz, $CDCl_3$) δ 8.16 (d, *J* = 8.9 Hz, 1H), 8.13 (d, *J* = 8.9 Hz, 1H), 7.82–7.76 (m, 2H), 7.75 (d, *J* = 1.5 Hz, 1H), 7.71 (td, *J* = 7.8, 1.0 Hz, 1H), 7.65 (dd, *J* = 8.1, 1.5 Hz, 1H), 7.50 (t, *J* = 7.5 Hz, 1H), 6.95 (d, *J* = 8.1 Hz, 1H), 6.04 (s, 2H) ppm; ^{13}C{^{1}H} NMR (100 MHz, $CDCl_3$) δ 156.6, 148.8, 148.3, 148.1, 136.6, 134.0, 129.6, 129.5, 127.4, 126.9, 126.0, 121.7, 118.6, 108.4, 107.9, 101.3 ppm; GC-MS for $C_{16}H_{11}NO_2$, m/z = 249 (M^+). ^{1}H and ^{13}C NMR spectral data are in good agreement with the literature values.[232]

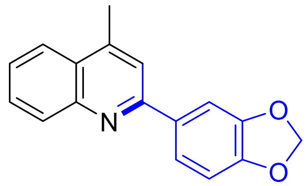

5-9r

2-(Benzo[d][1,3]dioxol-5-yl)-4-methylquinoline (5-9r): A 1,4-dioxane (2.0 mL) solution of complex **2-10** (9 mg, 3 mol %), **2-16** (8 mg, 10 mol %), 2'-aminoacetophenone (68 mg, 0.5 mmol), and (±)-3-amino-3-benzo[1,3]dioxol-5-yl-propionic acid (146 mg, 0.7 mmol) was stirred at 140 °C for 20 h. The product **5-9r** was isolated by column chromatography on silica gel (hexanes/EtOAc = 100:1–5:1; TLC: R_f = 0.6 (20% EtOAc in hexanes)). Yield = 73 mg (56%). Data for **5-9r:** ^{1}H NMR (400 MHz, $CDCl_3$) δ 8.13 (d, J = 8.4 Hz, 1H), 7.96 (d, J = 8.4 Hz, 1H), 7.74–7.60 (m, 4H), 7.52 (t, J = 7.5 Hz, 1H), 6.94 (d, J = 8.1 Hz, 1H), 6.03 (s, 2H), 2.73 (s, 3H) ppm; ^{13}C{^{1}H} NMR (100 MHz, $CDCl_3$) δ 156.3, 148.6, 148.2, 147.9, 144.6, 134.2, 130.0, 129.3, 127.0, 125.7, 123.5, 121.6, 119.3, 108.4, 107.8, 101.3, 19.0 ppm; GC-MS for $C_{17}H_{13}NO_2$, m/z = 263 (M^+).

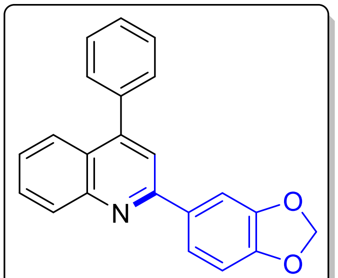

5-9s

2-(Benzo[d][1,3]dioxol-5-yl)-4-phenylquinoline (5-9s): A 1,4-dioxane (2.0 mL) solution of complex **2-10** (9 mg, 3 mol %), **2-16** (8 mg, 10 mol %), 2-aminobenzophenone (99 mg, 0.5 mmol), and (±)-3-amino-3-benzo[1,3]dioxol-5-yl-propionic acid (146 mg, 0.7 mmol) was stirred at 140 °C for 20 h. The product **5-9s** was isolated by column chromatography on silica gel (hexanes/EtOAc = 100:1–5:1; TLC: R_f = 0.6 (20% EtOAc in hexanes)). Yield = 114 mg (70%). Data for **5-9s:** ^{1}H NMR (400 MHz, $CDCl_3$) δ 8.20 (d, J = 8.4 Hz, 1H), 7.88 (d, J = 8.4 Hz, 1H), 7.78 (d, J = 1.1 Hz, 1H), 7.74 (s, 1H), 7.73–7.66 (m, 2H), 7.61–7.49 (m, 5H), 7.46 (dd, J = 7.6, 7.6 Hz, 1H), 6.95 (dd, J = 8.2 Hz, 1H), 6.04 (s, 2H), ppm; ^{13}C{^{1}H} NMR (100 MHz, $CDCl_3$) δ 156.2, 149.0, 148.8, 148.6, 148.3, 138.4, 134.0, 129.9, 129.5, 129.5, 128.5, 128.4, 126.1, 125.6, 125.6, 121.7, 118.9, 108.4, 107.9, 101.3 ppm; GC-MS for $C_{22}H_{15}NO_2$, m/z = 325 (M^+). HRMS (ESI-TOF) m/z: $[M + H]^+$ Calcd for $C_{22}H_{15}NO_2H$; 326.1176 Found 326.1156.

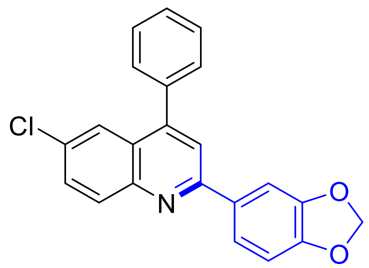

5-9t

2-(Benzo[d][1,3]dioxol-5-yl)-6-chloro-4-phenylquinoline (5-9t): A 1,4-dioxane (2.0 mL) solution of complex **2-10** (9 mg, 3 mol %), **2-16** (8 mg, 10 mol %), 5-chloro-2-aminobenzophenone (116 mg, 0.5 mmol), and (±)-3-amino-3-benzo[1,3]dioxol-5-yl-propionic acid (146 mg, 0.7 mmol) was stirred at 140 °C for 20 h. The product **5-9t** was isolated by column chromatography on silica gel (hexanes/EtOAc = 100:1–5:1; TLC: R_f = 0.7 (20% EtOAc in hexanes)). Yield = 89 mg (50%). Data for **5-9t:** ^1H NMR (400 MHz, $CDCl_3$) δ 8.12 (d, J = 9.0 Hz, 1H), 7.84 (s, 1H), 7.75 (d, J = 6.9 Hz, 2H), 7.65 (t, J = 9.4 Hz, 2H), 7.60–7.49 (m, 5H), 6.93 (d, J = 8.1 Hz, 1H), 6.03 (s, 2H) ppm; $^{13}C\{^1H\}$ NMR (100 MHz, $CDCl_3$) δ 156.2, 149.0, 148.4, 148.2, 147.0, 137.7, 133.5, 131.8, 131.4, 130.3, 129.4, 128.7, 128.6, 126.2, 124.4, 121.7, 119.5, 108.4, 107.7, 101.4 ppm; GC-MS for $C_{22}H_{14}ClNO_2$, m/z = 359 (M^+). HRMS (ESI-TOF) m/z: $[M + H]^+$ Calcd for $C_{22}H_{14}ClNO_2H$; 360.0786 Found 360.0773.

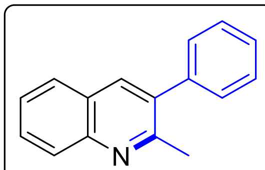

5-9u-a

2-Methyl-3-phenylquinoline (5-9u-a): A 1,4-dioxane (2.0 mL) solution of complex **2-10** (9 mg, 3 mol %), **2-16** (8 mg, 10 mol %), 2-aminobenzaldehyde (61 mg, 0.5 mmol), and (±)-3-amino-4-phenylbutanoic acid (125 mg, 0.7 mmol) was stirred at 140 °C for 20 h. The product **5-9u-a** was isolated by column chromatography on silica gel (hexanes/EtOAc = 100:1–5:1; TLC: R_f = 0.5 (20% EtOAc in hexanes)). Yield = 71 mg

(65%). Data for **5-9u-a:** ^{1}HNMR (400 MHz, $CDCl_3$) δ 8.07 (d, *J* = 8.5 Hz, 1H), 7.96 (s, 1H), 7.79 (d, *J* = 8.1 Hz, 1H), 7.70 (t, *J* = 7.7 Hz, 1H), 7.54–7.38 (m, 6H), 2.68 (s, 3H) ppm; $^{13}C\{^{1}H\}$ NMR (100 MHz, $CDCl_3$) δ 157.3, 147.0, 139.9, 136.1, 135.7, 129.3, 129.2, 128.4, 128.4, 127.6, 127.4, 126.8, 126.0, 24.6 ppm; GC-MS for $C_{16}H_{13}N$, m/z = 219 (M^+). ^{1}H and ^{13}C NMR spectral data are in good agreement with the literature values.[233]

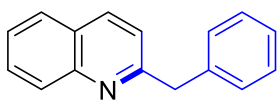

5-9u-b

2-(Phenylmethyl)quinoline (5-9u-b): A 1,4-dioxane (2.0 mL) solution of complex **2-10** (9 mg, 3 mol %), **2-16** (8 mg, 10 mol %), 2-aminobenzaldehyde (61 mg, 0.5 mmol), and (±)-3-amino-4-phenylbutanoic acid (125 mg, 0.7 mmol) was stirred at 140 °C for 20 h. The product **5-9u-b** was isolated by column chromatography on silica gel (hexanes/EtOAc = 100:1–51; TLC: R_f = 0.3 (20% EtOAc in hexanes)). Yield = 37 mg (34%). Data for **5-9u-b:** ^{1}H NMR (400 MHz, $CDCl_3$) δ 8.07 (d, *J* = 8.5 Hz, 1H), 8.01 (d, *J* = 8.5 Hz, 1H), 7.75 (d, *J* = 8.1 Hz, 1H), 7.69 (dd, *J* = 7.7, 7.7 Hz, 1H), 7.48 (dd, *J* = 7.5, 7.5 Hz, 1H), 7.33–7.18 (m, 6H), 4.34 (s, 2H) ppm; $^{13}C\{^{1}H\}$ NMR (100 MHz, $CDCl_3$) δ 161.2, 147.7, 139.2, 136.5, 129.5, 129.2, 128.9, 128.6, 127.5, 126.7, 126.5, 126.0, 121.5, 45.5 ppm; GC-MS for $C_{16}H_{13}N$, m/z = 219 (M^+). ^{1}H and ^{13}C NMR spectral data are in good agreement with the literature values.[234]

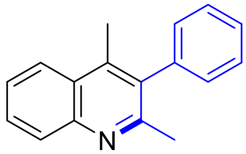

5-9v

2,4-Dimethyl-3-phenylquinoline (5-9v): A 1,4-dioxane (2.0 mL) solution of complex **2-10** (9 mg, 3 mol %), **2-16** (8 mg, 10 mol %), 2'-aminoacetophenone (68 mg, 0.5 mmol), and (±)-3-amino-4-phenylbutanoic acid (125 mg, 0.7 mmol) was stirred at 140 °C for 20 h. The product **5-9v** was isolated by column chromatography on silica gel (hexanes/EtOAc = 100:1–5:1; TLC: R_f = 0.6 (20% EtOAc in hexanes)). Yield = 85 mg (73%). Data for **5-9v:** ^{1}H NMR (400 MHz, $CDCl_3$) δ 8.06 (d, J = 8.4 Hz, 1H), 8.00 (d, J = 8.4 Hz, 1H), 7.69 (t, J = 7.6 Hz, 1H), 7.58–7.46 (m, 3H), 7.45–7.38 (m, 1H), 7.24–7.17 (m, 2H), 2.43 (s, 3H), 2.39 (s, 3H) ppm; ^{13}C{^{1}H} NMR (100 MHz, $CDCl_3$) δ 157.6, 146.6, 141.2, 139.5, 134.9, 129.3, 129.1, 128.9, 128.7, 127.4, 126.7, 125.7, 124.1, 25.4, 15.9 ppm; GC-MS for $C_{17}H_{15}N$, m/z = 233 (M^+). ^{1}H and ^{13}C NMR spectral data are in good agreement with the literature values.[188]

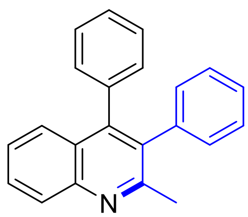

5-9w

2-Methyl-3,4-diphenylquinoline (5-9w): A 1,4-dioxane (2.0 mL) solution of complex **2-10** (9 mg, 3 mol %), **2-16** (8 mg, 10 mol %), 2-aminobenzophenone (99 mg, 0.5 mmol), and (±)-3-amino-4-phenylbutanoic acid (125 mg, 0.7 mmol) was stirred at 140 °C for 20 h. The product **5-9w** was isolated by column chromatography on silica gel (hexanes/EtOAc = 100:1–5:1; TLC: R_f = 0.5 (20% EtOAc in hexanes)). Yield = 106 mg (72%). Data for **5-9w:** ^{1}H NMR (400 MHz, $CDCl_3$) δ 8.12 (d, J = 8.4 Hz, 1H), 7.69 (t, J = 7.6 Hz, 1H), 7.50 (d, J = 8.4 Hz, 1H), 7.39 (t, J = 7.6 Hz, 1H), 7.32–7.15 (m, 6H), 7.14–7.02 (m, 4H), 2.55 (s, 3H) ppm; ^{13}C{^{1}H} NMR (100 MHz, $CDCl_3$) δ 157.8, 147.0, 146.5, 138.6, 136.7, 134.0, 130.1, 130.0, 129.1, 128.6, 127.9, 127.6, 127.2, 126.8, 126.6, 126.3, 125.8, 25.4 ppm; GC-MS for $C_{22}H_{17}N$, m/z = 295 (M^+). ^{1}H and ^{13}C NMR spectral data are in good agreement with the literature values.[188]

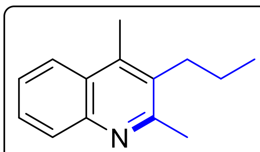

5-9x

2,4-Dimethyl-3-propylquinoline (5-9x): A 1,4-dioxane (2.0 mL) solution of complex **2-10** (9 mg, 3 mol %), **2-16** (8 mg, 10 mol %), 2'-aminoacetophenone (68 mg, 0.5 mmol), and (±)-3-aminoheptanoic acid (102 mg, 0.7 mmol) was stirred at 140 °C for 20 h. The product **5-9x** was isolated by column chromatography on silica gel (hexanes/EtOAc = 100:1–5:1; TLC: R_f = 0.7 (20% EtOAc in hexanes)). Yield = 95 mg (95%). Data for **5-9x:** ^{1}H NMR (400 MHz, $CDCl_3$) δ 7.97 (t, *J* = 9.7 Hz, 2H), 7.61 (t, *J* = 7.8 Hz, 1H), 7.49 (t, *J* = 7.8 Hz, 1H), 2.86–2.78 (m, 2H), 2.75 (s, 3H), 2.64 (s, 3H), 1.64–1.53 (m, 2H), 1.07 (t, *J* = 7.3 Hz, 3H) ppm; ^{13}C{^{1}H} NMR (100 MHz, $CDCl_3$) δ 158.2, 145.6, 140.6, 132.4, 128.9, 128.1, 127.3, 126.6, 125.4, 123.6, 31.8, 24.1, 23.0, 14.5, 14.2 ppm (two carbon signals obscured or overlapping); GC-MS for $C_{14}H_{17}N$, m/z = 199 (M^+). ^{1}H and ^{13}C NMR spectral data are in good agreement with the literature values.[235]

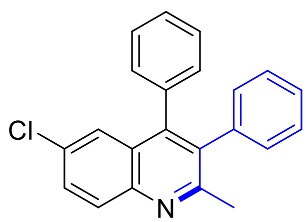

5-9y-a

6-Chloro-2-methyl-3,4-diphenylquinoline (5-9y-a): A 1,4-dioxane (2.0 mL) solution of complex **2-10** (9 mg, 3 mol %), **2-16** (8 mg, 10 mol %), 5-chloro-2-aminobenzophenone (116 mg, 0.5 mmol), and (±)-3-amino-4-phenylbutanoic acid (125 mg, 0.7 mmol) was stirred at 140 °C for 20 h. The product **5-9y-a** was isolated by column chromatography on silica gel (hexanes/EtOAc = 100:1–5:1; TLC: R_f = 0.6 (20% EtOAc in hexanes)). Yield = 143 mg (87%). Data for **5-9y-a:** ^{1}H NMR (400 MHz, $CDCl_3$) δ 8.03 (d, *J* = 9.0 Hz, 1H), 7.60 (dd, *J* = 9.0, 2.0 Hz, 1H), 7.45 (d, *J* = 2.0 Hz, 1H), 7.26–7.14 (m, 6H), 7.10–6.97 (m, 4H), 2.51 (s, 3H) ppm; ^{13}C{^{1}H} NMR (100 MHz, $CDCl_3$) δ 158.2, 145.8, 145.4, 138.2, 136.0, 134.9, 131.6, 130.3, 129.9, 129.9, 129.8, 127.9, 127.9, 127.5, 127.1, 127.0, 125.3, 25.4 ppm; GC-MS for $C_{22}H_{16}ClN$, m/z = 329 (M^+). ^{1}H and ^{13}C NMR spectral data are in good agreement with the literature values.[188]

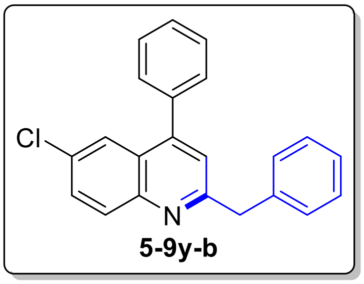

2-Benzyl-6-chloro-4-phenylquinoline (5-9y-b): A 1,4-dioxane (2.0 mL) solution of complex **2-10** (9 mg, 3 mol %), **2-16** (8 mg, 10 mol %), 5-chloro-2-aminobenzophenone (116 mg, 0.5 mmol), and (±)-3-amino-4-phenylbutanoic acid (125 mg, 0.7 mmol) was stirred at 140 °C for 20 h. The product **5-9y-b** was isolated by column chromatography on silica gel (hexanes/EtOAc = 100:1–5:1; TLC: R_f = 0.4 (20% EtOAc in hexanes)). Yield = 19 mg (12%). Data for **5-9y-b:** ^{1}H NMR (400 MHz, $CDCl_3$) δ 8.09 (d, J = 9.0 Hz, 1H), 7.82 (d, J = 1.7 Hz, 1H), 7.65 (dd, J = 9.0, 1.7 Hz, 1H), 7.57–7.38 (m, 5H), 7.36–7.18 (m, 6H), 4.36 (s, 2H) ppm; ^{13}C{^{1}H} NMR (100 MHz, $CDCl_3$) δ 161.0, 148.1, 146.7, 138.8, 137.4, 131.9, 131.0, 130.2, 129.4, 129.2, 128.7, 128.6, 126.6, 126.1, 124.5, 122.4, 45.5 ppm (one carbon signal obscured or overlapping); GC-MS for $C_{22}H_{16}ClN$, m/z = 329 (M^+). HRMS (ESI-TOF) m/z: $[M + H]^+$ Calcd for $C_{22}H_{16}ClNH$; 330.1044 Found 330.1039.

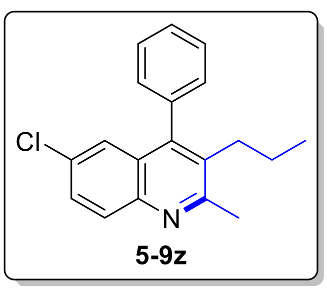

6-Chloro-2-methyl-4-phenyl-3-propylquinoline (5-9z): A 1,4-dioxane (2.0 mL) solution of complex **2-10** (9 mg, 3 mol %), **2-16** (8 mg, 10 mol %), 5-chloro-2-aminobenzophenone (116 mg, 0.5 mmol), and (±)-3-aminoheptanoic acid (102 mg, 0.7 mmol) was stirred at 140 °C for 20 h. The product **5-9z** was isolated by column chromatography on silica gel (hexanes/EtOAc = 100:1–5:1; TLC: R_f = 0.6 (20% EtOAc in hexanes)). Yield = 124 mg (84%). Data for **5-9z:** ^{1}H NMR (400 MHz, $CDCl_3$) δ 7.94 (d, J = 9.0 Hz, 1H), 7.60–7.44 (m, 4H), 7.22 (d, J = 7.1 Hz, 2H), 7.19 (d, J = 1.9 Hz, 1H), 2.79 (s, 3H), 2.56–2.45 (m, 2H), 1.51–1.37 (m, 2H), 0.82

(t, *J* = 7.3 Hz, 3H) ppm; $^{13}C\{^1H\}$ NMR (100 MHz, $CDCl_3$) δ 159.0, 145.7, 144.4, 136.7, 133.2, 131.2, 130.0, 129.2, 129.1, 128.5, 128.0, 127.9, 125.0, 32.5, 23.8, 23.5, 14.5 ppm; GC-MS for $C_{19}H_{18}ClN$, m/z = 295 (M^+). HRMS (ESI-TOF) m/z: $[M + H]^+$ Calcd for $C_{19}H_{18}ClNH$; 296.1201 Found 296.1177.

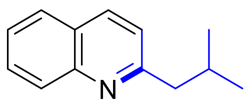

5-9aa

2-(2-Methylpropyl)quinoline (5-9aa): A 1,4-dioxane (2.0 mL) solution of complex **2-10** (9 mg, 3 mol %), **2-16** (8 mg, 10 mol %), 2-aminobenzaldehyde (61 mg, 0.5 mmol), and (±)-3-amino-5-methylhexanoic acid (102 mg, 0.7 mmol) was stirred at 140 °C for 20 h. The product **5-9aa** was isolated by column chromatography on silica gel (hexanes/EtOAc = 100:1–5:1; TLC: R_f = 0.6 (20% EtOAc in hexanes)). Yield = 79 mg (85%). Data for **5-9aa:** ^1H NMR (400 MHz, $CDCl_3$) δ 8.03 (d, *J* = 8.4 Hz, 2H), 7.75 (d, *J* = 8.2 Hz, 1H), 7.66 (t, *J* = 7.6 Hz, 1H), 7.46 (t, *J* = 7.6 Hz, 1H), 7.25 (d, *J* = 8.4 Hz, 1H), 2.83 (d, *J* = 7.6 Hz, 2H), 2.19 (nonet, *J* = 6.8 Hz, 1H), 0.96 (d, *J* = 6.8 Hz, 6H) ppm; $^{13}C\{^1H\}$ NMR (100 MHz, $CDCl_3$) δ 162.2, 147.9, 135.9, 129.2, 128.8, 127.4, 126.7, 125.6, 122.0, 48.3, 29.4, 22.5 ppm; GC-MS for $C_{13}H_{15}N$, m/z = 185 (M^+). ^1H and ^{13}C NMR spectral data are in good agreement with the literature values.[236]

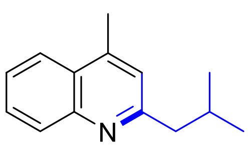

5-9ab

4-Methyl-2-(2-methylpropyl)quinoline (5-9ab): A 1,4-dioxane (2.0 mL) solution of complex **2-10** (9 mg, 3 mol %), **2-16** (8 mg, 10 mol %), 2'-aminoacetophenone (68 mg, 0.5 mmol), and (±)-3-amino-5-methylhexanoic acid (102 mg, 0.7 mmol) was stirred at 140 °C for 20 h. The product **5-9ab** was isolated by column chromatography on silica gel (*n*-hexane/EtOAc = 100:1–5:1; TLC: R_f = 0.6 (20% EtOAc in hexanes)). Yield = 62 mg (62%). Data for **5-9ab:** ^1H NMR (400 MHz, $CDCl_3$) δ 8.05 (d, *J* = 8.4 Hz, 1H), 7.94 (d, *J*

= 8.4 Hz, 1H), 7.66 (t, J = 7.4 Hz, 1H), 7.49 (t, J = 7.6 Hz, 1H), 7.10 (s, 1H), 2.80 (d, J = 7.4 Hz, 2H) 2.66 (m, 3H), 2.20 (dt, J = 13.6, 6.7 Hz, 1H), 0.97 (d, J = 6.7 Hz, 6H) ppm; $^{13}C\{^1H\}$ NMR (100 MHz, $CDCl_3$) δ 161.9, 147.7, 143.8, 129.3, 128.9, 126.7, 125.3, 123.5, 122.7, 48.2, 29.4, 22.5, 18.7 ppm; GC-MS for $C_{14}H_{17}N$, m/z = 199 (M^+). ^1H and ^{13}C NMR spectral data are in good agreement with the literature values.[237]

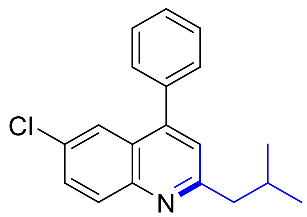
5-9ac

6-Chloro-2-isobutyl-4-phenylquinoline (5-9ac): A 1,4-dioxane (2.0 mL) solution of complex **2-10** (9 mg, 3 mol %), **2-16** (8 mg, 10 mol %), 5-chloro-2-aminobenzophenone (116 mg, 0.5 mmol), and (±)-3-amino-5-methylhexanoic acid (102 mg, 0.7 mmol) was stirred at 140 °C for 20 h. The product **5-9ac** was isolated by column chromatography on silica gel (hexanes/EtOAc = 100:1–5:1; TLC: R_f = 0.7 (20% EtOAc in hexanes). Yield = 114 mg (77%). Data for **5-9ac:** ^1H NMR (400 MHz, $CDCl_3$) δ 8.04 (d, J = 9.0 Hz, 1H), 7.84 (s, 1H), 7.60 (dd, J = 9.0, 1.4 Hz, 1H), 7.55–7.37 (m, 5H), 7.22 (s, 1H), 2.86 (d, J = 7.4 Hz, 2H), 2.24 (nonet, J = 6.8 Hz, 1H), 1.00 (d, J = 6.8 Hz, 6H) ppm; $^{13}C\{^1H\}$ NMR (100 MHz, $CDCl_3$) δ 162.0, 147.4, 146.7, 137.5, 131.5, 130.8, 129.9, 129.3, 128.6, 128.5, 125.9, 124.3, 122.9, 48.1, 29.3, 22.5 ppm; GC-MS for $C_{19}H_{18}ClN$, m/z = 295 (M^+). HRMS (ESI-TOF) m/z: $[M + H]^+$ Calcd for $C_{19}H_{18}ClNH$; 296.1201 Found 296.1167.

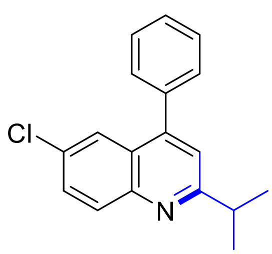
5-9ad

6-Chloro-2-isobutyl-4-phenylquinoline (5-9ad): A 1,4-dioxane (2.0 mL) solution of complex **2-10** (9 mg, 3 mol %), **2-16** (8 mg, 10 mol %), 5-chloro-2-aminobenzophenone (116 mg, 0.5 mmol), and (±)-β-leucine (92 mg, 0.7 mmol) was stirred at 140 °C for 20 h. The product **5-9ad** was isolated by column chromatography on silica gel (hexanes/EtOAc = 100:1–5:1; TLC: R_f = 0.7 (20% EtOAc in hexanes)). Yield = 71 mg, (51%). Data for **5-9ad:** ^{1}H NMR (400 MHz, $CDCl_3$) δ 8.07 (d, *J* = 9.0 Hz, 1H), 7.85 (s, 1H), 7.60 (dd, *J* = 9.0, 1.4 Hz, 1H), 7.55–7.42 (m, 5H), 7.31 (s, 1H), 3.29 (septet, *J* = 6.9 Hz, 1H), 1.44 (d, *J* = 6.9 Hz, 6H) ppm; $^{13}C\{^{1}H\}$ NMR (100 MHz, $CDCl_3$) δ 167.3, 147.8, 146.5, 137.6, 131.4, 130.9, 129.8, 129.3, 128.6, 128.4, 126.0, 124.2, 120.2, 37.1, 22.4 ppm; GC-MS for $C_{18}H_{16}ClN$, m/z = 281 (M^+). HRMS (ESI-TOF) m/z: $[M + H]^+$ Calcd for $C_{18}H_{16}ClNH$; 282.1044 Found 282.1010.

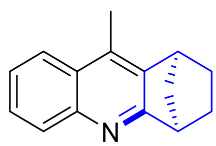
5-9ae

(1S,4R)-9-Methyl-1,2,3,4-tetrahydro-1,4-methanoacridine (5-9ae): A 1,4-dioxane (2.0 mL) solution of complex **2-10** (9 mg, 3 mol %), **2-16** (8 mg, 10 mol %), 2'-aminoacetophenone (68 mg, 0.5 mmol), and 3-aminobicyclo[2.2.1]heptane-2-carboxylic acid (109 mg, 0.7 mmol) was stirred at 140 °C for 20 h. The product **5-9ae** was isolated by column chromatography on silica gel (hexanes/EtOAc = 100:1–5:1; TLC: R_f = 0.3 (20% EtOAc in hexanes)). Yield = 89 mg, (85%). Data for **5-9ae:** ^{1}H NMR (400 MHz, $CDCl_3$) δ 8.00 (d, *J* = 8.3 Hz, 1H), 7.89 (d, *J* = 8.3 Hz, 1H), 7.59 (t, *J* = 7.6 Hz, 1H), 7.47 (t, *J* = 7.6 Hz, 1H), 3.65 (s, 1H), 3.51 (s, 1H), 2.59 (s, 3H), 2.09–1.99 (m, 2H), 1.89 (d, *J* = 9.3 Hz, 1H), 1.70 (d, *J* = 9.3 Hz, 1H), 1.47–1.40 (m, 1H), 1.33–1.23 (m, 1H) ppm; $^{13}C\{^{1}H\}$ NMR (100 MHz, $CDCl_3$) δ 169.6, 146.3, 137.9, 133.2, 129.1, 127.6, 127.6, 125.0, 123.6, 46.2, 45.8, 40.3, 26.9, 25.8, 14.1 ppm; GC-MS for $C_{15}H_{15}N$, m/z = 209 (M^+). HRMS (ESI-TOF) m/z: $[M + H]^+$ Calcd for $C_{15}H_{15}NH$; 210.1277 Found 210.1252.

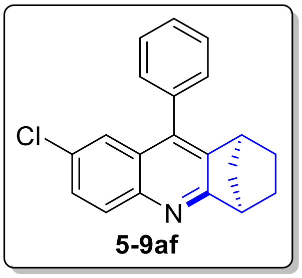

(1S,4R)-7-Chloro-9-phenyl-1,2,3,4-tetrahydro-1,4-methanoacridine (5-9af): A 1,4-dioxane (2.0 mL) solution of complex **2-10** (9 mg, 3 mol %), **2-16** (8 mg, 10 mol %), 5-chloro-2-aminobenzophenone (116 mg, 0.5 mmol), and 3-aminobicyclo[2.2.1]heptane-2-carboxylic acid (109 mg, 0.7 mmol) was stirred at 140 °C for 20 h. The product **5-9af** was isolated by column chromatography on silica gel (hexanes/EtOAc = 100:1–5:1; TLC: R_f = 0.4 (20% EtOAc in hexanes)). Yield = 138 mg, (90%). Data for **5-9af:** ^{1}H NMR (400 MHz, $CDCl_3$) δ 7.97 (d, J = 8.9 Hz, 1H), 7.62 (s, 1H), 7.58–7.45 (m, 4H), 7.45–7.27 (m, 2H), 3.57 (s, 1H), 3.38 (s, 1H), 2.13–1.92 (m, 3H), 1.68 (d, J = 9.3 Hz, 1H), 1.52 (t, J = 10.3 Hz, 1H), 1.40–1.31 (m, 1H) ppm; ^{13}C{^{1}H} NMR (100 MHz, $CDCl_3$) δ 170.3, 145.2, 138.6, 137.4, 135.3, 131.1, 130.4, 129.7, 129.4, 128.5, 128.2, 127.3, 124.7, 46.5, 45.8, 40.9, 27.4, 25.7 ppm; GC-MS for $C_{20}H_{16}ClN$, m/z = 305 (M^+). HRMS (ESI-TOF) m/z: $[M + H]^+$ Calcd for $C_{20}H_{16}ClNH$; 306.1044 Found 306.1013.

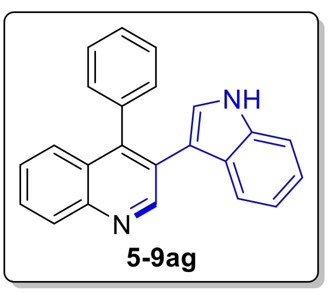

3-(1H-Indol-2-yl)-4-phenylquinoline (5-9ag): A 1,4-dioxane (2.0 mL) solution of complex **2-10** (9 mg, 3 mol %), **2-16** (8 mg, 10 mol %), 2-aminobenzophenone (99 mg, 0.5 mmol), and tryptamine (112 mg, 0.7 mmol) was stirred at 140 °C for 20 h. The product **5-9ag** was isolated by column chromatography on silica gel (hexanes/EtOAc = 100:1–5:1; TLC: R_f = 0.3 (20% EtOAc in hexanes)). Yield = 64 mg, (40%). Data for **5-9ag:** ^{1}H NMR (400 MHz, $CDCl_3$) δ 9.26 (s. 1H), 8.42 (brs, 1H), 8.20 (d, J = 8.4 Hz, 1H), 7.72–7.66 (m, 2H), 7.63 (d, J = 8.4 Hz, 1H), 7.45 (t, J = 7.6 Hz, 1H), 7.37–7.31 (m, 4H), 7.27–7.24 (m, 2H), 7.20 (t, J = 7.6 Hz, 1H), 7.13 (t, *J* = 7.6 Hz, 1H), 6.64 (d, *J* = 2.5 Hz, 1H) ppm; $^{13}C\{^1H\}$ NMR (100 MHz, $CDCl_3$) δ 152.2, 146.6, 145.7, 137.1, 135.7, 130.1, 129.1, 128.7, 128.2, 127.9, 127.7, 126.9, 126.8, 126.7, 126.4, 125.1, 122.4, 120.4, 119.3, 113.1, 111.3 ppm; GC-MS for $C_{23}H_{16}N_2$, m/z = 320 (M^+). HRMS (ESI-TOF) m/z: $[M + H]^+$ Calcd for $C_{23}H_{16}N_2H$; 321.1386 Found 321.1382.

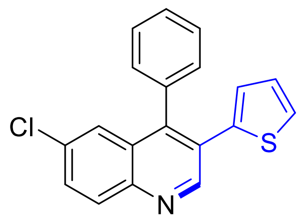

5-9ah

6-Chloro-4-phenyl-3-(thiophen-2-yl)quinoline (5-9ah): A 1,4-dioxane (2.0 mL) solution of complex **2-10** (9 mg, 3 mol %), **2-16** (8 mg, 10 mol %), 5-chloro-2-aminobenzophenone (116 mg, 0.5 mmol), and 2-thiopheneethylamine (89 mg, 0.7 mmol) was stirred at 140 °C for 20 h. The product **5-9ah** was isolated by column chromatography on silica gel (hexanes/EtOAc = 100:1–5:1; TLC: R_f = 0.4 (20% EtOAc in hexanes)). Yield = 68 mg, (42%). Data for **5-9ah:** ^1H NMR (400 MHz, $CDCl_3$) δ 9.15 (s, 1H), 8.12 (d, *J* = 8.9 Hz, 1H), 7.62 (dd, *J* = 8.9, 2.3 Hz, 1H), 7.52–7.44 (m, 4H), 7.27–7.24 (m, 3H), 6.98–6.91 (m, 2H) ppm; $^{13}C\{^1H\}$ NMR (100 MHz, $CDCl_3$) δ 150.7, 150.7, 144.9, 139.0, 135.4, 133.3, 130.6, 130.3, 130.0, 128.9, 128.8, 128.5, 128.0, 127.7, 127.1, 127.1, 125.5 ppm; GC-MS for $C_{19}H_{12}ClNS$, m/z = 321 (M^+). HRMS (ESI-TOF) m/z: $[M + H]^+$ Calcd for $C_{19}H_{12}ClNSH$; 322.0452 Found 322.0444.

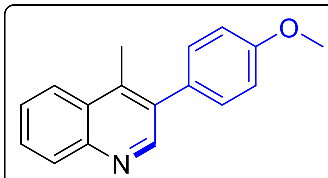

5-9am

3-(4-Methoxyphenyl)-4-methylquinoline (5-9am): A 1,4-dioxane (2.0 mL) solution of complex **2-10** (9 mg, 3 mol %), **2-16** (8 mg, 10 mol %), 2'-aminoacetophenone (68 mg, 0.5 mmol), and 2-(4-methoxyphenyl)ethanamine (106 mg, 0.7 mmol) was stirred at 140 °C for 20 h. The product **5-9am** was isolated by column chromatography on silica gel (hexanes/EtOAc = 100:1–5:1; TLC: R_f = 0.3 (20% EtOAc in hexanes)). Yield = 44 mg, (35%). Data for **5-9am:** [1]H NMR (400 MHz, $CDCl_3$) δ 8.78 (s, 1H), 8.16 (dd, *J* = 8.4, 0.8 Hz, 1H), 8.08 (dd, *J* = 1.4, 0.6 Hz, 1H), 7.73 (dd, *J* = 6.9, 1.4 Hz, 1H), 7.62 (dd, *J* = 6.9, 1.4 Hz, 1H), 7.33 (d, *J* = 8.8 Hz, 2H), 7.04 (d, *J* = 8.8 Hz, 2H), 3.89 (s, 3H), 2.66 (s, 3H) ppm; $^{13}C\{^1H\}$ NMR (100 MHz, $CDCl_3$) δ 159.2, 151.4, 146.4, 141.1, 134.1, 131.1, 130.7, 129.6, 128.9, 128.0,126.8, 124.2, 113.9, 55.4, 15.7 ppm; GC-MS for $C_{17}H_{15}NO$, m/z = 249 (M^+). HRMS (ESI-TOF) m/z: $[M + H]^+$ Calcd for $C_{17}H_{15}NOH$; 250.1149 Found 250.1144.

6.5.5.2 Characterization of the Dihydroquinazolin-4(1H)-one Compounds Listed in Table 5.6

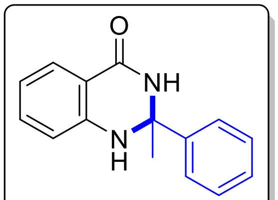

5-10a

2-Methyl-2-phenyl-2,3-dihydroquinazolin-4(1H)-one (**5-10a**): A 1,4-dioxane (2.0 mL) solution of complex **2-10** (9 mg, 3 mol %), **2-12** (12 mg, 10 mol %), 2-aminobenzamide (68 mg, 0.5 mmol) and (±)-α-methylbenzylamine (85 mg, 0.7 mmol) was stirred at 140 °C for 20 h. The product **5-10a** was isolated by column chromatography on silica gel (hexanes/EtOAc = 50:1–5:1; TLC: R_f = 0.3 (50% EtOAc in hexanes)). Yield = 110 mg (82%). Data for **5-10a**: [1]H NMR (400 MHz, DMSO-d_6) δ 8.80 (brs, 1H), 7.65 (brs, 1H), 7.53–7.46 (m, 3H), 7.31–7.24 (m, 2H), 7.23–7.14 (m, 2H), 6.77 (d, *J* = 8.2 Hz, 1H), 6.57 (t, *J* = 7.6 Hz, 1H), 1.64 (s, 3H) ppm; $^{13}C\{^1H\}$ NMR (100 MHz, DMSO-d_6) δ 164.0, 147.7, 147.3, 133.5, 128.1, 127.4, 127.2, 125.3, 117.0, 115.1, 114.4, 70.3, 30.8 ppm; GC-MS for $C_{15}H_{14}N_2O$, m/z = 238 (M^+). ^1H and ^{13}C NMR spectral data are in good agreement with the literature values.[238]

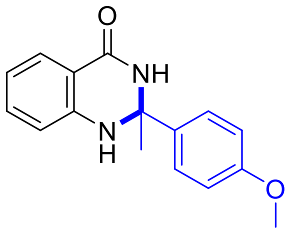

5-10b

2-(4-Methoxyphenyl)-2-methyl-2,3-dihydroquinazolin-4(1H)-one (**5-10b**): A 1,4-dioxane (2.0 mL) solution of complex **2-10** (9 mg, 3 mol %), **2-12** (12 mg, 10 mol %), 2-aminobenzamide (68 mg, 0.50 mmol) and (*S*)-(−)-1-(4-methoxyphenyl)ethylamine (106 mg, 0.70 mmol) was stirred at 140 °C for 20 h. The product **5-10b** was isolated by column chromatography on silica gel (hexanes/EtOAc = 50:1–5:1; TLC: R_f = 0.2 (50% EtOAc in hexanes)). Yield = 124 mg (93%). Data for **5-10b**: ^{1}H NMR (400 MHz, $CDCl_3$) δ 7.88–7.73 (m, 2H), 7.43 (d, *J* = 8.7 Hz, 2H), 7.24 (td, *J* = 7.4, 1.4 Hz, 1H), 6.78–6.66 (m, 4H), 5.24 (brs, 1H), 3.69 (s, 3H), 1.82 (s, 3H) ppm; ^{13}C{^{1}H} NMR (100 MHz, $CDCl_3$) δ 165.0, 159.0, 146.0, 137.4, 133.9, 128.1, 126.5, 118.6, 115.2, 114.8, 113.6, 70.5, 55.1, 29.9 ppm; GC-MS for $C_{16}H_{16}N_2O_2$, m/z = 268 (M^+). ^{1}H and ^{13}C NMR spectral data are in good agreement with the literature values.[239]

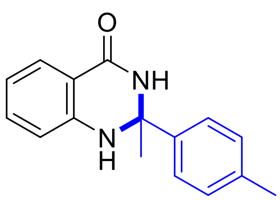

5-10c

2-Methyl-2-(p-tolyl)-2,3-dihydroquinazolin-4(1H)-one (**5-10c**): A 1,4-dioxane (2.0 mL) solution of complex **2-10** (9 mg, 3 mol %), **2-12** (12 mg, 10 mol %), 2-aminobenzamide (68 mg, 0.5 mmol) and 1-(4-methylphenyl)ethylamine (95 mg, 0.7 mmol) was stirred at 140 °C for 20 h. The product **5-10c** was isolated by column chromatography on silica gel (hexanes/EtOAc = 50:1–5:1; TLC: R_f = 0.2 (50% EtOAc in hexanes)). Yield = 113 mg (92%). Data for **5-10c**: ^{1}H NMR (400 MHz, DMSO-d_6) δ 8.72 (br s, 1H), 7.57 (brs, 1H), 7.47 (d, *J* = 7.8 Hz, 1H), 7.36 (d, *J* = 7.9 Hz, 2H), 7.19 (t, *J* = 7.6 Hz, 1H), 7.07 (d, *J* = 7.9 Hz, 2H), 6.74 (d, *J* = 8.1 Hz, 1H), 6.56 (t, *J* = 7.4 Hz, 1H), 2.20 (s, 3H), 1.61 (s, 3H) ppm; ^{13}C{^{1}H} NMR (100 MHz, DMSO) δ 163.8, 147.2, 144.7, 136.1, 133.2, 128.5, 127.2, 125.1, 116.7, 115.1, 114.3, 70.0, 30.7, 20.5 ppm; GC-MS for $C_{16}H_{16}N_2O$, m/z = 252 (M^+). ^{1}H and ^{13}C NMR spectral data are in good agreement with the literature values.[238-239]

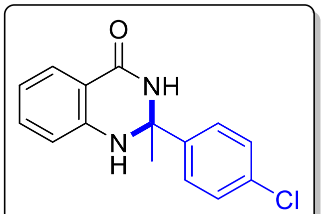

5-10d

2-(4-Chlorophenyl)-2-methyl-2,3-dihydroquinazolin-4(1*H*)-one (**5-10d**): A 1,4-dioxane (2.0 mL) solution of complex **2-10** (9 mg, 3 mol %), **2-12** (12 mg, 10 mol %), 2-aminobenzamide (68 mg, 0.5 mmol) and 1-(4-chlorophenyl)ethylamine (109 mg, 0.7 mmol) was stirred at 140 °C for 20 h. The product **5-10d** was isolated by recrystallization (50% EtOAc/CH_2Cl_2 in hexanes). Yield = 108 mg (79%). Data for **5-10d**: ^{1}H NMR (400 MHz, $CDCl_3$) δ 8.81 (brs, 1H), 7.67 (brs, 1H), 7.55–7.45 (m, 3H), 7.36 (d, *J* = 8.6 Hz, 2H), 7.21 (dd, *J* = 7.6, 1.4 Hz, 1H), 6.77 (d, *J* = 8.1 Hz, 1H), 6.59 (td, *J* = 7.6, 1.0 Hz, 1H), 1.64 (s, 3H) ppm; ^{13}C{^{1}H} NMR (100 MHz, $CDCl_3$) δ 160.2, 143.4, 143.1, 129.9, 128.3, 124.4, 123.7, 123.6, 113.5, 111.4, 110.8, 66.4, 26.9 ppm; GC-MS for $C_{15}H_{13}ClN_2O$, m/z = 272 (M^+). ^{1}H and ^{13}C NMR spectral data are in good agreement with the literature values.[238, 240]

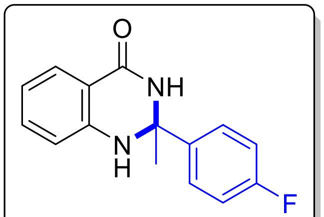

5-10e

2-(4-Fluorophenyl)-2-methyl-2,3-dihydroquinazolin-4(1H)-one (**5-10e**): A 1,4-dioxane (2.0 mL) solution of complex **2-10** (9 mg, 3 mol %), **2-12** (12 mg, 10 mol %), 2-aminobenzamide (68 mg, 0.5 mmol) and 4-fluoro-α-methylbenzylamine (97 mg, 0.7 mmol) was stirred at 140 °C for 20 h. The product **5-10e** was isolated by column chromatography on silica gel (hexanes/EtOAc = 50:1–5:1; TLC: R_f = 0.2 (50% EtOAc in hexanes)). Yield = 85 mg (66%). Data for **5-10e**: ^{1}H NMR (400 MHz, DMSO-d_6) δ 8.80 (br s, 1H), 7.65 (brs, 1H), 7.57–7.45 (m, 3H), 7.24–7.18 (m, 1H), 7.17–7.06 (m, 2H), 6.76 (d, J = 8.0 Hz, 1H), 6.59 (t, J = 7.5 Hz, 1H), 1.63 (s, 3H) ppm; $^{13}C\{^1H\}$ NMR (100 MHz, DMSO-d_6) δ 163.8, 161.22 (d, J_{CF} = 243.4 Hz), 147.0, 143.86 (d, J_{CF} = 2.9 Hz), 133.4, 127.3, 127.2, 117.0, 115.0, 114.72 (d, J_{CF} = 21.3 Hz), 114.3, 69.9, 30.7 ppm; GC-MS for $C_{15}H_{13}FN_2O$, m/z = 256 (M^+). ^1H and ^{13}C NMR spectral data are in good agreement with the literature values.[102]

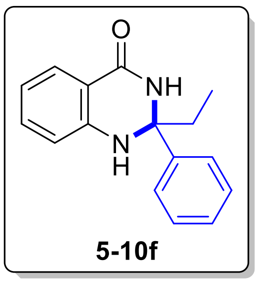

2-Ethyl-2-phenyl-2,3-dihydroquinazolin-4(1H)-one (**5-10f**): A 1,4-dioxane (2.0 mL) solution of complex **2-10** (9 mg, 3 mol %), **2-12** (12 mg, 10 mol %), 2-aminobenzamide (68 mg, 0.5 mmol) and α-ethylbenzylamine (95 mg, 0.7 mmol) was stirred at 140 °C for 20 h. The product **5-10f** was isolated by column chromatography on silica gel (hexanes/EtOAc = 110:1–5:1; TLC: R_f = 0.3 (50% EtOAc in hexanes)). Yield = 106 mg (84%). Data for **5-10f**: ^1H NMR (400 MHz, $CDCl_3$) δ 7.87 (brs, 1H), 7.82 (d, J = 7.9 Hz, 1H), 7.45 (d, J = 7.5 Hz, 2H), 7.37–7.08 (m, 4H), 6.82–6.64 (m, 2H), 4.97 (brs, 1H), 2.09 (q, J = 7.4 Hz, 2H), 0.97 (t, J = 7.4 Hz, 3H) ppm; $^{13}C\{^1H\}$ NMR (100 MHz, $CDCl_3$) δ 165.4, 146.1, 144.8, 133.9, 128.4, 128.3, 127.6, 125.4, 118.7, 115.5, 114.8, 73.7, 35.5, 8.1 ppm; GC-MS for $C_{16}H_{16}N_2O$, m/z = 252 (M^+). HRMS (ESI-TOF) m/z: $[M + H]^+$ Calcd for $C_{16}H_{16}N_2OH$; 253.1335 Found 253.1326.

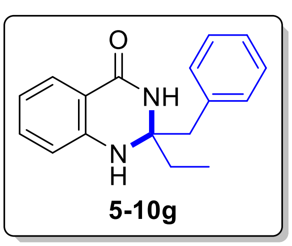

2-Benzyl-2-ethyl-2,3-dihydroquinazolin-4(1H)-one (**5-10g**): A 1,4-dioxane (2.0 mL) solution of complex **2-10** (9 mg, 3 mol %), **2-12** (12 mg, 10 mol %), 2-aminobenzamide (68 mg, 0.5 mmol) and (±)-1-phenylbutan-2-amine (104 mg, 0.7 mmol) was stirred at 140 °C for 20 h. The product **5-10g** was isolated by recrystallization (50% EtOAc/CH_2Cl_2 in hexanes). Yield = 101 mg (76%). Data for **5-10g**: ^1H NMR (400 MHz,

$CDCl_3$) δ 7.90 (dd, *J* = 7.8, 1.3 Hz, 1H), 7.41–7.17 (m, 4H), 7.15–7.07 (m, 2H), 6.81 (t, *J* = 7.4 Hz, 1H), 6.67 (brs, 1H), 6.63 (d, *J* = 8.1 Hz, 1H), 4.17 (brs, 1H), 3.20 (d, *J* = 13.3 Hz, 1H), 2.95 (d, *J* = 13.3 Hz, 1H), 1.72–1.62 (m, 2H), 1.04 (t, *J* = 7.4 Hz, 3H) ppm; $^{13}C\{^1H\}$ NMR (100 MHz, $CDCl_3$) δ 164.6, 146.1, 135.4, 134.1, 130.4, 128.4, 128.3, 127.0, 118.4, 114.5, 114.4, 72.3, 46.5, 31.3, 7.8 ppm; GC-MS for $C_{17}H_{18}N_2O$, m/z = 266 (M^+). HRMS (ESI-TOF) m/z: $[M + H]^+$ Calcd for $C_{17}H_{18}N_2Na$; 289.1311 Found 289.1325.

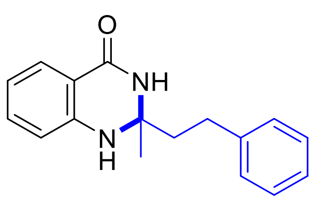

5-10h

2-Methyl-2-phenethyl-2,3-dihydroquinazolin-4(1H)-one (**5-10h**): A 1,4-dioxane (2.0 mL) solution of complex **2-10** (9 mg, 3 mol %), **2-12** (12 mg, 10 mol %), 2-aminobenzamide (68 mg, 0.5 mmol) and 3-amino-1-phenylbutane (104 mg, 0.7 mmol) was stirred at 140 °C for 20 h. The product **5-10h** was isolated by column chromatography on silica gel (hexanes/EtOAc = 50:1–5:1; TLC: R_f = 0.3 (50% EtOAc in hexanes)). Yield = 112 mg (84%). Data for **5-10h**: ^1H NMR (400 MHz, $CDCl_3$) δ 7.87 (d, *J* = 7.7 Hz, 1H), 7.43 (brs, 1H), 7.28–7.20 (m, 3H), 7.19–7.08 (m, 3H), 6.78 (d, *J* = 7.5 Hz, 1H), 6.52 (d, *J* = 8.0 Hz, 1H) 4.19 (brs, 1H), 2.85–2.68 (m, 2H), 2.16–1.99 (m, 2H), 1.55 (s, 3H) ppm; $^{13}C\{^1H\}$ NMR (100 MHz, $CDCl_3$) δ 164.7, 146.0, 141.1, 133.9, 128.5, 128.3, 128.2, 126.0, 118.4, 114.5, 114.3, 69.8, 43.6, 30.4, 28.3 ppm; GC-MS for $C_{17}H_{18}N_2O$, m/z = 266 (M^+). ^1H and ^{13}C NMR spectral data are in good agreement with the literature values.[239]

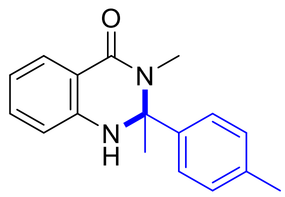

5-10i

2,3-Dimethyl-2-(*p*-tolyl)-2,3-dihydroquinazolin-4(1H)-one (5-10i): A 1,4-dioxane (2.0 mL) solution of complex **2-10** (9 mg, 3 mol %), **2-12** (12 mg, 10 mol %), 2-amino-N-methylbenzamide (75 mg, 0.5 mol %) and 1-(4-methylphenyl)ethylamine (95 mg, 0.7 mmol) was stirred at 140 °C for 20 h. The product **5-10i** was isolated by column chromatography on silica gel (hexanes/EtOAc = 50:1–5:1; TLC: R_f = 0.3 (50% EtOAc in hexanes)). Yield = 117 mg (88%). Data for **5-10i**: ^{1}H NMR (400 MHz, $CDCl_3$) δ 7.56 (d, *J* = 7.7 Hz, 1H), 7.39 (brs, 1H), 7.26 (d, *J* = 7.9 Hz, 2H), 7.20–7.05 (m, 3H), 6.69–6.55 (m, 2H), 2.93 (s, 3H), 2.23 (s, 3H), 1.83 (s, 3H) ppm; ^{13}C{^{1}H} NMR (100 MHz, $CDCl_3$) δ 176.5, 163.3, 146.0, 141.5, 137.0, 133.1, 128.9, 127.5, 125.6, 117.0, 114.1, 74.4, 28.9, 26.8, 20.5 ppm; GC-MS for $C_{17}H_{18}N_2O$, m/z = 266 (M^+). HRMS (ESI-TOF) m/z: $[M + H]^+$ Calcd for $C_{17}H_{18}N_2ONa$; 289.1311 Found 289.1306.

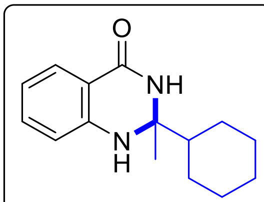

5-10j

2-Cyclohexyl-2-methyl-2,3-dihydroquinazolin-4(1H)-one (5-10j): A 1,4-dioxane (2.0 mL) solution of complex **2-10** (9 mg, 3 mol %), **2-12** (12 mg, 10 mol %), 2-aminobenzamide (68 mg, 0.5 mmol) and (S)-(+)-α-methylcyclohexanemethylamine (89 mg, 0.7 mmol) was stirred at 140 °C for 20 h. The product **5-10j** was isolated by column chromatography on silica gel (hexanes/EtOAc = 50:1–5:1; TLC: R_f = 0.3 (50% EtOAc in hexanes)). Yield = 98 mg (80%). Data for **5-10j**: ^{1}H NMR (400 MHz, DMSO) δ 7.87 (brs, 1H), 7.51 (dd, *J* = 7.7, 1.6 Hz, 1H), 7.17 (td, *J* = 7.7, 1.6 Hz, 1H), 6.65 (d, *J* = 8.1 Hz, 1H), 6.60 (brs, 1H), 6.56–6.52 (m, 1H), 1.80–1.65 (m, 4H), 1.59–1.50 (m, 2H), 1.29 (s, 3H), 1.13–0.95 (m, 5H) ppm; ^{13}C{^{1}H} NMR (100 MHz, DMSO) δ 163.0, 147.1, 133.3, 127.1, 115.8, 113.7, 113.5, 71.3, 47.9, 26.7, 26.4, 26.1, 26.0, 26.0, 24.9 ppm; GC-MS for $C_{15}H_{20}N_2O$, m/z = 244 (M^+). HRMS (ESI-TOF) m/z: $[M + H]^+$ Calcd for $C_{15}H_{20}N_2OH$; 245.1648 Found 245.1622. ^{1}H and ^{13}C NMR spectral data are in good agreement with the literature values.[241]

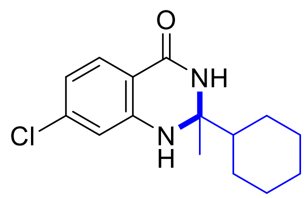

5-10k

7-Chloro-2-cyclohexyl-2-methyl-2,3-dihydroquinazolin-4(1H)-one (**5-10k**): A 1,4-dioxane (2.0 mL) solution of complex **2-10** (9 mg, 3 mol %), **2-12** (12 mg, 10 mol %), 2-amino-4-chlorobenzamide (85 mg, 0.5 mmol) and (S)-(+)-α-methylcyclohexanemethylamine (89 mg, 0.7 mmol) was stirred at 140 °C for 20 h. The product **5-10k** was isolated by column chromatography on silica gel (hexanes/EtOAc = 50:1–5:1; TLC: R_f = 0.3 (50% EtOAc in hexanes)). Yield = 122 mg (88%). Data for **5-10k**: ^{1}H NMR (400 MHz, DMSO) δ 8.01 (brs, 1H), 7.50 (d, J = 8.3 Hz, 1H), 6.90 (brs, 1H), 6.69 (d, J = 2.0 Hz, 1H), 6.55 (dd, J = 8.3, 2.0 Hz, 1H), 1.80–1.66 (m, 4H), 1.59–1.48 (m, 2H), 1.30 (s, 3H), 1.14–0.93 (m, 5H) ppm; ^{13}C{^{1}H} NMR (100 MHz, DMSO) δ 162.0, 148.0, 137.7, 129.0, 115.7, 112.5, 112.2, 71.6, 48.2, 26.6, 26.3, 25.9, 25.9, 25.0 ppm; GC-MS for $C_{15}H_{19}ClN_2O$, m/z = 278 (M^+). HRMS (ESI-TOF) m/z: $[M + H]^+$ Calcd for $C_{15}H_{19}ClN_2OH$; 279.1259 Found 279.1255.

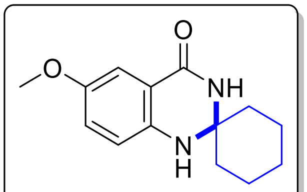

5-10l

6'-Methoxy-1'H-spiro[cyclohexane-1,2'-quinazolin]-4'(3'H)-one (**5-10l**): A 1,4-dioxane (2.0 mL) solution of complex **2-10** (9 mg, 3 mol %), **2-12** (12 mg, 10 mol %), 2-amino-5-methoxybenzamide (83 mg, 0.5 mmol) and cyclohexylamine (69 mg, 0.7 mmol) was stirred at 140 °C for 20 h. The product **5-10l** was isolated by recrystallization (50% EtOAc/CH_2Cl_2 in hexanes). Yield = 120 mg (98%). Data for **5-10l**:

^{1}H NMR (400 MHz, DMSO) δ 7.95 (brs, 1H), 7.13 (d, *J* = 3.0 Hz, 1H), 6.89 (dd, *J* = 8.7, 3.0 Hz, 1H), 6.79 (d, *J* = 8.7 Hz, 1H), 6.25 (brs, 1H), 3.66 (s, 3H),1.80–1.69 (m, 2H), 1.65–1.34 (m, 7H), 1.27–1.17 (m, 1H) ppm; ^{13}C{^{1}H} NMR (100 MHz, DMSO) δ 163.3, 151.1, 141.2, 121.3, 116.4, 115.2, 109.9, 68.0, 55.3, 38.9, 36.9, 24.8, 21.0 ppm; GC-MS for $C_{14}H_{18}N_2O_2$, m/z = 246 (M^+). HRMS (ESI-TOF) m/z: $[M + H]^+$ Calcd for $C_{14}H_{18}N_2O_2H$; 247.1441 Found 247.1408.

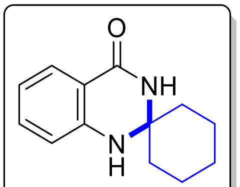
5-10m

1'H-spiro[cyclohexane-1,2'-quinazolin]-4'(3'H)-one (**5-10m**): A 1,4-dioxane (2.0 mL) solution of complex **2-10** (9 mg, 3 mol %), **2-12** (12 mg, 10 mol %), 2-aminobenzamide (68 mg, 0.5 mmol) and cyclohexylamine (69 mg, 0.7 mmol) was stirred at 140 °C for 20 h. The product **5-10m** was isolated by recrystallization (50% EtOAc/CH_2Cl_2 in hexanes; TLC: R_f = 0.3 (50% EtOAc in hexanes)). Yield = 104 mg (96%). Data for **5-10m**: ^{1}H NMR (400 MHz, DMSO) δ 7.93 (brs, H), 7.56 (d, *J* = 7.4 Hz, 1H), 7.21 (t, *J* = 7.3 Hz, 1H), 6.80 (d, *J* = 8.0 Hz, 1H), 6.70–6.49 (m, 2H), 1.80–1.68 (m, 2H), 1.67–1.48 (m, 6H), 1.46–1.36 (m, 1H), 1.31–1.16 (m, 1H) ppm; ^{13}C{^{1}H} NMR (100 MHz, DMSO) δ 163.3, 146.8, 133.2, 127.2, 116.6, 114.6, 114.5, 67.9, 37.2, 24.7, 20.9 ppm; GC-MS for $C_{13}H_{16}N_2O$, m/z = 216 (M^+). ^{1}H and ^{13}C NMR spectral data are in good agreement with the literature values.[242]

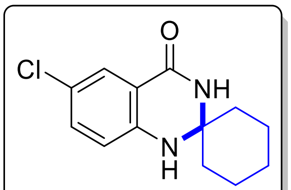
5-10n

6'-Chloro-1'H-spiro[cyclohexane-1,2'-quinazolin]-4'(3'H)-one (**5-10n**): A 1,4-dioxane (2.0 mL) solution of complex **2-10** (9 mg, 3 mol %), **2-12** (12 mg, 10 mol %), 2-amino-5-chlorobenzamide (85 mg, 0.5 mmol) and cyclohexylamine (69 mg, 0.7 mmol) was stirred at 140 °C for 20 h. The product **5-10n** was isolated by recrystallization (50% EtOAc/CH_2Cl_2 in hexanes; TLC: R_f = 0.3 (50% EtOAc in hexanes)). Yield = 104 mg (83%). Data for **5-10n**: ^{1}H NMR (400 MHz, DMSO) δ 8.12 (brs, 1H), 7.50 (d, J = 2.6 Hz, 1H), 7.23 (dd, J = 8.7, 2.6 Hz, 1H), 6.90–6.79 (m, 2H), 1.79–1.69 (m, 2H), 1.66–1.46 (m, 6H), 1.45–1.37 (m, 1H), 1.28–1.17 (m, 1H) ppm; ^{13}C{^{1}H} NMR (100 MHz, DMSO) δ 162.1, 145.5, 132.9, 126.3, 120.2, 116.6, 115.6, 68.1, 37.1, 24.6, 20.9 ppm; GC-MS for $C_{13}H_{15}ClN_2O$, m/z = 250 (M^+). HRMS (ESI-TOF) m/z: $[M + H]^+$ Calcd for $C_{13}H_{15}ClN_2OH$; 251.0946 Found 251.0912.

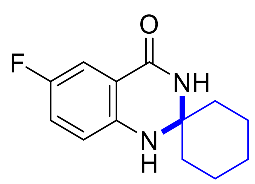

5-10o

6'-Fluoro-1'H-spiro[cyclohexane-1,2'-quinazolin]-4'(3'H)-one (**5-10o**): A 1,4-dioxane (2.0 mL) solution of complex **2-10** (9 mg, 3 mol %), **2-12** (12 mg, 10 mol %), 2-amino-5-fluorobenzamide (77 mg, 0.5 mmol) and cyclohexylamine (69 mg, 0.7 mmol) was stirred at 140 °C for 20 h. The product **5-10o** was isolated by recrystallization (50% EtOAc/CH_2Cl_2 in hexanes; TLC: R_f = 0.3 (50% EtOAc in hexanes)). Yield = 98 mg (84%). Data for **5-10o**: ^{1}H NMR (400 MHz, DMSO) δ 8.10 (brs, 1H), 7.26 (dd, J = 9.1, 3.1 Hz, 1H), 7.11 (td, J = 8.8, 3.1 Hz, 1H), 6.84 (dd, J = 8.8, 4.5 Hz, 1H), 6.60 (brs, 1H), 1.80–1.69 (m, 2H), 1.65–1.36 (m, 7H), 1.28–1.18 (m, 1H) ppm; ^{13}C{^{1}H} NMR (100 MHz, DMSO) δ 162.3, 154.4 (d, J_{CF} = 132.8 Hz), 143.4 (d, J_{CF} = 0.8 Hz), 120.5 (d, J_{CF} = 23.0 Hz), 116.2 (d, J_{CF} = 7.0 Hz), 115.1 (d, J_{CF} = 7.0 Hz), 112.2 (d, J_{CF} = 23.0 Hz), 68.0, 36.9, 24.6, 20.9 ppm; GC-MS for $C_{13}H_{15}FN_2O$, m/z = 234 (M^+). HRMS (ESI-QTOF) m/z: $[M + H]^+$ Calcd for $C_{13}H_{15}FN_2OH$; 235.1241 Found 235.1235.

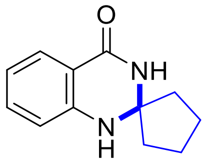

5-10p

1'H-spiro[cyclopentane-1,2'-quinazolin]-4'(3'H)-one (**5-10p**): A 1,4-dioxane (2.0 mL) solution of complex **2-10** (9 mg, 3 mol %), **2-12** (12 mg, 10 mol %), 2-aminobenzamide (68 mg, 0.5 mmol) and cyclopentylamine (60 mg, 0.7 mmol) was stirred at 140 °C for 20 h. The product **5-10p** was isolated by recrystallization (50% EtOAc/CH_2Cl_2 in hexanes; TLC: R_f = 0.2 (50% EtOAc in hexanes)). Yield = 85 mg (84%). Data for **5-10p**: ^{1}H NMR (400 MHz, $CDCl_3$) δ 8.11 (brs, 1H), 7.58 (d, J = 7.7 Hz, 1H), 7.21 (td, J = 7.7, 1.5 Hz, 1H), 6.74 (brs, 1H), 6.70 (d, J = 8.1 Hz, 1H), 6.62 (t, J = 7.4 Hz, 1H), 1.85–1.74 (m, 4H), 1.70–1.61 (m, 4H) ppm; ^{13}C{^{1}H} NMR (100 MHz, $CDCl_3$) δ 163.6, 147.6, 133.1, 127.3, 116.6, 114.6, 114.4, 77.1, 39.3, 22.0 ppm; GC-MS for $C_{12}H_{14}N_2O$, m/z = 202 (M^+). ^{1}H and ^{13}C NMR spectral data are in good agreement with the literature values.[242]

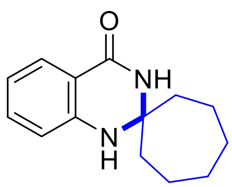

5-10q

1'H-spiro[cycloheptane-1,2'-quinazolin]-4'(3'H)-one (**5-10q**): A 1,4-dioxane (2.0 mL) solution of complex **2-10** (9 mg, 3 mol %), **2-12** (12 mg, 10 mol %), 2-aminobenzamide (68 mg, 0.5 mmol) and cycloheptylamine (79 mg, 0.7 mmol) was stirred at 140 °C for 20 h. The product **5-10q** was isolated by recrystallization (50% EtOAc/CH_2Cl_2 in hexanes; TLC: R_f = 0.3 (50% EtOAc in hexanes)). Yield = 86 mg (75%). Data for **5-10q**: ^{1}H NMR (400 MHz, DMSO) δ 7.85 (dd, J = 7.8, 1.6 Hz, 1H), 7.29–7.23 (m, 1H), 6.87 (brs, 1H), 6.81–6.75 (m, 1H), 6.62 (d, J = 8.1 Hz, 1H), 4.43 (brs, 1H), 2.06–1.95 (m, 4H), 1.64–1.44 (m, 8H) ppm; ^{13}C{^{1}H} NMR (100 MHz, DMSO) δ 164.1, 145.6, 133.7, 128.2, 118.5, 115.2, 114.8, 72.4, 41.4, 29.0, 21.5 ppm; GC-MS for $C_{14}H_{18}N_2O$, m/z = 230 (M^+). HRMS (ESI-TOF) m/z: $[M + H]^+$ Calcd for $C_{14}H_{18}N_2OH$; 231.1492 Found 231.1489.

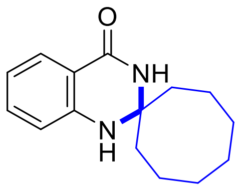

5-10r

1'H-spiro[cyclooctane-1,2'-quinazolin]-4'(3'H)-one (**5-10r**): A 1,4-dioxane (2.0 mL) solution of complex **2-10** (9 mg, 3 mol %), **2-12** (12 mg, 10 mol %), 2-aminobenzamide (68 mg, 0.5 mmol) and cyclooctylamine (89 mg, 0.7 mmol) was stirred at 140 °C for 20 h. The product **5-10r** was isolated by recrystallization (50% EtOAc/CH_2Cl_2 in hexanes; TLC: R_f = 0.3 (50% EtOAc in hexanes)). Yield = 97 mg (80%). Data for **5-10r**: ^{1}H NMR (400 MHz, DMSO) δ 7.85 (ddd, *J* = 7.7, 1.6, 0.4 Hz, 1H), 7.27 (dd, *J* = 7.7, 1.6 Hz, 1H), 6.79 (dd, *J* = 7.3, 1.0 Hz, 1H), 6.61 (ddd, *J* = 8.1, 1.0, 0.4 Hz, 1H), 6.53 (brs, 1H), 4.31 (brs, 1H), 2.10–1.96 (m, 4H), 1.74–1.42 (m, 10H) ppm; ^{13}C{^{1}H} NMR (100 MHz, DMSO) δ 164.0, 145.5, 133.8, 128.3, 118.5, 115.2, 114.7, 71.9, 36.0, 27.9, 24.5, 21.4 ppm; GC-MS for $C_{15}H_{20}N_2O$, m/z = 244 (M^+). HRMS (ESI-TOF) m/z: $[M + H]^+$ Calcd for $C_{15}H_{20}N_2OH$; 245.1648 Found 245.1622.

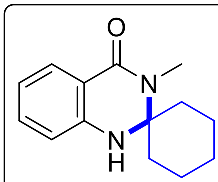

5-10s

3'-Methyl-1'H-spiro[cyclohexane-1,2'-quinazolin]-4'(3'H)-one (**5-10s**): A 1,4-dioxane (2.0 mL) solution of complex **2-10** (9 mg, 3 mol %), **2-12** (12 mg, 10 mol %), 2-amino-N-methylbenzamide (75 mg, 0.5 mmol) and cyclohexylamine (69 mg, 0.7 mmol) was stirred at 140 °C for 20 h. The product **5-10s** was isolated by recrystallization (50% EtOAc/CH_2Cl_2 in hexanes). Yield = 99 mg (86%). Data for **5-10s**: ^{1}H NMR (400 MHz, $CDCl_3$) δ 7.89 (dd, *J* = 7.7, 1.3 Hz, 1H), 7.26 (td, *J* = 7.7, 1.3 Hz, 1H), 6.81 (d, *J* = 7.6 Hz, 1H), 6.67 (d, *J* = 8.0 Hz, 1H), 4.61 (brs, 1H), 3.07 (s, 3H), 2.06–1.98 (m, 2H), 1.77–1.68 (m, 5H), 1.49–1.37 (m, 2H), 1.24–1.12 (m, 1H) ppm; ^{13}C{^{1}H} NMR (100 MHz, $CDCl_3$) δ 163.7, 143.9, 133.0, 128.6, 118.9, 116.8, 114.7, 71.9, 32.9, 26.5, 24.5, 22.3

ppm; GC-MS for $C_{14}H_{18}N_2O$, m/z = 230 (M^+). HRMS (ESI-TOF) m/z: $[M + H]^+$ Calcd for $C_{14}H_{18}N_2ONa$; 253.1311 Found 253.1302.

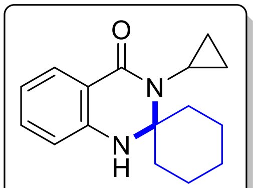

5-10t

3'-Cyclopropyl-1'H-spiro[cyclohexane-1,2'-quinazolin]-4'(3'H)-one (**5-10t**): A 1,4-dioxane (2.0 mL) solution of complex **2-10** (9 mg, 3 mol %), **2-12** (12 mg, 10 mol %), 2-amino-N-cyclopropylbenzamide (88 mg, 0.5 mmol) and cyclohexylamine (69 mg, 0.7 mmol) was stirred at 140 °C for 20 h. The product **5-10t** was isolated by column chromatography on silica gel (hexanes/EtOAc = 40:1–10:1; TLC: R_f = 0.4 (50% EtOAc in hexanes)). Yield = 69 mg (54%). Data for **5-10t**: ^{1}H NMR (400 MHz, $CDCl_3$) δ 7.92 (dd, *J* = 7.8, 1.4 Hz, 1H), 7.27 (td, *J* = 7.6, 1.4 Hz, 1H), 6.82 (t, *J* = 7.6 Hz, 1H), 6.66 (d, *J* = 8.1 Hz, 1H), 4.63 (brs, 1H), 2.36–2.14 (m, 3H), 2.03–1.92 (m, 2H), 1.80–1.68 (m, 3H), 1.50–1.33 (m, 2H), 1.28–1.19 (m, 1H), 1.05–0.93 (m, 2H), 0.85–0.78 (m, 2H) ppm; ^{13}C{^{1}H} NMR (100 MHz, $CDCl_3$) δ 166.5, 144.2, 133.3, 128.6, 118.9, 117.3, 114.7, 74.2, 42.0, 33.4, 24.6, 22.7, 9.4 ppm; GC-MS for $C_{16}H_{20}N_2O$, m/z = 256 (M^+). HRMS (ESI-TOF) m/z: $[M + H]^+$ Calcd for $C_{16}H_{20}N_2OH$; 257.1648 Found 257.1641.

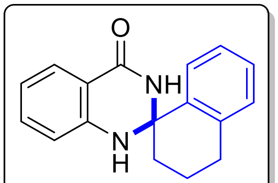

5-10u

3,4-Dihydro-1'H,2H-spiro[naphthalene-1,2'-quinazolin]-4'(3'H)-one (**5-10u**): A 1,4-dioxane (2.0 mL) solution of complex **2-10** (9 mg, 3 mol %), **2-12** (12 mg, 10 mol %), 2-aminobenzamide (68 mg, 0.5 mmol) and (S)-(+)-1,2,3,4-tetrahydro-1-naphthylamine (103 mg, 0.7 mmol) was stirred at 140 °C for 20 h. The product **5-10u** was isolated by column chromatography on silica gel (hexanes/EtOAc = 110:1–5:1; TLC: R_f = 0.3 (50% EtOAc in hexanes)). Yield = 92 mg (70%). Data for **5-10u**: ^{1}H NMR (400 MHz, $CDCl_3$) δ 8.03–7.72 (m, 2H), 7.43–6.98 (m, 4H), 6.81 (t, *J* =

7.6 Hz, 1H), 6.60 (d, J = 8.0 Hz, 1H), 5.90 (brs, 1H), 4.71 (brs, 1H), 2.88–2.71 (m, 2H), 2.34–2.23 (m, 1H), 2.21–2.11 (m, 1H), 1.92–1.76 (m, 2H) ppm; $^{13}C\{^1H\}$ NMR (100 MHz, $CDCl_3$) δ 163.5, 145.3, 137.9, 137.7, 134.1, 129.0, 128.9, 128.5, 128.3, 126.7, 118.5, 114.5, 114.3, 69.9, 37.0, 29.2, 19.0 ppm; GC-MS for $C_{17}H_{16}N_2O$, m/z = 264 (M^+). HRMS (ESI-TOF) m/z: $[M + H]^+$ Calcd for $C_{17}H_{16}N_2OH$; 265.1335 Found 265.1329.

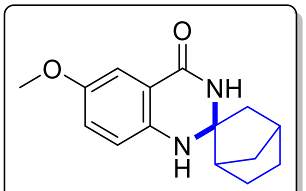

5-10v

(1R,4S)-6'-Methoxy-1'H-spiro[bicyclo[2.2.1]heptane-2,2'-quinazolin]-4'(3'H)-one (**5-10v**): A 1,4-dioxane (2.0 mL) solution of complex **2-10** (9 mg, 3 mol %), **2-12** (12 mg, 10 mol %), 2-amino-5-methoxybenzamide (83 mg, 0.5 mmol) and exo-2-aminonorbornane (78 mg, 0.7 mmol) was stirred at 140 °C for 20 h. The product **5-10v** was isolated by recrystallization (50% EtOAc/CH_2Cl_2 in hexanes; TLC: R_f = 0.1 (50% EtOAc in hexanes)). Yield = 87 mg (76%). Data for **5-10v**: ^1H NMR (400 MHz, DMSO) δ 8.22 (brs, 1H), 7.13 (t, J = 2.7 Hz, 1H), 6.95–6.83 (m, 1H), 6.79–6.68 (m, 1H), 6.52 (d, J = 16.5 Hz, 1H), 3.67 (s, 3H), 2.31–2.16 (m, 1H), 2.15–2.05 (m, 1H), 1.89–1.63 (m, 2H), 1.54–1.06 (m, 6H) ppm; $^{13}C\{^1H\}$ NMR (100 MHz, DMSO) δ 163.7, 151.1, 141.9, 121.3, 116.1, 115.8, 110.0, 75.5, 55.4, 45.7, 45.4, 36.7, 35.2, 27.8, 22.2 ppm; GC-MS for $C_{15}H_{18}N_2O_2$, m/z = 258 (M^+). HRMS (ESI-TOF) m/z: $[M + H]^+$ Calcd for $C_{15}H_{18}N_2O_2H$; 259.1441 Found 259.1413.

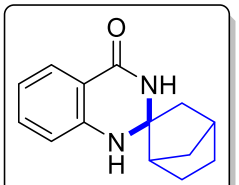

5-10w

(1R,4S)-1'H-Spiro[bicyclo[2.2.1]heptane-2,2'-quinazolin]-4'(3'H)-one (**5-10w**): A 1,4-dioxane (2.0 mL) solution of complex **2-10** (9 mg, 3 mol %), **2-12** (12 mg, 10 mol %), 2-aminobenzamide (68 mg, 0.5 mmol) and exo-2-aminonorbornane (78 mg, 0.7 mmol) was stirred at 140 °C for 20 h. The product **5-10w** was isolated by recrystallization (50%

$EtOAc/CH_2Cl_2$ in hexanes; TLC: R_f = 0.1 (50% EtOAc in hexanes)). Yield = 97 mg (79%). Data for **5-10w**: ^1H NMR (400 MHz, DMSO) δ 8.22 (brs, 1H), 7.59 (d, *J* = 7.6 Hz, 1H), 7.21 (t, *J* = 7.3 Hz, 1H), 6.85 (d, *J* = 11.8 Hz, 1H), 6.76 (dd, *J* = 17.3, 8.0 Hz, 1H), 6.63 (t, *J* = 7.3 Hz, 1H), 2.36–2.15 (m, 1H), 2.15–2.06 (m, 1H), 1.91–1.67 (m, 2H), 1.59–1.51 (m, 1H), 1.51–1.16 (m, 4H), 1.11 (d, *J* = 9.7 Hz, 1H) ppm; $^{13}C\{^1H\}$ NMR (100 MHz, DMSO) δ 163.8, 147.5, 133.1, 127.4, 116.6, 115.4, 114.4, 75.2, 46.1, 45.3, 36.7, 35.2, 27.7, 22.1 ppm; GC-MS for $C_{14}H_{16}N_2O$, m/z = 228 (M^+). ^1H and ^{13}C NMR spectral data are in good agreement with the literature values.[243]

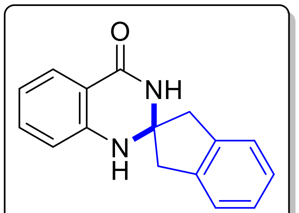

5-10x

1,3-Dihydro-1'H-spiro[indene-2,2'-quinazolin]-4'(3'H)-one (**5-10x**): A 1,4-dioxane (2.0 mL) solution of complex **2-10** (9 mg, 3 mol %), **2-12** (12 mg, 10 mol %), 2-aminobenzamide (68 mg, 0.5 mmol) and 2-aminoindane (67 mg, 0.7 mmol) was stirred at 140 °C for 20 h. The product **5-10x** was isolated by recrystallization (50% $EtOAc/CH_2Cl_2$ in hexanes). Yield = 98 mg (78%). Data for **5-10x**: ^1H NMR (400 MHz, DMSO) δ 8.36 (brs, 1H), 7.63 (d, *J* = 7.7 Hz, 1H), 7.27–7.15 (m, 5H), 7.09 (brs, 1H), 6.78–6.64 (m, 2H), 3.22 (ABq, *J* = 16.2 Hz, 4H) ppm; $^{13}C\{^1H\}$ NMR (100 MHz, DMSO) δ 163.7, 147.2, 139.6, 133.3, 127.4, 126.8, 124.8, 117.1, 114.9, 114.7, 76.9, 46.6 ppm; GC-MS for $C_{16}H_{14}N_2O$, m/z = 250 (M^+). ^1H and ^{13}C NMR spectral data are in good agreement with the literature values.[244]

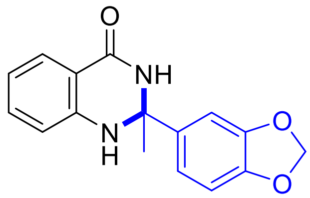

5-10y

2-(Benzo[d][1,3]dioxol-5-yl)-2-methyl-2,3-dihydroquinazolin-4(1H)-one (**5-10y**): A 1,4-dioxane (2.0 mL) solution of complex **2-10** (9 mg, 3 mol %), **2-12** (12 mg, 10 mol %), 2-aminobenzamide (34 mg, 0.25 mmol) and 3-amino-3-benzo[1,3]dioxol-5-yl-propionic acid (73 mg, 0.35 mmol) was stirred at 140 °C for 20 h. The product **5-10y** was isolated by column chromatography on silica gel (hexanes/EtOAc = 50:1–5:1; TLC: R_f = 0.1 (50% EtOAc in hexanes)). Yield = 55 mg (77%). Data for **5-10y**: ^{1}H NMR (400 MHz, DMSO) δ 8.72 (brs, 1H), 7.57 (brs, 1H), 7.49 (d, J = 7.7 Hz, 1H), 7.21 (td, J = 7.7, 1.3 Hz, 1H), 7.06 (d, J = 1.6 Hz, 1H), 6.92 (dd, J = 8.1, 1.6 Hz, 1H), 6.79 (d, J = 8.1 Hz, 1H), 6.76 (d, J = 8.1 Hz, 1H), 6.58 (t, J = 7.7 Hz, 1H), 5.93 (d, J = 1.8 Hz, 2H), 1.61 (s, 3H) ppm; ^{13}C{^{1}H} NMR (100 MHz, DMSO) δ 164.0, 147.3, 147.2, 146.3, 141.9, 133.4, 127.3, 118.5, 117.0, 115.1, 114.4, 107.5, 106.0, 101.1, 70.2, 30.9 ppm; GC-MS for $C_{16}H_{14}N_2O_3$, m/z = 282 (M^+). HRMS (ESI-TOF) m/z: $[M + H]^+$ Calcd for $C_{16}H_{14}N_2O_3H$; 283.1077 Found 283.1057.

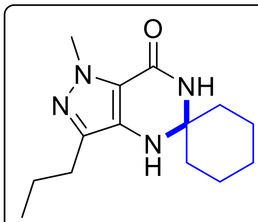

5-10z

1'-Methyl-3'-propyl-1',4'-dihydrospiro[cyclohexane-1,5'-pyrazolo[4,3-d]pyrimidin]-7'(6'H)-one (**5-10z**): A 1,4-dioxane (2.0 mL) solution of complex **2-10** (9 mg, 3 mol %), **2-12** (12 mg, 10 mol %), 4-amino-1-methyl-3-n-propyl-5-pyrazolecarboxamide (91 mg, 0.5 mmol) and cyclohexylamine (69 mg, 0.7 mmol) was stirred at 140 °C for 20 h. The product **5-10z** was isolated by column chromatography on silica gel (hexanes/EtOAc = 40:1–10:1; TLC: R_f = 0.3 (50% EtOAc in hexanes)). Yield = mg (96%). Data for **5-10z**: ^{1}H NMR (400 MHz, $CDCl_3$) δ 6.14 (brs, 1H), 4.03 (s, 3H), 2.52 (t, J = 7.5 Hz, 2H), 1.92–1.82 (m, 2H), 1.75–1.46 (m, 10H), 1.44–1.35 (m, 1H), 0.93

(t, *J* = 7.4 Hz, 2H) ppm; $^{13}C\{^1H\}$ NMR (100 MHz, $CDCl_3$) δ 158.5, 140.9, 130.1, 123.9, 71.7, 38.0, 36.7, 27.7, 25.1, 22.1, 21.9, 13.8 ppm; GC-MS for $C_{14}H_{22}N_4O$, m/z = 262 (M^+). HRMS (ESI-TOF) m/z: $[M + H]^+$ Calcd for $C_{14}H_{22}N_4OH$; 263.1866 Found 263.1862.

6.5.5.3 Characterization of Compounds Listed in Table 5.7

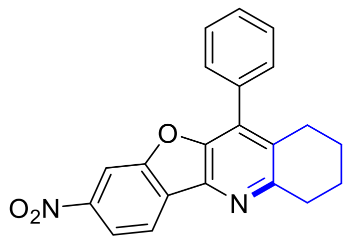

5-9ai

8-Nitro-11-phenyl-1,2,3,4-tetrahydrobenzofuro[3,2-b]quinoline (5-9ai): A 1,4-dioxane (2.0 mL) solution of complex **2-10** (9 mg, 3 mol %), **2-16** (8 mg, 10 mol %), (3-amino-6-nitrobenzofuran-2-yl)(phenyl)methanone (141 mg, 0.5 mmol), and (1S,2R)-2-aminocyclohexanecarboxylic acid (100 mg, 0.7 mmol) was stirred at 140 °C for 20 h. The product **5-9ai** was isolated by column chromatography on silica gel (hexanes/EtOAc = 100:1–5:1; TLC: R_f = 0.6 (50% EtOAc in hexanes)). Yield = 146 mg, (85%). Data for **5-9ai:** ^1H NMR (400 MHz, $CDCl_3$) δ (s, 1H), 8.34–8.26 (m, 2H), 7.62–7.49 (m, 3H), 7.49–7.40 (m, 2H), 3.21 (t, *J* = 6.6 Hz, 2H), 2.80 (t, *J* = 6.3 Hz, 2H), 2.03–1.95 (m, 2H), 1.85–1.78 (m, 2H) ppm; $^{13}C\{^1H\}$ NMR (100 MHz, $CDCl_3$) δ 155.8, 155.8, 149.2, 147.3, 138.9, 133.4, 132.2, 131.4, 129.3, 129.3, 128.8, 128.7, 120.9, 118.7, 108.4, 33.3, 28.0, 22.7, 22.6 ppm; GC-MS for $C_{21}H_{16}N_2O_3$, m/z = 344 (M^+). HRMS (ESI-TOF) m/z: $[M + H]^+$ Calcd for $C_{21}H_{16}N_2O_3H$; 345.1234 Found 345.1205.

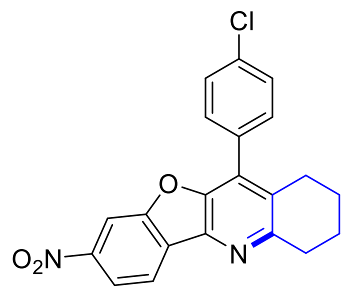

5-9aj

11-(4-Chlorophenyl)-8-nitro-1,2,3,4-tetrahydrobenzofuro[3,2-b]quinoline (5-9aj): A 1,4-dioxane (2.0 mL) solution of complex **2-10** (9 mg, 3 mol %), **2-16** (8 mg, 10 mol %), (3-amino-6-nitrobenzofuran-2-yl)(4-chlorophenyl)methanone (158 mg, 0.5 mmol), and (1S,2R)-2-aminocyclohexanecarboxylic acid (100 mg, 0.7 mmol) was stirred at 140 °C for 20 h. The product **5-9aj** was isolated by column chromatography on silica gel (hexanes/EtOAc = 100:1–5:1; TLC: R_f = 0.5 (50% EtOAc in hexanes)). Yield = 167 mg, (88%). Data for **5-9aj:** ^{1}H NMR (400 MHz, $CDCl_3$) δ 8.34 (s, 1H), 8.30–8.26 (m, 2H), 7.55 (d, J = 8.4 Hz, 2H), 7.40 (d, J = 8.4 Hz, 2H), 3.20 (t, J = 6.6 Hz, 2H), 2.77 (t, J = 6.3 Hz, 2H), 2.02–1.95 (m, 2H), 1.85–1.78 (m, 2H) ppm; ^{13}C{^{1}H} NMR (100 MHz, $CDCl_3$) δ 155.9, 155.9, 149.0, 147.4, 139.1, 135.0, 132.1, 131.2, 130.7, 130.6, 129.2, 129.1, 121.0, 118.9, 108.4, 33.3, 28.0, 22.7, 22.6 ppm; GC-MS for $C_{21}H_{15}ClN_2O_3$, m/z = 378 (M^+). HRMS (ESI-TOF) m/z: $[M + H]^+$ Calcd for $C_{21}H_{15}ClN_2O_3H$; 379.0844 Found 378.0818.

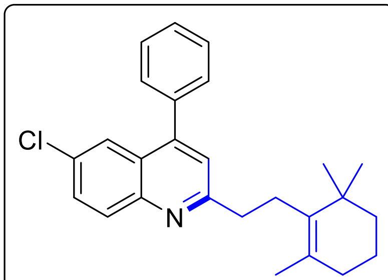

5-9ak

6-Chloro-4-phenyl-2-(2-(2,6,6-trimethylcyclohex-1-en-1-yl)ethyl)quinoline (5-9ak): A 1,4-dioxane (2.0 mL) solution of complex **2-10** (9 mg, 3 mol %), **2-16** (8 mg, 10 mol %), 5-chloro-2-aminobenzophenone (116 mg, 0.5 mmol), and in-situ generated 1-(4-(2,6,6-trimethylcyclohex-1-en-1-yl)but-2-en-2-yl)pyrrolidine (173 mg, 0.7 mmol) was stirred at 140 °C for 20 h. The product **5-9ak** was isolated by column chromatography on silica gel (hexanes/EtOAc = 100:1–5:1; TLC: R_f = 0.6 (50% EtOAc in hexanes)). Yield = 115 mg, (59%). Data for **5-9ak:** ^{1}H NMR (400 MHz, $CDCl_3$) δ 8.06 (d, *J* = 9.0 Hz, 1H), 7.82 (d, *J* = 2.1 Hz, 1H), 7.62 (dd, *J* = 9.0, 2.1 Hz, 1H), 7.58–7.47 (m, 5H), 7.26 (s, 1H), 3.09–3.01 (m, 2H), 2.53–2.47 (m, 2H), 1.96 (t, *J* = 6.2 Hz, 2H), 1.71 (s, 3H), 1.63–1.58 (m, 2H), 1.49–1.44 (m, 2H), 1.08 (s, 6H) ppm; $^{13}C\{^{1}H\}$ NMR (100 MHz, $CDCl_3$) δ 162.8, 147.7, 146.9, 137.7, 136.4, 135.9, 131.5, 131.0, 129.9, 129.4, 128.7, 128.5, 128.0, 127.8, 126.0, 124.4, 122.1, 44.5, 39.7, 35.1, 32.8, 28.7, 28.4, 22.2, 20.1, 19.5 ppm; GC-MS for $C_{26}H_{28}ClN$, m/z = 389 (M^+). HRMS (ESI-TOF) m/z: $[M + H]^+$ Calcd for $C_{26}H_{28}ClNH$; 390.1983 Found 390.1980.

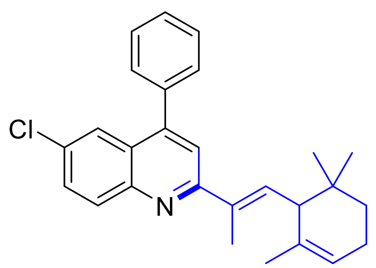

5-9al

6-Chloro-4-phenyl-2-(1-(2,6,6-trimethylcyclohex-2-en-1-yl)prop-1-en-2-yl)quinoline (5-9al): A 1,4-dioxane (2.0 mL) solution of complex **2-10** (9 mg, 3 mol %), **2-16** (8 mg, 10 mol %), 5-chloro-2-aminobenzophenone (116 mg, 0.5 mmol), and 1-(3-methyl-4-(2,6,6-trimethylcyclohex-2-en-1-yl)buta-1,3-dien-2-yl)pyrrolidine (181 mg, 0.7 mmol) was stirred at 140 °C for 20 h. The product **5-9al** was isolated by column chromatography on silica gel (hexanes/EtOAc = 100:1–5:1; TLC: R_f = 0.4 (20% EtOAc in hexanes)). Yield = 124 mg, (61%). Data for **5-9al:** ^{1}H NMR (400 MHz, $CDCl_3$) δ 8.06 (d, *J* = 9.0 Hz, 1H), 7.77 (d, *J* = 2.3 Hz, 1H), 7.61 (dd, *J* = 9.0, 2.3 Hz, 1H), 7.58–7.45 (m, 6H), 6.22 (dd, *J* = 10.9, 0.9 Hz, 1H), 5.44 (s, 1H), 2.80 (dd, *J* = 10.9 Hz, 1H), 2.37 (d, *J* = 0.9 Hz, 3H), 2.11–2.04 (m, 2H), 1.63 (s, 3H), 1.60–1.54 (m, 1H), 1.30–1.22 (m, 1H), 0.99 (s, 3H), 0.89 (s, 3H) ppm; $^{13}C\{^{1}H\}$ NMR (100 MHz, $CDCl_3$) δ 159.9, 147.3, 146.6, 138.0, 136.3, 135.8, 134.7, 131.5, 131.5, 130.0, 129.4, 128.7, 128.5, 126.2, 124.3, 121.0, 119.4, 50.2, 33.0, 32.0, 27.3, 27.2, 23.1, 23.0, 14.7 ppm; GC-MS for $C_{27}H_{28}ClN$, m/z =

401 (M^+). HRMS (ESI-TOF) m/z: $[M + H]^+$ Calcd for $C_{27}H_{28}ClNH$; 402.1983 Found 402.1997.

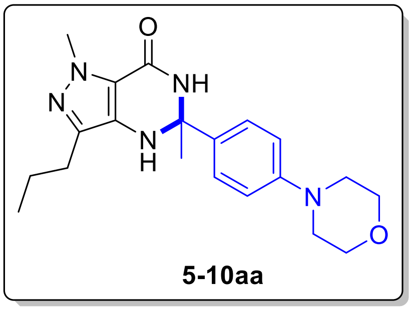

1,5-Dimethyl-5-(4-morpholinophenyl)-3-propyl-1,4,5,6-tetrahydro-7H-pyrazolo[4,3-d]pyrimidin-7-one (**5-10aa**): A 1,4-dioxane (2.0 mL) solution of complex **2-10** (9 mg, 3 mol %), **2-12** (12 mg, 10 mol %), 4-amino-1-methyl-3-n-propyl-5-pyrazolecarboxamide (91 mg, 0.5 mmol) and 1-[4-(4-morpholinyl)phenyl]ethanamine (144 mg, 0.7 mmol) was stirred at 140 °C for 20 h. The product **5-10aa** was isolated by column chromatography on silica gel (hexanes/EtOAc = 40:1–10:1; TLC: R_f = 0.2 (50% EtOAc in hexanes)). Yield = 143 mg (77%). Data for **5-10aa**: ^{1}H NMR (400 MHz, $CDCl_3$) δ 7.93 (d, J = 8.9 Hz 2H), 7.01 (brs, 1H), 6.91 (d, J = 8.9 Hz 2H), 6.05 (brs, 1H), 4.14 (s, 1H), 3.88–3.81 (m, 4H), 3.31–3.22 (m, 4H), 2.31 (t, J = 7.7 Hz 2H), 2.22 (s, 3H), 1.64–1.54 (m, 2H), 0.86 (t, J = 7.4 Hz 3H) ppm; $^{13}C\{^1H\}$ NMR (100 MHz, $CDCl_3$) δ 168.7, 162.0, 153.1, 140.1, 132.6, 128.7, 124.5, 113.9, 66.5, 47.8, 39.7, 30.8, 28.4, 21.5, 17.9, 14.0 ppm; GC-MS for $C_{20}H_{27}N_5O_2$, m/z = 369 (M^+). HRMS (ESI-TOF) m/z: $[M + H]^+$ Calcd for $C_{20}H_{27}N_5O_2H$; 370.2238 Found 370.257.2232.

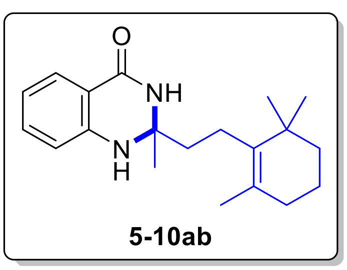

2-Methyl-2-(2-(2,6,6-trimethylcyclohex-1-en-1-yl)ethyl)-2,3-dihydroquinazolin-4(1H)-one (**5-10ab**): A 1,4-dioxane (2.0 mL) solution of complex **2-10** (9 mg, 3 mol %), **2-12** (12 mg, 10 mol %), 2-aminobenzamide (68 mg, 0.5 mmol) and in-situ generated 1-(4-(2,6,6-trimethylcyclohex-1-en-1-yl)but-2-en-2-yl)pyrrolidine (173 mg, 0.7 mmol) was stirred at 140 °C for 20 h. The product **5-10ab** was isolated by column chromatography on silica gel (hexanes/EtOAc = 40:1–10:1; TLC: R_f = 0.2 (50% EtOAc in hexanes)). Yield = 109 mg (70%). Data for **5-10ab**: ^{1}H NMR (400 MHz, $CDCl_3$) δ 7.84 (dd, *J* = 7.8, 1.2 Hz, 1H), 7.41 (brs, 1H), 7.25 (td, *J* = 7.8, 1.5 Hz, 1H), 6.76 (t, *J* = 7.8 Hz, 1H), 6.62 (d, *J* = 8.0 Hz, 1H), 4.31 (brs, 1H), 2.21–2.03 (m, 2H), 1.93–1.72 (m, 4H), 1.68–1.55 (m, 1H), 1.53 (s, 3H), 1.51 (s, 3H), 1.51–1.38 (m, 1H), 1.37–1.29 (m, 2H), 0.93 (s, 3H), 0.91 (s, 3H) ppm; $^{13}C\{^1H\}$ NMR (100 MHz, $CDCl_3$) δ 164.7, 146.1, 135.6, 133.7, 128.2, 127.5, 118.3, 114.6, 114.4, 69.9, 41.8, 39.6, 34.9, 32.7, 28.5, 28.5, 27.7, 22.6, 19.7, 19.3 ppm; GC-MS for $C_{20}H_{28}N_2O$, m/z = 312 (M^+). HRMS (ESI-TOF) m/z: $[M + H]^+$ Calcd for $C_{20}H_{28}N_2OH$; 313.2274 Found 313.2272.

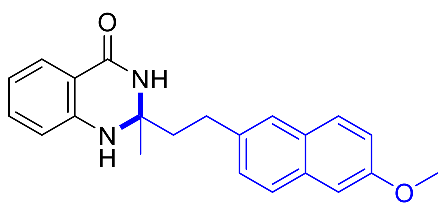

5-10ac

2-(2-(6-Methoxynaphthalen-2-yl)ethyl)-2-methyl-2,3-dihydroquinazolin-4(1H)-one (**5-10ac**): A 1,4-dioxane (2.0 mL) solution of complex **2-10** (9 mg, 3 mol %), **2-12** (12 mg, 10 mol %), 2-aminobenzamide (68 mg, 0.5 mmol) and in-situ generated 1-(4-(6-methoxynaphthalen-2-yl)but-2-en-2-yl)pyrrolidine (197 mg, 0.7 mmol) was stirred at 140 °C for 20 h. The product **5-10ac** was isolated by column chromatography on silica gel (hexanes/EtOAc = 40:1–10:1; TLC: R_f = 0.2 (50% EtOAc in hexanes)). Yield = 148 mg (86%). Data for **5-10ac**: ^{1}H NMR (400 MHz, $CDCl_3$) δ 8.12 (brs, 1H), 7.72 (d, *J* = 9.2 Hz, 2H), 6.32 (d, *J* = 7.6 Hz, 1H), 7.58 (s, 1H), 7.31 (d, *J* = 8.4 Hz, 1H), 7.27–7.21 (m, 2H), 7.11 (dd, *J* = 9.2, 2.2 Hz, 1H), 6.78 (brs, 1H), 6.72 (d, *J* = 8.0 Hz, 1H), 6.63 (t, *J* = 7.5 Hz, 1H), 3.84 (s, 3H), 3.43 (s, 3H), 2.91–2.76 (m, 2H), 2.09–1.93 (m, 2H) ppm; $^{13}C\{^1H\}$ NMR (100 MHz, $CDCl_3$) δ 163.3, 156.8, 147.3, 137.1, 133.4, 132.7, 128.8, 128.7, 127.8, 127.2, 126.8, 125.7, 118.5, 116.4, 114.2, 113.6, 105.8, 69.1, 55.1, 43.0, 29.9, 28.2 ppm; GC-MS for $C_{22}H_{22}N_2O_2$, m/z = 346 (M^+). HRMS (ESI-TOF) m/z: $[M + H]^+$ Calcd for $C_{22}H_{22}N_2O_2H$; 347.1754 Found 347.1750.

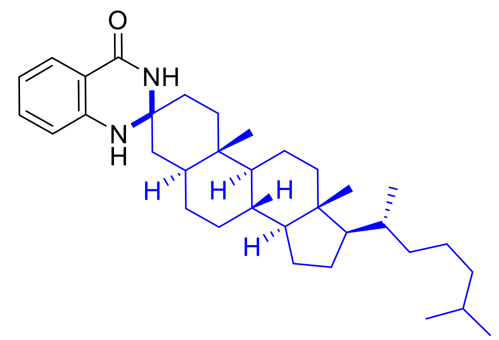

5-10ad

(8S,9R,10R,13S,14R,17S)-10,13-Dimethyl-17-((S)-6-methylheptan-2-yl)-1,2,4,5,6,7,8,9,10,11,12,13,14,15,16,17-hexadecahydro-1'H-spiro[cyclopenta[a]phenanthrene-3,2'-quinazolin]-4'(3'H)-one (**5-10ad**): A 1,4-dioxane (2.0 mL) solution of complex **2-10** (5 mg, 3 mol %), **2-12** (6 mg, 10 mol %), 2-aminobenzamide (34 mg, 0.25 mmol) and in-situ generated 1-((8S,9R,10R,13S,14R,17S)-10,13-dimethyl-17-((S)-6-methylheptan-2-yl)-4,5,6,7,8,9,10,11,12,13,14,15,16,17-tetradecahydro-1H-cyclopenta[a]phenanthren-3-yl)pyrrolidine (176 mg, 0.4 mmol) was stirred at 140 °C for 20 h. The product **5-10ad** was isolated by column chromatography on silica gel (hexanes/EtOAc = 40:1–10:1; TLC: R_f = 0.1 (50% EtOAc in hexanes)). Yield = 113 mg (90%). Data for **5-10ad**: ^1H NMR (400 MHz, DMSO) δ 8.03 (brs, 1H), 7.78 (s, 1H), 7.52 (d, J = 7.6 Hz, 1H), 6.83 (d, J = 8.1 Hz, 1H), 6.71 (brs, 1H), 6.61–6.58 (m, 1H), 1.95–1.90 (m, 1H), 1.80–1.74 (m, 2H), 1.64–1.56 (m, 2H), 1.51–1.42 (m, 6H), 1.36–1.25 (m, 6H), 1.20–1.02 (m, 1H), 0.99–0.92 (m, 3H), 0.88–0.85 (m, 3H), 0.84–0.81 (m, 6H), 0.75 (s, 3H), 0.62–0.56 (m, 3H) ppm; $^{13}C\{^1H\}$ NMR (100 MHz, DMSO) δ 163.7, 147.0, 133.5, 127.4, 116.8, 115.1, 114.6, 68.8, 56.6, 56.2, 55.4, 53.3, 42.6, 36.1, 35.7, 35.5, 35.4, 33.5, 33.4, 32.0, 32.0, 31.9, 28.3, 27.9, 24.3, 23.7, 23.1, 22.9, 21.1, 19.0, 12.3, 11.7, 11.6 ppm; GC-MS for $C_{34}H_{52}N_2O$, m/z

= 504 (M^+). HRMS (ESI-TOF) m/z: $[M + H]^+$ Calcd for $C_{34}H_{52}N_2OH$; 505.4152 Found 505.4144.

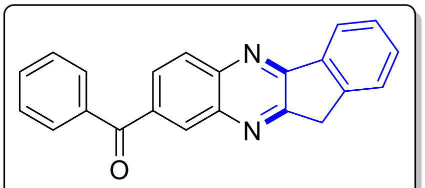

5-11q

(11H-Indeno[1,2-b]quinoxalin-8-yl)(phenyl)methanone (5-11q): A 1,4-dioxane (2.0 mL) solution of complex **2-10** (9 mg, 3 mol %), **2-16** (8 mg, 10 mol %), (3,4-diaminophenyl)(phenyl)methanone (106 mg, 0.5 mmol) and in-situ generated 4-(1H-inden-2-yl)morpholine (121 mg, 0.6 mmol) was stirred at 140 °C for 20 h. The product **5-11q** was isolated by column chromatography on silica gel (hexanes/EtOAc = 40:1–10:1; TLC: R_f = 0.5 (20% EtOAc in hexanes)). Yield = 127 mg (79%). Data for **5-11q**: ^{1}H NMR (400 MHz, $CDCl_3$) δ 8.48 (s, 1H), 8.29 (d, *J* = 6.9 Hz, 1H), 8.26–8.20 (m, 2H), 7.92–7.89 (m, 2H), 7.68 (d, *J* = 7.1 Hz, 1H), 7.65–7.61 (m, 1H), 7.59–7.52 (m, 4H), 4.17 (m, 2H) ppm; $^{13}C\{^1H\}$ NMR (100 MHz, $CDCl_3$) δ 195.7, 160.6, 156.3, 144.2, 143.9, 140.2, 137.6, 137.3, 137.1, 132.7, 132.2, 131.9, 130.1, 129.6, 129.3, 128.4, 128.3, 125.9, 123.1, 35.9 ppm; GC-MS for $C_{22}H_{14}N_2O$, m/z = 322 (M^+). HRMS (ESI-TOF) m/z: $[M + H]^+$ Calcd for $C_{22}H_{14}N_2OH$; 323.1179 Found 323.1177.

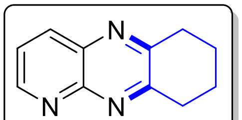

5-11o

Phenyl(6,7,8,9-tetrahydrophenazin-2-yl)methanone (5-11r): A 1,4-dioxane (2.0 mL) solution of complex **2-10** (9 mg, 3 mol %), **2-16** (8 mg, 10 mol %), (3,4-diaminophenyl)(phenyl)methanone (106 mg, 0.5 mmol) and 1-pyrrolidino-1-cyclohexene (91 mg, 0.6 mmol) was stirred at 140 °C for 20 h. The product **5-11r** was isolated by column chromatography on silica gel (hexanes/EtOAc = 40:1–10:1; TLC: R_f = 0.3 (20% EtOAc in hexanes)). Yield = 62 mg (67%). Data for **5-11r**: ^{1}H NMR (400 MHz, $CDCl_3$) δ 9.01 (dd, *J* = 4.1, 1.6 Hz, 1H), 8.26

(dd, *J* = 8.3, 1.6 Hz, 1H), 7.57 (dd, *J* = 8.3, 4.2 Hz, 1H), 3.25–3.11 (m, 4H), 2.06–1.96 (m, 4H) ppm; $^{13}C\{^{1}H\}$ NMR (100 MHz, $CDCl_3$) δ 157.8, 155.6, 152.8, 150.0, 137.1, 135.9, 124.2, 33.4, 33.0, 22.5, 22.3 ppm; GC-MS for $C_{11}H_{11}N_3$, m/z = 185 (M^+). ^1H and ^{13}C NMR spectral data are in good agreement with the literature values.[245]

7.0 Bibliography

1. Hartwig, J. F., Carbon−Heteroatom Bond-Forming Reductive Eliminations of Amines, Ethers, and Sulfides. *Acc. Chem. Res.* **1998,** *31*, 852-860.

2. Ho, T. C., Hydrodenitrogenation Catalysis. *Catal. Rev.* **1988,** *30*, 117-160.

3. (a) Ouyang, K.; Hao, W.; Zhang, W.-X.; Xi, Z., Transition-Metal-Catalyzed Cleavage of C–N Single Bonds. *Chem. Rev.* **2015,** *115*, 12045-12090; (b) Wang, Q.; Su, Y.; Li, L.; Huang, H., Transition-metal catalysed C–N bond activation. *Chem. Soc. Rev.* **2016,** *45*, 1257-1272; (c) Wang, Z.-X.; Yang, B., Chemical transformations of quaternary ammonium salts via C–N bond cleavage. *Org. Biomol. Chem.* **2020,** *18*, 1057-1072; (d) Pound, S. M.; Watson, M. P., Asymmetric synthesis via stereospecific C–N and C–O bond activation of alkyl amine and alcohol derivatives. *Chem. Commun.* **2018,** *54*, 12286-12301; (e) Liu, C.; Szostak, M., Twisted Amides: From Obscurity to Broadly Useful Transition-Metal-Catalyzed Reactions by N−C Amide Bond Activation. *Chem. Eur. J.* **2017,** *23*, 7157-7173; (f) Desnoyer, A. N.; Love, J. A., Recent advances in well-defined, late transition metal complexes that make and/or break C–N, C–O and C–S bonds. *Chem. Soc. Rev.* **2017,** *46*, 197-238.

4. Lawrence, S. A., *Amines: Synthesis, Properties and Applications*. Cambridge University Press: Cambridge, U.K., 2004.

5. (a) Shilov, A. E.; Shul'pin, G. B., Activation of C−H Bonds by Metal Complexes. *Chem. Rev.* **1997,** *97*, 2879-2932; (b) Davies, H. M. L.; Beckwith, R. E. J., Catalytic Enantioselective C−H Activation by Means of Metal−Carbenoid-Induced C−H Insertion. *Chem. Rev.* **2003,** *103* , 2861-2904; (c) Godula, K.; Sames, D., C-H Bond Functionalization in Complex Organic Synthesis. *Science* **2006,** *312*, 67-72; (d) Basu, D.; Kumar, S.; V, S. S.; Bandichhor, R., Transition metal catalyzed C-H activation for the synthesis of medicinally relevant molecules: A Review. *J. Chem. Sci.* **2018,** *130*, 71.

6. (a) Cornella, J.; Zarate, C.; Martin, R., Metal-catalyzed activation of ethers via C–O bond cleavage: a new strategy for molecular diversity. *Chem. Soc. Rev.* **2014,** *43*, 8081-8097; (b) Kim, J.; Lee, D.-H.; Kalutharage, N.; Yi, C. S., Selective Catalytic Synthesis of Unsymmetrical Ethers from the Dehydrative Etherification of Two Different Alcohols. *ACS Catal.* **2014,** *4*, 3881-3885.

7. Miyazaki, Y.; Ohta, N.; Semba, K.; Nakao, Y., Intramolecular Aminocyanation of Alkenes by Cooperative Palladium/Boron Catalysis. *J. Am. Chem. Soc.* **2014,** *136*, 3732-3735.

8. Smith, A. M.; Whyman, R., Review of Methods for the Catalytic Hydrogenation of Carboxamides. *Chem. Rev.* **2014,** *114*, 5477-5510.

9. Balaraman, E.; Gnanaprakasam, B.; Shimon, L. J. W.; Milstein, D., Direct Hydrogenation of Amides to Alcohols and Amines under Mild Conditions. *J. Am. Chem. Soc.* **2010,** *132*, 16756-16758.

10. Cabrero-Antonino, J. R.; Alberico, E.; Drexler, H.-J.; Baumann, W.; Junge, K.; Junge, H.; Beller, M., Efficient Base-Free Hydrogenation of Amides to Alcohols and Amines Catalyzed by Well-Defined Pincer Imidazolyl–Ruthenium Complexes. *ACS Catal.* **2016,** *6*, 47-54.

11. Papa, V.; Cabrero-Antonino, J. R.; Alberico, E.; Spanneberg, A.; Junge, K.; Junge, H.; Beller, M., Efficient and selective hydrogenation of amides to alcohols and amines using a well-defined manganese–PNN pincer complex. *Chem. Sci.* **2017,** *8*, 3576-3585.

12. Garg, J. A.; Chakraborty, S.; Ben-David, Y.; Milstein, D., Unprecedented iron-catalyzed selective hydrogenation of activated amides to amines and alcohols. *Chem. Commun.* **2016,** *52*, 5285-5288.

13. Schneck, F.; Assmann, M.; Balmer, M.; Harms, K.; Langer, R., Selective Hydrogenation of Amides to Amines and Alcohols Catalyzed by Improved Iron Pincer Complexes. *Organometallics* **2016,** *35*, 1931-1943.

14. Rezayee, N. M.; Samblanet, D. C.; Sanford, M. S., Iron-Catalyzed Hydrogenation of Amides to Alcohols and Amines. *ACS Catal.* **2016,** *6*, 6377-6383.

15. Jayarathne, U.; Zhang, Y.; Hazari, N.; Bernskoetter, W. H., Selective Iron-Catalyzed Deaminative Hydrogenation of Amides. *Organometallics* **2017,** *36*, 409-416.

16. Rasu, L.; John, J. M.; Stephenson, E.; Endean, R.; Kalapugama, S.; Clément, R.; Bergens, S. H., Highly Enantioselective Hydrogenation of Amides via Dynamic Kinetic Resolution Under Low Pressure and Room Temperature. *J. Am. Chem. Soc.* **2017,** *139*, 3065-3071.

17. Artús Suàrez, L.; Culakova, Z.; Balcells, D.; Bernskoetter, W. H.; Eisenstein, O.; Goldberg, K. I.; Hazari, N.; Tilset, M.; Nova, A., The Key Role of the Hemiaminal Intermediate in the Iron-Catalyzed Deaminative Hydrogenation of Amides. *ACS Catal.* **2018,** *8*, 8751-8762.

18. Balaraman, E.; Ben-David, Y.; Milstein, D., Unprecedented Catalytic Hydrogenation of Urea Derivatives to Amines and Methanol. *Angew. Chem. Int. Ed.* **2011,** *50*, 11702-11705.

19. Das, U. K.; Kumar, A.; Ben-David, Y.; Iron, M. A.; Milstein, D., Manganese Catalyzed Hydrogenation of Carbamates and Urea Derivatives. *J. Am. Chem. Soc.* **2019,** *141*, 12962-12966.

20. Li, Y.; Wang, Z.; Wu, X.-F., Palladium-Catalyzed Carbonylative Direct Transformation of Benzyl Amines under Additive-Free Conditions. *ACS Catal.* **2018,** *8*, 738-741.

21. Yu, H.; Gao, B.; Hu, B.; Huang, H., Charge-Transfer Complex Promoted C–N Bond Activation for Ni-Catalyzed Carbonylation. *Org. Lett.* **2017,** *19*, 3520-3523.

22. Zhang, Z.; Wang, H.; Qiu, N.; Kong, Y.; Zeng, W.; Zhang, Y.; Zhao, J., Synthesis of Triarylmethanes via Palladium-Catalyzed Suzuki Coupling of Trimethylammonium Salts and Arylboronic Acids. *J. Org. Chem.* **2018,** *83*, 8710-8715.

23. Han, C.; Zhang, Z.; Xu, S.; Wang, K.; Chen, K.; Zhao, J., Palladium-Catalyzed Hiyama Coupling of Benzylic Ammonium Salts via C–N Bond Cleavage. *J. Org. Chem.* **2019,** *84* , 16308-16313.

24. Xu, S.; Zhang, Z.; Han, C.; Hu, W.; Xiao, T.; Yuan, Y.; Zhao, J., Palladium-Catalyzed Coupling of Terminal Alkynes with Benzyl Ammonium Salts. *J. Org. Chem.* **2019,** *84*, 12192-12197.

25. Xu, Y.-N.; Zhu, M.-Z.; Tian, S.-K., Chiral α-Amino Acid/Palladium-Catalyzed Asymmetric Allylation of α-Branched β-Ketoesters with Allylic Amines: Highly Enantioselective Construction of All-Carbon Quaternary Stereocenters. *J. Org. Chem.* **2019,** *84*, 14936-14942.

26. Huang, C.-Y.; Doyle, A. G., Electron-Deficient Olefin Ligands Enable Generation of Quaternary Carbons by Ni-Catalyzed Cross-Coupling. *J. Am. Chem. Soc.* **2015,** *137*, 5638-5641.

27. Yu, X.-Y.; Zhou, Q.-Q.; Wang, P.-Z.; Liao, C.-M.; Chen, J.-R.; Xiao, W.-J., Dual Photoredox/Nickel-Catalyzed Regioselective Cross-Coupling of 2-Arylaziridines and Potassium Benzyltrifluoroborates: Synthesis of β-Substitued Amines. *Org. Lett.* **2018,** *20*, 421-424.

28. Hao, W.; Wu, X.; Sun, J. Z.; Siu, J. C.; MacMillan, S. N.; Lin, S., Radical Redox-Relay Catalysis: Formal [3+2] Cycloaddition of N-Acylaziridines and Alkenes. *J. Am. Chem. Soc.* **2017,** *139*, 12141-12144.

29. Kalutharage, N.; Yi, C. S., Deaminative and Decarboxylative Catalytic Alkylation of Amino Acids with Ketones. *Angew. Chem. Int. Ed.* **2013,** *52*, 13651-13655.

30. Hugelshofer, C. L.; Palani, V.; Sarpong, R., Oxazaborinines from Vinylogous N-Allylic Amides: Reactivities of Underexplored Heterocyclic Building Blocks. *Org. Lett.* **2018,** *20*, 2649-2653.

31. Wenkert, E.; Han, A.-L.; Jenny, C.-J., Nickel-induced conversion of carbon–nitrogen into carbon–carbon bonds. One-step transformations of aryl, quaternary ammonium salts into alkylarenes and biaryls. *J. Chem. Soc., Chem. Commun.* **1988,** 975-976.

32. Yu, S.; Liu, S.; Lan, Y.; Wan, B.; Li, X., Rhodium-Catalyzed C–H Activation of Phenacyl Ammonium Salts Assisted by an Oxidizing C–N Bond: A Combination of Experimental and Theoretical Studies. *J. Am. Chem. Soc.* **2015,** *137*, 1623-1631.

33. Greenhalgh, M. D.; Thomas, S. P., Iron-Catalyzed, Highly Regioselective Synthesis of α-Aryl Carboxylic Acids from Styrene Derivatives and CO2. *J. Am. Chem. Soc.* **2012,** *134*, 11900-11903.

34. Moragas, T.; Gaydou, M.; Martin, R., Nickel-Catalyzed Carboxylation of Benzylic C−N Bonds with CO2. *Angew. Chem. Int. Ed.* **2016,** *55*, 5053-5057.

35. Guisán-Ceinos, M.; Martín-Heras, V.; Tortosa, M., Regio- and Stereospecific Copper-Catalyzed Substitution Reaction of Propargylic Ammonium Salts with Aryl Grignard Reagents. *J. Am. Chem. Soc.* **2017,** *139*, 8448-8451.

36. (a) Katritzky, A. R.; De Ville, G.; Patel, R. C., Carbon-alkylation of simple nitronate anions by N-substituted pyridiniums. *Tetrahedron* **1981,** *37*, 25-30; (b) Katritzky, A. R.; Marson, C. M., Pyrylium Mediated Transformations of Primary Amino Groups into Other Functional Groups. New Synthetic Methods (41). *Angew. Chem. Int. Ed.* **1984,** *23*, 420-429.

37. Basch, C. H.; Liao, J.; Xu, J.; Piane, J. J.; Watson, M. P., Harnessing Alkyl Amines as Electrophiles for Nickel-Catalyzed Cross Couplings via C–N Bond Activation. *J. Am. Chem. Soc.* **2017,** *139*, 5313-5316.

38. Plunkett, S.; Basch, C. H.; Santana, S. O.; Watson, M. P., Harnessing Alkylpyridinium Salts as Electrophiles in Deaminative Alkyl–Alkyl Cross-Couplings. *J. Am. Chem. Soc.* **2019,** *141*, 2257-2262.

39. Martin-Montero, R.; Yatham, V. R.; Yin, H.; Davies, J.; Martin, R., Ni-catalyzed Reductive Deaminative Arylation at sp3 Carbon Centers. *Org. Lett.* **2019,** *21*, 2947-2951.

40. Jiang, X.; Zhang, M.-M.; Xiong, W.; Lu, L.-Q.; Xiao, W.-J., Deaminative (Carbonylative) Alkyl-Heck-type Reactions Enabled by Photocatalytic C−N Bond Activation. *Angew. Chem. Int. Ed.* **2019,** *58*, 2402-2406.

41. He, R.-D.; Li, C.-L.; Pan, Q.-Q.; Guo, P.; Liu, X.-Y.; Shu, X.-Z., Reductive Coupling between C–N and C–O Electrophiles. *J. Am. Chem. Soc.* **2019,** *141*, 12481-12486.

42. Nagae, H.; Xia, J.; Kirillov, E.; Higashida, K.; Shoji, K.; Boiteau, V.; Zhang, W.; Carpentier, J.-F.; Mashima, K., Asymmetric Allylic Alkylation of β-Ketoesters via C–N Bond Cleavage of N-Allyl-N-methylaniline Derivatives Catalyzed by a Nickel–Diphosphine System. *ACS Catal.* **2020**, *10*, 5828-5839.

43. Hu, X.-Q.; Hu, Z.; Zhang, G.; Sivendran, N.; Gooßen, L. J., Catalytic C–N and C–H Bond Activation: ortho-Allylation of Benzoic Acids with Allyl Amines. *Org. Lett.* **2018,** *20*, 4337-4340.

44. Cui, M.; Liu, J.-H.; Lu, X.-Y.; Lu, X.; Zhang, Z.-Q.; Xiao, B.; Fu, Y., Iron-mediated remote C–H bond benzylation of 8-aminoquinoline amides. *Tetrahedron Lett.* **2017,** *58*, 1912-1916.

45. Ueno, S.; Chatani, N.; Kakiuchi, F., Ruthenium-Catalyzed Carbon−Carbon Bond Formation via the Cleavage of an Unreactive Aryl Carbon−Nitrogen Bond in Aniline Derivatives with Organoboronates. *J. Am. Chem. Soc.* **2007,** *129*, 6098-6099.

46. Koreeda, T.; Kochi, T.; Kakiuchi, F., Cleavage of C−N Bonds in Aniline Derivatives on a Ruthenium Center and Its Relevance to Catalytic C−C Bond Formation. *J. Am. Chem. Soc.* **2009,** *131*, 7238-7239.

47. Cong, X.; Fan, F.; Ma, P.; Luo, M.; Chen, H.; Zeng, X., Low-Valent, High-Spin Chromium-Catalyzed Cleavage of Aromatic Carbon–Nitrogen Bonds at Room Temperature: A Combined Experimental and Theoretical Study. *J. Am. Chem. Soc.* **2017,** *139*, 15182-15190.

48. Wang, X.; Huang, Y.; Xu, Y.; Tang, X.; Wu, W.; Jiang, H., Palladium-Catalyzed Denitrogenative Synthesis of Aryl Ketones from Arylhydrazines and Nitriles Using O2 as Sole Oxidant. *J. Org. Chem.* **2017,** *82*, 2211-2218.

49. Tu, Y.; Yuan, L.; Wang, T.; Wang, C.; Ke, J.; Zhao, J., Palladium-Catalyzed Oxidative Carbonylation of Aryl Hydrazines with CO and O2 at Atmospheric Pressure. *J. Org. Chem.* **2017,** *82*, 4970-4976.

50. Cao, Z.-C.; Xie, S.-J.; Fang, H.; Shi, Z.-J., Ni-Catalyzed Cross-Coupling of Dimethyl Aryl Amines with Arylboronic Esters under Reductive Conditions. *J. Am. Chem. Soc.* **2018,** *140*, 13575-13579.

51. Zhang, Z.-B.; Ji, C.-L.; Yang, C.; Chen, J.; Hong, X.; Xia, J.-B., Nickel-Catalyzed Kumada Coupling of Boc-Activated Aromatic Amines via Nondirected Selective Aryl C–N Bond Cleavage. *Org. Lett.* **2019,** *21*, 1226-1231.

52. Chen, Q.; Gao, F.; Tang, H.; Yao, M.; Zhao, Q.; Shi, Y.; Dang, Y.; Cao, C., Sonogashira Cross-Coupling of Aryltrimethylammonium Salts. *ACS Catal.* **2019,** *9*, 3730-3736.

53. Feng, B.; Yang, Y.; You, J., Palladium-catalyzed denitrative Sonogashira-type cross-coupling of nitrobenzenes with terminal alkynes. *Chem. Commun.* **2020,** *56*, 790-793.

54. Xu, J.-X.; Zhao, F.; Yuan, Y.; Wu, X.-F., Ruthenium-Catalyzed Carbonylative Coupling of Anilines with Organoboranes by the Cleavage of Neutral Aryl C–N Bond. *Org. Lett.* **2020,** *22*, 2756-2760.

55. Xu, J.-X.; Zhao, F.; Franke, R.; Wu, X.-F., Ruthenium-catalyzed Suzuki coupling of anilines with alkenyl borates via selective aryl CN bond cleavage. *Catal. Commun.* **2020,** *140*, 106009.

56. Zhu, F.; Tao, J.-L.; Wang, Z.-X., Palladium-Catalyzed C–H Arylation of (Benzo)oxazoles or (Benzo)thiazoles with Aryltrimethylammonium Triflates. *Org. Lett.* **2015,** *17*, 4926-4929.

57. Wang, D.-Y.; Kawahata, M.; Yang, Z.-K.; Miyamoto, K.; Komagawa, S.; Yamaguchi, K.; Wang, C.; Uchiyama, M., Stille coupling via C–N bond cleavage. *Nat. Commun.* **2016,** *7*, 12937.

58. Zhou, Y.; Lin, L.; Wang, Y.; Zhu, J.; Song, Q., Cu-Catalyzed Aromatic Metamorphosis of 3-Aminoindazoles. *Org. Lett.* **2019,** *21*, 7630-7634.

59. Wang, M.; Zhang, X.; Zhuang, Y.-X.; Xu, Y.-H.; Loh, T.-P., Pd-Catalyzed Intramolecular C–N Bond Cleavage, 1,4-Migration, sp3 C–H Activation, and Heck Reaction: Four Controllable Diverse Pathways Depending on the Judicious Choice of the Base and Ligand. *J. Am. Chem. Soc.* **2015,** *137*, 1341-1347.

60. Gong, T.-J.; Xiao, B.; Cheng, W.-M.; Su, W.; Xu, J.; Liu, Z.-J.; Liu, L.; Fu, Y., Rhodium-Catalyzed Directed C–H Cyanation of Arenes with N-Cyano-N-phenyl-p-toluenesulfonamide. *J. Am. Chem. Soc.* **2013,** *135*, 10630-10633.

61. Yu, D.-G.; Gensch, T.; de Azambuja, F.; Vásquez-Céspedes, S.; Glorius, F., Co(III)-Catalyzed C–H Activation/Formal SN-Type Reactions: Selective and Efficient Cyanation, Halogenation, and Allylation. *J. Am. Chem. Soc.* **2014,** *136*, 17722-17725.

62. Li, J.; Ackermann, L., Cobalt-Catalyzed C□H Cyanation of Arenes and Heteroarenes. *Angew. Chem. Int. Ed.* **2015,** *54*, 3635-3638.

63. Miyaura, N.; Suzuki, A., Palladium-Catalyzed Cross-Coupling Reactions of Organoboron Compounds. *Chem. Rev.* **1995,** *95*, 2457-2483.

64. (a) Kaiser, D.; Bauer, A.; Lemmerer, M.; Maulide, N., Amide activation: an emerging tool for chemoselective synthesis. *Chem. Soc. Rev.* **2018,** *47*, 7899-7925; (b) Dander, J. E.; Garg, N. K., Breaking Amides using Nickel Catalysis. *ACS Catal.* **2017,** *7*, 1413-1423; (c) Takise, R.; Muto, K.; Yamaguchi, J., Cross-coupling of aromatic esters and amides. *Chem. Soc. Rev.* **2017,** *46*, 5864-5888; (d) Meng, G.; Shi, S.; Szostak, M., Cross-Coupling of Amides by N–C Bond Activation. *Synlett* **2016,** *27*, 2530-2540.

65. Pattabiraman, V. R.; Bode, J. W., Rethinking amide bond synthesis. *Nature* **2011,** *480*, 471-479.

66. Weires, N. A.; Baker, E. L.; Garg, N. K., Nickel-catalysed Suzuki–Miyaura coupling of amides. *Nat. chem.* **2016,** *8*, 75-79.

67. Simmons, B. J.; Weires, N. A.; Dander, J. E.; Garg, N. K., Nickel-Catalyzed Alkylation of Amide Derivatives. *ACS Catal.* **2016,** *6*, 3176-3179.

68. Boit, T. B.; Weires, N. A.; Kim, J.; Garg, N. K., Nickel-Catalyzed Suzuki–Miyaura Coupling of Aliphatic Amides. *ACS Catal.* **2018,** *8*, 1003-1008.

69. (a) Li, X.; Zou, G., Acylative Suzuki coupling of amides: acyl-nitrogen activation via synergy of independently modifiable activating groups. *Chem. Commun.* **2015,** *51*, 5089-5092; (b) Li, X.; Zou, G., Palladium-catalyzed acylative cross-coupling of amides with diarylborinic acids and sodium tetraarylborates. *J. Organomet. Chem.* **2015,** *794*, 136-145.

70. (a) Meng, G.; Szostak, M., Sterically Controlled Pd-Catalyzed Chemoselective Ketone Synthesis via N–C Cleavage in Twisted Amides. *Org. Lett.* **2015,** *17*, 4364-4367; (b) Meng, G.; Szostak, M., Palladium-catalyzed Suzuki–Miyaura coupling of amides by carbon–nitrogen cleavage: general strategy for amide N–C bond activation. *Org. Biomol. Chem.* **2016,** *14*, 5690-5707.

71. (a) Liu, C.; Meng, G.; Liu, Y.; Liu, R.; Lalancette, R.; Szostak, R.; Szostak, M., N-Acylsaccharins: Stable Electrophilic Amide-Based Acyl Transfer Reagents in Pd-Catalyzed Suzuki–Miyaura Coupling via N–C Cleavage. *Org. Lett.* **2016,** *18*, 4194-4197; (b) Karthik, S.; Gandhi, T., Palladium(II)/N-Heterocyclic Carbene-Catalyzed Direct C–H Acylation of Heteroarenes with N-Acylsaccharins. *Org. Lett.* **2017,** *19*, 5486-5489.

72. Luo, Z.; Liu, T.; Guo, W.; Wang, Z.; Huang, J.; Zhu, Y.; Zeng, Z., N-Acyl-5,5-dimethylhydantoin, a New Mild Acyl-Transfer Reagent in Pd Catalysis: Highly Efficient Synthesis of Functionalized Ketones. *Org. Process Res. Dev.* **2018,** *22*, 1188-1199.

73. Kadam, A. A.; Metz, T. L.; Qian, Y.; Stanley, L. M., Ni-Catalyzed Three-Component Alkene Carboacylation Initiated by Amide C–N Bond Activation. *ACS Catal.* **2019,** *9*, 5651-5656.

74. Liu, X.; Hsiao, C.-C.; Guo, L.; Rueping, M., Cross-Coupling of Amides with Alkylboranes via Nickel-Catalyzed C–N Bond Cleavage. *Org. Lett.* **2018,** *20*, 2976-2979.

75. Yu, C.-G.; Matsuo, Y., Nickel-Catalyzed Deaminative Acylation of Activated Aliphatic Amines with Aromatic Amides via C–N Bond Activation. *Org. Lett.* **2020,** *22*, 950-955.

76. Meng, G.; Szostak, M., General Olefin Synthesis by the Palladium-Catalyzed Heck Reaction of Amides: Sterically Controlled Chemoselective N-C Activation. *Angew. Chem. Int. Ed.* **2015,** *54*, 14518-14522.

77. Shi, S.; Meng, G.; Szostak, M., Synthesis of Biaryls through Nickel-Catalyzed Suzuki–Miyaura Coupling of Amides by Carbon–Nitrogen Bond Cleavage. *Angew. Chem. Int. Ed.* **2016,** *55*, 6959-6963.

78. Meng, G.; Szostak, M., Rhodium-Catalyzed C–H Bond Functionalization with Amides by Double C–H/C–N Bond Activation. *Org. Lett.* **2016,** *18*, 796-799.

79. Srimontree, W.; Chatupheeraphat, A.; Liao, H.-H.; Rueping, M., Amide to Alkyne Interconversion via a Nickel/Copper-Catalyzed Deamidative Cross-Coupling of Aryl and Alkenyl Amides. *Org. Lett.* **2017,** *19*, 3091-3094.

80. Chen, J.; Xu, M.; Yu, S.; Xia, Y.; Lee, S., Nickel-Catalyzed Claisen Condensation Reaction between Two Different Amides. *Org. Lett.* **2020,** *22*, 2287-2292.

81. Yada, A.; Okajima, S.; Murakami, M., Palladium-Catalyzed Intramolecular Insertion of Alkenes into the Carbon–Nitrogen Bond of β-Lactams. *J. Am. Chem. Soc.* **2015,** *137*, 8708-8711.

82. Medina, J. M.; Moreno, J.; Racine, S.; Du, S.; Garg, N. K., Mizoroki–Heck Cyclizations of Amide Derivatives for the Introduction of Quaternary Centers. *Angew. Chem. Int. Ed.* **2017,** *56*, 6567-6571.

83. Zhang, J.; Xu, B.; Wu, W.; Liu, T., Theoretical insight into the mechanisms of palladium-catalyzed intramolecular insertion of alkenes into the carbon-nitrogen bond of β-lactam. *J. Organomet. Chem.* **2018,** *864*, 37-43.

84. Li, R.; Xu, H.; Zhao, N.; Jin, X.; Dang, Y., Origins of Chemoselectivity in the Ni-Catalyzed Biaryl and Pd-Catalyzed Acyl Suzuki–Miyaura Cross-Coupling of N-Acetyl-Amides. *J. Org. Chem.* **2020,** *85*, 833-840.

85. Ni, S.; Zhang, W.; Mei, H.; Han, J.; Pan, Y., Ni-Catalyzed Reductive Cross-Coupling of Amides with Aryl Iodide Electrophiles via C–N Bond Activation. *Org. Lett.* **2017,** *19*, 2536-2539.

86. van de Kuil, L. A.; Grove, D. M.; Gossage, R. A.; Zwikker, J. W.; Jenneskens, L. W.; Drenth, W.; van Koten, G., Mechanistic Aspects of the Kharasch Addition Reaction Catalyzed by Organonickel(II) Complexes Containing the Monoanionic Terdentate Aryldiamine Ligand System [C6H2(CH2NMe2)2-2,6-R-4]. *Organometallics* **1997,** *16*, 4985-4994.

87. Zhuo, J.; Zhang, Y.; Li, Z.; Li, C., Nickel-Catalyzed Direct Acylation of Aryl and Alkyl Bromides with Acylimidazoles. *ACS Catal.* **2020,** *10*, 3895-3903.

88. Meng, G.; Shi, S.; Szostak, M., Palladium-Catalyzed Suzuki–Miyaura Cross-Coupling of Amides via Site-Selective N–C Bond Cleavage by Cooperative Catalysis. *ACS Catal.* **2016,** *6*, 7335-7339.

89. Shi, S.; Xu, K.; Jiang, C.; Ding, Z., ZnCl2-Catalyzed [3 + 2] Cycloaddition of Benzimidates and 2H-Azirines for the Synthesis of Imidazoles. *J. Org. Chem.* **2018,** *83*, 14791-14796.

90. Zhou, Y.; Wang, Y.; Song, Z.; Nakano, T.; Song, Q., Cu-catalyzed C–N bond cleavage of 3-aminoindazoles for the C–H arylation of enamines. *Org. Chem. Front.* **2020,** *7*, 25-29.

91. Qin, G.; Li, L.; Li, J.; Huang, H., Palladium-Catalyzed Formal Insertion of Carbenoids into Aminals via C–N Bond Activation. *J. Am. Chem. Soc.* **2015,** *137*, 12490-12493.

92. Feng, J.-J.; Lin, T.-Y.; Wu, H.-H.; Zhang, J., Transfer of Chirality in the Rhodium-Catalyzed Intramolecular Formal Hetero-[5 + 2] Cycloaddition of Vinyl Aziridines and Alkynes: Stereoselective Synthesis of Fused Azepine Derivatives. *J. Am. Chem. Soc.* **2015,** *137*, 3787-3790.

93. Li, B.; Xu, H.; Wang, H.; Wang, B., Rhodium-Catalyzed Annulation of Tertiary Aniline N-Oxides to N-Alkylindoles: Regioselective C–H Activation, Oxygen-Atom Transfer, and N-Dealkylative Cyclization. *ACS Catal.* **2016,** *6*, 3856-3862.

94. Gao, B.; Huang, H., Palladium-Catalyzed Hydroaminocarbonylation of Alkynes with Tertiary Amines via C–N Bond Cleavage. *Org. Lett.* **2017,** *19*, 6260-6263.

95. Rao, C.; Mai, S.; Song, Q., Cu-Catalyzed Synthesis of 3-Formyl Imidazo[1,2-a]pyridines and Imidazo[1,2-a]pyrimidines by Employing Ethyl Tertiary Amines as Carbon Sources. *Org. Lett.* **2017,** *19*, 4726-4729.

96. He, Y.; Zheng, Z.; Liu, Q.; Song, G.; Sun, N.; Chai, X., Tunable Synthesis of 2-Ene-1,4-diones, 4-Hydroxycyclopent-2-en-1-ones, and 2-(Furan-3-yl)acetamides via Palladium-Catalyzed Cascade Reactions of Allenols. *J. Org. Chem.* **2018,** *83*, 12514-12526.

97. (a) Gazizov, A. S.; Smolobochkin, A. V.; Anikina, E. A.; Strelnik, A. G.; Burilov, A. R.; Pudovik, M. A., Acid-Mediated C–N Bond Cleavage in 1-Sulfonylpyrrolidines: An Efficient Route towards Dibenzoxanthenes, Diarylmethanes, and Resorcinarenes. *Synlett* **2018,** *29*, 467-472; (b) Jiang, H.; He, J.; Liu, T.; Yu, J.-Q., Ligand-Enabled γ-C(sp3)–H Olefination of Amines: En Route to Pyrrolidines. *J. Am. Chem. Soc.* **2016,** *138*, 2055-2059.

98. Chen, H.; Yang, H.; Li, N.; Xue, X.; He, Z.; Zeng, Q., Palladium-Catalyzed C–N Cross-Coupling of NH-Heteroarenes and Quaternary Ammonium Salts via C–N Bond Cleavage. *Org. Process Res. Dev.* **2019,** *23*, 1679-1685.

99. Cai, W.; Wu, J.; Zhang, H.; Jalani, H. B.; Li, G.; Lu, H., Rh-Catalyzed Chemoselective [4 + 1] Cycloaddition Reaction toward Diverse 4-Methyleneprolines. *J. Org. Chem.* **2019,** *84*, 10877-10891.

100. Nicolle, S. M.; Lewis, W.; Hayes, C. J.; Moody, C. J., Stereoselective Synthesis of Highly Substituted Tetrahydrofurans through Diverted Carbene O-H Insertion Reaction. *Angew. Chem. Int. Ed.* **2015,** *54*, 8485-8489.

101. Xia, Y.; Liu, Z.; Liu, Z.; Ge, R.; Ye, F.; Hossain, M.; Zhang, Y.; Wang, J., Formal Carbene Insertion into C–C Bond: Rh(I)-Catalyzed Reaction of Benzocyclobutenols with Diazoesters. *J. Am. Chem. Soc.* **2014,** *136*, 3013-3015.

102. Baker, E. L.; Yamano, M. M.; Zhou, Y.; Anthony, S. M.; Garg, N. K., A two-step approach to achieve secondary amide transamidation enabled by nickel catalysis. *Nat. Commun.* **2016,** *7*, 11554.

103. Meng, G.; Lei, P.; Szostak, M., A General Method for Two-Step Transamidation of Secondary Amides Using Commercially Available, Air- and Moisture-Stable Palladium/NHC (N-Heterocyclic Carbene) Complexes. *Org. Lett.* **2017,** *19*, 2158-2161.

104. Yu, S.; Shin, T.; Zhang, M.; Xia, Y.; Kim, H.; Lee, S., Nickel/Briphos-Catalyzed Direct Transamidation of Unactivated Secondary Amides Using Trimethylsilyl Chloride. *Org. Lett.* **2018,** *20*, 7563-7566.

105. McGuire, J. L., *Pharmaceuticals: Classes, Therapeutic Agents, Areas of Application*. Wiley-VCH: 2000; Vol. 1-4.

106. Elangovan, S.; Neumann, J.; Sortais, J.-B.; Junge, K.; Darcel, C.; Beller, M., Efficient and selective N-alkylation of amines with alcohols catalysed by manganese pincer complexes. *Nat. Commun.* **2016,** *7*, 12641-12649.

107. (a) Seyden-Penne, J., *Reductions by the Alumino- and Borohydrides in Organic Synthesis*. 2nd Edition ed.; Wiley: New York, 1997; (b) Shen, Q.; Hartwig, J. F., [(CyPF-tBu)PdCl2]: An Air-Stable, One-Component, Highly Efficient Catalyst for Amination of Heteroaryl and Aryl Halides. *Org. Lett.* **2008,** *10*, 4109-4112; (c) Green, R. A.; Hartwig, J. F., Palladium-Catalyzed Amination of Aryl Chlorides and Bromides with Ammonium Salts. *Org. Lett.* **2014,** *16*, 4388-4391; (d) Ruiz-Castillo, P.; Blackmond, D. G.; Buchwald, S. L., Rational Ligand Design for the Arylation of Hindered Primary Amines Guided by Reaction Progress Kinetic Analysis. *J. Am. Chem. Soc.* **2015,** *137*, 3085-3092; (e) Fors, B. P.; Watson, D. A.; Biscoe, M. R.; Buchwald, S. L., A Highly Active Catalyst for Pd-Catalyzed Amination Reactions: Cross-Coupling Reactions Using Aryl Mesylates and the Highly Selective Monoarylation of Primary Amines Using Aryl Chlorides. *J. Am. Chem. Soc.* **2008,** *130*, 13552-13554.

108. Sperotto, E.; van Klink, G. P. M.; van Koten, G.; de Vries, J. G., The mechanism of the modified Ullmann reaction. *Dalton Trans.* **2010,** *39*, 10338-10351.

109. Huang, L.; Arndt, M.; Gooßen, K.; Heydt, H.; Gooßen, L. J., Late Transition Metal-Catalyzed Hydroamination and Hydroamidation. *Chem. Rev.* **2015,** *115*, 2596-2697.

110. Kosugi, M.; Kameyama, M.; Migita, T., Palladium-Catalyzed Aromatic Amination of Aryl Bromides with N,N-Di-ethylamino-tributyltin. *Chem. Lett.* **1983,** *12*, 927-928.

111. Dale Boger, L.; Panek, J. S., Palladium (O) mediated β-carboline synthesis: Preparation of the CDE ring system of lavendamycin. *Tetrahedron Lett.* **1984,** *25*, 3175-3178.

112. Paul, F.; Patt, J.; Hartwig, J. F., Palladium-catalyzed formation of carbon-nitrogen bonds. Reaction intermediates and catalyst improvements in the hetero cross-coupling of aryl halides and tin amides. *J. Am. Chem. Soc.* **1994,** *116*, 5969-5970.

113. Guram, A. S.; Buchwald, S. L., Palladium-Catalyzed Aromatic Aminations with in situ Generated Aminostannanes. *J. Am. Chem. Soc.* **1994,** *116*, 7901-7902.

114. Wagaw, S.; Rennels, R. A.; Buchwald, S. L., Palladium-Catalyzed Coupling of Optically Active Amines with Aryl Bromides. *J. Am. Chem. Soc.* **1997,** *119*, 8451-8458.

115. Li, Z.; Legras, L.; Kumar, A.; Vachhani, D. D.; Sharma, S. K.; Parmar, V. S.; Van der Eycken, E. V., Microwave-assisted synthesis of 4H-benzo[f]imidazo[1,4]diazepin-6-ones via a post-Ugi copper-catalyzed intramolecular Ullmann coupling. *Tetrahedron Lett.* **2014,** *55*, 2070-2074.

116. Bordwell, F. G., Equilibrium acidities in dimethyl sulfoxide solution. *Acc. Chem. Res.* **1988,** *21*, 456-463.

117. Nishikawa, D.; Hirano, K.; Miura, M., Asymmetric Synthesis of α-Aminoboronic Acid Derivatives by Copper-Catalyzed Enantioselective Hydroamination. *J. Am. Chem. Soc.* **2015,** *137*, 15620-15623.

118. (a) Hamid, M. H. S. A.; Slatford, P. A.; Williams, J. M. J., Borrowing Hydrogen in the Activation of Alcohols. *Adv. Synth. Catal.* **2007,** *349*, 1555-1575; (b) Dobereiner, G. E.; Crabtree, R. H., Dehydrogenation as a Substrate-Activating Strategy in Homogeneous Transition-Metal Catalysis. *Chem. Rev.* **2010,** *110*, 681-703; (c) Guillena, G.; Ramón, D. J.; Yus, M., Hydrogen Autotransfer in the N-Alkylation of Amines and Related Compounds using Alcohols and Amines as Electrophiles. *Chem. Rev.* **2010,** *110*, 1611-1641; (d) Yang, Q.; Wang, Q.; Yu, Z., Substitution of alcohols by N-nucleophiles via transition metal-catalyzed dehydrogenation. *Chem. Soc. Rev.* **2015,** *44*, 2305-2329.

119. (a) Yan, T.; Feringa, B. L.; Barta, K., Iron catalysed direct alkylation of amines with alcohols. *Nat. Commun.* **2014,** *5*, 5602; (b) Rösler, S.; Ertl, M.; Irrgang, T.; Kempe, R., Cobalt-Catalyzed Alkylation of Aromatic Amines by Alcohols. *Angew. Chem. Int. Ed.* **2015,** *54*, 15046-15050; (c) Mukherjee, A.; Nerush, A.; Leitus, G.; Shimon, L. J. W.; Ben David, Y.; Espinosa Jalapa, N. A.; Milstein, D., Manganese-Catalyzed Environmentally Benign Dehydrogenative Coupling of Alcohols and Amines to Form Aldimines and H_2: A Catalytic and Mechanistic Study. *J. Am. Chem. Soc.* **2016,** *138*, 4298-4301; (d) Vellakkaran, M.; Singh, K.; Banerjee, D., An Efficient and Selective Nickel-Catalyzed Direct N-Alkylation of Anilines with Alcohols. *ACS Catal.* **2017,** *7*, 8152-8158.

120. (a) Baxter, E. W.; Reitz, A. B., Reductive Aminations of Carbonyl Compounds with Borohydride and Borane Reducing Agents. In *Organic Reactions*, 2002; Vol. 59, p 1−715; (b) Gomez, S.; Peters, J. A.; Maschmeyer, T., The Reductive Amination of Aldehydes and Ketones and the Hydrogenation of Nitriles: Mechanistic Aspects and Selectivity Control. *Adv. Synth. Catal.* **2002,** *344*, 1037-1057; (c) P, T. R.; S, V. S.; Jyoti, P.; K., T. V., Recent Development on Catalytic Reductive Amination and Applications. *Curr. Org. Chem.* **2008,** *12*, 1093-1115.

121. (a) Hollmann, D.; Bähn, S.; Tillack, A.; Beller, M., A General Ruthenium-Catalyzed Synthesis of Aromatic Amines. *Angew. Chem. Int. Ed.* **2007,** *46*, 8291-8294; (b) Hollmann, D.; Bähn, S.; Tillack, A.; Beller, M., N-Dealkylation of aliphatic amines and selective synthesis of monoalkylated aryl amines. *Chem. Commun.* **2008**, 3199–3201.

122. Zhao, X.; Liu, D.; Guo, H.; Liu, Y.; Zhang, W., C–N Bond Cleavage of Allylic Amines via Hydrogen Bond Activation with Alcohol Solvents in Pd-Catalyzed Allylic Alkylation of Carbonyl Compounds. *J. Am. Chem. Soc.* **2011,** *133*, 19354-19357.

123. Wang, L.-M.; Kobayashi, K.; Arisawa, M.; Saito, S.; Naka, H., Pd/TiO_2-Photocatalyzed Self-Condensation of Primary Amines To Afford Secondary Amines at Ambient Temperature. *Org. Lett.* **2019,** *21*, 341-344.

124. Xi, Z.-W.; Yang, L.; Wang, D.-Y.; Pu, C.-D.; Shen, Y.-M.; Wu, C.-D.; Peng, X.-G., Visible-Light Photocatalytic Synthesis of Amines from Imines via Transfer Hydrogenation Using Quantum Dots as Catalysts. *J. Org. Chem.* **2018,** *83*, 11886-11895.

125. (a) Yi, C. S.; Zeczycki, T. N.; Guzei, I. A., Highly Cooperative Tetrametallic Ruthenium-μ-Oxo-μ-Hydroxo Catalyst for the Alcohol Oxidation Reaction. *Organometallics* **2006,** *25*, 1047-1051; (b) Yi, C. S.; Lee, D. W., Regioselective Intermolecular Coupling Reaction of Arylketones and Alkenes Involving C–H Bond Activation Catalyzed by an in Situ Formed Cationic Ruthenium Hydride Complex. *Organometallics* **2009,** *28*, 4266-4268; (c) Kwon, K.-H.; Lee, D. W.; Yi, C. S., Chelate-Assisted Oxidative Coupling Reaction of Arylamides and Unactivated Alkenes: Mechanistic Evidence for Vinyl C–H Bond Activation Promoted by an Electrophilic Ruthenium Hydride Catalyst. *Organometallics* **2010,** *29*, 5748-5750.

126. (a) Arachchige, P. T. K. Ruthenium Catalyzed Deaminative Coupling Reaction of Amines Via C-N Bond Activation. Marquette University, Milwaukee WI, 2017; (b) Arachchige, P. T. K.; Lee, H.; Yi, C. S., Synthesis of Symmetric and Unsymmetric Secondary Amines from the Ligand-Promoted Ruthenium-Catalyzed Deaminative Coupling Reaction of Primary Amines. *J. Org. Chem.* **2018,** *83*, 4932–4947.

127. (a) Singleton, D. A.; Thomas, A. A., High-Precision Simultaneous Determination of Multiple Small Kinetic Isotope Effects at Natural Abundance. *J. Am. Chem. Soc.* **1995,** *117*, 9357-9358; (b) Frantz, D. E.; Singleton, D. A.; Snyder, J. P., ^{13}C Kinetic Isotope Effects for the Addition of Lithium Dibutylcuprate to Cyclohexenone. Reductive Elimination Is Rate-Determining. *J. Am. Chem. Soc.* **1997,** *119*, 3383-3384; (c) Nowlan, D. T.; Gregg, T. M.; Davies, H. M. L.; Singleton, D. A., Isotope Effects and the Nature of Selectivity in Rhodium-Catalyzed Cyclopropanations. *J. Am. Chem. Soc.* **2003,** *125*, 15902-15911.

128. (a) Brown, R. S.; Ulan, J. G., Hydrolysis of imidazole-containing amide acetals. *J. Am. Chem. Soc.* **1983,** *105*, 2382-2388; (b) Manoharan, T. S.; Brown, R. S., 1-(1-Ethoxyethyl): an effective protecting group for imidazole nitrogen. *J. Org. Chem.* **1988,** *53*, 1107-1110; (c) Fast, W.; Wang, Z.; Benkovic, S. J., Familial Mutations and Zinc Stoichiometry Determine the Rate-Limiting Step of Nitrocefin Hydrolysis by Metallo-β-lactamase from Bacteroides fragilis. *Biochemistry* **2001,** *40*, 1640-1650; (d) Reyes, M. B.; Carpenter, B. K., Mechanism of Thermal Deazetization of 2,3-Diazabicyclo[2.2.1]hept-2-ene and Its Reaction Dynamics in Supercritical Fluids. *J. Am. Chem. Soc.* **2000,** *122*, 10163-10176.

129. Eubanks, J. R. I.; Sims, L. B.; Fry, A., Carbon isotope effect studies of the mechanism of the Hofmann elimination reaction of para-substituted (2-phenylethyl-1-14C)- and (2-phenylethyl-2-14C)-trimethylammonium bromides. *J. Am. Chem. Soc.* **1991,** *113* , 8821-8829.

130. Marlier, J. F.; Robins, L. I.; Tucker, K. A.; Rawlings, J.; Anderson, M. A.; Cleland, W. W., A Kinetic and Isotope Effect Investigation of the Urease-Catalyzed Hydrolysis of Hydroxyurea. *Biochemistry* **2010,** *49* , 8213-8219.

131. (a) Wu, J.-C.; Song, R.-J.; Wang, Z.-Q.; Huang, X.-C.; Xie, Y.-X.; Li, J.-H., Copper-Catalyzed C-H Oxidation/Cross-Coupling of α-Amino Carbonyl Compounds. *Angew. Chem. Int. Ed.* **2012,** *51*, 3453-3457; (b) Tian, J.-S.; Loh, T.-P., Copper-Catalyzed Rearrangement of Tertiary Amines through Oxidation of Aliphatic C-H Bonds

in Air or Oxygen: Direct Synthesis of α-Amino Acetals. *Angew. Chem. Int. Ed.* **2010,** *49*, 8417-8420; (c) Guo, S.; Qian, B.; Xie, Y.; Xia, C.; Huang, H., Copper-Catalyzed Oxidative Amination of Benzoxazoles via C−H and C−N Bond Activation: A New Strategy for Using Tertiary Amines as Nitrogen Group Sources. *Org. Lett.* **2011,** *13*, 522-525; (d) Wan, J.-P.; Zhou, Y.; Cao, S., Domino Reactions Involving the Branched C–N and C═C Cleavage of Enaminones Toward Pyridines Synthesis. *J. Org. Chem.* **2014,** *79*, 9872-9877.

132. (a) Theophanides, T.; Harvey, P. D., Structural and spectroscopic properties of metal-urea complexes. *Coord. Chem. Rev.* **1987,** *76*, 237-264; (b) Borovik, A. S., Bioinspired Hydrogen Bond Motifs in Ligand Design: The Role of Noncovalent Interactions in Metal Ion Mediated Activation of Dioxygen. *Acc. Chem. Res.* **2005,** *38*, 54-61; (c) Shao, J.-Y.; Gong, Z.-L.; Zhong, Y.-W., Bridged cyclometalated diruthenium complexes for fundamental electron transfer studies and multi-stage redox switching. *Dalton Trans.* **2018,** *47*, 23-29.

133. Jaber, M.; Robinson, S. W.; Missale, C.; Caron, M. G., Dopamine receptors and brain function. *Neuropharmacology* **1996,** *35*, 1503-1519.

134. (a) Mukaiyama, T.; Kobayashi, S., Tin(II) Enolates in the Aldol, Michael, and Related Reactions. In *Organic Reactions*, 1994; Vol. 46, pp 1-103; (b) Smith, M. B.; March, J., *Advanced Organic Chemistry: Reactions, Mechanisms and Structure*. Wiley-Interscience: New York, , 2007.

135. (a) Obora, Y., Recent Advances in α-Alkylation Reactions using Alcohols with Hydrogen Borrowing Methodologies. *ACS Catal.* **2014,** *4*, 3972-3981; (b) Zhang, Z.; Li, W.-D. Z.; Li, Y., Novel Approach for the Stereocontrolled Construction of Eudesmane Skeleton: A Concise Synthesis of (±)-Balanitol. *Org. Lett.* **2001,** *3*, 2555-2557; (c) Stork, G.; Niu, D.; Fujimoto, A.; Koft, E. R.; Balkovec, J. M.; Tata, J. R.; Dake, G. R., The First Stereoselective Total Synthesis of Quinine. *J. Am. Chem. Soc.* **2001,** *123*, 3239-3242; (d) Lim, H. N.; Xing, D.; Dong, G., Transition-Metal-Catalyzed Ketone α-Alkylation and Alkenylation with Simple Alkenes and Alkynes through a Dual Activation Strategy. *Synlett.* **2019,** *30*, 674-684.

136. (a) Larock, R. C., *Comprehensive Organic Transformations: A Guide to Functional Group Preparations*. Wiley: 1999; (b) Von Oettingen, W. F., *The halogenated hydrocarbons of industrial and toxicological importance*. Elsevier: Amsterdam, 1964.

137. (a) Stork, G.; Landesman, H. K., A New Alkylation of Carbonyl Compounds. *J. Am. Chem. Soc.* **1956,** *78* (19), 5128-5129; (b) Stork, G.; Terrell, R.; Szmuszkovicz, J., A New Synthesis of 2-Alkyl and 2-Acyl Ketones. *J. Am. Chem. Soc.* **1954,** *76*, 2029-2030; (c) Solomons, T. W. G.; Fryhle, C. B.; Snyder, S. A., *Organic chemistry*. 2014; (d) Stork, G.; Brizzolara, A.; Landesman, H.; Szmuszkovicz, J.; Terrell, R., The Enamine Alkylation and Acylation of Carbonyl Compounds. *J. Am. Chem. Soc.* **1963,** *85*, 207-222.

138. (a) Guillena, G.; Ramón, D. J.; Yus, M., Alcohols as Electrophiles in C–C Bond-Forming Reactions: The Hydrogen Autotransfer Process. *Angew. Chem. Int. Ed.* **2007,**

46, 2358-2364; (b) Chelucci, G., Ruthenium and osmium complexes in CC bond-forming reactions by borrowing hydrogen catalysis. *Coord. Chem. Rev.* **2017,** *331*, 1-36; (c) Huang, F.; Liu, Z.; Yu, Z., C-Alkylation of Ketones and Related Compounds by Alcohols: Transition-Metal-Catalyzed Dehydrogenation. *Angew. Chem. Int. Ed.* **2016,** *55*, 862-875.

139. (a) Elangovan, S.; Sortais, J.-B.; Beller, M.; Darcel, C., Iron-Catalyzed α-Alkylation of Ketones with Alcohols. *Angew. Chem. Int. Ed.* **2015,** *54*, 14483-14486; (b) Zhang, G.; Wu, J.; Zeng, H.; Zhang, S.; Yin, Z.; Zheng, S., Cobalt-Catalyzed α-Alkylation of Ketones with Primary Alcohols. *Org. Lett.* **2017,** *19*, 1080-1083; (c) Chakraborty, S.; Daw, P.; Ben David, Y.; Milstein, D., Manganese-Catalyzed α-Alkylation of Ketones, Esters, and Amides Using Alcohols. *ACS Catal.* **2018,** *8*, 10300-10305.

140. Smith, L. B.; Armstrong, R. J.; Matheau-Raven, D.; Donohoe, T. J., Chemo- and Regioselective Synthesis of Acyl-Cyclohexenes by a Tandem Acceptorless Dehydrogenation-[1,5]-Hydride Shift Cascade. *J. Am. Chem. Soc.* **2020,** *142*, 2514-2523.

141. Huang, Z.; Lim, H. N.; Mo, F.; Young, M. C.; Dong, G., Transition metal-catalyzed ketone-directed or mediated C–H functionalization. *Chem. Soc. Rev.* **2015,** *44*, 7764-7786.

142. (a) Pirnot, M. T.; Rankic, D. A.; Martin, D. B. C.; MacMillan, D. W. C., Photoredox Activation for the Direct β-Arylation of Ketones and Aldehydes. *Science* **2013,** *339*, 1593-1596; (b) Petronijević, F. R.; Nappi, M.; MacMillan, D. W. C., Direct β-Functionalization of Cyclic Ketones with Aryl Ketones via the Merger of Photoredox and Organocatalysis. *J. Am. Chem. Soc.* **2013,** *135*, 18323-18326.

143. Okada, M.; Fukuyama, T.; Yamada, K.; Ryu, I.; Ravelli, D.; Fagnoni, M., Sunlight photocatalyzed regioselective β-alkylation and acylation of cyclopentanones. *Chem. Sci.* **2014,** *5*, 2893-2898.

144. (a) Wang, X.; Pei, T.; Han, X.; Widenhoefer, R. A., Palladium-Catalyzed Intramolecular Hydroalkylation of Unactivated Olefins with Dialkyl Ketones. *Org. Lett.* **2003,** *5*, 2699-2701; (b) Qian, H.; Pei, T.; Widenhoefer, R. A., Development, Scope, and Mechanism of the Palladium-Catalyzed Intramolecular Hydroalkylation of 3-Butenyl β-Diketones. *Organometallics* **2005,** *24*, 287-301; (c) Xiao, Y.-P.; Liu, X.-Y.; Che, C.-M., Efficient Gold(I)-Catalyzed Direct Intramolecular Hydroalkylation of Unactivated Alkenes with α-Ketones. *Angew. Chem. Int. Ed.* **2011,** *50*, 4937-4941.

145. Mo, F.; Dong, G., Regioselective ketone α-alkylation with simple olefins via dual activation. *Science* **2014,** *345*, 68-72.

146. Klauck, F. J. R.; James, M. J.; Glorius, F., Deaminative Strategy for the Visible-Light-Mediated Generation of Alkyl Radicals. *Angew. Chem. Int. Ed.* **2017,** *56*, 12336-12339.

147. Sun, S.-Z.; Romano, C.; Martin, R., Site-Selective Catalytic Deaminative Alkylation of Unactivated Olefins. *J. Am. Chem. Soc.* **2019,** *141*, 16197-16201.

148. Fu, M.-C.; Shang, R.; Zhao, B.; Wang, B.; Fu, Y., Photocatalytic decarboxylative alkylations mediated by triphenylphosphine and sodium iodide. *Science* **2019,** *363*, 1429-1434.

149. Kirinde Arachchige, P. T.; Yi, C. S., Synthesis of Quinazoline and Quinazolinone Derivatives via Ligand-Promoted Ruthenium-Catalyzed Dehydrogenative and Deaminative Coupling Reaction of 2-Aminophenyl Ketones and 2-Aminobenzamides with Amines. *Org. Lett.* **2019,** *21*, 3337-3341.

150. (a) Ritleng, V.; Sirlin, C.; Pfeffer, M., Ru-, Rh-, and Pd-Catalyzed C−C Bond Formation Involving C−H Activation and Addition on Unsaturated Substrates: Reactions and Mechanistic Aspects. *Chem. Rev.* **2002,** *102*, 1731-1770; (b) Kakiuchi, F.; Kochi, T.; Mizushima, E.; Murai, S., Room-Temperature Regioselective C−H/Olefin Coupling of Aromatic Ketones Using an Activated Ruthenium Catalyst with a Carbonyl Ligand and Structural Elucidation of Key Intermediates. *J. Am. Chem. Soc.* **2010,** *132*, 17741-17750.

151. (a) Frantz, D. E.; Singleton, D. A., Isotope Effects and the Mechanism of Chlorotrimethylsilane-Mediated Addition of Cuprates to Enones. *J. Am. Chem. Soc.* **2000,** *122*, 3288-3295; (b) Singleton, D. A.; Wang, Z., Isotope Effects and the Nature of Enantioselectivity in the Shi Epoxidation. The Importance of Asynchronicity. *J. Am. Chem. Soc.* **2005,** *127*, 6679-6685; (c) Hirschi, J. S.; Takeya, T.; Hang, C.; Singleton, D. A., Transition-State Geometry Measurements from 13C Isotope Effects. The Experimental Transition State for the Epoxidation of Alkenes with Oxaziridines. *J. Am. Chem. Soc.* **2009,** *131*, 2397-2403.

152. (a) Leber, P. A.; Baldwin, J. E., Thermal [1,3] Carbon Sigmatropic Rearrangements of Vinylcyclobutanes. *Acc. Chem. Res.* **2002,** *35*, 279-287; (b) Baldwin, J. E.; Leber, P. A., Molecular rearrangements through thermal [1,3] carbon shifts. *Org. Biomol. Chem.* **2008,** *6*, 36-47.

153. (a) Marion, N.; Nolan, S. P., Propargylic Esters in Gold Catalysis: Access to Diversity. *Angew. Chem. Int. Ed.* **2007,** *46* (16), 2750-2752; (b) Rao, W.; Susanti, D.; Chan, P. W. H., Gold-Catalyzed Tandem 1,3-Migration/[2 + 2] Cycloaddition of 1,7-Enyne Benzoates to Azabicyclo[4.2.0]oct-5-enes. *J. Am. Chem. Soc.* **2011,** *133*, 15248-15251; (c) Chen, C.; Zou, Y.; Chen, X.; Zhang, X.; Rao, W.; Chan, P. W. H., Gold-Catalyzed Tandem 1,3-Migration/Double Cyclopropanation of 1-Ene-4,n-diyne Esters to Tetracyclodecene and Tetracycloundecene Derivatives. *Org. Lett.* **2016,** *18*, 4730-4733; (d) Ren, Y.; Lin, Z., Theoretical Studies on Rh-Catalyzed Cycloisomerization of Homopropargylallene-Alkynes through C(sp3)–C(sp) Bond Activation. *ACS Catal.* **2020,** *10*, 1828-1837.

154. (a) Grigg, R. D.; Van Hoveln, R.; Schomaker, J. M., Copper-Catalyzed Recycling of Halogen Activating Groups via 1,3-Halogen Migration. *J. Am. Chem. Soc.* **2012,** *134*, 16131-16134; (b) Kazem Shiroodi, R.; Dudnik, A. S.; Gevorgyan, V., Stereocontrolled 1,3-Phosphatyloxy and 1,3-Halogen Migration Relay toward Highly Functionalized 1,3-Dienes. *J. Am. Chem. Soc.* **2012,** *134*, 6928-6931; (c) Van Hoveln, R. J.; Schmid, S. C.; Tretbar, M.; Buttke, C. T.; Schomaker, J. M., Formal asymmetric hydrobromination of styrenes via copper-catalyzed 1,3-halogen migration. *Chem. Sci.* **2014,** *5*, 4763-4767; (d)

Van Hoveln, R.; Hudson, B. M.; Wedler, H. B.; Bates, D. M.; Le Gros, G.; Tantillo, D. J.; Schomaker, J. M., Mechanistic Studies of Copper(I)-Catalyzed 1,3-Halogen Migration. *J. Am. Chem. Soc.* **2015,** *137*, 5346-5354.

155. (a) Khan, I.; Ibrar, A.; Ahmed, W.; Saeed, A., Synthetic approaches, functionalization and therapeutic potential of quinazoline and quinazolinone skeletons: The advances continue. *Eur. J. Med. Chem.* **2015,** *90*, 124-169; (b) Gupta, T.; Rohilla, A.; Pathak, A.; Akhtar, M. J.; Haider, M. R.; Yar, M. S., Current perspectives on quinazolines with potent biological activities: A review. *Synth. Commun.* **2018,** *48*, 1099-1127.

156. (a) Akduman, B.; Crawford, E. D., Terazosin, doxazosin, and prazosin: current clinical experience. *Urology* **2001,** *58*, 49-54; (b) McConnell, J. D.; Roehrborn, C. G.; Bautista, O. M.; Andriole, G. L.; Dixon, C. M.; Kusek, J. W.; Lepor, H.; McVary, K. T.; Nyberg, L. M.; Clarke, H. S.; Crawford, E. D.; Diokno, A.; Foley, J. P.; Foster, H. E.; Jacobs, S. C.; Kaplan, S. A.; Kreder, K. J.; Lieber, M. M.; Lucia, M. S.; Miller, G. J.; Menon, M.; Milam, D. F.; Ramsdell, J. W.; Schenkman, N. S.; Slawin, K. M.; Smith, J. A., The Long-Term Effect of Doxazosin, Finasteride, and Combination Therapy on the Clinical Progression of Benign Prostatic Hyperplasia. *N. Engl. J. Med.* **2003,** *349*, 2387-2398.

157. (a) Pao, W.; Miller, V. A., Epidermal Growth Factor Receptor Mutations, Small-Molecule Kinase Inhibitors, and Non–Small-Cell Lung Cancer: Current Knowledge and Future Directions. *J. Clin. Oncol.* **2005,** *23*, 2556-2568; (b) Miller, V. A.; Kris, M. G.; Shah, N.; Patel, J.; Azzoli, C.; Gomez, J.; Krug, L. M.; Pao, W.; Rizvi, N.; Pizzo, B.; Tyson, L.; Venkatraman, E.; Ben-Porat, L.; Memoli, N.; Zakowski, M.; Rusch, V.; Heelan, R. T., Bronchioloalveolar Pathologic Subtype and Smoking History Predict Sensitivity to Gefitinib in Advanced Non–Small-Cell Lung Cancer. *J. Clin. Oncol.* **2004,** *22*, 1103-1109.

158. (a) Geyer, C. E.; Forster, J.; Lindquist, D.; Chan, S.; Romieu, C. G.; Pienkowski, T.; Jagiello-Gruszfeld, A.; Crown, J.; Chan, A.; Kaufman, B.; Skarlos, D.; Campone, M.; Davidson, N.; Berger, M.; Oliva, C.; Rubin, S. D.; Stein, S.; Cameron, D., Lapatinib plus Capecitabine for HER2-Positive Advanced Breast Cancer. *N. Engl. J. Med.* **2006,** *355*, 2733-2743; (b) Johnston, S.; Pippen, J.; Pivot, X.; Lichinitser, M.; Sadeghi, S.; Dieras, V.; Gomez, H. L.; Romieu, G.; Manikhas, A.; Kennedy, M. J.; Press, M. F.; Maltzman, J.; Florance, A.; O'Rourke, L.; Oliva, C.; Stein, S.; Pegram, M., Lapatinib Combined With Letrozole Versus Letrozole and Placebo As First-Line Therapy for Postmenopausal Hormone Receptor–Positive Metastatic Breast Cancer. *J. Clin. Oncol.* **2009,** *27*, 5538-5546.

159. (a) Amin, K. M.; Kamel, M. M.; Anwar, M. M.; Khedr, M.; Syam, Y. M., Synthesis, biological evaluation and molecular docking of novel series of spiro [(2H,3H) quinazoline-2,1′ - cyclohexan]-4(1H)- one derivatives as anti-inflammatory and analgesic agents. *Eur. J. Med. Chem.* **2010,** *45*, 2117-2131; (b) Furman, R. R.; Sharman, J. P.; Coutre, S. E.; Cheson, B. D.; Pagel, J. M.; Hillmen, P.; Barrientos, J. C.; Zelenetz, A. D.; Kipps, T. J.; Flinn, I.; Ghia, P.; Eradat, H.; Ervin, T.; Lamanna, N.; Coiffier, B.; Pettitt, A. R.; Ma, S.; Stilgenbauer, S.; Cramer, P.; Aiello, M.; Johnson, D. M.; Miller, L.

L.; Li, D.; Jahn, T. M.; Dansey, R. D.; Hallek, M.; O'Brien, S. M., Idelalisib and Rituximab in Relapsed Chronic Lymphocytic Leukemia. *N. Engl. J. Med.* **2014,** *370*, 997-1007; (c) Kshirsagar, U. A., Recent developments in the chemistry of quinazolinone alkaloids. *Org. Biomol. Chem.* **2015,** *13*, 9336-9352.

160. (a) Terrett, N. K.; Bell, A. S.; Brown, D.; Ellis, P., Sildenafil (VIAGRATM), a potent and selective inhibitor of type 5 cGMP phosphodiesterase with utility for the treatment of male erectile dysfunction. *Bioorg. Med. Chem. Lett.* **1996,** *6*, 1819-1824; (b) Goldstein, I.; Lue, T. F.; Padma-Nathan, H.; Rosen, R. C.; Steers, W. D.; Wicker, P. A., Oral Sildenafil in the Treatment of Erectile Dysfunction. *N. Engl. J. Med.* **1998,** *338*, 1397-1404.

161. (a) Connolly, D. J.; Cusack, D.; O'Sullivan, T. P.; Guiry, P. J., Synthesis of quinazolinones and quinazolines. *Tetrahedron* **2005,** *61*, 10153-10202; (b) Khan, I.; Ibrar, A.; Abbas, N.; Saeed, A., Recent advances in the structural library of functionalized quinazoline and quinazolinone scaffolds: Synthetic approaches and multifarious applications. *Eur. J. Med. Chem.* **2014,** *76*, 193-244.

162. Fang, J.; Zhou, J.; Fang, Z., Synthesis of 2-substituted quinazolines via iridium catalysis. *RSC Adv.* **2013,** *3*, 334-336.

163. Qiu, G.; Lu, Y.; Wu, J., A concise synthesis of 4-imino-3,4-dihydroquinazolin-2-ylphosphonates via a palladium-catalyzed reaction of carbodiimide, isocyanide, and phosphite. *Org. Biomol. Chem.* **2013,** *11*, 798-802.

164. (a) Liu, X.; Fu, H.; Jiang, Y.; Zhao, Y., A Simple and Efficient Approach to Quinazolinones under Mild Copper-Catalyzed Conditions. *Angew. Chem. Int. Ed.* **2009,** *48*, 348-351; (b) Wang, C.; Li, S.; Liu, H.; Jiang, Y.; Fu, H., Copper-Catalyzed Synthesis of Quinazoline Derivatives via Ullmann-Type Coupling and Aerobic Oxidation. *J. Org. Chem.* **2010,** *75*, 7936-7938; (c) Xu, W.; Jin, Y.; Liu, H.; Jiang, Y.; Fu; Hua, Copper-Catalyzed Domino Synthesis of Quinazolinones via Ullmann-Type Coupling and Aerobic Oxidative C−H Amidation. *Org. Lett.* **2011,** *13*, 1274-1277; (d) Malakar, C. C.; Baskakova, A.; Conrad, J.; Beifuss, U., Copper-Catalyzed Synthesis of Quinazolines in Water Starting from o-Bromobenzylbromides and Benzamidines. *Chem. – A Eur. J.* **2012,** *18*, 8882-8885; (e) Omar, M. A.; Conrad, J.; Beifuss, U., Copper-catalyzed domino reaction between 1-(2-halophenyl)methanamines and amidines or imidates for the synthesis of 2-substituted quinazolines. *Tetrahedron* **2014,** *70*, 3061-3072.

165. (a) Han, B.; Yang, X.-L.; Wang, C.; Bai, Y.-W.; Pan, T.-C.; Chen, X.; Yu, W., CuCl/DABCO/4-HO-TEMPO-Catalyzed Aerobic Oxidative Synthesis of 2-Substituted Quinazolines and 4H-3,1-Benzoxazines. *J. Org. Chem.* **2012,** *77*, 1136-1142; (b) Chen, Z.; Chen, J.; Liu, M.; Ding, J.; Gao, W.; Huang, X.; Wu, H., Unexpected Copper-Catalyzed Cascade Synthesis of Quinazoline Derivatives. *J. Org. Chem.* **2013,** *78*, 11342-11348; (c) Liu, Q.; Zhao, Y.; Fu, H.; Cheng, C., Copper-Catalyzed Sequential N-Arylation and Aerobic Oxidation: Synthesis of Quinazoline Derivatives. *Synlett* **2013,** *24*, 2089-2094; (d) Wang, X.; He, D.; Huang, Y.; Fan, Q.; Wu, W.; Jiang, H., Copper-Catalyzed Synthesis of Substituted Quinazolines from Benzonitriles and 2-

Ethynylanilines via Carbon–Carbon Bond Cleavage Using Molecular Oxygen. *J. Org. Chem.* **2018,** *83*, 5458-5466.

166. (a) Wiedemann, S. H.; Ellman, J. A.; Bergman, R. G., Rhodium-Catalyzed Direct C−H Addition of 3,4-Dihydroquinazolines to Alkenes and Their Use in the Total Synthesis of Vasicoline. *J. Org. Chem.* **2006,** *71*, 1969-1976; (b) Mohammed, S.; Vishwakarma, R. A.; Bharate, S. B., Iodine Catalyzed Oxidative Synthesis of Quinazolin-4(3H)-ones and Pyrazolo[4,3-d]pyrimidin-7(6H)-ones via Amination of sp3 C–H Bond. *J. Org. Chem.* **2015,** *80*, 6915-6921; (c) Wang, X.; Jiao, N., Rh- and Cu-Cocatalyzed Aerobic Oxidative Approach to Quinazolines via [4 + 2] C–H Annulation with Alkyl Azides. *Org. Lett.* **2016,** *18*, 2150-2153; (d) Gutiérrez-Bonet, Á.; Remeur, C.; Matsui, J. K.; Molander, G. A., Late-Stage C–H Alkylation of Heterocycles and 1,4-Quinones via Oxidative Homolysis of 1,4-Dihydropyridines. *J. Am. Chem. Soc.* **2017,** *139*, 12251-12258.

167. Liang, Y.; Tan, Z.; Jiang, H.; Zhu, Z.; Zhang, M., Copper-Catalyzed Oxidative Multicomponent Annulation Reaction for Direct Synthesis of Quinazolinones via an Imine-Protection Strategy. *Org. Lett.* **2019,** *21*, 4725-4728.

168. Dömling, A.; Wang, W.; Wang, K., Chemistry and Biology Of Multicomponent Reactions. *Chem. Rev.* **2012,** *112*, 3083-3135.

169. (a) Chen, X.-W.; Zhao, H.; Chen, C.-L.; Jiang, H.-F.; Zhang, M., Hydrogen-Transfer-Mediated α-Functionalization of 1,8-Naphthyridines by a Strategy Overcoming the Over-Hydrogenation Barrier. *Angew. Chem. Int. Ed.* **2017,** *56*, 14232-14236; (b) Chen, X.; Zhao, H.; Chen, C.; Jiang, H.; Zhang, M., Transfer hydrogenative para-selective aminoalkylation of aniline derivatives with N-heteroarenes via ruthenium/acid dual catalysis. *Catal. Commun.* **2018,** *54*, 9087-9090.

170. Liang, T.; Tan, Z.; Zhao, H.; Chen, X.; Jiang, H.; Zhang, M., Aerobic Copper-Catalyzed Synthesis of Benzimidazoles from Diaryl- and Alkylamines via Tandem Triple C–H Aminations. *ACS Catal.* **2018,** *8*, 2242-2246.

171. Xie, H.; Liao, Y.; Chen, S.; Chen, Y.; Deng, G.-J., Copper-catalyzed efficient direct amidation of 2-methylquinolines with amines. *Org. Biomol. Chem.* **2015,** *13*, 6944-6948.

172. Chatterjee, T.; Kim, D. I.; Cho, E. J., Base-Promoted Synthesis of 2-Aryl Quinazolines from 2-Aminobenzylamines in Water. *J. Org. Chem.* **2018,** *83*, 7423-7430.

173. (a) Williamson, T. A., The chemistry of quinazoline. In *Chemistry of Heterocyclic Compounds*, Elderfield, R. C., Ed.; John Wiley & Sons: New York, 1957; Vol. 6, p 324−376; (b) Ferrini, S.; Ponticelli, F.; Taddei, M., Convenient Synthetic Approach to 2,4-Disubstituted Quinazolines. *Org. Lett.* **2007,** *9*, 69-72; (c) Hensbergen, A. W.; Mills, V. R.; Collins, I.; Jones, A. M., An expedient synthesis of oxazepino and oxazocino quinazolines. *Tetrahedron Lett.* **2015,** *56*, 6478-6483.

174. (a) Martins, M. A. P.; Frizzo, C. P.; Moreira, D. N.; Buriol, L.; Machado, P., Solvent-Free Heterocyclic Synthesis. *Chem. Rev.* **2009,** *109*, 4140-4182; (b) Candeias, N.

R.; Branco, L. C.; Gois, P. M. P.; Afonso, C. A. M.; Trindade, A. F., More Sustainable Approaches for the Synthesis of N-Based Heterocycles. *Chem. Rev.* **2009,** *109*, 2703-2802.

175. (a) Xu, L.; Jiang, Y.; Ma, D., Synthesis of 3-Substituted and 2,3-Disubstituted Quinazolinones via Cu-Catalyzed Aryl Amidation. *Org. Lett.* **2012,** *14*, 1150-1153; (b) Wei, H.; Li, T.; Zhou, Y.; Zhou, L.; Zeng, Q., Copper-Catalyzed Domino Synthesis of Quinazolin-4(3H)-ones from (Hetero)arylmethyl Halides, Bromoacetate, and Cinnamyl Bromide. *Synthesis* **2013,** *45*, 3349-3354; (c) Li, F.; Lu, L.; Liu, P., Acceptorless Dehydrogenative Coupling of o-Aminobenzamides with the Activation of Methanol as a C1 Source for the Construction of Quinazolinones. *Org. Lett.* **2016,** *18*, 2580-2583; (d) Upadhyaya, K.; Thakur, R. K.; Shukla, S. K.; Tripathi, R. P., One-Pot Copper(I)-Catalyzed Ligand/Base-Free Tandem Cyclooxidative Synthesis of Quinazolinones. *J. Org. Chem.* **2016,** *81*, 5046-5055.

176. (a) Hakim Siddiki, S. M. A.; Kon, K.; Touchy, A. S.; Shimizu, K.-i., Direct synthesis of quinazolinones by acceptorless dehydrogenative coupling of o-aminobenzamide and alcohols by heterogeneous Pt catalysts. *Catal. Sci. Technol.* **2014,** *4*, 1716-1719; (b) Zhang, W.; Meng, C.; Liu, Y.; Tang, Y.; Li, F., Auto-Tandem Catalysis with Ruthenium: From o-Aminobenzamides and Allylic Alcohols to Quinazolinones via Redox Isomerization/Acceptorless Dehydrogenation. *Adv. Synth. Catal.* **2018,** *360*, 3751-3759.

177. (a) Jiang, X.; Tang, T.; Wang, J.-M.; Chen, Z.; Zhu, Y.-M.; Ji, S.-J., Palladium-Catalyzed One-Pot Synthesis of Quinazolinones via tert-Butyl Isocyanide Insertion. *J. Org. Chem.* **2014,** *79*, 5082-5087; (b) Qian, C.; Liu, K.; Tao, S.-W.; Zhang, F.-L.; Zhu, Y.-M.; Yang, S.-L., Palladium-Catalyzed Oxidative Three-Component Coupling of Anthranilamides with Isocyanides and Arylboronic Acids: Access to 2,3-Disubstituted Quinazolinones. *J. Org. Chem.* **2018,** *83*, 9201-9209.

178. Bhargava Reddy, M.; Prasanth, K.; Anandhan, R., Visible-light induced copper(i)-catalyzed oxidative cyclization of o-aminobenzamides with methanol and ethanol via HAT. *Org. Biomol. Chem.* **2020,** *18*, 9601-9605.

179. Tian, Q.; Zhang, J.; Xu, L.; Wei, Y., Synthesis of quinazolin-4(3H)-ones via electrochemical decarboxylative cyclization of α-keto acids with 2-aminobenzamides. *Molecular Catal.* **2021,** *500*, 111345.

180. Kalutharage, N.; Yi, C. S., Chemoselective Formation of Unsymmetrically Substituted Ethers from Catalytic Reductive Coupling of Aldehydes and Ketones with Alcohols in Aqueous Solution. *Org. Lett.* **2015,** *17*, 1778-1781.

181. Yi, C. S.; Lee, D. W., Efficient Dehydrogenation of Amines and Carbonyl Compounds Catalyzed by a Tetranuclear Ruthenium-μ-oxo-μ-hydroxo-hydride Complex. *Organometallics* **2009,** *28*, 947-949.

182. Broere, D. L. J.; Plessius, R.; van der Vlugt, J. I., New avenues for ligand-mediated processes – expanding metal reactivity by the use of redox-active catechol, o-aminophenol and o-phenylenediamine ligands. *Chem. Soc. Rev.* **2015,** *44*, 6886-6915.

183. (a) Yeung, C. S.; Dong, V. M., Catalytic Dehydrogenative Cross-Coupling: Forming Carbon−Carbon Bonds by Oxidizing Two Carbon−Hydrogen Bonds. *Chem. Rev.* **2011,** *111* (3), 1215-1292; (b) Girard, S. A.; Knauber, T.; Li, C.-J., The Cross-Dehydrogenative Coupling of C–H Bonds: A Versatile Strategy for C–C Bond Formations. *Angew. Chem. Int. Ed.* **2014,** 53, 74-100.

184. Zhang, G.-F.; Zhang, S.; Pan, B.; Liu, X.; Feng, L.-S., 4-Quinolone derivatives and their activities against Gram positive pathogens. *Eur. J. Med. Chem.* **2018,** *143*, 710-723.

185. Lee, E.; Han, S.; Jin, G. H.; Lee, H. J.; Kim, W.-Y.; Ryu, J.-H.; Jeon, R., Synthesis and anticancer activity of aminodihydroquinoline analogs: Identification of novel proapoptotic agents. *Bioorg. Med. Chem. Lett.* **2013,** *23*, 3976-3978.

186. Insuasty, B.; Montoya, A.; Becerra, D.; Quiroga, J.; Abonia, R.; Robledo, S.; Vélez, I. D.; Upegui, Y.; Nogueras, M.; Cobo, J., Synthesis of novel analogs of 2-pyrazoline obtained from [(7-chloroquinolin-4-yl)amino]chalcones and hydrazine as potential antitumor and antimalarial agents. *Eur. J. Med. Chem.* **2013,** *67*, 252-262.

187. Sharma, R.; Kour, P.; Kumar, A., A review on transition-metal mediated synthesis of quinolines. *J. Chem. Sci.* **2018,** *130*, 73.

188. Kong, L.; Yu, S.; Zhou, X.; Li, X., Redox-Neutral Couplings between Amides and Alkynes via Cobalt(III)-Catalyzed C–H Activation. *Org. Lett.* **2016,** *18*, 588-591.

189. (a) Cho, C. S.; Oh, B. H.; Kim, J. S.; Kim, T.-J.; Shim, S. C., Synthesis of quinolines ruthenium-catalysed amine exchange reaction between anilines and trialkylamines. *Chem. Commun.* **2000**, 1885-1886; (b) Cho, C. S.; Kim, J. S.; Oh, B. H.; Kim, T.-J.; Shim, S. C.; Yoon, N. S., Ruthenium-Catalyzed Synthesis of Quinolines from Anilines and Allylammonium Chlorides in an Aqueous Medium via Amine Exchange Reaction. *Tetrahedron* **2000,** *56*, 7747-7750.

190. Aramoto, H.; Obora, Y.; Ishii, Y., N-Heterocyclization of Naphthylamines with 1,2- and 1,3-Diols Catalyzed by an Iridium Chloride/BINAP System. *J. Org. Chem.* **2009,** *74*, 628-633.

191. Vardhan Reddy, K. H.; Brion, J.-D.; Messaoudi, S.; Alami, M., Synthesis of Biheterocycles Based on Quinolinone, Chromone, and Coumarin Scaffolds by Palladium-Catalyzed Decarboxylative Couplings. *J. Org. Chem.* **2016,** *81*, 424-432.

192. Wu, G. Y., *Amino Acids :Biochemistry and Nutrition*. CRC Press: New York, 2013.

193. Conti, P.; Tamborini, L.; Pinto, A.; Blondel, A.; Minoprio, P.; Mozzarelli, A.; De Micheli, C., Drug Discovery Targeting Amino Acid Racemases. *Chem. Rev.* **2011,** *111*, 6919-6946.

194. (a) Notz, W.; Tanaka, F.; Barbas, C. F., Enamine-Based Organocatalysis with Proline and Diamines: The Development of Direct Catalytic Asymmetric Aldol,

Mannich, Michael, and Diels−Alder Reactions. *Acc. Chem. Res.* **2004,** *37* (8), 580-591; (b) Mukherjee, S.; Yang, J. W.; Hoffmann, S.; List, B., Asymmetric Enamine Catalysis. *Chem. Rev.* **2007,** *107*, 5471-5569.

195. Turner, N. J., Enantioselective Oxidation of C–O and C–N Bonds Using Oxidases. *Chem. Rev.* **2011,** *111*, 4073-4087.

196. Xiang, J.-C.; Wang, Z.-X.; Cheng, Y.; Xia, S.-Q.; Wang, M.; Tang, B.-C.; Wu, Y.-D.; Wu, A.-X., Divergent Synthesis of Functionalized Quinolines from Aniline and Two Distinct Amino Acids. *J. Org. Chem.* **2017,** *82*, 9210-9216.

197. Yang, D.; Zhao, D.; Mao, L.; Wang, L.; Wang, R., Copper/DIPEA-Catalyzed, Aldehyde-Induced Tandem Decarboxylation–Coupling of Natural α-Amino Acids and Phosphites or Secondary Phosphine Oxides. *J. Org. Chem.* **2011,** *76*, 6426-6431.

198. Zhang, W.; Wang, C.; Wang, Q., Copper-Catalyzed Decarboxylative Functionalization of Conjugated β,γ-Unsaturated Carboxylic Acids. *ACS Catal.* **2020,** *10*, 13179-13185.

199. Li, H.-H.; Li, J.-Q.; Zheng, X.; Huang, P.-Q., Photoredox-Catalyzed Decarboxylative Cross-Coupling of α-Amino Acids with Nitrones. *Org. Lett.* **2021,** *23*, 876-880.

200. Wen, H.; Ge, R.; Qu, Y.; Sun, J.; Shi, X.; Cui, W.; Yan, H.; Zhang, Q.; An, Y.; Su, W.; Yang, H.; Kuai, L.; Satz, A. L.; Peng, X., Synthesis of 1,2-Amino Alcohols by Photoredox-Mediated Decarboxylative Coupling of α-Amino Acids and DNA-Conjugated Carbonyls. *Org. Lett.* **2020,** *22*, 9484-9489.

201. Zhang, Z.; Qin, Z.; Chang, W.; Li, J.; Fan, R.; Wu, X.; Guo, R.; Xie, X.; Zhou, L., Nickel-Catalyzed Decarboxylative Cyclization of Isatoic Anhydrides with Carbodiimides: Synthesis of 2,3-Dihydroquinazolin-4(1H)-ones. *Adv. Synth. Catal.* **2020,** *362*, 2864-2869.

202. Yamaguchi, K.; Kawaguchi, S.-i.; Sonoda, M.; Tanimori, S.; Ogawa, A., Copper-catalyzed tandem reaction directed toward synthesis of 2,2-disubstituted quinazolinones from vinyl halides and 2-aminobenzamides. *Tetrahedron Lett.* **2017,** *58*, 4043-4047.

203. Dolomanov, O. V.; Bourhis, L. J.; Gildea, R. J.; Howard, J. A. K.; Puschmann, H., OLEX2: a complete structure solution, refinement and analysis program. *Journal of Applied Crystallography* **2009,** *42*, 339-341.

204. Bourhis, L. J.; Dolomanov, O. V.; Gildea, R. J.; Howard, J. A. K.; Puschmann, H., The anatomy of a comprehensive constrained, restrained refinement program for the modern computing environment - Olex2 dissected. *Acta Crystallographica Section A* **2015,** *71*, 59-75.

205. Sheldrick, G., SHELXT - Integrated space-group and crystal-structure determination. *Acta Crystallographica Section A* **2015,** *71*, 3-8.

206. Hamid, M. H. S. A.; Allen, C. L.; Lamb, G. W.; Maxwell, A. C.; Maytum, H. C.; Watson, A. J. A.; Williams, J. M. J., Ruthenium-Catalyzed N-Alkylation of Amines and Sulfonamides Using Borrowing Hydrogen Methodology. *J. Am. Chem. Soc.* **2009,** *131*, 1766-1774.

207. Shan, S. P.; Xiaoke, X.; Gnanaprakasam, B.; Dang, T. T.; Ramalingam, B.; Huynh, H. V.; Seayad, A. M., Benzimidazolin-2-ylidene N-heterocyclic carbene complexes of ruthenium as a simple catalyst for the N-alkylation of amines using alcohols and diols. *RSC Adv.* **2015,** *5*, 4434-4442.

208. Goriya, Y.; Kim, H. Y.; Oh, K., o-Naphthoquinone-Catalyzed Aerobic Oxidation of Amines to (Ket)imines: A Modular Catalyst Approach. *Org. Lett.* **2016,** *18*, 5174-5177.

209. Li, K.; Weber, A. E.; Tseng, L.; Malcolmson, S. J., Diastereoselective and Enantiospecific Synthesis of 1,3-Diamines via 2-Azaallyl Anion Benzylic Ring-Opening of Aziridines. *Org. Lett.* **2017,** *19*, 4239-4242.

210. B.;, J. A. M. J.; Peralta, J. E.; Bearpark, M.; Heyd, J. J.; Brothers, E.; Kudin, K. N.; Staroverov, V. N.; Kobayashi, R.; Normand, J.; Raghavachari, K.; Rendell, A.; Burant, J. C.; Iyengar, S. S.; Tomasi, J.; Cossi, M.; Rega, N.; Millam, J. M.; Klene, M.; Knox, J. E.; J. B. Cross V. B, F. O.; R., O. Y.; Cammi; Pomelli, C.; Ochterski, J. W.; Martin, R. L.; Morokuma, K.; Zakrzewski, V. G.; Voth, G. A.; Salvador, P.; Dannenberg, J. J.; Dapprich, S.; Daniels, A. D.; Farkas, O.; Foresman, J. B.; Ortiz, J. V.; Cioslowski, J.; Fox, D. J., Gaussian, Inc., A. J. A. Gaussian 16, Revision C.01.

211. Zhao, Y.; Truhlar, D. G., A new local density functional for main-group thermochemistry, transition metal bonding, thermochemical kinetics, and noncovalent interactions. *J. Chem. Phys.* **2006,** *125*, 194101.

212. Weigend, F.; Ahlrichs, R., Balanced basis sets of split valence, triple zeta valence and quadruple zeta valence quality for H to Rn: Design and assessment of accuracy. *Phy. Chem. Chem. Phys.* **2005,** *7*, 3297-3305.

213. Andrae, D.; Häußermann, U.; Dolg, M.; Stoll, H.; Preuß, H., Energy-adjustedab initio pseudopotentials for the second and third row transition elements. *Theoretica chimica acta* **1990,** *77*, 123-141.

214. (a) Cancès, E.; Mennucci, B.; Tomasi, J., A new integral equation formalism for the polarizable continuum model: Theoretical background and applications to isotropic and anisotropic dielectrics. *J. Chem. Phys.* **1997,** *107*, 3032-3041; (b) Tomasi, J.; Mennucci, B.; Cammi, R., Quantum Mechanical Continuum Solvation Models. *Chem. Rev.* **2005,** *105*, 2999-3094.

215. Bauernschmitt, R.; Ahlrichs, R., Stability analysis for solutions of the closed shell Kohn–Sham equation. *J. Chem. Phys.* **1996,** *104*, 9047-9052.

216. Fukui, K., The path of chemical reactions - the IRC approach. *Acc. Chem. Res.* **1981,** *14*, 363-368.

217. Portela-Cubillo, F.; Scott, J. S.; Walton, J. C., Microwave-Promoted Syntheses of Quinazolines and Dihydroquinazolines from 2-Aminoarylalkanone O-Phenyl Oximes. *J. Org. Chem.* **2009,** *74*, 4934-4942.

218. He, K.-H.; Tan, F.-F.; Zhou, C.-Z.; Zhou, G.-J.; Yang, X.-L.; Li, Y., Acceptorless Dehydrogenation of N-Heterocycles by Merging Visible-Light Photoredox Catalysis and Cobalt Catalysis. *Angew. Chem. Int. Ed.* **2017,** *56*, 3080-3084.

219. Jin, J.; MacMillan, D. W. C., Alcohols as alkylating agents in heteroarene C–H functionalization. *Nature* **2015,** *525*, 87-90.

220. (a) Youn, S. W.; Yoo, H. J.; Lee, E. M.; Lee, S. Y., Metal-Free One-Pot Synthesis of (Tetrahydro)Quinolines through Three-Component Assembly of Arenediazonium Salts, Nitriles, and Styrenes. *Adv. Synth. Catal.* **2018,** *360*, 278-283; (b) Wolf, C.; Ekoue-Kovi, K., Palladium-Catalyzed Suzuki–Miyaura Cross-Coupling Using Phosphinous Acids and Dialkyl(chloro)phosphane Ligands. *Eur. J. Org. Chem.* **2006,** *2006*, 1917-1925.

221. Prasan Ojha, D.; Ramaiah Prabhu, K., Pd-Catalyzed Cross-Coupling Reactions of Hydrazones: Regioselective Synthesis of Highly Branched Dienes. *J. Org. Chem.* **2013,** *78*, 12136-12143.

222. Ren, X.; Han, S.; Gao, X.; Li, J.; Zou, D.; Wu, Y.; Wu, Y., Direct arylation for the synthesis of 2-arylquinolines from N-methoxyquinoline-1-ium tetrafluoroborate salts and arylboronic acids. *Tetrahedron Lett.* **2018,** *59*, 1065-1068.

223. Xiao, F.; Chen, Y.; Liu, Y.; Wang, J., Sequential catalytic process: synthesis of quinoline derivatives by AuCl3/CuBr-catalyzed three-component reaction of aldehydes, amines, and alkynes. *Tetrahedron* **2008,** *64*, 2755-2761.

224. Martínez, R.; Ramón, D. J.; Yus, M., RuCl2(dmso)4 Catalyzes the Solvent-Free Indirect Friedländer Synthesis of Polysubstituted Quinolines from Alcohols. *Eur. J. Org. Chem.* **2007,** *2007*, 1599-1605.

225. Mohammadpoor-Baltork, I.; Tangestaninejad, S.; Moghadam, M.; Mirkhani, V.; Anvar, S.; Mirjafari, A., Microwave-Promoted Alkynylation-Cyclization of 2-Aminoaryl Ketones: A Green Strategy for the Synthesis of 2,4-Disubstituted Quinolines. *Synlett* **2010,** *2010*, 3104-3112.

226. Augustine, J. K.; Bombrun, A.; Venkatachaliah, S., An efficient catalytic method for the Friedländer annulation mediated by peptide coupling agent propylphosphonic anhydride (T3P®). *Tetrahedron Lett.* **2011,** *52*, 6814-6818.

227. Chen, X.; Qiu, S.; Wang, S.; Wang, H.; Zhai, H., Blue-light-promoted carbon–carbon double bond isomerization and its application in the syntheses of quinolines. *Org. Biomol. Chem.* **2017,** *15*, 6349-6352.

228. (a) Sénéchal-David, K.; Hemeryck, A.; Tancrez, N.; Toupet, L.; Williams, J. A. G.; Ledoux, I.; Zyss, J.; Boucekkine, A.; Guégan, J.-P.; Le Bozec, H.; Maury, O.,

Synthesis, Structural Studies, Theoretical Calculations, and Linear and Nonlinear Optical Properties of Terpyridyl Lanthanide Complexes: New Evidence for the Contribution of f Electrons to the NLO Activity. *J. Am. Chem. Soc.* **2006,** *128*, 12243-12255; (b) Fang, L.; Yu, J.; Liu, Y.; Wang, A.; Wang, L., Homogeneous catalysis, heterogeneous recycling: a new family of branched molecules with hydrocarbon or fluorocarbon chains for the Friedländer synthesis of quinoline under solvent-free conditions. *Tetrahedron* **2013,** *69*, 11004-11009.

229. Sridharan, V.; Ribelles, P.; Ramos, M. T.; Menéndez, J. C., Cerium(IV) Ammonium Nitrate Is an Excellent, General Catalyst for the Friedländer and Friedländer−Borsche Quinoline Syntheses: Very Efficient Access to the Antitumor Alkaloid Luotonin A. *J. Org. Chem.* **2009,** *74*, 5715-5718.

230. Palimkar, S. S.; Siddiqui, S. A.; Daniel, T.; Lahoti, R. J.; Srinivasan, K. V., Ionic Liquid-Promoted Regiospecific Friedlander Annulation: Novel Synthesis of Quinolines and Fused Polycyclic Quinolines. *J. Org. Chem.* **2003,** *68*, 9371-9378.

231. Muscia, G. C.; Bollini, M.; Carnevale, J. P.; Bruno, A. M.; Asís, S. E., Microwave-assisted Friedländer synthesis of quinolines derivatives as potential antiparasitic agents. *Tetrahedron Lett.* **2006,** *47*, 8811-8815.

232. Korivi, R. P.; Cheng, C.-H., Nickel-Catalyzed Cyclization of 2-Iodoanilines with Aroylalkynes: An Efficient Route for Quinoline Derivatives. *J. Org. Chem.* **2006,** *71*, 7079-7082.

233. Saunthwal, R. K.; Patel, M.; Verma, A. K., Metal- and Protection-Free [4 + 2] Cycloadditions of Alkynes with Azadienes: Assembly of Functionalized Quinolines. *Org. Lett.* **2016,** *18*, 2200-2203.

234. Kumar, G. S.; Kumar, P.; Kapur, M., Traceless Directing-Group Strategy in the Ru-Catalyzed, Formal [3 + 3] Annulation of Anilines with Allyl Alcohols: A One-Pot, Domino Approach for the Synthesis of Quinolines. *Org. Lett.* **2017,** *19*, 2494-2497.

235. Stopka, T.; Niggemann, M., Metal free carboamination of internal alkynes – an easy access to polysubstituted quinolines. *Chem. Commun.* **2016,** *52*, 5761-5764.

236. Lewis, J. C.; Bergman, R. G.; Ellman, J. A., Rh(I)-Catalyzed Alkylation of Quinolines and Pyridines via C−H Bond Activation. *J. Am. Chem. Soc.* **2007,** *129*, 5332-5333.

237. Zhang, L.; Liu, Z.-Q., Molecular Oxygen-Mediated Minisci-Type Radical Alkylation of Heteroarenes with Boronic Acids. *Org. Lett.* **2017,** *19*, 6594-6597.

238. Das, S.; Santra, S.; Jana, S.; Zyryanov, G. V.; Majee, A.; Hajra, A., The Remarkable Cooperative Effect of a Brønsted-Acidic Ionic Liquid in the Cyclization of 2-Aminobenzamides with Ketones. *Eur. J. Org. Chem.* **2017,** *2017*, 4955-4962.

239. Hu, B.-Q.; Wang, L.-X.; Yang, L.; Xiang, J.-F.; Tang, Y.-L., Copper-Catalyzed Intramolecular C–C Bond Cleavage To Construct 2-Substituted Quinazolinones. *Eur. J. Org. Chem.* **2015,** *2015*, 4504-4509.

240. Wang, X.-S.; Yang, K.; Zhou, J.; Tu, S.-J., Facile Method for the Combinatorial Synthesis of 2,2-Disubstituted Quinazolin-4(1H)-one Derivatives Catalyzed by Iodine in Ionic Liquids. *J. Comb. Chem.* **2010,** *12*, 417-421.

241. Patil, N. T.; Lakshmi, P. G. V. V.; Singh, V., AuI-Catalyzed Direct Hydroamination/Hydroarylation and Double Hydroamination of Terminal Alkynes. *Eur. J. Org. Chem.* **2010,** *2010*, 4719-4731.

242. Luo, Y.; Wu, Y.; Wang, Y.; Sun, H.; Xie, Z.; Zhang, W.; Gao, Z., Ethanol promoted titanocene Lewis acid catalyzed synthesis of quinazoline derivatives. *RSC Adv.* **2016,** *6*, 66074-66077.

243. Revathy, K.; Lalitha, A., p-TSA-catalyzed synthesis of spiroquinazolinones. *J. Iran. Chem. Soc.* **2015,** *12*, 2045-2049.

244. Rambabu, D.; Kiran Kumar, S.; Yogi Sreenivas, B.; Sandra, S.; Kandale, A.; Misra, P.; Basaveswara Rao, M. V.; Pal, M., Ultrasound-based approach to spiro-2,3-dihydroquinazolin-4(1H)-ones: their in vitro evaluation against chorismate mutase. *Tetrahedron Lett.* **2013,** *54*, 495-501.

245. Hameed, A.; Zehra, S. T.; Shah, S. J. A.; Khan, K. M.; Alharthy, R. D.; Furtmann, N.; Bajorath, J.; Tahir, M. N.; Iqbal, J., Syntheses, Cholinesterases Inhibition, and Molecular Docking Studies of Pyrido[2,3-b]pyrazine Derivatives. *Chem. Biol. Drug Des.* **2015,** *86*, 1115-1120.

246. Bahuguna, A.; Sharma, R.; Sagara, P. S.; Ravikumar, P. C. Exploration of Aberrant Behaviour of Grignard Reagents with Indole-3-carboxaldehyde: Application to the Synthesis of Turbomycin B and Vibrindole A Derivatives. *Synlett* **2017**, *28*, 117-121.

8.0 ANNEX

8.1 Future Directions

We have been able to demonstrate the ligand enabled catalytic protocol for deaminative coupling reactions of amines to generate number of synthetically and pharmaceutically useful scaffolds. Also, we observed the following set of new coupling reactions which are potentially developed in the future.

8.1.1 Synthesis of Quinolones

We recently observed a new deaminative and dehydrative cyclization reaction to produce Quinolone derivatives of amino ketones with amines.

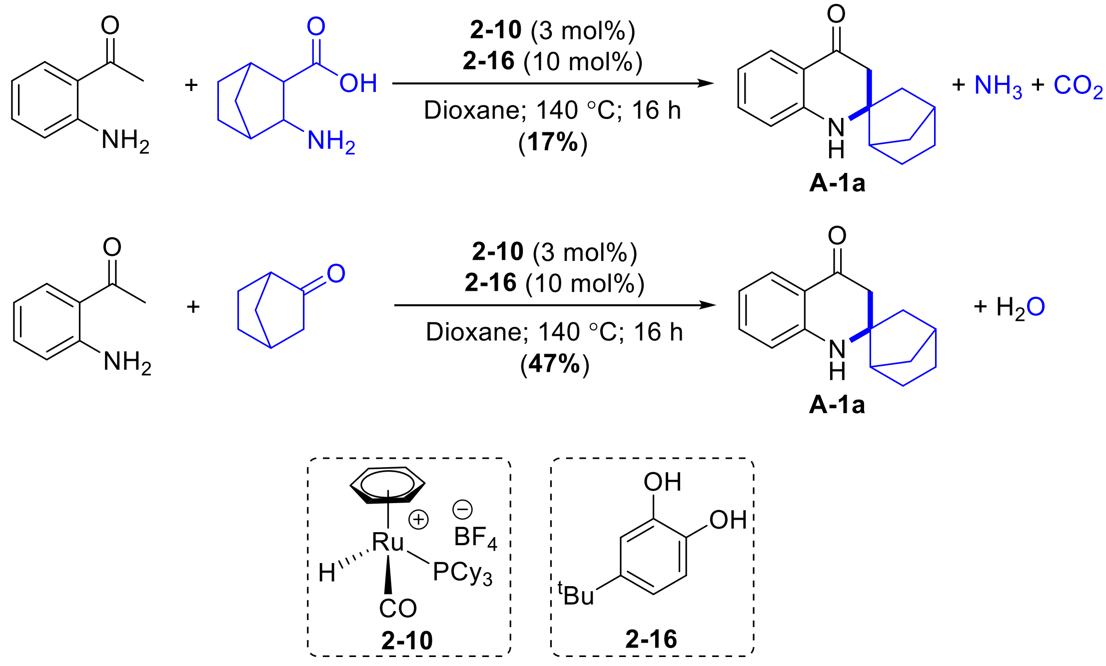

Characterization of the Quinolone Products

A 1,4-dioxane (2.0 mL) solution of complex **2-10** (9 mg, 3 mol %), **2-16** (8 mg, 10 mol %), 2-aminophenylethanone (68 mg, 0.5 mmol), and 2-Norbornanone (56 mg, 0.5 mmol) was stirred at 140 °C for 20 h. The product **4-12p** was isolated by column chromatography on silica gel (hexanes/EtOAc = 50:1–10:1; Yield = 53 mg (47%).

NMR data for 1'H-spiro[bicyclo[2.2.1]heptane-2,2'-quinolin]-4'(3'H)-one (A-1a): ^{1}H NMR (400 MHz, $CDCl_3$) δ 7.78 (dd, *J* = 7.9, 1.6 Hz, 1H), 7.27 (dd, *J* = 7.6, 1.6 Hz, 1H), 6.68 (td, *J* = 7.5, 1.0 Hz, 1H), 6.63 (d, *J* = 8.3 Hz, 1H), 4.39 (brs, 1H), 2.68 (s, 2H), 2.40 (s, 1H), 2.26 (s, 1H), 1.79–1.72 (m, 1H), 1.68–1.51 (m, 3H), 1.45–1.36 (m, 1H), 1.32–1.21 (m, 3H) ppm; ^{13}C{^{1}H} NMR (100 MHz, $CDCl_3$) δ 194.2, 150.8, 135.3, 127.3, 119.0, 117.5, 115.6, 62.1, 49.8, 45.9, 42.5, 37.0, 36.5, 28.3, 22.8 ppm; GC-MS for $C_{15}H_{17}NO$, m/z = 227 (M^+). HRMS (ESI-TOF) m/z: $[M + H]^+$ Calcd for $C_{15}H_{17}NOH$ 228.1383, Found 228.1358.

X-ray Crystallographic Data for the Product A-1a:

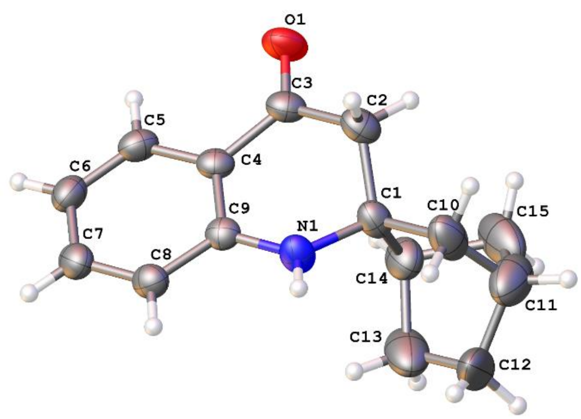

Molecular Structure of **A-1a**

Experimental Features: Pale-yellow needles. The dataset was collected at 100K with an Oxford SuperNova diffractometer using Cu(Kα) radiation.

Structure Description: The centrosymmetric crystal contains a racemic mixture of RRS and SSR diastereomers (RRS is shown on the picture). The dihydropyridine ring has a sofa conformation with the spiro-carbon C1 deviating from the rest. However, the sofa is distorted toward C1,C2-half-chair (C1 deviates by 0.484 Å and C2 deviates by -0.231 Å from the plane of the remaining 4 atoms). The norbornane moiety is disordered. The nature of the disorder is unclear. One of possibilities is a ~20% impurity of a rearranged by-product.

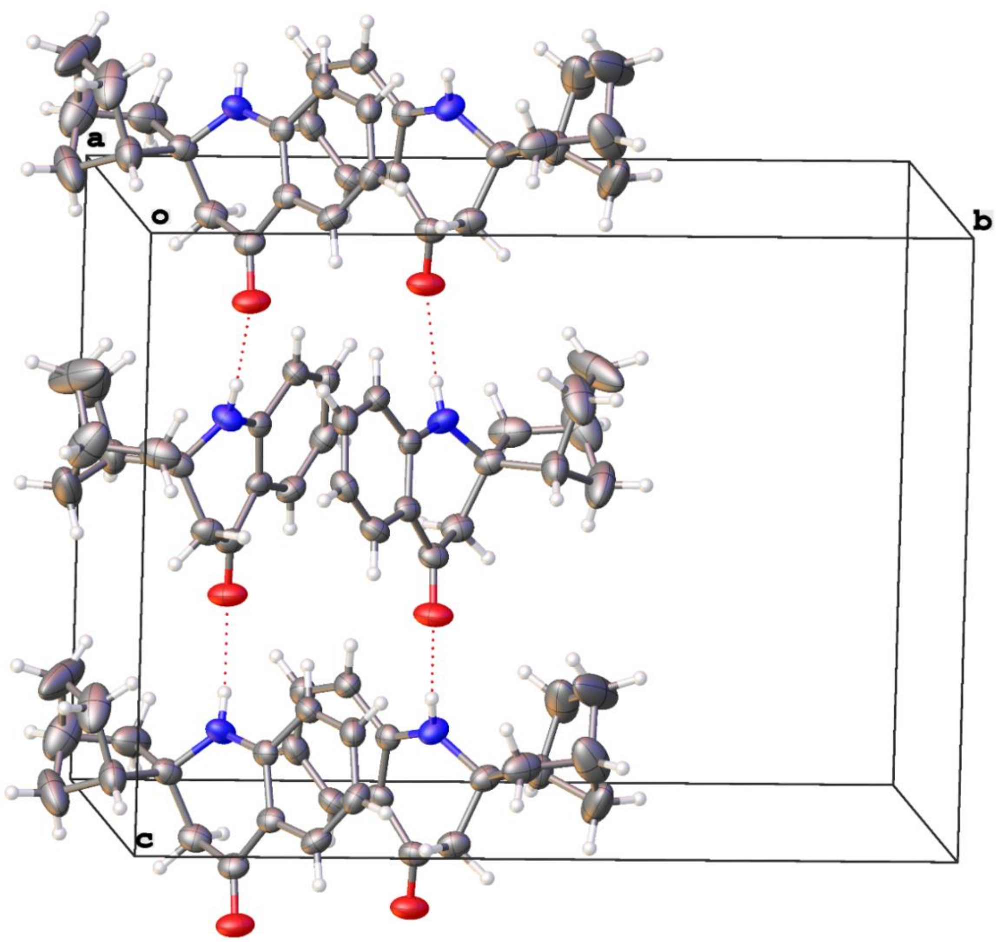

Crystal Packing of A-1a: The molecules form H-bonded chains along z axis.

Table A.1 Crystal data and structure refinement for A-1a.

Identification code	yi4a
Empirical formula	$C_{15}H_{17}NO$
Formula weight	227.29
Temperature/K	101(2)
Crystal system	orthorhombic
Space group	Pccn
a/Å	10.72779(14)
b/Å	17.0827(3)
c/Å	12.9832(2)
α/°	90
β/°	90
γ/°	90
Volume/Å^3	2379.29(6)
Z	8
ρ_{calc}g/cm^3	1.269
μ/mm^{-1}	0.618
F(000)	976.0
Crystal size/mm^3	0.441 × 0.057 × 0.042
Radiation	CuKα (λ = 1.54184)
2Θ range for data collection/°	9.736 to 141.376
Index ranges	$-13 \leq h \leq 12$, $-20 \leq k \leq 20$, $-11 \leq l \leq 15$
Reflections collected	11454
Independent reflections	2249 [R_{int} = 0.0178, R_{sigma} = 0.0114]
Data/restraints/parameters	2249/0/154
Goodness-of-fit on F^2	1.076
Final R indexes [I>=2σ (I)]	R_1 = 0.0830, wR_2 = 0.2083
Final R indexes [all data]	R_1 = 0.0875, wR_2 = 0.2120
Largest diff. peak/hole / e Å^{-3}	1.00/-0.46

Synthesis of A-1b;

(1R,2R,3S,4S)-3-chloro-1'H-spiro[bicyclo[2.2.1]heptane-2,2'-quinolin]-4'(3'H)-one

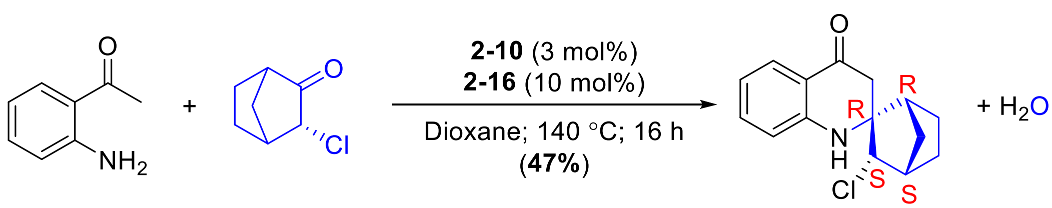

A-1b

X-ray Crystallographic Data for the Product A-1b:

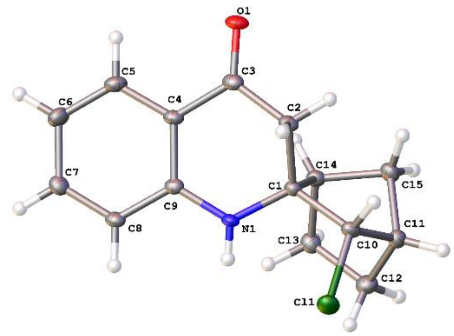

Molecular Structure of **A-1b**

Experimental Features: Colorless thin needles. The dataset was collected at 100K with an Oxford SuperNova diffractometer using Cu(Kα) radiation.

Structure Description: The molecule represents a diastereomer with Cl substituent in norbornane moiety oriented trans to its methylene bridge. The centrosymmetric crystals contain a racemic mixture of it. Interestingly, the imino group has a pyramidal configuration – its H atom deviates by 0.38 Å from the CNC plane.

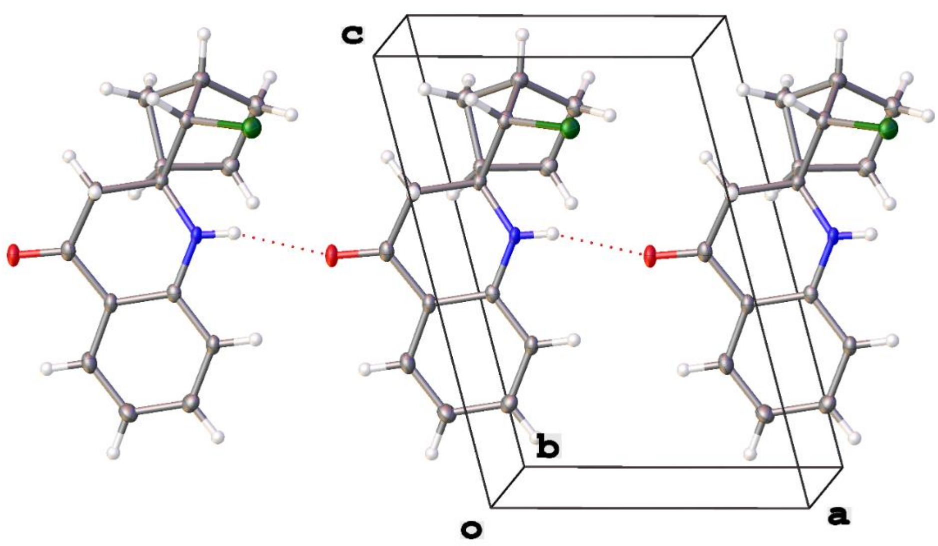

Crystal Packing of A-1b: In the crystal, the molecules form translational H-bonded chain along x axis.

Table A.2 Crystal data and structure refinement for yi4i.

Identification code	yi4i
Empirical formula	$C_{15}H_{16}ClNO$
Formula weight	261.74
Temperature/K	100.00(14)
Crystal system	monoclinic
Space group	$P2_1/c$
a/Å	6.92048(14)
b/Å	18.3728(3)
c/Å	10.1341(2)
α/°	90
β/°	104.567(2)
γ/°	90
Volume/Å^3	1247.11(4)
Z	4
ρ_{calc}g/cm^3	1.394
μ/mm^{-1}	2.590
F(000)	552.0
Crystal size/mm^3	0.465 × 0.042 × 0.018
Radiation	CuKα (λ = 1.54184)
2Θ range for data collection/°	9.628 to 141.19
Index ranges	$-8 \le h \le 8$, $-22 \le k \le 22$, $-12 \le l \le 12$
Reflections collected	11770
Independent reflections	2369 [R_{int} = 0.0280, R_{sigma} = 0.0190]
Data/restraints/parameters	2369/0/167
Goodness-of-fit on F^2	1.050
Final R indexes [I>=2σ (I)]	R_1 = 0.0370, wR_2 = 0.1003
Final R indexes [all data]	R_1 = 0.0402, wR_2 = 0.1037
Largest diff. peak/hole / e Å^{-3}	0.33/-0.33

8.1.2 Synthesis of Flavanones

To further extend the synthetic utility of ligand-promoted C–N bond coupling reactions, we have been exploring the coupling reactions of 2-hydroxoketones with primary amines which led to the formation of flavanone products **A-2**. Scope and mechanistic investigations are currently underway in our laboratory. A 1,4-dioxane (2.0 mL) solution of complex **2-10** (9 mg, 3 mol %), **2-12** (8 mg, 10 mol %), 2-hydroxyketone (0.5 mmol), and primary amine (0.5 mmol) was stirred at 120 °C for 20 h. The products were isolated by column chromatography on silica gel (hexanes/EtOAc = 100:1–10:1).

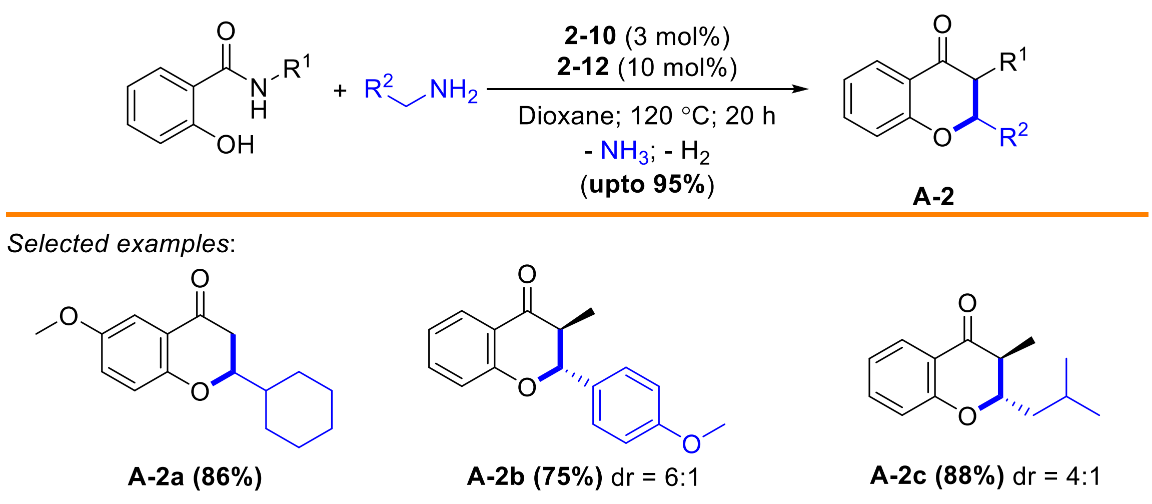

NMR Data for the Products

2-cyclohexyl-6-methoxychroman-4-one (A-2a) ^{1}H NMR (400 MHz, $CDCl_3$) δ 7.28 (d, *J* = 3.2 Hz, 1H), 7.07 (dd, *J* = 9.0, 3.2 Hz, 1H), 6.90 (d, *J* = 9.0 Hz, 1H), 4.19–4.10 (m, 1H), 3.79 (s, 3H), 2.71–2.60 (m, 2H), 2.00–1.94 (m, 1H), 1.82–1.68 (m, 5H), 1.32–1.09 (m, 5H) ppm; $^{13}C\{^{1}H\}$ NMR (100 MHz, $CDCl_3$) δ 193.3, 156.6, 153.8, 125.2, 120.7, 119.2, 107.1, 82.1, 55.8, 41.7, 40.1, 28.3, 28.2, 26.3, 25.9, 25.9 ppm; GC-MS for $C_{16}H_{20}O_3$, m/z = 260 (M^+). HRMS (ESI-TOF) m/z: $[M + H]^+$ Calcd for $C_{16}H_{20}O_3$; 261.1485 Found 261.1490.

2-(4-methoxyphenyl)-3-methylchroman-4-one (A-2b) : ^{1}HNMR (400MHz, $CDCl_3$) δ 7.92 (d, *J* = 8.1 Hz, 1H), 7.48 (t, *J* = 8.1 Hz, 1H), 7.39 (d, *J* = 8.6 Hz, 2H), 7.04 (t, *J* = 7.5 Hz, 1H), 7.01–6.93 (m, 3H), 5.01 (d, *J* = 12.4 Hz, 1H), 3.84 (s, 3H), 3.08–2.97 (m, 1H), 1.00 (d, *J* = 6.8 Hz, 3H) ppm; $^{13}C\{^1H\}$ NMR (100 MHz, $CDCl_3$) δ 207.1, 161.3, 135.8, 130.1, 128.7, 127.2, 121.4, 120.3, 117.9, 114.1, 85.2, 55.3, 46.3, 30.9, 10.3 ppm; GC-MS for $C_7H_{16}O_3$, m/z = 268 (M^+). HRMS (ESI-TOF) m/z: $[M + H]^+$ Calcd for 269.1172 Found 269.1171.

2-isobutyl-3-methylchroman-4-one (A-2c) ^{1}H NMR (400 MHz, $CDCl_3$) δ 7.87 (dd, *J* = 7.8, 1.7 Hz, 1H), 7.48–7.43 (m, 1H), 7.02–6.93 (m, 2H), 4.20 (dt, *J* = 10.2, 2.9 Hz, 1H), 2.57 (dq, *J* = 10.2, 7.0 Hz, 1H), 2.09–1.98 (m, 1H), 1.84–1.76 (m, 1H), 1.51–1.42 (m, 1H), 1.22 (d, *J* = 7.0 Hz, 3H), 1.00–0.94 (m, 6H) ppm; $^{13}C\{^1H\}$ NMR (100 MHz, $CDCl_3$) δ 195.1, 160.8, 135.7, 127.2, 121.0, 120.2, 117.8, 80.7, 45.7, 42.0, 24.1, 23.7, 21.5, 11.0 ppm; GC-MS for $C_{14}H_{18}O_2$, m/z = 218 (M^+). HRMS (ESI-TOF) m/z: $[M + H]^+$ Calcd for $C_{14}H_{18}O_2$; 219.1380 Found 1375.

8.1.3 C-C Bond Activation Reaction

To further extend the synthetic utility of ligand-promoted C–N bond activated C-C bond formation reactions, we have been exploring the coupling reaction of 1-(1-Ethyl-1H-indol-3-yl)ethanone with tryptamine led to the formation of C-C bond activated homocoupling product **A-3**. A 1,4-dioxane (2.0 mL) solution of complex **2-10** (9 mg, 3 mol %), **2-12** (8 mg, 10 mol %), (0.5 mmol), and tryptamine (0.7 mmol) was stirred at 130 °C for 20 h. The products were isolated by column chromatography on silica gel (hexanes/EtOAc = 40:1–5:1).

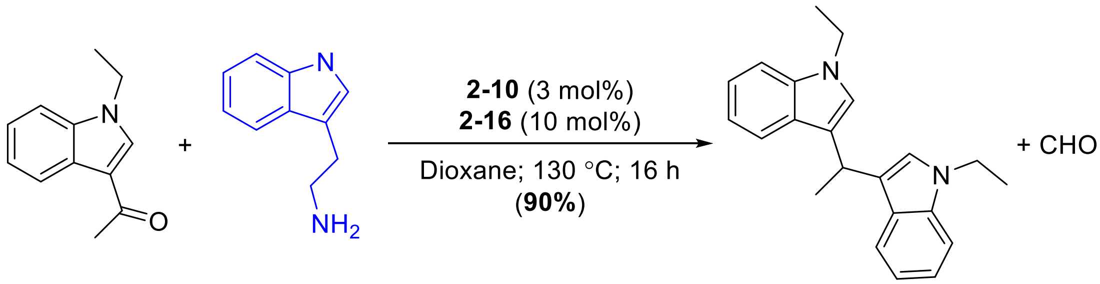

A-3

NMR Data for 3,3'-(ethane-1,1-diyl)bis(1-ethyl-1H-indole) (A-3) ^{1}H NMR (400 MHz, $CDCl_3$) δ 7.58 (d, *J* = 8.0 Hz, 2H), 7.32 (d, *J* = 8.3 Hz, 2H), 7.18 (t, *J* = 7.8 Hz, 2H), 7.02 (t, *J* = 7.6 Hz, 2H), 6.85 (s, 2H), 4.67 (d, *J* = 7.1 Hz, 1H), 4.10 (q, *J* = 7.4 Hz, 4H), 1.80 (d, *J* = 7.1 Hz, 3H), 1.41 (t, *J* = 7.4 Hz, 6H) ppm; ^{13}C{^{1}H} NMR (100 MHz, $CDCl_3$) δ 136.3, 127.4, 124.3, 121.0, 120.3, 119.9, 118.3, 109.1, 40.7, 28.1, 22.1, 15.5 ppm; GC-MS for $C_{22}H_{24}N_2$, m/z = 316 (M^+).[246]

8.1.4 C-C Bond Formation via Alkene Insertion Reaction

To further extend the ligand-promoted C–C bond formation reactions, we have been exploring the coupling reaction of 1,2-dimethylindole with olefin led to the formation of olefin inserted product **A-4** in 60% yield. This protocol would be promising in generating substituted indole derivatives. A 1,4-dioxane (2.0 mL) solution of complex **2-10** (9 mg, 3 mol %), **2-12** (8 mg, 10 mol %), (0.5 mmol), 1,2-Dimethylindole and styrene (0.5 mmol) was stirred at 130 °C for 20 h. The products were isolated by column chromatography on silica gel (hexanes/EtOAc = 40:1–5:1).

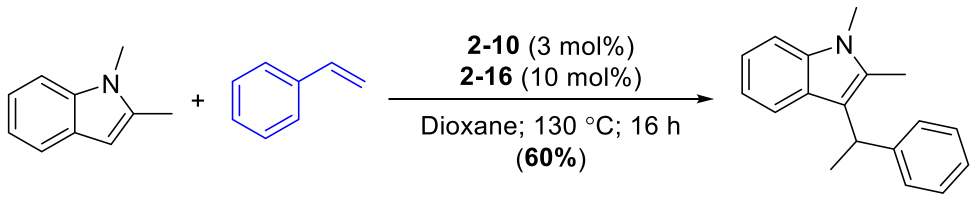

A-4

NMR Data for 1,2-dimethyl-3-(1-phenylethyl)-1H-indole (A-4) ^{1}H NMR (400 MHz, $CDCl_3$) δ 7.47 (d, *J* = 7.9 Hz, 1H), 7.40 (d, *J* = 7.9 Hz, 1H), 7.33–7.28 (m, 3H), 7.22–7.16 (m, 2H), 7.03 (td, *J* = 7.4, 0.9 Hz, 1H), 4.51 (q, *J* = 7.4 Hz, 1H), 3.69 (s, 3H), 2.39 (s, 3H), 1.84 (d, *J* = 7.4 Hz, 3H) ppm; ^{13}C{^{1}H} NMR (100 MHz, $CDCl_3$) δ146.3, 136.7, 132.4, 128.0, 128.0, 127.3, 125.5, 120.2, 119.3, 118.5, 115.4, 108.6, 35.7, 29.4, 20.7, 10.5 ppm; GC-MS for $C_{18}H_{19}N$, m/z = 249 (M^+).

8.1.5 Transamidation Reactions

The coupling reaction of 2-hydroxybenzamide with primary amines led to the formation of N-substituted amide product **A-5** in 95% yield via C-N bond activation. A 1,4-dioxane (2.0 mL) solution of complex **2-10** (9 mg, 3 mol %), **2-12** (8 mg, 10 mol %), 2-hydroxybenzamide (0.5 mmol), and primary amine (0.6 mmol) was stirred at 130 °C for 20 h. The products were isolated by column chromatography on silica gel (hexanes/EtOAc = 60:1–5:1).

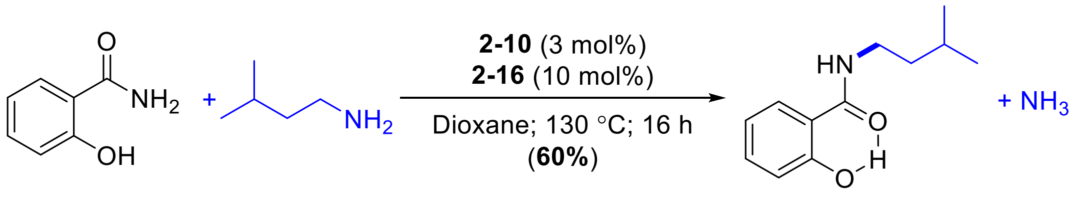

NMR Data for 2-hydroxy-N-isopentylbenzamide (A-5) ^{1}H NMR (400 MHz, $CDCl_3$) δ 12.44 (brs, 1H), 7.41–7.32 (m, 2H), 6.97 (d, J = 8.3 Hz, 1H), 6.82 (t, J = 6.7 Hz, 1H), 6.40 (brs, 1H), 3.48–3.42 (m, 2H), 1.67 (septet, J = 6.7 Hz, 1H), 1.55–1.47 (m, 2H), 0.94 (d, J = 6.7 Hz, 3H) ppm; ^{13}C{^{1}H} NMR (100 MHz, $CDCl_3$) δ 169.9, 161.4, 134.0, 125.2, 118.6, 118.5, 114.3, 38.2, 38.0, 25.9, 22.4 ppm; GC-MS for $C_{12}H_{17}NO_2$, m/z = 207 (M^+).

8.1.6 Synthesis of Quinoline Derivatives with Primary Amines

As an extension for the reaction described in chapter 5, 2-aminophenylethanones with β-amino acids are effective in formation of quinoline products. The reaction was carried out with the in-situ generated complex **2-10** (9 mg, 3 mol %), **2-12** (8 mg, 10 mol %) with 2-aminophenylethanone and branched amines. This protocol selectively generated the substituted quinoline products shown in **Table 5.5**. This catalytic protocol unveils the synthesis of quinoline derivatives via atom economical fashion than the reaction with β-amino acids which are quite rare and expensive.

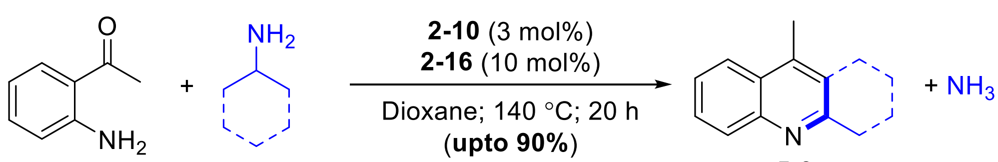

The reaction of aniline derivatives with allyl amine were tested for the potential synthesis of quinoline derivatives. The reaction of aniline derivatives (0.5 mmol), allyl amine (1.5 mmol) with isolated ruthenium catecholate **2-11** yielded the 1 to 2 coupling products in reasonable yields.

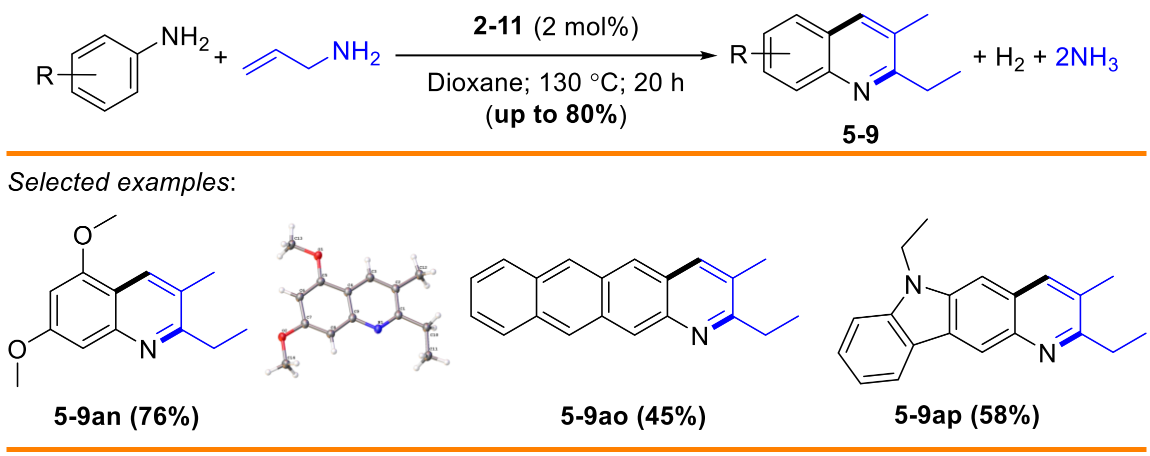

However, the reaction of 3,5-dimethoxy aniline (0.5 mmol) with 2-Methyl-2-propen-1-amine (1 mmol) yielded the 1 to 1 coupling product **5-9aq** over 90% yield.

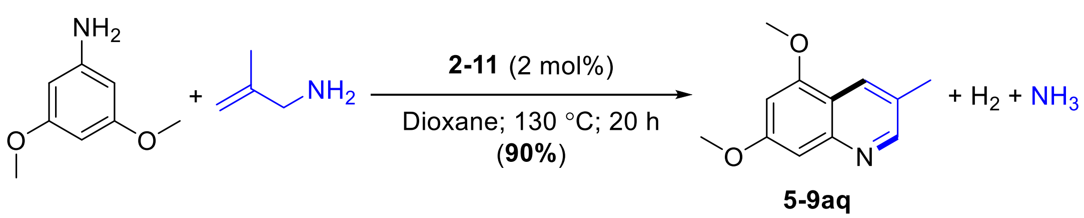

NMR Data for the Quinoline Products.

2-Ethyl-5,7-dimethoxy-3-methylquinoline (5-9an): ^{1}H NMR (400 MHz, $CDCl_3$) δ 8.11 (s, 1H), 6.97 (d, *J* = 2.1 Hz, 1H), 6.43 (d, *J* = 2.1 Hz, 1H), 3.93 (s, 3H), 3.91 (s, 3H), 2.94 (q, *J* = 7.6 Hz, 2H), 2.43 (d, *J* = 0.8 Hz, 3H), 1.33 (t, *J* = 7.6 Hz, 3H) ppm; $^{13}C\{^{1}H\}$ NMR (100 MHz, $CDCl_3$) δ 163.7, 160.3, 155.4, 148.5, 130.7, 126.0, 115.3, 99.0, 97.2, 55.6, 55.5, 29.4, 18.9, 13.0 ppm; GC-MS for $C_{14}H_{17}NO_2$, m/z = 231 (M^+). HRMS (ESI-TOF) m/z: $[M + H]^+$ Calcd for $C_{14}H_{17}NO_2H$ 232.1332; Found 232.1330.

2-ethyl-3-methylnaphtho[2,3-g]quinoline (5-9ao): ^{1}H NMR (400 MHz, $CDCl_3$) δ 9.06 (s, 1H), 8.78 (s, 1H), 8.39 (s, 1H), 8.13–8.10 (m, 1H), 8.08–8.04 (m, 1H), 7.97 (d, *J* = 9.3 Hz, 1H), 7.86 (d, *J* = 9.3 Hz, 1H), 7.59–7.55 (m, 2H), 3.06 (q, *J* = 7.6 Hz, 2H), 2.62 (s, 3H), 1.41 (t, *J* = 7.6 Hz, 3H) ppm; ^{13}C{^{1}H} NMR (100 MHz, $CDCl_3$) δ 132.0, 131.9, 131.8, 130.3, 129.9, 129.4, 128.2, 127.9, 127.9, 127.1, 127.0, 126.1, 126.0, 125.9, 124.1, 121.3, 120.6, 29.7, 19.3, 13.1 ppm; GC-MS for $C_{20}H_{17}N$, m/z = 271 (M^+). HRMS (ESI-TOF) m/z: $[M + H]^+$ Calcd for $C_{20}H_{17}NH$ 272.1434; Found 272.1429.

2,6-diethyl-3-methyl-6H-pyrido[3,2-b]carbazole (5-9ap): ^{1}H NMR (400 MHz, $CDCl_3$) δ 8.20 (s, 1H), 8.10 (d, *J* = 7.7 Hz, 1H), 7.90 (dd, *J* = 1.7, 0.7 Hz, 1H), 7.47 (td, *J* = 7.7, 1.2 Hz, 1H), 7.37–7.35 (m, 1H), 7.23 (td, *J* = 7.4, 1.0 Hz, 1H), 6.12 (td, *J* = 7.4, 0.1 Hz, 1H), 4.36 (q, *J* = 7.3 Hz, 2H), 2.37 (pentet, *J* = 7.5 Hz, 2H), 2.06 (s, 3H), 1.44 (t, *J* = 7.3 Hz, 3H), 1.12 (t, *J* = 7.5 Hz, 3H) ppm; ^{13}C{^{1}H} NMR (100 MHz, $CDCl_3$) δ 163.6, 145.6, 144.5, 140.4, 138.3, 136.2, 125.7, 123.4, 123.1, 120.5, 119.9, 118.7, 112.2, 108.6, 108.5, 37.6, 22.1, 13.8, 13.5, 11.4 ppm; GC-MS for $C_{20}H_{20}N_2$, m/z = 288 (M^+). HRMS (ESI-TOF) m/z: $[M + H]^+$ Calcd for $C_{20}H_{20}N_2H$ 289.1699; Found 289.1687.

5,7-Dimethoxy-3-methyl-quinoline (5-9aq): ^{1}H NMR (400 MHz, $CDCl_3$) δ 8.64 (d, *J* = 2.2 Hz, 1H), 8.21–8.16 (m, 1H), 6.97 (d, *J* = 2.2 Hz, 1H), 6.47 (d, *J* = 2.2 Hz, 1H), 3.93 (s, 3H), 3.91 (s, 3H), 2.45 (s, 3H) ppm; ^{13}C{^{1}H} NMR (100 MHz, $CDCl_3$) δ 160.3, 155.4, 152.6, 148.5, 129.5, 127.3, 116.4, 99.5, 98.1, 55.7, 55.4, 18.5 ppm; GC-MS for

$C_{12}H_{13}NO_2$, m/z = 203 (M^+). HRMS (ESI-TOF) m/z: $[M + H]^+$ Calcd for $C_{12}H_{13}NO_2H$ 204.1019; Found 204.1014.

Also, it has been found that the three-component coupling reaction of 3,5-dimethoxy aniline (0.5 mmol), allyl amine (0.5 mmol) and enamine (0.5 mmol) afforded the tri substituted quinoline product **5-9ao**. This catalytic protocol enables to synthesize complex quinoline products.

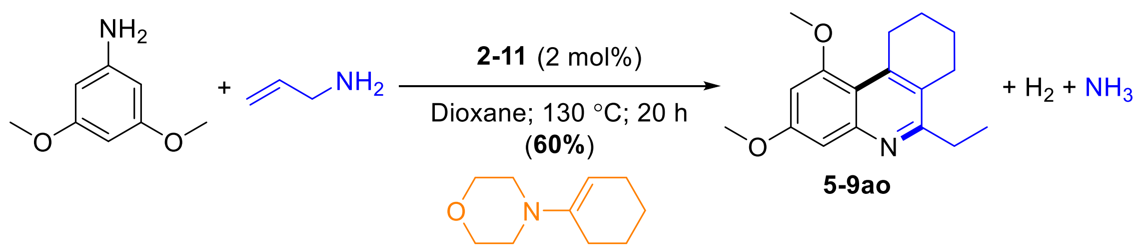

8.1.7 Detection of Zwitterionic Ruthenium Hydride Complex A-6

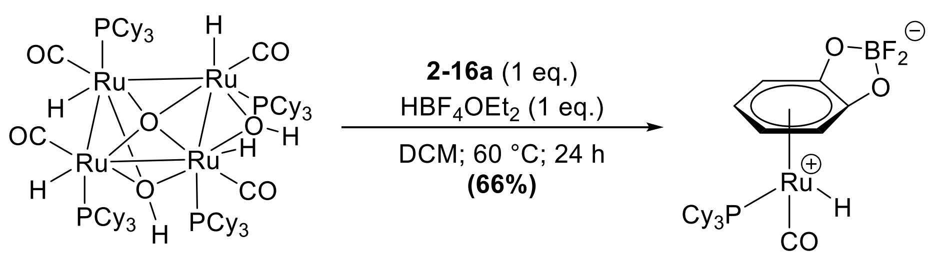

In a glove box, complex **2-9** (200 mg, 0.12 mmol) and 5,5-ditertiarybutylcatechol (107 mg, 0.48 mmol) was dissolved in dichloromethane (10 mL) in a 25 mL Schlenk tube equipped with a Teflon screw-cap stopcock and a magnetic stirring bar. The tube was brought out of the box, and $HBF_4{\cdot}OEt_2$ (64 μL, 0.48 mmol) was added via syringe under N_2 stream. The color of the solution was changed from dark red to pale yellow immediately. After stirring for 24 h at 60 ºC, the mixture was filtered through a celite bed. Then, the solvent was removed under vacuum, and the residue was dissolved by adding acetone (10 mL). The solution was recrystallized from acetone/pentanes yielded the product **A-6** as a light greenish prism shaped crystals. A suitable colorless prism shaped crystal with the dimension of $0.553 \times 0.278 \times 0.167$ mm^3 was selected and analyzed. The dataset was collected with an Oxford SuperNova diffractometer using Mo(Kα) radiation at 100K.

Structure description: The Ru(I) ion has a tripod coordination with η^6-coordinated adduct of pyrocatechol with BF_2 and carbonyl, phosphine and hydride (not localized) "legs". It exists in an eclipsed conformation. The positions of the carbonyl group and presumed hydride ligand are statistically interchanged in the crystal by 20%. This results in the respective disorder of adjacent t-butyl and cyclohexyl groups (see below).

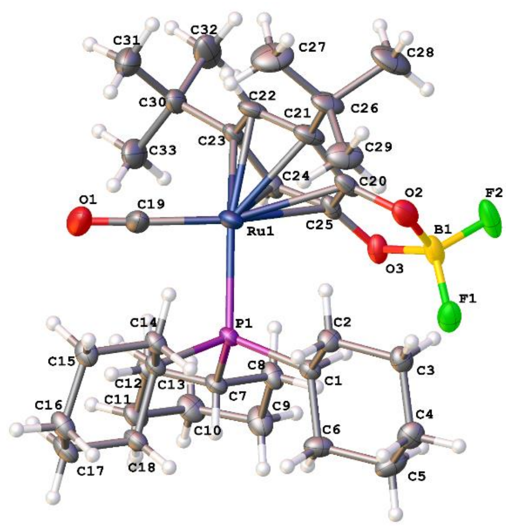

Molecular Structure of **A-6**

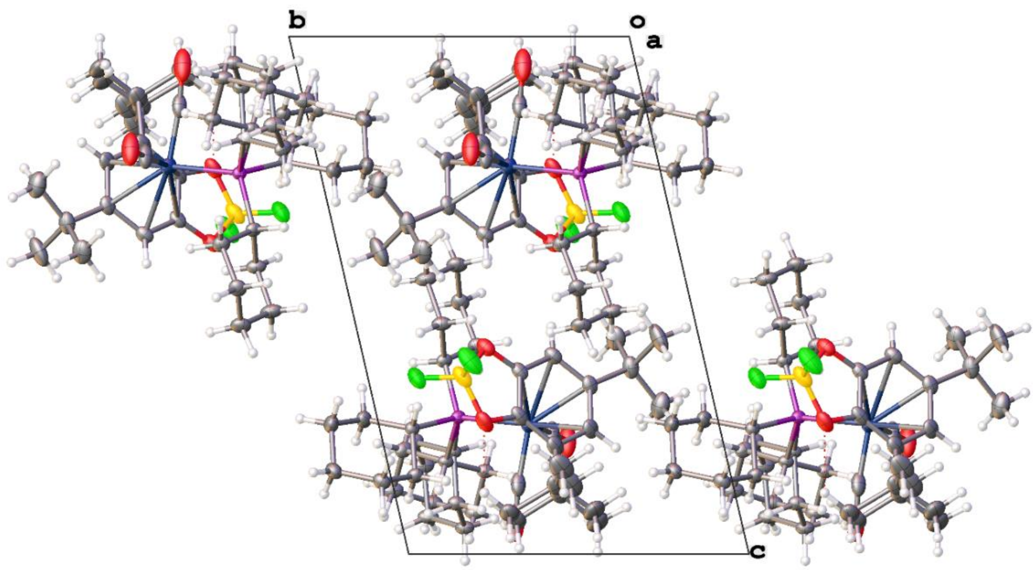

Crystal Packing of **A-6**

Evaluation of the activity and selectivity of the complex **A-6** towards deaminative coupling reactions potentially useful in the future research.

Table A-3 Crystal data and structure refinement for yi4p.

Identification code	yi4p
Empirical formula	$C_{33}H_{53}BO_3F_2PRu$
Formula weight	678.60
Temperature/K	100.00(10)
Crystal system	triclinic
Space group	P-1
a/Å	10.6805(2)
b/Å	11.3363(3)
c/Å	15.9739(3)
α/°	97.0035(18)
β/°	99.7171(18)
γ/°	116.984(2)
Volume/Å^3	1654.85(7)
Z	2
ρ_{calc}g/cm^3	1.362
μ/mm^{-1}	0.564

F(000)	714.0
Crystal size/mm^3	0.553 × 0.278 × 0.167
Radiation	MoKα (λ = 0.71073)
2Θ range for data collection/°	6.724 to 59.408
Index ranges	$-14 \leq h \leq 13$, $-14 \leq k \leq 15$, $-22 \leq l \leq 21$
Reflections collected	37384
Independent reflections	8536 [R_{int} = 0.0296, R_{sigma} = 0.0272]
Data/restraints/parameters	8536/0/416
Goodness-of-fit on F^2	1.049
Final R indexes [I>=2σ (I)]	R_1 = 0.0332, wR_2 = 0.0724
Final R indexes [all data]	R_1 = 0.0383, wR_2 = 0.0755
Largest diff. peak/hole / e Å^{-3}	1.40/-1.68

8.2 Data for the Computational DFT Study

N-ethyl isopropenyl amine

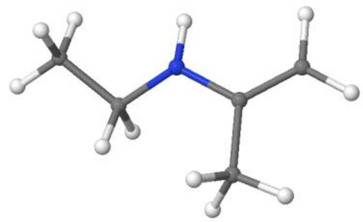

1\1\GINC-COMET-10-22\FOpt\RM06L\Gen\C5H11N1\TALIPOVM\28-Aug-
2020\0\\#P
M06L/chkbasis opt(verytight) freq scf(fermi,xqc,maxcyc=200) nosym int
(grid=ultrafine) Geom(AllCheck) Guess(read) SCRF(Check)\\Title\\0,1\H,
5.99036121,7.7948961512,3.0055959123\H,8.0426186173,6.601994675,3.5699
734068\C,4.0084380283,9.3556195012,3.2193760815\C,7.4260033456,6.17056
04989,4.3796641651\N,5.5335428156,7.6266031909,3.9001607531\H,7.013065
0633,8.0354350479,5.3865471627\C,4.4949025809,8.5120052839,4.157331946
9\C,6.4514792133,7.1867379379,4.9313152028\H,8.1158291866,5.8164399715
,5.1633570111\H,6.8951475943,5.2957009627,3.9658108971\C,3.9033345705,
8.4346454385,5.5299142851\H,5.8705288044,6.7313073955,5.7537501621\H,3
.0233487675,9.0903049685,5.6154918306\H,4.6263630387,8.741727831,6.308
4835713\H,3.5891524426,7.4036490314,5.7777329065\H,4.4509638192,9.4177
806555,2.216473412\H,3.1285409019,9.9726114584,3.4251612929\\Version=E
S64L-G16RevC.01\HF=-251.6351738\RMSD=8.757e-10\RMSF=2.201e-06\Dipole=0
.6158143,-0.3297556,0.3410726\Quadrupole=10.1837344,-14.1815684,3.9978
34,5.2898997,6.6362494,2.3746248\PG=C01 [X(C5H11N1)]\\@

Sigmatropic TS (no catalyst, closed-shell)

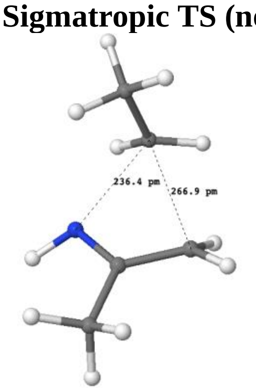

1\1\GINC-COMET-10-48\FTS\RM06L\GenECP\C5H11N1\TALIPOVM\28-Aug-
2020\0\\
#P M06L/genECP opt(verytight,ts,calcfc,noeigentest) freq scf(fermi,xqc
,maxcyc=200) nosym int(grid=ultrafine)\\Title\\0,1\H,3.1301474274,-0.1
527300349,-0.4114938471\N,0.2231414641,-0.9474375151,-0.5525956473\C,-

1.8426848461,0.2008148178,-0.588553968\H,0.0063646894,1.7175391892,-0.
97647437\C,0.5164291603,1.3445157761,-0.0859382249\H,-1.508544195,-1.0
612967977,1.0766742618\H,-1.9649704905,-0.4904631389,-1.4252586797\C,-
2.2075819772,-0.2655254902,0.7546750354\H,-2.2040366037,0.5392931745,1
.5066149941\H,-3.2148647824,-0.7363979158,0.7427109501\H,2.4758995275,
-1.2934598856,0.7987646175\C,2.3849102707,-0.2692959331,0.3971497023\H
,2.672741329,0.4376177698,1.1939084608\C,0.9916959965,0.0298459447,-0.
1089666115\H,-2.0008630286,1.251695811,-0.8473240813\H,0.9881895898,2.
1071342511,0.5504551367\H,0.7752664689,-1.7373000229,-0.925187729\\Ver
sion=ES64L-G16RevC.01\HF=-251.4998791\RMSD=6.440e-09\RMSF=7.118e-07\Di
pole=-0.1196629,-0.1605764,-0.0842516\Quadrupole=2.2205326,-0.9825844,
-1.2379482,-1.0880221,0.5139797,0.3762335\PG=C01 [X(C5H11N1)]\\@

Pentan-2-imine

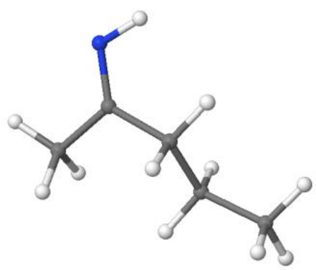

1\1\GINC-COMET-05-67\FOpt\RM06L\Gen\C5H11N1\TALIPOVM\28-Aug-
2020\0\\#P
M06L/chkbasis opt(verytight) freq scf(fermi,xqc,maxcyc=200) nosym int
(grid=ultrafine) Geom(AllCheck) Guess(read) SCRF(Check)\\Title\\0,1\H,
6.0168274351,8.0133237468,3.0985796929\H,8.7954205499,9.6826132594,7.1
204360421\C,6.8114489014,8.8543065414,5.3215416091\C,8.687327563,8.589
1208099,7.0014450548\N,5.1600354591,8.0321063304,3.6695617255\C,5.4393
012953,8.4372371956,4.8499610206\C,7.2675254683,8.2105237479,6.6282897
848\H,8.9985493378,8.1211373826,7.9512206186\H,9.4080687123,8.27280359
74,6.2258006924\C,4.3353051128,8.5276531291,5.8595318497\H,6.580307677
5,8.5011136051,7.4458510581\H,7.1815233615,7.1091557405,6.5436015881\H
,7.5485197448,8.6454573125,4.5221855374\H,6.8104707078,9.9573653726,5.
4519592801\H,4.4591355319,7.7621163993,6.6478251941\H,3.3589991267,8.3
690185633,5.3762801166\H,4.3353240147,9.5069172662,6.3729291351\\Versi
on=ES64L-G16RevC.01\HF=-251.649995\RMSD=8.844e-09\RMSF=3.363e-06\Dipol
e=0.7669129,0.3055568,0.717208\Quadrupole=3.1148202,-3.3702769,0.25545
67,14.6730337,12.45728,13.8620527\PG=C01 [X(C5H11N1)]\\@

3-20a (*N*-ethyl isopropenyl amine + catalyst system)

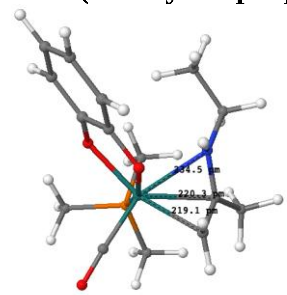

1\1\GINC-COMET-05-08\FOpt\RM06L\Gen\C15H24N1O3P1Ru1\TALIPOVM\27-Aug-20
20\0\\#P M06L/chkbasis opt(verytight) freq scf(fermi,xqc,maxcyc=200) n
osym int(grid=ultrafine) Geom(AllCheck) Guess(read) SCRF(Check)\\Title
\\0,1\Ru,3.9380945103,7.0207662807,2.5873546804\P,2.6366749729,5.65672
78128,3.9630800673\O,1.4483618032,7.360072282,0.982165757\O,4.71724318
62,5.1982846543,1.9717795515\O,5.4167794282,7.7180992124,1.2630023029\
C,1.1926257362,6.2927104584,4.8810447615\C,3.5794406929,4.7134676448,5
.2109944341\C,1.9173959837,4.3291570139,2.9476191403\C,2.4334670553,7.
2012575692,1.5857682989\C,5.755670365,5.3699931114,1.1466676837\C,6.49
65880713,4.286437727,0.6562729643\C,7.5861581751,4.4942845096,-0.19671
37349\H,8.1591532277,3.6346157492,-0.56544686\C,7.9373928902,5.7904888
687,-0.5760751481\C,7.2010117291,6.8822368986,-0.1026789096\H,7.459615
564,7.9082827095,-0.3933951146\C,6.117899052,6.6929826159,0.7667698921
\H,1.4916457546,7.0091845794,5.6625916938\H,0.6369989858,5.4667074799,
5.3597674557\H,0.5146335252,6.812322988,4.1823081688\H,3.94785468,5.35
94215163,6.0250631615\H,4.4456262147,4.2451681737,4.7130055336\H,2.952
9880664,3.9217685233,5.6596358987\H,1.169318731,4.7470036802,2.2532402
353\H,1.4351386194,3.558121165,3.5737976522\H,2.7281180348,3.880241701
4,2.3501315834\H,6.1859060869,8.1171766438,3.158837961\H,8.0483274016,
6.5595778958,3.6105774787\C,3.9130250916,9.1497296972,3.1030806119\C,7
.3810105732,6.099568713,4.3611207165\N,5.6656052282,7.7800783358,3.980
2462062\H,7.0584353877,7.8843681688,5.5620215083\C,4.4474447569,8.4363
526219,4.1964322133\C,6.4742457716,7.1278353454,4.9984640732\H,8.01612
59061,5.6152887272,5.1208726972\H,6.7919082343,5.3234414206,3.84244645
66\C,3.8853129653,8.4972194596,5.5770564028\H,5.7995514538,6.649021763
,5.7268594516\H,2.8683534356,8.9174406027,5.5547519402\H,4.506279895,9
.1712093481,6.1983204147\H,3.852161609,7.5256219841,6.0964003708\H,4.5
731666471,9.564346834,2.3299633704\H,2.9725885714,9.6873574635,3.27181
90263\H,6.2028125308,3.2744111178,0.9625217863\H,8.7884933985,5.959428
9322,-1.2472038354\\Version=ES64L-G16RevC.01\HF=-1301.9868378\RMSD=9.2
88e-09\RMSF=1.728e-06\Dipole=-1.3134139,0.4388931,4.718466\Quadrupole=
-35.1294639,0.6352357,34.4942283,-5.9722805,33.6839245,60.8853252\PG=C
01 [X(C15H24N1O3P1Ru1)]\\@

TS-3-20a (3-20a→ 3-21a): (*N*-ethyl isopropenyl amine + catalyst system)

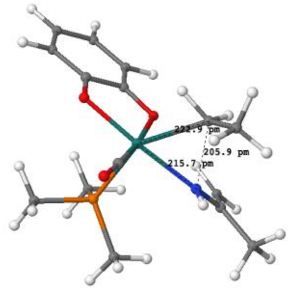

1\1\GINC-COMET-05-15\FTS\RM06L\Gen\C15H24N1O3P1Ru1\TALIPOVM\27-Aug-202
0\0\\#P M06L/chkbasis opt(verytight,ts,calcfc,noeigentest) freq scf(fe
rmi,xqc,maxcyc=200) nosym int(grid=ultrafine) Geom(AllCheck) Guess(rea
d) SCRF(Check)\\Title\\0,1\Ru,-0.1811469883,0.7218890706,0.0551740935\
P,-1.3807861939,-1.2248622312,0.2909470106\O,-2.6426218982,2.331142391
8,0.6782285787\O,1.5089854252,-0.2821287717,-0.6517551481\O,-0.5728880
45,0.6823491078,-1.9648676867\C,-1.8067511077,-1.6633894763,2.00007831
73\C,-0.4942396287,-2.6628999251,-0.3668049375\C,-2.9576347238,-1.1998
313676,-0.6086865489\C,-1.6761255116,1.7150826031,0.4628931467\C,1.465
8934713,-0.4939900846,-1.9536927034\C,2.4433690007,-1.2218588168,-2.65
36291271\C,2.3076583206,-1.4379340767,-4.0251496055\H,3.0814478983,-1.
9970950718,-4.5648847572\C,1.1895139928,-0.9497979239,-4.7148240634\C,
0.1988799661,-0.2392002277,-4.0370259082\H,-0.6822326174,0.1518576735,
-4.5598306681\C,0.3318926424,0.0109692892,-2.6613756748\H,-0.879734597
4,-1.8334969504,2.5738912908\H,-2.4206528019,-2.5810123907,2.022878013
6\H,-2.3704202721,-0.8417553838,2.473652629\H,0.4538256958,-2.79456447
17,0.1798677825\H,-0.253937531,-2.4983941511,-1.431798299\H,-1.1094982
543,-3.5752256302,-0.272211811\H,-3.615926928,-0.4150099655,-0.2004126
984\H,-3.4708480192,-2.1751740075,-0.536793368\H,-2.7614383582,-0.9636
157575,-1.6676023707\H,1.0905838864,-1.125263726,-5.7927248082\H,3.308
7122427,-1.6053944601,-2.0997650092\H,2.6146313663,-1.7492850221,2.902
5280643\H,-0.0065683446,3.6539747583,1.8030169697\H,1.4370229331,1.020
8935374,4.6459457331\C,2.00486109,-1.0966094676,2.2687583522\C,1.05503
75333,3.3497691454,1.7869071456\H,2.0985228561,-1.1737678264,1.1799820
38\C,1.1229287715,0.006588654,4.3352978232\C,1.2045429738,-0.160280250
2,2.8425896738\H,1.3977008739,3.2088010634,2.8253288476\H,1.6177580741
,4.2102476057,1.3736504233\H,2.2746594765,1.6633832301,1.0256682969\C,
1.2896206336,2.1437061852,0.9415932271\H,0.0872859608,-0.1313995108,4.
7019522241\H,1.7647665424,-0.7178172238,4.8608884135\N,0.4124239696,0.
7076043524,2.128687948\H,1.0937475899,2.3695344305,-0.1512060016\H,-0.
1397213659,1.3171610701,2.7291351519\\Version=ES64L-G16RevC.01\HF=-130
1.9100589\RMSD=5.084e-09\RMSF=4.670e-07\Dipole=-1.1110278,-0.5418275,2
.5053295\Quadrupole=-2.7449171,5.3961331,-2.6512161,10.7072466,2.20788
69,2.9487214\PG=C01 [X(C15H24N1O3P1Ru1)]\\@

3-21a: (*N*-ethyl isopropenyl amine + catalyst system)

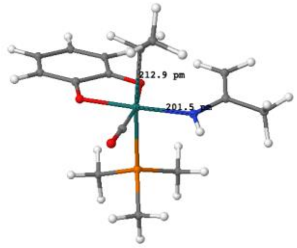

1\1\GINC-COMET-05-16\FOpt\UM06L\Gen\C15H24N1O3P1Ru1\TALIPOVM\27-Aug-20
20\0\\#P M06L/chkbasis opt(verytight) freq scf(fermi,xqc,maxcyc=200) n
osym int(grid=ultrafine) Geom(AllCheck) Guess(read) SCRF(Check)\\Title
\\0,1\Ru,-0.1395015921,0.6507959787,0.4050411946\P,-1.5676352865,-1.43
94682635,0.4665004488\O,-2.3239275704,2.493601457,1.263912079\O,1.2758
407659,-0.6646786629,-0.624834689\O,-0.6002346991,0.9222728999,-1.5899
147796\C,-3.1507190239,-1.3998551713,1.3757353726\C,-0.6782808097,-2.8
371813778,1.2307486221\C,-2.0335891303,-2.0845217045,-1.175785651\C,-1
.4514423406,1.7829707743,0.9589296544\C,1.2085861362,-0.540536774,-1.9
040245841\C,2.0445630908,-1.2424981161,-2.8101568856\C,1.8789077831,-1
.0746434245,-4.1726617693\H,2.5344482478,-1.612329919,-4.8679362651\C,
0.8759684459,-0.2184557309,-4.6904925265\C,0.0333830597,0.4741520621,-
3.8413498901\H,-0.7500309125,1.1392395191,-4.2211083146\C,0.1802529199
,0.3344129007,-2.4405497435\H,-2.9685727711,-1.1028894889,2.4234018236
\H,-3.6627938638,-2.3789879528,1.3702733139\H,-3.820469161,-0.64528572
38,0.9286880963\H,-0.4416974947,-2.5964601687,2.2815621577\H,0.2783413
382,-2.9903168091,0.7027085639\H,-1.2657221808,-3.7726279222,1.2003308
943\H,-2.6435034429,-1.337317728,-1.711363777\H,-2.6014147374,-3.02982
05349,-1.1044040425\H,-1.1243882323,-2.2638850604,-1.7763374563\H,0.77
1286211,-0.106073964,-5.7756086656\H,2.8163348863,-1.9050964561,-2.403
0414377\H,3.491372039,-1.0309558132,2.6984490718\H,0.4014566887,3.9294
681599,1.082960757\H,1.3844486534,0.7567081953,4.8341755681\C,2.619852
2982,-0.6234574954,2.1749626696\C,1.3039780449,3.309481542,1.239128584
\H,2.6303511361,-0.5959894235,1.0811243104\C,1.5301777149,-0.248099302
,4.3960917439\C,1.5379235,-0.1897916252,2.8934271799\H,1.2865017764,2.
9705446935,2.2932071323\H,2.1771004992,3.9873381636,1.1397675333\H,2.3
073234527,1.5696803669,0.4283180145\C,1.3711989367,2.1456925079,0.2817
103138\H,0.7047951319,-0.8833376509,4.76850641\H,2.4721600074,-0.65433
89923,4.7956564618\N,0.4142197013,0.3195883392,2.3141757107\H,1.366395
5475,2.4888117666,-0.7722512107\H,-0.2401647637,0.6480619293,3.0268280
058\\Version=ES64L-G16RevC.01\HF=-1301.9450029\S2=0.633175\S2-1=0.\S2A
=0.044837\RMSD=5.275e-09\RMSF=4.225e-07\Dipole=-0.6694411,-2.0812759,0
.9569175\Quadrupole=-2.7015089,-6.1941715,8.8956804,5.0052175,-0.01042
29,-1.6187703\PG=C01 [X(C15H24N1O3P1Ru1)]\\@

TS-3-22a (3-21a→3-22a): (*N*-ethyl isopropenyl amine + catalyst system)

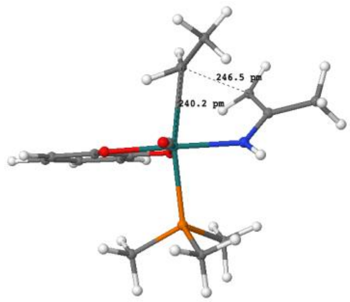

1\1\GINC-COMET-05-51\FTS\RM06L\Gen\C15H24N1O3P1Ru1\TALIPOVM\27-Aug-202
0\0\\#P M06L/chkbasis opt(verytight,ts,calcfc,noeigentest) freq scf(fe
rmi,xqc,maxcyc=200) nosym int(grid=ultrafine) Geom(AllCheck) Guess(rea
d) SCRF(Check)\\Title\\0,1\Ru,4.5315162419,7.3272562892,3.4478668999\P
,3.1173752823,5.4839478635,3.4618590712\O,2.3610057686,9.1782255764,4.
3781980395\O,5.9229114125,6.0292058131,2.4991844114\O,4.1685361301,7.6
994612951,1.4573403093\C,1.6179180954,5.6010881555,4.4844424248\C,3.97
68623326,4.0049853683,4.0677998542\C,2.5300272979,5.0375917912,1.80455
32256\C,3.2280697283,8.4769940581,4.0402397688\C,5.9084302046,6.143913
4319,1.190362525\C,6.730911704,5.39083721,0.3324342888\C,6.6477170625,
5.5643403286,-1.0485569124\H,7.3079339439,4.9870402655,-1.7071664388\C
,5.7294563348,6.469376644,-1.601278719\C,4.8856772687,7.2079580319,-0.
7736602327\H,4.1551915245,7.9142411704,-1.185810482\C,4.9680723404,7.0
639221758,0.6219493744\H,1.8896579616,5.8208102484,5.5312348242\H,1.04
41625673,4.6578748657,4.4615553567\H,0.9749301414,6.4198519196,4.12072
69922\H,4.3060118412,4.1699492709,5.1070342236\H,4.8757771012,3.841375
891,3.4511803599\H,3.3242546621,3.1150556841,4.0249357286\H,1.93637194
64,5.8643692972,1.3820548099\H,1.9190412374,4.1180891829,1.8343141922\
H,3.3953675515,4.8731534853,1.1387170545\H,5.6730616369,6.5966338497,-
2.6888620466\H,7.4427257848,4.6837881919,0.7752732979\H,8.2747704528,7
.1668254144,5.4634710869\H,5.4902894342,9.5159666095,5.6132791133\H,5.
5380041621,7.5324784009,7.9145836222\C,7.2759866375,6.9424829795,5.065
9769497\C,6.2334196156,9.8309902934,4.8522341149\H,7.2096041633,6.4819
397285,4.0811896062\C,6.3739565628,7.0034094694,7.4228991614\C,6.18858
57997,6.9066516849,5.937884225\H,7.1842233892,10.0002211064,5.38779580
16\H,5.877061199,10.8114550869,4.4741856261\H,7.3883872547,8.688581470
8,3.3430864538\C,6.3807494717,8.8283165927,3.755590026\H,6.4503020604,
6.0019835102,7.8862369988\H,7.3079603573,7.5360323595,7.6678025285\N,4
.9590673369,6.879382434,5.4277717175\H,5.7081607346,9.0066659067,2.878
9639581\H,4.2219062635,6.9162495969,6.1332368088\\Version=ES64L-G16Rev
C.01\HF=-1301.9087146\RMSD=9.355e-09\RMSF=1.064e-06\Dipole=-1.0414478,
-1.4535617,2.4592903\Quadrupole=-8.3772572,-29.8524105,38.2296677,-16.
347474,19.2549374,21.55849\PG=C01 [X(C15H24N1O3P1Ru1)]\\@

3-22a: (*N*-ethyl isopropenyl amine + catalyst system)

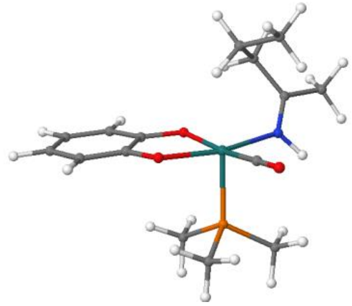

1\1\GINC-COMET-05-66\FOpt\RM06L\Gen\C15H24N1O3P1Ru1\TALIPOVM\27-Aug-20
20\0\\#P M06L/chkbasis opt(verytight) freq scf(fermi,xqc,maxcyc=200) n
osym int(grid=ultrafine) Geom(AllCheck) Guess(read) SCRF(Check)\\Title
\\0,1\Ru,-0.3251680693,0.3307436991,0.2287240365\P,-1.8619624413,-1.29
11178729,0.163903045\O,-2.484194489,2.3316407254,0.8732127807\O,1.3009
818274,-0.806912866,-0.3263722839\O,-0.4465009116,0.5093077021,-1.8293
767067\C,-2.5337861446,-1.8786695729,1.7550313236\C,-1.2161754471,-2.7
890100274,-0.6362713884\C,-3.3378145436,-0.8644679162,-0.8072960056\C,
-1.6410430435,1.5575147113,0.6349373049\C,1.3908704216,-0.961062808,-1
.6431128\C,2.3407139184,-1.7889685555,-2.2588955209\C,2.3660026871,-1.
9211149081,-3.6503049541\H,3.1187971512,-2.5642319847,-4.1224240582\C,
1.4326131666,-1.2392260847,-4.4375360411\C,0.4696326985,-0.4204100977,
-3.8413763297\H,-0.2682811684,0.1214541346,-4.4458545807\C,0.442041415
1,-0.2597504244,-2.4468923828\H,-1.7300768063,-2.3192314039,2.36916976
96\H,-3.3113017804,-2.6477684257,1.5985470406\H,-2.981237536,-1.036459
2566,2.3109442432\H,-0.3692947206,-3.1916158138,-0.0572325525\H,-0.838
7595685,-2.5342435554,-1.6426106472\H,-2.002477222,-3.5591088052,-0.72
9898551\H,-3.8791277986,-0.0317198147,-0.3278982797\H,-4.0178230413,-1
.7290523632,-0.907454839\H,-3.0153233166,-0.5292787077,-1.8070861718\H
,1.4522685356,-1.3458506937,-5.5291626858\H,3.0609689281,-2.3214806641
,-1.6248763738\H,3.3334143313,1.3227606458,2.5631437555\H,0.484966908,
2.980260622,2.3378947693\H,0.9381181483,-0.4126699319,4.6928419392\C,2
.5066776913,1.0155428848,1.8962328547\C,1.4126917382,3.3229972595,1.84
3772066\H,2.9146215895,0.2304347439,1.2325461442\C,1.758915865,0.09416
29205,4.1593626041\C,1.4309168457,0.386906033,2.7354402783\H,2.0868211
999,3.7120657168,2.6294579563\H,1.1376420807,4.1708476107,1.1937985221
\H,2.9638107488,2.5927908569,0.5229278028\C,2.0719710706,2.2113075488,
1.0525150068\H,2.6633963354,-0.5378882598,4.2234225903\H,2.0026335639,
1.0307888195,4.6947554442\N,0.2713014141,0.1226843634,2.2340391739\H,1
.4014844272,1.8836670307,0.2239930159\H,-0.3749866585,-0.2743172141,2.
9215996852\\Version=ES64L-G16RevC.01\HF=-1302.0121025\RMSD=9.027e-09\R
MSF=8.931e-07\Dipole=-0.6282483,-1.0526919,3.7810144\Quadrupole=2.3806
783,-3.3783337,0.9976554,13.5268424,9.1382723,-2.354226\PG=C01 [X(C15H
24N1O3P1Ru1)]\\@

3-20b: (*N*-benzyl-1-phenylethen-1-amine + catalyst system, X=Y=H)

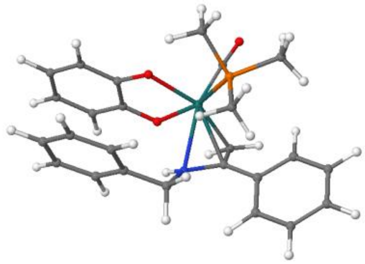

1\1\GINC-COMET-07-02\FOpt\RM06L\Gen\C25H28N1O3P1Ru1\TALIPOVM\29-Aug-20
20\0\\#P M06L/chkbasis opt(verytight) freq scf(fermi,xqc,maxcyc=200) n
osym int(grid=ultrafine) Geom(AllCheck) Guess(read) SCRF(Check)\\Title
\\0,1\Ru,4.1232894679,7.1121277536,2.6907596468\P,2.8942740433,5.60896
30063,4.0482719483\O,1.6419589587,7.2241759541,1.0431680349\O,5.024433
5758,5.3937077455,1.9713026133\O,5.5458671231,7.9599892906,1.390271197
6\C,1.1040145119,5.8654811993,4.3296558592\C,3.5005533574,5.2059360714
,5.7258535025\C,2.8914004863,3.9748131812,3.2440501175\C,2.6226567591,
7.1616112391,1.6704240049\C,5.9975218651,5.6578466352,1.0994973262\C,6
.7451535895,4.6438458072,0.4871030193\C,7.7713725537,4.9625475658,-0.4
075779354\H,8.3574195465,4.1585195664,-0.8703286625\C,8.0458871443,6.2
974114899,-0.7124736235\C,7.2913946397,7.3204320141,-0.1270591831\H,7.
4861608277,8.3746799728,-0.3613738565\C,6.2721005286,7.0165928454,0.78
50080684\H,0.9120294046,6.6896674526,5.0333011726\H,0.657240208,4.9469
261339,4.7494385672\H,0.5994794058,6.0949892784,3.376110766\H,3.492474
5221,6.0884314986,6.3875198465\H,4.5306247267,4.8176902508,5.661593170
5\H,2.8660981788,4.4230904995,6.17905894\H,2.4348225873,4.0545379483,2
.2435206987\H,2.3227338975,3.2472384976,3.8495911692\H,3.926953177,3.6
327184079,3.0996049632\H,6.2878773219,8.3729341093,3.3264318125\C,3.97
73360298,9.2281564097,3.1981992793\N,5.7786303357,7.9867520217,4.13108
02983\C,4.5174908831,8.5703411139,4.3310644312\C,6.5904067031,7.213638
5963,5.0642403482\H,4.6504909308,9.6607721626,2.4468547048\H,3.0247591
664,9.7523722063,3.3293766852\H,6.5211546466,3.6010976225,0.7450564193
\H,8.8469734651,6.5497000847,-1.4184707446\C,7.4887413601,6.2517678417
,4.3313512643\C,7.4718551768,4.8862741342,4.6305860581\H,6.791908881,4
.5074861509,5.4046812245\C,8.3170259904,3.9996622366,3.9625246205\H,8.
2866771842,2.9313242087,4.2059644194\C,9.1903950799,4.4713999457,2.983
8960404\H,9.8437106105,3.7749358343,2.4458026653\C,9.2189936931,5.8317
162216,2.6791488044\H,9.8893514087,6.2087976769,1.8992156558\C,8.37505
8695,6.713645745,3.3490178661\H,8.4130202981,7.7815631123,3.0941974906
\H,5.917272691,6.6724924157,5.7489826823\H,7.203234012,7.8950044071,5.
6907429283\C,3.8678498797,8.635020536,5.6564179987\C,4.5967169263,8.74
02551384,6.8517444849\H,5.6890648604,8.7721623568,6.8334968339\C,3.942
2543398,8.8466545472,8.0797290106\H,4.5344526856,8.9281199295,8.998114
5332\C,2.5505348579,8.8593934127,8.1415027824\H,2.0394911616,8.9357658

87,9.1074566569\C,1.8135934271,8.7932709982,6.9555585596\H,0.718122528
3,8.8218238483,6.9851785638\C,2.4649541588,8.6900696502,5.7327445276\H
,1.8794755246,8.6372781325,4.8076597228\\Version=ES64L-G16RevC.01\HF=-
1685.129787\RMSD=9.147e-09\RMSF=1.940e-06\Dipole=-1.2989432,0.0209542,
4.389873\Quadrupole=-30.5545374,-6.9139902,37.4685276,-12.2633375,26.6
875364,56.5316007\PG=C01 [X(C25H28N1O3P1Ru1)]\\@

TS-3-20b (3-20b→TS-3-20b): (*N*-benzyl-1-phenylethen-1-amine + catalyst system, X=Y=H)

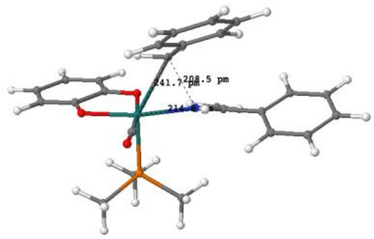

1\1\GINC-COMET-04-01\FTS\RM06L\Gen\C25H28N1O3P1Ru1\TALIPOVM\30-Aug-202
0\0\\#P M06L/chkbasis opt(verytight,ts,calcfc,noeigentest) freq scf(fe
rmi,xqc,maxcyc=200) nosym int(grid=ultrafine) Geom(AllCheck) Guess(rea
d) SCRF(Check)\\Title\\0,1\Ru,-0.3241194607,0.7454282876,0.0899513455\
P,-1.556825557,-1.1398127391,0.3371250123\O,-2.6606142381,2.3493652715
,1.085696313\O,1.2709200019,-0.2362926205,-0.8406107566\O,-0.893501732
5,0.8583497571,-1.9022737297\C,-3.2295493881,-1.0373834778,-0.36469903
87\C,-1.8014127902,-1.6650017455,2.0596051249\C,-0.8033989934,-2.56709
79116,-0.4934343878\C,-1.7380365393,1.7339877638,0.7209590967\C,1.1119
727219,-0.3512049579,-2.144025007\C,2.011710329,-1.0416320884,-2.97516
84591\C,1.7589646478,-1.1523229162,-4.3414290472\H,2.4712063553,-1.683
3693096,-4.9842775117\C,0.5985098098,-0.5926827669,-4.8973056642\C,-0.
3160750102,0.0820733592,-4.0913441804\H,-1.2270381732,0.5263726266,-4.
5100405763\C,-0.0684215314,0.2272685155,-2.7139206576\H,-3.8102633646,
-0.2541393854,0.1505357677\H,-3.760990115,-2.0010802619,-0.2709930112\
H,-3.1545928777,-0.7604721023,-1.4293401757\H,-2.3197014363,-0.8708001
12,2.6234075469\H,-0.8217770147,-1.8466357106,2.53455633\H,-2.40337159
13,-2.5897989543,2.1075118295\H,-0.6746005353,-2.3471249656,-1.5676796
948\H,-1.4392927552,-3.4632537177,-0.3825327789\H,0.1930149629,-2.7642
839746,-0.0657933168\H,0.4081470056,-0.6859256706,-5.973238704\H,2.910
5318944,-1.4796937458,-2.5247509781\H,2.7354912635,-1.8585831569,2.481
7451186\C,2.0986083049,-1.1432526909,1.9513674044\H,2.0261300614,-1.19
87967511,0.8596279827\C,1.4256819343,-0.181574605,2.646826463\C,1.4280
930731,2.2183044381,0.8671566003\N,0.5800878366,0.7153260288,2.0379131
525\H,0.1769311596,1.3711533609,2.7054993544\C,1.5942211471,-0.0300149
465,4.1182698881\C,0.5185724522,0.3509668812,4.9378414214\H,-0.4754998
656,0.5080903511,4.4992120528\C,0.6826571709,0.506273566,6.3132710532\
H,-0.1738429488,0.7970337219,6.9323644625\C,1.9282364139,0.2844093349,

6.9005710848\H,2.059678947,0.4105753732,7.981268131\C,3.0060506009,-0.
0981979341,6.1002394194\H,3.991225716,-0.2676400899,6.5501970185\C,2.8
404197149,-0.2530159625,4.7257846003\H,3.6982446272,-0.5287305537,4.10
11103084\C,1.2380586776,3.3696089193,1.726958748\H,1.0799668692,2.3825
875836,-0.181719939\H,2.3870988865,1.6871928106,0.8894485264\C,1.98482
3509,3.5080681027,2.916169147\C,1.7903367278,4.6017041212,3.7511802032
\C,0.8466720145,5.5794438801,3.4199045546\C,0.0992554477,5.4564964231,
2.2459146092\C,0.2893485824,4.3618692623,1.4090975417\H,-0.3013193526,
4.2635783692,0.4894471197\H,2.7194688851,2.7360187078,3.1791855308\H,2
.377849361,4.6949310478,4.6715792426\H,0.6931787297,6.4399485077,4.080
8820859\H,-0.6400905712,6.220919452,1.9824164229\\Version=ES64L-G16Rev
C.01\HF=-1685.0695171\RMSD=5.623e-09\RMSF=1.687e-06\Dipole=-0.6101857,
-0.467597,2.6885371\Quadrupole=-2.5174341,2.8829675,-0.3655334,7.68429
85,5.4834976,6.8637016\PG=C01 [X(C25H28N1O3P1Ru1)]\\@

3-21b: (*N*-benzyl-1-phenylethen-1-amine + catalyst system, X=Y=H)

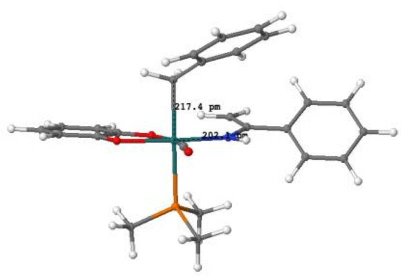

1\1\GINC-COMET-07-11\FOpt\UM06L\Gen\C25H28N1O3P1Ru1\TALIPOVM\29-Aug-20
20\0\\#P M06L/chkbasis opt(verytight) freq scf(fermi,xqc,maxcyc=200) n
osym int(grid=ultrafine) Geom(AllCheck) Guess(read) SCRF(Check)\\Title
\\0,1\Ru,0.0327885503,0.7070197456,0.2388003636\P,-1.4786725399,-1.250
9215469,0.4531519963\O,-2.0604166255,2.6966053625,0.9931328329\O,1.358
5405163,-0.7331636703,-0.7392706449\O,-0.4075273146,0.9308890531,-1.76
45484587\C,-3.0110304068,-1.0412439622,1.4196003123\C,-0.6451333452,-2
.6573814083,1.2581780341\C,-2.0508947018,-1.9377959293,-1.1355966556\C
,-1.2194469307,1.9345048212,0.7347919962\C,1.2874900957,-0.6695172243,
-2.0228993616\C,2.0681381072,-1.4666328914,-2.898666677\C,1.9008861436
,-1.3507497832,-4.2660630118\H,2.5128925902,-1.9619524409,-4.939775728
3\C,0.9517810928,-0.4542850123,-4.8175660651\C,0.1648422865,0.33212371
14,-3.9978438349\H,-0.5752366321,1.0304640689,-4.4036162954\C,0.315883
4516,0.2468000878,-2.5933164793\H,-2.7631960275,-0.6925304776,2.437425
5205\H,-3.5859598476,-1.9814163605,1.4974776516\H,-3.6472971757,-0.271
6046693,0.9501695854\H,-0.3679544119,-2.3868270486,2.2915815447\H,0.28
6765021,-2.8865078539,0.7139171843\H,-1.2857108368,-3.5572192608,1.282
605045\H,-2.6274475859,-1.1757612203,-1.6867015783\H,-2.680358399,-2.8
344752348,-0.9927079049\H,-1.1812296189,-2.2133747228,-1.7577230112\H,

0.8451717307,-0.3862066948,-5.906086871\H,2.7988664057,-2.1586911401,-
2.4659406695\H,3.4168144548,-1.3190546494,2.6296820819\C,2.6248034924,
-0.793131934,2.0862657816\C,1.6642494945,3.2239516929,1.056808841\H,2.
6251375926,-0.8279210974,0.9921756996\C,1.6279413802,-0.1510484139,2.7
791823022\H,2.5547730577,1.4945286447,0.1405074515\C,1.6593467123,2.13
84162718,0.0603724983\N,0.5771162573,0.4643549714,2.1701320661\H,1.572
368376,2.513201099,-0.9756957872\H,0.0396653546,1.0091985289,2.8466023
889\C,1.6616747468,-0.0951825746,4.2651616889\C,0.4808897099,-0.206587
9094,5.0162479534\H,-0.4772471735,-0.3656903255,4.5043836092\C,0.50982
62657,-0.1505466742,6.4085734297\H,-0.4225319117,-0.2501810116,6.97599
91178\C,1.7213478364,0.024792406,7.0771895789\H,1.7450692318,0.0738666
267,8.1717215288\C,2.9028330135,0.1402728346,6.3427812941\H,3.85816006
59,0.2885215104,6.8592290881\C,2.8734055979,0.0792800436,4.9514731077\
H,3.8027760859,0.1926561766,4.3802270048\C,2.3787785055,3.1058842862,2
.2651760028\C,0.9150605712,4.4014660198,0.8646713997\C,0.8703372792,5.
4005709346,1.8328486896\C,2.3311655707,4.101670667,3.2395606125\C,1.57
40361118,5.2559516048,3.0319958911\H,2.9914032251,2.2100512378,2.43197
34202\H,0.3467134142,4.5218451006,-0.0676152026\H,0.2775116883,6.30558
57028,1.6514316018\H,1.5363031879,6.0411114769,3.796153907\H,2.8977972
132,3.976228455,4.1711041331\\Version=ES64L-G16RevC.01\HF=-1685.105171
1\S2=0.647919\S2-1=0.\S2A=0.053605\RMSD=9.476e-09\RMSF=1.112e-06\Dipol
e=-1.044887,-2.5111266,0.6974784\Quadrupole=-0.8911454,-12.5040508,13.
3951963,0.9905467,0.6800306,-1.3656514\PG=C01 [X(C25H28N1O3P1Ru1)]\\@

TS-3-21b (3-21b→TS-3-21b): (*N*-benzyl-1-phenylethen-1-amine + catalyst system, X=Y=H)

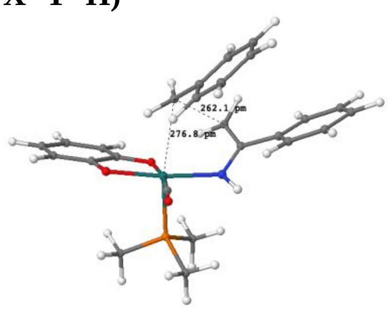

1\1\GINC-COMET-07-24\FTS\RM06L\Gen\C25H28N1O3P1Ru1\TALIPOVM\29-Aug-
202
0\0\\#P M06L/chkbasis opt(verytight,ts,calcfc,noeigentest) freq scf(fe
rmi,xqc,maxcyc=200) nosym int(grid=ultrafine) Geom(AllCheck) Guess(rea
d) SCRF(Check)\\Title\\0,1\Ru,4.2977258143,7.1166793826,3.3430558622\P
,2.9657060683,5.2720264674,3.2804275176\O,2.0306948202,8.8278692826,4.
3014094503\O,5.7583141052,5.9381095488,2.3537436776\O,4.0322751279,7.6
645559887,1.3761398553\C,1.4619165961,5.2989894451,4.2985287353\C,3.87
44045181,3.7981839304,3.8218751323\C,2.410616325,4.8998949157,1.594335
5345\C,2.935506231,8.181823256,3.9498933947\C,5.8010381119,6.156284142

5,1.0607456316\C,6.6757036237,5.4875940539,0.1833992531\C,6.6629978914
,5.7883642394,-1.1762791626\H,7.3610181122,5.2774101678,-1.850284523\C
,5.7676943234,6.7404006926,-1.6918334448\C,4.8761567927,7.3979704183,-
0.849232334\H,4.1645398452,8.1380337394,-1.2336878496\C,4.8788319549,7
.1178735316,0.5295586104\H,1.7272561491,5.4801552634,5.3542135316\H,0.
9215676744,4.3384174862,4.2311380489\H,0.7924905896,6.1106066152,3.968
7366642\H,4.1886893041,3.9277201629,4.8706655631\H,4.7825449775,3.6950
073986,3.2059419287\H,3.2525340244,2.8897386547,3.7307994976\H,1.77800
95309,5.7202544177,1.2183330426\H,1.8465053446,3.9510395906,1.56051599
3\H,3.2882944883,4.8204844579,0.9290092747\H,5.7689958972,6.9656700929
,-2.7647934323\H,7.3714661691,4.7479915273,0.5971114528\H,8.0991882317
,6.7524305026,5.3876124619\C,7.0884318972,6.5689965284,5.0068318734\C,
6.4235998837,9.6581433411,4.7616932438\H,6.9792287836,6.1144630576,4.0
216428327\C,5.9894937517,6.73789602,5.8388993924\H,7.491690098,8.40661
63283,3.313870006\C,6.5129602534,8.7452472731,3.6649943519\N,4.7513481
505,6.6972919894,5.3240804867\H,5.7650418169,8.8447694754,2.8570342861
\H,4.0243870819,6.8165315729,6.0293790024\C,6.1715020887,7.14797997,7.
250767061\C,5.269986011,8.0391155716,7.8571809397\C,5.4724871451,8.485
2099628,9.1606566065\C,6.5799621343,8.047577176,9.8881059909\C,7.48339
54503,7.1593931859,9.3003504301\C,7.2811605887,6.7152880489,7.99629647
61\H,7.987565881,6.0079912326,7.5455567144\H,4.4254992284,8.4370608249
,7.2800869421\H,4.7679349604,9.1976824071,9.6055377683\H,6.7422024329,
8.401216293,10.9128685488\H,8.3529345678,6.8058418942,9.8666062023\C,5
.2465450988,10.405843684,5.0074162326\C,7.509978873,9.8510038222,5.653
6736332\C,7.4245088598,10.7396472068,6.7134807094\C,5.1645435557,11.29
8572284,6.0707209257\C,6.2482597289,11.4680467945,6.9352728398\H,8.279
8746846,10.8631390747,7.3885319012\H,6.1793790692,12.1619197391,7.7809
324109\H,8.4286461361,9.2707357472,5.4997524965\H,4.3943984133,10.2937
847942,4.3264993374\H,4.2417807329,11.8697353275,6.2271609901\\Version
=ES64L-G16RevC.01\HF=-1685.0759273\RMSD=5.111e-09\RMSF=9.586e-07\Dipol
e=-1.043133,-1.5677281,1.9421431\Quadrupole=-4.2901403,-31.2293855,35.
5195258,-19.6005788,16.135455,20.5572816\PG=C01 [X(C25H28N1O3P1Ru1)]\\
@

3-22b: (*N*-benzyl-1-phenylethen-1-amine + catalyst system, X=Y=H)

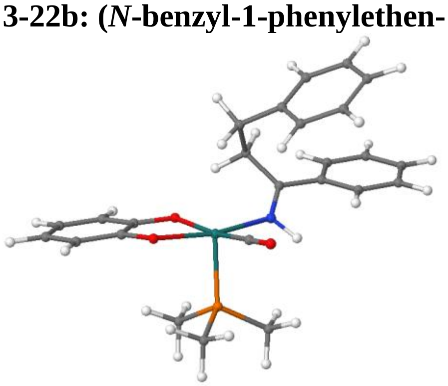

1\1\GINC-COMET-07-40\FOpt\RM06L\Gen\C25H28N1O3P1Ru1\TALIPOVM\29-Aug-20
20\0\\#P M06L/chkbasis opt(verytight) freq scf(fermi,xqc,maxcyc=200) n
osym int(grid=ultrafine) Geom(AllCheck) Guess(read) SCRF(Check)\\Title
\\0,1\Ru,-0.2312873787,0.2927805343,0.0727248499\P,-1.7600184466,-1.33
57924265,0.2107605724\O,-2.3049594258,2.2845848642,0.9732743917\O,1.31
77233564,-0.8055822197,-0.719402899\O,-0.5996051161,0.5302202731,-1.94
25647611\C,-2.2372903726,-1.9158976449,1.8719158922\C,-1.2006713398,-2
.8335361805,-0.6524324542\C,-3.3409215144,-0.9228826239,-0.5854116318\
C,-1.4931299271,1.5136860247,0.636374186\C,1.2343385013,-0.94243616,-2
.0374734226\C,2.0915125312,-1.7612005189,-2.7870383006\C,1.929229115,-
1.8646686684,-4.1704684216\H,2.6074870019,-2.5010629323,-4.7517239253\
C,0.903951352,-1.1619791428,-4.8144157106\C,0.032865443,-0.3522057576,
-4.0828080589\H,-0.7732647548,0.2059779258,-4.5744212908\C,0.191441488
3,-0.2238395737,-2.6934135637\H,-1.3562913431,-2.3123373558,2.40436469
29\H,-2.9971276551,-2.715378198,1.8079540275\H,-2.6580589772,-1.081367
358,2.459221694\H,-0.2981908331,-3.2371709205,-0.1651953252\H,-0.93339
01702,-2.5805593469,-1.6940184238\H,-1.9929635889,-3.6032394648,-0.660
7030395\H,-3.819928771,-0.07952554,-0.0603740044\H,-4.0282161955,-1.78
7461771,-0.585048332\H,-3.1441779352,-0.6085713165,-1.6238478293\H,0.7
798989576,-1.2474924385,-5.9008992978\H,2.8869866796,-2.3074296782,-2.
2650007626\H,3.8058602266,0.4717208337,2.1029848153\C,2.8423775199,0.5
672700725,1.5759438038\H,2.8340122487,-0.1443205162,0.7343131536\C,1.7
092315779,0.2683871741,2.5141988117\C,2.7087568449,1.9997899583,1.0276
63235\N,0.5124113433,0.1175001056,2.0370239174\H,-0.1801198762,-0.0249
654273,2.778025842\C,2.4977819466,3.0112198583,2.1213660685\C,1.250869
485,3.6197283318,2.3087655056\H,0.440442915,3.4135184046,1.5964679982\
C,1.0267341667,4.4790158008,3.3860912688\H,0.0435555403,4.9478415404,3
.5116498852\C,2.0488588197,4.7388589445,4.2984958336\H,1.8744127199,5.
4107954952,5.1469224012\C,3.298935669,4.1419691818,4.1209582\H,4.10997
96613,4.3438662976,4.8306919969\C,3.5188574191,3.2884717853,3.04177589
94\H,4.5033047644,2.8181417794,2.9137772045\H,1.8612653951,2.039079781
9,0.3116818865\H,3.614345321,2.2290599938,0.4364488754\C,1.9417130684,
0.3058138039,3.9716686342\C,3.1281221315,-0.1908018564,4.537839917\H,3
.8845965911,-0.6608118891,3.8993257687\C,3.3429364413,-0.11942839,5.91
15806607\H,4.2675781624,-0.5246946963,6.3375652855\C,2.3891229346,0.47
00809134,6.7426244105\H,2.5680162262,0.5412876609,7.8213701297\C,1.210
8411572,0.9775075095,6.1925528257\H,0.4669658762,1.4619134635,6.834915
2287\C,0.986311752,0.890808646,4.8221762359\H,0.07972127,1.3393230539,
4.3966054489\\Version=ES64L-G16RevC.01\HF=-1685.161995\RMSD=7.020e-09\
RMSF=5.326e-07\Dipole=-0.4354104,-1.3000696,3.8569295\Quadrupole=5.136
3366,-9.0880154,3.9516788,8.3955383,10.2702352,1.1744259\PG=C01 [X(C25
H28N1O3P1Ru1)]\\@

3-20c: (X=CF3)

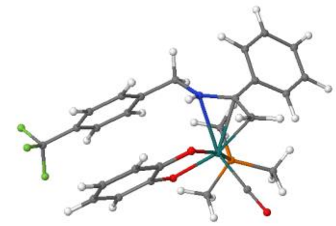

1\1\GINC-COMET-05-06\FOpt\RM06L\Gen\C26H27F3N1O3P1Ru1\TALIPOVM\30-
Aug-
2020\0\\#P M06L/chkbasis opt(verytight) freq scf(fermi,xqc,maxcyc=200)
nosym int(grid=ultrafine) Geom(AllCheck) Guess(read) SCRF(Check)\\Tit
le\\0,1\Ru,4.1326425686,7.0854542316,2.7099388046\P,2.8921133235,5.599
9819379,4.0783733776\O,1.6673690596,7.157708359,1.035914173\O,5.060227
6051,5.3619085301,2.0368787933\O,5.5559515207,7.9210903612,1.402313434
1\C,1.098822673,5.862106066,4.3319820653\C,3.4713865818,5.2198246622,5
.7714084204\C,2.9006631601,3.9556054249,3.2954721613\C,2.6408882348,7.
1097229791,1.6747755456\C,6.0382632427,5.6180774303,1.1676398664\C,6.8
009362114,4.5993731945,0.5812562073\C,7.8367680084,4.9113650168,-0.304
5520978\H,8.4397938944,4.1050683682,-0.7390939367\C,8.1052067077,6.243
1874206,-0.6273206358\C,7.3330558832,7.2701075402,-0.0729492865\H,7.52
18106676,8.3214740083,-0.3242498012\C,6.3023288675,6.9737497314,0.8289
843102\H,0.8987012613,6.700896217,5.0158920306\H,0.6461231695,4.952678
7961,4.7650248807\H,0.6062859935,6.0720976751,3.3678266158\H,3.4596176
819,6.1123513265,6.4190658848\H,4.498940327,4.8220114335,5.7330766885\
H,2.8238083531,4.4491484626,6.2267353702\H,2.448934491,4.0211920117,2.
2916830965\H,2.3318973954,3.2326313494,3.9063528601\H,3.9381282899,3.6
156233813,3.1594841557\H,6.2831945848,8.3806059492,3.3248563101\C,3.96
52739299,9.2069261039,3.1852279154\N,5.7784170727,8.0006603418,4.13550
51477\C,4.5093936994,8.5701729511,4.3285220223\C,6.5941150701,7.224583
454,5.0618748922\H,4.636357392,9.6365770212,2.4302017273\H,3.007837682
6,9.7244436292,3.3067999686\H,6.5887421146,3.5588012196,0.8574641485\H
,8.9167342643,6.4891798034,-1.3234041156\C,7.4883630205,6.2774290194,4
.3049579599\C,7.397404497,4.8945584699,4.4918698113\H,6.6684752434,4.4
862349878,5.2022412144\C,8.2219703734,4.0267050415,3.7844670088\H,8.13
51511364,2.9440627771,3.9296792108\C,9.1521770708,4.535086376,2.874649
0144\C,10.0198530417,3.5722945779,2.1226636862\C,9.25815608,5.91058385
79,2.6805887412\H,9.9719637261,6.3109614019,1.9551072313\C,8.428207466
6,6.771751334,3.3930634772\H,8.5207756906,7.8531226336,3.2256752343\H,
5.9258911173,6.6724115355,5.7425755845\H,7.2112185564,7.8981878052,5.6
918035838\C,3.8616723184,8.6437041446,5.6536578912\C,4.5933592144,8.75
1757224,6.8469056661\H,5.6857709139,8.7821934864,6.8261677931\C,3.9417
345302,8.864277415,8.0758635389\H,4.535820281,8.9486077586,8.992720094
5\C,2.5501774377,8.8797648887,8.1401949138\H,2.0412570362,8.9612492605
,9.1068134011\C,1.8104858696,8.8098908241,6.9560971017\H,0.715175492,8
.8405035661,6.9880023514\C,2.4589173983,8.7009083712,5.7323180194\H,1.

87094249,8.6456249727,4.8090652066\F,10.7362811751,4.161002877,1.15856
35265\F,9.2979984258,2.5931653219,1.5484148314\F,10.8964794141,2.95643
36829,2.9437929058\\Version=ES64L-G16RevC.01\HF=-2021.888525\RMSD=7.25
8e-09\RMSF=2.238e-06\Dipole=-2.1625039,0.8604916,4.7881383\Quadrupole=
-55.3732165,10.3211543,45.0520621,-5.4258216,28.9924409,63.8609022\PG=
C01 [X(C26H27F3N1O3P1Ru1)]\\@

TS(3-20c→TS3-20c): (X=CF3)

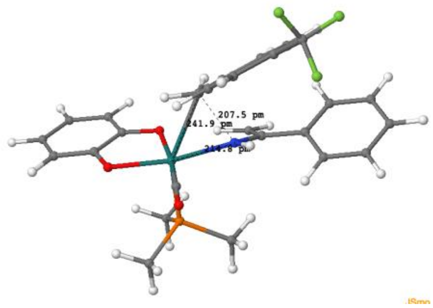

1\1\GINC-COMET-03-59\FTS\RM06L\Gen\C26H27F3N1O3P1Ru1\TALIPOVM\02-
Sep-2
020\0\\#P M06L/chkbasis opt(verytight,ts,calcfc,noeigentest) freq scf(
fermi,xqc,maxcyc=200) nosym int(grid=ultrafine) Geom(AllCheck) Guess(r
ead) SCRF(Check)\\Title\\0,1\Ru,-0.4115673092,0.7053541961,0.032719418
1\P,-1.5783153984,-1.2205169376,0.2953120522\O,-2.8055443035,2.2475320
993,0.9903708506\O,1.2265929755,-0.2311284227,-0.8655277955\O,-0.96381
91471,0.7685750247,-1.9663105234\C,-3.2626630734,-1.1753514755,-0.3829
493612\C,-1.7779183183,-1.7516150527,2.0213597741\C,-0.7864867432,-2.6
20757074,-0.5452595017\C,-1.8629139191,1.6549833762,0.6399108846\C,1.0
909687719,-0.3629221714,-2.169108203\C,2.0293952721,-1.024728417,-2.98
10047385\C,1.7994121213,-1.1578989225,-4.3484260558\H,2.5401991757,-1.
6663585528,-4.9769323376\C,0.6247114708,-0.6493370473,-4.9253677009\C,
-0.3267783894,-0.0037725765,-4.1398508262\H,-1.2483924739,0.3998006948
,-4.5756523304\C,-0.1041315262,0.1638218787,-2.7601680926\H,-3.8659652
453,-0.4199141178,0.1475405017\H,-3.754986467,-2.1596796484,-0.2907104
108\H,-3.213447524,-0.8872520565,-1.4461156396\H,-2.3146291406,-0.9754
998771,2.5929373826\H,-0.7853046484,-1.8981787504,2.481194411\H,-2.346
4660576,-2.6968034376,2.078749976\H,-0.6762488742,-2.3963012236,-1.620
6500699\H,-1.3914498262,-3.5373133101,-0.428547349\H,0.220318641,-2.78
61884199,-0.1287428348\H,0.4536964897,-0.7603131352,-6.0027573126\H,2.
9383578336,-1.42237939,-2.5140159175\H,2.7574815087,-1.7267386937,2.49
77285835\C,2.0863580123,-1.0585959597,1.9484174254\H,2.0084788652,-1.1
55067954,0.8598581636\C,1.3764596309,-0.1037591497,2.6159852598\C,1.31
54051604,2.221068382,0.7904000161\N,0.4911736408,0.7354836087,1.981150
134\H,0.0588602395,1.3871518811,2.6343285973\C,1.5508049494,0.11987383
44,4.0773955481\C,0.4652540035,0.4856043204,4.8905796884\H,-0.54168039
44,0.5612639559,4.4595213848\C,0.6378994342,0.7307161351,6.2517505215\

H,-0.2252992578,1.0097792336,6.8667314943\C,1.9019034853,0.6148460425,
6.8300445604\H,2.0403765695,0.8141066587,7.898710943\C,2.9888389594,0.
2430338011,6.0368551481\H,3.9873284068,0.154327098,6.4804653492\C,2.81
45273172,-0.002479463,4.6767592289\H,3.678449527,-0.2664345033,4.05507
03317\C,1.2175972577,3.3317559252,1.717607439\H,0.8930396255,2.4391869
351,-0.2204515725\H,2.2648315258,1.67647387,0.7230204059\C,2.103130346
7,3.4180646186,2.8106929675\C,1.9964438616,4.4472673433,3.7366460086\C
,1.0001810314,5.4166697979,3.5872619263\C,0.1155709154,5.3502625729,2.
5037532101\C,0.2207826302,4.3190630301,1.5812188404\H,-0.4779150424,4.
2676945429,0.7372433461\H,2.8805832602,2.6540441798,2.9318343975\H,2.6
892106568,4.4989434329,4.5823301456\C,0.8434991905,6.5354619781,4.5715
033997\H,-0.6611944772,6.1142314998,2.3867223569\F,0.8876808615,7.7355
127151,3.9661583759\F,1.7941368652,6.5289715367,5.514455073\F,-0.34351
29333,6.4747295402,5.2028730522\\Version=ES64L-G16RevC.01\HF=-2021.823
6631\RMSD=6.242e-09\RMSF=1.780e-06\Dipole=-0.4850654,-1.7771924,1.7313
066\Quadrupole=8.6386,-8.5157748,-0.1228252,7.1786965,4.8333793,-7.999
5013\PG=C01 [X(C26H27F3N1O3P1Ru1)]\\@

3-20c: (X=CF3)

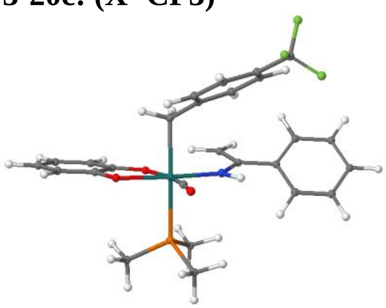

1\1\GINC-COMET-05-37\FOpt\UM06L\Gen\C26H27F3N1O3P1Ru1\TALIPOVM\30-Aug-
2020\0\\#P M06L/chkbasis opt(verytight) freq scf(fermi,xqc,maxcyc=200)
nosym int(grid=ultrafine) Geom(AllCheck) Guess(read) SCRF(Check)\\Tit
le\\0,1\Ru,0.0340372386,0.7122301754,0.2488170785\P,-1.4791581715,-1.2
31990116,0.4571866291\O,-2.0610179057,2.7013323451,0.9996195002\O,1.35
90321453,-0.7311789858,-0.7253349966\O,-0.4063320744,0.9311725849,-1.7
580288468\C,-3.0080338511,-1.020246231,1.4274657875\C,-0.6454730386,-2
.642970441,1.2528187075\C,-2.0559397838,-1.9056811919,-1.1347997712\C,
-1.2209958139,1.9381105666,0.7429552562\C,1.2909700732,-0.6687062281,-
2.0088713229\C,2.0747077222,-1.466581456,-2.8814555106\C,1.9110390275,
-1.3519995719,-4.2488948373\H,2.5248758445,-1.9635306577,-4.9205210904
\C,0.9627102926,-0.4559961636,-4.8042043045\C,0.1730981232,0.331020232
3,-3.9885644576\H,-0.5659675765,1.0284772875,-4.3974781503\C,0.3198076
902,0.2472097729,-2.58302473\H,-2.758255576,-0.6755072688,2.4461012343
\H,-3.5839450396,-1.9599031074,1.5029505412\H,-3.6441356448,-0.2486530
979,0.9611506864\H,-0.3697914897,-2.3802014154,2.2885401707\H,0.286873

9153,-2.8680229921,0.707689173\H,-1.2862106796,-3.5427222865,1.2699762
713\H,-2.6300066979,-1.137757495,-1.6802074742\H,-2.6895651203,-2.7998
232294,-0.9952217088\H,-1.1889668328,-2.1825528376,-1.7599886639\H,0.8
594738094,-0.3895379646,-5.893097988\H,2.8043806995,-2.1578437103,-2.4
458890576\H,3.4348258007,-1.2873433943,2.6330367888\C,2.6385841953,-0.
7650999798,2.0923436588\C,1.6604040596,3.229537384,1.0400374993\H,2.64
08107906,-0.792903366,0.9980765523\C,1.6330766215,-0.1389566402,2.7885
115941\H,2.5609853823,1.5095378821,0.1218193277\C,1.6620052975,2.14808
01733,0.0449314058\N,0.5791118685,0.4706256741,2.1795053274\H,1.562690
2939,2.5219771935,-0.9896943864\H,0.0280609532,0.9979231109,2.85910307
72\C,1.6630442442,-0.0911082851,4.2747340217\C,0.4814417913,-0.2130304
826,5.0229180811\H,-0.4750043194,-0.376833406,4.5094055044\C,0.5073898
491,-0.1616185995,6.4154181381\H,-0.4253794693,-0.268633932,6.98065448
36\C,1.7164507156,0.0192286469,7.0868818088\H,1.7375623536,0.065570489
8,8.1814981851\C,2.898719675,0.1444076621,6.3554725056\H,3.851898946,0
.2971423645,6.8743959048\C,2.8724973934,0.0880720298,4.9639404519\H,3.
8027581497,0.2088899668,4.3956401424\C,2.374294405,3.1122239996,2.2516
390039\C,0.9049343518,4.4034941562,0.8522070793\C,0.84623069,5.3974844
701,1.8220154179\C,2.3170423977,4.0984333255,3.2274738957\C,1.54753493
85,5.2495185012,3.0223944229\H,2.9933519197,2.2217613175,2.4183128939\
H,0.3376189637,4.5270478938,-0.0793205274\H,0.2472282824,6.2973865265,
1.6480093775\C,1.5169397519,6.2972631711,4.0848642835\H,2.8792180338,3
.9792108668,4.1621180533\F,0.6634120092,7.294802971,3.8075887845\F,2.7
279510681,6.861854612,4.2760565254\F,1.1567073106,5.7915371794,5.28240
25919\\Version=ES64L-G16RevC.01\HF=-2021.8634583\S2=0.672746\S2-1=0.\S
2A=0.059107\RMSD=4.176e-09\RMSF=1.262e-06\Dipole=-1.1377285,-3.7200539
,-0.3031565\Quadrupole=9.067006,-22.74467,13.677664,-2.6912182,-2.0871
157,-17.0661072\PG=C01 [X(C26H27F3N1O3P1Ru1)]\\@

3-20c: (X=OMe)

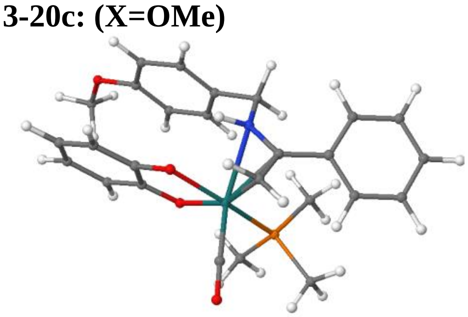

1\1\GINC-COMET-02-26\FOpt\RM06L\Gen\C26H30N1O4P1Ru1\TALIPOVM\30-Aug-20
20\0\\#P M06L/chkbasis opt(verytight) freq scf(fermi,xqc,maxcyc=200) n
osym int(grid=ultrafine) Geom(AllCheck) Guess(read) SCRF(Check)\\Title
\\0,1\Ru,4.1813110483,7.0085458737,2.7486856934\P,2.9018015274,5.58433
50747,4.1453572404\O,1.7537886631,7.0540652837,1.0211943405\O,5.087559
4479,5.2524563801,2.1203006766\O,5.6436388147,7.7926784922,1.455832409

1\C,1.100592421,5.8564656213,4.3243785666\C,3.4156196545,5.277925596,5
.8751823052\C,2.9331242052,3.9034748672,3.4428582881\C,2.7137010605,7.
0140672832,1.6818102926\C,6.0769650212,5.4771173063,1.2563546564\C,6.8
13751475,4.4334397902,0.6783609057\C,7.8570402811,4.7082513582,-0.2108
98732\H,8.4384780869,3.8826958724,-0.6405524968\C,8.1584089379,6.02924
3181,-0.5473110044\C,7.4105247438,7.0801390348,-0.0044660969\H,7.62474
6732,8.1235028963,-0.2683163912\C,6.3747752773,6.8205484901,0.90208334
95\H,0.8787336878,6.7373789124,4.9458240468\H,0.6334198226,4.976000070
4,4.7998501776\H,0.6400552302,6.0045884123,3.3333268288\H,3.3733905985
,6.1958873669,6.484339765\H,4.4462812825,4.8866948204,5.8992843614\H,2
.7526268489,4.5227198548,6.3343073687\H,2.5267792433,3.9216006203,2.41
80159404\H,2.3344714443,3.2131599923,4.0631258122\H,3.9731214425,3.552
343841,3.3692981968\H,6.3230058957,8.3002364123,3.3738459652\C,4.01739
62364,9.1470884738,3.1485016927\N,5.7968629953,7.9702307832,4.19351763
99\C,4.5301660081,8.5535485626,4.3285976162\C,6.5977798985,7.233007411
8,5.1700245251\H,4.7104650011,9.5442928474,2.3957334018\H,3.0594457973
,9.6723074593,3.2240761933\H,6.558396475,3.4023161935,0.9562364174\H,8
.9756605108,6.248566875,-1.2454310983\C,7.5239429589,6.2923945273,4.45
37058487\C,7.3112522729,4.913684905,4.4470164288\H,6.4681144992,4.4893
238875,5.0068568944\C,8.1413039549,4.0525382924,3.7314078114\H,7.93358
22084,2.9785544571,3.7400464757\C,9.2030003741,4.5754506214,2.98310681
58\O,10.0472997742,3.8316280751,2.2361824543\C,9.4331046913,5.95869241
24,2.9857092316\H,10.2616737157,6.3521921446,2.3884995785\C,8.60406004
43,6.7977988226,3.7135250723\H,8.7963307629,7.8796499496,3.6988649329\
H,5.9154201325,6.6877663789,5.8430643986\H,7.1784360296,7.9400965755,5
.7971355476\C,3.8422768451,8.6748786331,5.6302912511\C,4.5374377281,8.
8124829868,6.8422852093\H,5.6299351199,8.8306044239,6.8550711894\C,3.8
494534111,8.9671635154,8.0466293664\H,4.4161636308,9.0732508851,8.9784
716933\C,2.4568230394,8.9958963683,8.0678279356\H,1.9191007074,9.11009
81456,9.0154130446\C,1.7533786689,8.8962560545,6.8638701478\H,0.657846
4189,8.9356042281,6.8609109836\C,2.4381212798,8.7458619868,5.664533658
1\H,1.8777376423,8.6661747492,4.7260868822\C,9.7907818252,2.4571958258
,2.118350472\H,9.8800019503,1.937503712,3.0921938917\H,10.5487153004,2
.0556524957,1.4299050811\H,8.7842291966,2.2685536292,1.6982888493\\Ver
sion=ES64L-G16RevC.01\HF=-1799.5518969\RMSD=7.161e-09\RMSF=5.609e-07\D
ipole=-1.4927613,-0.3173901,4.2632773\Quadrupole=-33.3758944,-5.540793
5,38.9166879,-21.3842499,24.5840716,53.9401143\PG=C01 [X(C26H30N1O4P1R
u1)]\\@

TS(6→6’): (X= OMe)

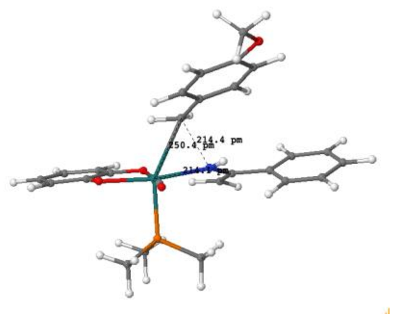

1\1\GINC-COMET-02-31\FTS\RM06L\Gen\C26H30N1O4P1Ru1\TALIPOVM\31-Aug-202
0\0\\#P M06L/chkbasis opt(verytight,ts,calcfc,noeigentest) freq scf(fe
rmi,xqc,maxcyc=200) nosym int(grid=ultrafine) Geom(AllCheck) Guess(rea
d) SCRF(Check)\\Title\\0,1\Ru,-0.3431232995,0.7292441693,0.0978246814\
P,-1.5740662287,-1.1430199596,0.3398276997\O,-2.662630073,2.3428003089
,1.1155272751\O,1.261041093,-0.2357869437,-0.8304344418\O,-0.897836558
1,0.8637266214,-1.9043958348\C,-3.243961718,-1.0470940405,-0.372092874
5\C,-1.8325412873,-1.6700804455,2.060954484\C,-0.8166751272,-2.5733998
933,-0.4837343267\C,-1.7489639974,1.718887669,0.7380359218\C,1.1090410
258,-0.3473530404,-2.1357425359\C,2.0146750513,-1.0341986514,-2.962966
8554\C,1.7744836046,-1.1380709121,-4.3326265333\H,2.491712118,-1.66702
02682,-4.971785342\C,0.6200443526,-0.5736499274,-4.8948279375\C,-0.300
5832774,0.0982685776,-4.0923629326\H,-1.2073360269,0.545804028,-4.5171
216816\C,-0.0668731913,0.2354302628,-2.7115233963\H,-3.8283209673,-0.2
623580935,0.136845615\H,-3.7754519629,-2.0108490869,-0.2784484585\H,-3
.1630611963,-0.7735314468,-1.4372056694\H,-2.3627980365,-0.8789040319,
2.6181361655\H,-0.8555462159,-1.8416628885,2.5452776205\H,-2.427118074
1,-2.599960093,2.1060351969\H,-0.6761719138,-2.3524574957,-1.556343112
2\H,-1.4553873493,-3.4684796603,-0.3799441785\H,0.1749857999,-2.773214
0441,-0.0463411493\H,0.4380166161,-0.6609893449,-5.9728398952\H,2.9094
024927,-1.4750294019,-2.5067571266\H,2.6993083942,-1.8823959202,2.5025
037939\C,2.0719508047,-1.1648346387,1.9636454217\H,1.9958191666,-1.232
7614382,0.8728529837\C,1.4145596379,-0.1824275578,2.6468193581\C,1.473
9457664,2.2756193349,0.8584261631\N,0.5815394755,0.7170467952,2.028877
8446\H,0.1923066557,1.3870456128,2.6907057247\C,1.5916795489,-0.015174
1585,4.1158611517\C,0.5221282857,0.38478219,4.9344463995\H,-0.47179853
3,0.5432966532,4.4959032572\C,0.6924742516,0.5568071778,6.3070978102\H
,-0.1594356335,0.8618974399,6.9257316442\C,1.9387145801,0.3334373067,6
.8926821908\H,2.0753299593,0.4730749809,7.9711099081\C,3.0104447352,-0
.0681598935,6.0934865055\H,3.9959753934,-0.2392812432,6.5421371128\C,2
.8382889397,-0.2400558252,4.7217166828\H,3.6912285718,-0.5314025956,4.
0973477051\C,1.2559847188,3.4133768416,1.7069347096\H,1.1080235205,2.3
909760115,-0.1850826624\H,2.4170788856,1.7212605804,0.9113766492\C,1.9
779357872,3.5716555099,2.9154121133\C,1.7536060448,4.6515646374,3.7455

144244\C,0.7907178989,5.621600759,3.4032459353\C,0.0596371102,5.483091
8593,2.2117296212\C,0.2925155372,4.3908945002,1.3863813625\H,-0.288903
6628,4.2848436515,0.4618689278\H,2.7240102726,2.8171835947,3.195530440
2\H,2.3100063211,4.7779222875,4.6797855069\O,0.6386131625,6.6355038033
,4.2724156047\H,-0.6942383292,6.2212211545,1.9242222253\C,-0.310469082
2,7.6363611629,3.9857892289\H,-0.2638638528,8.3528848848,4.8175942419\
H,-1.3323248208,7.2187192134,3.9235139655\H,-0.0723551648,8.1607733601
,3.0419756701\\Version=ES64L-G16RevC.01\HF=-1799.4920138\RMSD=6.053e-0
9\RMSF=1.153e-06\Dipole=-0.9044863,0.7002787,2.963368\Quadrupole=-8.54
77919,16.6464729,-8.098681,3.0103779,2.5106199,12.1569015\PG=C01 [X(C2
6H30N1O4P1Ru1)]\\@

6': (X= OMe)

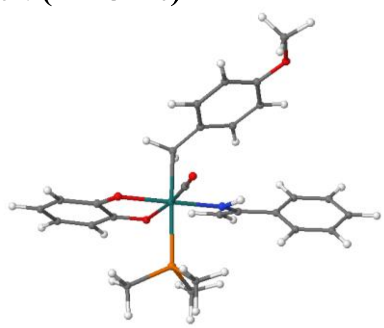

1\1\GINC-COMET-02-30\FOpt\UM06L\Gen\C26H30N1O4P1Ru1\TALIPOVM\30-Aug-20
20\0\\#P M06L/chkbasis opt(verytight) freq scf(fermi,xqc,maxcyc=200) n
osym int(grid=ultrafine) Geom(AllCheck) Guess(read) SCRF(Check)\\Title
\\0,1\Ru,0.0192275142,0.7028662846,0.2117055367\P,-1.472656065,-1.2680
058967,0.4466913886\O,-2.0777208312,2.6937794171,0.9527376577\O,1.3581
071803,-0.7308345584,-0.7515912615\O,-0.4132315529,0.9163079799,-1.791
0475116\C,-3.0109919448,-1.0568871262,1.4034807364\C,-0.6328318196,-2.
6573205064,1.2745301284\C,-2.0317183749,-1.9814380796,-1.1351351947\C,
-1.237184717,1.9290324425,0.6984604\C,1.2896335791,-0.6771779363,-2.03
67587615\C,2.075800506,-1.4762337769,-2.9050397146\C,1.9110944507,-1.3
70871369,-4.2742089\H,2.5280531808,-1.9835839967,-4.9420728862\C,0.958
8488963,-0.4838949469,-4.8335104641\C,0.165921229,0.3039092616,-4.0197
846247\H,-0.5773635283,0.9953358793,-4.431681349\C,0.3152410443,0.2292
179933,-2.6151314109\H,-2.7696972344,-0.6915326639,2.417046157\H,-3.57
9477943,-1.9999866944,1.4928631842\H,-3.6507867419,-0.2986484008,0.920
4433222\H,-0.3586296367,-2.3692752277,2.3039821906\H,0.3010647643,-2.8
898237069,0.7351955875\H,-1.2687661942,-3.5600762278,1.3117139885\H,-2
.6160213604,-1.2335344315,-1.6973133371\H,-2.6500935066,-2.8844277639,
-0.9834462347\H,-1.1563870123,-2.2531245948,-1.7510621378\H,0.85365339
41,-0.4235349813,-5.9226574556\H,2.8092949979,-2.1614682256,-2.4660217
405\H,3.4061819873,-1.2909723208,2.6320614219\C,2.6133640098,-0.773692

9931,2.0815659025\C,1.6424741105,3.2332305375,1.0445155924\H,2.6151651
667,-0.8205536407,0.9878968522\C,1.613174544,-0.1276559627,2.765654283
6\H,2.5373129555,1.5031938041,0.1349318594\C,1.6413460836,2.1455345083
,0.0510075896\N,0.5598732169,0.4766008359,2.1497261687\H,1.5572857888,
2.5161224498,-0.9869014234\H,0.0217446596,1.0288828105,2.8194456677\C,
1.6454763278,-0.0552422103,4.2511060745\C,0.4644860459,-0.1625201369,5
.0024664185\H,-0.4923778106,-0.3312183498,4.4912921095\C,0.4917465968,
-0.0898639768,6.3940814216\H,-0.4408264898,-0.1863810497,6.9617545531\
C,1.7017893623,0.0985207177,7.0617990263\H,1.724160784,0.1613064651,8.
1556653087\C,2.8835047326,0.2100702995,6.3271610733\H,3.8376281911,0.3
689088901,6.8426992139\C,2.855691511,0.1322255807,4.9366722333\H,3.785
0716204,0.2428700892,4.3648511647\C,2.3497800708,3.1221205891,2.260101
4576\C,0.8972548409,4.4093576703,0.8573024823\C,0.8406172204,5.4174631
41,1.8188810098\C,2.3005877474,4.1119751281,3.2325798311\C,1.541481962
6,5.271936737,3.0236033654\H,2.9639698995,2.2294916445,2.4368127888\H,
0.3293200115,4.5360852182,-0.0741987413\H,0.244749291,6.313701148,1.61
93310853\O,1.5476128241,6.1897565933,4.0255418242\H,2.8540869815,4.011
7023052,4.1733079875\C,0.8012973808,7.3624583758,3.8480342903\H,1.1565
140336,7.9498428409,2.9787750006\H,0.9357768781,7.9615918985,4.7608260
604\H,-0.2773548107,7.1486622161,3.7151817526\\Version=ES64L-G16RevC.0
1\HF=-1799.523566\S2=0.62997\S2-1=0.\S2A=0.049306\RMSD=9.082e-09\RMSF=
9.530e-07\Dipole=-1.2824148,-1.8017841,0.7256765\Quadrupole=-5.1119069
,-2.0582252,7.1701321,-1.0177303,-1.8014107,1.0263735\PG=C01 [X(C26H30
N1O4P1Ru1)]\\@

6: (Y=CF3)

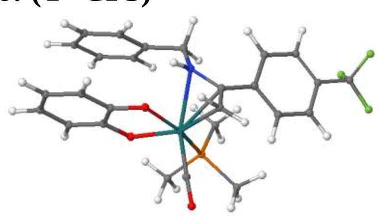

1\1\GINC-COMET-02-34\FOpt\RM06L\Gen\C26H27F3N1O3P1Ru1\TALIPOVM\30-
Aug-
2020\0\\#P M06L/chkbasis opt(verytight) freq scf(fermi,xqc,maxcyc=200)
nosym int(grid=ultrafine) Geom(AllCheck) Guess(read) SCRF(Check)\\Tit
le\\0,1\Ru,4.1204382697,7.1105883233,2.6995468435\P,2.8968832428,5.598
2677358,4.0581468464\O,1.6336278908,7.2212096059,1.0590300266\O,5.0173
49179,5.396422713,1.9731367127\O,5.5370011993,7.9599478487,1.395214166
7\C,1.1046721431,5.848781294,4.3300160884\C,3.4969041483,5.204294998,5
.7400943705\C,2.9078317781,3.9624863426,3.2587441959\C,2.6150697886,7.
1583527381,1.6837044363\C,5.991750557,5.6601205494,1.1025992922\C,6.73
81063071,4.6461321862,0.4886784588\C,7.7635498887,4.9666979613,-0.4055
941342\H,8.3501300875,4.163795601,-0.8693737418\C,8.0371281664,6.30234

59686,-0.7095364315\C,7.2829497992,7.3248216916,-0.1237971667\H,7.4767
944144,8.3791449832,-0.3579481379\C,6.2651840107,7.0189820006,0.789416
6029\H,0.9041563622,6.6797683902,5.0232544338\H,0.6610530141,4.9331738
417,4.7592831055\H,0.601957626,6.0642967808,3.3723485182\H,3.479445692
7,6.0870187872,6.4011064362\H,4.5294354524,4.8217814911,5.6838999219\H
,2.8645534516,4.4190628376,6.1919133745\H,2.4589900613,4.0364344689,2.
2543772725\H,2.3373707826,3.2351860153,3.8627892352\H,3.9456418815,3.6
233102111,3.1242575752\H,6.2874398809,8.3860944274,3.337221589\C,3.967
8122995,9.2242460755,3.195718502\N,5.7759196867,7.9938465236,4.1371386
942\C,4.5085372507,8.5676046435,4.3305682147\C,6.5860122787,7.22042984
2,5.071854988\H,4.6425500063,9.6619830704,2.4487494608\H,3.0127502632,
9.7449955944,3.3233401841\H,6.5139545806,3.6031618671,0.745102847\H,8.
8379527455,6.5551818532,-1.4155015912\C,7.4840591659,6.2582874093,4.33
88226765\C,7.46248896,4.8917849667,4.6330451209\H,6.7816449817,4.51203
94897,5.4058502204\C,8.3050170069,4.0050295871,3.9618547219\H,8.271480
557,2.9359927769,4.2015718375\C,9.1800003958,4.477636682,2.9851404957\
C,9.2133642645,5.8390481644,2.6856534711\H,9.8858254281,6.2169349795,1
.9079341244\C,8.3723329244,6.7212306446,3.35877592\H,8.4142382293,7.79
00786036,3.1084532287\H,5.9114157236,6.6782232103,5.7545557349\H,7.198
1887263,7.9009675636,5.7000577233\C,3.8571484576,8.6383600324,5.652906
1302\C,4.5856277444,8.7489646619,6.8499557095\H,5.6774489302,8.7825046
063,6.8343997381\C,3.9335402193,8.856994015,8.0738402466\H,4.519903610
4,8.942730368,8.9956095195\C,2.538586709,8.8669091902,8.1335853073\C,1
.8720439772,8.9655061829,9.4721826372\C,1.8002005884,8.7978079337,6.94
91876669\H,0.7064372513,8.8247638963,6.9822319629\C,2.4550117809,8.692
1298111,5.729686537\H,1.8672286556,8.6367531036,4.8068450916\H,9.83135
75022,3.7811318705,2.444804022\F,0.5370010971,8.99371317,9.3782786074\
F,2.2522874195,10.0724855159,10.1326282061\F,2.1957455063,7.9238423024
,10.2600921521\\Version=ES64L-G16RevC.01\HF=-2021.8833074\RMSD=5.483e-
09\RMSF=1.663e-06\Dipole=-0.6877164,-0.2616849,3.0375818\Quadrupole=-1
0.3497151,-2.3965905,12.7463056,-4.4503251,27.8316293,31.9807054\PG=C0
1 [X(C26H27F3N1O3P1Ru1)]\\@

TS(6→6'): (Y=CF3)

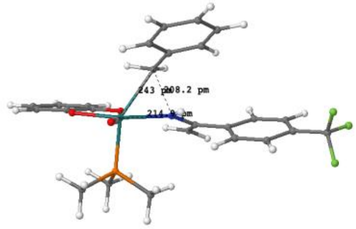

1\1\GINC-COMET-02-58\FTS\RM06L\Gen\C26H27F3N1O3P1Ru1\TALIPOVM\31-
Aug-2
020\0\\#P M06L/chkbasis opt(verytight,ts,calcfc,noeigentest) freq scf(
fermi,xqc,maxcyc=200) nosym int(grid=ultrafine) Geom(AllCheck) Guess(r

ead) SCRF(Check)\\Title\\0,1\Ru,-0.2212807326,0.7545974343,0.050603208
9\P,-1.3581869801,-1.194122108,0.254459318\O,-2.6484209407,2.223470413
,1.0389648474\O,1.4343910605,-0.1273400528,-0.8707216643\O,-0.77156489
58,0.8641872389,-1.9463563265\C,-3.0373336105,-1.1564379483,-0.4374841
767\C,-1.5671828638,-1.7742906175,1.9640869747\C,-0.5388848624,-2.5606
186943,-0.6149967682\C,-1.691992007,1.6605797073,0.6770898325\C,1.2998
589245,-0.2304609372,-2.1779440331\C,2.2473018501,-0.8579152507,-3.005
9003462\C,2.0188811868,-0.9613247864,-4.3767415269\H,2.7673588341,-1.4
42888015,-5.0172959435\C,0.8366735031,-0.4572988577,-4.9406495664\C,-0
.1241546552,0.1541329764,-4.1384107389\H,-1.0524763801,0.5539124277,-4
.5635772516\C,0.097129224,0.2915105643,-2.7556189926\H,-3.655864435,-0
.423539101,0.1069304273\H,-3.5162222429,-2.1497242333,-0.3754489273\H,
-2.9827131545,-0.8392184641,-1.49208343\H,-2.1205932258,-1.0210784538,
2.5503443222\H,-0.5771464254,-1.9201762682,2.4296625937\H,-2.123221977
6,-2.728224683,1.9913250222\H,-0.4210487368,-2.3056757141,-1.682777041
2\H,-1.1322931193,-3.48814072,-0.5295367652\H,0.4660982546,-2.72352048
74,-0.1930748058\H,0.6662123109,-0.5443876994,-6.0203715133\H,3.162785
6622,-1.2528056875,-2.5492235606\H,2.9612981847,-1.7059560848,2.438561
5868\C,2.2896220637,-1.0205053674,1.9120566282\H,2.2226654849,-1.07241
59959,0.8197475064\C,1.5586938866,-0.1048045443,2.6107499635\C,1.45629
01633,2.3094746147,0.8696872384\N,0.6697522995,0.7520954387,2.00606916
93\H,0.225255916,1.3771222437,2.676532398\C,1.7098378364,0.0345263162,
4.0846490174\C,0.6136018141,0.3630457217,4.9020420672\H,-0.3834639158,
0.4869704615,4.4617313035\C,0.7601111534,0.5065418074,6.2763785837\H,-
0.1079283676,0.7545923825,6.8977254166\C,2.0122244665,0.3243429338,6.8
702410358\C,2.141275887,0.504428153,8.3518685682\C,3.1107439239,-0.007
1512518,6.0761211338\H,4.0950551308,-0.1453426848,6.5341306897\C,2.957
4126389,-0.148638673,4.7000067206\H,3.8315175055,-0.3828788733,4.08231
8411\C,1.2102673887,3.4336155674,1.7501048317\H,1.0976587517,2.4719397
231,-0.1752771582\H,2.4393699204,1.8238159004,0.8833691086\C,1.9604209
088,3.5937925484,2.9345633794\C,1.7106190158,4.6579083734,3.792669747\
C,0.7072425289,5.5838195826,3.4891094583\C,-0.043125011,5.4398444474,2
.3193477727\C,0.2022986784,4.3745099365,1.4595130385\H,-0.3902764618,4
.2596745809,0.5430684624\H,2.7450408384,2.8642376768,3.1733445805\H,2.
301525927,4.7693620095,4.7088200971\H,-0.8281670216,6.164698923,2.0772
669831\H,0.5100619063,6.4209105078,4.1682025195\F,1.8722878636,1.77052
62285,8.7219606737\F,3.3693218666,0.2137917196,8.8002281025\F,1.275207
2628,-0.2759863054,9.0227577969\\Version=ES64L-G16RevC.01\HF=-2021.824
2565\RMSD=7.647e-09\RMSF=8.371e-07\Dipole=-0.747459,-0.6355906,1.29116
11\Quadrupole=7.110139,14.7574956,-21.8676346,6.3263972,-0.0609642,5.1
967673\PG=C01 [X(C26H27F3N1O3P1Ru1)]\\@

6': (Y=CF3)

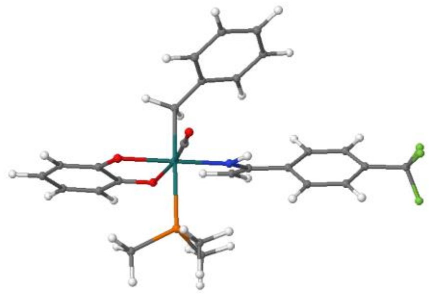

1\1\GINC-COMET-02-49\FOpt\UM06L\Gen\C26H27F3N1O3P1Ru1\TALIPOVM\30-Aug-
2020\0\\#P M06L/chkbasis opt(verytight) freq scf(fermi,xqc,maxcyc=200)
nosym int(grid=ultrafine) Geom(AllCheck) Guess(read) SCRF(Check)\\Tit
le\\0,1\Ru,0.0305592738,0.7040312267,0.2359646016\P,-1.4861277869,-1.2
525197262,0.4534331406\O,-2.061640979,2.6957775472,0.9884771461\O,1.35
55556596,-0.7377196364,-0.7393549891\O,-0.4046619675,0.9281185295,-1.7
657269294\C,-3.013892944,-1.0394154178,1.4258985834\C,-0.6522809773,-2
.6612442285,1.2538240291\C,-2.0651791197,-1.9345161425,-1.1346424806\C
,-1.2214497283,1.9334367601,0.7302035421\C,1.2874808389,-0.6745078481,
-2.0227188289\C,2.0681862872,-1.473161289,-2.897228603\C,1.9031573016,
-1.3555172122,-4.264356345\H,2.5148989512,-1.9672738458,-4.9377195756\
C,0.9565395852,-0.4564431308,-4.8172147208\C,0.1695277983,0.3310391748
,-3.9991866972\H,-0.5683671001,1.0310241731,-4.4058874052\C,0.31840368
51,0.2440834733,-2.594476153\H,-2.7618886918,-0.6920507844,2.443185570
5\H,-3.5902701265,-1.978546366,1.5051350018\H,-3.6505204737,-0.2684034
746,0.9592695592\H,-0.3709149763,-2.392221219,2.2864682911\H,0.2769398
97,-2.8924368102,0.7059319791\H,-1.294977156,-3.559456184,1.2801365496
\H,-2.6416265032,-1.169888732,-1.6822425761\H,-2.6967126863,-2.8295853
518,-0.9911613526\H,-1.1985886544,-2.2117160386,-1.7602833601\H,0.8524
300951,-0.3877967722,-5.9058815174\H,2.7967869167,-2.1669370251,-2.463
8574116\H,3.4184607524,-1.3132748048,2.6310824519\C,2.6239023178,-0.79
39446242,2.0852304977\C,1.668358725,3.2146049573,1.0652134787\H,2.6196
403067,-0.8420130587,0.9916948146\C,1.6279423855,-0.1482799481,2.77318
30066\H,2.5553052268,1.4874435138,0.1410085192\C,1.6606588068,2.132811
2201,0.0648581578\N,0.5704064674,0.4616263061,2.168664441\H,1.57234751
31,2.5113837589,-0.9697049782\H,0.0374100343,1.0132808892,2.8428582605
\C,1.6688430756,-0.0864240541,4.2585358834\C,0.491954456,-0.2053284692
,5.0166415137\H,-0.4681913661,-0.3716752654,4.5125676982\C,0.526513933
5,-0.1469636064,6.4045186148\H,-0.3984751257,-0.2523427018,6.982528208
2\C,1.7432539688,0.0403230414,7.0664169692\C,1.748761898,0.0851686734,
8.5643737758\C,2.9209263456,0.1650913401,6.3283640004\H,3.8744272296,0
.3232502801,6.841446012\C,2.8807210487,0.1006679656,4.9384246187\H,3.8
06942809,0.2216300318,4.3648996186\C,2.3908496652,3.0944696748,2.26860
28144\C,0.9154074108,4.3910038707,0.8811814946\C,0.8746099873,5.387036

6213,1.8525782692\C,2.3476027759,4.0875416097,3.2461208951\C,1.5863242
46,5.2404237279,3.0467731625\H,3.0080940624,2.2002766973,2.4274050368\
H,0.3415954206,4.5133209353,-0.0474519158\H,0.2789468553,6.2913710179,
1.6776030892\H,2.9215833327,3.9621180464,4.1731525953\H,1.5520303554,6
.0233333638,3.8132994427\F,2.9529390466,0.3879790124,9.0656117113\F,1.
3839609637,-1.0980216737,9.093160337\F,0.8776086508,0.9937980014,9.036
8384564\\Version=ES64L-G16RevC.01\HF=-2021.8596257\S2=0.623499\S2-1=0.
\S2A=0.048585\RMSD=4.922e-09\RMSF=1.220e-06\Dipole=-1.1138553,-2.48525
44,-0.7927694\Quadrupole=10.4833332,-1.0904406,-9.3928927,1.139899,-3.
7582985,-1.3883986\PG=C01 [X(C26H27F3N1O3P1Ru1)]\\@

6: (Y= OMe)

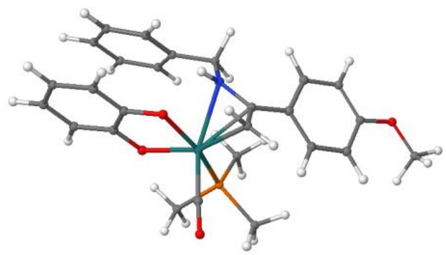

1\1\GINC-COMET-04-58\FOpt\RM06L\Gen\C26H30N1O4P1Ru1\TALIPOVM\30-Aug-20
20\0\\#P M06L/chkbasis opt(verytight) freq scf(fermi,xqc,maxcyc=200) n
osym int(grid=ultrafine) Geom(AllCheck) Guess(read) SCRF(Check)\\Title
\\0,1\Ru,4.1063819437,7.0931468476,2.6568761629\P,2.872343419,5.596987
2711,4.0060111426\O,1.6460425013,7.1765693718,0.978759062\O,5.04097220
41,5.3767272706,1.9687351158\O,5.5417170737,7.9466166717,1.3735119781\
C,1.08495146,5.8594778437,4.3023392378\C,3.4916103104,5.1848819287,5.6
763645579\C,2.8543762767,3.9674135195,3.1925219\C,2.6208214714,7.12728
40595,1.6178423727\C,6.0157450269,5.6456934059,1.100421986\C,6.7788611
29,4.6356844517,0.5004308072\C,7.809573818,4.9583419775,-0.3878619878\
H,8.4065868782,4.1568816141,-0.841055835\C,8.074564871,6.2937837523,-0
.6982372596\C,7.3057032654,7.3128958566,-0.1244807934\H,7.4930662385,8
.3676852589,-0.3627188821\C,6.2806341692,7.0054076091,0.7798860351\H,0
.9024912899,6.6773921144,5.0158076747\H,0.6353131862,4.9389014337,4.71
48182106\H,0.5763499924,6.1019922768,3.3540459668\H,3.4870677852,6.065
4437812,6.3409895752\H,4.52276135,4.8010805058,5.6001213326\H,2.863961
0647,4.3978160772,6.1318651096\H,2.3785518426,4.0547310727,2.201485387
3\H,2.2976699003,3.2340755651,3.8022396636\H,3.8879713496,3.6291751016
,3.0260651251\H,6.2521818613,8.3660057937,3.3064447537\C,3.94095089,9.
2102489383,3.167195142\N,5.7446182169,7.9896556685,4.1170906495\C,4.48
25898667,8.569866618,4.308956591\C,6.5570917007,7.2310741269,5.0605312
731\H,4.6138634882,9.641749355,2.4149176855\H,2.9861986601,9.731953271
4,3.291970607\H,6.5628608705,3.592379566,0.7631308922\H,8.879016672,6.
5495636968,-1.3991998518\C,7.4725457893,6.2720717313,4.3454796376\C,7.

4856088152,4.914736014,4.6804523354\H,6.8139953581,4.5422677838,5.4648
53804\C,8.3505599158,4.0296316416,4.0362150519\H,8.343478113,2.9676321
615,4.307617261\C,9.2143939823,4.4948612522,3.0459529077\C,9.212798220
2,5.846927454,2.7054327935\H,9.874923732,6.2181354702,1.9157011675\C,8
.3486778023,6.7274765996,3.3511695804\H,8.3631590406,7.7883237698,3.06
65966119\H,5.8845123591,6.6877379287,5.7441647336\H,7.1582660086,7.922
9345488,5.6870216383\C,3.8277442051,8.6275373461,5.6299749781\C,4.5427
86984,8.7283195277,6.837966343\H,5.6351966366,8.7585781972,6.836306531
3\C,3.8885128969,8.8364824112,8.0572540341\H,4.4528228422,8.9202279435
,8.9915488974\C,2.4879040921,8.8570798618,8.1174698458\O,1.938109243,8
.950788854,9.3438236623\C,1.7573684765,8.7931822853,6.9205218422\H,0.6
635696376,8.8257123418,6.9239925958\C,2.4284334633,8.6901938628,5.7074
2372\H,1.8412808047,8.6426708636,4.7830469145\H,9.8838834068,3.7992845
797,2.526891712\C,0.5358189368,8.9996124168,9.4483382972\H,0.119437236
4,9.880603049,8.9249575324\H,0.3075125775,9.0785584884,10.5204716401\H
,0.0658173801,8.0824079423,9.0462525431\\Version=ES64L-G16RevC.01\HF=-
1799.5503615\RMSD=6.044e-09\RMSF=1.555e-06\Dipole=-2.0761464,0.2041578
,4.7169652\Quadrupole=-37.8218361,-3.2686381,41.0904741,-24.0147725,16
.4476295,63.0690917\PG=C01 [X(C26H30N1O4P1Ru1)]\\@

TS(6→6'): (Y= OMe)

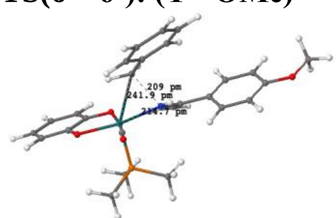

1\1\GINC-COMET-04-51\FTS\RM06L\Gen\C26H30N1O4P1Ru1\TALIPOVM\31-Aug-
202
0\0\\#P M06L/chkbasis opt(verytight,ts,calcfc,noeigentest) freq scf(fe
rmi,xqc,maxcyc=200) nosym int(grid=ultrafine) Geom(AllCheck) Guess(rea
d) SCRF(Check)\\Title\\0,1\Ru,-0.1826207508,0.7843336944,0.0489696369\
P,-1.3952223725,-1.1162573336,0.270644434\O,-2.5454885047,2.3488676914
,1.0444331508\O,1.4302439157,-0.1691164717,-0.8816958713\O,-0.74017829
62,0.910166071,-1.9470170099\C,-3.0598081366,-1.0291360843,-0.45271511
49\C,-1.6570447685,-1.6536130135,1.9869111371\C,-0.6137611558,-2.52945
66748,-0.5581011874\C,-1.6123533077,1.7490756394,0.6802007651\C,1.2815
04363,-0.2723638204,-2.1871571489\C,2.1953660592,-0.9428421716,-3.0192
772132\C,1.9540326794,-1.0415736837,-4.3886226392\H,2.6773468287,-1.55
69596148,-5.0318989321\C,0.7909028866,-0.4900429428,-4.946800717\C,-0.
1375430337,0.164863506,-4.1401133861\H,-1.0508156815,0.6026708011,-4.5
606926599\C,0.0981664367,0.2980403349,-2.7593694723\H,-3.6560676264,-0
.2557927306,0.0597396573\H,-3.5813055902,-1.9994281979,-0.3721853427\H
,-2.9740972077,-0.7442047321,-1.5144191884\H,-2.1938111103,-0.86900158

31,2.5469401453\H,-0.6817021163,-1.8247059941,2.4744851662\H,-2.247612
7044,-2.5863030515,2.0222460619\H,-0.4703324927,-2.2996372057,-1.62843
89277\H,-1.241122596,-3.4335045119,-0.4638223246\H,0.3778881401,-2.718
1808464,-0.1157263721\H,0.6092787114,-0.5738723106,-6.0250434041\H,3.0
962559188,-1.3747453165,-2.5669619106\H,2.8585428324,-1.8345085332,2.4
348209222\C,2.2298753385,-1.1097290955,1.9072273556\H,2.1744671217,-1.
1460094574,0.8137794237\C,1.5524329681,-0.1553183791,2.6096310823\C,1.
549228007,2.2721244312,0.8469286757\N,0.7101223208,0.745569952,2.00088
51585\H,0.3017099965,1.3956573315,2.6708702372\C,1.710937358,-0.013710
5562,4.0809614516\C,0.6349814465,0.3680992998,4.9045904549\H,-0.358297
6477,0.5354765057,4.4678389968\C,0.7853305798,0.5115884754,6.275985133
9\H,-0.0582924113,0.7991568286,6.9120162237\C,2.0297901173,0.276902533
,6.8796974027\O,2.0886158006,0.4436735451,8.2194733874\C,3.114504412,-
0.105708782,6.0793481262\H,4.1010225213,-0.2866157535,6.5165692184\C,2
.9449275422,-0.2447172214,4.7025655506\H,3.8099105749,-0.5209673937,4.
0878689678\C,1.3343262336,3.4145758174,1.7124509837\H,1.2082503993,2.4
376297983,-0.2039302224\H,2.5147893062,1.7535939133,0.8754821088\C,2.0
66741822,3.5561346702,2.9102320249\C,1.8480849023,4.6414742295,3.75008
98962\C,0.893952349,5.6078774773,3.4155836304\C,0.1603214435,5.4817379
268,2.2332703581\C,0.3746437913,4.3953953419,1.3915629682\H,-0.2054679
523,4.2944089783,0.4654846567\H,2.8089948032,2.7924306752,3.176094974\
H,2.4243563648,4.7369147772,4.6773592035\H,-0.587508718,6.2369699971,1
.967157756\H,0.7211109197,6.4615166615,4.0806686891\C,3.3129701811,0.2
062755638,8.8666138189\H,3.652171135,-0.8380104326,8.7283197149\H,3.13
97472345,0.3875134121,9.9370391436\H,4.1042884191,0.8923580162,8.50907
11937\\Version=ES64L-G16RevC.01\HF=-1799.4896074\RMSD=7.669e-09\RMSF=1
.493e-06\Dipole=-0.044483,-0.6147803,3.1311668\Quadrupole=-2.2410324,-
1.9159616,4.156994,7.1244791,17.2713394,5.315906\PG=C01 [X(C26H30N1O4P
1Ru1)]\\@

6’: (Y= OMe)

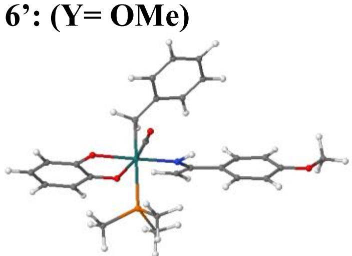

1\1\GINC-COMET-04-71\FOpt\UM06L\Gen\C26H30N1O4P1Ru1\TALIPOVM\30-
Aug-20
20\0\\#P M06L/chkbasis opt(verytight) freq scf(fermi,xqc,maxcyc=200) n
osym int(grid=ultrafine) Geom(AllCheck) Guess(read) SCRF(Check)\\Title
\\0,1\Ru,0.0380251685,0.7103813997,0.2357563266\P,-1.4614647778,-1.251
6641297,0.4748792761\O,-2.0536622106,2.6934325868,1.0106170549\O,1.355
3440955,-0.72897208,-0.7549136179\O,-0.4294078004,0.9271662918,-1.7630

213132\C,-2.9857061125,-1.0434316388,1.454579728\C,-0.6152561331,-2.65
11635718,1.278907585\C,-2.0468444131,-1.9494929945,-1.1044059058\C,-1.
2125913189,1.9338499678,0.744366264\C,1.268011018,-0.6682370588,-2.037
9834645\C,2.0402025148,-1.4649955741,-2.9214074663\C,1.8558109856,-1.3
536716595,-4.2872015594\H,2.4615089234,-1.9648739582,-4.9666410203\C,0
.8971344334,-0.4620342492,-4.8291526192\C,0.1178770354,0.3239523065,-4
.001389328\H,-0.6296138805,1.0187313374,-4.3997429103\C,0.2864839357,0
.2431199389,-2.5986489458\H,-2.7301005359,-0.6855724019,2.467259024\H,
-3.5549295413,-1.9859623974,1.5449669549\H,-3.6303928243,-0.2805355099
,0.9856219714\H,-0.328380381,-2.3741596666,2.3079438961\H,0.3119250067
,-2.8800332878,0.7265398156\H,-1.2526777196,-3.5528845442,1.314621412\
H,-2.6329339898,-1.1930483833,-1.6531755551\H,-2.6702909163,-2.8485641
768,-0.9504823561\H,-1.1822543198,-2.2237228441,-1.7341428483\H,0.7765
389471,-0.3971181525,-5.9164360314\H,2.7784271117,-2.1535918807,-2.495
8266348\H,3.463105352,-1.2942525058,2.5786850628\C,2.6653259501,-0.762
695561,2.0491927403\C,1.6680362483,3.2372386898,1.0246292751\H,2.66065
29498,-0.7766980678,0.9547537022\C,1.668560971,-0.136795676,2.75988366
55\H,2.554876609,1.5111342244,0.0991949014\C,1.6547017557,2.1496872907
,0.0304258425\N,0.6102048004,0.4750548876,2.1609200886\H,1.5513796125,
2.5222157318,-1.0049434203\H,0.0761007532,1.0159233896,2.8432882337\C,
1.713323111,-0.0915540185,4.2432920788\C,0.5400778958,-0.1998258071,5.
0119841354\H,-0.4268965938,-0.3498526753,4.5142210574\C,0.5756560317,-
0.154914748,6.3975444792\H,-0.3380873347,-0.2523241769,6.9928038596\C,
1.7971896777,0.0096728997,7.0680503319\O,1.7405841362,0.0471458028,8.4
169370699\C,2.9772327555,0.1239209716,6.3205786945\H,3.9439596558,0.26
57287947,6.8126927763\C,2.9236404959,0.0707524483,4.9288586234\H,3.853
6046532,0.1834378979,4.3582715715\C,2.3982212191,3.1244979581,2.224144
1525\C,0.9114786134,4.4112909573,0.8401903855\C,0.8746839102,5.4119594
276,1.8071411764\C,2.3584279944,4.1216690168,3.1973934114\C,1.59397919
61,5.2725359611,2.9975966377\H,3.0159025605,2.2311191084,2.3851492293\
H,0.3304764383,4.5274466272,-0.0848167201\H,0.2754906463,6.3139828508,
1.6317294048\H,2.9367756134,3.9995808067,4.1222398281\H,1.5621931883,6
.0587375397,3.7609870977\C,2.9410228708,0.206330455,9.1301265267\H,3.6
449984954,-0.6249098254,8.9350020961\H,2.6721130607,0.2049481403,10.19
60661013\H,3.4372244064,1.1645875149,8.8854081709\\Version=ES64L-G16Re
vC.01\HF=-1799.5254149\S2=0.656209\S2-1=0.\S2A=0.055649\RMSD=5.874e-09
\RMSF=1.388e-06\Dipole=-0.4534503,-2.4646092,1.2599705\Quadrupole=-1.4
502717,-17.7977583,19.24803,1.2871997,12.1746681,-0.3218521\PG=C01 [X(
C26H30N1O4P1Ru1)]\\@

Radical Fragment 1

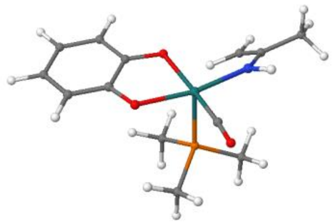

1\1\GINC-COMET-10-
21\FOpt\UM06L\GenECP\C13H19N1O3P1Ru1(2)\TALIPOVM\28-
Aug-2020\0\\#P M06L/genECP opt(verytight) freq scrf(pcm,solvent=1,4-di
oxane) scf(fermi,xqc,maxcyc=200) nosym int(grid=ultrafine)\\Title\\0,2
\Ru,-1.4637864544,0.2746258517,-0.6217650294\P,-1.8433250825,-1.587047
3665,0.5972869716\O,-4.4123769928,0.5494222321,-1.143064634\O,-1.17284
70801,-0.9435958734,-2.2742769803\O,0.6044989752,0.1760151649,-0.71069
35341\C,-2.4065193377,-1.2725471342,2.2921398169\C,-0.3429857652,-2.59
74021292,0.7589939907\C,-3.0690125039,-2.7164101063,-0.1222750006\C,-3
.2735396996,0.473427621,-0.9047883716\C,0.0816649026,-1.2854794821,-2.
4620117529\C,0.4940650673,-2.2116499514,-3.4392026345\C,1.8463055343,-
2.5020670983,-3.5860412742\H,2.1683402332,-3.2191367162,-4.3502751722\
C,2.8038656048,-1.8816040689,-2.7641345845\C,2.4187285356,-0.968088205
5,-1.7871842178\H,3.1548325059,-0.4775728454,-1.139852036\C,1.05683020
03,-0.6601827481,-1.6157082165\H,-1.6675755989,-0.6364534466,2.8105203
026\H,-2.5293645604,-2.2188389349,2.8482464036\H,-3.3705033576,-0.7377
309465,2.2704353211\H,0.4415441039,-2.0390700793,1.2947242075\H,0.0462
05899,-2.8551137917,-0.2418565034\H,-0.5630417004,-3.5306166535,1.3072
361598\H,-4.0535620535,-2.2230841254,-0.1772347303\H,-3.1600523372,-3.
6372026684,0.4808059452\H,-2.7593088104,-2.9778782824,-1.1477328052\H,
-2.269860031,2.2915645649,0.87984772\C,0.4151102466,1.0716474839,2.230
9787987\N,-1.4726579156,1.6539206437,0.8614368943\C,-0.6244688736,1.89
73429207,1.901627642\C,-0.9096270349,3.1363010046,2.7041727508\H,-0.83
30870909,4.0426778351,2.0760861429\H,-0.2093614639,3.2505732757,3.5461
918498\H,-1.9354956125,3.1196263697,3.1173389652\H,1.0849723003,1.3284
814836,3.0580790918\H,0.6415269992,0.1824662055,1.6340532544\H,-0.2655
31016,-2.6804919821,-4.0756395174\H,3.8660992648,-2.1211380208,-2.8931
552341\\Version=ES64L-G16RevC.01\HF=-1222.8286686\S2=0.765559\S2-1=0.\
S2A=0.750165\RMSD=6.618e-09\RMSF=4.077e-06\Dipole=-0.9723417,-0.863777
1,2.3565395\Quadrupole=-3.7492347,8.5066154,-4.7573807,3.4594508,-6.86
22332,-0.7893385\PG=C01 [X(C13H19N1O3P1Ru1)]\\@

Radical Fragment 2

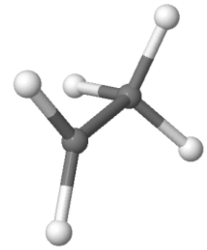

1\1\GINC-COMET-10-34\FOpt\UM06L\GenECP\C2H5(2)\TALIPOVM\28-Aug-2020\0\
\#P M06L/genECP opt(verytight) freq scrf(pcm,solvent=1,4-dioxane) scf(
fermi,xqc,maxcyc=200) nosym int(grid=ultrafine)\\Title\\0,2\H,4.384849
2594,3.8343261595,0.8157036869\C,3.7706381063,3.951082724,-0.095684622
8\H,2.9346352855,1.8750913026,0.1205883044\C,2.7347077184,2.9028030593
,-0.208430679\H,4.4865681863,3.9399750169,-0.9476103742\H,3.336052011,
4.967151918,-0.0802332209\H,1.8358394331,3.0618398198,-0.8176730943\\V
ersion=ES64L-G16RevC.01\HF=-79.0699757\S2=0.756411\S2-1=0.\S2A=0.75002
4\RMSD=5.472e-09\RMSF=1.068e-06\Dipole=0.110727,0.0587785,-0.0553348\Q
uadrupole=0.6681616,0.288862,-0.9570236,0.9468041,0.0785304,-0.608149\
PG=C01 [X(C2H5)]\\@

Radical Fragment 3

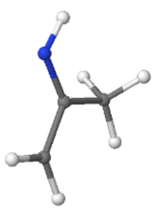

1\1\GINC-COMET-10-36\FOpt\UM06L\GenECP\C3H6N1(2)\TALIPOVM\28-Aug-2020\
0\\#P M06L/genECP opt(verytight) freq scrf(pcm,solvent=1,4-dioxane) sc
f(fermi,xqc,maxcyc=200) nosym int(grid=ultrafine)\\Title\\0,2\H,3.1232
069079,-0.6309771825,-0.3208757943\N,0.3981145481,-0.799842443,-0.9600
887402\H,-0.4125927492,1.6038239896,-0.5695186595\C,0.5419854266,1.361
8663227,-0.0872180185\H,2.2531546759,-1.0993415643,1.1519685083\C,2.38
9189292,-0.2784727586,0.4253170684\H,2.8370775699,0.5734058517,0.96220
8767\C,1.0786641522,0.0654047492,-0.2379483923\H,1.0499024723,2.136918
3586,0.4982917064\H,0.9059277042,-1.6963353233,-0.9827764453\\Version=
ES64L-G16RevC.01\HF=-172.4482853\S2=0.775006\S2-1=0.\S2A=0.7502\RMSD=3
.041e-09\RMSF=4.116e-06\Dipole=0.8032785,0.0949672,0.5203757\Quadrupol
e=1.2380319,1.3481094,-2.5861413,-1.3188939,-0.0712861,0.1592876\PG=C0
1 [X(C3H6N1)]\\@